

**New Synthetic Strategies for Semiconducting
Polymers: Incorporation of Tin, Boron and
Gold as Metalfunctionalities
and Dinucleophile Synthesis**

Dissertation

Zur Erlangung des Doktorgrades
der Mathematisch-Naturwissenschaftlichen Fakultät
der Christian-Albrechts-Universität zu Kiel

vorgelegt von

Annika C. J. Heinrich

Kiel 2015

1. Gutachterin: Prof. Dr. Anne Staubitz

2. Gutachterin: Prof. Dr. Thisbe K. Lindhorst

Tag der mündlichen Prüfung: 13. Juli 2015

Zum Druck genehmigt: 13. Juli 2015

gez. Prof. Dr. Wolfgang J. Duschl, Dekan

Die vorliegende Arbeit wurde unter Anleitung von
Prof. Dr. Anne Staubitz
am Otto Diels-Institut für Organische Chemie
der Christian-Albrechts-Universität zu Kiel
in der Zeit von Januar 2012 bis Mai 2015 angefertigt.

Hiermit erkläre ich, Annika C. J. Heinrich, an Eides statt, dass ich die vorliegende Dissertation selbstständig und nur mit den angegebenen Hilfsmitteln angefertigt habe. Inhalt und Form dieser Arbeit sind, abgesehen von der Beratung durch meine Betreuerin Prof. Dr. Anne Staubitz, durch mich eigenständig erarbeitet und verfasst worden. Die Arbeit entstand unter der Einhaltung der Regeln guter wissenschaftlicher Praxis der Deutschen Forschungsgemeinschaft. Weder die gesamte Arbeit noch Teile davon habe ich an anderer Stelle im Rahmen eines Prüfungsverfahrens eingereicht. Dies ist mein erster Promotionsversuch.

Kiel, den 28. Mai 2015

(Annika C. J. Heinrich)

“Nur der Versuch ist schlüssig,
niemals aber die unbewiesene Behauptung.“

Robert Boyle

In tief empfundener Liebe und Dankbarkeit für meine Eltern.

Ich weiß, ihr seid immer um mich, aber ich wünschte, ihr könntet bei mir sein!

Danksagung

Ich möchte mich an dieser Stelle bei allen bedanken, die mich während der letzten Jahre und damit bei der Anfertigung dieser Arbeit unterstützt haben.

An erster Stelle gilt mein herzlicher Dank Prof. Dr. Anne Staubitz. Vielen Dank für die interessante, anspruchsvolle und spannende Themenstellung dieser Arbeit, die so manches unerwartete Ergebnis geliefert hat und deine ausgezeichnete Betreuung. Durch deine scheinbar unerschöpfliche Motivation und dein Engagement hast du es immer wieder geschafft, mich zu begeistern, an meine Grenzen und darüber hinaus zu führen. Danke für dein Vertrauen und deine Unterstützung in allen Situationen!

Ein weiteres großes Dankeschön gilt der Deutschen Bundesstiftung Umwelt (DBU), die mir durch ein Promotionsstipendium über drei Jahre diese Doktorarbeit finanziert hat. Die jährlichen Seminare und Veranstaltungen wie die Verleihung der Umweltpreise haben mir immer viel Spaß gebracht: Ich habe vor Allem durch die interdisziplinären Vorträge viel gelernt und durfte viele nette Menschen kennen lernen.

Vielen Dank auch an Prof. Dr. Thisbe K. Lindhorst für die Übernahme des Zweitgutachtens. Ich möchte mich auch bei allen Institutsangehörigen für die schöne Zeit bedanken, bei der spektroskopischen Abteilung um Prof. Dr. Frank Sönnichsen für ihre Mühe bei der Anfertigung meiner Messungen, allen voran Gitta und Marion für die Erfüllung so mancher Sonderwünsche und die vielen spontanen Messungen, die ihr mir ermöglicht habt! Vielen Dank auch an Prof. Dr. Christian Näther und seine Mitarbeiter für die Anfertigung der Röntgenstrukturanalysen, thanks to Dr. Paul Gates for measuring all the high resolution mass spectra.

Meinen Praktikanten/Bachelor-Student(innen) Birk, Mischa, Julia, Elly und Marscha möchte ich sehr für ihre Arbeit und die gemeinsame Zeit danken, ebenso dem gesamten Arbeitskreis Staubitz! Danke für die schöne und witzige Zeit mit euch vor, während und nach den Frühstücksrunden. Mein besonderer Dank gilt hier Julian, nicht nur für die sehr schönen gemeinsamen Jahre im Labor (und deine Hilfe wenn z. B. mal wieder was zu weit oben stand) sondern auch für die fachlichen Gespräche und das engagierte Korrekturlesen dieser Arbeit!

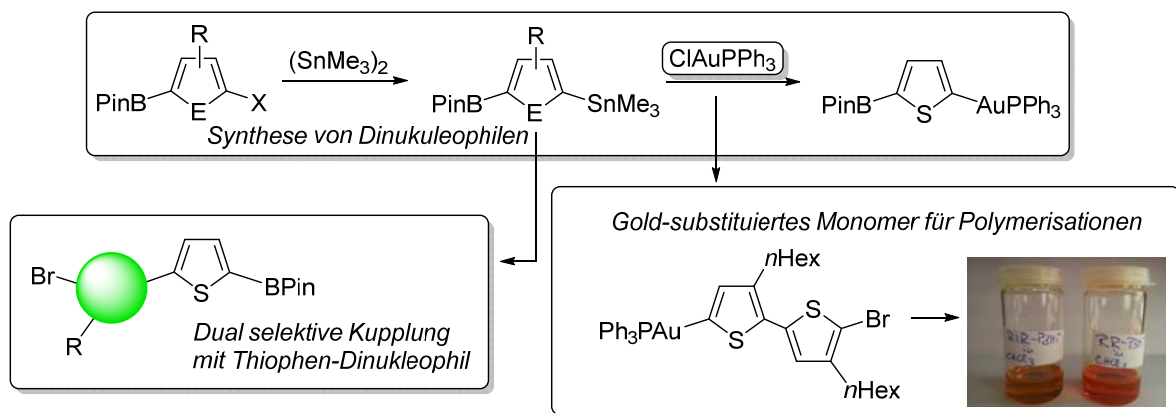
Viel zu deutlich musste ich spüren, wie wichtig Familie und Freunde sind. Ihr verdient meinen größten Dank: Milena, Astrid, Jette, Sophie und alle anderen, die mich aufgefangen haben, vor Allem in den letzten Monaten! Egal was war, ihr habt mich unterstützt wo ihr konntet, mir zugehört und ob nötig oder nicht, mich bei einem schönen spontanen Ausritt oder Kaltgetränk abgelenkt! Ilse, danke für deine Unterstützung (und damit ist nicht nur das Korrekturlesen der Arbeit gemeint)!

Meine Eltern haben mir so vieles ermöglicht und dafür bin ich euch so dankbar! Ich hätte euch so gerne noch so viel zurückgegeben und noch viel mehr Zeit mit euch verbracht. Ihr fehlt mir einfach unglaublich! Zum Glück habt ihr mir Basti zur Seite gestellt, der gerade mehr als erfolgreich die Aufgaben des großen Bruders annimmt und meistert. Ich weiß, dass ich alles andere als einfach bin und genau deshalb bin so froh, dass du da bist und ich mich immer auf dich verlassen kann!

Jörn, du warst in den letzten Jahren ein ganz besonderer Teil meines Lebens und immer an meiner Seite! Danke dafür und dass es dich gibt und einfach für alles, was wir gemeinsam erleben durften. Du hast mich immer unterstützt, mir den Rücken frei gehalten und an mich geglaubt – egal, was war!

Zusammenfassung

In dieser Arbeit wurde eine generell anwendbare Methode zur Synthese von dinukleophilen Verbindungen entwickelt, die sowohl mit Zinn als auch mit Bor funktionalisiert sind. Am Beispiel eines Thiophenderivates konnte die Methode einer sowohl Nukleophil- als auch Elektrophil-selektiven Kreuzkupplung erfolgreich gezeigt werden. Diese Art der Reaktion erlaubt es, unterschiedliche Aromaten miteinander zu verbinden, wobei die Produkte jeweils noch über eine Bor- und eine Halogenfunktion verfügen. Am Beispiel elektronen- armer, -reicher und neutraler Dielektrophile konnte die allgemeine Anwendbarkeit der Reaktion gezeigt werden. Die Produkte eignen sich unter anderem für die Verwendung als Monomere in Polymerisationsreaktionen und damit für die Synthese halbleitender Polymere.

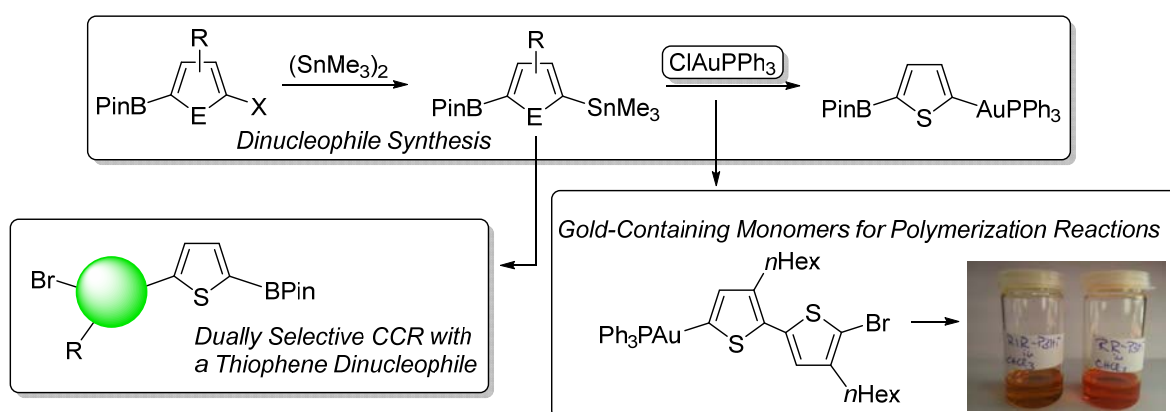


Darüber hinaus konnte die erste Verbindung einer weiteren Klasse von Dinukleophilen synthetisiert werden: Es gelang, ein Thiophenderivat herzustellen, welches sowohl über eine Bor- als auch eine Goldfunktion verfügt. Goldorganyle wurden bisher nur selten stöchiometrisch verwendet. Es zeigt sich allerdings, dass diese unter milden Reaktionsbedingungen und mit guten Ausbeuten Kreuzkupplungsreaktionen eingehen. Damit eignet sich diese neue sowohl Gold- als auch Bor-funktionalisierte Verbindung ebenfalls für eine potentielle dual-selektive Kreuzkupplung.

Die Synthese von hoch definiertem, regio regulärem Poly(3-hexylthiophen) (P3HT) erfolgt über die Methode der lebenden Polymerisation mit sowohl halogen- als auch metallfunktionalisierten Monomeren. Problematisch ist bisher jedoch die Synthese stabiler, isolierbarer Monomere. Es wurde daher ein Monomer entwickelt, welches aus zwei Hexylthiophen-Einheiten besteht und einerseits eine nukleophile Goldgruppe und andererseits eine Bromidgruppe als elektrophile Funktionalität trägt. Dieses ist luft- und feuchtigkeitsstabil. Ein Katalysatorscreening für die Polymerisation ergab, dass je nach Katalysator zwei Typen von Polymeren gebildet werden konnten. Beide waren zwar regio regulär, aber dennoch deutlich voneinander unterschiedlich: Zum einen ergab sich ein HH-TT-P3HT, zum anderen konnte das erwartete HT-P3HT erhalten werden (HH = Head-to-Head, TT = Tail-to-Tail, HT = Head-to-Tail). Diese erfolgreichen Polymerisationsreaktionen brachten zahlreiche neue Einblicke und Erkenntnisse in Bezug auf Kupplungsreaktionen mit Goldorganylen mit sich.

Abstract

In this thesis a general method for the synthesis of dinucleophilic compounds, containing both a stannyl and a boron moiety, was developed. Using a thiophene derivative as dinucleophile, it was possible to show that a both nucleophile and electrophile selective cross-coupling reaction could be performed successfully. This type of reaction allows the combination of different aromatic systems, where the products still contain both a halogen and a boron functionality. It was shown for electron poor, rich and neutral dielectrophiles that this reaction can be used as a general method. The resulting products can be used, besides other potential applications, as monomers in polymerization reactions and thus for the synthesis of semiconducting polymers.



Furthermore the first compound of another class of dinucleophiles could be successfully synthesized: A thiophene derivative which contains both a boron and a gold moiety as metal functional groups. Organogold reagents have been rarely used in stoichiometric amounts so far. It was shown that these compounds perform cross-coupling reactions under mild reaction conditions and in high yields. Therefore this type of both gold and boron functionalized dinucleophiles are suitable for a potential use in dually-selective cross-coupling reactions.

The synthesis of well-defined regio regular poly(3-hexylthiophene) (P3HT) is generally performed by using the method of living polymerization. Monomers for these reactions generally contain both a halogen and a metal functionality. Until now the synthesis of monomers that are stable and can be isolated before use is a problem. Therefore a monomer was synthesized, which was comprised of two hexylthiophene units and which contained gold moiety as functional groups as well as a bromide as electrophile functionality. This monomer was stable to air and moisture. A catalyst screening of the polymerization reaction gave two different polymers as products, depending on the catalyst species used. Both polymers showed high regio regularities but were considerably different from each other: On the one hand HH-TT-P3HT was obtained, on the other hand the expected HT-P3HT could be isolated (HH = Head-to-Head, TT = Tail-to-Tail, HT = Head-to-Tail). These successful polymerization reactions gave new insights and findings especially on cross-coupling reactions of organogold reagents.

Abbreviations

A	area
ATR	attenuated total reflectance
Boc	<i>tert</i> -butyloxycarbonyl
calcd.	calculated
CI	chemical ionization
COSY	correlated spectroscopy
CV	column volume
d	doublet (NMR)
DCM	dichloromethane
dd	doublet of doublets (NMR)
Decomp. temp.	decomposition temperature
DMF	<i>N,N</i> -dimethylformamide
EI	electron ionization
ESI	electron spray ionization
FT	fourier transform
GC	gas chromatography
GC-MS	gas chromatography-mass spectrometry
GPC	gel permeations chromatography
HH	head-to-head
HMBC	heteronuclear multiple bond coherence
HOMO	highest occupied molecular orbital
HRMS	high resolution mass spectrometry
HSQC	heteronuclear single quantum coherence
HT	head-to-tail
Ind	indole scaffold
IR	infrared
LDA	lithium diisopropylamide
LUMO	lowest occupied molecular orbital
m	medium (concerning the intensity) (IR)
m	multiplet (NMR)
MALDI	matrix-assisted laser desorption/ionization
M_n	number average molecular weight
M.p.	melting point
M_w	weight average molecular weight
MW	microwave
MS	mass spectrometry
n	amount of substance
NMR	nuclear magnetic resonance
PDI	polydispersity index
Phe	benzene scaffold
Pyr	pyridine scaffold
OFET	organic field effect transistor
OLED	organic light emitting diode
OSC	organic solar cell
P3AT	poly(3-alkyl)thiophene
Pin	pinacol

PS	polystyrene
rir	regio irregular
R _f	response factor
R _r	regio regular
rt	room temperature
s	strong (concerning the intensity) (IR)
s	singlet (NMR)
t	triplet (NMR)
THF	tetrahydrofuran
TMEDA	tetramethylethylenediamine
TMS	tetramethylsilane
TOC	table of contents
TOF	time of flight
Tph	thiophene
TT	tail-to-tail
UV-Vis	ultraviolet-visible
w	weak (concerning the intensity) (IR)

A Guide to This Thesis

This thesis is divided into 6 chapters (see Table of Contents). One part of the results in this thesis and a short review article has been published in a peer reviewed journal, and the original publication can be found in the subsections of chapter 3 (“Results and Discussion”). The majority of the other results are described and put into context in the form of manuscripts. The corresponding “Supporting Information” (SI), which includes all experimental data of the manuscripts or publication can be found in subsections of chapter 5 (“Experimental Section”). In addition to the overall “Summary and Outlook” (Chapter 4), each subsection contains its own outlook with further experiments. The details for these can also be found in the SI, placed directly after the SI-part for the corresponding manuscript. As every publication has its own introduction, chapter 1 (“Introduction”) provides some general information on the topics of cross-coupling reactions and semiconducting polymers.

Every publication or manuscript starts with its own numbering concerning figures, schemes, tables and compounds. To allow a clear identification of each compound, molecules of chapter 3.1 are specified in the outlook as **P1-X**, where the prefix **P** stands for publication; compounds of chapter 3.2 are specified as **M1-X**, where the prefix **M** stands for manuscript. The same procedure was done for chapter 3.3, where compounds are specified as **M2-X** and in chapter 3.4, where **P2-X** is used. For all other compounds, figures, tables and schemes a continuous numbering can be found.

Table of Contents

1 Introduction.....	1
1.1 Organic Semiconductors.....	1
1.2 Polythiophenes	3
1.2.1 Characteristics and Analysis of Poly(3-alkylthiophenes)	4
1.2.2 Synthesis of Poly(3-alkylthiophenes).....	5
1.3 Cross-Coupling Reactions	8
1.4 Selectivity in Cross-Coupling Reactions	8
1.5 Elemental Gold and Gold in Reactions	11
1.5.1 Gold as Catalyst Species.....	11
1.5.2 Stoichiometric use of Organogold Reagents	12
1.5.3 Gold Compared to Other Metals	14
1.6 Synthesis of Organogold Reagents	15
1.7 Gold Recycling.....	15
2 Objectives.....	17
2.1 Selective Cross-Coupling Reactions on Aromatic Dinucleophiles	17
2.2 Synthesis of Aromatic Dinucleophiles	18
2.3 Gold-Containing Thiophene-Type Monomers for Polymerization Reactions	19
3 Results and Discussion	20
3.1 Chemoselective Cross-Coupling Reactions.....	20
3.1.1 Nucleophile and Electrophile Selective Cross-Coupling Reactions.....	20
3.1.2 Further Experiments and Outlook	25
3.2 Aromatic Dinucleophiles.....	27
3.2.1 Synthesis of Aromatic Dinucleophiles.....	27
3.2.1.1 Introduction	28
3.2.1.2 Synthesis of Tin-Boron Functionalized Dinucleophiles.....	29

3.2.1.3 Synthesis of Gold-Boron Functionalized Dinucleophiles	34
3.2.1.4 Conclusion	41
3.2.1.5 References	41
3.2.2 An Outlook: Cross-Coupling Reactions on Aromatic Dinucleophiles.....	43
3.2.2.1 Attempted Nucleophile Selective Cross-Coupling Reactions of Tin-Boron Functionalized Dinucleophiles	43
3.2.2.2 Attempted Electrophile- and Nucleophile Selective Cross-Coupling Reactions of Tin-Boron Functionalized Dinucleophiles	45
3.2.2.3 Further Planned Syntheses of Both Organogold- and Boronic Ester Difunctionalized Dinucleophiles.....	47
3.2.2.4 Attempted Nucleophile Selective Cross-Coupling Reactions on Organogold-Boron Functionalized Thiophene.....	48
3.3 Gold-Functionalized Thiophene-Type Monomers in Polymerization Reactions.....	50
3.3.1 Manuscript on Gold-Functionalized Thiophene-Type Monomers in Polymerization Reactions	50
3.3.1.1 Introduction	52
3.3.1.2 Synthesis of a Novel Organogold Monomer.....	53
3.3.1.3 Organogold Cross-Coupling	55
3.3.1.4 Synthesis of an Organogold Bithiophene Monomer	56
3.3.1.5 Polymerization Reactions	57
3.3.1.6 Regio Regular HT-P3HT	61
3.3.1.7 Potential Causes for a Slow Initiation Process.....	62
3.3.1.8 Testing Further Characteristics of a Living Polymerization	67
3.3.1.9 Conclusion.....	69
3.3.1.10 References	70
3.3.2 Outlook and Further Experiments	73

3.3.2.1 Polymerization Reactions of Improved Gold Containing Monomer	73
3.3.2.2 Recycling	74
3.4 Minireview on (Triphenylphosphine)gold(I) Chloride	76
4 Summary and Outlook.....	79
5 Experimental Section.....	85
5.1 Supporting Information on Chapter 3.1.	85
5.1.1 Supporting Information for <i>Org. Lett.</i> 2013 , <i>15</i> , 4666-4669.	85
5.1.2 Further Experimental Data on Chapter 3.1	136
5.2 Supporting Information on Chapter 3.2	157
5.2.1 Supporting Information for the Manuscript <i>Aromatic Dinculeophiles</i>	157
5.2.2 Further Experimental Data on Chapter 3.2	213
5.3 Supporting Information for Chapter 3.3.....	219
5.3.1 Supporting Information for the Manuscript <i>Gold-Functionalized Thiophene-Type Monomers in Polymerization Reactions</i>	219
5.3.2 Further Experimental Data for Chapter 3.3	287
6 References.....	290

1 Introduction

The Nobel Prize is one of the most important awards scientists can receive. The outstanding work of the chemistry Nobel laureates of 2000^[1] and 2010^[2] is of high importance for both industry and researchers in the field of synthetic organic chemistry and organic electronic devices: In 2010, Heck,^[3] Negishi^[4] and Suzuki^[5] were honored with the Nobel Prize for their work on palladium catalyzed cross-coupling reactions.^[2] In 2000, Heeger, MacDiarmid and Shirakawa were awarded this a prestigious prize for the discovery and development of conductive polymers.^[1]

1.1 Organic Semiconductors

Semiconducting polymers can be used for a large variety of applications. For example they can be incorporated into organic electronics like organic solar cells (OSCs),^[6] organic field effect transistors (OFETs)^[6b, 7] and light emitting diodes (OLEDs).^[8] One of the latest developments in the field of entertainment industry is a curved OLED television set (Figure 1).



Figure 1. LG presents their curved OLED TV as new class of home entertainment (reproduced with permission from LG, © 2015).^[9]

The general benefits arising from the use of semiconducting organic polymers, and generally organic semiconductors, can be clarified by the example of this technical achievement: Devices can be produced in thin shapes, they are lightweight and flexible, manufacturing costs and power consumption are low.^[10] Concerning TVs this is why the former cathode ray tubes (CRTs) have been largely replaced by flat screen monitors like OLED TVs (Figure 1). These benefits also apply to solar cells: organic solar cells can be easily processed by roll-to-roll inkjet printing.^[11] If they are printed onto a plastic film, the whole solar cell is as flexible as the film. This procedure makes them potentially cheap in comparison to their inorganic analogues. Both kinds of solar cells have their own advantages: The inorganic crystalline

silicon solar cells have efficiencies up to 26 %^[12] and are used on roofs or in solar fields. In contrast to this organic solar cells have lower efficiencies of 11 % at present,^[12b, 13] but because of their transparency and flexibility, they can be used in other complementary areas. It is conceivable that they can be used on clothing, and they are already used as mobile photovoltaic charger for mobile phones (Figure 2). Research groups are working on improved materials and efficiencies.



Figure 2. A shoulder bag, bearing organic solar cells on the surface allowing to charge an electrical device like a mobile phone induced by sunlight.

The first conducting polymer, doped polyacetylene, was discovered in 1977 by Heeger, MacDiarmid and Shirakawa.^[1a, 14] The general principle of a semiconducting polymer is that it is made up of a large planar conjugated pi-system. In the case of polyacetylene, the cause for its semiconducting properties can be envisioned like this: The polymer contains a system of conjugated double bonds: if these p-orbitals form an overlap, the sp^2 hybridized carbon atoms split up into bonding (π) and anti-bonding (π^*) orbitals, also called HOMO (highest occupied molecular orbital) and LUMO (lowest unoccupied molecular orbital). In the case of ethylene the two electrons in the p_z orbitals of the carbon atoms form the π -bond of the double bond. They occupy the lower-energy HOMO (Figure 3).^[15] For 1,3-butadiene there are four p_z -orbitals to consider: These p_z orbitals form four molecular orbitals where two are occupied and two are unoccupied. This principle can be applied for an infinite number of orbitals, as in the case of a long polymer chain. The resulting energy levels of the different π and π^* orbitals are getting closer to each other and finally they form so called bands: a valence band that is formed of the π orbitals and a conduction band that is formed of the π^* orbitals. Based on this simple model one would expect that the highest level of the valence band and lowest level of the conduction band eventually overlap each other for long polymer chains, but it is not the case concerning semiconducting organic polymers: The Peierls distortion leads to partial localization of electrons by distorting the geometry of the conjugated π -system.^[16]

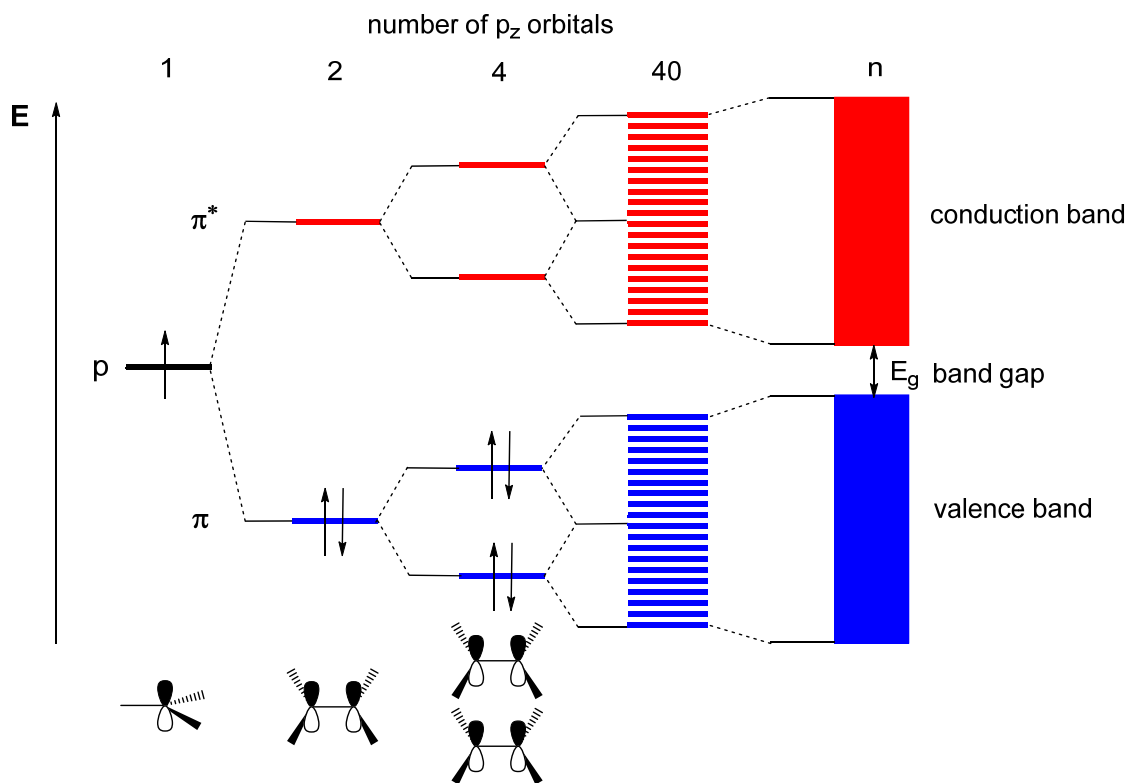


Figure 3. This schematic energy diagram shows the formation of a valence band and a conduction band in a sp^2 -hybridized system as it exists in semiconducting polymers.^[15]

The energy gap between the conduction band and the valence band is called band gap. Conductivity is possible when electrons of the valence band can move into the conduction band by thermal or photochemical excitation. This can happen if both bands overlap, for example in case of metals. Concerning semiconductors, the band gap is narrow which means that electrons can move into the conduction band by thermal or photochemical excitation.^[17] Concerning insulators the conducting band is energetically too far away, and thus not possible to reach even for excited electrons.^[18] Modern conducting organic materials are typically not doped and have intrinsically low band gaps.^[19]

1.2 Polythiophenes

It has been shown that different aromatic systems like polyethylene dioxythiophenes,^[20] fluorenebenzothiazoles,^[21] poly(pyrroles)^[22] and poly(*para*-phenylenes)^[23] can be used as semiconducting polymers. At present thiophene based polymers are considered to be the most promising for applications in organic solar cells.^[24] In general most polymers based on aromatic monomers include alkyl chains in order to afford a good solubility of the polymer and as a result an easily processable material is generated. Nowadays 2,5-poly(3-alkyl)-thiophenes (P3ATs) belong to the best investigated and used polymers.^[19, 25]

1.2.1 Characteristics and Analysis of Poly(3-alkylthiophenes)

The monomers themselves, 3-alkyl-thiophenes, are asymmetric. Therefore three different types of 2/5-linkage can be found in the polymer backbone: head-to-tail (HT), head-to-head (HH) and tail-to-tail (TT) (Figure 4).^[26]

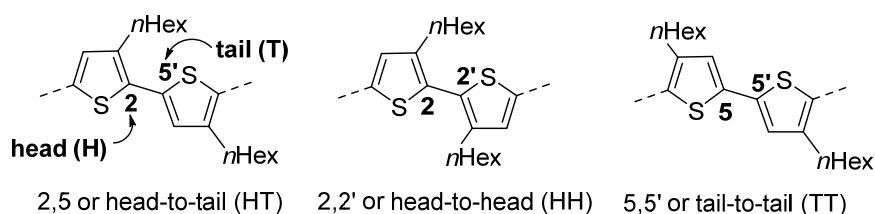


Figure 4. 2,5-Poly(3-alkyl)thiophene can be linked in different ways.

Commonly the sterically hindered 2-position is designated as “head”, the less hindered 5-position as “tail”. These coupling abbreviations can be used as prefix to specify the polymer itself. It is important which kind of polymer is formed in a reaction: the properties of pure HT-P3AT significantly differ from the polymers where HT, HH and TT couplings are also found. Spectroscopy allows an exact characterization of the polymers regarding the structure itself. ¹H NMR spectroscopy shows broad signals which are typical for polymers. Concerning only HT-coupled polymers there is one clear signal in the aromatic region (at 6.9 ppm) for the proton in 4-position of the thiophene ring and one signal in the alkyl region (at 2.7 ppm) for the first methylene group of the alkyl chain that is directly located on the thiophene ring. In contrast to this, TT- and HH-coupling gives shifted signals in the aromatic region (7.0 ppm) and a further signal in the alkyl region (at 2.5 ppm), caused by an interaction of the neighboring alkyl chains (compare Chapter 5.4). UV-Vis spectroscopy shows an absorption maximum of $\lambda_{\text{max}} = 449$ nm for HT-P3HT (poly-(3-hexylthiophene)); other P3ATs show absorption maxima of $\lambda_{\text{max}} = 442$ -456 nm in solution. A polymer with HH or TT defects shows a decreased absorption at lower wavelengths.^[19]

All these differences result from the polymer structure itself and the electronic differences of the regioisomers.^[19, 27] If only HT couplings are present, a regio regular polymer is formed with a planar and linear polymer backbone with a delocalized electronic system (Figure 5, green). If all types of linkage are obtained, a regio irregular polymer is formed. Here the alkyl chains of the thiophene blocks are disordered. The interaction of the chains in the case of a HH coupling leads to a twist of the planes of the heterocycles of at least 30 ° against each

other (Figure 5, red).^[28] This twist results in torsional defects with a lowered delocalization of the π electrons.^[19]

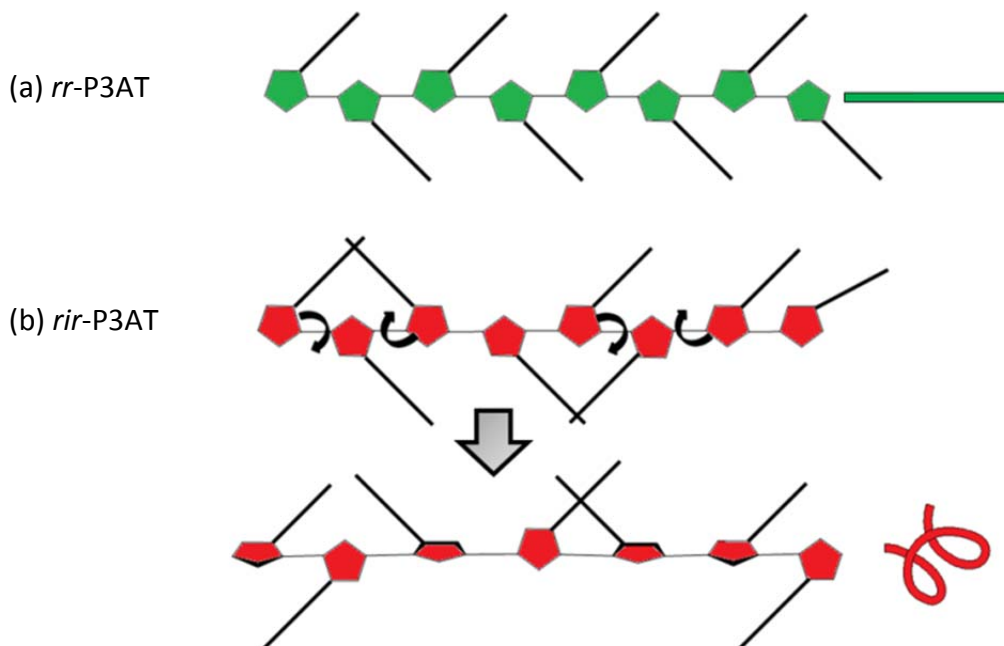


Figure 5. In general regio regular (a) and regio irregular P3AT (b) show different electronic properties. The planar backbone of the regio regular P3AT has a linear structure. The disordered alkyl chains in the regio irregular P3AT cause a twisted polymer backbone.

1.2.2 Synthesis of Poly(3-alkylthiophenes)

Regio irregular polymers are obtained, if step growth polycondensation polymerization reactions are used for the synthesis (Figure 6).^[29] Here monomers of the type X-monomer-X **1** react with another monomer of the type M-monomer-M **2**, often in a Stille^[30] or Suzuki^[30b, 30f, 31] cross-coupling reaction. High molecular weights can only be obtained at nearly full conversion of the monomers. The reason is the mechanism of this type of polymerization. After every coupling event, the catalyst leaves the polymer chain and performs another random coupling. With this, a large number of low molecular weight chains are present in the reaction mixture even at conversion values of > 75% conversion. When most monomers have reacted, more and more chain-chain coupling reactions are catalyzed with the result of an abruptly fast growth of the polymer chains (Figure 6, **3**).^[29]

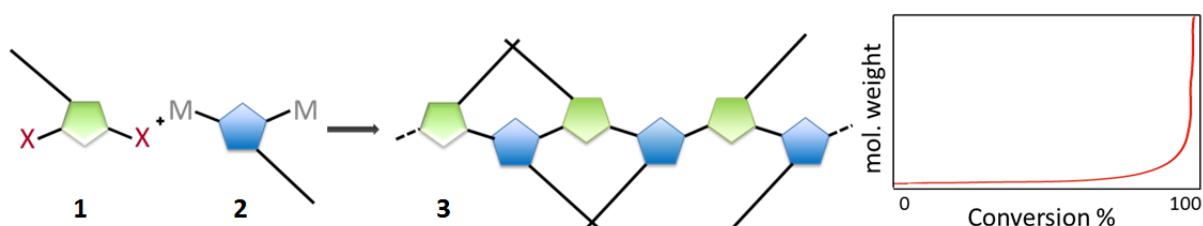


Figure 6. Schematic polymerization principle for a step growth polycondensation reaction.

If only HT coupling in P3AT is found, polymers are described as regio regular. In this type of polymer the backbone forms a planar conjugated system of well delocalized π electrons which results in a good conductivity. Independently of each other Yokozawa and McCulloch developed the living polymerization process for the synthesis of P3HT (Figure 7).^[24a, 32] They prepared a monomer *in situ* that contains both a halogen and a metal functionality on the same molecule **4**. $[\text{Ni}(\text{dppp})\text{Cl}_2]$ as catalytic species led to a polymer **5** with a very high proportion of regio regular HT connections in the backbone. Furthermore, the polymers obtained showed high molecular weights and a low polydispersity index (PDI). In addition, the end group of the polymer chain could be controlled, which gives access to block copolymers.^[33]

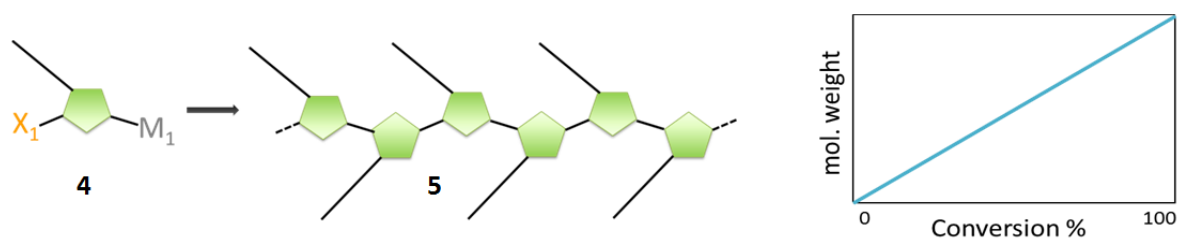
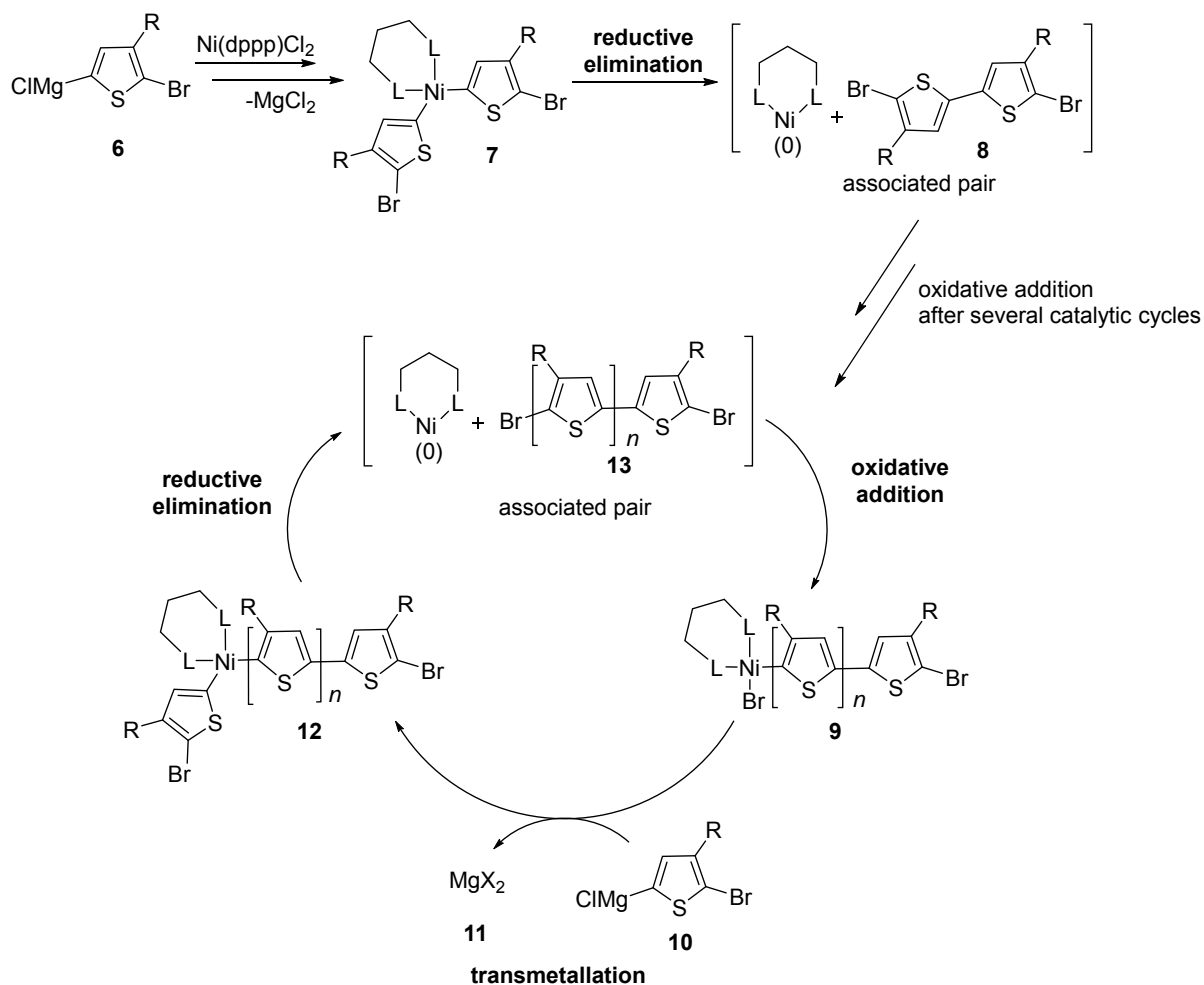


Figure 7. Schematic polymerization principle for a living chain growth polymerization reaction and its reaction kinetic.

Formally this polymerization is also a polycondensation reaction, and should follow the kinetics of a step growth polymerization, but kinetic studies showed the behavior of a living chain growth polymerization. Characteristic for this type of growth is the linear relationship between the conversion of the monomer and the molecular weight (Figure 7).^[24a, 32]

Even if the molecular mechanism is not completely understood by now, its special feature is the unusual reaction behavior of the catalyst species.^[34] The first coupling reaction is a very quickly initiated homo coupling of two monomers **6**, where the Ni (II) catalyst **7** becomes a Ni (0) species **8** after reductive elimination. This species forms a so-called associated pair **8**, **13**: the catalyst stays on the polymer chain. The further sequential steps are typical for cross-coupling reactions and are repeated in a catalytic cycle: Oxidative addition of the catalyst species to the polymer chain **9**, transmetalation and reductive elimination lead to a well-defined polymer (Scheme 1, **12**). The first approaches for such living polymerization were made by using zinc and magnesium as metal functionalities, but similar reactions were demonstrated with tin^[35] and boronic esters^[36] as metal functionalities. In the latter cases the process was not living, although regio regular polymers were obtained.



Scheme 1. Proposed mechanism for the living polymerization.^[19]

If a palladium catalyst is used for the polymerization of the same monomers, the reaction follows the kinetic of a step growth polymerization. The reason for this is that in contrast to the nickel species palladium typically does not form an associated pair that stays together: after the coupling event the palladium species leaves the polymer chain.^[19] This is a disadvantage of this method regarding the fact that only at nearly full conversion of the monomer, high molecular weights can be observed. However, today, there is only one example of a fluorene system with the metal functional group being a boronic ester, where a palladium catalyst can perform a living polymerization process as well, for example when the metal functional group on the monomer is M = boron.^[21]

For many applications it is important that the band gap of the material in a device is low or that it can be tuned. It has been shown that the combination of an electron rich and an electron deficient heterocycle in the polymer backbone leads to a lower band gap.^[37] One possibility to combine heterocycles in the polymer backbone is to use different monomers of

the types X-Monomer1-X (**1**) and M-Monomer2-M (**2**) in a step growth polymerization reaction (see Figure 6).^[29] This method allows the easy combination of different heterocycles, but disadvantages like low molecular weights and high PDIs limit their use in electronic devices, where well-defined polymers are required. If monomers of the type X-heterocycle1-heterocycle2-M were available, the advantages of both polymerization types could be combined: regio regular polymers containing different heterocycles in the polymer backbone could be synthesized with a low PDI at high molecular weights via controlled living chain growth.

1.3 Cross-Coupling Reactions

Both the living chain growth polymerization and the step growth polymerization reactions are based on the principle of cross-coupling reactions. Cross-coupling reactions are the most efficient way to form new carbon-carbon bonds, providing access to highly complex molecular structures from simple building blocks.^[38] The importance of this reaction type was underlined by awarding Heck,^[3] Negishi^[4] and Suzuki^[5] with the Nobel Prize in 2010 for their work on palladium catalyzed cross-coupling reactions.^[2] The connection of sp^- , sp^2 - and sp^3 - hybridized carbon atoms by using transition metals catalysts is essential for both laboratory research and industrial production.^[39]

Many different types of cross-coupling reactions are known, but the reaction principle is almost always the same.^[40] An electrophile R-X (X= I, Br, Cl, OTf, etc.) reacts in a transition metal catalyzed cycle with a nucleophile R-M in generally high yields, where M represents different metal functional groups: Alkyl, vinyl or aryl derivatives can be functionalized by halogen-metal exchange or direct metalation *in situ* with tin (Stille,^[39b, 41] Migita^[42]), boron (Suzuki,^[43] Miyaura^[5]), silicon (Hiyama^[44]), zinc (Negishi^[4]) and magnesium (Kumada,^[45] Corriu^[46]).

1.4 Selectivity in Cross-Coupling Reactions

It is well established that the order of reactivity of the electrophilic coupling partner decreases for the different leaving groups I > OTf > Br >> Cl.^[47] This order is generally found in most types of cross coupling reaction like in Stille or Suzuki type reactions, but exceptions can be found as well: For example in iron-catalyzed Kumada cross-coupling reactions where an order of Cl > OTf > Br > I was found.^[48] This feature has been used for the development of

electrophile selective cross-coupling reactions.^[49] In contrast to this, nucleophile selective cross-coupling reactions have been rarely investigated, most of them on non-aromatic dinucleophiles.^[21, 50] On the one hand (alkene) substrates (**14**) with both a tin and a boron functionality are often used in order to perform a Stille- selective cross-coupling reaction.^[51] On the other hand compounds with two boron functionalities with different boronic ester groups can be found in order to use their different reactivity (**15**).^[52]

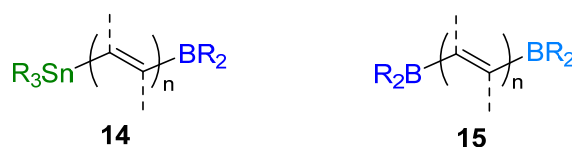
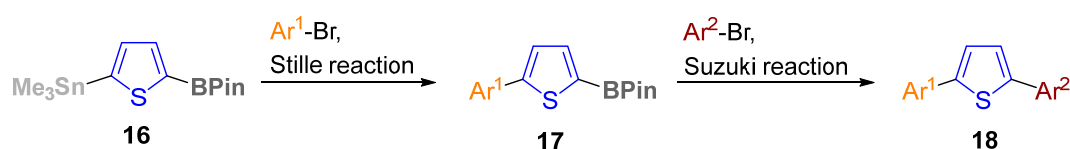


Figure 8. Reported non-aromatic dinucleophiles **14** and **15** that are used for nucleophile-selective cross-coupling reactions.^[51-52]

However nucleophile selective cross-coupling reactions on aromatic dinucleophiles are almost undeveloped.^[21, 50a, 53] The different reaction conditions of Stille and Suzuki-Miyaura reactions have been used a few times, but until 2012, there was only one report published where a nucleophile selective cross-coupling reaction on a tin- and boron-containing aromatic compound, *para*-Bu₃Sn-C₆H₄-B(OR)₂, was used.^[53] In 2012 J. Linshoeft performed the first systematic study of a nucleophile selective cross-coupling reaction on a single aromatic substrate (Scheme 2).^[50a] A thiophene derivative **16** containing both a trimethyl tin group in 2-position and a boronic ester functional group in 5-position was used for Stille coupling reactions with different brominated electrophiles in excellent chemoselectivity and very good yields. A nucleophile-selective sequential one-pot reaction was developed, in which the different reactivities of the Stille and Suzuki-Miyaura cross-coupling reactions could be harnessed.



Scheme 2. Nucleophile-selective cross-coupling reaction.^[50a]

The reason for this only very recent development of nucleophile selective cross-coupling reactions is the lack of synthetic methods for dinucleophilic compounds with different metal functionalities. Linshoeft *et al.* used 2,5-(di-trimethyltin)thiophene as starting material for the synthesis of the dinucleophile **16**. By using one equivalent of methyllithium and

subsequent quenching with an isopropylboronic ester, the product could be isolated in a yield of 55%.^[54] Yamamoto *et al.* synthesized *para*-Bu₃Sn-C₆H₄-B(OR)₂ by using *para*-Br-C₆H₄-B(OMIDA)₂ as starting material, where the *N*-methyliminodiacetic acid (MIDA) group on the boron was used as protecting group during the lithiation. The whole reaction was run at low temperatures of -78 °C to avoid a cleavage of the protecting group: A halogen lithium exchange was performed and a subsequent addition of trimethyltin chloride led to the tin- and boron functionalized species.^[53]

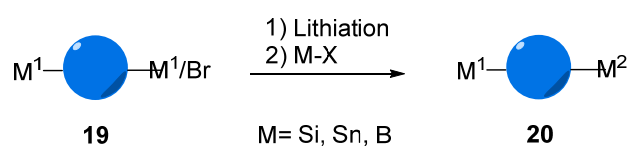
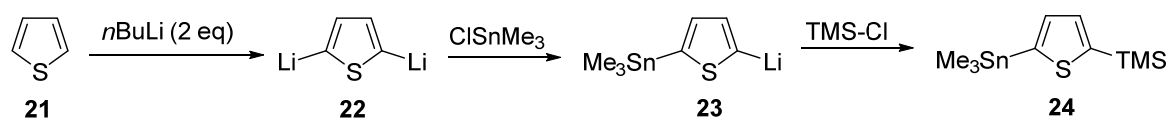


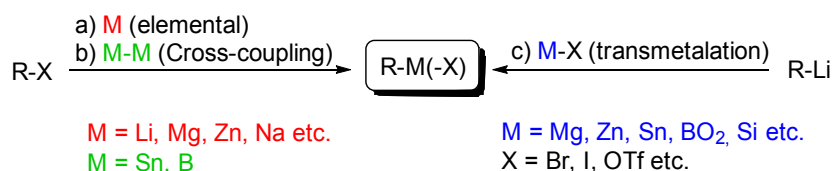
Figure 9. Dinucleophiles can be synthesized by using metalated starting materials.

Another type of synthesis was described by Müller and coworkers who synthesized a thiophene derivative containing tin and silicon as metal functionalities **24**. Thiophene (**21**) was lithiated in 2- and 5 position (**22**). By adding one equivalent trimethyltin chloride a lithium-tin exchange was performed in one position (**23**). Subsequent quenching with trimethylsilyl chloride gave the dinucleophile **24**.^[55]



Scheme 3. Schematic principle for the synthesis of **24** by performing a one-pot-reaction.

This type of one-pot reaction method might be used for other symmetric aromatic systems, although it is possible that reaction conditions have to be adapted. In contrast to this asymmetric aromatic systems like 3-alkyl thiophene might give a mixture of dinucleophiles, because of a lack of site selectivity. In general metal functional groups are introduced by lithiation of a halogenated compound (R-Li) and a subsequent lithium-metal exchange, direct metalation *in situ* or by a cross-coupling between a halogenated (R-X) and a *bis*-metalated species (M-M) like *bis*(trimethyl)ditin, (SnMe₃)₂, or *bis*(pinacolato)diboron, (BPin)₂ (Scheme 4).^[56]



Scheme 4. General synthetic methods for introducing metal- functionalities.

If dinucleophiles are used in nucleophile selective cross-coupling reactions, both metal functionalities should have a different reaction behavior: For example, the distinction between tin and boron is successful, because in contrast to Stille reactions, a successful Suzuki reaction requires a base.^[54]

1.5 Elemental Gold and Gold in Reactions

Gold in its elemental form has always fascinated mankind. One of the most famous art objects was manufactured 3300 years ago and is made of 24 pounds of solid gold: the burial mask of Tutankhamun, which can be visited in the Egyptian museum in Cairo (Figure 10).^[57] Until today gold is used for the manufacture of jewelry, it is also well known as material for tooth crowns in dental medicine. In recent clinical investigations it has been shown that it can be used in anti-cancer therapy without any problems of allergic reactions as gold (0) is biocompatible.^[58] Furthermore it is used in industry and electronics because of its excellent properties as conductor. It is chemically inert which includes stability against most acids and minimizes the risk of corrosion. As it is a very soft metal, it can be processed very easily.

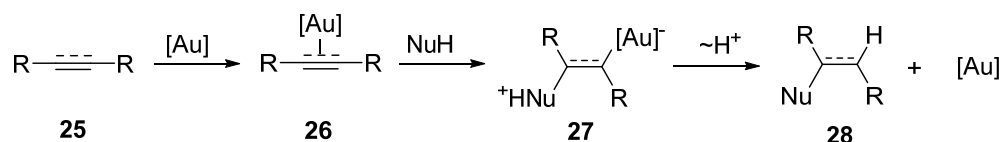


Figure 10. Burial mask of Tutankhamun.^[57]

1.5.1 Gold as Catalyst Species

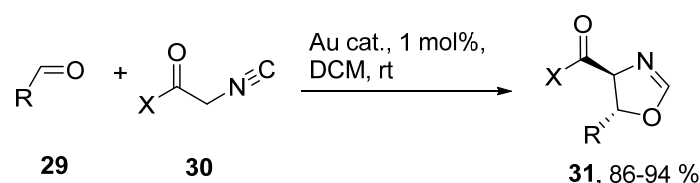
In contrast to its use in its elemental form gold was largely ignored in catalysis research,^[59] although there was no apparent reason for it: gold(I) reagents have the same electron configuration as Ni(0) and Pd(0); the electronic configuration of gold(III) is equal to that of Ni(II) and Pd(II). However in the last couple of decades, the use of catalytic gold has been rapidly developed: Today gold(I) reagents play an increasingly important role in organic chemistry. For example they are used as Lewis acids for the activation of carbon-carbon multiple bonds which are in most cases present in alkynes, allenes or olefins **25** by a nucleophilic attack: Gold coordinates on the π -system of the starting material. With this a nucleophile (NuH) can coordinate on the activated multiple bond **26** and forms a new

carbon-carbon bond **27**. Then the gold leaves and by replacement with a proton, a neutral new compound **28** is observed as well as the gold, which can act in another activation process (Scheme 5).^[60]



Scheme 5. Activation of multiple bonds by a gold(I) complex.^[60]

Cyclization reactions can be gold-catalyzed by activation of carbonyl groups and alcohols.^[61] On the one hand intramolecular cyclization reactions can be obtained if the nucleophilic group is in conjugation to the double bond resulting in conjugated systems. On the other hand intermolecular asymmetric catalytic reactions as the aldol reaction of aldehydes with isocyanoacetates can be performed (Scheme 6).^[62] Here both the aldehyde **29** and the triple bond of the isocyanate **30** are activated by coordination on the gold catalyst. The oxygen of the isocyanate group is subsequently deprotonated by an amino-ligand of the catalyst species, which indicates an intermolecular aldol reaction of the pre-oriented isocyanate and the aldehyde and forms a new 5-membered ring. By leaving of the gold catalyst an oxazoline derivative **31** can be found as formed product.

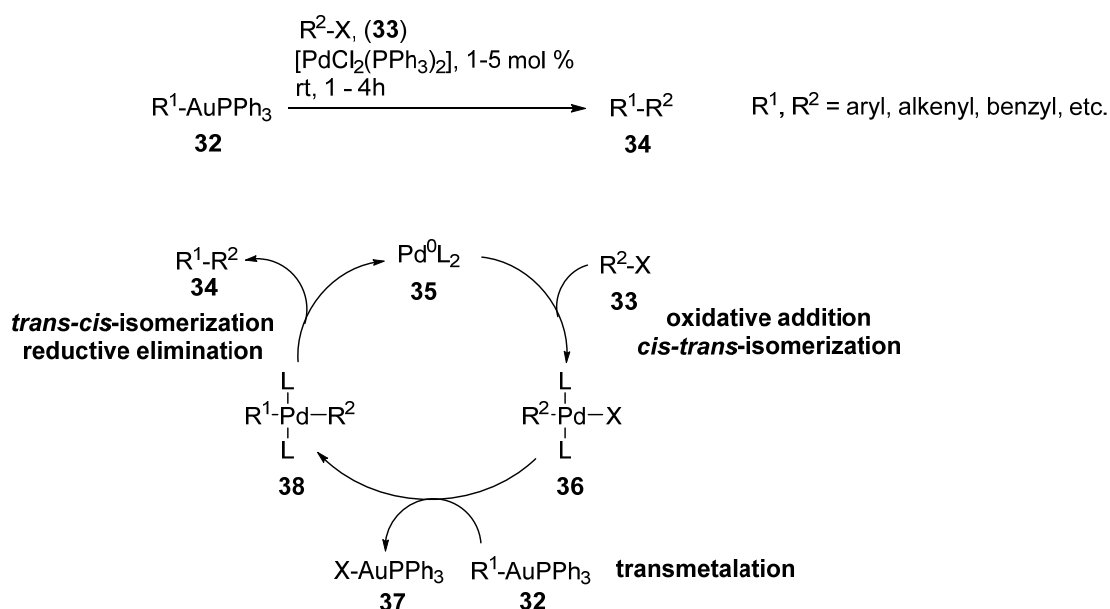


Scheme 6. Catalytic asymmetric aldol reaction of aldehydes **29** and isocyanoacetates **30**.^[63]

1.5.2 Stoichiometric use of Organogold Reagents

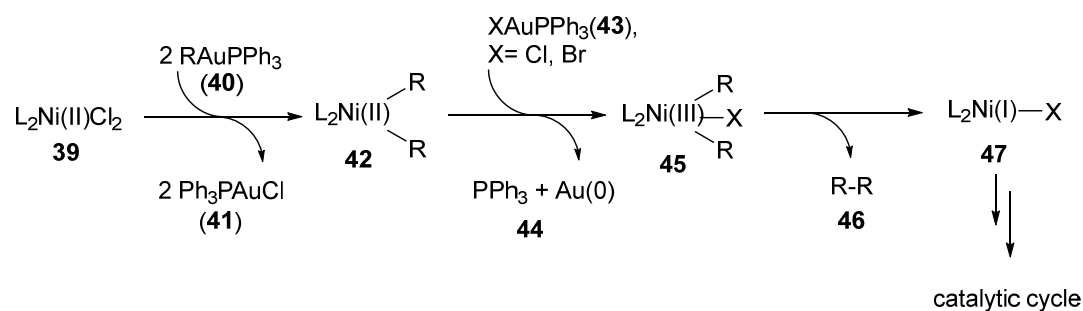
In contrast to the use of gold as catalyst species, the use of stoichiometric amounts of organogold(I) reagents in cross-coupling reactions is found only occasionally.^[64] In the beginning these reactions were performed in order to investigate the mechanism of gold-catalysis. Up to now few studies are present in the literature.^[64d, 65] By these it was observed that organogold(I) reagents are efficient nucleophiles in cross-coupling reactions with electrophiles: Gold has been demonstrated that palladium-catalyzed cross-coupling reactions with organogold reagents proceed in high yields and under mild reaction conditions with alkynes.^[64b, 66] It can also be used in gold dual-catalyzed rearrangement and

cross-coupling reactions.^[67] In contrast to other metal containing nucleophiles like zinc or magnesium many organogold cross-coupling reagents have an important advantage: With triphenylphosphine as ligand on the gold atom, the majority of compounds is stable in air, which makes them very easy to handle and to work with.^[59a] Most of the cross-coupling reactions can be performed under mild reaction conditions and give the coupling products in high yields by using nickel or palladium catalyst species.^[64b, 64d] Different substituents like aryl, alkenyl and benzyl reagents have been presented in these reactions. The mechanism seems similar to other cross-coupling reactions: First an oxidative addition of the catalyst species **35** takes place with the electrophile **33**. Subsequently a transmetalation with the nucleophilic gold species **32** takes place. The last step is the reductive elimination, where the catalyst leaves the coupling product **34** and starts a new cycle (Scheme 7).



Scheme 7. Example for palladium-catalyzed cross-coupling reactions with organogold reagents.^[66b]

The nickel-catalyzed cross-coupling reaction mechanism seems to work in similar ways to other metal nucleophiles that are well explored: First the active nickel(I) species **47** has to be formed *in situ*. This happens by a successive double transmetalation of the organogold reagent **40** and **43** to the used nickel catalyst **39**, giving the first coupling product **46** after reductive elimination. The resulting nickel(I) species **47** performs the coupling events with other organogold species **40** in a catalytic cycle as well (Scheme 8).^[64d]



Scheme 8. First proposed steps of nickel-catalyzed cross-coupling reactions with organogold species where Ni(I)/Ni(III) species are active in the catalytic cycle.^[64d]

1.5.3 Gold Compared to Other Metals

In contrast to other organometallic compounds the research on organogold compounds has just started in the last decade and is becoming progressively more intensive.^[59] The stoichiometric use of organogold reagents offers great potential: Bulky phosphine ligands on the gold atom make the whole compound in general stable towards air and makes them easy to isolate by crystallization.^[59a] This is a great advantage in contrast to organozinc or -magnesium species that are generally synthesized *in situ* by transmetalation reactions.^[4, 45-46] The problem arising from this latter process is that the reagent formation is that cannot be controlled. For Grignard reagents it is known that depending on solvent, concentration and temperature, different aggregates and reagent compositions can be obtained. The use of this undefined mixture in further reactions is a problem when unexpected errors occur: For such reagents it is difficult to determine if the problem is one of the reaction itself or if there were problems with reagent formation.

Other common organometallic compounds that are used for coupling reactions and that avoid these complication contain boron (Suzuki^[43]) or silicon (Hiyama^[44]). Both reactions are well explored, but in contrast offer to the use of organogold reagents a potential disadvantage: A base needs to be added for a successful coupling reaction. Especially in natural products synthesis, where often base labile protecting groups are used, these types of base induced coupling reactions may cause problems as some protecting groups for esters, aldehydes, alcohols, amines are cleaved by a base.^[68]

When a Stille^[41] or Migita^[42] coupling reaction is performed, organotin compounds are used. These reactions require no additional reactants like a base, but these compounds have another disadvantage: Organotin reagents are very toxic to organisms!^[69] Organogold reagents are, like most heavy metal containing reagents, toxic as well. In case of an

intoxication a chelation therapy can ameliorate the condition.^[70] In contrast to stannanes however they are safe enough to be used in low concentration for research in anti-cancer medicine. For this research toxicity studies gave the results that soluble gold salts are toxic to the liver and kidneys.^[71]

Until it was known that gold (I) complexes offer a cardiovascular toxicity,^[72] phosphine containing gold(I) reagents have been long time used against rheumatoid arthritis.^[73] Gold (III) reagents are the most toxic compounds among organogold species which makes them a good candidate in anti-cancer research.^[58] Today gold nanoparticles are frequently used in clinical research because of their non-toxicity.^[58, 70]

1.6 Synthesis of Organogold Reagents

Organogold reagents are generally synthesized by using halogenated goldphosphines **49** as precursors, mostly ClAuPPh₃, which can be synthesized from elemental gold.^[59a] By quenching lithiated species with a gold chloride the organogold reagent **50** is formed by a transmetalation reaction.^[64c] Organolithium reagents are generally used for the synthesis of other metal-containing compounds by transmetalation: Boronic ester, zinc and tin moieties for example can be introduced on this way as well.

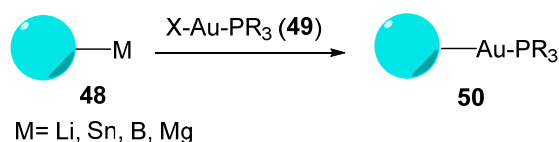


Figure 11. Organogold reagents can be synthesized by metal-metal exchange reactions.

In contrast to many other metals gold can perform metal-metal exchange reactions not only with lithium but with stannylated^[74] and boronated^[64a] compounds as well as with Grignard reagents^[67b] (Figure 11; compare Chapter 3.4). By using organic salts like dithiocarbamates, gold chloride forms the corresponding organogold carbamate.^[75]

1.7 Gold Recycling

As gold belongs to the more expensive metals, an efficient way to save costs can be by using immobilized gold that can be recycled. It is well established that catalysts can be immobilized on a surface.^[76] This method has been even used for gold(I) catalysis: a NHC-ligand that is covalently bonded to silica gel was used as linker to the active gold species (Figure 12, **51**).^[76a]

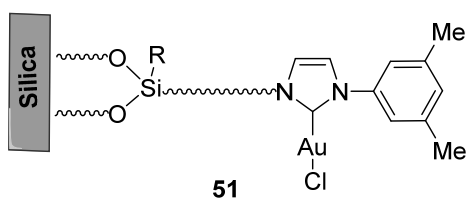


Figure 12. Schematic drawing of an immobilized gold-catalyst.^[76a]

The catalyst itself, which was used in this case for a Suzuki-coupling reaction, could be recovered by filtration after the reaction has performed. Therefore reusability and activity has been shown for immobilized gold catalysts. Future development will show if it is possible to use an immobilization in cases where the gold compound is used in stoichiometric amounts.

2 Objectives

2.1 Selective Cross-Coupling Reactions on Aromatic Dinucleophiles

Organic semiconducting materials used in applications are often made of thiophene based polymers or oligomers. The polymer length as well as the combination with different heterocycles in the polymer backbone allows a modification of the polymers' properties (see Chapter 1). For applications like organic solar cells and other electronic devices, well-defined polymers with low polydispersities, high molecular weights and high regio regularities are demanded. The so called "living" polymerization which was developed in 2004 by Yokozawa and McCullough gives access to these kinds of polymers.^[32c, 77] Monomers suitable for these transition metal catalyzed cross-coupling living polymerization must contain both a metal functional group (M) and a halogen functional group (X), M-monomer-X, which is a synthetic challenge for any but the simplest aromatic rings (compare Chapter 1). The lack of adequate general synthetic methodology to prepare more complex monomers that combine two different heterocycles, X-heterocycle-heterocycle-M **54** has prevented further research on these materials (Figure 13). In order to obtain these kinds of monomers, a both nucleophile- and electrophile selective cross-coupling reaction should be developed. A dinucleophile containing two different metal functionalities **53** should react selectively with an electrophile **52** that contains two different halogen functionalities to give the required monomers **54**. That an only nucleophile selective reaction itself works in high yields was shown by J. Linshoeft *et al.* in 2012 by using a thiophene derivative as dinucleophile containing both a stannyl and a boron functionality.^[50a]

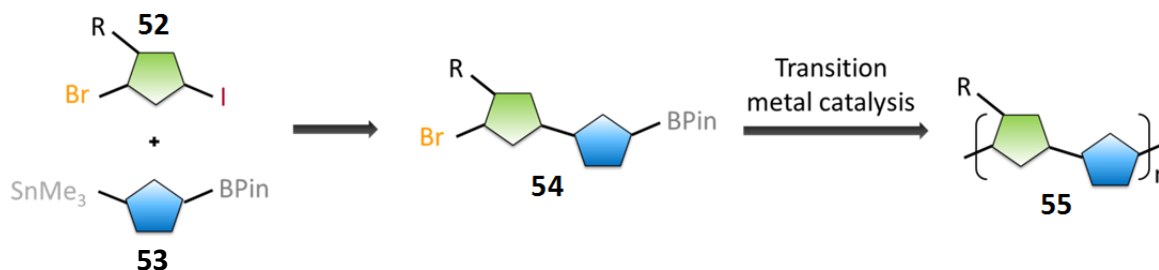


Figure 13. The objective for the first project was to synthesize monomers **54** containing both a metal functional group and a halogen in a both nucleophile and electrophile selective cross-coupling reaction.

If this kind of selective reaction leads to the required functionalized monomers **54**, polymerization reactions were to be performed (Figure 13, **55**), and the obtained polymer(s) will have to be characterized. A thiophene derivative was to be used to establish, if such a dually- selective cross-coupling reaction can be performed successfully.

2.2 Synthesis of Aromatic Dinucleophiles

As next step further aromatic dinucleophiles (Figure 14, **56** and **57**) should be synthesized and used in similar selective cross-coupling reactions in order to obtain a large variety of different monomers that can be eventually used in polymerization reactions. If it is possible, different electron rich and electron poor aromatic (hetero)cycles could be combined by this method and on that way, new polymers would be easily available.

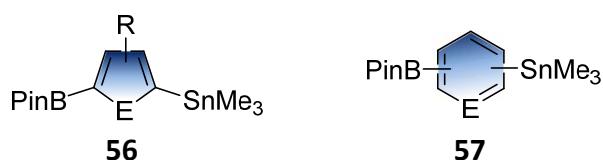


Figure 14. Further dinucleophiles **56** and **57** containing both a stannyl and a boron functional group would give access to new monomers for polymerization reactions, if they are used in a nucleophile- and electrophile selective cross-coupling reaction (E = N, S, C, O, etc.).

An environmental disadvantage of these dinucleophiles is the use of tin as one of the metal functionalities because of the toxicity associated with organotin reagents. As consequence on this a further project would be the replacement of the toxic tin^[69] by other metal functionalities. One requirement is to isolate the dinucleophiles, which is why air sensitive zinc and magnesium cannot be used as metal functionalities in this case. In the last decade research on the topic of gold catalysis^[59] and increasingly cross-coupling with organogold compounds, albeit mostly from the perspective of gaining mechanistic understanding, became of high interest.^[64] Therefore, a further aim was to test if gold as a metal functional group could be combined with other metal functional groups to prepare a new class of aromatic dinucleophile. For this reason it was the aim to synthesize both gold and boron functionalized dinucleophiles (Figure 15, **58** and **59**, E = N, S, C, O, etc.).

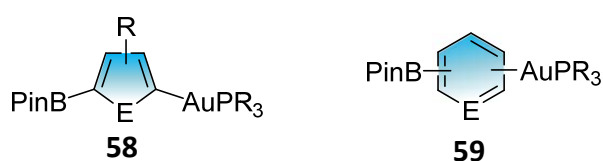


Figure 15. Is it possible to synthesize dinucleophiles containing gold and boron as metal functionalities?

2.3 Gold-Containing Thiophene-Type Monomers for Polymerization Reactions

Today monomers of the type M-monomer-X that can be used for the synthesis of semiconducting polymers were synthesized with different metal functionalities like zinc, magnesium, tin and boron.^[78] However gold has not been used as a metal functional group in such cross-coupling polymerizations, despite potential advantages such as air- and moisture stability, which makes these compounds isolable. It was therefore planned to synthesize air stable aromatic organogold compounds Au-monomer-X **60** that can be used in polymerization reactions. As the polymer poly(3-*n*-hexyl)thiophene (P3HT, **61**) is very well investigated, an organogold thiophene building block should be synthesized that would give P3HT in a polymerization reaction (Figure 16).

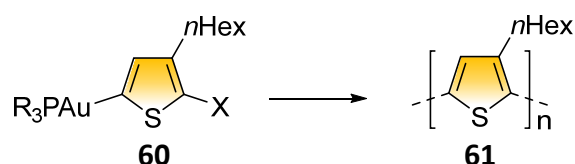


Figure 16. Does a polymerization work with gold as metal functionality on the monomer?

This would not only simplify the characterization of the polymer formed in this reaction: also performing of the kinetic studies and the comparison with the data of the P3HT that is made by using the common standard methods are the topics of this last project.

3 Results and Discussion

3.1 Chemoselective Cross-Coupling Reactions

3.1.1 Nucleophile and Electrophile Selective Cross-Coupling Reactions

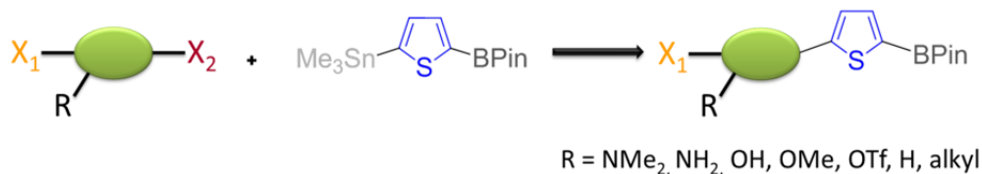
“Dual Selectivity: Electrophile and Nucleophile Selective Cross-Coupling Reactions on a Single Aromatic Substrate”

A. C. J. Heinrich, B. Thiedemann, P. J. Gates, A. Staubitz, *Org. Lett.* **2013**, *15*, 4666-4669.

Reprinted with permission from ACS Publications. © 2013 American Chemical Society.

DOI: 10.1021/ol401923j

Abstract: The development of a high yielding, both nucleophile and electrophile selective cross-coupling reaction with aromatic rings is presented. The reaction is general with respect to functional groups. Furthermore, the products still contain a boronic ester and a bromide. These two functional groups allow them to be easy-to-prepare, highly complex starting materials for further reactions and avoid protecting group transformations.



TOC Graphic. A both nucleophile and electrophile selective cross-coupling reaction was developed.

Scientific contribution to this paper

In this project I carried out all syntheses and experimental work with the following support by the coauthors: B. Thiedemann worked under my guidance / supervision on the optimization of the selective cross-coupling reaction during his “F3” internship. P. J. Gates recorded all high resolution mass spectra. A. Staubitz and I wrote the article together. Compounds **65**, **66** and **67** (Outlook) were prepared by M. Ried under my supervision during an internship.

The work is based on the following publication, where I was responsible for the synthesis and optimization of the tin and boron functionalized thiophene **1** during my diploma thesis:

J. Linshoef, A. C. J. Heinrich, S. A. W. Segler, P. J. Gates, A. Staubitz, *Org. Lett.* **2012**, *14*, 5644 -5647.

Dual Selectivity: Electrophile and Nucleophile Selective Cross-Coupling Reactions on a Single Aromatic Substrate

Annika C. J. Heinrich,[†] Birk Thiedemann,[†] Paul J. Gates,[‡] and Anne Staubitz^{*†}

Otto Diels-Institut für Organische Chemie, Universität Kiel, Otto-Hahn-Platz 4, 24118 Kiel, Germany, and School of Chemistry, University of Bristol, Bristol BS8 1TS, United Kingdom

astaubitz@oc.uni-kiel.de

Received July 9, 2013

ABSTRACT



The development of a high yielding, both nucleophile and electrophile selective cross-coupling reaction with aromatic rings is presented. The reaction is general with respect to functional groups. Furthermore, the products still contain a boronic ester and a bromide. These two functional groups allow them to be easy-to-prepare, highly complex starting materials for further reactions, avoiding protecting group transformations.

Cross-coupling reactions are very efficient for the formation of new carbon–carbon bonds.¹ For such reactions, it is well established that the order of reactivity of the electrophilic coupling partner decreases for the leaving groups I > OTf > Br ≫ Cl.² This has already been used to great advantage for the development of electrophile

selective cross-coupling reactions.³ However, nucleophile selective cross-coupling reactions on aromatic dinucleophiles are almost undeveloped.⁴

We recently addressed this synthetic problem by the first systematic study of a nucleophile selective cross-coupling reaction on a single aromatic substrate.^{4b,5} It was possible to synthesize a thiophene derivative **1** with both a trimethyl tin group in the 2-position and a boronic ester functional group in the 5-position. Using this compound, excellent chemoselectivity was observed in Stille coupling reactions with different brominated electrophiles in excellent yields.^{4b,5}

The challenge was now to extend the degree of chemoselectivity even further: was it possible to develop both a

[†] Universität Kiel.

[‡] University of Bristol.

(1) (a) Suzuki, A. *Angew. Chem., Int. Ed.* **2011**, *50*, 6722. (b) Suzuki, A. *Angew. Chem.* **2011**, *123*, 6854. (c) Diederich, F.; Meijere, A. d. *Metal-Catalyzed Cross-Coupling Reactions*, 2nd ed.; Wiley-VCH: Weinheim, 2004. (d) Nicolaou, K. C.; Bulger, P. G.; Sarlah, D. *Angew. Chem., Int. Ed.* **2005**, *44*, 4442. (e) Nicolaou, K. C.; Bulger, P. G.; Sarlah, D. *Angew. Chem.* **2005**, *117*, 4516. (f) Chen, X.; Engle, K. M.; Wang, D.-H.; Yu, J.-Q. *Angew. Chem., Int. Ed.* **2009**, *48*, 5094. (g) Chen, X.; Engle, K. M.; Wang, D.-H.; Yu, J.-Q. *Angew. Chem.* **2009**, *121*, 5196. (h) Pouy, M. J.; Stanley, L. M.; Hartwig, J. F. *J. Am. Chem. Soc.* **2009**, *131*, 11312.

(2) Miyaura, N.; Suzuki, A. *Chem. Rev.* **1995**, *95*, 2457.

(3) (a) Wu, X.-F.; Anbarasan, P.; Neumann, H.; Beller, M. *Angew. Chem., Int. Ed.* **2010**, *49*, 7316. (b) Wu, X.-F.; Anbarasan, P.; Neumann, H.; Beller, M. *Angew. Chem.* **2010**, *122*, 7474. (c) Lou, S.; Fu, G. C. *J. Am. Chem. Soc.* **2010**, *132*, 1264. (d) Martin, R.; Rivero, M. R.; Buchwald, S. L. *Angew. Chem., Int. Ed.* **2006**, *45*, 7079. (e) Martin, R.; Rivero, M. R.; Buchwald, S. L. *Angew. Chem.* **2006**, *118*, 7237. (f) Mosrin, M.; Knochel, P. *Chem.—Eur. J.* **2009**, *15*, 1468. (g) Aranyos, A.; Old, D. W.; Kiyomori, A.; Wolfe, J. P.; Sadighi, J. P.; Buchwald, S. L. *J. Am. Chem. Soc.* **1999**, *121*, 4369. (h) Bonnamour, J.; Piedrafitra, M.; Bolm, C. *Adv. Synth. Catal.* **2010**, *352*, 1577. (i) Boyer, A.; Isono, N.; Lackner, S.; Lautens, M. *Tetrahedron* **2010**, *66*, 6468. (j) Cho, G. Y.; Rémy, P.; Jansson, J.; Moessner, C.; Bolm, C. *Org. Lett.* **2004**, *6*, 3293. (k) Shen, Q.; Hartwig, J. F. *J. Am. Chem. Soc.* **2007**, *129*, 7734. (l) Kienle, M.; Unsinn, A.; Knochel, P. *Angew. Chem., Int. Ed.* **2010**, *49*, 4751. (m) Kienle, M.; Unsinn, A.; Knochel, P. *Angew. Chem.* **2010**, *122*, 4860.

(4) (a) Yamamoto, Y.; Seko, T.; Nemoto, H. *J. Org. Chem.* **1989**, *54*, 4736–4737. (b) Linshoef, J.; Heinrich, A. C. J.; Segler, S. A. W.; Gates, P. J.; Staubitz, A. *Org. Lett.* **2012**, *14*, 5644. (c) Elmalem, E.; Kiriy, A.; Huck, W. T. S. *Macromolecules* **2011**, *44*, 9057. On nonaromatic dinucleophiles, chemoselective reactions have also been reported: (d) Cai, M.-Z.; Zhou, Z.; Wang, P.-P. *Synthesis* **2006**, 789. (n) *Synthesis* **2006**, 2006, 789. (e) Sorg, A.; Brückner, R. *Angew. Chem., Int. Ed.* **2004**, *43*, 4523. (f) Cai, M.-Z.; Wang, Y.; Wang, P.-P. *J. Organomet. Chem.* **2008**, *693*, 2954. (g) Iannazzo, L.; Vollhardt, K. P. C.; Malacria, M.; Aubert, C.; Gandon, V. *Eur. J. Org. Chem.* **2011**, *2011*, 3283. (h) Ogima, M.; Hyuga, S.; Hara, S.; Suzuki, A. *Chem. Lett.* **1989**, 1959. (i) Malan, C.; Morin, C. *Synlett* **1996**, 167. (j) Pihko, P. M.; Koskinen, A. M. P. *Synlett* **1999**, 1966. (k) Ros Laó, A.; López-Rodríguez, R.; Estepa, B.; Álvarez, E.; Fernández, R.; Lassaletta, J. M. *J. Am. Chem. Soc.* **2012**, *134*, 4573. (l) Zhou, H.; Moberg, C. *J. Am. Chem. Soc.* **2012**, *134*, 15992. (m) Singidi, R. R.; RajanBabu, T. V. *Org. Lett.* **2010**, *12*, 2622.

(5) For a highlight on this work, see: Knochel, P.; Barl, N. M. *Synfacts* **2013**, *9*, 204.

nucleophile and electrophile selective cross-coupling reaction? In such a reaction, a dinucleophile **M1**-Heterocycle**1**-**M2** would selectively react with a dielectrophile **X1**-Heterocycle**2**-**X2** so that only one of four potential products would be formed without the use of protecting group chemistry.

In this way, the reaction would become even more useful: Not only would the final product still contain a nucleophilic group for cross-coupling reactions but also an electrophilic site would be retained alongside any functional groups present on the aromatic rings that are tolerant toward cross-coupling reactions.

In such a reaction, it is vital to achieve not only good but quantitative selectivity, because all possible products are so similar in molecular weight and structure that their separation would be difficult or impossible. To develop a nucleophile *and* electrophile cross-coupling reaction, dinucleophile **1** was used.

As a test reaction, **1** was initially reacted with the easily accessible dielectrophile **2** which contains a bromide substituent in the 2-position and an iodide substituent in the 5-position. We screened over 40 different reaction conditions (solvents, temperatures, reaction times, catalysts, catalyst loadings; for details see Supporting Information (SI) Table SI-1).

Encouragingly, in all of those reactions—although decomposition products and low conversions did occur—the only cross-coupling product was **5a**, where the iodide had reacted in a Stille reaction. Due to this extensive screening, it was possible to identify conditions which gave excellent selectivity and a yield of 95%, using DMF as the solvent, [Pd(PPh₃)₄] as the catalyst (5 mol %) at 55 °C, and a reaction time of 18 h (Table 1, entry 1). Alternatively, at 70 °C, the reaction time could be shortened to 15 h with a yield of 96% (Table 1, entry 2). However, when we attempted to transfer these conditions to the reaction of **1** with the alkylated dielectrophile **3**, the reaction was no longer selective with respect to the electrophile: not only the iodide but also the bromide had reacted under these reaction conditions to give **4b** (Table 1, entries 3–4). This was surprising, given the increased steric bulk of the hexyl group adjacent to the bromide, and is probably due to electronic effects. Although the undesired side product **4b** occurred only in small amounts, this impurity can be expected to cause substantial problems: Its reactivity as an electrophilic cross-coupling partner compared to **5b** would be higher. Because it was not possible to separate **4b** and **5b**, it was essential to reoptimize the entire reaction. The ratio of **4b** to **5b** was independent of the catalyst loading (Table 1, entries 3–6), and therefore, low catalyst loadings of 1–2 mol % were selected for further optimizations. A breakthrough was achieved by using a microwave apparatus as the heat source. With a catalyst loading of 1–2 mol %, quantitative selectivity was found in all cases (Table 1, entries 7–11).

While a high reaction temperature of 120 °C led to product decomposition with longer reaction times (entries 9 and 10), the reaction gave quantitative yields at 80 °C after 3 h 30 min (Table 2, entry 7). Equally good conditions included a temperature of 100 °C, for either

20 min with 2 mol % or 30 min with 1 mol % of the catalyst (Table 2, entries 8 and 11).

Table 1. Stille Coupling Reaction with a Reagent with Competing Electrophilic Sites



entry	starting material	cat. loading (mol %)	temp (°C)	time	yield 5 (%) ^{a,b}	normalized ratio 5a : 4 ^c
1	2	5	70	15 h	96	>99.7: <i>n</i> ^d
2	2	5	55	18 h	95	>99.7: <i>n</i> ^d
3	3	5	70	18 h	68	93:7
4	3	5	55	39 h	73	94:6
5	3	2	55	30 h	79	94:6
6	3	10	55	30 h	76	94:6
7	3	2	80 (MW)	3.5h	>99	>99.7: <i>n</i> ^d
8	3	2	100 (MW)	20 min	>99	>99.7: <i>n</i> ^d
9	3	2	120 (MW)	20 min	95	>99.7: <i>n</i> ^d
10	3	2	120 (MW)	30 min	85	>99.7: <i>n</i> ^d
11	3	1	100 (MW)	30 min	>99	>99.7: <i>n</i> ^d

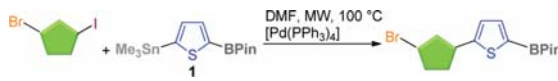
^aThe reaction was controlled at regular intervals by GC, using triisopropylbenzene as internal calibration standard. ^bIf the yield is < 100%, unidentified side products were formed. The starting material was fully converted in all cases. MW = microwave. ^cThe amount of the undesired nonselective coupling product was calculated by NMR analysis (see Figure SI 3). ^dThe limit of detection was estimated by comparative integration of the NMR signals to baseline to be *n* < 0.3% (see Figure SI 3). Where *n* is indicated in the table, no byproduct peak could be detected.

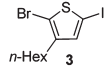
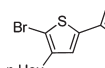
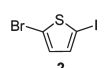
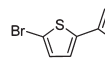
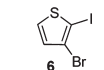
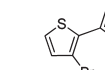
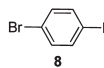
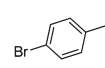
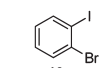
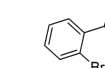
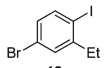
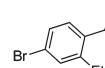
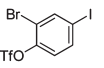
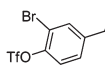
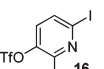
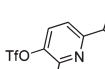
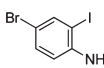
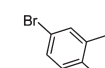
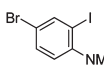
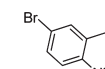
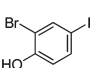
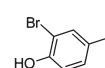
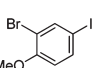
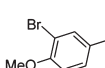
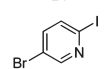
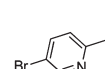
It was now important to prove that this second set of conditions really did represent a general method for cross-coupling with different dielectrophiles.

Therefore, a variety of different electrophiles containing two or even three different electrophilic functionalities (for their synthesis see SI) were reacted with the dinucleophile **1** at 100 °C in the microwave using 2 mol % of [Pd(PPh₃)₄] as the catalyst (Table 2). Thiophene dielectrophiles **2** and **3** gave the product in 20 min in high yields of 89% and 95% respectively, but if the bromide was in an *ortho*-position to the iodide (**6**), the reaction time had to be prolonged to 2 h (entries 1–3) to achieve a similar yield of 79%. This substituent effect in the *ortho*-position could also be observed for phenyl dielectrophiles **8**, **10**, and **12** where the reaction with the *ortho*-substituted **10** took more than four times as long (**12** twice as long) as the *para*-substituted **8** to proceed to completion (entries 4–6).

This effect is presumably induced by steric hindrance (compare for example entries 2 and 3 or entries 4 and 5).⁶ However, despite this difference in reactivity, all of those

(6) (a) Suzuki, A. *Chem. Commun.* **2005**, 4759. (b) Watanabe, T.; Miyaura, N.; Suzuki, A. *Synlett* **1992**, 207.

Table 2. Performing Stille Cross-Coupling Reactions with Various Dielectrophiles^a


entry	dielectrophile	product	time (min)	isolated yield (%)
1			20	95
2			20	89
3			120	79
4			60	84
5			270	75
6			120	79
7			90	79
8			300	82
9			120	75
10			210	73
11			60	65
12			120	83
13			300	81

^aThe reactions were performed in a 1 mmol scale: electrophile (1.00 mmol), nucleophile (1.00 mmol), and the catalyst [Pd(PPh₃)₄] (2 mol %) were dissolved in DMF (4 mL) and stirred at 100 °C in the microwave for the specified time.

dielectrophiles gave complete selectivity and high yields (> 75%). The products of these reactions are particularly interesting, as they lead to regioisomers: it is well

established in medicinal chemistry,⁷ agrochemistry,⁸ and materials chemistry⁹ that regioisomers of otherwise the same molecules can have dramatic effects on the bioactivity of a compound or, respectively, on the materials properties of the material derived from it.¹⁰ Starting materials **14** and **16** are trielectrophiles, with an iodide, a trifluoromethylsulfonyl group, and a bromide present, and even in those cases, only the desired cross-coupling products **15** and **17** were obtained in excellent yields of 79% and 82% respectively (entries 7 and 8). Such compounds are highly valuable because the additional electrophilic group can be used for further modifications. The reaction appears to be very robust toward both electron-rich and -deficient dielectrophiles: amine substituted starting materials (**18** and **20**, entries 9 and 10), a phenol (**22**, entry 11), and a methoxysubstituted reagent (**24**, entry 12) react in similar yields (> 65%) to electron-deficient starting materials such as pyridines (**16** and **26**, entries 8 and 13, yields > 81%). The relatively long reaction times for the latter of 5 h are likely to be a consequence of catalyst deactivation due to the lone pair of the nitrogen of the pyridine *ortho* to the reacting iodide.¹¹

The development of this dually selective coupling reaction led to compounds comprised of two aromatic (hetero)cycles, containing a boronic ester, a bromide, and one other functionality.

A further aspect was to test if the reaction was electrophile selective even with competing electrophiles: in the reactions discussed so far, the first substitution during the coupling reaction changes the reactivity of the second electrophilic site.

To prove that selectivity can be demonstrated even if entirely equal electrophiles were used, equimolar amounts of competing arylbromides and -iodides (Table 3) were used. For these electrophiles, 2-halothiophenes (**28a** and **28b**), halobenzenes (**30a** and **30b**), and 2-halopyridines (**32a** and **32b**), in the order of increasing electron deficiency, only the aryl iodide reacted—with quantitative selectivity and in high yields (78–92%), although the more electron-deficient substrates required longer reaction times.

The compounds prepared via this nucleophile and electrophile selective cross-coupling reaction bear both an electrophilic and a nucleophilic group. They therefore resemble monomers that can be used for living cross-coupling polymerization reactions to give semiconducting

(7) (a) Chaurasia, C. S.; Li, K.; Doughty, M. B. *J. Med. Chem.* **1993**, *36*, 272. (b) Rao, P. N. P.; Uddin, J.; Knaus, E. E. *J. Med. Chem.* **2004**, *47*, 3972. (c) Cosyn, L.; Palaniappan, K. K.; Kim, S.-K.; Duong, H. T.; Gao, Z.-G.; Jacobson, K. A.; Calenbergh, S. V. *J. Med. Chem.* **2006**, *49*, 7373. (d) Bailly, C.; Dassonneville, L.; Colson, P.; Houssier, C.; Fukasawa, K.; Nishimura, S.; Yoshinari, T. *Cancer Res.* **1999**, *59*, 2853.

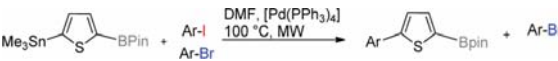
(8) Ladner, D. W. *Pestic. Sci.* **1990**, *29*, 317.

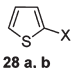
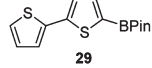
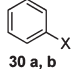
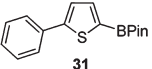
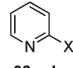
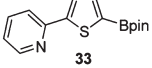
(9) Dubey, R. K.; Efimov, A.; Lemmetyinen, H. *Chem. Mater.* **2011**, *23*, 778.

(10) From single molecule conductivity measurements, the importance of positional connectivity is well known, but bulk measurements barely exist, due to the inaccessibility of such materials so far. See: Lemasson, F.; Berton, N.; Tittmann, J.; Hennrich, F.; Kappes, M. M.; Mayor, M. *Macromolecules* **2012**, *45*, 713.

(11) Solano, C.; Svensson, D.; Olomi, Z.; Jensen, J.; Wendt, O. F.; Wärnmark, K. *Eur. J. Org. Chem.* **2005**, 3510.

Table 3. Stille Coupling Reaction with Competitive Electrophiles (Yield Estimated by GC)^a



entry	electrophiles ^[b]	product	time (min)	conv ^[c] I:Br	yield ^[d] (%)
1	 28 a, b	 29	20	100: n ^e	78
2	 30 a, b	 31	20	100: n ^f	92
3	 32 a, b	 33	300	100: n ^g	89

^aThe dinucleophile (1.00 mmol) the bromide (1.00 mmol) and the iodide (1.00 mmol) reacted under the described reaction conditions for the specified reaction time. ^bX = Br (a) or I (b), 1:1. ^cThe conversion was monitored by GC and reported in % with respect to the standard, triisopropylbenzene. ^dThe yield was isolated. ^eThe method detection limit (see SI):¹² n = 0.4%; the unselective product was not observed. ^fThe method detection limit (see SI):¹² n = 0.4%; the unselective product was not observed. ^gThe method detection limit (see SI):¹² n = 0.7%; the unselective product was not observed.

polymers.¹³ Because thiophene and its derivatives¹⁴ belong to the best understood semiconducting polymers, we chose compound **5b** as the monomer for a proof-of-concept polymerization. Upon addition of a solution of a catalyst, [Pd(PtBu₃)₂], in THF to a solution of the monomer **5b** in

(12) Wisconsin Department of Natural Resources 1996, *Analytical Detection Limit Guidance and Laboratory Guide for Determining Method Detection Limits*, Wisconsin Department of Natural Resources Laboratory Certification Program, PUBL-TS-056-96.

(13) (a) Sheina, E. E.; Liu, J.; Iovu, M. C.; Laird, D. W.; McCullough, R. D. *Macromolecules* **2004**, *37*, 3526. (b) Yokoyama, A.; Miyakoshi, R.; Yokozawa, T. *Macromolecules* **2004**, *37*, 1169. (c) Zhang, H.-H.; Xing, C.-H.; Hu, Q.-S. *J. Am. Chem. Soc.* **2013**, *134*, 13156.

(14) (a) Mishra, A.; Ma, C.-Q.; Bäuerle, P. *Chem. Rev.* **2009**, *109*, 1141. (b) Perepichka, I. F.; Perepichka, D. F. *Handbook of Thiophene-based Materials: Applications in Organic Electronics and Photonics*; Wiley-VCH: Weinheim, 2009. (c) Roncali, J. *Chem. Rev.* **1992**, *92*, 711. (d) Marsella, M. J.; Swager, T. M. *J. Am. Chem. Soc.* **1993**, *115*, 12214. (e) Osaka, I.; McCullough, R. D. *Acc. Chem. Res.* **2008**, *41*, 1202. (f) Thompson, B. C.; Fréchet, J. M. J. *Angew. Chem., Int. Ed.* **2007**, *47*, 58. (g) Thompson, B. C.; Fréchet, J. M. J. *Angew. Chem.* **2007**, *120*, 62.

THF in the presence of a base, the reaction mixture changed its color from light green to dark red within 6 min and a dark red precipitate formed. As Suzuki cross-coupling reactions with arylbromides catalyzed by [Pd(PtBu₃)₂] typically do not show such a color change, it is likely to be indicative of the formation of an elongated π -system. The product could be isolated by precipitation in a yield of the crude product of 61%. Although the material was too poorly soluble to obtain an NMR spectrum, by MALDI-MS, we could detect oligomers of up to 10 repeating units (M = 2483 m/z). The low solubility of polymer may be attributed to the absence of an alkyl chain on every other thiophene unit, compared to the soluble P3HT. This may lead to an increased propensity for crystallization of the polymer.

In conclusion, we developed the first nucleophile and electrophile selective one-pot cross-coupling reaction on aromatic rings. We found high selectivities for a broad range of electrophiles, high yields, and comparatively short reaction times. The type of product which is now available is highly functionalized with substituents that are still reactive toward further transformations, without any additional protection group operations. This new reaction strategy allows the convergent syntheses of complex molecules which is particularly useful if a large library of building blocks is desired, for example for screening the biological potency of a class of compounds or testing the influence of regioisomers on the performance of a material. In principle, the products of this reaction may be polymerized. Although the solubility of the resulting polymer was low, oligomers could be unequivocally identified. Work is ongoing to increase the solubility of the polymers, to exploit the wide range of new monomers which are now accessible and to establish conditions where this process can become a living polymerization.

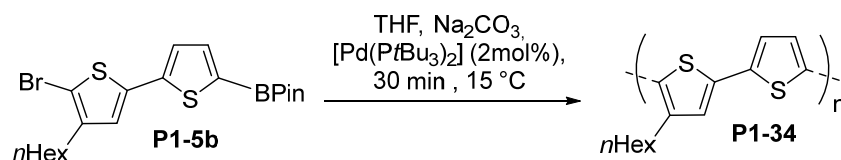
Acknowledgment. A.H. thanks the Deutsche Bundesstiftung Umwelt (DBU) for a Ph.D. scholarship.

Supporting Information Available. Experimental section and NMR spectra are included in the Supporting Information. This material is available free of charge via the Internet at <http://pubs.acs.org>.

The authors declare no competing financial interest.

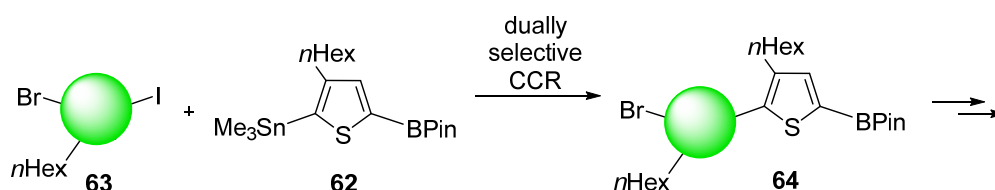
3.1.2 Further Experiments and Outlook

The method of a dually-selective cross-coupling reaction could be developed successfully. One of the resulting products **P1-5b** was used as monomer in a polymerization reaction. A dark red polymer **P1-34** was observed, but this precipitated from solution (see SI, Chapter 5).



Scheme 9. Polymerization of monomer **P1-5b** gave an insoluble polymer **P1-34**.

Therefore the aim of future work on this project is to improve the solubility of the polymer. On the one hand a further hexyl chain on the second and presently unsubstituted thiophene moiety in **P1-5b**, the monomer, would lead to P3HT in a polymerization reaction. The polymer is well characterized and soluble.^[19] For this strategy it would be necessary to introduce the alkyl chain in the dinucleophile **62**.

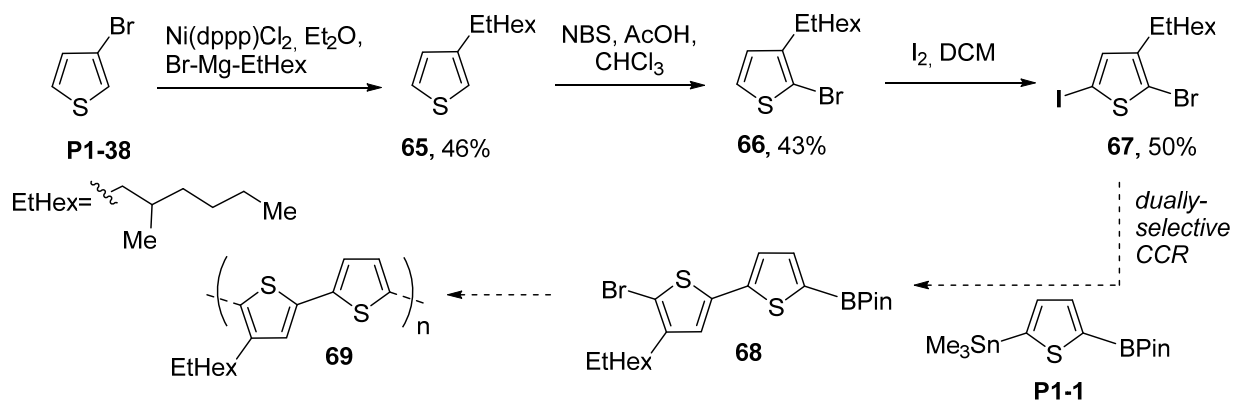


Scheme 10. If an alkyated dinucleophile **62** can be synthesized, the monomer **64** could be synthesized by a dually-selective cross coupling reaction and would give a soluble polymer in a polymerization reaction.

As described in Chapter 3.2 (see below) the synthesis of the dinucleophile **62** was successful. S. Urrego-Riveros is continuing work now on the synthesis of new monomers that are made of this thiophene dinucleophile **62** and electrophiles that are alkyated **63** (Scheme 10). In order to obtain a polymer **64** with alternated aromatic systems in the backbone, other dielectrophilic heterocycles can be envisioned, for example alkyated pyridines or benzenes.

A further concept to improve the solubility of polymers is to introduce a branched, racemic alkyl chain on the backbone of the polymer. The synthesis of the corresponding starting material starts with the alkylation of 3-bromothiophene **P1-38** in a Kumada cross-coupling with the Grignard-compound to give **65**. Bromination followed by iodination leads to compound **67**. Further work on this project will include further improvement of the yields of the individual steps for the synthesis of the dielectrophile, the combination of this

dielectrophile with various dinucleophiles like **P1-1** and eventually polymerization (Scheme 11).



Scheme 11. A dielectrophile with a branched alkyl chain (**67**) might lead to improved solubility of the polymer.^[79]

As a long term goal, polymerization should be optimized to proceed under living conditions and the resulting diverse range of polymers will be analyzed for their performance in devices.

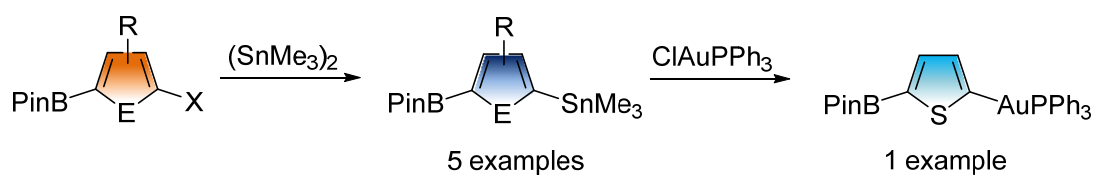
3.2 Aromatic Dinucleophiles

3.2.1 Synthesis of Aromatic Dinucleophiles

This chapter was written in unset manuscript form with the view of a timely publication of these results. For further desirable experiments for this project see Chapter 3.2.5.

A. C. J. Heinrich, P. J. Gates, C. Näther, A. Staubitz

Abstract: The synthesis of aromatic dinucleophiles was developed. On the one hand a high yielding general method for the synthesis of tin-boron functionalized dinucleophiles is presented. By using the tin-boron functionalized thiophene derivative as starting material it was possible to synthesize the first example of a gold-boron difunctionalized derivative in a high yield by performing a simple transmetalation reaction under mild reaction conditions.



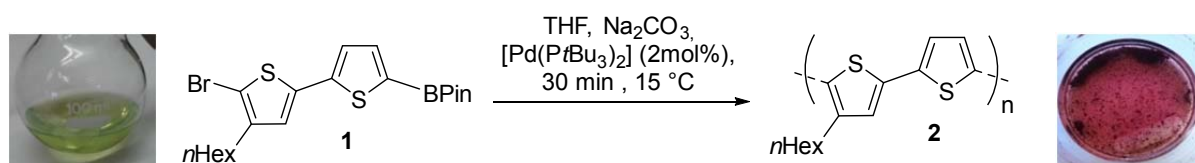
TOC Graphic. The synthesis of aromatic dinucleophiles was developed successfully.

Scientific contribution to this manuscript

In this project I carried out all syntheses and experimental work with support of the following people: C. Näther carried out the X-ray crystallography measurements. P. J. Gates recorded all high resolution mass spectra.

3.2.1.1 Introduction

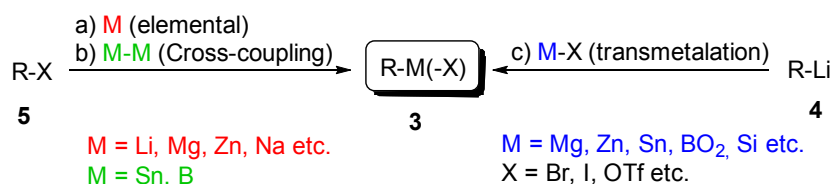
We recently presented a method by which a dinucleophilic thiophene derivative could be reacted in an electrophile- and nucleophile selective cross-coupling with thiophene dielectrophiles as well as pyridine and benzene dielectrophiles (Chapter 3.1).^[1] In one example we could demonstrate that it was possible to polymerize the resulting dithiophene **1** to give a dark red polymer (Scheme 1, **2**). However because this dinucleophile had not enough solubilizing side chains, it precipitated from solution.



Scheme 1. Polymerization of the green monomer **1** give a polymer that precipitates as dark red solid from solution (CHCl_3).

In order to improve the solubility of a polymer one aim was to introduce an alkyl chain into the dinucleophiles. Another aim concerned the dinucleophilic aromatic compound itself: For many applications it is important that the band gap of the material in a device is low or that it can be tuned. It has been shown that the combination of an electron rich and an electron deficient heterocycle in the polymer backbone leads to a lower band gap.^[2] With a larger variety of dinucleophiles, the general long term goal should be attainable: The synthesis of polymers with alternating heterocycles in the polymer backbone. The synthesis of other aromatic dinucleophiles was required to obtain a whole library of new monomers,.

In general metal functional groups are introduced to a molecule **3** by lithiation of a halogenated compound (R-Li, **4**) and a subsequent lithium-metal exchange, direct metalation *in situ* or by a cross-coupling between a halogenated (R-X, **5**) and a *bis*-metalated species (M-M) like *bis*-(trimethyl)ditin, $(\text{SnMe}_3)_2$, or *bis*-(pinacolato)diboron, $(\text{BPin})_2$ (Scheme 2).^[3]



Scheme 2. General synthetic methods are shown for introducing metal-functionalities.

The amount and variety of aromatic dinucleophilic compounds **7** is significantly limited.^[4] The reason for this is the lack of synthetic methods for the synthesis of dinucleophilic

compounds with different metal functionalities **7**. It has been shown by three examples that a (selective) lithium-metal exchange can be successfully used for the dinucleophile synthesis (Figure 1, **7**).^[4b, 4c] In one case the different metal functionalities were introduced by subsequently addition of the reagents to obtain the tin-silicon functionalized dinucleophile.^[5]

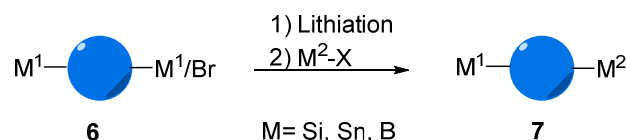
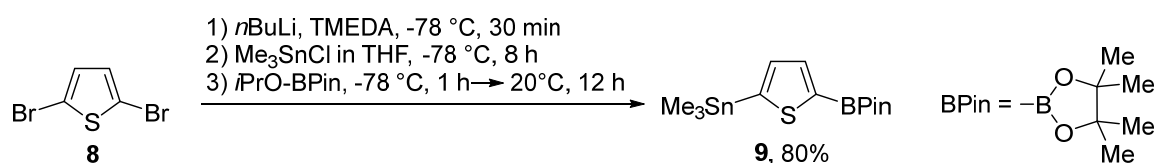


Figure 1. Dinucleophiles **7** can be synthesized by using metalated starting materials **6**.

This type of one-pot reaction method might be used for other symmetric aromatic systems, although it is possible that reaction conditions have to be adapted. In contrast to this, asymmetric aromatic systems like 3-alkyl thiophene might give a mixture of dinucleophiles because of a lack of site selectivity.

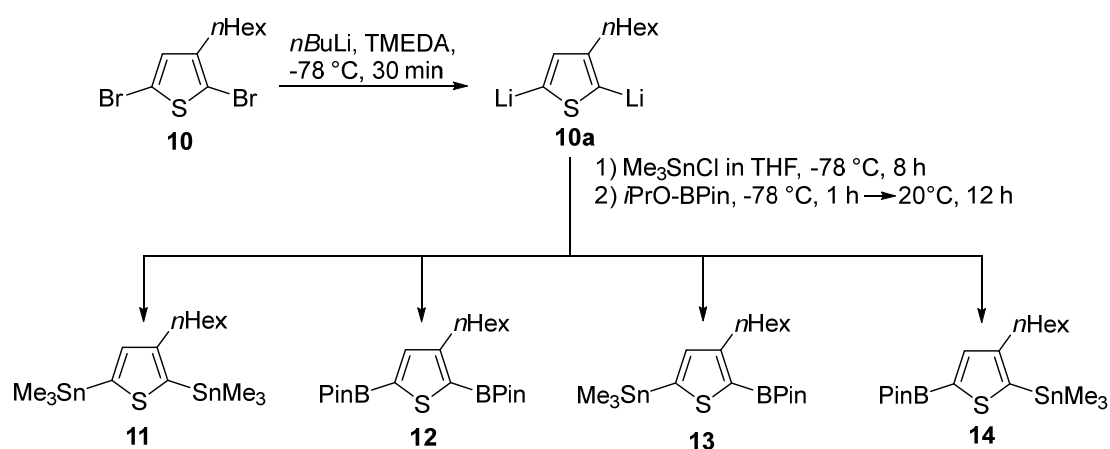
3.2.1.2 Synthesis of Tin-Boron Functionalized Dinucleophiles

We could show that the combination of tin and a boronic ester as metal functional groups on an aromatic substrate allows their use for nucleophile selective cross-coupling reactions.^[1, 4b] The synthesis of the published dinucleophile **9** was optimized by us previously^[6] using the symmetrical 2,5-dibrominated thiophene **8** as starting material, similar to the method described by Müller.^[5] The reaction itself was a one-pot reaction, where both the 2- and 5- position was lithiated at low temperatures. By adding first trimethyltinchloride and subsequently the isopropyl pinacole boronic ester (*i*PrOBPin) the product **9** was obtained in a good yield of 80% (Scheme 3).^[6] However, the purification was laborious, as the side product, a 2,5-diboronated thiophene, had to be removed by sublimation at 20 °C before the product itself could be isolated by sublimation. This procedure is very time consuming, but other purification methods were unsuccessful: The product did not crystallize and the tin group was unstable on silica.



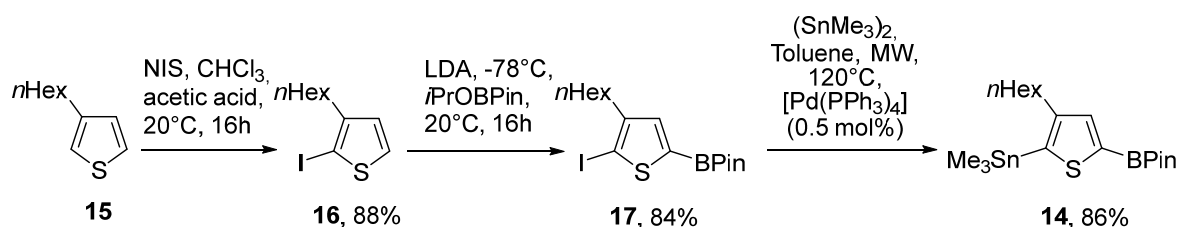
Scheme 3. One pot synthesis of the unsubstituted thiophene dinucleophile **9**.^[6]

For obtain a soluble polymer we showed that one hexyl chain every second aromatic unit is insufficient. Consequently, a thiophene dinucleophile (**13** and **14**) should contain an alkyl chain in 3- or 4-position (Scheme 4): However when the one-pot-reaction conditions of Scheme 1 were transferred to the unsymmetrical 2,5-dibrominated *n*-hexylthiophene **10**, the reaction failed (Scheme 4). A mixture of different metalated thiophene species was found: The distannylated- and the diboronated species (**11** and **12**) were observed as well as the two possible mixed-metalated species (**13** and **14**). Although the lithiation itself was successful on both the 2- and 5-position to **10a**, the first lithium-tin exchange was obviously not selective for one position of the thiophene derivative **10**, explaining derivatives **11** and **12**. The occurrence of **11** can be explained by a double transmetalation with trimethyltin chloride: The first lithium-tin exchange will be performed in 2-position. If the trimethyltin species is added faster than the lithium-tin exchange itself occurs: At this point, there is an excess of unreacted trimethyltin chloride in the reaction mixture, because another lithium-tin exchange takes place in 5-position. As a result on this, **12** is observed as well: As the double lithiated species **10a** has reacted in parts with two tin electrophiles, some double lithiated thiophene species **10a** is left in the mixture that can perform a double transmetalation with the boronic ester in 2-an 5 position to give **12**. A successive lithium-tin exchange in 2-position followed by lithium boron exchange in 5-position explains the formation of the desired compound **14** whereas a successive lithium-tin exchange in 5-position followed by a lithium boron exchange in 2-position would give rise to compound **13**, suggesting little selectivity for the exchange reactions.



Scheme 4. One-pot synthesis of the alkylated thiophene dinucleophile **13** or **14** failed, an undefined mixture of all presented species **11-14** was found.

The result was a mixture of all described species (**11-14**) that could not be separated from each other. A qualitative analysis was performed by GC-MS, but the quantity of each formed species could not be established due to their similar electronic structures (NMR). As this transfer of the one-pot reaction conditions to an unsymmetrical derivative was not easily possible, another method to introduce both the stannyl and the boron functionality into a substance had to be developed. When using trimethyltin chloride as metalation agent a lithium-tin exchange is required (Scheme 5). This pathway would be avoided, if di(trimethyltin), $(\text{SnMe}_3)_2$, was used. In this case a palladium catalyzed cross-coupling reaction (Stille-Kelly coupling)^[7] can be carried out on a halogenated species (Scheme 2). We speculated that it should be possible to use a precursor **17** that already contains a boron functionality to form the desired dinucleophile **14**. It was anticipated that the boron functional group in **17** should be inert under the coupling reaction conditions, because no additional base is required in Stille-Kelly-couplings (Scheme 5). This was indeed the case: First 3-*n*-hexyl-thiophene **15** was iodinated in 2-position by using *N*-iodosuccinimide (NIS).^[4a] The resulting product **16** was selectively lithiated in 5-position with the bulky base lithium diisopropylamide (LDA). This procedure efficiently avoids iodine-lithium exchange due to the size of the lithium base. Subsequent quenching with isopropylpinacole boronic ester (*i*PrOBPin) gave compound **17**, which could be isolated in a very good yield of 93%. This compound **17**, containing both a boron and a halogen functionality, was used as precursor for the last step: The cross-coupling reaction with the ditin species $(\text{SnMe}_3)_2$ was performed in a microwave apparatus at 120 °C, using $[\text{Pd}(\text{PPh}_3)_4]$ as catalyst species and toluene as solvent. After 20 minutes, the reaction was complete and the product **14** could be isolated without extensive purification steps. Washing with water removed the catalyst and the remaining tin species, which was used in an excess of 1.2 equivalents.

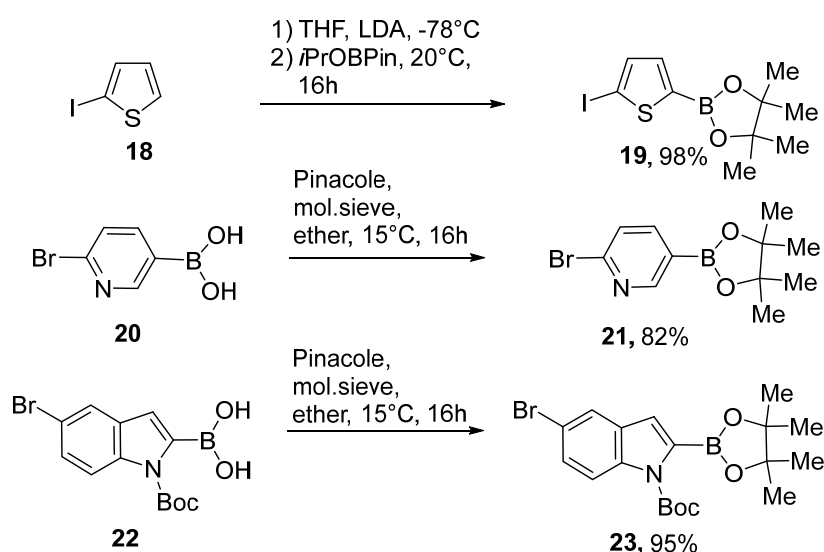


Scheme 5. Synthesis of the alkylated thiophene dinucleophile **14**.

If a catalyst loading of 5 mol% was used, it was not possible to separate the remaining triphenyl ligands in the mixture completely from the desired product **14**. By reducing the

catalyst loading to 0.5 mol% the reaction proceeded equally well and gave the product **14** without impurities in a yield of 86% as oil. Thus, the first asymmetric alkylated dinucleophile could be realized (Scheme 5). Now it had to be established if this presented method can be used as a general method for the synthesis that allows access to other (hetero)cyclic aromatic systems.

The easiest way to test it was the transfer of the reaction conditions to the unsubstituted tin and boron functionalized thiophene **9** (Table 1, entry 1). The both halogenated and boronated thiophene derivative **19** was synthesized similarly to the alkylated compound **17** and could be isolated in a yield of 98% (Scheme 6).

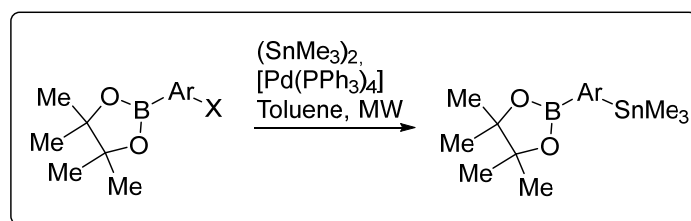


Scheme 6. The precursor **19** was synthesized similar to **17** by lithiation and subsequent quenching with a boronic ester, **21** and **23** were synthesized by an esterification of the boronic acids with pinacol.

As additional aromatic systems, phenyl, indole and pyridine derivatives were chosen. In order to simplify the reaction and to show that this method can be used as a general procedure for the synthesis of aromatic dinucleophiles, these derivatives did not contain any alkyl chain at this point of development. Therefore, the precursors were either commercially available in the case of the phenyl derivative or easy to synthesize by transferring the boronic acid into the pinacoleboronic ester (Scheme 6). These reactions gave high yields of 82% for the pyridine derivative (**21**) and 99% for the indole derivative (**23**).^[8] The coupling reaction of **19** with $(\text{SnMe}_3)_2$ in a microwave apparatus gave the desired dinucleophile **9** in an excellent yield of 95% (Table 1, entry 1). For the synthesis of the pyridine and indole dinucleophiles themselves the corresponding boronic esters **21** and **23** were used as starting

materials in the coupling reaction with $(\text{SnMe}_3)_2$. Due to the different electronic structures of the used aromatic systems, it was not surprising that the reaction time had to be adapted for each species (Table 1).

Table 1. Synthesis of aromatic dinucleophiles.



Entry	Product	Reaction time	Temperature	Yield (isolated)
1	 9	20 min	120 °C	95%
2	 14	20 min	120 °C	86%
3	 24	30 min	120 °C	93%
4	 25	60 min	120 °C	96%
5	 26	180 min	120 °C	<25%, not isolated
6	 26	180 min	100 °C	54%

In case of the benzene derivative **24** the product was obtained in a very good yield of 93% by prolonging the reaction time to 30 minutes (Table 1, entry 3). The indole derivative **25** was isolated in an excellent yield of 96% in a reaction time of 60 minutes (Table 1, entry 4). The pyridine derivative **26** did not react as expected: Although at 120 °C, the starting material was completely consumed after 180 min (Table 1, entry 5), the product had formed in a lower yield of <25%. However, an undetermined by-product that was formed perhaps by decomposition of the product could not be removed from the product. Consequently, the

temperature was lowered to 100 °C. After 180 min a conversion of 60% (calculated by NMR) was observed (Table 1, entry 6). Here a mixture of starting material **21** and product **26** could be isolated. The starting material could be removed by sublimation to afford the product in a yield of 54%. Attempts to prolong the reaction time in order to obtain higher conversion failed: Either the starting material or the product started to decompose again in this case.

Finally, the aromatic dinucleophiles **9**, **14**, **24**, **25**, and **26** could be synthesized in good to excellent yields. With this, a general method for the synthesis of dinucleophilic compounds that contain tin and a boronic ester as metal functionalities on the same substrate could be developed. As precursor for this method aromatic systems containing a halogen and a boronic ester must be available. This synthetic route offers access to further aromatic dinucleophilic systems that can be synthesized in future work.

3.2.1.3 Synthesis of Gold-Boron Functionalized Dinucleophiles

In order to synthesize other dinucleophiles with potentially new and different reactivity patterns, it was envisioned to replace tin by another metal functionality. Similar to the tin-boron functionalized thiophene dinucleophile **9** we wished to differentiate between the two metal functionalities in a coupling reaction. Another attribute should be the stability of the dinucleophile itself: In order to obtain a well characterized, easy to handle compound, a species was required that could be isolated and, in an ideal case, handled without inert atmosphere. For this reason lithium, magnesium and zinc were not considered to be suitable alternative metal functionalities for this project. Organosilicon compounds are stable and can be isolated. But to perform a Hiyama coupling reaction, a base is needed similar to the Suzuki coupling reaction.^[1, 4b, 9] Nevertheless, it could be difficult to find reaction conditions where it can be distinguished selectively between silicon and boronic esters. In addition silicon functional groups are found to be not very reactive. Searching for alternative metals that could be used in coupling reactions, gold was considered as a possible metal functional group: Even if the total amount of isolated aromatic organogold compounds is limited until now, most of them are stable in air. Cross-coupling reactions have been demonstrated so that these reactions may proceed in high yields without any need of a base, which would compete with the cross-coupling of the boronic ester.^[10]

Organogold reagents are generally synthesized by using halogenated goldphosphines **27** as precursors. The organogold reagent **28** is commonly formed by transmetalation reactions. In

contrast to many other metals, gold can perform metal-metal exchange reactions not only with lithium^[10c] but with stannylated^[11] and boronated^[10a] compounds as well as with Grignard reagents^[12] (Figure 2, **29**; compare Chapter 3.3). By using organic salts like dithiocarbamates, gold chloride forms the corresponding organogold carbamate.^[13]

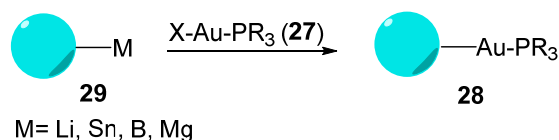
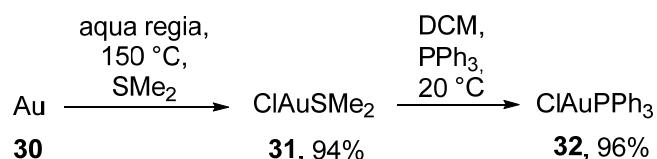


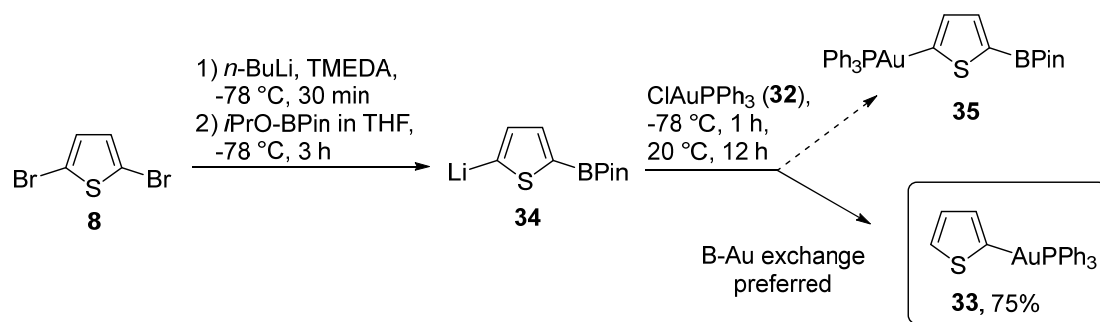
Figure 2. Orgaogold reagents **29** can be synthesized by metal-metal exchange reactions.

For the synthesis of the desired organogold species we chose ClAuPPh₃ (**32**) as a reactant. This could be synthesized directly from elemental gold in a two-step synthesis,^[14] giving the product **32** in an excellent yield of 92% (Scheme 7). The bulky phenyl ligands make the compound stable and thus easy to handle in reactions.^[14] Only light exposure should be omitted to avoid decomposition especially of intermediate **31**. Another advantage is that organogold compounds that contain triphenylphosphine ligands can be purified by crystallization in most cases.



Scheme 7. Synthesis of (triphenylphosphine)gold **32** chloride from elemental gold.^[14]

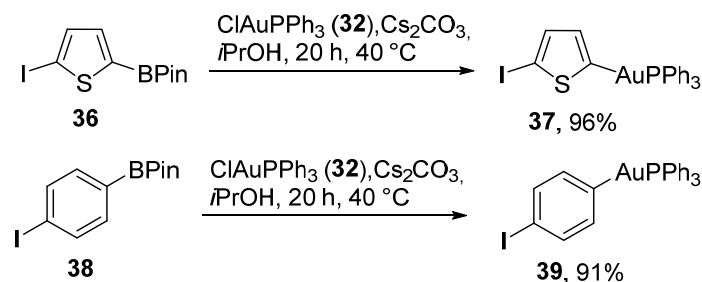
To obtain dinucleophiles containing a boronic ester and gold as metal functionalities, several approaches were considered. As it is known that lithium-gold exchange reactions are high yielding reactions in general, such a route was attempted initially for the dibrominated thiophene **8**. In analogy to the synthesis of the tin-boron functionalized dinucleophile **9** (Scheme 8), both 2- and 5-position were lithiated. By adding successively the boronic ester and then the gold chloride it was expected to obtain the dinucleophile (Scheme 8, **35**). However instead of the expected product **35**, surprisingly **33** was obtained in a yield of 75% (Scheme 8). A possible explanation is that the gold chloride **32** performs a preferred metal exchange with the boronic ester instead of with lithium. We speculate that a possible explanation can be found in the HSAB (hard and soft acids and bases) theory: Li⁺ is characterized as hard acid, whereas Au⁺ is characterized as a soft acid. A boronic ester is described softer than lithium and thus possibly preferred for the exchange with gold.



Scheme 8. Planned synthesis of the dinucleophile **35** starting from 2,5-dibromothiophene (**11**) failed; no product was observed. Compound **33** was isolated instead of the expected product.

Switching the order of addition of the boronic ester and the gold chloride to the lithiated thiophene did also not give the expected product, **33** could be isolated in a yield of 30% by crystallization. In this case the issue can be the reaction time of addition (3 h) or stirring (5 h), which will need to be adapted, similar to the tin-boron functionalized thiophene **9**, (Chapter 3.1): Either for the time of addition for the gold chloride ClAuPPh₃ (**32**) or the time of stirring when the addition of the gold compound is completed. Therefore, this route was not pursued further for the time remaining.

Considering these results, alternative routes had to be divided: Reactions are known where **32** performs an exchange with stannyl^[11] and boron^[10a] groups under mild reaction conditions. In one reported case, a boronic ester was exchanged by **32** on a thiophene derivative containing two boron functional groups, 2,2'-bithiophene-5,5'-diboronic acid bis(pinacol) ester. In this reaction it was found out that Cs₂CO₃ as a base had to be present. The mild reaction conditions of 40 °C in dry isopropanol as solvent gave the product in yields > 80%.^[15] These reaction conditions could be transferred to the reaction of compound **36** as starting material, where the product **37** could be isolated in a yield of 96% (Scheme 9). Likewise, **38** could be used as starting material resulting **39** in a yield of 91%. It is important to note that the iodo group was entirely unaffected. This is vital for further transformations of these compounds to the desired monomers that contains of the type X-heterocycle1-heterocycle2-M.



Scheme 9. Test reaction for a boron-gold exchange reaction. The iodide functionality was used to determine, if this functional group influences the reaction.

The compounds were characterized by standard analytical methods and single crystals could be obtained. The molecular structures of **37** and **39** were determined by X-ray crystallography. The thiophenyl gold complex **37** (Figure 3, a) is similar to the structure of 2-triphenylphosphine-gold(I)thiophene.^[16] The Au1-C1 [2.039 (5) Å] and Au1-P1 [2.2936 (12) Å] bond length differ only slightly from each other. The expected linear C1-Au1-P1 angle was found to be 178.01°. The three angles between the gold Au1-P1-phenyl-C11, C21 and C31 were found to be 114.38°, 114.53° and 110.53°.

The iodophenyl gold complex **39** (Figure 3, b) shows similarities to the thiophene **37** as well. The Au1-C1 [2.043 (4) Å] and Au1-P1 [2.2888 (12) Å] bond length are nearly equal. Here as well the expected linear C1-Au1-P1 angle was found to be 174.16° and the three angles between the gold Au1-P1-phenyl-C11, C21 and C31 were found to be 115.51°, 110.91° and 113.69° respectively.

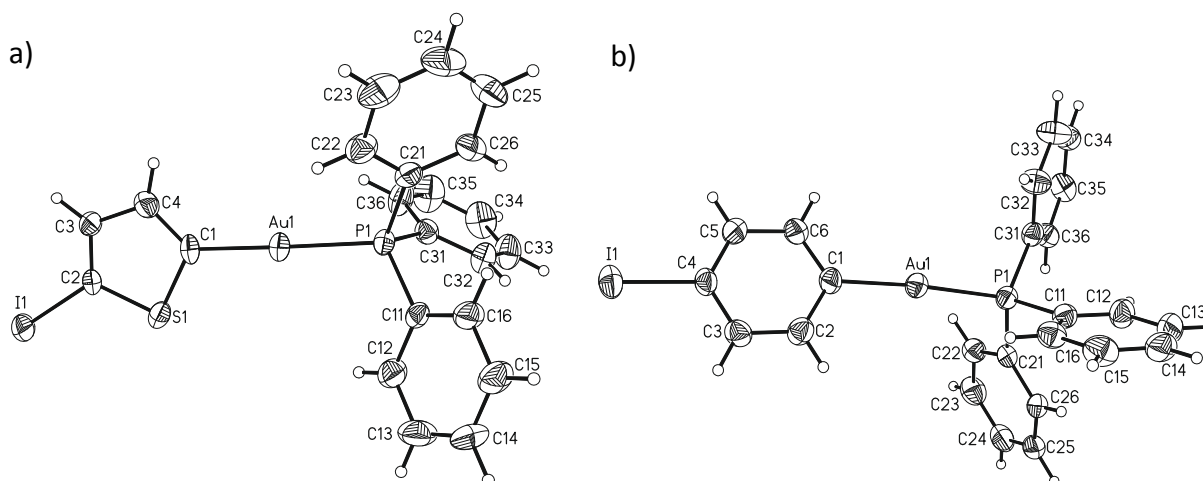
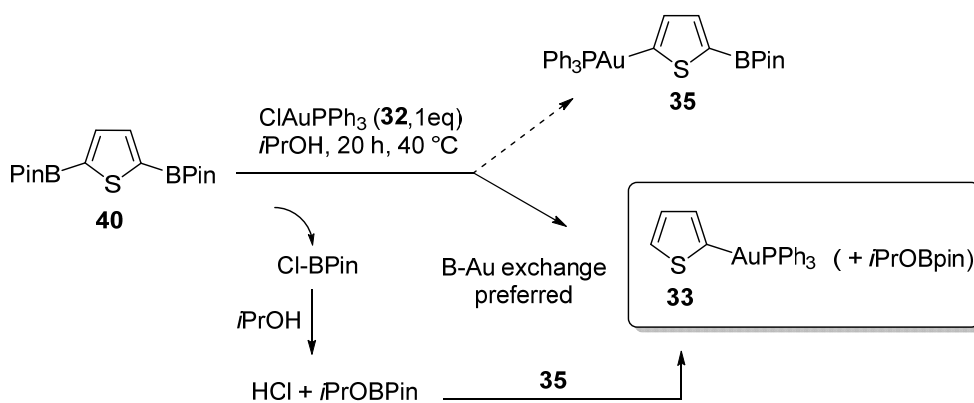


Figure 3. Molecular structure of **37** (a) and **39** (b), ellipsoids show 50% probability levels. Selected bond distances for **37** [Å]: C1-Au1 2.039 (5), P1-Au1 2.2936 (12). Selected angles [°]: C1-Au1-P1 178.201. Selected bond distances for **39** [Å]: C1-Au1 2.043 (4), P1-Au1 2.2888 (12). Selected angles [°]: C1-Au1-P1 174.2160.

Based on the apparently facile boron-gold exchange that proceeded without the need of a lithium compound, a further approach to the synthesis of a gold and boron functionalized dinucleophile **35** was to use a diboronated species **40**. By adding just one equivalent of the gold chloride, only one of the two boron functionality should exchange (Scheme 10). As it turned out, this approach failed: Both boronic esters were removed, even if only one gold substituent is found in the final product. ^1H and ^{31}P NMR (41.4 ppm) confirmed the identity of (triphenyl-phosphine(gold))thiophene (**33**) as formed product in a yield of 45% by crystallization. We speculate that the boron-gold-exchange is a very fast reaction. The boronic ester chloride formed in this reaction might subsequently react with the solvent to form the boronic ester *i*PrOBPin and hydrochloric acid. The latter might lead to a cleavage of the second boron functionality of the thiophene starting material.

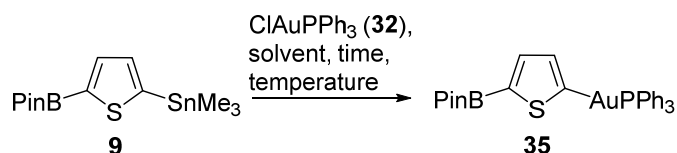


Scheme 10. Synthesis of the gold and boron functionalized dinucleophile **35** from the diboronated species **40** failed.

Not only lithium and boronic esters are known for metal-metal exchange reactions with gold chlorides: There are two different methods described in the literature where a stannyl group also undergoes such an exchange. In these cases no base is required (Table 2, entries 1 and 2). When using the tin-boron functionalized dinucleophile **9** as starting material, the boronic ester should stay stable while the tin exchanges with the chloride **32**. For all reactions, 1.0 equivalents of the gold chloride **32** were used and the reaction was performed under inert conditions with dry and degassed solvents. When toluene was used as solvent, the reaction was heated to $70\text{ }^\circ\text{C}$ for 16 h (Table 2, entry 1). After 1 h all reactants were dissolved. When dichloromethane was used as solvent, the reaction was performed at $20\text{ }^\circ\text{C}$, where all reactants were dissolved immediately (Table 2, entry 2). In both reactions no product could be observed. Besides starting material, a crude ^{31}P NMR spectrum showed again the 2-

(triphenylphosphinegold)-thiophene (**33**) as one of the compounds formed. Therefore, the boronic ester does not require a base for the exchange reaction with gold which results in no selectivity in both cases.

Table 2. Synthesis of thiophene **35** from the tin-boron dinucleophile **9**.



Entry	Solvent	Time	Temperature	Yield
1	Toluene	16 h	70 °C	-
2	DCM	2 h	20 °C	-
3	<i>i</i> PrOH	20 h	40 °C	76%

In contrast to the exchange reactions of boron by gold in toluene and DCM, the reaction in isopropanol is performed with the addition of a base in the literature. Wondering if this is necessary to obtain a boron-gold exchange, the reaction with the dinucleophile **9** was performed in isopropanol as solvent, merely without addition of the base (Table 2, entry 3). The reaction was heated to 40 °C and stirred for 20 h at this temperature. Both the gold chloride **32** and the tin-boron difunctionalized thiophene derivative **9** were hardly soluble in isopropanol. During the whole reaction, a white precipitate was visible in the mixture. Despite this low solubility the expected product **35** could be isolated in a good yield of 76%. Purification was simple: Isopropanol was removed *in vacuo*. The white residue was diluted in DCM and filtered over Celite. The generated tin species, likely to be Me_3SnOH , could be removed by filtration over Celite. Removal of the solvent gave the pure product **35**. The solid could be crystallized by dissolving in a minimum of DCM which was layered with hexane. In addition to standard analysis, the molecular structure of **35** was determined by X-ray crystallography, as single crystals were observed (Figure 4). For the first time it was possible to synthesize a dinucleophile containing gold and boron on the same aromatic ring.

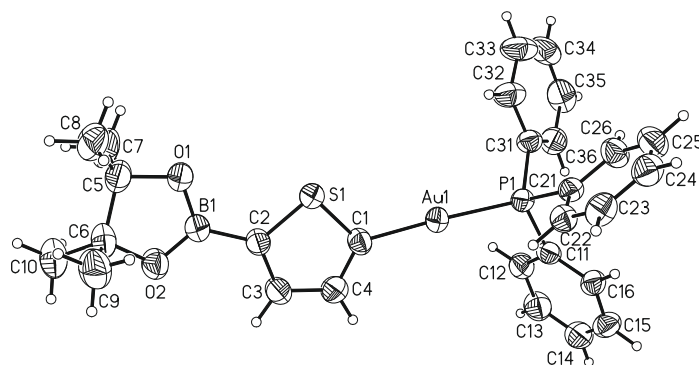
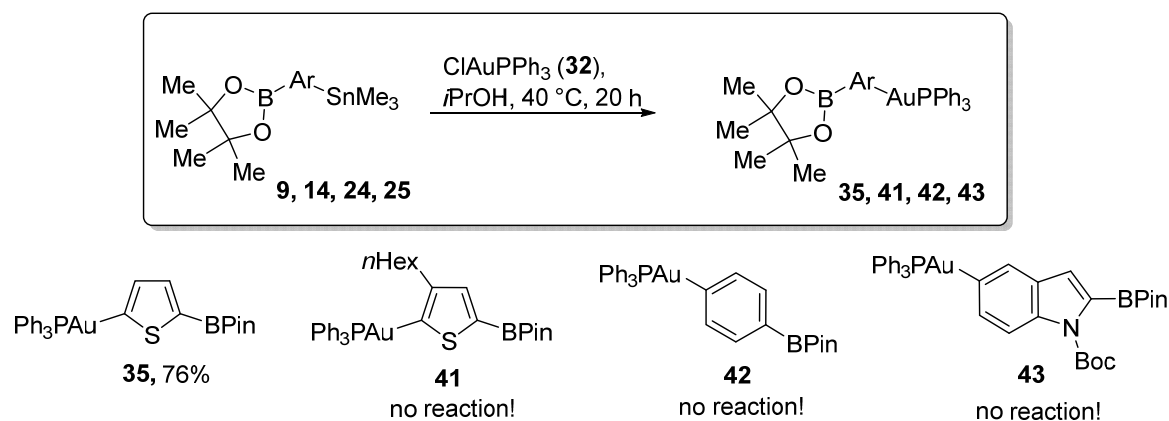


Figure 4. Molecular structure of **35**, ellipsoids show 50% probability levels. Selected bond distances for **35** [Å]: C1-Au1 2.036 (6), P1-Au1 2.2792 (12), C2-B1 1.534 (8). Selected angles [°]: C1-Au1-P1 176.99, O1-B-O2 113.4.

The thiophene gold complex **35** (Figure 4) was similar to the structure of 2-triphenylphosphine-gold(I)thiophene.^[16] The Au1-C1 [2.036 (6) Å] and Au1-P1 [2.2792 (14) Å] bond length differed only slightly from each other. The expected linear C1-Au1-P1 angle was found to be 176.99°. The triangle between the gold Au1-P1-phenyl-C11, C21 and C33 were found to be 110.81°, 113.35° and 115.80° respectively. The B-C2 had a bond length of 1.534(8) Å. The B-O1 [1.375 (7) Å] and B-O2 [1.348 (8) Å] bond length were in the same range. The angles of C2-B-O1 (123.4 Å) and C2-B-O2 (123.2 Å) were found to be the same. The angle between O1-B-O2 was found to be 113.4°.

As the synthesis of the gold-boron functionalized thiophene dinucleophile **35** was successful by starting from the corresponding tin-boron functionalized derivative **9**, the other available aromatic tin-boron functionalized dinucleophiles **14**, **24** and **25** should be used as starting materials as well (compare Chapter 3.2.1). Surprisingly no product could be observed: The benzene-, indole- and hexylthiophene derivatives (**14**, **24** and **25**) did not give the expected products (Scheme 11, **41**, **42**, **43**). Mainly starting material could be observed. The crucial aspect of the success of this reaction seemed to be the solubility of the starting materials. For the derivative **35**, the starting material **9** was poorly soluble in isopropanol. However, all other tin and boron functionalized dinucleophiles **14**, **24** and **25** were soluble in isopropanol, even if 2 h were required for the indole derivative **25**. The dissolved dinucleophiles do obviously not react under these conditions, a reason for this is not evident at the moment.



Scheme 11. The selective gold-tin exchange is only successful for the unsubstituted thiophene derivative **35**.

3.2.1.4 Conclusion

In conclusion we could demonstrate a general method for the synthesis of aromatic nucleophiles containing both a tin and a boron functional group. By using both halogenated and boronated starting materials that are either commercially available or in general easy to synthesize, the tin moiety was introduced by performing a Stille-Kelly coupling reaction. The both tin and boron difunctionalized thiophene (**9**), hexylthiophene (**14**), phenyl (**24**), indole (**26**) and pyridine (**26**) products could be isolated in overall very good yields. Further aromatic dinucleophiles will be synthesized using this method in future work. With these new compounds, dually-selective cross-coupling reactions could lead to improved monomers that would give new, soluble polymers. Another approach gave the first example of dinucleophile that contains both gold and a boron functional group in an excellent yield, starting from the corresponding tin-boron functionalized system. Further work will establish nucleophile selective cross-coupling reactions for such substrates as well, which will provide a new tool for chemoselective synthesis.

Acknowledgements

We thank the DECHEMA for financial support. A. C. J. Heinrich thanks the Deutsche Bundesstiftung Umwelt (DBU) for a Ph. D. scholarship.

3.2.1.5 References

- [1] A. C. J. Heinrich, B. Thiedemann, P. J. Gates, A. Staubitz, *Org. Lett.* **2013**, *15*, 4666.
- [2] U. Salzner, O. Karalti, S. Durdađi, *J. Mol. Model.* **2006**, *12*, 687.
- [3] (a) E. Riedel, *Moderne Anorganische Chemie, Vol. 1*, de Gruyter, Berlin, **1999**; (b) R. Brückner, *Rektionsmechanismen, Vol. 2*, Spektrum Verlag, Heidelberg, **2002**.

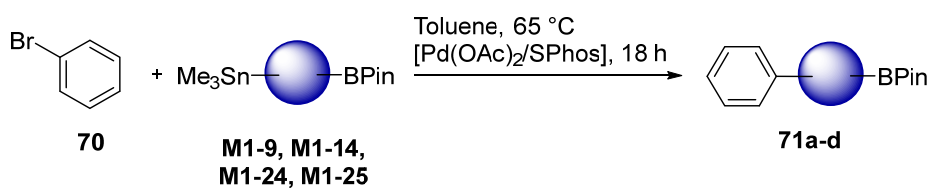
-
- [4] (a) E. Elmalem, A. Kiriya, W. T. S. Huck, *Macromolecules* **2011**, *44*, 9057; (b) J. Linshoef, A. C. J. Heinrich, S. A. W. Segler, P. J. Gates, A. Staubitz, *Org. Lett.* **2012**, *14*, 5644; (c) Y. Yamamoto, T. Seko, H. Nemoto, *J. Org. Chem.* **1989**, *54*, 4736.
- [5] C. Muschelknautz, C. Dostert, T. J. J. Müller, *Synlett* **2010**, *2010*, 415.
- [6] A. C. J. Heinrich, *Diploma Thesis* **2011**, University of Kiel.
- [7] (a) T. R. Kelly, Q. Li, V. Bhushan, *Tetrahedron Lett.* **1990**, *31*, 161; (b) R. Grigg, A. Teasdale, V. Sridharan, *Tetrahedron Lett.* **1991**, *32*, 3859.
- [8] C. G. Watson, V. K. Aggarwal, *Org. Lett.* **2013**, *15*, 1346.
- [9] (a) A. Suzuki, *Angew. Chem. Int. Ed.* **2011**, *50*, 6722; (b) F.-S. Han, *Chem. Soc. Rev.* **2013**, *42*, 5270; (c) N. Miyaura, A. Suzuki, *Chem. Rev.* **1995**, *95*, 2457; (d) S. R. Chemler, D. Trauner, S. J. Danishefsky, *Angew. Chem. Int. Ed.* **2001**, *40*, 4544.
- [10] (a) F. Rominger, T. D. Ramamurthi, A. S. K. Hashmi, *J. Organomet. Chem.* **2009**, *694*, 592; (b) Y. Shi, S. D. Ramgren, S. A. Blum, *Organometallics* **2009**, *28*, 1275; (c) L.-P. Liu, G. B. Hammond, *Chem. Soc. Rev.* **2012**, *41*, 3129; (d) J. J. Hirner, S. A. Blum, *Organometallics* **2011**, *30*, 1299.
- [11] N. Meyer, S. Sivanathan, F. Mohr, *J. Organomet. Chem.* **2011**, *694*, 592.
- [12] Y. Shi, K. E. Roth, S. D. Ramgren, S. A. Blum, *J. Am. Chem. Soc.* **2009**, *131*, 18022.
- [13] F. K. Keter, I. A. Guzei, M. Nell, W. E. v. Zyl, J. Darkwa, *Inorg. Chem.* **2014**, *53*, 2058.
- [14] A. Heinrich, *Synlett* **2015**, *26*, 1135.
- [15] C. Lothschütz, R. Döpp, M. Rudolph, T. D. Ramamurthi, F. Rominger, A. S. K. Hashmi, *Angew. Chem.* **2009**, *121*, 8392.
- [16] K. A. Porter, A. Schier, H. Schmidbaur, *Organometallics* **2003**, *22*, 4922.

3.2.2 An Outlook: Cross-Coupling Reactions on Aromatic Dinucleophiles

As described in Chapter 3.1 of this thesis it was possible to use newly synthesized dinucleophiles in cross-coupling reactions. In this chapter the optimized reaction conditions for the tin-boron functionalized thiophene derivative **M1-9** were used (compare Chapter 3.1): On the one hand in order to perform a nucleophile-selective cross-coupling reaction with 1-bromobenzene **44** as electrophile.^[50a] On the other hand 1-iodo-4-bromobenzene **48** was used as electrophile in order to perform a both nucleophile-and electrophile selective cross-coupling reaction.^[50m]

3.2.2.1 Attempted Nucleophile Selective Cross-Coupling Reactions of Tin-Boron Functionalized Dinucleophiles

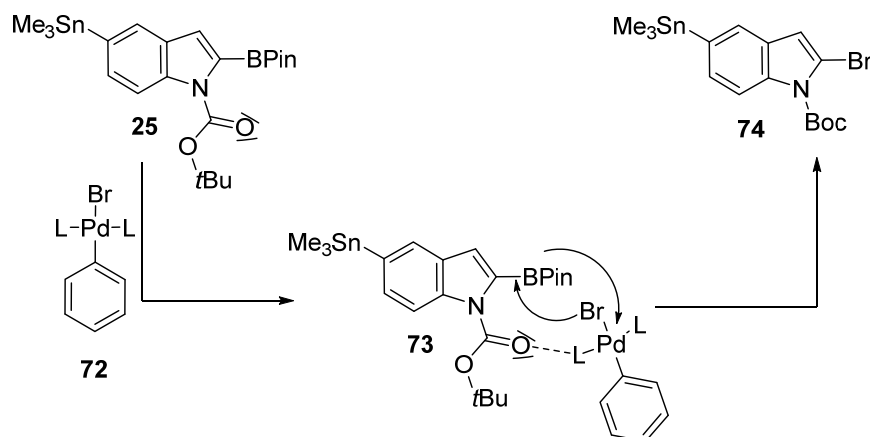
To simplify the identification of selective reaction conditions it was planned initially to perform merely a nucleophile-selective cross-coupling reaction, as it was presented by J. Linshoef in 2012.^[50a] Here a method of nucleophile-selective cross-coupling reaction was developed by using the thiophene derivative **M1-9** as starting material (Table 1, entry 1). The Stille reaction with aryl bromides was performed under mild reaction conditions in toluene as solvent at 65 °C and a catalyst system of [Pd(OAc)₂/SPhos]. The selective coupling reactions gave the products in high yields within 18 h of reaction time. To assess if these reaction conditions could be transferred to new dinucleophiles **M1-14**, **M1-24**, and **M1-25**, they were used under the same conditions with 1-bromobenzene (**44**) as electrophile (Table 1). For the workup all reactions were filtered over a short plug of silica in order to remove the palladium (decomposed catalyst species) from the remaining reaction mixture. For the alkylated thiophene dinucleophile **M1-14** as nucleophile, the crude ¹H NMR of the reaction mixture mainly showed starting material with impurities that were either formed by decomposition of the starting material on the silica or the impurities were caused by unremoved catalyst material (Table 1, entry 2). For phenyl dinucleophile **M1-24** as starting material, the result was similar: There was mainly starting material which could be recovered in a yield of 80% (Table 1, entry 3). There was no evidence that the cross-coupling reaction itself had taken place.

Table 1. Approaches for the nucleophile selective cross-coupling reaction.

Entry	Starting Material	Reaction time	Yield
1	 M1-9	18 h	83% ^a
2	 M1-14	18 h	-
3	 M1-24	18 h	-
4	 M1-25	18 h	-

^aTo compare the reactions this experiment is already reported in *Org. Lett.* **2012**.^[50a] The yield was isolated in this case, the conversion was not controlled by GC.

Similarities were found for the dimetalated indole derivative **M1-25** as starting material. GC-MS showed two species in the crude reaction mixture: On the one hand starting material could be identified (Table 1, entry 4). On the other hand a pure compound **74** could be isolated and characterized by ¹H NMR and mass spectrometry, whose genesis cannot be easily explained (Scheme 12): The indole species **74** with a bromide substituent in 2-position where the boronic ester was situated previously. In the reaction a metal-halogen exchange must have taken place. This is an unusual reaction; while oxidative brominations of aromatic boronic acids have been described,^[80] in such cases a Br⁺ equivalent or Br⁻ and an oxidation source is always present.^[81]



Scheme 12. Until now it is unclear how compound **74** was formed. A possibility is an oxidation by the catalyst which transferred the bromine into the Boc-protected intermediate.

One explanation might be that the carbonyl function of the protection group coordinates to the catalyst complex **72**. If this happens, the catalyst may perform a ligand exchange: The boronic ester leaves the indole, and a bromide is substituted in this position (Scheme 12).

For all reactions (Table 1), starting material could be identified as main species in the mixture. In addition to this the catalyst species decomposed after 18 h at 65 °C or even earlier. It is therefore expected that increasing the reaction time will not give any improvement of the yields. Finally, improved reaction conditions have to be developed for the nucleophile selective cross-coupling reaction as well.

3.2.2.2 Attempted Electrophile- and Nucleophile Selective Cross-Coupling Reactions of Tin-Boron Functionalized Dinucleophiles

In 2013 (Chapter 3.1) the method of a both nucleophile and electrophile selective cross-coupling reaction was developed using the tin- and boron functionalized thiophene derivative **M1-9** as dinucleophilic species.^[50m] To obtain the high selectivity described in this publication, a large amount of optimization work had been performed. With a range of new dinucleophiles in hand we wished to analyze, if these reaction conditions could be transferred to these new synthesized aromatic dinucleophiles **M1-14**, **M1-25** and **M1-26**.

On behalf of it, the coupling reactions were performed in the microwave at 100 °C with $[\text{Pd}(\text{PPh}_3)_4]$ as a catalyst (2 mol%) in DMF and 1-bromo-4-iodobenzene (**75**) as dielectrophile (Table 2). For the unsubstituted thiophene derivative **M1-9** the reaction gave the product completely selective in an isolated yield of 84 % (Table 2, entry 1, compare Chapter 3.1). When using the alkylated thiophene dinucleophile **M1-14**, the reaction time was extended.

After 60 minutes the conversion was incomplete at only 13% (Table 2, entry 2). After an additional 3 h the reaction mixture showed a conversion of 27%. However a black precipitate was formed indicating that the palladium catalyst had decomposed (Table 2, entry 3). By mass spectrometry it was found out that the reaction was unselective: Besides some unidentified decomposition species, both the undesired bromo-coupled product and the desired iodo-coupled product were found to be the main coupling products; an exact ratio of the two coupling products could not be determined by ^1H NMR spectroscopy due to the remaining by-products that gave signals in the aromatic region as well. This unselective coupling behavior was unexpected, especially because the aromatic system was still a thiophene and thus extremely similar to compound **M1-9**.

Table 2. Approaches for the nucleophile- and electrophile-selective cross-coupling reaction.

Reaction scheme: 4-bromoiodobenzene (**75**) + Me_3Sn -[Aromatic]-BPin (M1-9, M1-14, M1-24, M1-25) $\xrightarrow[\text{[Pd(PPh}_3)_4]]{\text{DMF, MW, 100 }^\circ\text{C}}$ Br-[Aromatic]-BPin (**76a-d**)

Entry	Starting Material	Reaction time	Conversion (GC)	Yield
1	<p>M1-9</p>	60 min	>84%	84% ^a
2	<p>M1-14</p>	1 h	13 %	-
3	<p>M1-14</p>	4 h	27%	-
4	<p>M1-24</p>	1 h	31%	-
5	<p>M1-24</p>	17 h	100%	-
6	<p>M1-25</p>	90 min	100%	-

^aTo compare the reactions, this experiment is already reported in *Org. Lett.* **2013**.^[50m] The yield was isolated in this case, the conversion was not controlled by GC.

As in the case of the alkylated thiophene derivative **M1-14**, for the phenyl derivative **M1-24** it was found that a longer reaction time was required: After 1 h, a conversion of 31% of the starting material was found (Table 2, entry 4). After 17 h a full conversion of **M1-24** was obtained. Also as in the previous case a mixture of both possible cross-coupling species was found in an undefinable ratio (Table 2, entry 5). The reaction with the indole dinucleophile **M1-25** as starting material was stopped after 90 minutes (Table 1, entry 6), when the catalyst decomposed visibly after this time. In the case of the indole derivative **M1-25** a mixture of two similar species was found after column chromatography in one fraction, where the expected iodo-coupled product was found to be the main-product (> 80%). By mass spectroscopy it was confirmed that these two species are both possible cross-coupled products. In addition the Boc-protection group of the indole had been removed.

In summary it was not possible to transfer the optimized reaction conditions that were developed for the thiophene dinucleophile **M1-9** to the other dinucleophiles. For each nucleophile, new and improved reaction conditions have to be found to obtain a selective cross-coupling reaction. In addition to this, another protecting group than Boc has to be used to make the indole derivative stable.

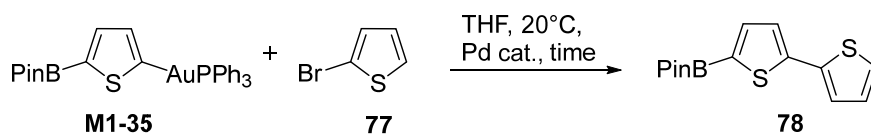
3.2.2.3 Further Planned Syntheses of Both Organogold- and Boronic Ester Difunctionalized Dinucleophiles

Although the synthesis of further gold- and boron functionalized dinucleophiles could not be demonstrated at the time of writing, it was possible to isolate the thiophene derivative **M1-35**. A transfer of the newly designed method to further reagents was unsuccessful until now, but a further investigation of this reaction type will likely lead to further gold-boron dinucleophilic compounds, because they appear to be stable, isolatable compounds. As solubility of the starting materials seems to have a high impact on this reaction type, polar solvents like methanol solvents might be a good alternative to the hitherto used isopropanol. Methanol is more polar than isopropanol and may lead to a lower solubility of the remaining tin and boron functionalized dinucleophiles in this solvent and thus to the formation of the desired both gold- and boron containing products **M1-41**, **M1-42**, **M1-43**. Temperature and reaction time will effect this reaction as well and might lead to the desired products.

3.2.2.4 Attempted Nucleophile Selective Cross-Coupling Reactions on Organogold-Boron Functionalized Thiophene

Similar to the both alkyltin and boron difunctionalized dinucleophile **M1-9** the new-type dinucleophile **M1-35** was used in cross-coupling reactions with the electrophile **77** to evaluate, if nucleophile-selective cross-coupling reactions would be possible (Table 3).

Table 3. Attempts to perform a nucleophile-selective cross-coupling reaction with organogold and boron thiophene **M1-35** as starting material.



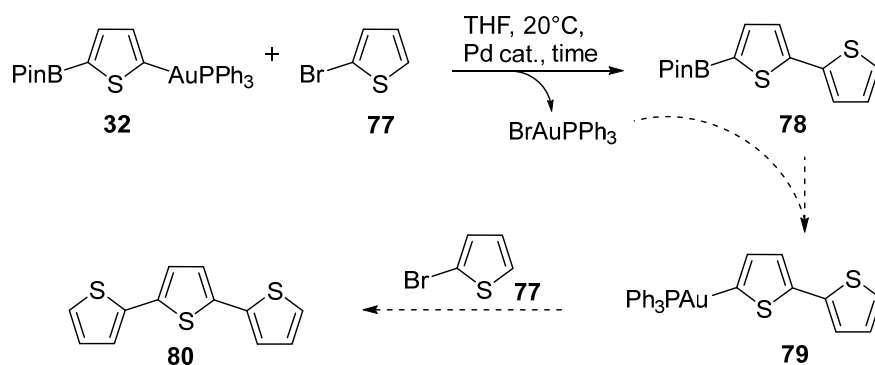
Entry	Catalyst	Time	Conversion ^a	Yield
1	[Pd(dppf)Cl ₂]	5 h	59%	-
2	[Pd(dppf)Cl ₂]	30 h	65%	-
3	[Pd(PtBu ₃) ₂]	1 h	80%	-
4	[Pd(PtBu ₃) ₂]	5 h	80%	-
5	[Pd(PtBu ₃) ₂]	30 h	79%	-

^aThe conversion was measured by GC and was based on the consumption of the electrophile **78**.

All reactions were performed in THF as solvent due to a good solubility of the starting materials and were stirred at 20 °C for the specified reaction time. The conversion was based on the consumption of the electrophile **77**. When [Pd(dppf)Cl₂] was used as catalyst, the conversion was 59% after 5 h and increased only slightly to 65% after 30 h (Table 3, entry 1 and 2). At this point of time, a black precipitate was found in the reaction mixture, which indicates that the catalytic species had decomposed. When using [Pd(PtBu₃)₂] as catalyst, the reaction appeared to be much faster (Table 3, entries 3-5). After 1 h a conversion of 80% was obtained which did not increase after a longer reaction time.

Although the conversion was high when [Pd(PtBu₃)₂] was used as catalyst, it was not possible to isolate product **78**, which has been confirmed to be formed by GC-MS, but only in small amounts. In fact ¹H NMR spectroscopy showed a number of different aromatic species. It was not possible to separate them from each other by crystallization or column chromatography. This is why here it can only be speculated that the first coupling reaction, the coupling of the gold moiety with the electrophile works well. As leaving group BrAuPPh₃

is formed, which is similar to ClAuPPh_3 (**M1-32**). This compound has been used to perform a boron-gold exchange successfully. With this knowledge it can be possible that after a first coupling reaction a boron-gold exchange on **78** has occurred to **79**, which might have subsequently performed another coupling reaction with the electrophile **77** to give **80** (Scheme 13). This would explain, why it was not possible to separate the species due to their similar properties.



Scheme 13. In the coupling reaction $[\text{BrAuPPh}_3]$ is formed. This might perform a boron-gold exchange which would lead to compound **80** which can take part in another coupling reaction.

This was just a first attempt on this new dinucleophile **M1-35**, further reaction conditions and studies have to be performed to determine how the reaction proceeds in detail. It is very promising however that the cross-coupling of the dinucleophile itself seems to proceed. If the resulting gold halogenide could be sequestered, the reaction could be terminated after the first desired coupling. Alternatively, if the electrophile can be modified in such a way that another species than a halogenide is formed, selectivity might be achieved. It has not been shown until now, but an alternative conceivable leaving group might be a pseudo-halide, for example, a trifluoromethylsulfonyl group.

3.3 Gold-Functionalized Thiophene-Type Monomers in Polymerization Reactions

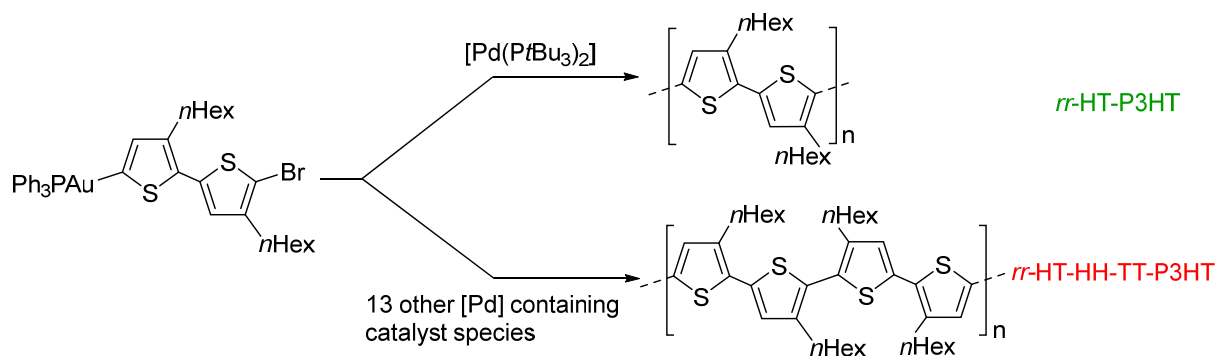
3.3.1 Manuscript on Gold-Functionalized Thiophene-Type Monomers in Polymerization Reactions

“An Unexpected Twist: The Journey to a Gold-based Method for the Synthesis of Highly Regio Regular Head-to-Tail Poly-3-Hexylthiophene and its Counterpart Regio Regular Head-to-Head/Head-to-Tail/Tail-to-Tail Poly-3-Hexylthiophene”

A. C. J. Heinrich, P. J. Gates, C. Näther, A. Staubitz

This chapter was written in manuscript form with the view of a timely publication of these results. For further desirable experiments for this project see Chapter 3.3.2.

ABSTRACT: Present routes for the synthesis of regio regular P3HT are far from ideal: They are either based on zinc or magnesium containing monomers that cannot be isolated or on monomers that contain highly toxic tin. Alternatively they rely on Suzuki cross-coupling methods under polar conditions that prevent the formation of long polymer chains. In this work, the first approach for the synthesis of monomers containing gold as metal functional group is presented. These nonpolar, stable monomers, which are much less toxic than tin-containing monomers, can be easily isolated. Using $[\text{Pd}(\text{PtBu}_3)_2]$ as catalyst the polymerization follows a (living) chain growth polymerization kinetic, although the polydispersity index is relatively high ($\text{PDI}=2$). The reason for this is likely to be a slow initiation that is dependent on the length of the initial monomer. Ligand scrambling experiments revealed that a further cause for the slow initiation is a rapid ligand exchange between the catalyst and the phosphine ligand at the gold monomer. Almost all other catalysts lead exclusively to head-to-head and tail-to-tail couplings, giving highly regio regular HH-TT-P3HT. These polymerizations follow a step growth kinetic. The experimental data are substantiated by theoretical calculations.



TOC Graphic. Polymerization of the monomer leads to different regio regular polymers by using different catalyst species.

Scientific contribution to this project

In this project I carried out all syntheses and experimental work with support of the following people: C. Näther carried out the X-ray crystallography measurement. P. J. Gates recorded all high resolution mass spectra. A. Staubitz performed the DFT calculations.

3.3.1.1 Introduction

Generally semiconducting polymers are synthesized by step growth polymerizations,^[1] where a monomer of type X-monomer-X (with X = halogen) reacts with a monomer of type M-monomer-M (with M = metal), most often in Suzuki^[2] and Stille^[2a, 2e, 3] coupling reactions. Such monomers are readily available and therefore different aromatic systems can be alternated in the polymer backbone. This allows tuning the band gap width;^[4] however molecular weight, polydispersity and regio regularity (in the case of asymmetrically substituted monomers) cannot be controlled, as there are 4 different possibilities of the two monomers to react with each other. In the case of poly-3-alkylthiophenes (P3ATs) prepared using this strategy the alkyl chains are disordered (regio irregular) which leads to a twisted polymer backbone and results in impairing electron delocalization (Figure 1, red, (b)).^[5] In 2004 a method for the “living” chain growth polymerization of aromatic heterocycles was introduced, which revolutionized the synthesis of semiconducting polymers.^[6] In contrast to step growth polymerizations, this method leads to planar polymer systems with much lower polydispersities, high molecular weights and high regio regularities (Figure 1, green, (a)).^[7]

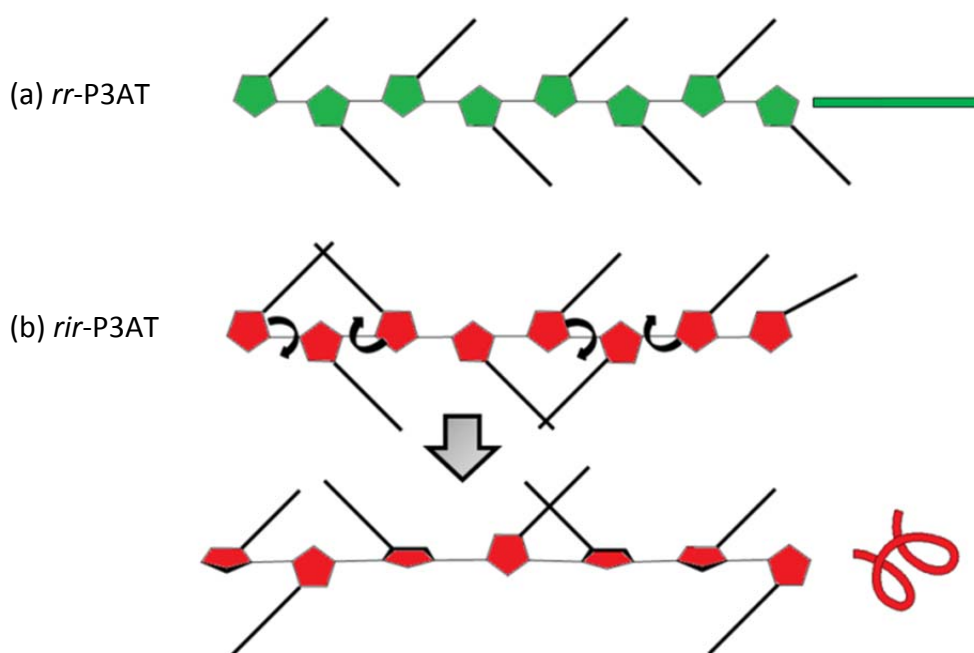


Figure 1. In general regio regular (a) and regio irregular P3AT (b) show different electronic properties. The planar backbone of the regio regular P3AT has a linear structure. The disordered alkyl chains in the regio irregular P3AT cause a twisted polymer backbone.

All these factors substantially influence and improve the electronic properties of the bulk material and therefore device performance.^[8] Despite of these undoubted advantages, until

now, there are only very few (hetero)aromatic monomers available for living polymerizations,^[9] thiophenes being a notable exception.^[10] In fact there is only one example, where the monomer is a combination of different heterocycles.^[11] Monomers suitable for the transition metal catalyzed cross-coupling living polymerization (CCLP) must contain both a metal functional group and a halogen functional group M-monomer-X (Figure 2, **1**), which is a synthetic challenge for any but the simplest aromatic rings.

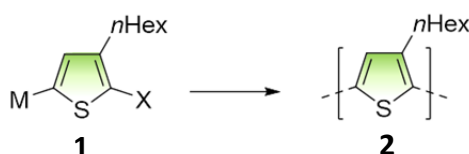


Figure 2. Monomers for the living polymerization must contain both a metal functional group and a halogen. P3HT (**2**) is the best described organic semiconducting polymer.

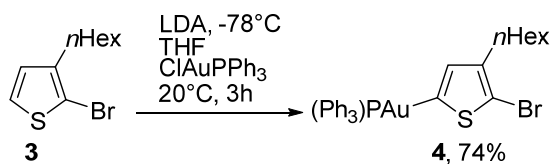
Besides magnesium and zinc, tin is used as often as boronic esters as metal functionalities for the synthesis of organic semiconducting polymers. Examples are known for thiophenes,^[12] fluorenes,^[13] fluorenebenzothiazoles^[11] and polyparaphenylenes.^[14] Whereas zinc and magnesium containing monomers have the disadvantage that they have to be prepared *in situ*, tin containing monomers can be isolated. However they are very toxic.^[15] Boronic esters on the other hand may lead to a limitation of the chain length, due to the basic aqueous reaction mixture that is generally needed for Suzuki coupling reactions, which may lead to a premature precipitation of the growing, non-polar polymer chain.^[16] Other metal functionalities have been rarely used for this field of research and there are no reports on polymerizations with organogold monomers which are expected to be less toxic than tin-containing monomers. On top of that these nonpolar, stable monomers can be easily isolated.

Only in very recent years organogold species have been researched in detail. The focus hereby has been on reactions that are catalytic in gold.^[17] Cross-coupling reactions with stoichiometric organogold species are very rare and have not at all been investigated for polymerization reactions.^[18] In most cases the examined organogold species was used for the investigation of the different steps in gold catalysis.

3.3.1.2 Synthesis of a Novel Organogold Monomer

To investigate the suitability of gold(I) compounds as monomers for polymerization reactions we synthesized compound **4**, which is analogous to the established monomers **1**. This

monomer was expected to give the well-established poly(3-hexyl)thiophene (P3HT, **2**), facilitating the analysis and optimization of the reaction.



Scheme 1. Synthesis of compound **4**.

The synthesis of compound **4** was achieved by selectively lithiating 2-bromo-3-hexylthiophene **3**^[12] in 5-position with the bulky base LDA and transmetalation with the organogold(I) reagent ClAuPPh₃ (Scheme 1).^[17d] Crystallization in hexane led to the product in a good yield of 74%. As it is often observed for organogold(I) compounds, **4** was stable under air conditions. The molecular structure of **4** was determined by X-ray crystallography (Figure 3): The gold complex **4** is similar to the structure of 2-triphenylphosphine-gold(I)thiophene.^[19] The Au1-C1 [2.035 (5) Å] was slightly shorter than the Au1-P1 [2.2804 (11) Å] bond length.

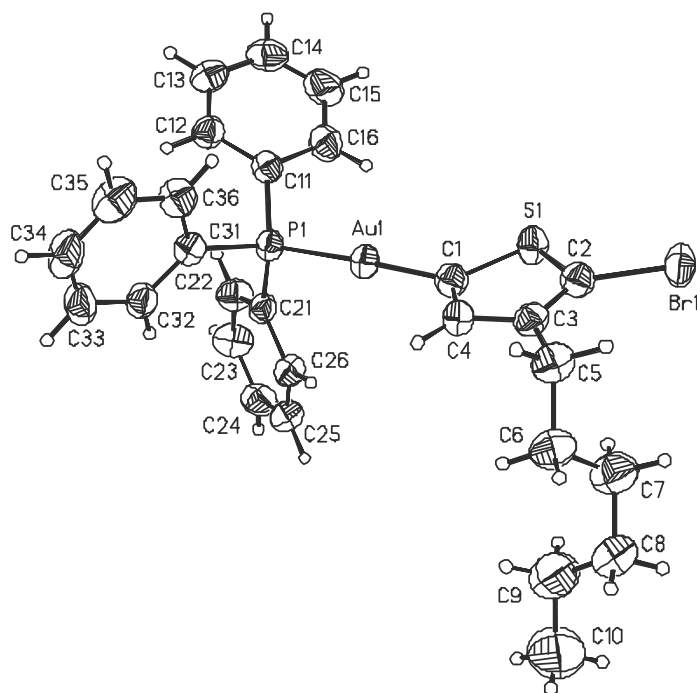


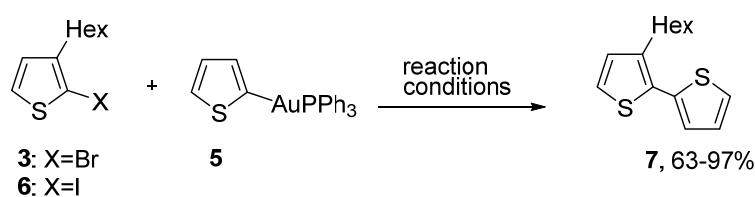
Figure 3. ORTEP drawing of **4**, ellipsoids show 50% probability levels. Selected bond distances [Å]: C1-Au1 2.035(5), P1-Au1 2.2804 (11). Selected angles [°]: C1-Au1-P1 177.21 (13).

The C-Au-P angle was almost linear with 177.21°, which is very common for this type of compound due to the very efficient s-p and s-d orbital mixing for heavy atoms such as gold.^[18a] On the phosphorus atom a tetrahedral geometry was observed with Au-P-C angles

averaging around 115° and 111°, suggesting a strong donation of the phosphorus lone pair to the gold atom.^[20]

3.3.1.3 Organogold Cross-Coupling

Before the polymerization reactions were carried out, it was necessary to find suitable reaction conditions for the intramolecular cross-coupling reaction of a gold-containing thiophene species without the complication of the polymerization reaction. With **5** as nucleophile and 3-*n*-hexyl-2-bromo-thiophene (**3**) and 3-*n*-hexyl-2-iodothiophene (**6**) as electrophiles various conditions were screened (40 reactions, Scheme 2, full screening see SI Table SI 1). All reactions proceeded in high yields around 90% almost irrespective of temperature, solvent and solubility. Unexpectedly the brominated species **3** gave higher yields in a coupling reaction than the iodide **6**. This is an unusual observation as aryl iodides tend to be more reactive than aryl bromides in cross-coupling reactions,^[16c] but exceptions have been reported in the case of Kumada cross-coupling reactions with iron catalysts.^[21]



Scheme 2. Gold cross-coupling reaction with simple starting materials led to optimized reaction conditions.

Having this monomer and suitable reaction conditions in hand the next step was to perform the polymerization of **4** to P3HT. To our surprise under none of the previously successful reaction conditions a reaction occurred (see SI table SI2). A thorough literature search revealed that little was known about reactivity trends for stoichiometric gold reagents. One report^[22] described cross-coupling reactions with organogold species with different electrophiles, giving generally very good yields, but in one case, when an electron rich electrophile was used, no reaction was observed. The case of a monomer such as **4** is special, because the gold and the halogen are bound on the same molecule. As the gold atom has a lower electronegativity ($\chi=2.4$)^[23] than thiophenyl ($\chi=2.56$)^[24] we speculated that the whole thiophene ring could be too electron rich to react with itself as electrophilic component. Therefore the use of a bithiophene as monomer (**8**), containing gold in 2- and a halogen in 5'-position, seemed a more reactive monomer as we reasoned that the impact of

the gold atom on the electrophilic site would be reduced by both distance and statistically (ratio gold atom / thiophene units). In this molecule **8** the gold and the halogen are still on the same substrate, but on different thiophene rings, which could lead to a more suitable electronic structure (Figure 4).

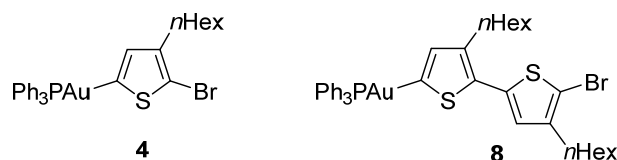
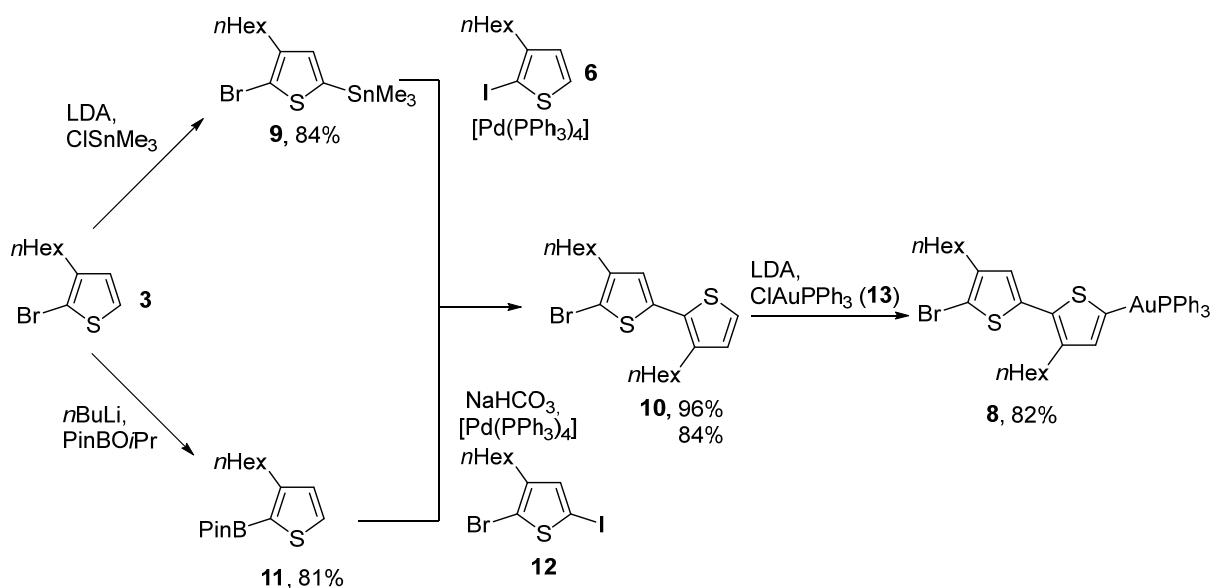


Figure 4. The improved monomer **8** containing two thiophene units could lead to a polymer.

3.3.1.4 Synthesis of an Organogold Bithiophene Monomer

To test this hypothesis we synthesized bithiophene **8** starting from **3**, which was lithiated in 5-position and then quenched with trimethyltin chloride to obtain the stannylated compound **9** in a yield of 87% (Scheme 3). In a subsequent electrophile selective cross-coupling reaction with **6**, the precursor molecule **10** was isolated in a yield of 96%. In an alternative route, the starting material **3** was used in a halogen-metal exchange reaction and by quenching with an isopropylboronic pinacol ester compound **11** was isolated, which could be used again in a electrophile selective cross-coupling reaction with **12** to afford **10** in a yield of 84%. The precursor **10** was lithiated in 5'-position at 0 °C and by quenching with ClAuPPh₃ (**13**) the new monomer **8** could be isolated in a good yield of 82% by crystallization in hexane (Scheme 3).



Scheme 3. Synthesis of the bithiophene monomer **8**.

3.3.1.5 Polymerization Reactions

With monomer **8**, polymerization reactions were screened using a range of very different catalysts. The catalyst loading was 5 mol% in all cases and THF was used as solvent under *reflux* reaction conditions. With the exception of two catalyst complexes (Table 1, entry 4 and 5) all catalyst species gave a polymer as product. A detailed analysis of the ^1H NMR spectra of these polymers showed a repeating unit of 5 monomers (10 thiophene rings), a recurring amount of HH-TT coupling of 5:3:2^[25] can be found (see Figure 5, red spectrum). The signals of the first methylene groups of the hexylchains, which are located on the thiophene, show different shifts for HT (2.8 ppm) and HH (2.6 ppm) couplings. For TT couplings no hexyl-groups are located adjacent to each other and no separated signal is visible.

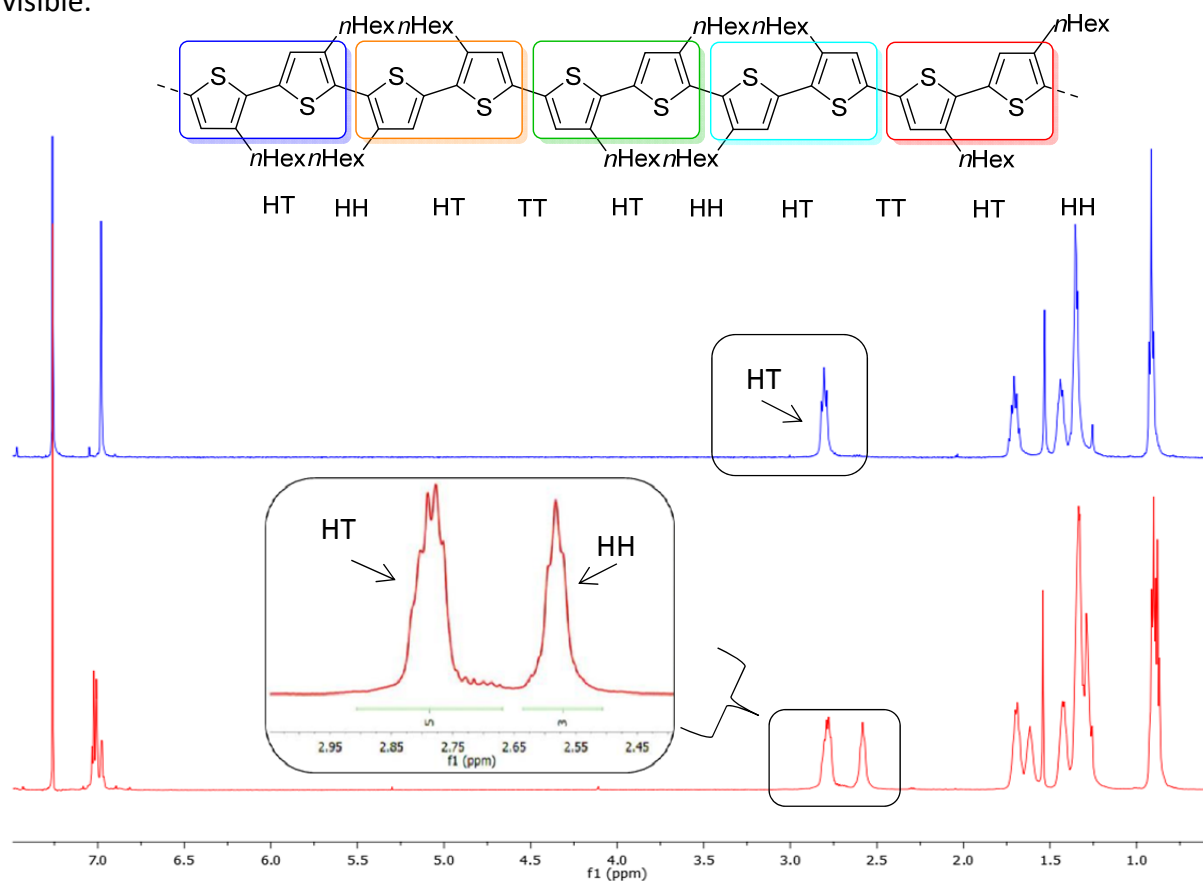
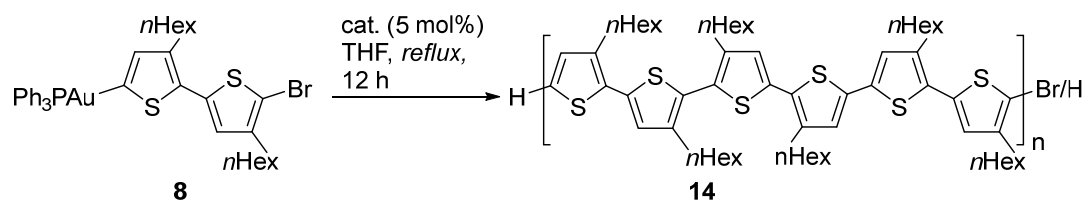


Figure 5. A repeating unit of 5 monomers contains 10 thiophene units (colored boxes). The ^1H NMR spectrum of this polymer is shown in red and the different shifts for HT (2.8 ppm) and HH (2.6 ppm) couplings are shown in a bigger size. The blue trace shows a ^1H spectrum of a completely *rr*-HT-P3HT.

These features are indicative of a highly regio regular P3HT, but one in which only HH and TT coupling had occurred instead of the expected regio regular HT coupling we had expected. The PDIs were between 1.5 to 3.5 and increased with the molecular weight (with maximum

M_w values of 55.000) (Table 1, entry 1, conventional GPC at 20°C, calibrated against PS^[26]). This was the case despite the substantial steric and electronic differences of the catalysts (monodentate vs. bidentate, phosphines vs. *N*-heterocyclic carbenes, Pd(II) and Pd(0) precursors). In uncontrolled step growth polymerizations to form P3HT, a regio random cross-coupling pattern would be expected.

Table 1. Catalyst screening with **8** as monomer.



Entry	Catalyst ^a	Polymer ^b	M_n^c	M_n^d	M_w^c	M_w^d	PDI ^c
1	[Pd(dppf)Cl ₂ ·CH ₂ Cl ₂]	HH-TT ^e	16000	10000	55700	34800	3.5
2	[Pd(PPh ₃) ₄]	HH-TT ^e	2200	1370	3400	2100	1.5
3	[Pd(PtBu ₂ Ph) ₂]	HH-TT ^e	16700	10400	39800	25000	2.4
4	[[(<i>i</i> Pr)Pd(NQ)] ₂]	-	400	250	1800	1100	4.1
5	[[(<i>i</i> Mes)Pd(NQ)] ₂]	-	380	240	850	500	2.2
6	[(<i>i</i> Pr)Pd(allyl)Cl]	HH-TT ^e	1150	720	1800	1100	1.6
7	[(<i>i</i> Mes)Pd(allyl)Cl]	HH-TT ^e	1800	1100	3300	2100	1.8
8	[(<i>S</i> iPr)Pd(allyl)Cl]	HH-TT ^e	1300	800	2600	500	2.0
9	[(<i>S</i> iPr)Pd(cinnamyl)Cl]	HH-TT ^e	7800	4800	18200	11000	2.3
10	[[(<i>i</i> Pr)PdCl ₂] ₂]	HH-TT ^e	9000	5600	23100	14400	2.6
11	[(<i>i</i> Mes)Pd(vs)]	HH-TT ^e	9000	5600	25500	16000	2.8
12	[(<i>S</i> iMes)Pd(vs)]	HH-TT ^e	9500	5900	28700	18000	3.0
13	[Pd(dippf)(vs)tol]	HH-TT ^e	1500	900	2800	1800	1.8

^aFull molecular structure of the catalysts can be found in the SI. ^bDetermined by ¹H NMR spectroscopy: Integration of the first methylene groups of the hexyl chain that are located directly on the thiophene. ^cDetermined by GPC, using polystyrene as standard. ^dDivided with factor 1.6 to correct calibration against PS.^[26] ^eThe Polymer structure was found in a ratio of HH-TT, 5:3:2.^[25]

As all of these polymerization reactions seemed to follow a similar type of polymerization, kinetic studies were performed exemplary on [Pd(PtBu₂Ph)₂] as catalyst species. Here the reaction kinetic followed a typical step growth polymerization (Figure 6): In the beginning of

the reaction the molecular weight increased only very slowly. Then a rapid growth of the molecular weight was observed, yielding high molecular weights, but high PDIs as well.

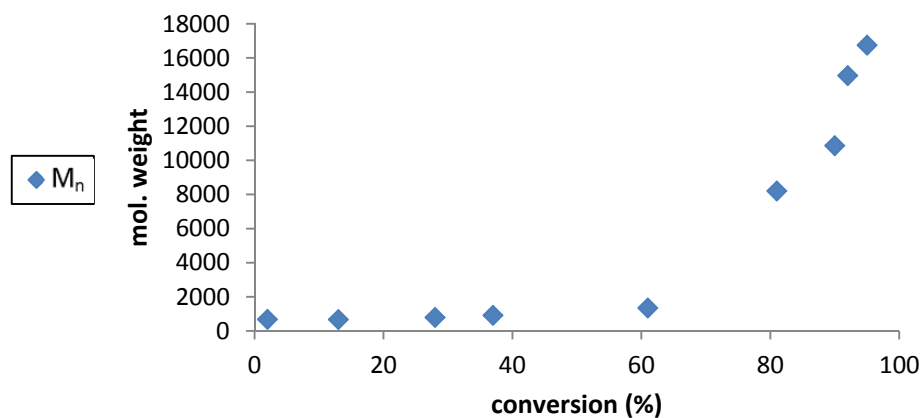
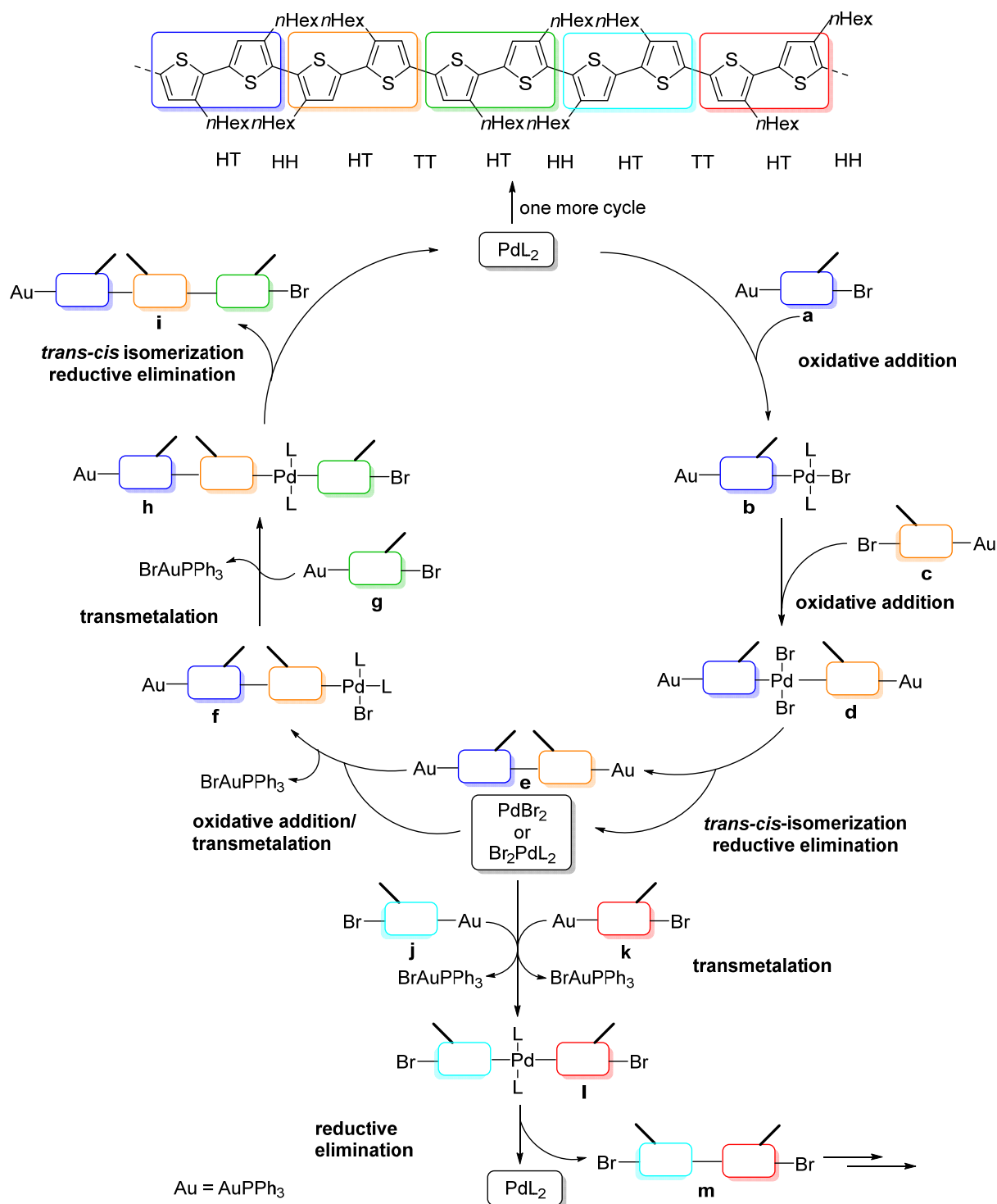


Figure 6. Kinetic studies for the polymerization of **8**, using $[\text{Pd}(\text{PtBu}_2\text{Ph})_2]$ as catalyst species. The conversion was calculated by ^1H NMR spectroscopy.

These results were unexpected in more than one respect: A monomer that contains both a metal functional group and a halogen on the same substrate, should lead to a regio regular polymer as product, even if the process is not living. This high degree of HH and TT couplings is highly unusual for P3HT, as the HT coupling should be preferred due to the steric hindrance of the alkyl chain.^[5b, 27] To explain the occurrence of such a well-defined HH / TT polymer one possible hypothesis might be a polymer formation entirely by homocoupling reactions (Scheme 4). Following this hypothesis, in the first step the palladium (0) species would perform an oxidative addition on the electrophilic side of the monomer **a** to give the Pd(II) intermediate **b**. Instead of performing a transmetalation as it is common for coupling reactions, another oxidative addition with another monomer **c** would occur to form palladium species **d**. By reductive elimination of the palladium (II) species as PdBr_2L_2 (or PdL_2), a new carbon-carbon bond would be formed by homocoupling to give a species containing two gold moieties (**e**). Then the newly formed Pd(II) species would perform a transmetalation with **e** and BrAuPPh_3 would leave and the intermediate **f**, which was detected to be formed (see Chapter 3.3.2.2). Then, another monomer (**g**) would react in a simple transmetalation reaction as a nucleophile and by reductive elimination the PdL_2 (0) species would be re-formed as well as the newly coupled leaving group **i**. By performing one more cycle a pentamer (out of 10 thiophene units) should be formed which represents the spectroscopic unit that is detected by ^1H NMR spectroscopy (Figure 5). As additional reaction a double transmetalation reaction of the gold moieties of two monomers **j** and **k** with the

palladium (II) species is possible which form intermediate **I**. By reductive elimination Pd (0) leaves as well as the dibrominated species **m** which can react as electrophile in the catalytic cycle as well to form the repeating unit in the polymer.

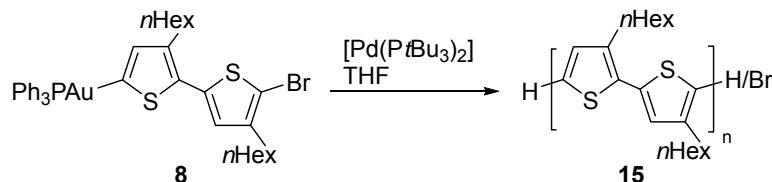


Scheme 4. Proposed mechanism for the formation of the regio regular HH-TT-P3HT **14**.

3.3.1.6 Regio Regular HT-P3HT

Surprisingly, only with $[\text{Pd}(\text{PtBu}_3)_2]$ as catalyst we found a completely regio regular HT-HT polymer **15** (Table 2, entry 1) with a PDI of 2 and a molecular weight of 14 kDa (M_n). For a controlled living polymerization process higher catalyst loadings should lead to lower molecular weights (with ideally one palladium complex per growing chain). Therefore the reaction was performed with 2 mol% and 5 mol% of catalyst species, but the molecular weights were comparable (Table 2, entries 1 and 2). Another aspect was the effect of the temperature on the polymerization. Therefore we performed the reaction at 45 °C and 66 °C (Table 2, entry 1 and 3), which also gave comparable results. In all cases a molecular weight (M_n) of 13 to 16 kDa was found with PDIs of 2 to 2.5. In contrast to this, when toluene was used as a solvent to allow a reaction temperature of 90 °C, we observed molecular weight of 15 kDa (M_n) a much higher and PDI of 5.2 (Table 2, entry 4). It is likely that this was caused by increased homocoupling of polymer chains due to the higher temperature; the polymer was still regio regular within the detection limits of the NMR spectrometer.

Table 2. Polymerization reactions with **8** as monomer.



Entry	Catalyst Loading (mol%)	T	M_n^a	M_n^c	M_w^a	M_w^c	PDI ^a
1	5	66 °C	22700	14200	46200	28800	2.0
2	2	66 °C	25200	15700	64400	40200	2.5
3	2	45 °C	20600	12800	46800	29200	2.3
4	2	90 °C ^b	23700	15000	122800	76700	5.2

The reactions were quenched with 1M HCl in MeOH after 15 h. ^aDetermined by GPC. ^bToluene was used as solvent. ^cDivided by factor 1.6 to correct calibration against PS.^[26]

We also performed kinetic studies in THF with a catalyst loading of 5 mol%. They showed a fast monomer conversion, which followed a nearly linear chain growth (Figure 7) and ended after 200 minutes of reaction time at which point the PDI remained constant at ca. 2. This protocol established a new method for the synthesis of a semiconducting polymer by using an organogold monomer **8** as starting material. The PDI of 2 was comparatively high, but this

could be a result of a slow initiation in case of the bithiophene **8** as monomer: If the initiation process for a living polymerization reaction is slow, not all polymer chains start growing at the same time, which leads to a broader molecular weight distribution.

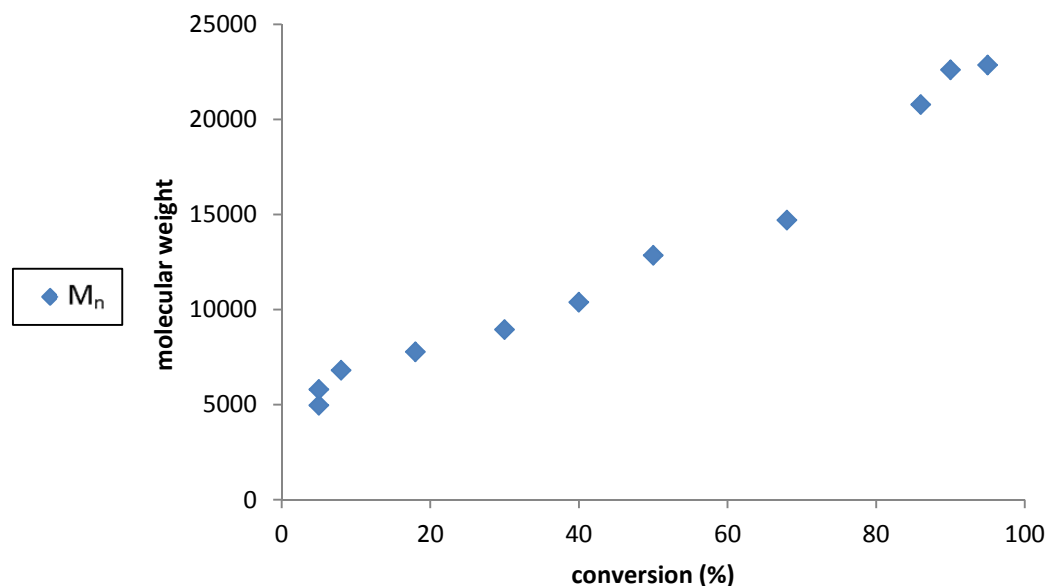


Figure 7. The conversion of the monomer **8** was calculated by integration of the aromatic region of the corresponding ^1H NMR spectra. The error will be significant in this graphic due to the exchange of the phosphine ligands that occurs in the reaction. Nevertheless it is visible that the chain growth is likely to be linear.

3.3.1.7 Potential Causes for a Slow Initiation Process

a) Stability of the Monomer Against Phosphine Exchange Reactions

As it was somewhat unusual that only this catalyst would give regio regular HT-P3HT, it was important to investigate which special feature was the reason of this behavior. As it is known that the ligand PtBu_3 dissociates from palladium with ease,^[28] a possible cause could be that the PPh_3 ligand on the gold in the monomer would exchange with the PtBu_3 from the catalyst. As there was comparatively little catalyst existent it could be one reason for an overall slow initiation event, where chains would be initiated not simultaneously but sequentially - once such an exchange had taken place. Therefore as a control reaction we tested, if the triphenylphosphine ligands of the gold species **8** performed an exchange with the *tert*butylphosphine ligands of the catalyst species $[\text{Pd}(\text{P}(\text{tBu}_3)_2)]$ by adding the phosphine ligand without use of the palladium catalyst itself. Two reactions were performed: In the first reaction monomer **8** (9 eq) was dissolved in $\text{THF-}d_8$ and tri(*tert*butyl)-phosphine (1 eq) was added. These ratios are the same as for the polymerization reactions with 10 mol% of

catalyst. The reactions were monitored by ^{31}P NMR spectroscopy. When the first NMR spectra were recorded, the signal of the tri(*tert*butyl)-phosphine at 63 ppm had already disappeared. A new signal was visible at 92.5 ppm. The signal ratio stayed constant over the period of 3 h indicating that a ligand exchange took place to give a stable equilibrium. To prove that the new signal resulted from the formation of compound **16**, another experiment was performed, where tri(*tert*butyl)phosphine was used in an excess (9:1): here, the signal of the starting material **8** at 43 ppm disappeared entirely (see Figure 9). The spectrum displayed peaks at 92.5 ppm indicative of the newly formed compound **16** at, a peak at 63 ppm, which could be attributed to the excess tri(*tert*butyl)phosphine and as triphenylphosphine is liberated its signal at -5.4 ppm (Figure 8).

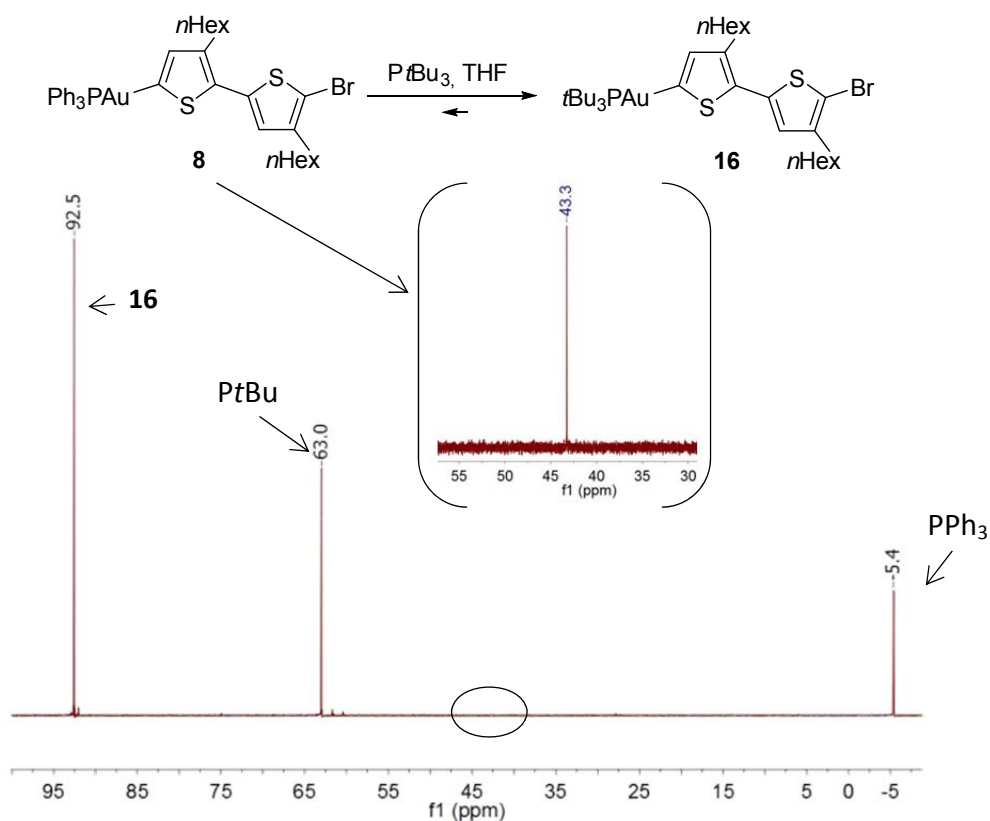


Figure 8. Test for ligand exchange reaction. In this case PtBu_3 (63.0 ppm) was used in an excess (9:1) to the monomer **8** (not visible at 43.3 ppm). As the whole monomer was converted into the organogold species **16** (92.5 ppm), PPh_3 dissociated (-5.4 ppm).

This experiment suggests that an entirely different process takes place in the case of $[\text{Pd}(\text{PtBu}_3)_2]$ as opposed to all other catalysts that were analyzed: When using $[\text{Pd}(\text{PtBu}_3)_2]$ as catalyst species, the butyl ligands are exchanged with the phenyl phosphine ligands of the gold species. Because of that it can be assumed that the active species that takes part in the polymerization is in fact compound **16**, which is formed *in situ*. In case of the monomer **4**,

where no polymerization could be observed under any conditions, the same experiments were performed to test if a ligand exchange takes place: In an NMR tube, both the monomer **4** and tri(*tert*butyl)phosphine were dissolved in deuterated THF. The ^{31}P NMR measurements show that the phosphine ligand of the monomer **4** does perform an exchange with ligand tri(*tert*butyl)phosphine to give compound **17** (Figure 9, c) and d)) in both cases: In the first case PtBu_3 was used in an excess with respect to the monomer **4** (9:1, Figure 9, a)).

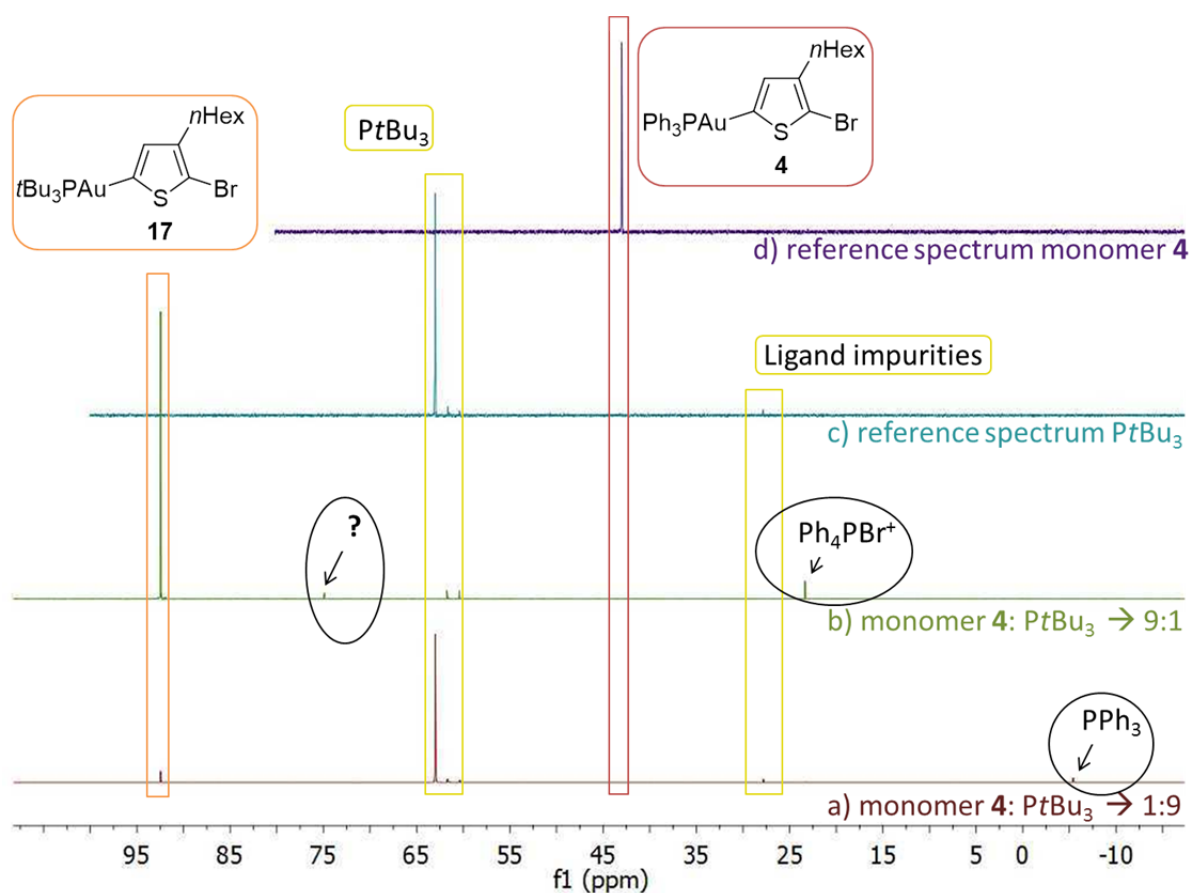


Figure 9. Ligand exchange reaction with monomer **4**. Reference spectra show the monomer **4** (spectrum d), 43 ppm) and the ligand itself, PtBu_3 (spectrum c), 63 ppm). In experiment a), PtBu_3 was used in an excess (9:1) with respect to the monomer **4** (no longer visible at 43.3 ppm). As the whole monomer was converted into the organogold species **17** (92.5 ppm), PPh_3 dissociated (-5.4 ppm). In reaction b) the monomer **4** (no longer visible at 43.3 ppm) was used in an excess (9:1) with respect to PtBu_3 (no longer visible at 63.0 ppm). The newly formed expected organogold species **17** was formed. However in addition to this, the excess of **4** was converted to another undefined species (74 ppm); the formation of $[\text{Ph}_4\text{PBr}^+]^{[29]}$ was confirmed as well (24 ppm).

The spectrum showed the expected species resulting from the exchange: A newly formed species **17**, containing a tritertbutylphosphine ligand on the gold moiety was visible (92 ppm) and the monomer **4** was completely transformed into this species (no signal at 43 ppm for **4**). The ligand leaving the gold species **4**, PPh_3 , was detected as well (-5 ppm). As

expected the PtBu_3 phosphine was visible as well as due to its use in excess (at 63 ppm with its impurities at 27, 60 and 61 ppm - these impurities were already present in the commercially available batch). These findings are consistent with the experiments with the monomer **8**. The reversed approach, where the monomer **4** was used in an excess with respect to PtBu_3 (9:1, Figure 9, b)), gave the expected new species **17** as well as a result of the expected ligand exchange. Surprisingly however the monomer **4**, which should still be present due to its use in an excess, was no longer detectable. Instead of this, new species were formed in addition to **17**: The signal at 23 ppm could be identified as $[\text{Ph}_4\text{PBr}^+]$,^[29] the new species at 73 ppm could not be identified.^[30] In addition it seemed as if the signals of the impurities already present in the batch of the commercially obtained ligand showed an increased intensity (60 and 61 ppm). We speculate that these signals might correspond to $t\text{Bu}_2\text{PBr}$ and $t\text{BuPBr}_2$, impurities resulting of the synthesis of the ligand PtBu_3 itself.

a) DFT calculations: Lower Rate of Initiation due to Electronic Factors

In order to prove this theory and to understand these results, we analyzed the monomer **16** and related structures by DFT calculations (for computational details see SI, Chapter 5). For this purpose, the structures of compounds **a-e** with their tri(*tert*butylphosphine) ligand ($t\text{Bu}_3\text{P}$), which appear to be the relevant species in solution, were optimized and compared (Figure 10). Our initial hypothesis, i. e. that the partial negative charge on the carbon atom adjacent to the reacting bromide would decrease with increasing numbers of thiophenyl units in the ring was analyzed by comparing the NBO charges (NBO = natural bond order). Although they were indeed increasingly less negative (-0.347, -0.340, -0.339, -0.338, -0.337, respectively), the effect was small and unlikely to be the primary cause of the observed reactivity.

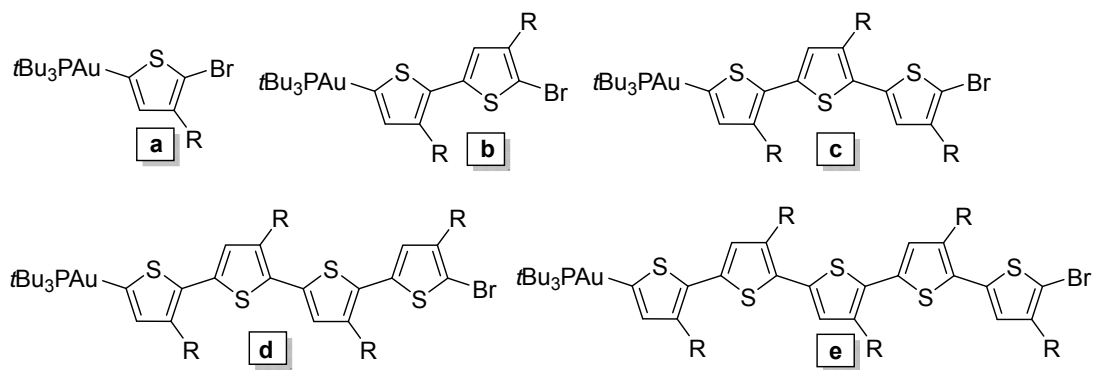


Figure 10. Growing polymer chains with $t\text{Bu}_3\text{P}$ -ligands on the Au atom. To simplify the calculations ethyl groups were used instead of *n*-hexyl chains.

A second hypothesis was formed based on the seminal work of Allen and Locklin and co-workers.^[31] They suggest that at least in nickel catalyzed McCullough polymerizations, η^2 -bound π -complexes are relatively stable intermediates and that their formation is the first irreversible step of the polymerization. Therefore, if this step is fast, initiation will be fast and a living mechanism should be observed. The first step of a coupling cycle is the coordination of the electrophilic component to the transition metal center. If in our case, where a palladium catalyst is used, the formation of the η^2 -bound π -complex is the decisive step, we have to consider the π^* orbitals of the (*t*Bu₃P) ligands of the monomers: these π^* orbitals provide in our case the LUMOs with which the catalyst interacts. The lower the LUMO, the easier is the reaction with the completely filled d^{10} -orbitals of the palladium complex. Our calculations gave the outcome that the longer the thiophenyl chains are, the lower is the energy of this LUMO. The energy distinction between **a** (Figure 10, one thiophene unit) and **b** (Figure 10, two thiophene units) was found to be the most striking. This high energy of the LUMO of **a** might be the reason for our experimental result that **4** (which is transformed to **17** under the reaction conditions) does not react in a polymerization reaction, whereas **8** (which is transformed to **16** under the reaction conditions) does give the required polymer due to its LUMOs lower and obviously suitable energy (Figure 11).

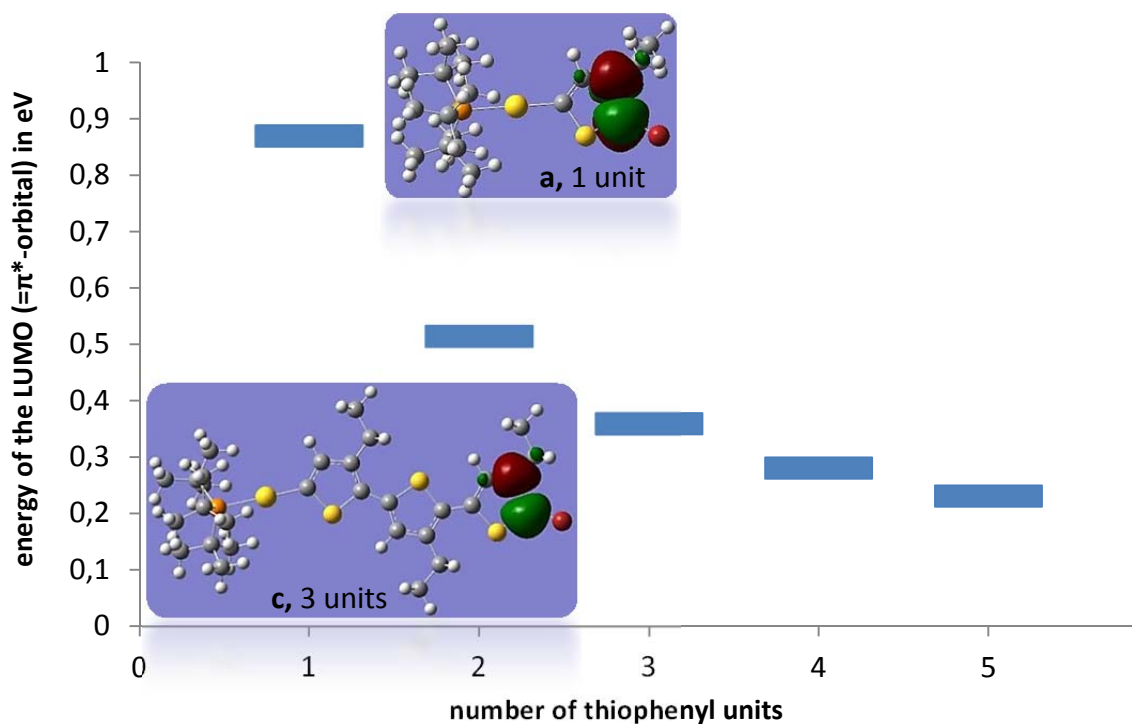


Figure 11. Energy levels of the LUMO (π^* orbitals) decreases the more thiophene units are present in the monomer. The gap between one and two units is striking.

3.3.1.8 Testing Further Characteristics of a Living Polymerization

Another special characteristic of a living polymerization is the associated pair that is formed between the growing polymer chain and catalyst species: The catalyst stays at the end of the chain and thus an elongation is possible by adding more monomers (see Chapter 1). To find out if the chain ends in the polymerization mixture were active and thus to obtain further proof for a living polymerization process, **4** was added to the reaction mixture, where the monomer **8** is converted to the polymer **15** after some polymerization had already taken place. If this would lead to the incorporation of the monomer **4** into the growing chain and in view of the fact that **4** does not polymerize by itself, this would be highly suggestive of the fact that the length of the first monomer, where the first the oxidative addition of the catalyst to the π^* -bond takes place, is the crucial factor in determining the kinetics of the initiation (see above).

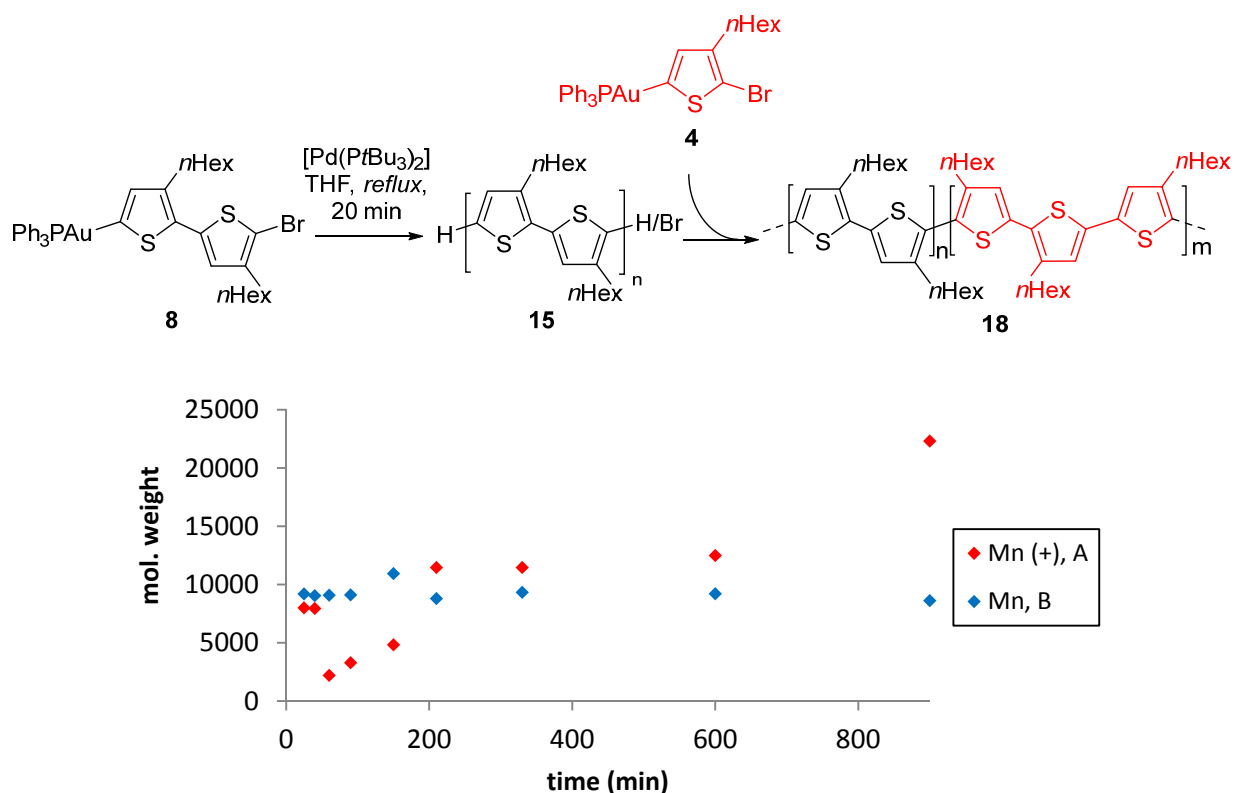


Figure 12. Comparing kinetic studies: After 20 minutes, compound **4** was added (M_n (+), red). M_n : 13900 kDa, M_w : 36400 kDa, PDI: 2.6. The molecular weights were divided by factor 1.6 to correct calibration against PS.^[26]

Once the rate limiting step of the initiation has been overcome the addition of monomer **4** (in the reaction mixture transformed **17**) to a reaction mixture of the bithiophene **8** (in the reaction mixture transformed **16**) should lead to a continued reaction consuming **17** and

longer polymer chains are observed than without any addition of new monomers. The experiment to prove this hypothesis was to perform a polymerization reaction with the addition of **8** (in the reaction mixture transformed **16**) and after 20 minutes: When most of the bithiophene monomers **16** were consumed, half of the polymerization mixture was added to a solution of monomer **4** in THF (reaction mixture (A), red, M_n (+)), whereas the other half ((B), blue, M_n) was left undisturbed as control reaction. The molecular weights of both reactions were analyzed and compared (Figure 12). The control reaction (B) gave the expected M_n of 10 kDa after 120 min and a PDI of 2.5 (Figure 12, blue, M_n). In (A), an immediate decrease of the average molecular weight was observed and a strong increase of the PDI to 4. It was followed by an increasing of the molecular weight up to a M_n of 14 kDa, as it was expected (calculated molecular weight based on incorporation of **4** = 20 kDa), where the PDI was found to be 2.6. These findings confirm that the chain end of the polymerization mixture of **16** was still active. ^1H NMR analysis of the samples showed that the control reaction mixture (B) produced an entirely regio regular HT-P3HT **15** as expected. However, the situation was different for (A): It can safely be assumed that up to the point of adding the second monomer **4** (in the reaction mixture transformed **17**) the polymer was formed as regio regular HT-P3HT, which can easily be shown by ^1H NMR spectroscopy (Figure 13, blue). The second part of the polymer was completely different as the NMR shows a substantial amount of HH coupling. This would mean that the monomer **17** was introduced into the polymer backbone as a series of homo-coupling reactions (compare Figure 13, **18**).

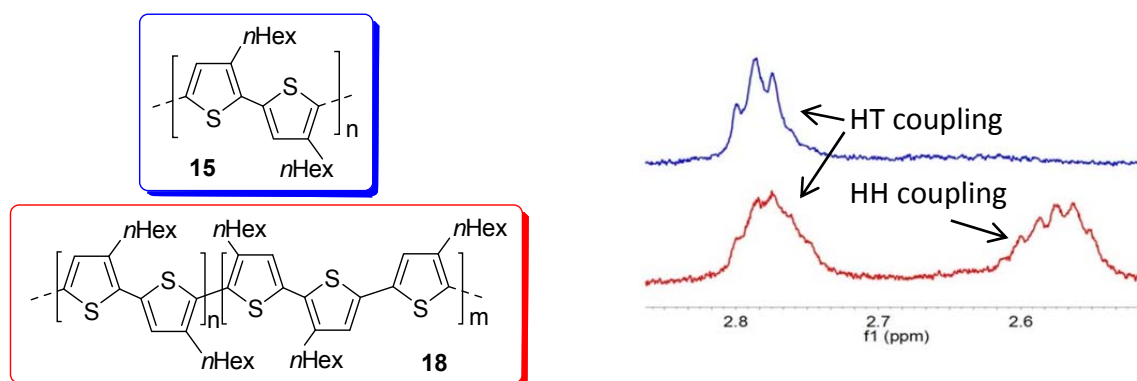


Figure 13. Different 2/5 couplings are visible in the ^1H NMR spectra of the different structured polymers. The NMR spectra show the signals for the first methylene groups of the hexylchain that are located on the thiophene. Blue: Regio regular polymer **15** at 600 min (only monomer **8**), red: Regio irregular polymer **18** at 600 min (after 20 min, monomer **4** was added).

3.3.1.9 Conclusion

In conclusion, it was successful to use gold as metal functionality for the preparation of monomers that can be used for the synthesis of organic semiconducting polymers: Two types of monomers of one and two thiophene units could be synthesized in very good yields containing both a gold functional group and a halogen. Although the monomer with only one thiophene moiety did not polymerize, it was possible to synthesize a monomer of two thiophene units, gold as nucleophilic group. This monomer was successfully used for the synthesis of the semiconducting polymer P3HT: For 13 catalyst species we found different, but highly well-defined regio regular polymers with a HH-TT ratio of 5:3:2 with molecular weights up to 50 kDa at higher PDIs of 3.5. These polymerizations seem to follow the kinetic of a step growth polymerization. By using $[\text{Pd}(\text{PtBu}_3)_2]$ as catalyst species it was possible to synthesize regio regular HT-P3HT with a PDI of 2.0 and a molecular weight of 20 kDa. The kinetic of this polymerization seems to proceed with a nearly linear molecular weight / conversion relationship, suggesting chain growth polymerization. However, it was found that the tri(*tert*butylphosphine) ligand of the catalyst species performs an exchange with the phenylligands of the gold moiety of the monomers **4** and **8** (in the reaction mixture transformed **17** and **16**), although only monomer **8** gives a polymer in the reaction. This indicates that the reactive species that gives this type of regio regular HT-P3HT is formed *in situ*. The ligand exchange experiments confirm that even, if the ligand on gold is tri(*tert*butylphosphine), it is the length of the first monomer, which determines whether a polymerization can take place: The longer the monomer is, the lower is the energy of the π^* system. Additionally the ligand exchange reaction for the monomer **8** is completely selective whereas in the case monomer **4**, side products of the exchange were visible. These unexpected species might contribute to the failure of the polymerization reaction. With these results, it is absolutely necessary to repeat the polymerization reactions and the kinetic studies with the improved monomer **16**, which has to be synthesized as next step.

Acknowledgements

We thank the DECHEMA und Umicore Inc. for financial support. A. C. J. Heinrich thanks the Deutsche Bundesstiftung Umwelt (DBU) for a Ph. D. scholarship.

3.3.1.10 References

- [1] Y.-J. Cheng, S.-H. Yang, C.-S. Hsu, *Chem. Rev.* **2009**, *109*, 5868.
- [2] (a) W. Li, W. S. C. Roelofs, M. M. Wienk, R. A. J. Janssen, *J. Am. Chem. Soc.* **2012**, *134*, 13787; (b) A. Zhang, J. Sakamoto, A. D. Schlüter, *Chimia* **2008**, *62*, 776; (c) C. S. Fischer, M. C. Baier, S. Mecking, *J. Am. Chem. Soc.* **2013**, *135*, 1148; (d) F. Zhang, W. Mammo, L. M. Andersson, S. Admassie, M. R. Andersson, O. Inganäs, *Adv. Mater.* **2006**, *18*, 2169; (e) H. T. Black, A. Dadvand, S. Liu, V. S. Ashby, D. F. Perepichka, *J. Mater. Chem. C* **2013**, *1*, 260; (f) N. Berton, F. Lemasson, J. Tittmann, N. Stürzl, F. Hennrich, M. M. Kappes, M. Mayor, *Chem. Mater.* **2011**, *23*, 2237.
- [3] (a) B. Carsten, F. He, H. J. Son, T. Xu, L. Yu, *Chem. Rev.* **2011**, *111*, 1493; (b) J. Hou, Z. Tan, Y. Yan, Y. He, C. Yang, Y. Li, *J. Am. Chem. Soc.* **2006**, *128*, 4911; (c) Y. Liang, D. Feng, Y. Wu, S.-T. Tsai, G. Li, C. Ray, L. Yu, *J. Am. Chem. Soc.* **2009**, *131*, 7792; (d) H. Zhong, Z. Li, F. Deledalle, E. C. Fregoso, M. Shahid, Z. Fei, C. B. Nielsen, N. Yaacobi-Gross, S. Roszbauer, T. D. Anthopoulos, J. R. Durrant, M. Heeney, *J. Am. Chem. Soc.* **2013**, *135*, 2040.
- [4] (a) E. E. Havinga, W. t. Hoeve, H. Wynberg, *Synth. Met.* **1993**, *55-57*, 299; (b) M. Kertesz, C. H. Choi, S. Yang, *Chem. Rev.* **2005**, *105*, 3448; (c) S. V. Rocha, N. S. Finney, *Org. Lett.* **2010**, *12*, 2598; (d) H. A. M. v. Mullekom, J. A. J. M. Vekemans, E. E. Havinga, E. W. Meijer, *Mater. Sci. Eng. R.* **2001**, *32*, 1.
- [5] (a) J. L. Brédas, *J. Chem. Phys.* **1985**, *58*, 904; (b) I. F. Perepichka, D. F. Perepichka, *Handbook of Thiophene-Based Materials: Applications in Organic Electronics and Photonics*, 1st. ed., John Wiley & Sons, Ltd., Chichester, UK, **2009**.
- [6] (a) Although the living character of this type of polymerization was recognized in 2004, the polymerization itself has been reported much earlier: R. D. McCullough, R. D. Lowe, R., *J. Chem. Soc., Chem. Commun.* **1992**, *70*; (b) A. Yokoyama, R. Miyakoshi, T. Yokozawa, *Macromolecules* **2004**, *37*, 1169; (c) E. E. Sheina, J. Liu, M. C. Iovu, D. W. Laird, R. D. McCullough, *Macromolecules* **2004**, *37*, 3526; (d) R. D. M. I. Osaka, *Acc. Chem. Res.* **2008**, *41*, 1202; (e) V. Senkovskyy, M. Sommer, A. Kiriya, *Macromol. Rapid Commun.* **2011**, *32*, 1503; (f) K. Okamoto, C. K. Luscombe, *Polym. Chem.* **2011**, *2*, 2424.
- [7] (a) C.-C. Ho, Y.-C. Liu, S.-H. Lin, W.-F. Su, *Macromolecules* **2012**, *45*, 813; (b) J. Hollinger, P. M. DiCarmine, D. Karl, D. S. Seferos, *Macromolecules* **2012**, *45*, 3772; (c) T. Yokozawa, A. Yokoyama, *Chem. Rev.* **2009**, *109*, 5595; (d) R. H. Lohwasser, M. Thelakkat, *Macromolecules* **2011**, *44*, 3388.
- [8] (a) K. Tajima, Y. Suzuki, K. Hashimoto, *J. Phys. Chem. C* **2008**, *112*, 8507; (b) A. J. Heeger, *Chem. Soc. Rev.* **2010**, *39*, 2354; (c) D. Zhitomirsky, I. J. Kramer, A. J. Labelle, A. Fischer, R. Debnath, J. Pan, O. M. Bakr, E. H. Sargent, *Nano Lett.* **2012**, *12*, 1007; (d) P. Kohn, S. Huettner, H. Komber, V. Senkovskyy, R. Tkachov, A. Kiriya, R. H. Friend, U. Steiner, W. T. S. Huck, J.-U. Sommer, M. Sommer, *J. Am. Chem. Soc.* **2012**, *134*, 4790.
- [9] (a) C. R. Bridges, T. M. McCormick, G. L. Gibson, J. Hollinger, D. S. Seferos, *J. Am. Chem. Soc.* **2013**, *135*, 13212; (b) Y. Nanashima, A. Yokoyama, T. Yokozawa, *Macromolecules* **2012**, *45*, 2609; (c) T. Yokozawa, Y. Nanashima, Y. Ohta, *ACS Macro Lett.* **2012**, *1*, 862; (d) S. R. Lee, J. W. G. Bloom, S. E. Wheeler, A. J. McNeil, *Dalton Trans.* **2013**, *42*, 4218; (e) A. E. Javier, S. R. Varshney, R. D. McCullough, *Macromolecules* **2010**, *43*, 3233; (f) M. C. Stefan, A. E. Javier, I. Osaka, R. D. McCulloch, *Macromolecules* **2009**, *42*, 30; (g) M. Heeney, W. Zhang, D. J. Crouch, M. L. Chabinyc, S. Gordeyev, R. Hamilton, S. J. Higgins, I. McCullough, P. J. Skabara, D.

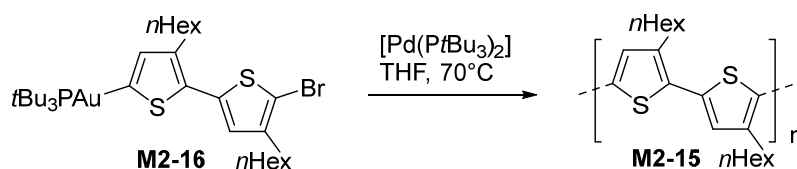
- Sparrowe, S. Tierney, *Chem. Commun.* **2007**, 5061; (h) A. Patra, Y. H. Wijsboom, S. S. Zade, M. Li, Y. Sheynin, G. Leitius, M. Bendikov, *J. Am. Chem. Soc.* **2008**, *130*, 6734; (i) J. Hollinger, A. A. Jahnke, N. Coombs, D. S. Seferos, *J. Am. Chem. Soc.* **2010**, *132*, 8546; (j) A. Yokoyama, H. Suzuki, Y. Kubota, K. Ohuchi, H. Higashimura, T. Yokozawa, *J. Am. Chem. Soc.* **2007**, *23*, 7236; (k) R. Miyakoshi, K. Shimono, A. Yokoyama, T. Yokozawa, *J. Am. Chem. Soc.* **2006**, *128*, 16012; (l) A. Yokoyama, A. Kato, R. Miyakoshi, T. Yokozawa, *Macromolecules* **2008**, *41*, 7271.
- [10] (a) R. Miyakoshi, K. Shimono, A. Yokoyama, T. Yokozawa, *J. Am. Chem. Soc.* **2006**, *128*, 16012; (b) L. Huang, S. Wu, Y. Qu, Y. Geng, F. Wang, *Macromolecules* **2008**, *41*, 8944; (c) M. C. Stefan, A. E. Javier, I. Osaka, R. D. McCullough, *Macromolecules* **2009**, *42*, 30; (d) L. Wen, B. C. Duck, P. C. Dastoor, S. C. Rasmussen, *Macromolecules* **2008**, *41*, 4576; (e) A. Yokoyama, A. Kato, R. Miyakoshi, T. Yokozawa, *Macromolecules* **2008**, *41*, 7271; (f) F. C. Krebs, V. Senkovskyy, A. Kiriy, *IEEE J. Sel. Top. Quant. Electron.* **2010**, *16*, 1821; (g) R. Matsidik, H. Komber, A. Luzio, M. Caironi, M. Sommer, *J. Am. Chem. Soc.* **2015**, *asap*.
- [11] E. Elmalem, A. Kiriy, W. T. S. Huck, *Macromolecules* **2011**, *44*, 9057.
- [12] T. Yokozawa, R. Suzuki, M. Nojima, Y. Ohta, A. Yokoyama, *Macromol. Rapid. Commun.* **2011**, *32*, 801.
- [13] (a) A. Yokoyama, H. Suzuki, Y. Kubota, K. Ohuchi, H. Higashimura, T. Yokozawa, *J. Am. Chem. Soc.* **2007**, *129*, 7236; (b) R. Grisorio, P. Mastroilli, G. P. Suranna, *Polym. Chem.* **2014**, *5*, 4304; (c) H.-H. Zhang, C.-H. Xing, Q.-S. Hu, *J. Am. Chem. Soc.* **2012**, *134*, 13156; (d) E. Elmalem, F. Biedermann, K. Johnson, R. H. Friend, W. T. S. Huck, *J. Am. Chem. Soc.* **2012**, *134*, 17769.
- [14] (a) T. Yokozawa, H. Kohno, Y. Ohta, A. Yokoyama, *Macromolecules* **2010**, *43*, 7095; (b) S. Kang, R. J. Ono, C. W. Bielawski, *J. Am. Chem. Soc.* **2013**, *135*, 4784.
- [15] (a) K. Kent, *Critical Reviews in Toxicology* **1996**, *26*; (b) M. Hoch, *Appl. Geochem.* **2001**, *16*, 719; (c) K. Appel, *Drug Metab. Rev.* **2004**, *36*, 763; (d) F. Grun, B. Blumberg, *Endocrinology* **2006**, *147*, 550.
- [16] (a) A. Suzuki, *Angew. Chem. Int. Ed.* **2011**, *50*, 6722; (b) F.-S. Han, *Chem. Soc. Rev.* **2013**, *42*, 5270; (c) N. Miyaura, A. Suzuki, *Chem. Rev.* **1995**, *95*, 2457; (d) S. R. Chemler, D. Trauner, S. J. Danishefsky, *Angew. Chem. Int. Ed.* **2001**, *40*, 4544; (e) A. C. J. Heinrich, B. Thiedemann, P. J. Gates, A. Staubitz, *Org. Lett.* **2013**, *15*, 4666.
- [17] (a) J. J. Hirner, Y. Shi, S. A. Blum, *Acc. Chem. Res.* **2011**, *44*, 603; (b) S. P. Nolan, *Acc. Chem. Res.* **2011**, *44*, 91; (c) A. S. K. Hashmi, *Chem. Rev.* **2007**, *107*, 3180; (d) A. Heinrich, *Synlett* **2015**, *asap*, DOI: 10.1055/s-0034-1380551; (e) A. S. K. Hashmi, C. Lothschütz, R. Döpp, M. Rudolph, T. D. Ramamurthi, F. Rominger, *Angew. Chem. Int. Ed.* **2009**, *48*, 8243; (f) P. Garcia, M. Malacria, C. Aubert, V. Gandon, L. Fensterbank, *ChemCatChem* **2010**, *2*, 493; (g) A. S. K. Hashmi, G. J. Hutchings, *Angew. Chem. Int. Ed.* **2006**, *45*, 47; (h) E. Jiménez-Núñez, A. M. Echavarren, *Chem. Rev.* **2008**, *108*, 3326.
- [18] (a) F. Rominger, T. D. Ramamurthi, A. S. K. Hashmi, *J. Organomet. Chem.* **2009**, *694*, 592; (b) Y. Shi, S. D. Ramgren, S. A. Blum, *Organometallics* **2009**, *28*, 1275; (c) L.-P.-. Liu, G. B. Hammond, *Chem. Soc. Rev.* **2012**, *41*, 3129; (d) J. J. Hirner, S. A. Blum, *Organometallics* **2011**, *30*, 1299.
- [19] K. A. Porter, A. Schier, H. Schmidbaur, *Organometallics* **2003**, *22*, 4922.
- [20] A. O. Borissova, A. A. Korlyukov, M. Y. Antipin, K. A. Lyssenko, *J. Phys. Chem. A* **2008**, *122*, 11519.
- [21] L. A. M. Mèndez, H. Krause, A. Fürstner, *J. Am. Chem. Soc.* **2002**, *124*, 13856.

- [22] C. Lothschütz, R. Döpp, M. Rudolph, T. D. Ramamurthi, F. Rominger, A. S. K. Hashmi, *Angew. Chem.* **2009**, *121*, 8392.
- [23] (a) W. M. Haynes, *CRC Handbook of Chemistry and Physics, Vol. 95. Ed.*, Taylor & Francis, **2014**; (b) L. Pauling, *J. Am. Chem. Soc.* **1932**, *54*, 3570.
- [24] S. Gronowitz, *The Chemistry of Heterocyclic Compounds, Thiophenes and Its Derivatives, Vol. 2.*, John Wiley & Sons, Inc., **1985**.
- [25] Although the TT coupling is not observable by ^1H NMR spectroscopy, it is implicit through the overall integration of the signals in the spectrum.
- [26] R. C. Hiorns, R. d. Bettignies, J. Leroy, S. Bailly, M. Firon, C. Sentein, A. Khoukh, H. Preud'homme, C. Dragon-Lartigau, *Adv. Funct. Mater.* **2006**, *16*, 2263.
- [27] T. A. Chen, R. D. Rieke, *J. Am. Chem. Soc.* **1992**, *114*, 10087.
- [28] L. He, *Synlett* **2015**, *26*, 40.
- [29] D. Marcoux, A. B. Charette, *Adv. Synth. Catal.* **2008**, *350*, 2967.
- [30] The species that were initially considered could be excluded due to their reported chemical shifts: PPh_2tBu , BrPPh_2 , BrPPh_2^+ , BrPtBu_2 , BrPPhtBu . For other species, no chemical shifts are reported, so that they cannot be confirmed or excluded at this point: $\text{BrPPh}_2\text{tBu}^+$, BrPPhtBu^+ , $\text{Br}_2\text{PPhtBu}^+$ or corresponding THF containing species.
- [31] S. K. Sontag, J. A. Bilbrey, N. E. Huddleston, G. R. Sheppard, W. D. Allen, J. Locklin, *J. Org. Chem.* **2014**, *79*, 1836.

3.3.2 Outlook and Further Experiments

3.3.2.1 Polymerization Reactions of Improved Gold Containing Monomer

All experiments indicate that the $[\text{Pd}(\text{PtBu}_3)_2]$ catalyst performs a ligand exchange with the organogold species **M2-8**. This reacts as the active species for the polymerization reaction. The experiment described in Chapter 3.4.7, in which an excess of the ligand $t\text{Bu}_3\text{P}$ was added to the monomer solution, has strong evidence for this theory. This exchange influences the reaction kinetic of the polymerization: The initiation is slow, which causes broad polydispersities in the living polymerization process. To circumvent the problem of slow initiation the bithiophene monomer **M2-16** has to be synthesized and used under the same reaction conditions for the polymerization reaction (Scheme 14).



Scheme 14. Monomer **M2-16** as starting material for the polymerization should give the *rr*-HT-P3HT **M2-15**. The initiation is expected to be faster and may result in a living polymerization.

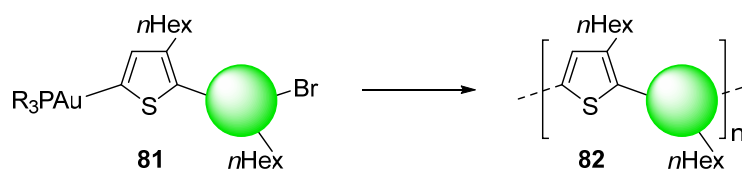
The synthesis of monomer **M2-16** *in situ* is obviously easily possible but in order to avoid any phenyl ligands that may influence the polymerization reaction, the monomer has to be synthesized and isolated before use. This should be possible by the synthesis of ClAuPtBu_3 as a reagent instead of ClAuPPh_3 (**M2-13**) in the last step of the monomer synthesis (Chapter 3.3.1.4, Scheme 3).

Another experiment that was left to do is another blank test similar to the one described in chapter 3.4.7 with monomer **8**. Instead of PtBu_3 , PPh_2Bu_2 was used as ligand in excess here. Derived from the results in chapter 3.4.5, where the *rr*-HH-TT (**M2-15**) was synthesized, it was expected that this ligand would not perform an exchange with the gold monomer. This would encourage the theory that the ligands on the gold species influence the polymerization kinetics. We found out however that we could observe an exchange of the ligands, although the equilibrium seemed to be less on the product side. This was observed for both ratios (9:1 or 1:9) of monomer **8** to ligand. In addition, for both cases the expected exchange species was not a single product: When the ratio of monomer to ligand (9:1) was used, Ph_4PBr^+ was found similar to the previous finding of the experiments on the monomer **4**. In the reverse case a much larger amount of different species was formed. It can only be

speculated about the reasons for this unusual behavior, but it is conceivable that the gold moiety might act as Lewis acid and therefore it induces a ligand exchange on the phosphorous atom of the ligands itself. As some Ph_4PBr^+ could be identified,^[29] we think that the bromide functional group of the monomer **8** is involved in an exchange reaction. It is very important to understand the mechanism of these exchange reactions. One concept might be testing different ligands with a simplified gold species like the already available thiophene **5**. If in this case more than the expected species occur as well, we would receive information about the involvement of the bromide functional group of our monomers **4** and **8**.

We found that the length of the monomer is decisive to the polymerization process and the kinetic. With this knowledge a monomer of three thiophene units would be necessary to be synthesized in order to compare kinetic studies of the monomers. Further projects based on these studies offer great potential, especially the idea to use other ligands on the gold moiety might give completely different results in polymerization reaction.

If the polymerization reaction itself is understood better, as well as the factors that obviously influence this reaction, other gold-containing monomers **81** can be polymerized. By combining thiophene and other heterocycles new well-defined polymers **82** would be available using this method (Scheme 15).



Scheme 15. Monomers of two different aromatic cycles, a halogen and a gold moiety **81** might give new well-defined polymers **82**.

3.3.2.2 Recycling

Another aspect of high importance is the possibility of recycling gold or a synthetically useful gold species. It is well established that catalysts can be immobilized on a surface.^[76a, 76b] Using this it is possible to recover the active metal species. This method has been even used for gold(I) catalysis: A ligand that is covalently bound to a surface was used as linker to the active gold species.^[76a] In contrast to this, the use of immobilized stoichiometric aryl gold organyles and their use in cross-coupling reactions have not been shown so far. In our case we expected that after the coupling reaction the newly formed gold species was BrAuPPh_3

(**83**) (compare Figure 17), because for both mechanisms it is proposed that BrAuPPh_3 is the leaving gold reagent. To confirm which kind of gold species is formed during the polymerization a quenching reaction of a typical polymerization (Chapter 3.3.1.6, Table 2) was performed by just adding methanol. With this, we were able to separate this projected species without the decomposition typically caused by the addition of HCl . A manual preparative column with GPC gel (PS beads) was performed for the separation of the polymer and the resulting gold species (Figure 17).

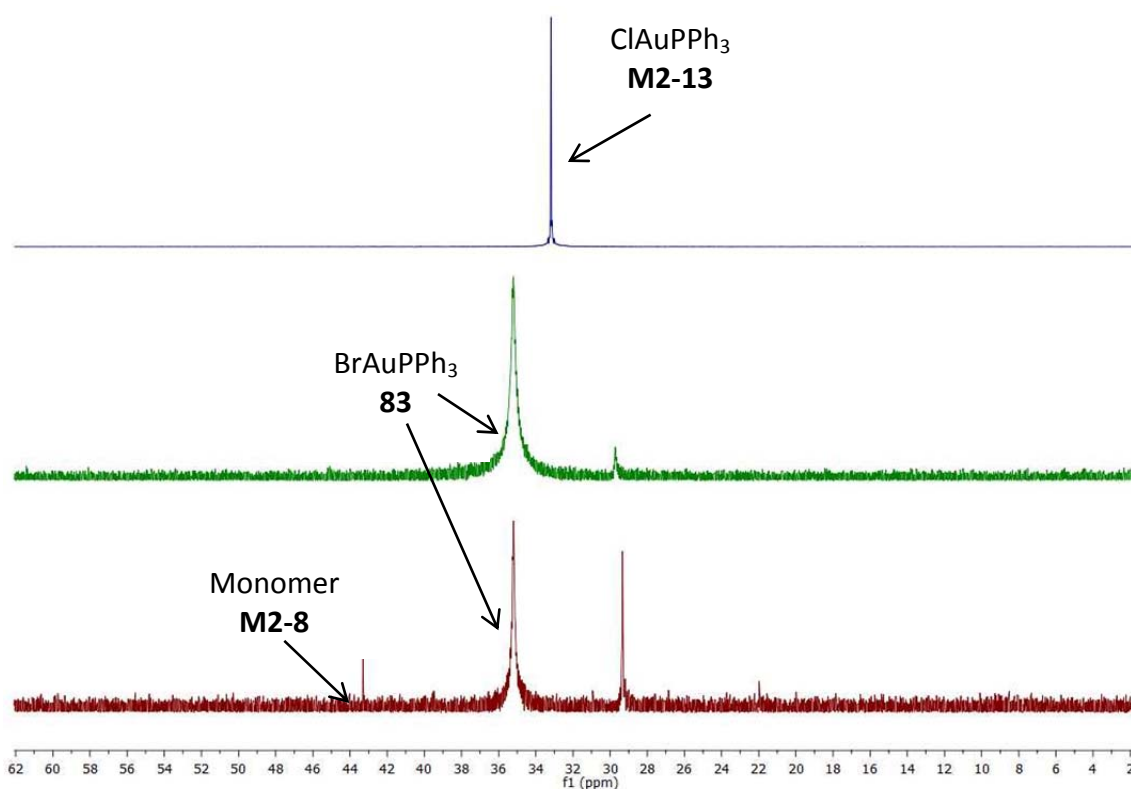


Figure 17. ^{31}P NMR of ClAuPPh_3 synthesized by ourselves (**M2-13**, blue), the commercially available BrAuPPh_3 (**83**, green) and the isolated gold species that was formed during the polymerization reaction (red).

The ^{31}P NMR shows that there are at least 3 species present: Traces of remaining monomer (**M2-8**, 43.3 ppm), BrAuPPh_3 (**83**, 35.2 ppm), which we expected to find and which is the main product. Another undefined species was found at 29.3 ppm (red spectrum). In green the ^{31}P NMR reference spectrum of BrAuPPh_3 (**83**) is shown bought from Alfa Aesar. In blue the ^{31}P NMR spectrum of ClAuPPh_3 synthesized by ourselves (**M2-13**) is shown. This result is the foundation for further experiments, where the gold species can either be attempted to be recycled: One possibility might be the immobilization of the gold with its ligands on a surface (compare Chapter 1).

3.4 Minireview on (Triphenylphosphine)gold(I) Chloride

“(Triphenylphosphine)gold(I) Chloride”

A. C. J. Heinrich, *Synlett* **2015**, 26,1135-1136.

Reprinted with permission from Georg Thieme Verlag. © Georg Thieme Verlag · New York.

DOI: 10.1055/s-0034-1380551.

Abstract: For the synthesis of all gold containing aromatic systems that I synthesized during my Ph. D. time, ClAuPPh₃ was used as precursor. The phenyl ligands make the organic compounds stable to air und therefore isolation is possible. It is a substantial advantage for all further reactions, especially the polymerization reactions, where the correct ratio between catalyst and monomer is of high importance. Triphenylphosphinegold(I) chloride (**35**) as reagent can be used for many different types of reaction and can be easily synthesized from elemental gold (**33**). In order to illustrate the many uses of this versatile reagent a “Spotlight” was written for a publication in the journal *Synlett*.



TOC Graphic. The “Spotlight” article presents an overview using ClAuPPh₃ in chemical reactions.

Scientific contribution to this paper

I wrote this article, the abstracts and schemes by myself.

(Triphenylphosphine)gold(I) Chloride

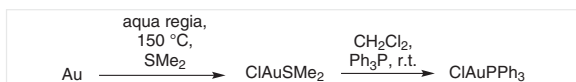
Annika C. J. Heinrich

Otto-Diels Institute for Organic Chemistry, University of Kiel, Otto-Hahn-Platz 4, 24098 Kiel, Germany
aheinrich@oc.uni-kiel.de

Published online: 01.04.2015

DOI: 10.1055/s-0034-1380551; Art ID: st-2015-v0520-v

(Triphenylphosphine)gold(I) chloride, ClAuPPh_3 , is a well characterized colorless complex¹ with a melting point of 236–240 °C² and it is soluble in most common organic solvents. Although it is commercially available, it is cheaper to prepare it directly from elemental gold in an easy, high-yielding two-step synthesis. In the first step, gold is dissolved in boiling *aqua regia* to form the gold(III) intermediate AuCl_4 in solution. By adding dimethyl sulfide, the complex ClAuSMe_2 precipitates as a white solid in an excellent yield of 93%.³



Scheme 1 Preparation of (triphenylphosphine)gold(I) chloride

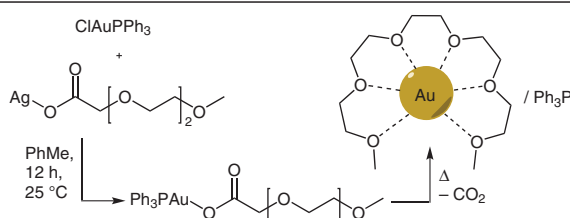
Annika Heinrich studied chemistry at the University of Kiel and there she obtained her diploma degree in 2011. At the moment, she is working as a Ph.D. student in the group of Professor Dr. Anne Staubitz at the Institute of Organic Chemistry in Kiel. Her research focuses on highly selective cross-coupling reactions and on the synthesis of semiconducting polymers. (Triphenylphosphine)gold(I) chloride is a frequently used reagent in her research: It is used for the synthesis of aromatic organogold compounds that can be used in cross-coupling reactions and polymerization reactions.



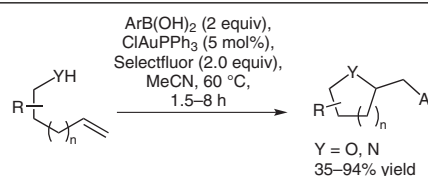
This precursor complex is dissolved in dichloromethane together with triphenylphosphine to form immediately the desired complex in a very good yield of 92% after precipitation by adding methanol.⁴ ClAuPPh_3 is a useful reagent in various types of reactions. It is often used in gold catalysis where it can act as co-catalyst or catalyst itself, or it can be used for the formation of more complex catalytic systems.⁵ ClAuPPh_3 can also be used for the synthesis of organogold compounds,⁶ which can perform cross-coupling reactions in a generally mild manner and with high tolerance towards functional groups. Herein, some applications of ClAuPPh_3 as reactant will be presented.

Table 1 Use of (Triphenylphosphine)gold(I) Chloride

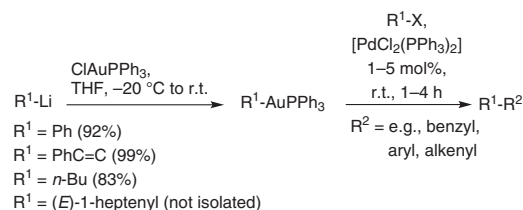
(A) ClAuPPh_3 can be used for the generation of gold nanoparticles. In the first step, gold chloride reacts with an ethylene glycol silver carboxylate in a transmetalation reaction. The resulting gold(I) complex generates the gold nanoparticle by thermal induction. The resulting nanoparticles do not need any further stabilizing or reducing reagents and have size diameters of 3–6 nm with narrow size distribution.⁷



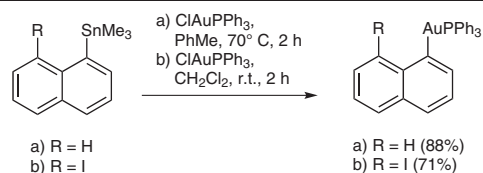
(B) Zhang et al. used ClAuPPh_3 as catalytic species for the formation of various saturated substituted O- and N-heterocycles. The homogeneous oxidative functionalization of terminal alkenes leads to a cyclization reaction that proceeds within short reaction times and under mild reaction conditions. In mechanistic studies they found that a conversion of $\text{C}(\text{sp}^3)\text{-Au}$ bonds into $\text{C}(\text{sp}^3)\text{-C}(\text{sp}^2)$ bonds is catalyzed by an $\text{Au}(\text{I})/\text{Au}(\text{III})$ system in a cross-coupling manner when using boronic acids as nucleophiles with Selectfluor as oxidant.⁸



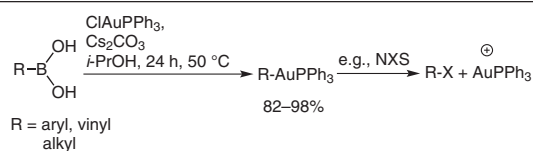
(C) Pérez-Sestelo and co-workers prepared different aryl-, alkynyl-, and alkylgold(I) compounds in very high yields using the corresponding lithiated organic species and ClAuPPh_3 as reagent. The organogold(I) compounds are used as nucleophiles in palladium-catalyzed cross-coupling reactions with various electrophiles under mild reaction conditions and in short reaction times.⁹



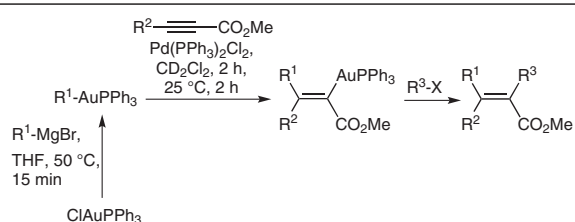
(D) Meyer et al. showed that trimethyltin-substituted naphthalene derivatives perform transmetalation reactions under very mild conditions using ClAuPPh₃ as reagent. One example showed the synthesis of a compound containing both a gold(I) moiety and an iodide function on the same molecule, which cannot be prepared using organolithium or Grignard reagents in this case.¹⁰



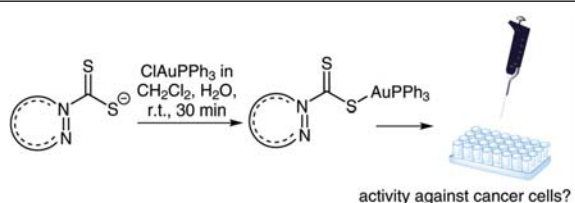
(E) Rominger et al. used boronic acid derivatives as precursors for the synthesis of organogold(I) phosphane complexes. They are prepared in good yields of 82–98% using ClAuPPh₃ as reagent. This method allows a higher tolerance towards functional groups than using lithiated species as reactants. As vinyl-, aryl- and heteroaryl-gold compounds are assumed to be intermediates in homogeneous gold catalysis, Rominger et al. used the prepared compounds to obtain more information about the mechanism of a catalytic cycle with gold.¹¹



(F) Blum and co-workers prepared vinyl and aryl organogold(I) compounds by treating the corresponding vinyl- or arylmagnesium bromides with ClAuPPh₃. These simple compounds were used for continuing steps of reactions: First they performed a regio- and diastereoselective palladium-catalyzed *syn*-carboauration of alkynes. In a further step, di- and trisubstituted olefins were synthesized by either performing palladium-catalyzed cross-coupling reactions or electrophilic trapping reactions. These reactions demonstrate the potential of the combination of gold and palladium in organic synthesis.¹²



(G) Keter et al. synthesized phosphinogold(I) dithiocarbamate complexes by using ClAuPPh₃ and similar gold(I) precursors and different potassium salts of the corresponding dithiocarbamates under mild conditions and in short reaction times. The resulting complexes were tested for their activity against human cervical epithelioid carcinoma (HeLa) cells, a type of cancer. The P-Au-S moiety seemed to play an important role for the activity.¹³



Acknowledgment

A. C. J. Heinrich sincerely thanks the Deutsche Bundesstiftung Umwelt (DBU) for a Ph.D. scholarship.

References

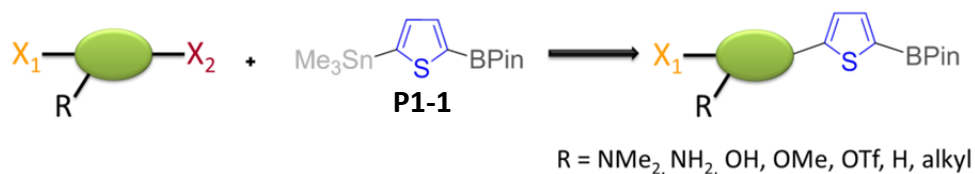
- Borissova, A. O.; Korlyukov, A. A.; Antipin, M. Y.; Lyssenko, K. A. *J. Phys. Chem. A* **2008**, *112*, 11519.
- Kouroulis, K. N.; Hadjikakou, S. K.; Kourkoumelis, N.; Kubicki, M.; Male, L.; Hursthouse, M.; Skoulika, S.; Metsios, A. K.; Tyurin, V. Y.; Dolganov, A. V.; Milaeva, E. R.; Hadjiliadis, N. *Dalton Trans.* **2009**, 10446.
- Brandys, M.-C.; Jennings, M. C.; Puddephatt, R. J. *Dalton Trans.* **2000**, 4601.
- Mézailles, N.; Ricard, L.; Gagosz, F. *Org. Lett.* **2005**, *7*, 4133.
- See for example: (a) Hashmi, A. S. K. *Chem. Rev.* **2007**, *107*, 3180. (b) Gorin, D. J.; Sherry, B. D.; Toste, F. D. *Chem. Rev.* **2008**, *108*, 3351. (c) Li, Z.; Brouwer, C.; He, C. *Chem. Rev.* **2008**, *108*, 3239.
- See for example: Liu, L.-P.; Hammond, G. B. *Chem. Soc. Rev.* **2012**, *41*, 3129.
- Tuchscherer, A.; Schaarschmidt, D.; Schulze, S.; Hietschold, M.; Lang, H. *Inorg. Chem. Commun.* **2011**, *14*, 676.
- Zhang, G.; Cui, L.; Wang, Y.; Zhang, L. *J. Am. Chem. Soc.* **2010**, *132*, 1474.
- Peña-López, M.; Ayán-Varela, M.; Sarandeses, L. A.; Pérez-Sestelo, J. *Chem. Eur. J.* **2010**, *16*, 9905.
- Meyer, N.; Sivanathan, S.; Mohr, F. J. *Organomet. Chem.* **2011**, *696*, 1244.
- Rominger, F.; Ramamurthi, T. D.; Hashmi, A. S. K. *J. Organomet. Chem.* **2009**, *694*, 592.
- Shi, Y.; Ramgren, S. D.; Blum, S. A. *Organometallics* **2009**, *28*, 1275.
- Keter, F. K.; Guzei, I. A.; Nell, M.; van Zyl, W. E.; Darkwa, J. *Inorg. Chem.* **2014**, *53*, 2058.

4 Summary and Outlook

The aim of this thesis was to find new synthetic strategies for the semiconducting polymers. One focus was on the synthesis of new aromatic dinucleophiles. With these compounds new monomers for polymerization reactions became available, containing both a halogen and a metal functional group. Another important aspect was the introduction of organogold compounds into the research field of polymer synthesis.

Nucleophile and Electrophile Selective Cross-Coupling Reactions

The process of a living polymerization leads to well-defined polymers: High molecular weights and low polydispersities can be reached simultaneously. The lack of adequate monomers that perform this kind of polymerization limits its increasing use in the synthesis of semiconducting polymers. It was one task of this work to develop a method for the synthesis of new type monomers that combine different (hetero)cycles and contain besides this both a halogen and a metal functional group. A tin- and boron functionalized thiophene derivative as dinucleophile **P1-1** was used in order to perform a *both* nucleophile and electrophile selective cross-coupling reaction following a general procedure which gave the products completely selective in high yields after an extensive optimization.



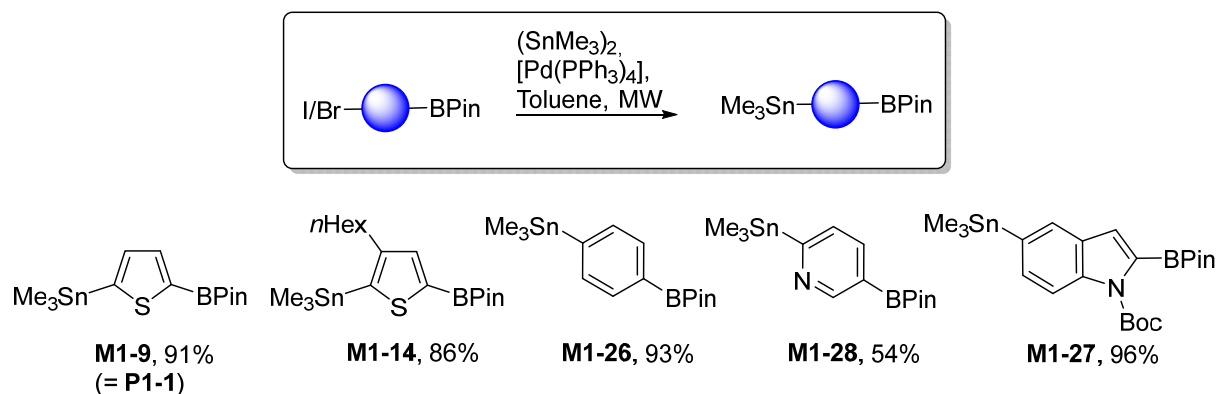
Scheme 17. It took more than 80 optimization reactions to find reaction conditions that proceed completely selective in high yields with 13 different electrophiles.

By using microwave conditions, 11 examples of electron poor, neutral and electron rich aromatic dielectrophiles and even 2 trielectrophiles could be used successfully to give the products in overall very good yields (Scheme 17). One of these products was successfully used as monomer in a polymerization reaction. Although the obtained polymer **P1-34** was insoluble, which made a further characterization and investigation of the polymer kinetic impossible, a branched alkyl chain on the dielectrophilic component might lead to an improved solubility. Another approach which will lead to an increase of the solubility of a resulting polymer, would include dinucleophiles that contain a solubilizing substituent like an alkyl or alkoxy chain.

Aromatic Tin-Boron Functionalized Dinucleophiles

In order to use the products of the successful selective cross-coupling reactions as monomers for polymerization reactions it was the task to synthesize further aromatic dinucleophilic compounds. The use of these compounds in a dually-selective cross-coupling reaction would lead to a whole library of new monomers, where different aromatic systems can be combined with each other in an easy way and with this they would give an access to new semiconducting polymers.

By developing a general method that uses aromatic systems containing both a halogen and a boron group as starting material, it was possible to synthesize four further dinucleophilic compounds in overall very good yields (Scheme 18) containing both a tin- and a boron functional group (**M1-14**, **M1-26**, **M1-27**, **M1-28**).



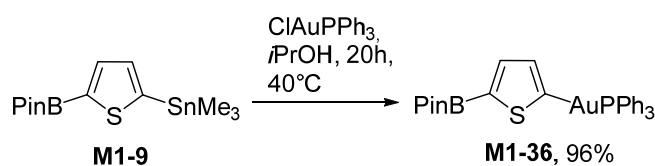
Scheme 18. Different dinucleophiles were available by using a general method, starting from the both halogenated and boronated corresponding species.

With these dinucleophiles dually-selective cross-coupling reactions were performed using the optimized reaction conditions of the unsubstituted thiophene derivative **P1-1**.^[50m] Surprisingly all attempts showed low conversions and non-selective coupling reactions. Even the attempt to use them in a just nucleophile selective coupling reaction proved to be difficult.^[54] As all aromatic systems are electronically and sterically different from each other, new reaction conditions for selective reactions have to be developed again for each compound. By screening different catalyst species, solvents, temperatures and reaction times it will be possible to find suitable conditions for each dinucleophile. The synthesis of further aromatic dinucleophiles like furans or benzothiadiazoles and others will be simple to perform as well as the alkylated derivatives. The resulting cross-coupling products of these dinucleophiles will contain both a halogen-functional group and a boron moiety. Especially

the products of the alkylated dinucleophiles will give new, soluble polymers in a polymerization reaction, which allow the combination of different aromatic systems in the polymer backbone in a simple way. Their analysis and characterization will be as important as kinetic studies on the polymerization process as well. If they show promising electronic properties, they will be incorporated into test devices. S. Urrego-Riveros is continuing the research on this topic at the moment.

Gold Containing Dinucleophiles

As Stille and Suzuki coupling reactions are well investigated, the combination of these two metals in a dinucleophile was advisable to perform a dually-selective cross-coupling reaction, for which there was no precedent in the literature. A combination of other metal functionalities and their use in nucleophile cross-coupling reactions has not been shown until now. Regarding the fact that organotin compounds are very toxic, it has always been planned to replace the toxic tin moiety by other metals. Besides a lower toxicity, this metal functionality had to be stable under air conditions which would make an isolation of the compound possible. Gold was found to be a suitable alternative in combination with boron, especially because it seemed to be possible to distinguish between gold and boron in a cross-coupling reaction. By performing a selective metal-exchange reaction it was possible to synthesize the thiophene derivative **M1-36** as first compound that contains both gold and a boron moiety starting from the dinucleophile **M1-9** (Scheme 19).

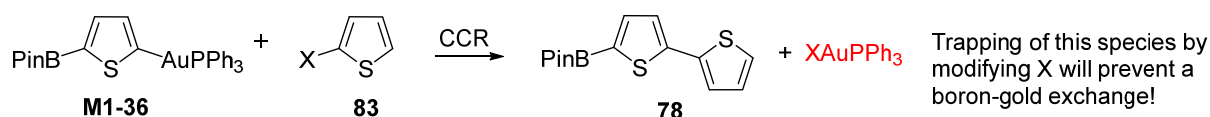


Scheme 19. Synthesis of the first both gold and boron difunctionalized dinucleophile.

To transfer these reaction conditions to the phenyl-, hexylthiophene- or indole derivatives (**M1-17**, **M1-26**, **M1-27**) remains a task for the future. The solubility of the reactants seems to have a high impact on this type of metal-transfer reaction. With this knowledge it could be possible to optimize these reaction conditions for other dinucleophilic compounds by replacing the solvent to a more polar system like methanol, varying the temperature and reaction time.

As the present synthesis of dinucleophile **M1-36** still relies on a toxic stannyl group, work is ongoing on routes that will avoid this functional group: With a better understanding of the reactivities of the reagents required to prepare dinucleophiles of type **M1-36**, one can be confident that this functionality can be avoided in the future. One approach might be to consider other metal-gold exchange reactions. Therefore a preferred exchange order of different metals has to be investigated, including metals like silicon and copper as well as metals that are introduced *in situ* like magnesium and zinc.

The use of this new dinucleophile **M1-36** in a nucleophile selective cross-coupling reaction led to a nearly full conversion of the electrophile. An isolation of the coupling product however has not been possible to date, as it seems that undesired (coupling) reactions occurred after the desired reaction.



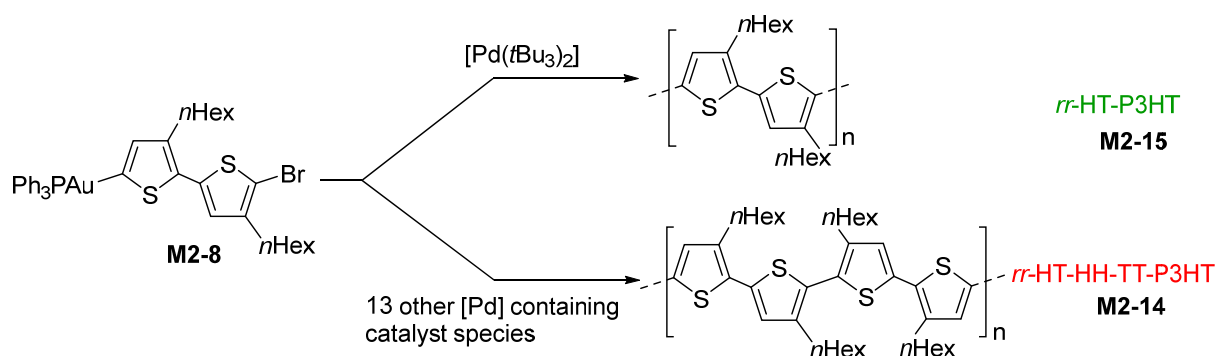
Scheme 20. A boron-gold exchange must be avoided. Modifying the electrophile might lead to success by the modification of the functional group X in **85**.

A particularly valuable insight is that the gold species that results from the catalytic cycle, BrAuPPh_3 may perform another metal exchange reaction with the boronic ester. This in turn was likely to be the cause of an undefined mixture of coupling products. This type of reaction shows a large potential for further developments: Optimization reactions have to be performed as well as mechanistic studies need to be made by isolation of intermediates. It is speculated that trapping the gold moiety might lead to a success in this case (Scheme 20). In general the reaction of gold with other metals seems to be a factor that requires further investigation studies.

Gold-Functionalized Thiophene-Type Monomers in Polymerization Reactions

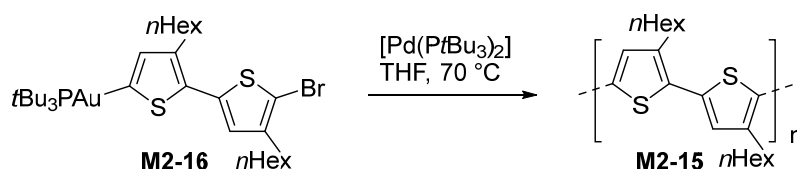
As it has never been shown before, it was planned to synthesize air stable aromatic organogold compounds containing besides a halogen functional group a gold moiety. With this the best conditions for a polymerization reaction were created that could follow the kinetics of a living polymerization type reaction. It was possible to synthesize such a monomer **M2-8** bearing two thiophene units that could be used with success in polymerization reactions. In a catalyst screening for the polymerization reaction two different polymers were found: Most catalysts gave regio regular HH-TT P3HT (Scheme 21,

M2-14) as product, only when $[\text{Pd}(\text{PtBu}_3)_2]$ was used as catalyst species the expected regio regular HT-P3HT was synthesized (Scheme 21, **M2-15**). Kinetic studies were performed and led to a number of unusual, unexpected discoveries: The polymerization to give **M2-14** appeared to be a step growth process; with $[\text{Pd}(\text{PtBu}_3)_2]$ it was chain growth. In the former cases the product seems to arise from homocoupling reactions that take place exclusively, whereas in the latter case the expected cross-coupling was observed.



Scheme 21. One monomer leads to two different, but well-defined regio-regular polymers by changing the catalyst.

The most interesting result was that the $[\text{Pd}(\text{PtBu}_3)_2]$ catalyst performs a ligand exchange reaction with the phenyl ligands of the gold monomer. It seems as if the reactive species that leads to the regio regular HT-P3HT, is formed *in situ*; nevertheless the reaction appears to be chain growth. To clarify the reason for this behavior and further improve the control of the reaction (by forcing a faster initiation event) the next step will be to synthesize and isolate the gold monomer **M2-16**, which appears to be formed immediately with the catalyst species. The synthesis of **M2-16** will proceed similar to the synthesis of the monomer **M2-8**, entirely with ClAuPtBu_3 as reactant instead of ClAuPPh_3 . The resulting monomer **M2-16** has to be used in a polymerization reaction in order to continue and complete the kinetic studies for this project (Scheme 22).



Scheme 22. The improved monomer **M2-16** with *tert*-butylphenyl ligands on the gold atom has to be synthesized and used in polymerization reactions in order to complete the kinetic studies for this project.

The described syntheses and methods are the basis of new semiconducting polymers and offer alternative routes for present syntheses. The monomers can be easily synthesized of two different aromatic systems and include a metal that allows isolation. It is a long term goal to transfer these methods to new and promising monomers. The resulting polymers will have to be tested on their properties in optoelectronic devices.

5 Experimental Section

5.1 Supporting Information on Chapter 3.1.

5.1.1 Supporting Information for *Org. Lett.* 2013, 15, 4666-4669.

Dual Selectivity: Electrophile *and* Nucleophile Selective Cross-Coupling Reactions on a Single Aromatic Substrate

Annika C. J. Heinrich, Birk Thiedemann, Paul J. Gates and Anne Staubitz*

*Otto Diels-Institut für Organische Chemie, Universität Kiel, Otto-Hahn-Platz 4, 24118 Kiel
(Germany)*

* astaubitz@oc.uni-kiel.de

Supporting Information

Abbreviations	S1
General Methods and Materials	S2
GC Optimization Reactions	S4
Syntheses	S15
NMR spectra	S34

Abbreviations

A	area
anhyd.	anhydrous
Ar	aryl
ATR	attenuated total reflectance
calcd.	calculated
CI	chemical ionization
COSY	correlated spectroscopy
d	doublet (NMR)
DEPT	distortionless enhancement by polarization transfer
DMF	<i>N,N</i> -dimethylformamide
dppe	1,2-bis(diphenylphosphino)ethane
dppf	1,1'-bis(diphenylphosphino)ferrocene
EA	elemental analysis
EI	electron ionization
Fur	furan
GC	gas chromatography
GC-MS	gas chromatography-mass spectrometry
HMBC	heteronuclear multiple bond coherence
HSQC	heteronuclear single quantum coherence
IR	infrared
LOQ	limit of quantification
m	medium (concerning the intensity) (IR)
m	multiplet (NMR)
MDL	method detection limit
M.p.	melting point
MS	mass spectrometry
MW	microwave
n	amount of substance
Naph	naphthalene
Pin	pinacol
Pyr	pyridine
RF	response factor
s	strong (concerning the intensity) (IR)
s	singlet (NMR)
SPhos	2-dicyclohexylphosphino-2',6'-dimethoxybiphenyl
t	triplet (NMR)
THF	tetrahydrofuran
TMEDA	<i>N,N,N',N'</i> -tetramethylethylenediamine
Tph	thiophene
w	weak (concerning the intensity) (IR)

General Methods and Materials

All syntheses were carried out using standard Schlenk techniques or in a glovebox under a dry and inert nitrogen atmosphere. Glassware and NMR-tubes were dried in an oven at 200 °C for at least 2 h prior to use. Reaction vessels were heated under vacuum and purged with nitrogen three times before adding reagents.

Analyses

¹H NMR, ¹³C NMR, ¹¹B NMR and ¹¹⁹Sn NMR spectra were recorded at 300 K.

¹H NMR spectra were recorded on a Bruker AC 200 (200 MHz) spectrometer, a Bruker ARX 300 (300 MHz) spectrometer or a Bruker DRX 500 (500 MHz) spectrometer. ¹³C NMR spectra were recorded on a Bruker AC 200 (50 MHz) spectrometer, a Bruker ARX 300 (75 MHz) spectrometer or a Bruker DRX 500 (125 MHz) spectrometer. ¹¹B NMR and ¹¹⁹Sn NMR spectra were recorded on a Bruker DRX 500 (160 MHz and 187 MHz) spectrometer.

¹H NMR and ¹³C NMR spectra were referenced against the solvent peak. ¹¹B NMR spectra were referenced against BF₃·OEt₂ in CDCl₃, the reference of the ¹¹⁹Sn NMR spectra was calculated based on the ¹H NMR signal of tetramethyl silane (TMS).

The exact assignment of the peaks was proved by ¹H, ¹³C DEPT and two-dimensional NMR spectroscopy such as ¹H COSY, ¹³C HSQC or ¹H/¹³C HMBC when possible.

All melting points were recorded on a LG1586 Electrothermal® IA6304 capillary melting point Apparatus and are uncorrected.

IR spectra were recorded on a Perkin Elmer Paragon 1000 FT-IR spectrometer with a A531-G Golden-Gate-ATR-unit.

EI/CI mass spectra were recorded on a Finnigan MAT 8200 or a Finnigan MAT 8230 apparatus.

Ultra High resolution ESI mass spectra were recorded on a Bruker Daltonics Apex IV Fourier transform Ion Cyclotron resonance mass spectrometer. The high resolution EI mass spectra was run on a VG Analytical Autospec apparatus.

The MALDI-ToF-ToF mass spectra were recorded on a Applied Biosystems 4700 Proteomics analyser spectrometer and a dithranol matrix in methanol. The polymer was dissolved in THF.

GC-MS analysis was performed on a Hewlett Packard 5890A gas chromatograph, equipped with a Hewlett Packard 5972A mass selective detector and an Agilent Technologies dimethylpolysiloxane column (19091S-931E, nominal length 15 m, 0.25 mm diameter, 0.25 μm grain size).

GC analysis was performed on an Agilent Technologies 6890N gas chromatograph, equipped with an Agilent Technologies 7683 Series Injector, an Agilent Technologies (5 %-phenyl)-methylpolysiloxane column (19091J-413, nominal length 30 m, 0.32 mm diameter, 0.25 μm grain size) and a flame ionization detector (FID).

All microwave irradiation reactions were carried out on a Biotage® Initiator+ SP Wave synthesis system, with continuous irradiation power from 0 to 300 W. All reactions were carried out in 5 mL oven-dried Biotage microwave vials sealed with an aluminum/Teflon® crimp top, which can be exposed to a maximum of 250 °C and 20 bar internal pressure. The reaction temperature was measured by an IR sensor on the outer surface of the process vial.

Chemicals

All reagents were used without further purification unless otherwise noted.

Compound	Supplier	Purity	Comment
1,3,5-Triisopropylbenzene	Alfa Aesar Inc.	96 %	distilled
1-Bromobenzene	ABCR	99.5 %	
1-Bromohexane	Sigma Aldrich Inc.	98 %	
1-Bromo-2-iodobenzene	ABCR Inc.	99 %	
1-Bromo-4-iodobenzene	ABCR Inc.	98 %	
1-Iodobenzene	Acros Inc.	98 %	
1-Iodophenol	Alfa Aesar Inc.	99 %	
2-Bromo-3-hydroxypyridine	Alfa Aesar Inc.	99 %	
2-Bromopyridine	VWR Inc.	99 %	
2-Bromothiophene	Sigma Aldrich Inc.	98 %	
2-Iodo-4-bromoaniline	Acros Inc.	98 %	
2-Iodopyridine	Acros Inc.	98 %	
2-Iodothiophene	Acros Inc.	98 %	
5-Bromo-2-iodopyridine	Alfa Aesar Inc.	97 %	
Acetic acid	Merck Inc.	99.8 %	anhydrous
Ammonium chloride	Grüssing Inc.	99.5 %	
Bromine	Acros Inc.	99.99 %	

Hydrobromic acid		Fischer Chemicals Inc.	48 %	
Hydrochloric acid		Grüssing	37 %	
Iodine		Grüssing	99.5 %	resublimed
Iodomethane		Alfa Aesar Inc.	99 %	distilled
K ₂ CO ₃		Fluca Inc.	99.99 %	
Magnesium		Merck Inc.	99.5 %	
Magnesium sulfate		Grüssing Inc.	99 %	
Mesitylene		Merck Inc.	98 %	
Methylithium		Acros Inc.	1.6 M in diethyl ether	
Molecular sieve, 3 Å		Alfa Aesar Inc.		
[Ni(dppp)Cl ₂]		ABCR Inc.	99 %	
<i>N</i> -Iodosuccinimide		Molekula	95 %	
<i>n</i> -Butyllithium		Acros Inc.	2.5 M in hexanes	
[Pd(OAc) ₂]		Strem Chemicals Inc.	>98 %	
[Pd(PPh ₃) ₄]		ABCR Inc.	99 %	
pinacol		ABCR Inc.	99 %	
<i>p</i> -Toluenesulfonic acid monohydrate	acid	Acros Inc.	98.5 %	
Sodium		Merck Inc.	≥ 99 %	
Sodium chloride		Grüssing Inc.	99.5 %	
Sodium sulfate		Grüssing Inc.	99 %	
SPhos		Strem Chemicals Inc.	>98 %	
Thiophene		VWR Inc.	99 %	distilled
TMEDA		Acros Inc.	99.5 %	
Trifluoromethanesulfonic anhyd.	acid	Sigma Aldrich Inc.	>99 %	
Triisopropyl borate		Strem Chemicals Inc.	>98 %	
Trimethyltin chloride		Acros Inc.	99 %	
Zinc		Merck Inc.	99.99 %	

Solvents

All solvents were used freshly distilled after refluxing for several hours over the specified drying agent under nitrogen and were stored in a J. Young's-tube. If no drying agent is noted, the solvents were only distilled for purification purposes.

Diethyl ether	-
Dioxane	Sodium with benzophenone as an indicator; stored over 3 Å molecular sieve
DMF	CaH ₂ ; stored over 3 Å molecular sieve
Ethyl acetate	-
<i>n</i> -Hexane	Sodium with benzophenone as an indicator; stored over 3 Å molecular sieve
Methanol	HPLC grade, used as received.
Pentane	-
Pyridine	Distilled from NaH, then dried and stored over 3 Å molecular sieve
THF	Sodium with benzophenone as an indicator; stored over 3 Å molecular sieve
Toluene	Sodium with benzophenone as an indicator; degassed by freeze-pump-thaw technique, stored over 3 Å molecular sieve

Chromatography

For the chromatographic purification, silica gel (Macherey-Nagel Inc., grain size 0.040 - 0.063 mm) was used. Thin layer chromatography was performed using pre-coated plates from Macherey-Nagel Inc., ALUGRAM[®] Xtra SIL G/UV254. Most chromatography purifications were carried out using an Interchim Puriflash 430 system, where cadriges of Interchim (silica HC, grain size 50 µm, 120 g or 80 g) were used.

GC Optimization Reactions

The yields for the optimization reactions were determined by GC by a multiple point internal standard method, using 1,3,5-triisopropylbenzene as a standard. The following equation was used for the calculation of the yields:

$$n(\text{analyte}) = \frac{A(\text{analyte})}{A(\text{standard})} \times \frac{n(\text{standard})}{RF}$$

where n is the amount of substance, A the integrated area and RF a system specific response factor.

For the calibration curve, known amounts of the analyte and 1,3,5-triisopropylbenzene were used. The response factor RF was obtained from the slope of the resulting calibration curve (Figures SI 1 and SI2).

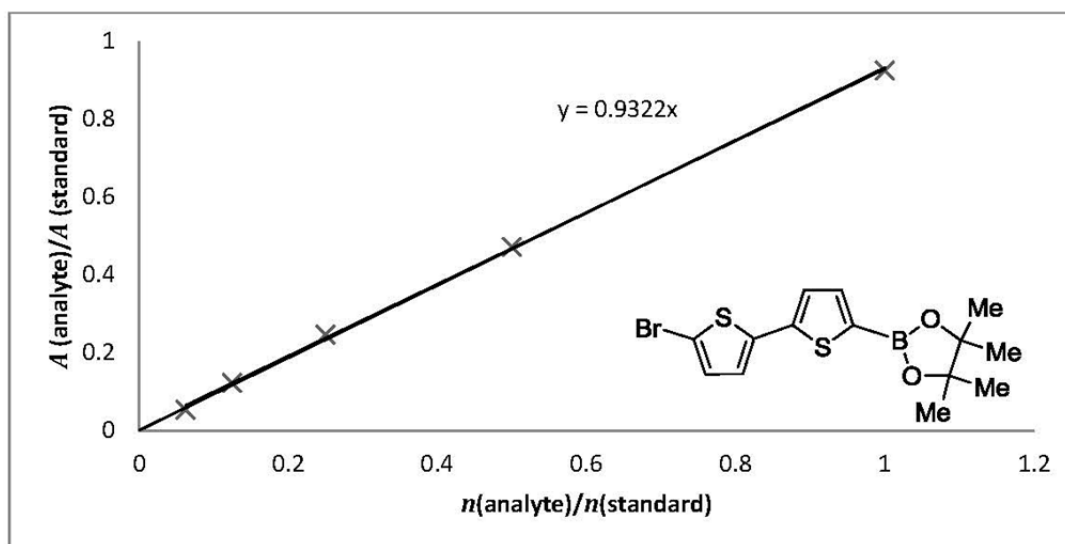


Figure SI 1. Calibration curve for 2-(5'-bromo[2,2'-bithiophen]-5-yl)-4,4,5,5-tetramethyl-1,3,2-dioxaborolane (**5a**), using 1,3,5-triisopropylbenzene as an internal standard.

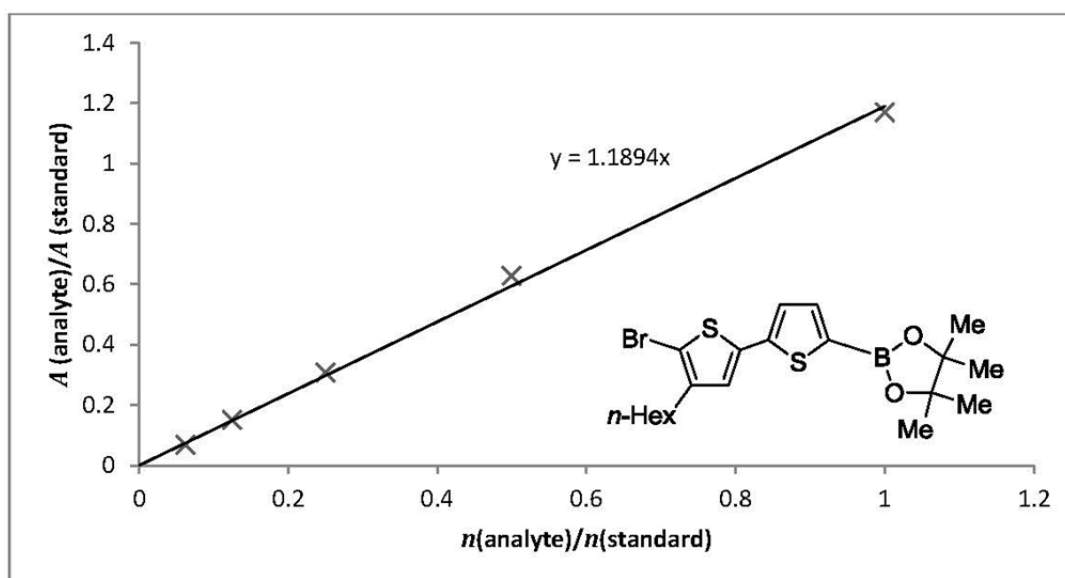


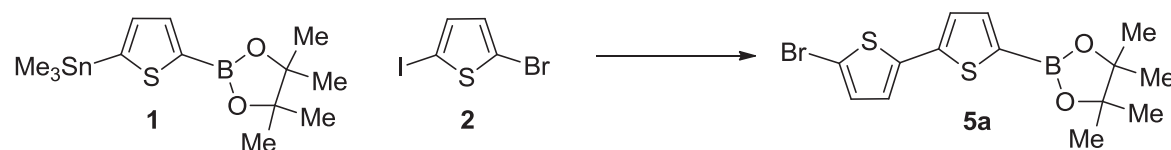
Figure SI 2. Calibration curve for 2-(4'-n-hexyl-5'-bromo[2,2'-bithiophen]-5-yl)-4,4,5,5-tetramethyl-1,3,2-dioxaborolane (**5b**), using 1,3,5-triisopropylbenzene as an internal standard.

*General Procedure 1.**Optimization reactions under thermal conditions:*

A solution of 4,4,5,5-tetramethyl-2-(5-(trimethylstannyl)thiophen-2-yl)-1,3,2-dioxaborolane (**1**) (186 mg, 0.50 mmol), the electrophile **2** or **3** (0.50 mmol), the catalyst (1-10 mol% and the internal standard 1,3,5-triisopropylbenzene (100 μ L, 86.0 mg, 0.43 mmol) were dissolved in the solvent and heated to the required temperature for the specified time. After certain time intervals, a sample (0.1 mL) was taken from each reaction vessel, filtered through a short plug of silica (5 x 3 mm; eluent: ethyl acetate) using a syringe filter, and was then used for GC analysis.

For all reaction conditions, the parameters were varied as specified in Table SI 1.

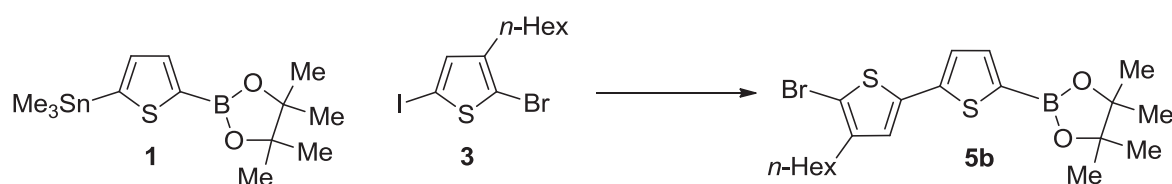
Table SI 1. Optimization reactions for the synthesis of 2-(5'-bromo[2,2'-bithiophen]-5-yl)-4,4,5,5-tetramethyl-1,3,2-dioxaborolane **5a**.



Entry	Solvent	Catalyst	Loading	T [°C]	t [h]	Yield [%]
1	Dioxane	[Pd(PPh ₃) ₄]	5 mol%	110	0.75	13
2	Dioxane	[Pd(PPh ₃) ₄]	5 mol%	110	1.33	23
3	Dioxane	[Pd(PPh ₃) ₄]	5 mol%	110	3	41
4	Dioxane	[Pd(PPh ₃) ₄]	5 mol%	110	6	53
5	Dioxane	[Pd(PPh ₃) ₄]	5 mol%	110	9	45
6	Dioxane	[Pd(PPh ₃) ₄]	5 mol%	55	6	0
7	Dioxane	[Pd(PPh ₃) ₄]	5 mol%	55	9	1
8	Dioxane	[Pd(PPh ₃) ₄]	5 mol%	55	12	2
9	Dioxane	[Pd(PPh ₃) ₄]	5 mol%	55	15	1
10	Dioxane	[Pd(OAc) ₂]/SPhos	1 mol%	110	0.75	8
11	Dioxane	[Pd(OAc) ₂]/SPhos	[Pd(OAc) ₂] 2 mol% SPhos 1 mol%	110	1.33	7
12	Dioxane	[Pd(OAc) ₂]/SPhos	[Pd(OAc) ₂] 2 mol% SPhos 1 mol%	110	3	8
13	Dioxane	[Pd(OAc) ₂]/SPhos	[Pd(OAc) ₂] 2 mol% SPhos 1 mol%	110	6	8
14	Dioxane	[Pd(OAc) ₂]/SPhos	[Pd(OAc) ₂] 2 mol% SPhos 1 mol%	110	9	6
15	Toluene	[[Pd(OAc) ₂]/SPhos	[Pd(OAc) ₂] 2 mol% SPhos 1 mol%	110	0.75	7
16	Toluene	[Pd(OAc) ₂]/SPhos	[Pd(OAc) ₂] 2 mol% SPhos 1 mol%	110	1.33	8
17	Toluene	[Pd(OAc) ₂]/SPhos	[Pd(OAc) ₂] 2 mol% SPhos 1 mol%	110	5	8
18	Toluene	[Pd(OAc) ₂]/SPhos	[Pd(OAc) ₂] 2 mol% SPhos 1 mol%	110	9	6
19	Toluene	[Pd(OAc) ₂]/SPhos	[Pd(OAc) ₂] 2 mol% SPhos 1 mol%	110	16	5
20	Toluene	[Pd(PPh ₃) ₄]	5 mol%	55	6	0

21	Toluene	[Pd(PPh ₃) ₄]	5 mol%	55	9	0
22	Toluene	[Pd(PPh ₃) ₄]	5 mol%	55	12	0
23	Toluene	[Pd(PPh ₃) ₄]	5 mol%	55	15	0
24	DMF	[Pd(PPh ₃) ₄]	5 mol%	55	6	50
25	DMF	[Pd(PPh ₃) ₄]	5 mol%	55	9	67
26	DMF	[Pd(PPh ₃) ₄]	5 mol%	55	12	87
27	DMF	[Pd(PPh ₃) ₄]	5 mol%	55	15	88
28	DMF	[Pd(PPh ₃) ₄]	5 mol%	55	18	95
29	DMF	[Pd(OAc) ₂]/SPhos	1 mol%	70	12	5
		[Pd(OAc) ₂]	2 mol%			
30	DMF	[Pd(OAc) ₂]/SPhos	1 mol%	70	15	5
		[Pd(OAc) ₂]	2 mol%			
31	DMF	[Pd(OAc) ₂]/SPhos	1 mol%	70	18	5
		[Pd(OAc) ₂]	2 mol%			
32	DMF	[Pd(OAc) ₂]/SPhos	1 mol%	70	21	5
		[Pd(OAc) ₂]	2 mol%			
33	DMF	[Pd(PPh ₃) ₄]	5 mol%	70	12	91
35	DMF	[Pd(PPh ₃) ₄]	5 mol%	70	15	96
36	DMF	[Pd(PPh ₃) ₄]	5 mol%	70	18	95
37	DMF	[Pd(PPh ₃) ₄]	5 mol%	70	21	95
38	Pyridine	[Pd(PPh ₃) ₄]	5 mol%	55	6	8
39	Pyridine	[Pd(PPh ₃) ₄]	5 mol%	55	9	17
40	Pyridine	[Pd(PPh ₃) ₄]	5 mol%	55	12	22
41	Pyridine	[Pd(PPh ₃) ₄]	5 mol%	55	15	25
42	Pyridine	[Pd(PPh ₃) ₄]	5 mol%	55	18	27
43	Pyridine	[Pd(PPh ₃) ₄]	5 mol%	70	18	52
44	Pyridine	[Pd(PPh ₃) ₄]	5 mol%	70	21	57
45	Pyridine	[Pd(PPh ₃) ₄]	5 mol%	70	12	60

Table SI 2a. Optimization reactions for the synthesis of 2-(3'-*n*-hexyl-5'-bromo[2,2'-bithiophen]-5-yl)-4,4,5,5-tetramethyl-1,3,2-dioxaborolane **5b** using reaction conditions described in General Procedure 1.



Entry	Solvent	Catalyst	Loading	<i>T</i> [°C]	<i>t</i> [h]	Yield [%]
1	DMF	[Pd(PPh ₃) ₄]	5 mol%	55	15	49
2	DMF	[Pd(PPh ₃) ₄]	5 mol%	55	18	60
3	DMF	[Pd(PPh ₃) ₄]	5 mol%	55	21	56
4	DMF	[Pd(PPh ₃) ₄]	5 mol%	55	24	64
5	DMF	[Pd(PPh ₃) ₄]	5 mol%	55	30	70
6	DMF	[Pd(PPh ₃) ₄]	5 mol%	55	39	74
7	DMF	[Pd(PPh ₃) ₄]	5 mol%	55	48	74
8	DMF	[Pd(PPh ₃) ₄]	2 mol%	55	15	64
9	DMF	[Pd(PPh ₃) ₄]	2 mol%	55	18	65
10	DMF	[Pd(PPh ₃) ₄]	2 mol%	55	21	70
11	DMF	[Pd(PPh ₃) ₄]	2 mol%	55	24	79
12	DMF	[Pd(PPh ₃) ₄]	2 mol%	55	30	80
13	DMF	[Pd(PPh ₃) ₄]	2 mol%	55	39	69
14	DMF	[Pd(PPh ₃) ₄]	2 mol%	55	48	68

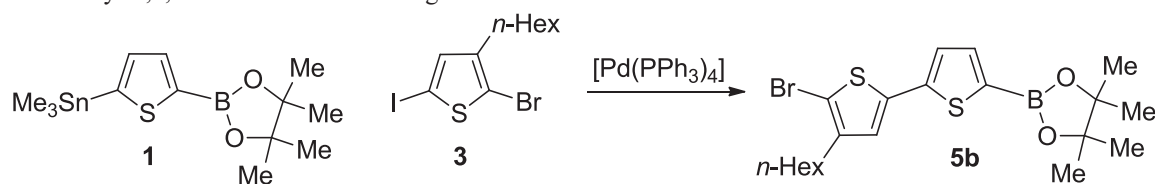
15	DMF	[Pd(PPh ₃) ₄]	10 mol%	55	15	45
16	DMF	[Pd(PPh ₃) ₄]	10 mol%	55	18	54
17	DMF	[Pd(PPh ₃) ₄]	10 mol%	55	21	63
18	DMF	[Pd(PPh ₃) ₄]	10 mol%	55	24	60
19	DMF	[Pd(PPh ₃) ₄]	10 mol%	55	30	77
20	DMF	[Pd(PPh ₃) ₄]	10 mol%	55	39	69
21	DMF	[Pd(PPh ₃) ₄]	10 mol%	55	48	67
22	DMF	[Pd(PPh ₃) ₄]	5 mol%	70	72	54
23	DMF	[Pd(PPh ₃) ₄]	5 mol%	70	15	67
24	DMF	[Pd(PPh ₃) ₄]	5 mol%	70	18	68

General Procedure 2.

Optimization reactions under microwave conditions:

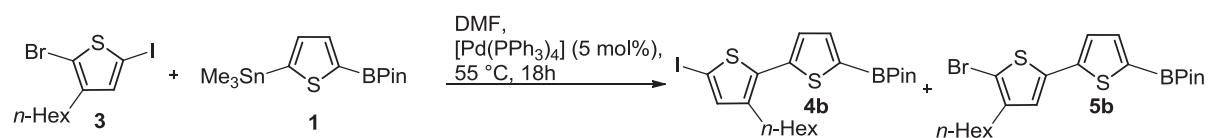
A solution of the electrophile **3** (372 mg, 1.00 mmol), 4,4,5,5-tetramethyl-2-(5-(trimethylstannyl)thiophen-2-yl)-1,3,2-dioxaborolane (**1**) (448 mg, 1.2 mmol), [Pd(PPh₃)₄] (20 mg, 2 mol%) and the internal standard 1,3,5-triisopropylbenzene (100 μ L, 86 mg, 0.43 mmol) in DMF (4 mL) was heated to 100 °C in a microwave apparatus. After 10, 20 and 30 minutes, a sample (0.1 mL) was taken from the reaction vessel, filtered through a short plug of silica (5 x 3 mm; eluent: ethyl acetate) using a syringe filter and was then used for GC analysis.

Table SI 2b. Optimization reactions for the synthesis of 2-(3'-*n*-hexyl-5'-bromo[2,2'-bithiophen]-5-yl)-4,4,5,5-tetramethyl-1,3,2-dioxaborolane **5b** using microwave reaction conditions.



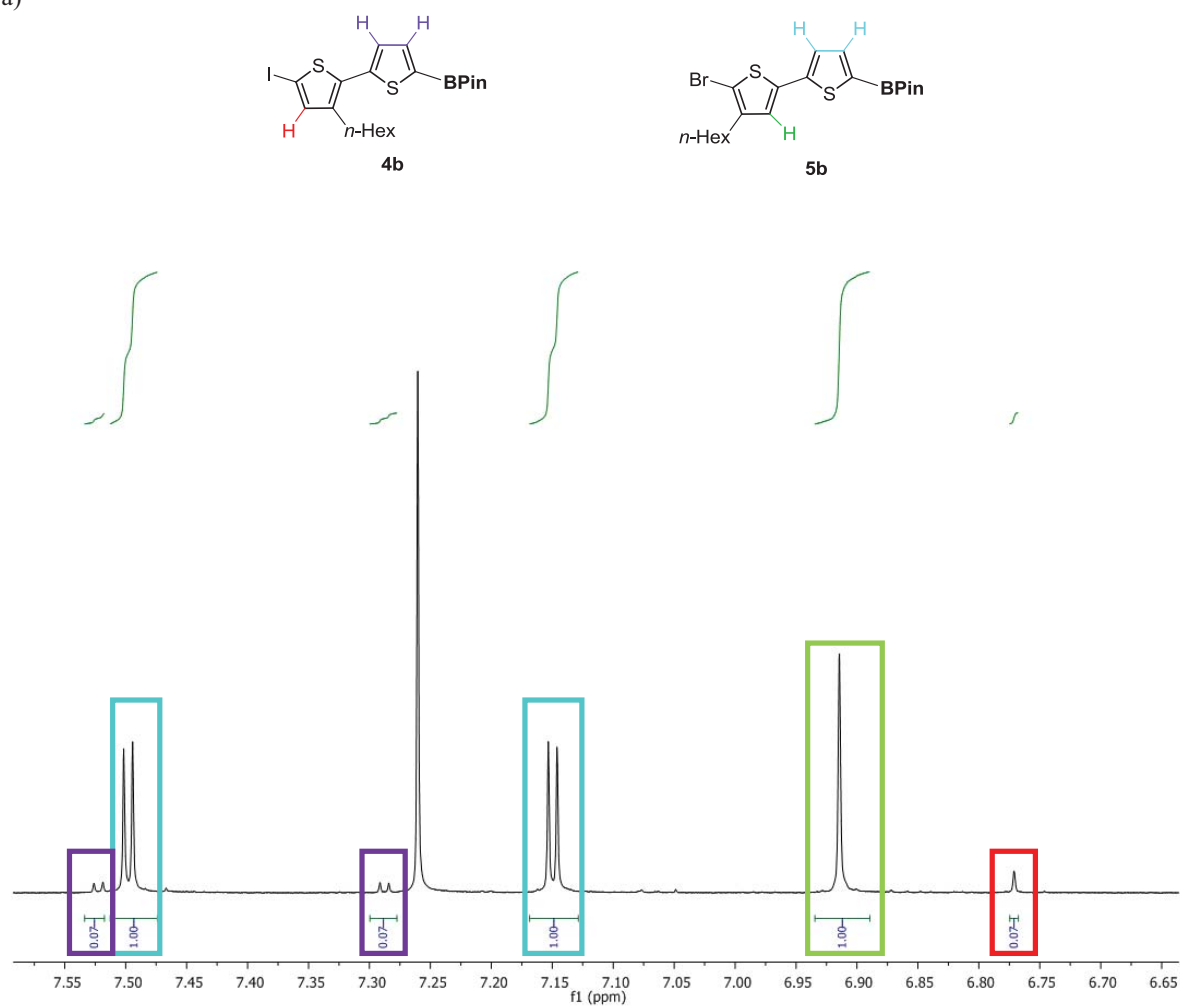
Entry	Solvent / mL	Catalyst-Loading	<i>T</i> [°C]	<i>t</i> [min]	Yield [%]
1	DMF/ 4	0.5 mol%	150	2	16
2	DMF/ 4	0.5 mol%	150	4	18
3	DMF/ 4	0.5 mol%	150	6	68
4	DMF/ 4	0.5 mol%	150	8	18
5	DMF/ 4	2 mol%	120	10	88
6	DMF/ 4	2 mol%	120	20	95
7	DMF/ 4	2 mol%	120	30	85
8	DMF/ 4	2 mol%	100	10	88
9	DMF/ 4	2 mol%	100	20	>99
10	DMF/ 4	2 mol%	100	30	>99
11	DMF/ 4	2 mol%	80	10	12
12	DMF/ 4	2 mol%	80	20	24
13	DMF/ 4	2 mol%	80	30	38
14	DMF/ 4	2 mol%	80	45	46
15	DMF/ 4	2 mol%	80	60	55
16	DMF/ 4	2 mol%	80	120	80
17	DMF/ 4	2 mol%	80	210	>99
18	DMF/ 2	2 mol%	100	20	>99
19	DMF/ 2	1 mol%	100	10	71
20	DMF/ 2	1 mol%	100	20	93
21	DMF/ 2	1 mol%	100	30	>99
22	DMF/ 2	1 mol%	100	45	>99
23	DMF/ 1	1 mol%	100	10	67
24	DMF/ 1	1 mol%	100	20	84
25	DMF/ 1	1 mol%	100	30	78

Example of an unselective coupling reaction:

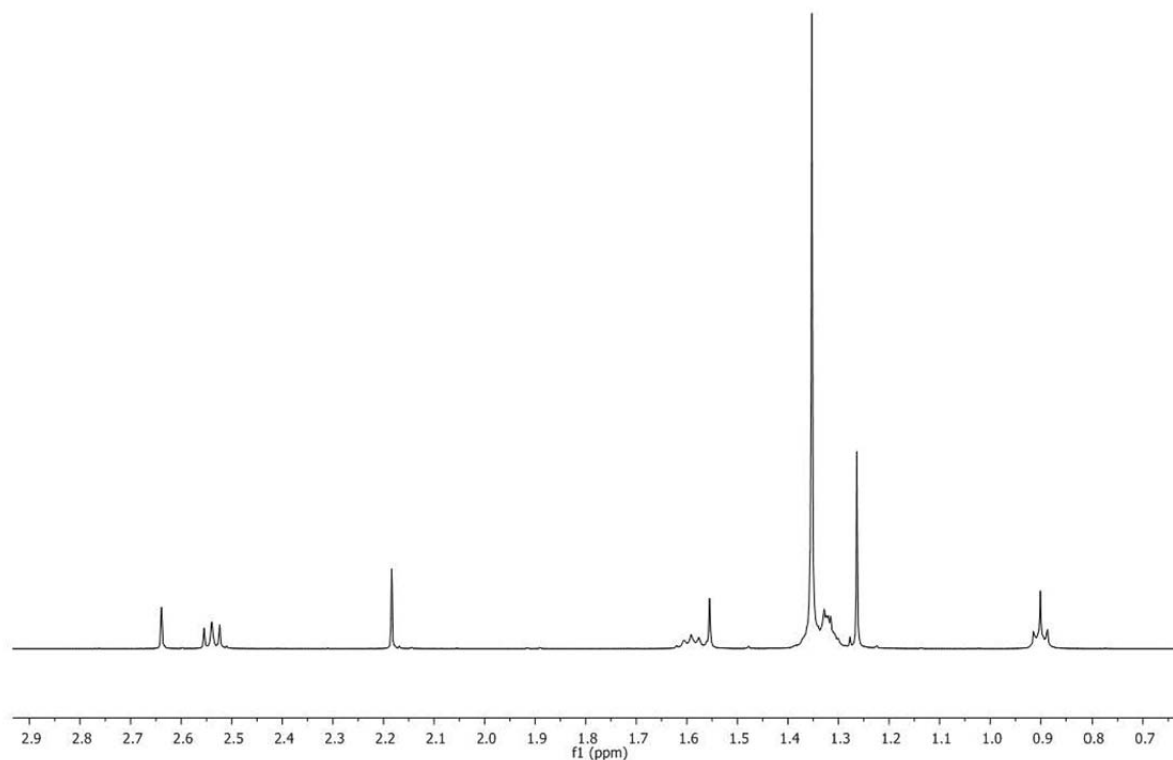


A solution of 4,4,5,5-tetramethyl-2-(5-(trimethylstannyl)thiophen-2-yl)-1,3,2-dioxaborolane (**1**) (186 mg, 0.50 mmol), the electrophile **3** (187 mg, 0.50 mmol), $[\text{Pd}(\text{PPh}_3)_4]$ (28 mg, 5 mol%) and the internal standard 1,3,5-triisopropylbenzene (100 μL , 86.0 mg, 0.43 mmol) were dissolved in DMF and heated to 55 °C for 18 h. Then, the mixture was cooled to 20 °C and diethyl ether (10 mL) was added to the solution. The aqueous layer was washed with brine (3 x 10 mL), dried over sodium sulfate and the solvent was removed in vacuo. The resulting green liquid was purified by column chromatography to afford the mixture of **4b** and **5b** (See Figure SI 3).

a)



b)



c)

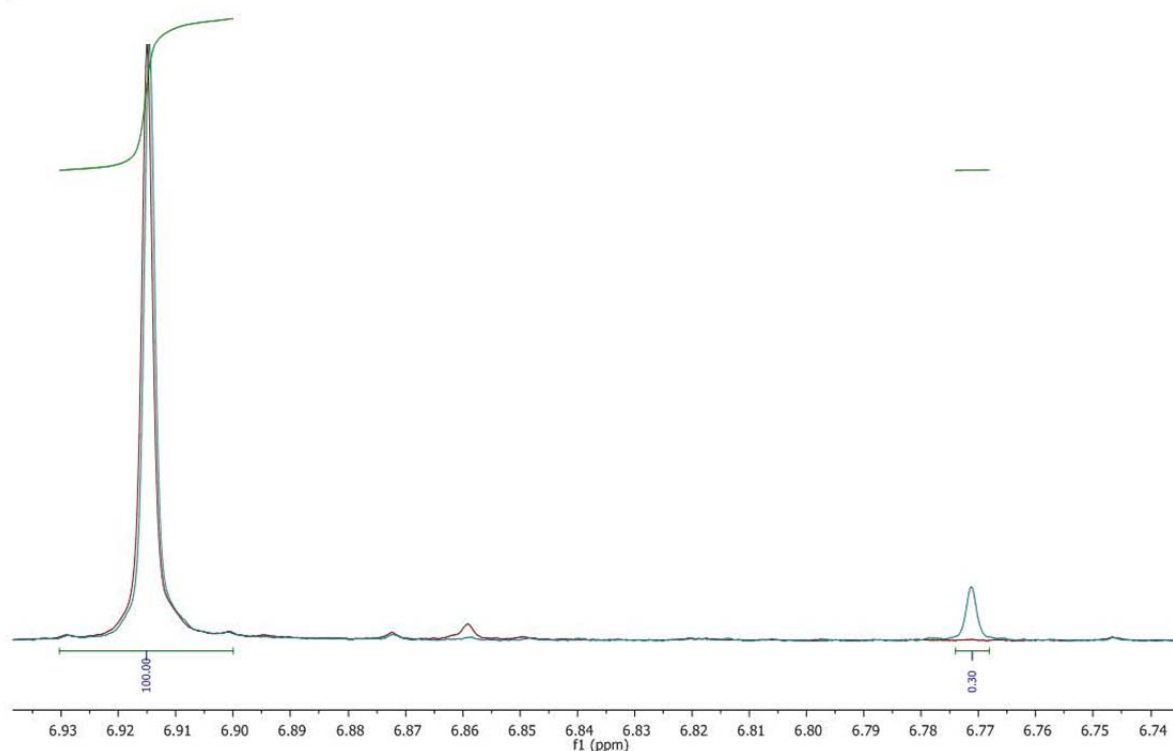


Figure SI 3. ^1H NMR spectrum of the purified mixture of **4b** and **5b**. a) Aryl region; b) Alkyl region; integration of the signals was impossible due to signal overlay. For a comparison with the pure **5b**, see page SI 37; c) Illustration of the detection limit of the NMR spectrometer: the peak on the left is assigned to the product **5b** (integration value: 100), the peak to the right is the corresponding peak of the corresponding byproduct **4b**. In case of the teal spectrum (compare figure 3a), the ratio of **5b** to **4b** is 100:7. In case of the red spectrum it is 100: 0.3. Therefore, the detection limit of the NMR spectrometer is $\geq 0.3\%$.

Reactions with Competing Electrophiles

The yields for the reactions with the competing electrophiles were determined by GC by a multiple point internal standard method, using 1,3,5-triisopropylbenzene as a standard. The following equation was used for the calculation of the yields:

$$n(\text{analyte}) = \frac{A(\text{analyte})}{A(\text{standard})} \times \frac{n(\text{standard})}{RF}$$

where n is the amount of substance, A the integrated area and RF a system specific response factor.

For the calibration curve, known amounts of the analyte and 1,3,5-triisopropylbenzene were used. The response factor RF was obtained from the slope of the resulting calibration curve (Figures SI 3- 8).

Typical procedure for the competitive reactions under microwave conditions:

A solution of 4,4,5,5-tetramethyl-2-(5-(trimethylstannyl)thiophen-2-yl)-1,3,2-dioxaborolane (**1**) (448 mg, 1.20 mmol), the competing electrophiles (each 1.00 mmol), $[\text{Pd}(\text{PPh}_3)_4]$ (23 mg, 2 mol%) and the internal standard 1,3,5-triisopropylbenzene (100 μL , 86.0 mg, 0.43 mmol) were dissolved in DMF (4 mL) and heated to 100 $^\circ\text{C}$ in a microwave apparatus. After 20 minutes, a sample (0.1 mL) was filtered through a short plug of silica (5 x 3 mm; eluent: ethyl acetate) using a syringe filter and was then used for GC analysis.

In case of pyridine as electrophile, the time had to be increased, see table SI 3.

Table SI 3. Reactions with competing electrophiles using microwave reaction conditions.

entry	electrophiles ^[b]	product	time (min)	conversion ^[c] I : Br	Yield (%)
1			20	100: n ^e	78 ^[d]
2			20	100: n ^f	92 ^[d]
3			20	23: n ^g	-
4			30	25: n ^g	-
5			60	43: n ^g	-
6			90	47: n ^g	-
7			150	66: n ^g	-
8			210	76: n ^g	-

9			250	86: n ^g	-
10			300	100: n ^g	89 ^[d]

^a The dinucleophile (1.00 mmol) the bromide (1.00 mmol) and the iodide (1.00 mmol) reacted under the described reaction conditions for the specified reaction time. ^b X = Br or I, 1:1. ^c The conversion was monitored by GC. ^d Isolated Yield. ^{e, f, g} The method limit of detection was determined to be: n^e = 0.4%; n^f = 0.4%, n^g = 0.7%. In none of the cases, the unselective product was observed.

Thiophene Derivatives

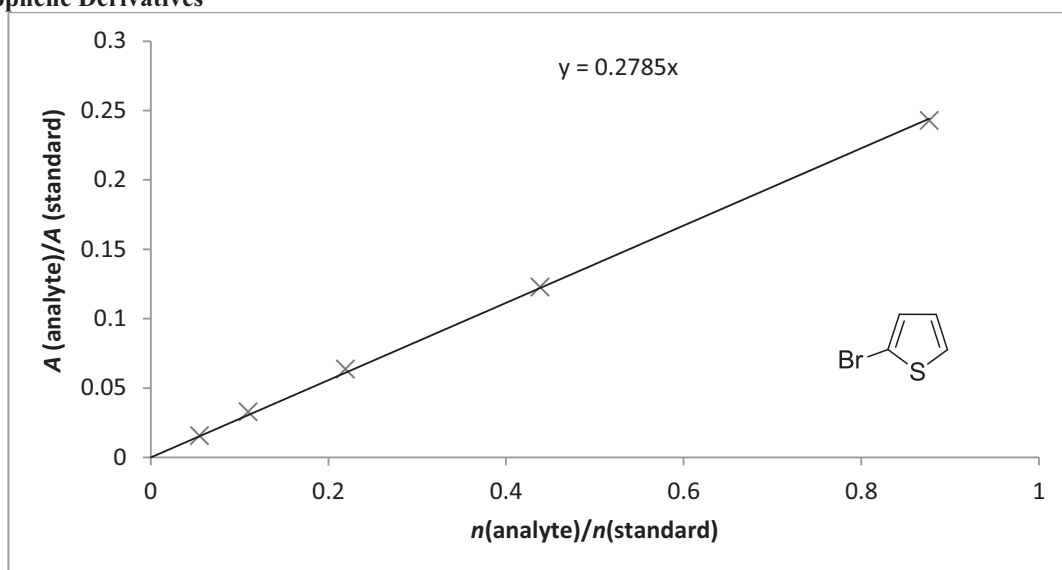


Figure SI 4. Calibration curve for 2-bromothiophene (**28a**), using 1,3,5-triisopropylbenzene as an internal standard.

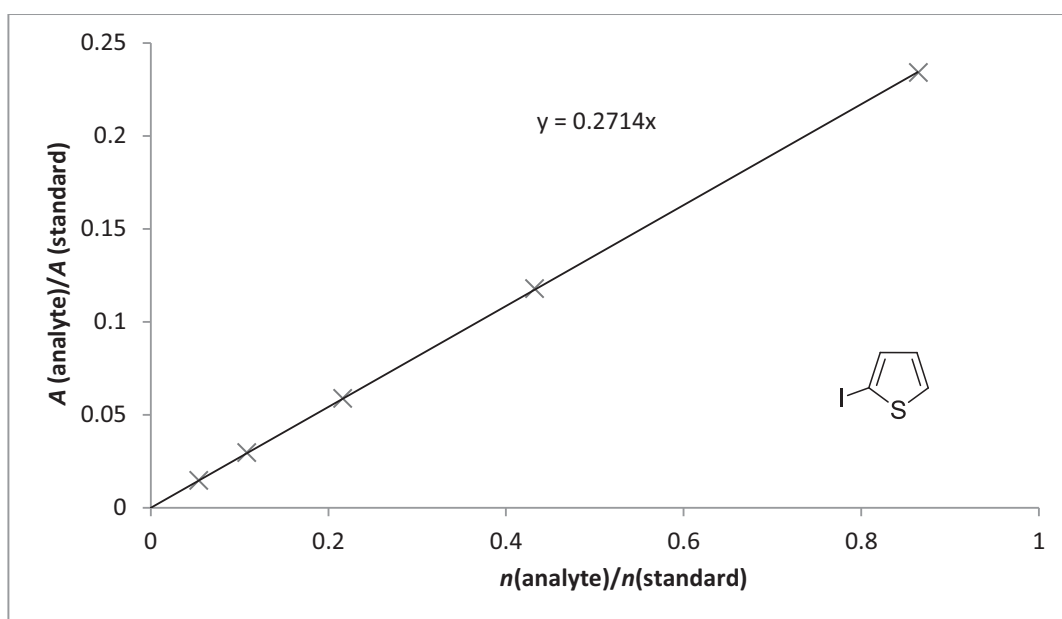


Figure SI 5. Calibration curve for 2-iodothiophene (**28b**), using 1,3,5-triisopropylbenzene as an internal standard.

Benzene Derivatives

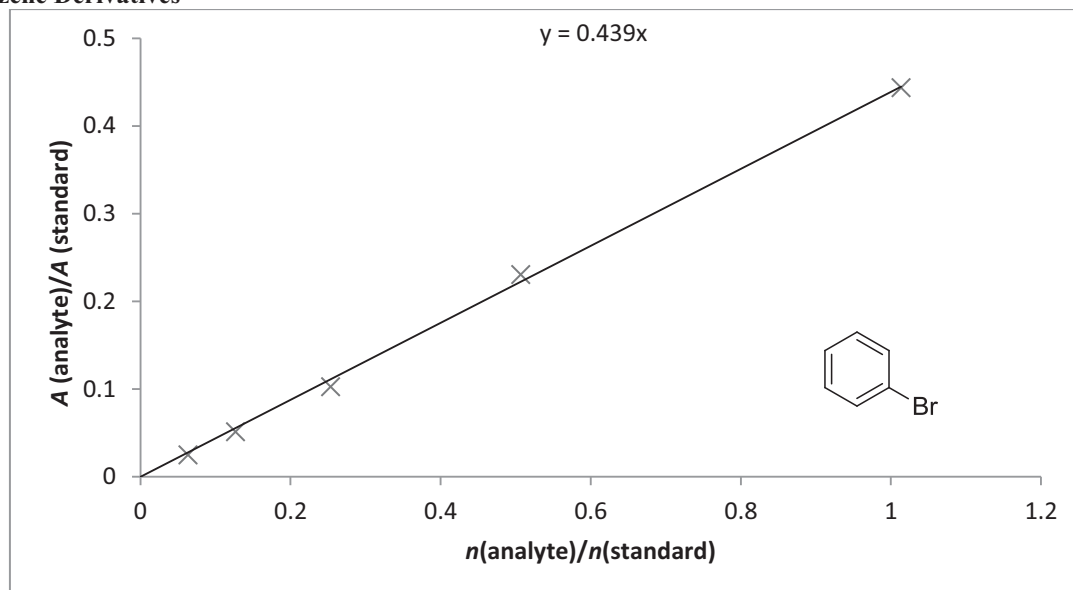


Figure SI 6. Calibration curve for 2-bromobenzene (30a), using 1,3,5-triisopropylbenzene as an internal standard.

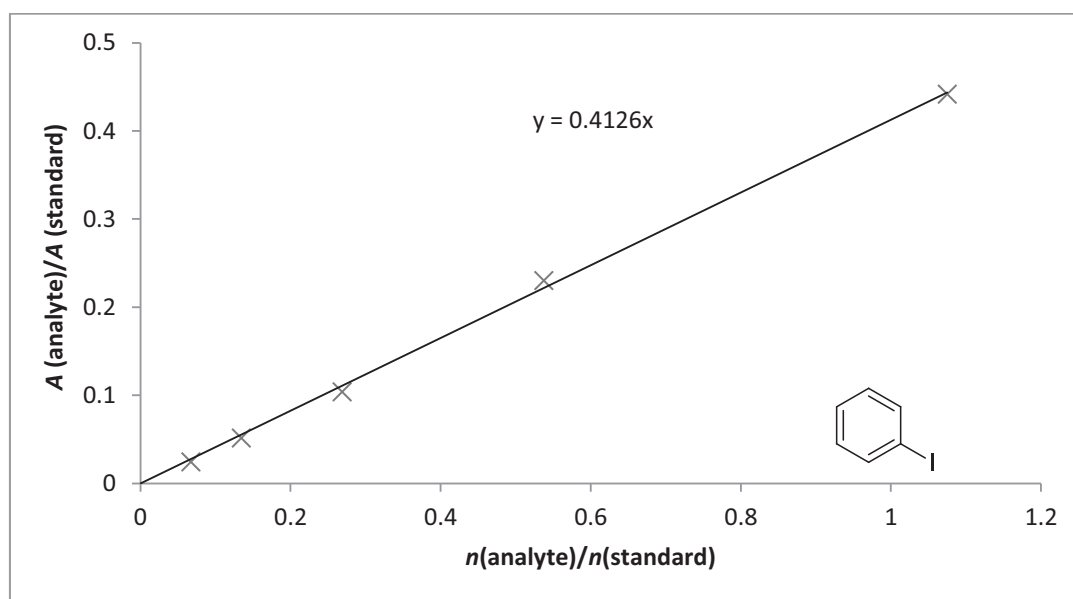


Figure SI 7. Calibration curve for 2-iodobenzene (30b), using 1,3,5-triisopropylbenzene as an internal standard.

Pyridine Derivatives

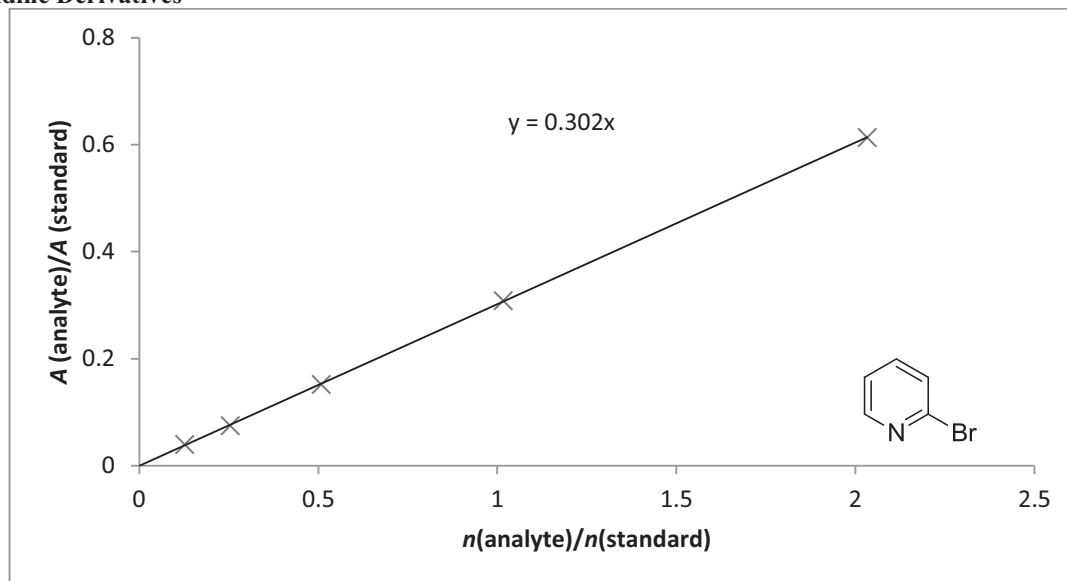


Figure SI 8. Calibration curve for 2-bromopyridine (**32a**), using 1,3,5-triisopropylbenzene as an internal standard.

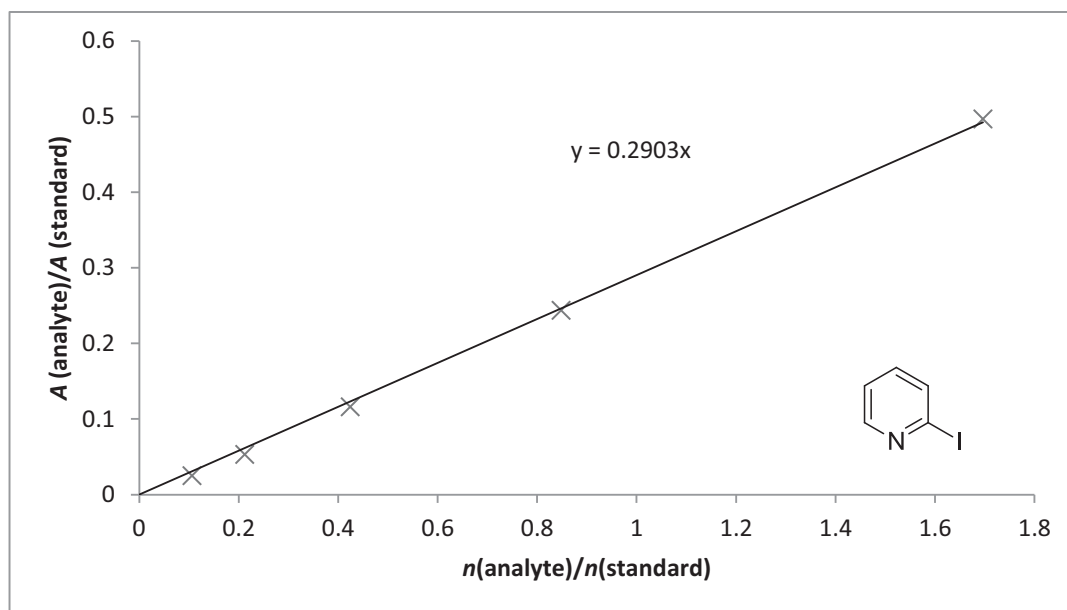


Figure SI 9. Calibration curve for 2-iodopyridine (**32b**), using 1,3,5-triisopropylbenzene as an internal standard.

The method detection limit (MDL) of **28b**, **30b** and **32b** was determined by preparing a series of solutions of each compound and analyzing them following an established protocol.¹

The following equation was used for the calculation ratio of calculated and measured yield:

$$\frac{A(\text{analyte})}{A(\text{standard}) \times RF} = \frac{n(\text{analyte})}{n(\text{standard})}$$

where n is the amount of substance, A the integrated area and RF a system specific response factor.

The standard deviation (S) was calculated using:

$$(S)^2 = \frac{1}{n-1} [\sum_{i=1}^n (x_i^2) - (\sum_{i=1}^n x_i)^2 / n],$$

Where in our case $x_i = 1$ to n with $n = 10$ where the values are the analytical results in % of analyte with respect to standard. These values were obtained from 10 samples per analyte which were diluted individually for each sample to a nominal concentration of, for **28b** = 4.8% analyte to standard (7.94 μmol /10 mL for the analyte); **30b** = 4.9% analyte to standard (8.08 μmol /10 mL for the analyte); **32b** = 4.8% analyte to standard (7.98 μmol /10 mL for the analyte). This led to values of S of for **28b** = 0.146%; **30b** = 0.146%;; **32b** = 0.241%.

The MDL is defined as

$$MDL = (S) \times (t),$$

Where the t is defined as the Student's t -value. In our case of 10 replicates and 9 degrees of freedom, the t -value is: 2.821.

The limit of quantification (LOQ) is defined as

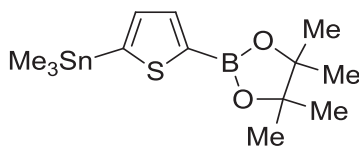
$$LOQ = 10 \times (S).$$

Compound	MDL in %	LOQ (%)
2-Iodothiophene (28b)	0.4	1.5
Iodobenzene (30b)	0.4	1.5
2-Iodopyridine(32b)	0.7	2.4

(1) Wisconsin Department of Natural Resources 1996, *Analytical Detection Limit Guidance and Laboratory Guide for Determining Method Detection Limits*, Wisconsin Department of Natural Resources Laboratory Certification Program, PUBL-TS-056-96.

Syntheses

4,4,5,5-Tetramethyl-2-(5-(trimethylstannyl)thiophen-2-yl)-1,3,2-dioxaborolane (1)



Methyl lithium (625 μL , 1.00 mmol, 1.60 M in diethyl ether) was added within 10 min to a suspension of 2,5-bis(trimethylstannyl)thiophene (410 mg, 1.00 mmol) in THF (6 mL) at $-100\text{ }^{\circ}\text{C}$. The slightly yellow solution was stirred for 2 h at $-78\text{ }^{\circ}\text{C}$. 2-Isopropoxy-4,4,5,5-tetramethyl-1,3,2-dioxaborolane (186 mg, 1.00 mmol) was slowly added at this temperature and stirred for 1 h. Then the reaction mixture was warmed to $20\text{ }^{\circ}\text{C}$ within 12 h without removing the cooling bath and was then quenched with water. The aqueous layer was washed with diethyl ether (3 x 20 mL). The combined organic layer were washed with brine (1 x 20 mL) and dried over sodium sulfate. The solvent was removed *in vacuo* and the crude product was purified by sublimation² ($30\text{ }^{\circ}\text{C}$, 2×10^{-2} mbar) to afford 205 mg (55 %) of a colorless solid.

Note: the compound was unstable to silica gel chromatography.

¹H NMR (500 MHz, CDCl_3): δ = 7.79 (d, 1 H, 3J = 3.2 Hz, Tph-H), 7.33 (d, 1 H, 3J = 3.2 Hz, Tph-H), 1.37 (s, 12 H, pin- CH_3), 0.40 (s, 9 H, $\text{Sn}(\text{CH}_3)_3$) ppm.

¹³C NMR (126 MHz, CDCl_3): δ = 146.5 (Tph-C), 137.8 (Tph-CH), 136.3 (Tph-CH), 84.1 (pin- $\text{C}(\text{CH}_3)_4$), 24.9 ($\text{BO}_2\text{C}(\text{CH}_3)_4$), -8.1 ($\text{Sn}(\text{CH}_3)_3$) ppm.³

¹¹⁹Sn NMR (187 MHz, CDCl_3): δ = -26.8 ppm.

¹¹B NMR (160 MHz, CDCl_3): δ = 28.8 ppm.

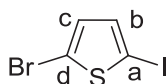
M.p.: $84\text{ }^{\circ}\text{C}$.

IR (ATR): $\tilde{\nu}$ = 2978 (m), 2920 (w), 1510 (s), 1418 (s), 1331 (s), 1254 (m), 1138 (s), 1064 (s), 1021 (m), 957 (m), 928 (m), 853 (m), 820 (m), 770 (s), 665 (s), 533 (s) cm^{-1} .

HRMS (ESI): m/z found 397.0432; calcd. for $\text{C}_{13}\text{H}_{23}\text{BNaO}_2\text{SSn}$ 397.0426.

The NMR data are in agreement with the our previous work.⁴

2-Bromo-5-iodothiophene (2)



In the dark, 2-bromothiophene (4.89 g, 30.0 mmol) was dissolved in a mixture of chloroform (40 mL) and acetic acid (20 mL). Then, *N*-iodosuccinimide (7.88 g, 35.0 mmol) was added and the reaction was allowed to proceed for 16 h at $20\text{ }^{\circ}\text{C}$. The solution was concentrated *in vacuo*, neutralized with NaHCO_3 (1M, 50 mL) and extracted with *n*-hexane. The combined organic layers were dried over magnesium sulfate and the solvent was removed *in vacuo*. Finally, the product was distilled (1 mbar, $70\text{ }^{\circ}\text{C}$) to yield 6.76 g (78 %) of a bright yellow solid.

¹H NMR (200 MHz, CDCl_3): δ = 7.01 (d, 1H, 3J = 3.8 Hz, Tph-H), 6.73 (d, 1H, 3J = 3.8 Hz, Tph-H) ppm.

¹³C NMR (50 MHz, CDCl_3): δ = 137.5 (Tph-CH), 131.7 (Tph-CH), 115.2 (Tph-C), 72.2 (Tph-C) ppm.

M.p.: $116\text{ }^{\circ}\text{C}$.

IR (ATR): $\tilde{\nu}$ = 3091 (w), 1731 (w), 1567 (w), 1508 (m), 1397 (m), 1202 (m), 968 (s), 929 (m), 780 (s) cm^{-1} .

MS (EI, 70 eV): m/z (%) = 290/288 (100/98) $[\text{M}]^+$, 163/161 (13/13) $[\text{M}-\text{I}]^+$.

MS (CI, isobutane): m/z (%) = 291/289 (45/50) $[\text{M}+\text{H}]^+$, 290/288 (95/100) $[\text{M}]^+$.

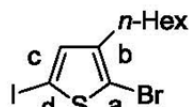
The NMR data are in agreement with the data found in the literature where a different preparation procedure for this compound was used.⁵

(2) An impurity sublimed first ($25\text{ }^{\circ}\text{C}$, 2×10^{-2} mbar).

(3) The carbon atom bound to boron was not visible due to the high quadrupole moment of the boron nucleus.

(4) J. Linshoef, A. C. J. Heinrich, S. A. W. Segler, P. J. Gates, A. Staubitz, *Org. Lett.* **2012**, *14*, 5644.

(5) B.T. Holmes, W. T. Pennington, T. W. Hanks, *Molecules* **2002**, *7*, 447.

2-Bromo-3-*n*-hexyl-5-iodothiophene (3)

2-Bromo-3-*n*-hexyl-5-iodothiophene was prepared similar to a method described Smeets et al.^[5] and was modified as follows:

In the dark, 2-bromo-3-*n*-hexylthiophene (566 mg, 2.30 mmol) was dissolved in a mixture of chloroform (20 mL) and acetic acid (10 mL). Then, *N*-iodosuccinimide (697 mg, 3.10 mmol) was added in one portion and the reaction was allowed to proceed for 16 h. The solution was neutralized using sodium hydrogen carbonate (1M, 50 mL) and extracted with *n*-hexane (3 x 15 mL). The combined organic layers were dried over magnesium sulfate and the solvent was removed *in vacuo*. The crude product was purified by Kugelrohr distillation (130 °C, 0.01 mbar) to yield 710 mg (83 %) of a yellow oil.

¹H NMR (200 MHz, CDCl₃): δ = 6.96 (s, 1H, Tph-*H*), 2.50 (t, 2H, ³J = 7.8 Hz, Tph-CH₂(CH₂)₄CH₃), 1.58-1.22 (m, 8H, Tph-CH₂(CH₂)₄CH₃), 0.95-0.84 (m, 3H, Tph-(CH₂)₅CH₃) ppm.

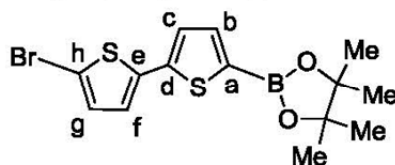
¹³C NMR (125 MHz, CDCl₃): δ = 144.3 (Tph-C-b), 138.0 (Tph-C-c), 111.7 (Tph-C), 70.9 (Thp-C), 31.6, 29.6, 29.2, 28.8, 22.6 (Tph-(CH₂)₅CH₃), 14.1 (Tph-(CH₂)₅CH₃) ppm.

IR (ATR): $\tilde{\nu}$ = 2952 (m), 2923 (s), 2953 (m), 1536 (w), 1458 (m), 1402 (m), 1376 (w), 1191 (m), 994 (s), 902 (m), 826 (s), 725 (m), 578 (w) cm⁻¹.

MS (EI, 70 eV): *m/z* (%) = 373/371 (29)/(27) [M]⁺, 300 (100) [M-BrC₅H₁₁]⁺.

MS (CI, isobutane): *m/z* (%) = 374/372 (100)/(95) [M + H]⁺.

The NMR data are in agreement with the data found in the literature.⁶

4,4,5,5-Tetramethyl-2-(5-(5-bromothiophen)thiophen-2-yl)-1,3,2-dioxaborolane (5a)

4,4,5,5-Tetramethyl-2-(5-(trimethylstannyl)thiophen-2-yl)-1,3,2-dioxaborolane (374 mg, 1.00 mmol), [Pd(PPh₃)₄] (23 mg, 2 mol%) and 2-bromo-5-iodothiophene (288 mg, 1.00 mmol) were dissolved in DMF (4 mL). The mixture was heated to 100 °C in a microwave apparatus for 20 min and was then filtered over a short plug of celite. The solvent was removed *in vacuo* and the crude product was purified by column chromatography (*n*-hexane, R_f = 0.40). Subsequent recrystallization from hexane gave the product as a pale green solid in a yield of 330 mg (89 %).

¹H NMR (500 MHz, CDCl₃): δ = 7.51 (d, 1H, ³J = 3.6 Hz, Tph-*H-c/f*), 7.17 (d, 1H, ³J = 3.6 Hz, Tph-*H-c/f*), 6.97 (m, 2H, Tph-*H-b, H-g*), 1.35 (s, 12H, pin-C(CH₃)₃) ppm.

¹³C NMR (125 MHz, CDCl₃): δ = 143.0 (Tph-C), 138.8 (Tph-C), 137.9 (Tph-CH), 130.7 (Tph-CH), 125.1 (Tph-CH), 124.4 (Tph-CH), 111.6 (Tph-C), 84.3 (pin-C(CH₃)₂), 24.8 (pin-C(CH₃)₃) ppm.³

¹¹B NMR (160 MHz, CDCl₃): δ = 28.9 ppm.

M.p.: 91 °C.

IR (ATR): $\tilde{\nu}$ = 2975 (w), 1515(m), 1463 (s), 1352 (s), 1339 (s), 1315 (s), 1264 (s), 1211 (m), 1141(s), 1064 (s), 1017 (m), 957 (w), 851 (s), 795 (s), 660 (s) cm⁻¹.

MS (EI, 70 eV): *m/z* (%) = 371/369 (100)/(95) [M]⁺.

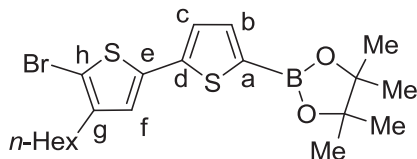
MS (CI, isobutane): *m/z* (%) = 372/370 (89)/(100) [M + H]⁺.

HRMS (ESI): *m/z* found 370.9941; calcd. for C₁₄H₁₇BBro₂S₂ 370.9949.

The NMR data are in agreement with the data found in the literature where the compound was prepared by a different, lower yielding procedure.⁷

(6) A. Smeets, K. V. d. Bergh, J. De-Winter, P. Gerbaux, T. Verbiest, G. Koeckelberghs, *Macromolecules* **2009**, *42*, 7638.

(7) O. Henze, D. Parker, W. J. Feast, *J. Mater. Chem.* **2003**, *13*, 1269.

4,4,5,5-Tetramethyl-2-(5-(5-bromo-3-*n*-hexylthiophen)thiophen-2-yl)-1,3,2-dioxaborolane (**5b**)

4,4,5,5-Tetramethyl-2-(5-(trimethylstannyl)thiophen-2-yl)-1,3,2-dioxaborolane (374 mg, 1.00 mmol), [Pd(PPh₃)₄] (23 mg, 2 mol%) and the 2-bromo-3-*n*-hexyl-5-iodothiophene (288 mg, 1.00 mmol) were dissolved in DMF (4 mL). The mixture was heated to 100 °C in a microwave apparatus for 20 min and was then filtered over a short plug of celite. The solvent was removed *in vacuo* and the crude product was purified by column chromatography (*n*-hexane, R_f = 0.7) to afford the product as a green oil in a yield of 351 mg (95 %).

¹H NMR (500 MHz, CDCl₃): δ = 7.43 (d, 1H, ³J = 3.6 Hz, Tph-*H*-b/c), 7.08 (d, 1H, ³J = 3.6 Hz, Tph-*H*-b/c), 6.84 (s, 1H, Tph-*H*-f), 2.48-2.43 (m, 2H, Tph-CH₂), 1.55-1.49 (m, 2H, Tph-CH₂CH₂), 1.29-1.27 (m, 18H, Tph-(CH₂)₂(CH₂)₃CH₃, pin-C(CH₃)₄), 0.82 (t, 3H, ³J = 6.4 Hz, alkyl-CH₃) ppm.

¹³C NMR (125 MHz, CDCl₃): δ = 143.4 (Tph-C-e/h), 143.0 (Tph-C-e/h), 137.9 (Tph-CH-b/c), 136.6 (Tph-C-d), 132.3 (Tph-C-g), 125.1 (Tph-C-f), 124.8 (Tph-C-b/c), 108.4 (Tph-C-a), 84.2 (pin-C(CH₃)₄), 31.6, 29.6, 29.5, 28.8, 22.6 (Tph-(CH₂)₅CH₃), 24.8 (pin-C(CH₃)₄), 14.1 (Tph-(CH₂)₅CH₃) ppm.

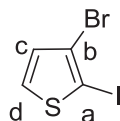
¹¹B NMR (160 MHz, CDCl₃): δ = 28.8 ppm.

IR (ATR): $\tilde{\nu}$ = 2926 (m), 2855 (w), 1523 (m), 1470 (s), 1425 (m), 1346 (s), 1286 (s), 1140 (s), 1065 (s), 1016 (m), 956 (w), 852 (s), 805 (m), 658 (w), 663 (s) cm⁻¹.

MS (EI, 70 eV): *m/z* (%) = 456/454 (82)/(74) [M]⁺, 305 (100) [M-Br-C₅H₁₁]⁺.

MS (CI, isobutane): *m/z* (%) = 457/455 (65)/(76) [M + H]⁺, 456/454 (100)/(81) [M - H + H]⁺.

HRMS (ESI): *m/z* found 455.0878; calcd. for C₂₀H₂₉BBRO₂S₂ 455.0879.

3-Bromo-2-iodothiophene (**6**)

In the dark, 3-bromo-thiophene (1.63 g, 10.0 mmol) was dissolved in a mixture of chloroform (20 mL) and acetic acid (10 mL). Then, *N*-iodosuccinimide (2.70 g, 12.0 mmol) was added in one portion and the reaction was allowed to proceed for 48 h at 20 °C. The solution was then concentrated *in vacuo*, neutralized with NaHCO₃ (1M, 50 mL) and extracted with *n*-hexane. The combined organic layers were dried over magnesium sulphate and the solvent was removed *in vacuo*. Finally, the product was distilled (Kugelrohr; 50°C, 0.02 mbar) to yield a bright orange oil in a yield of 1.65 g (57 %).

¹H NMR (200 MHz, CDCl₃): δ = 7.41 (d, 1H, ³J = 5.5 Hz, Tph-*H*), 6.90 (d, 1H, ³J = 5.5 Hz, Tph-*H*) ppm.

¹³C NMR (50 MHz, CDCl₃): δ = 132.1 (Tph-CH), 130.3 (Thp-CH), 120.6 (Thp-C-b) ppm.

IR (ATR): $\tilde{\nu}$ = 3103 (w), 1729 (w), 1568 (w), 1487 (m), 1385 (m), 1334 (s), 1142 (m), 957 (m), 853 (s), 696 (s), 643 (m), 578 (s) cm⁻¹.

MS (EI, 70 eV): *m/z* (%) = 289/287 (99/100) [M]⁺, 163/161 (13/13) [M - I]⁺.

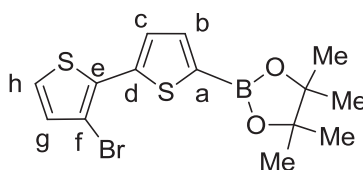
MS (CI, isobutane): *m/z* (%) = 290/289 (40/26) [M + H]⁺, 290/288 (77/100) [M]⁺.

HRMS (EI): *m/z* found 217.8102; calcd. for C₄H₂BrIS 287.8105.

The NMR data are in agreement with the data found in the literature where another procedure was performed.⁸

(8) M. J. Marsella, Z.-Q. Wang, R. J. Reid, K. Yoon, *Org. Lett.* **2001**, *3*, 885.

4,4,5,5-Tetramethyl-2-(5-(3-bromothiophen)thiophen-2-yl)-1,3,2-dioxaborolane (7)



4,4,5,5-Tetramethyl-2-(5-(trimethylstannyl)thiophen-2-yl)-1,3,2-dioxaborolane (374 mg, 1.00 mmol), [Pd(PPh₃)₄] (23 mg, 2 mol%) and the 3-bromo-2-iodothiophene (289 mg, 1.00 mmol) was dissolved in DMF (4 mL). The mixture was heated to 100 °C in a microwave apparatus for 120 min and was then filtered over a short plug of celite. The solvent was removed *in vacuo* and the crude product was purified by column chromatography (*n*-hexanes / ethyl acetate (9:1), R_f = 0.28) to afford the product as a pale green solid in a yield of 291 mg (79 %).

¹H NMR (500 MHz, CDCl₃): δ = 7.58 (d, 1H, ³J = 3.7 Hz, Tph-*H*-c), 7.49 (d, 1H, ³J = 3.7 Hz, Tph-*H*-b), 7.20 (d, 1H, ³J = 5.4 Hz, Tph-*H*-g), 7.02 (d, 1H, ³J = 5.4 Hz, Tph-*H*-h), 1.35 (s, 12H, pin-C(CH₃)₄) ppm.

¹³C NMR (500 MHz, CDCl₃): δ = 141.1 (Tph-*C*-e), 137.2 (Tph-*C*-c), 132.3 (Tph-*C*-d), 132.1 (Tph-*C*-h), 127.8 (Tph-*C*-b), 124.8 (Tph-*C*-g), 108.5 (Tph-*C*-f), 84.3 (pin-C(CH₃)₄), 24.8 (pin-C(CH₃)₄) ppm.³

¹¹B NMR (160 MHz, CDCl₃): δ = 28.8 ppm.

M.p.: 72 °C.

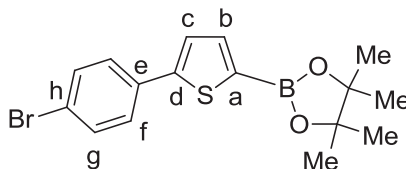
IR (ATR): $\tilde{\nu}$ = 2974 (m), 2929(w), 1506 (m), 1458 (s), 1325 (s), 1268 (s), 1212 (w), 1138 (s), 1065 (s), 1015 (m), 957 (w), 851 (s), 822 (s), 409 (s), 663 (s), 614 (m) cm⁻¹.

MS (EI, 70 eV): *m/z* (%) = 372/370 (100)/(88) [M]⁺.

MS (CI, isobutane): *m/z* (%) = 429/427 (24)/(17) [M + isobutane]⁺, 373/371 (100)/(99) [M + H]⁺.

HRMS (ESI): *m/z* found 370.9949; calcd. for C₁₄H₁₇BBro₂S₂ 370.9941.

4,4,5,5-Tetramethyl-2-(5-(4-bromophenyl)thiophen-2-yl)-1,3,2-dioxaborolane (9)



4,4,5,5-Tetramethyl-2-(5-(trimethylstannyl)thiophen-2-yl)-1,3,2-dioxaborolane (374 mg, 1.00 mmol), [Pd(PPh₃)₄] (23 mg, 2 mol%) and the 1-bromo-4-iodobenzene (283 mg, 1.00 mmol) were dissolved in DMF (4 mL). The mixture was heated to 100 °C in a microwave for 60 min and was then filtered over a short plug of celite. The solvent was removed *in vacuo* and the crude product was purified by column chromatography (*n*-hexanes / ethyl acetate (9:1), R_f = 0.28) to afford the product as a colorless solid in a yield of 308 mg (84 %).

¹H NMR (500 MHz, CDCl₃): δ = 7.59 (d, 1H, ³J = 3.6 Hz, Tph-*H*-b), 7.50 (apparent s, 4H, Ar-*H*), 7.36 (d, 1H, ³J = 3.6 Hz, Tph-*H*-c), 1.36 (s, 12H, pin-C(CH₃)₄) ppm.

¹³C NMR (125 MHz, CDCl₃): δ = 149.9 (Tph-*C*-d), 138.2 (Tph-*C*-b), 133.2 (Ar-*C*-e), 132.0 (Ar-*C*-f), 127.6 (Ar-*C*-g), 124.8 (Tph-*C*-c), 121.8 (Ar-*C*-h), 84.2 (pin-C(CH₃)₄), 24.8 (pin-C(CH₃)₄) ppm.³

¹¹B NMR (160 MHz, CDCl₃): δ = 28.7 ppm.

M.p.: 103 °C.

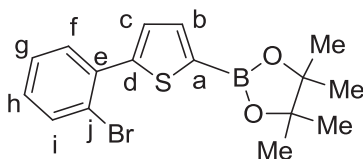
IR (ATR): $\tilde{\nu}$ = 2988 (m), 2928 (w), 1529 (m), 1451 (s), 1353 (s), 1327 (s), 1302 (s), 1141 (s), 1112 (m), 1067 (s), 1003 (m), 951 (w), 852 (m), 805 (s), 662 (s) cm⁻¹.

MS (EI, 70 eV): *m/z* (%) = 366/364 (52)/(100) [M]⁺.

MS (CI, isobutane): *m/z* (%) = 423/421 (29)/(26) [M + isobutane + H]⁺, 367/365 (100)/(99) [M + H]⁺.

HRMS (ESI): *m/z* found 365.0391; calcd. for C₁₆H₁₉BBro₂S 365.0377.

4,4,5,5-Tetramethyl-2-(5-(2-bromophenyl)thiophen-2-yl)-1,3,2-dioxaborolane (11)



4,4,5,5-Tetramethyl-2-(5-(trimethylstannyl)thiophen-2-yl)-1,3,2-dioxaborolane (374 mg, 1.00 mmol), [Pd(PPh₃)₄] (23 mg, 2 mol%) and the 1-bromo-2-iodothiophene (283 mg, 1.00 mmol) were dissolved in DMF (4 mL). The mixture was heated to 100 °C in a microwave for 270 min and was then filtered over a short plug of celite. The solvent was removed *in vacuo* and the crude product was purified by column chromatography (*n*-hexanes / ethyl acetate (9:1), R_f = 0.46) to afford the product as a colorless solid in a yield of 272 mg (75 %).

¹H NMR (600 MHz, CDCl₃): δ = 7.67 (dd, 1H, ³J = 8.0, ⁴J = 1.0 Hz, Ar-*H*-i), 7.62 (d, 1H, ³J = 3.5 Hz, Tph-*H*), 7.48 (dd, 1H, ³J = 7.7, ⁴J = 1.5 Hz, Ar-*H*-f), 7.37 (d, 1H, ³J = 3.5 Hz, Tph-*H*), 7.33 (td, 1H, ³J = 7.7, ⁴J = 1.0 Hz, Ar-*H*-g), 7.19 (td, 1H, ³J = 8.0, ⁴J = 1.5 Hz, Ar-*H*-h), 1.36 (s, 12H, pin-C(CH₃)₄) ppm.

¹³C NMR (150 MHz, CDCl₃): δ = 148.7 (Tph-C-d), 137.0 (Tph-CH), 135.3 (Ar-C-e), 133.7 (Ar-C-i), 131.9 (Ar-C-f), 129.2 (Ar-C-h, Tph-CH), 127.4 (Ar-C-g), 122.7 (Tph-C-j), 84.2 (pin-C(CH₃)₄), 24.8 (pin-C(CH₃)₄) ppm.³

¹¹B NMR (160 MHz, CDCl₃): δ = 28.9 ppm.

M.p.: 104 °C.

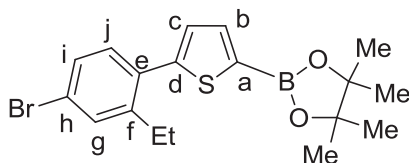
IR (ATR): $\tilde{\nu}$ = 2979 (w), 2930 (w), 1533 (m), 1482 (m), 1449 (s), 1351 (s), 1334 (s), 1298 (s), 1272 (m), 1140 (s), 1068 (m), 1019 (m), 854 (s), 819 (m), 756 (s), 749 (s), 664 (s) cm⁻¹.

MS (EI, 70 eV): *m/z* (%) = 366/364 (100)/(92) [M]⁺.

MS (CI, isobutane): *m/z* (%) = 423/421 (12)/(13) [M + isobutane + H]⁺, 367/365 (100)/(99) [M + H]⁺.

HRMS (ESI): *m/z* found 365.0381; calcd. for C₁₆H₁₉BBrO₂S 365.0377.

4,4,5,5-Tetramethyl-2-(5-(4-bromo-2-ethylphenyl)thiophen-2-yl)-1,3,2-dioxaborolane (13)



4,4,5,5-Tetramethyl-2-(5-(trimethylstannyl)thiophen-2-yl)-1,3,2-dioxaborolane (374 mg, 1.00 mmol), [Pd(PPh₃)₄] (23 mg, 2 mol%) and the 4-bromo-2-ethyl-1-iodobenzene (311 mg, 1.00 mmol) were dissolved in DMF (4 mL). The mixture was heated to 100 °C in a microwave for 120 min and was then filtered over a short plug of celite. The solvent was removed *in vacuo* and the crude product was purified by column chromatography (*n*-hexanes / ethyl acetate (9:1), R_f = 0.67) to afford the product as a colorless solid in a yield of 310 mg (79 %).

¹H NMR (500 MHz, CDCl₃): δ = 7.60 (d, 1H, ³J = 3.5 Hz, Tph-*H*-b), 7.44 (d, 1H, ³J = 2.0 Hz, Ar-*H*-g), 7.33 (dd, 1H, ³J = 8.2, ⁴J = 2.0 Hz, Ar-*H*-i), 7.21 (d, 1H, ³J = 8.2 Hz, Ar-*H*-j), 7.08 (d, 1H, ³J = 3.5 Hz, Tph-*H*-c), 2.71 (q, 2H, ³J = 7.5 Hz, Ar-CH₂), 1.36 (s, 12H, pin-C(CH₃)₄), 1.16 (t, 3H, ³J = 7.5 Hz, Ar-CH₂CH₃) ppm.

¹³C NMR (125 MHz, CDCl₃): δ = 148.8 (Tph-C-d), 144.6 (Ar-C-e), 137.3 (Tph-C-b), 132.7 (Ar-C-f), 132.3 (Ar-C-j), 131.8 (Ar-C-g), 128.8 (Ar-C-i), 128.2 (Tph-C-c), 122.4 (Ar-C-h), 84.2 (pin-C(CH₃)₄), 26.5 (Ar-CH₂), 24.8 (pin-C(CH₃)₄), 15.4 (Ar-CH₂CH₃) ppm.³

¹¹B NMR (160 MHz, CDCl₃): δ = 28.8 ppm.

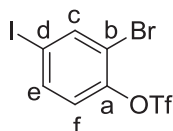
M.p.: 56 °C.

IR (ATR): $\tilde{\nu}$ = 2970 (W), 2927 (w), 2968 (w), 1535 (m), 1489 (w), 1449 (m), 1333 (s), 1293 (s), 1137 (s), 1067 (s), 1017 (m), 944 (m), 851 (m), 816 (s), 660 (s) cm⁻¹.

MS (EI, 70 eV): *m/z* (%) = 394/392 (100)/(99) [M]⁺.

MS (CI, isobutane): *m/z* (%) = 395/393 (100)/(98) [M + H]⁺.

HRMS (ESI): *m/z* found 393.0702; calcd. for C₁₈H₂₃BBrO₂S 393.0690.

2-Bromo-4-iodophenyl trifluoromethanesulfonate (14)

To a solution of 2-bromo-4-iodophenol (1.10 g, 3.68 mmol) and pyridine (1.88 mL) trifluoromethanesulfonic anhydride (690 μ L, 1.16 g, 4.09 mmol) was added at 0 °C over a course of 5 min. The resulting yellow mixture was stirred at 0 °C for 5 min and then allowed to warm to 20 °C and stirred for 25 h. The resulting mixture was poured into water (50 mL) and extracted with diethyl ether (3 x 50 mL). The ether extract was washed sequentially with water (1 x 50 mL), 10% aqueous hydrochloric acid solution (2 x 50 mL), water (1 x 50 mL) and a concentrated sodium chloride solution (1 x 50 mL), dried over magnesium sulfate and concentrated *in vacuo*. The residue was purified by column chromatography (pentane / ethyl acetate (20:1), R_f = 0.9) to yield 1.36 g (86 %) as a slightly yellow oil.

$^1\text{H NMR}$ (500 MHz, CDCl_3): δ = 8.03 (d, 4J = 2.1 Hz, 1 H, Ar-*H-c*), 7.71 (dd, 3J = 8.6 Hz, 4J = 2.1 Hz, 1H, Ar-*H-e*), 7.08 (d, 3J = 8.6 Hz, 1H, Ar-*H-f*) ppm.

$^{13}\text{C NMR}$ (125 MHz, CDCl_3): δ = 147.0 (Ar-*C-a*), 142.6 (Ar-*C-d*), 138.2 (Ar-*C-c*), 124.3 (Ar-*C-e*), 119.9 (OTf-*C*), 117.3 (Ar-*C-f*), 93.2 (Ar-*C-b*) ppm.⁹

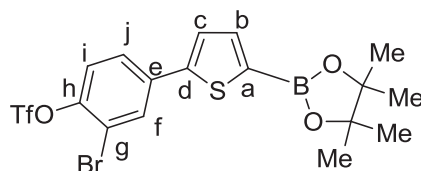
$^{19}\text{F NMR}$ (470 MHz, CDCl_3): δ = -73.2 ppm.

IR (ATR): $\tilde{\nu}$ = 3088 (w), 1559 (w), 1461 (m), 1426 (s), 1206 (s), 1132 (s), 1037 (s), 873 (s), 817 (m), 780 (m), 603 (s), 572 (m), 535 (m) cm^{-1} .

MS (EI, 70 eV): m/z (%) = 432/430 (99)/(100) $[\text{M}]^+$.

MS (CI, isobutane): m/z (%) = 432/430 (100)/(85) $[\text{M}]^+$.

HRMS (EI): m/z found 429.7977; calcd. for $\text{C}_7\text{H}_3\text{BrF}_3\text{IO}_3\text{S}$ 429.7983.

4,4,5,5-Tetramethyl-2-(5-(3-bromo-4-trifluoromethanesulfonatophenyl)-thio-phen-2-yl)-1,3,2-dioxaborolane (15)

4,4,5,5-Tetramethyl-2-(5-(trimethylstannyl)thiophen-2-yl)-1,3,2-dioxaborolane (374 mg, 1.00 mmol), $[\text{Pd}(\text{PPh}_3)_4]$ (23 mg, 2 mol%) and 2-bromo-4-iodophenyl trifluoromethane sulfonate (431 mg, 1.00 mmol) were dissolved in DMF (4 mL). The mixture was heated to 100 °C in a microwave for 90 min and was then filtered over a short plug of celite. The solvent was removed *in vacuo* and the crude product was purified by column chromatography (*n*-hexanes / ethyl acetate (9:1), R_f = 0.54) to afford the product as an off white solid in a yield of 403 mg (79 %).

$^1\text{H NMR}$ (500 MHz, CDCl_3): δ = 7.94 (d, 1H, 4J = 2.2 Hz, 1H, Ar-*H-f*), 7.64 – 7.59 (m, 2H, Ar-*H-j*, Tph-*H*), 7.39 (d, 1H, 3J = 3.6 Hz, Tph-*H*), 7.35 (d, 1H, 3J = 8.6 Hz, Ar-*H-i*), 1.36 (s, 12H, pin- $\text{C}(\text{CH}_3)_4$) ppm.

$^{13}\text{C NMR}$ (125 MHz, CDCl_3): δ = 147.1 (Ar-*C-h*), 146.2, 146.2 (Ar-*C-e*, Tph-*C-d*), 138.6 (Tph-*CH*), 135.9 (OTf-*C*), 131.6 (Ar-*C-f*), 126.4 (Ar-*C-j*), 126.1 (Tph-*CH*), 123.2 (Ar-*C-i*), 116.5 (Ar-*C-g*), 84.4 (pin- $\text{C}(\text{CH}_3)_4$), 24.8 (pin- $\text{C}(\text{CH}_3)_4$) ppm.^{3,9}

$^{11}\text{B NMR}$ (160 MHz, CDCl_3): δ = 28.6 ppm.

$^{19}\text{F NMR}$ (470 MHz, CDCl_3): δ = 73.2 ppm.

M.p.: 65 °C.

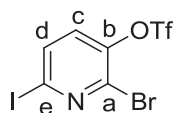
IR (ATR): $\tilde{\nu}$ = 2987 (w), 2935(w), 1531 (m), 1455 (m), 1425 (m), 1350 (s), 1327 (s), 1280 (s), 1134 (s), 1073 (m), 1023 (m), 886 (m), 875 (m), 813 (m), 785 (m), 664 (m), 602 (s) cm^{-1} .

MS (EI, 70 eV): m/z (%) = 514/512 (20)/(19) $[\text{M}]^+$, 381/379 (93)/(100) $[\text{M}-\text{SO}_2\text{CF}_3]^+$.

MS (CI, isobutane): m/z (%) = 571/569 (18)/(19) $[\text{M} + \text{isobutane} + \text{H}]^+$, 515/513 (100)/(95) $[\text{M} + \text{H}]^+$.

HRMS (ESI): m/z found 534.9649; calcd. for $\text{C}_{17}\text{H}_{17}\text{BBrF}_3\text{NaO}_5\text{S}_2$ 534.9638.

(9) The signal of the triflate group was not visible in the $^{13}\text{C NMR}$.

2-Bromo-6-iodopyridin-3-yl trifluoromethanesulfonate (16)

Trifluoromethanesulfonic anhydride (690 μL , 1.16 g, 4.09 mmol) was added over a course of 5 min to a solution of 4-bromo-6-iodopyridin-3-ol (1.10 g, 3.68 mmol) and pyridine (1.88 mL) at 0 °C. The resulting yellow mixture was stirred at 0 °C for 5 min and then allowed to warm to 20 °C and stirred for 25 h. The resulting mixture was poured into water (50 mL) and extracted with ethyl ether (3 x 50 mL). The ether extract was washed sequentially with water (2 x 30 mL), and a concentrated sodium chloride solution (2 x 30 mL), dried with magnesium sulfate and concentrated *in vacuo*. The residue was purified by column chromatography (*n*-hexanes / ethyl acetate (9:1), R_f = 0.5) to yield 1.43 g (94 %) of a slightly yellow oil.

$^1\text{H NMR}$ (500 MHz, CDCl_3): δ = 7.77 (d, 1H, 3J = 8.4 Hz, Pyr-*H*-d), 7.30 (d, 1H, 3J = 8.4 Hz, Pyr-*H*-c) ppm.

$^{13}\text{C NMR}$ (125 MHz, CDCl_3): δ = 145.2 (Pyr-*C*-b), 135.3 (Pyr-*C*-d), 131.7 (Pyr-*C*-c), 119.8 (Pyr-*C*-a), 117.2 (OTf-*C*), 113.6 (Pyr-*C*-e) ppm.⁹

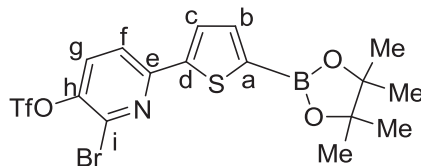
$^{19}\text{F NMR}$ (470 MHz, CDCl_3): δ = 72.9 ppm.

IR (ATR): $\tilde{\nu}$ = 3113 (w), 1551 (m), 1431 (m), 1403 (s), 1335 (m), 1204 (s), 1131 (s), 1100 (m), 1045 (s), 867 (s), 784 (s), 755 (s), 667 (m), 635 (m), 603 (s), 576 (s), 515 (m) cm^{-1} .

MS (EI, 70 eV): m/z (%) = 433/431 (79)/(100) $[\text{M}]^+$.

MS (CI, isobutane): m/z (%) = 434/432 (100)/(93) $[\text{M} + \text{H}]^+$.

HRMS (ESI): m/z found 430.7924; calcd. for $\text{C}_6\text{H}_2\text{BrINO}_3\text{S}$ 430.7936.

4,4,5,5-Tetramethyl-2-(5-(2-bromo-3-trifluoromethanesulfonate)pyridine-6-yl)-thiophen-2-yl)-1,3,2-dioxaborolane (17)

4,4,5,5-Tetramethyl-2-(5-(trimethylstannyl)thiophen-2-yl)-1,3,2-dioxaborolane (374 mg, 1.00 mmol), $[\text{Pd}(\text{PPh}_3)_4]$ (23 mg, 2 mol%) and the 2-bromo-6-iodopyridin-3-yl trifluoromethanesulfonate (432 mg, 1.00 mmol) were dissolved in DMF (4 mL). The mixture was heated to 100 °C in a microwave for 300 min and was then filtered over a short plug of celite. The solvent was removed *in vacuo* and the crude product was purified by column chromatography (*n*-hexanes / ethyl acetate (9:1), R_f = 0.42) to afford the product as a colorless solid in a yield of 420 mg (82 %).

$^1\text{H NMR}$ (500 MHz, CDCl_3): δ = 7.72 (d, 1H, 3J = 3.7 Hz, Tph-*H*), 7.64 – 7.61 (m, 2H, Pyr-*H*), 7.61 (d, 1H, 3J = 3.7 Hz, Tph-*H*), 1.36 (s, 12H, pin- $\text{C}(\text{CH}_3)_4$) ppm.

$^{13}\text{C NMR}$ (125 MHz, CDCl_3): δ = 155.5 (Pyr-*C*-h), 152.4 (Tph-*C*-d), 147.1 (Pyr-*C*-e), 142.9 (OTf-*C*), 137.9 (Tph-*CH*), 135.3 (Pyr-*C*-i), 131.2 (Pyr-*CH*), 128.2 (Tph-*CH*), 119.1 (Pyr-*CH*), 84.5 (pin- $\text{C}(\text{CH}_3)_4$), 24.8 (pin- $\text{C}(\text{CH}_3)_4$) ppm.^{3,9}

$^{11}\text{B NMR}$ (160 MHz, CDCl_3): δ = 28.6 ppm.

$^{19}\text{F NMR}$ (470 MHz, CDCl_3): δ = 73.0 ppm.

M.p.: 121 °C.

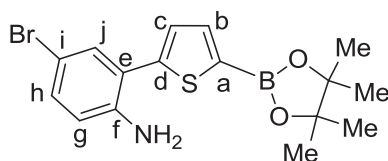
IR (ATR): $\tilde{\nu}$ = 2986(m), 1547 (w), 1531 (m), 1482 (w), 1421 (s), 1347 (s), 1321 (s), 1206 (s), 1135 (s), 1047 (m), 874 (m), 852 (m), 789 (m), 762 (m), 665 (m), 603 (s) cm^{-1} .

MS (EI, 70 eV): m/z (%) = 516/514 (100)/(84) $[\text{M}]^+$.

MS (CI, isobutane): m/z (%) = 516/514 (14)/(22) $[\text{M}]^+$, 456/454 (100)/(98) $[\text{M} - \text{CF}_3\text{O}_2\text{S} + \text{H}]^+$.

HRMS (ESI): m/z found 535.9608; calcd. for $\text{C}_{16}\text{H}_{16}\text{BBrF}_3\text{NNaO}_5\text{S}_2$ 535.9591.

5-Bromo-2-(5-(4,4,5,5-tetramethyl-1,3,2-dioxaborolan-2-yl)thiophen-2-yl)aniline (19)



4,4,5,5-Tetramethyl-2-(5-(trimethylstannyl)thiophen-2-yl)-1,3,2-dioxaborolane (374 mg, 1.00 mmol), [Pd(PPh₃)₄] (2 mol%, 23 mg) and the 2-iodo-4-bromoaniline (298 mg, 1.00 mmol) were dissolved in DMF (4 mL). The mixture was heated to 100 °C in the microwave for 120 min and was then filtered over a short plug of celite. The solvent was removed *in vacuo* and the crude product was purified by column chromatography (*n*-hexanes / ethyl acetate (9:1), R_f = 0.26) to afford the product as yellow oil in a yield of 285 mg (75 %).

¹H NMR (500 MHz, DMSO-d₆): δ = 6.73 (d, ³J = 3.6 Hz, 1H, Tph-H), 6.54 (d, ³J = 3.6 Hz, 1H, Tph-H), 6.45 (d, ⁴J = 2.4 Hz, 1H, Ar-H-j), 6.38 (dd, ³J = 8.7, ⁴J = 2.4 Hz, 1H, Ar-H-h), 5.93 (d, ³J = 8.7 Hz, 1H, Ar-H-g), 4.48 (s, 2H, NH₂), 0.47 (s, 12H, (pin-C(CH₃)₄)) ppm.

¹³C NMR (125 MHz, DMSO-d₆): δ = 147.1 (Tph-C-d), 145.4 (Ar-C-f), 138.5 (Tph-C-b), 132.2 (Ar-C-j), 131.9 (Ar-C-h), 128.1 (Tph-C-c), 120.3 (Ar-C-e), 118.3 (Ar-C-g), 107.4 (Ar-C-i), 84.5 (pin-C(CH₃)₄), 25.0 (pin-C(CH₃)₄) ppm.³

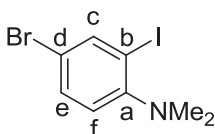
¹¹B NMR (160 MHz, CDCl₃): δ = 28.5 ppm.

IR (ATR): $\tilde{\nu}$ = 2978 (w), 1528 (m), 1453 (s), 1353 (s), 1257 (s), 1139 (s), 1072 (s), 1053 (m), 1018 (m), 852 (m), 806 (s), 681 (m), 663 (s) cm⁻¹.

MS (EI, 70 eV): *m/z* (%) = 381/379 (94)/(100) [M]⁺.

MS (CI, isobutane): *m/z* (%) = 381/379 (100)/(73) [M]⁺.

HRMS (ESI): *m/z* found 408.0799; calcd. for C₁₈H₂₄BBrNaO₂S 408.0799.

4-Bromo-2-iodo-*N,N*-dimethylaniline (20)

Potassium carbonate (1.38 g, 10.0 mmol) was added to a solution of the 2-iodo-4-bromoaniline (1.49, 5.00 mmol) and iodomethane (4.26 g, 30.0 mmol) in acetonitrile (30 mL). The resulting mixture was heated to reflux for 24 h. Water (30 mL) was added to the reaction mixture and the resulting solution was extracted with diethyl ether (3×30 mL). The combined organic layers were dried over anhydrous magnesium sulfate. The solvent was removed *in vacuo* and the residue was purified by flash column chromatography (*n*-hexanes / ethyl acetate (9:1), R_f = 0.53) as the eluent to afford 1.04 g (64 %) as pale orange oil.

¹H NMR (500 MHz, CDCl₃): δ = 7.95 (d, ⁴J = 2.3 Hz, 1H, Ar-H-c), 7.41 (dd, ³J = 8.5, ⁴J = 2.3 Hz, 1H, Ar-H-e), 6.93 (d, ³J = 8.5 Hz, 1H, Ar-H-f), 2.73 (s, 6H, N(CH₃)₂) ppm.

¹³C NMR (125 MHz, CDCl₃): δ = 154.0 (Ar-C-a), 142.0 (Ar-C-c), 131.9 (Ar-C-e), 121.4 (Ar-C-f), 116.4 (Ar-C-d), 97.4 (Ar-C-b), 44.8 (N(CH₃)₂) ppm.

IR (ATR): $\tilde{\nu}$ = 2940 (w), 2827 (m), 2779 (w), 1464 (s), 1449 (s), 1312 (m), 1156 (s), 1021 (s), 942 (m), 869 (m), 814 (s), 772 (s), 653 (m), 595 (s), 557 (s) cm⁻¹.

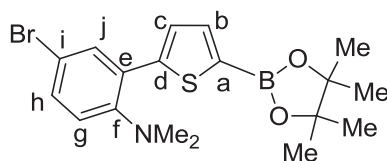
MS (EI, 70 eV): *m/z* (%) = 327/325 (90)/(100) [M]⁺.

MS (CI, isobutane): *m/z* (%) = 328/326 (100)/(99) [M+H]⁺.

HRMS (EI): *m/z* found 324.8953; calcd. for C₈H₉BrIN 324.8963.

The ¹H NMR spectral data are in good agreement with the literature data.¹⁰

(10) Y. Chen, C.-H. Cho, R. C. Larock, *Org. Lett.* **2009**, *11*, 173.

5-Bromo-*N,N*-dimethyl-2-(5-(4,4,5,5-tetramethyl-1,3,2-dioxaborolan-2-yl)thiophen-2-yl)aniline (21)

4,4,5,5-Tetramethyl-2-(5-(trimethylstannyl)thiophen-2-yl)-1,3,2-dioxaborolane (374 mg, 1.00 mmol), [Pd(PPh₃)₄] (2 mol%, 23 mg) and 4-Bromo-2-iodo-*N,N*-dimethylaniline (325 mg, 1.00 mmol) were dissolved in DMF (4 mL). The mixture was heated to 100 °C in a microwave for 210 min and was then filtered over a short plug of celite. The solvent was removed *in vacuo* and the crude product was purified by column chromatography (*n*-hexanes / ethyl acetate (9:1), R_f = 0.5) to afford the product as a colorless solid in a yield of 297 mg (73 %).

¹H NMR (500 MHz, CDCl₃): δ = 7.63 (d, ⁴J = 2.4 Hz, 1H, Ar-*H*-j), 7.57 (d, ³J = 3.6 Hz, 1H, Tph-*H*), 7.46 (d, ³J = 3.6 Hz, 1H, Tph-*H*), 7.32 (dd, ³J = 8.6, ⁴J = 2.4 Hz, 1H, Ar-*H*-h), 6.97 (d, ³J = 8.6 Hz, 1H, Ar-*H*-g), 2.60 (s, 6H, N(CH₃)₂), 1.36 (s, 12H, (pin-C(CH₃)₄)) ppm.

¹³C NMR (125 MHz, CDCl₃): δ = 150.4 (Ar-C-f), 147.4 (Tph-C-d), 136.8 (Tph-CH), 132.5 (Ar-C-g), 131.0 (Ar-C-i), 130.5 (Ar-C-e), 126.9 (Tph-CH), 121.1 (Ar-C-j), 115.3 (Ar-C-h), 84.0 (pin-C(CH₃)₄), 43.9 (N(CH₃)₂), 24.8 (pin-C(CH₃)₄) ppm.³

¹¹B NMR (160 MHz, CDCl₃): δ = 28.9 ppm.

M.p.: 41 °C.

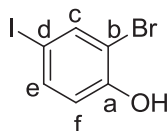
IR (ATR): $\tilde{\nu}$ = 2983 (w), 1526 (m), 1450 (m), 1348 (s), 1326 (s), 1297 (m), 1139 (s), 1074 (m), 852 (m), 821 (s), 665 (s) cm⁻¹.

MS (EI, 70 eV): *m/z* (%) = 409/407 (100)/(84) [M]⁺.

MS (CI, isobutane): *m/z* (%) = 466/464 (34)/(16) [M + isobutane + H]⁺, 409/407 (100)/(85) [M]⁺.

HRMS (ESI): *m/z* found 402.0318; calcd. for C₁₆H₁₉BBrNNaO₂S 402.0306.

2-Bromo-4-iodophenol (22)



4-Iodo-phenol (10.0 g, 45.4 mmol) was dissolved in methanol (60 mL). Bromine (2.57 mL, 49.9 mmol) was added dropwise at 0 °C over the course of 5 min. After 30 min, a saturated sodium thiosulfate solution (50 mL) was added, the reaction mixture was extracted with diethyl ether (3 x 50 mL), washed with water (1 x 50 mL), dried over sodium sulfate, and concentrated *in vacuo*. Purification by column chromatography (hexanes / dichloromethane (2:1), R_f = 0.56) gave the product in a yield of 11.2 g (83 %).

¹H NMR (500 MHz, DMSO-*d*₆): δ = 10.5 (s, 1H, Ar-OH), 7.75 (d, ³J = 2.1 Hz, 1H, Ar-*H*-c), 7.47 (dd, ³J = 8.5 Hz, ³J = 2.1 Hz, 1, Ar-*H*-e), 6.77 (d, ³J = 8.5 Hz, 1H, Ar-*H*-f).

¹³C NMR (125 MHz, DMSO-*d*₆): δ = 154.7 (Ar-C-a), 140.4 (Ar-C-e), 137.7 (Ar-C-c), 119.1 (Ar-C-f), 111.3 (Ar-C-b), 81.4 (Ar-C-d) ppm.

M.p.: 48 °C.

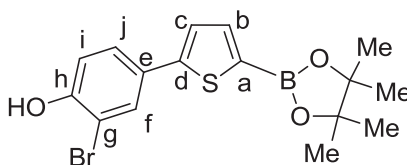
MS (EI, 70 eV): *m/z* (%) = 300/288 (100)/(93) [M]⁺.

MS (CI, isobutane): *m/z* (%) = 300/288 (100)/(85) [M]⁺.

IR (ATR): $\tilde{\nu}$ = 3365 (m), 3076 (w), 3053 (w), 1880 (w), 1737 (w), 1566 (s), 1464 (s), 1393 (m), 1328 (m), 1267 (m), 1243 (s), 1182 (s), 1036 (s), 871 (s), 809 (s), 675 (s), 606 (s), 541 (s) cm⁻¹.

HRMS (EI): *m/z* found 297.8496; calcd. for C₆H₄BrI 297.8490.

4,4,5,5-Tetramethyl-2-(5-(3-bromo-phen-4-ol)thiophen-2-yl)-1,3,2-dioxaborolane (23)



4,4,5,5-Tetramethyl-2-(5-(trimethylstannyl)thiophen-2-yl)-1,3,2-dioxaborolane (374 mg, 1.00 mmol), $[\text{Pd}(\text{PPh}_3)_4]$ (2 mol%, 23 mg) and 2-bromo-4-iodophenol (299 mg, 1.00 mmol) were dissolved in DMF (4 mL). The mixture was heated to 100 °C in a microwave for 60 min and was then filtered over a short plug of celite. The solvent was removed *in vacuo* and the crude product was purified by column chromatography (*n*-hexanes / ethyl acetate (9:1), $R_f = 0.15$) to afford the product as a colorless solid in a yield of 246 mg (65 %).

$^1\text{H NMR}$ (500 MHz, CD_2Cl_2): $\delta = 7.8$ (d, 1H, $^4J = 2.2$ Hz, Ar-*H*-f), 7.56 – 7.53 (m, 2H, Tph-*H*-b, Ar-*H*-j), 7.31 (d, 1H, $^3J = 3.6$ Hz, Tph-*H*-c), 7.06 (d, 1H, $^3J = 8.5$ Hz, Ar-*H*-i), 5.72 (s, 1H, Ar-*OH*), 1.36 (s, 12H, (pin-C(CH_3) $_4$)) ppm.

$^{13}\text{C NMR}$ (125 MHz, CD_2Cl_2): $\delta = 152.4$ (Ar-*C*-h), 149.4 (Tph-*C*-d), 138.2 (Tph-*C*-b), 129.8 (Ar-*C*-f), 128.7 (Ar-*C*-e), 127.3 (Ar-*C*-j), 124.4 (Tph-*C*-c), 116.6 (Ar-*C*-i), 110.7 (Ar-*C*-g), 84.3 (pin-C(CH_3) $_4$), 24.7 (pin-C(CH_3) $_4$) ppm.³

$^{11}\text{B NMR}$ (160 MHz, CDCl_3): $\delta = 28.7$ ppm.

M.p.: 58 °C.

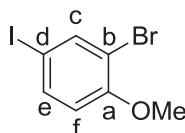
IR (ATR): $\tilde{\nu} = 2926$ (m), 2855 (w), 1523 (m), 1470 (s), 1425 (m), 1346 (s), 1286 (s), 1140 (s), 1065 (s), 1016 (m), 956 (w), 852 (s), 805 (m), 658 (w), 663 (s) cm^{-1} .

MS (EI, 70 eV): m/z (%) = 456/454 (82)/(74) $[\text{M}]^+$, 305 (100) $[\text{M}-\text{Br}-\text{C}_3\text{H}_{11}]^+$.

MS (CI, isobutane): m/z (%) = 457/455 (65)/(76) $[\text{M} + \text{H}]^+$, 456/454 (100)/(81) $[\text{M} - \text{H} + \text{H}]^+$.

HRMS (ESI): m/z found 403.0160; calcd. for $\text{C}_{16}\text{H}_{18}\text{BBrNaO}_3\text{S}$ 403.0145.

2-Bromo-4-iodo-1-methoxybenzene (24)



2-Bromo-4-iodophenol (600 mg, 2.01 mmol) was dissolved in THF (9 mL) and KOH (224 mg, 4.00 mmol) was added. The mixture was stirred for 30 min under nitrogen and the MeI (320 μL , 5.16 mmol) was added. After 16 hours, water (30 mL) and diethyl ether (30 mL) were added and the mixture was stirred for another 30 min. The organic phase was collected, and the aqueous phase was extracted with diethyl ether (2 x 30 mL). The combined organic extracts were dried with magnesium sulfate, filtered and concentrated *in vacuo*. The crude product was filtered over silica (40 g; *n*-hexane) to afford 437 mg (70 %) of the product as a colorless solid.

$^1\text{H NMR}$ (500 MHz, CDCl_3): $\delta = 7.82$ (d, $^4J = 2.1$ Hz, 1H, Ar-*H*-c), 7.55 (dd, $^3J = 8.6$, $^4J = 2.1$ Hz, 1H, Ar-*H*-e), 6.66 (d, $^3J = 8.6$ Hz, 1H, Ar-*H*-f), 3.87 (s, 3H, OCH_3) ppm.

$^{13}\text{C NMR}$ (125 MHz, CDCl_3): $\delta = 141.0$ (Ar-*C*-c), 137.3 (Ar-*C*-e), 113.3 (Ar-*C*-f), 113.0 (Ar-*C*-a), 101.6 (Ar-*C*-b), 86.6 (Ar-*C*-d), 56.3 (OCH_3) ppm.

M.p.: 82 °C.

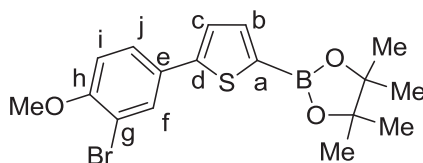
IR (ATR): $\tilde{\nu} = 3013$ (w), 2933 (w), 1570 (w), 1471 (m), 1456 (s), 1283 (s), 1247 (s), 1147 (m), 1047 (s), 1015 (s), 877 (m), 803 (s), 675 (m), 606 (m) cm^{-1} .

MS (EI, 70 eV): m/z (%) = 314/312 (100)/(94) $[\text{M}]^+$.

MS (CI, isobutane): m/z (%) = 315/313 (75)/(35) $[\text{M} + \text{H}]^+$.

HRMS (EI): m/z found 311.8656; calcd. for $\text{C}_7\text{H}_6\text{BrIO}$ 311.8647.

4,4,5,5-Tetramethyl-2-(5-(3-bromo-phen-4-methoxy)thiophen-2-yl)-1,3,2-dioxaborolane (25)



4,4,5,5-Tetramethyl-2-(5-(trimethylstannyl)thiophen-2-yl)-1,3,2-dioxaborolane (374 mg, 1.00 mmol), [Pd(PPh₃)₄] (2 mol%, 23 mg) and 2-bromo-4-iodo-1-methoxybenzene (313 mg, 1.00 mmol) were dissolved in DMF (4 mL). The mixture was heated to 100 °C in a microwave for 120 min and was then filtered over a short plug of celite. The solvent was removed *in vacuo* and the crude product was purified by column chromatography (*n*-hexanes / ethyl acetate (9:1), R_f = 0.22) to afford the product as a colorless solid in a yield of 327 mg (83 %).

¹H NMR (500 MHz, CDCl₃): δ = 7.84 (d, ⁴J = 2.2 Hz, 1H, Ar-*H*-f), 7.57 (d, ³J = 3.6 Hz, 1H, Tph-*H*), 7.54 (dd, ³J = 8.6, ⁴J = 2.2 Hz, 1H, Ar-*H*-j), 7.27 (d, ³J = 3.6 Hz, 1H, Tph-*H*), 6.91 (d, ³J = 8.6 Hz, 1H, Ar-*H*-i), 3.92 (s, 3H, OCH₃), 1.35 (s, 12H, (pin-C(CH₃)₄)) ppm.

¹³C NMR (125 MHz, CDCl₃): δ = 155.7 (Ar-C-h), 149.5 (Tph-C-d), 138.2 (Tph-C-b), 131.0 (Ar-C-f), 128.5 (Ar-C-e), 126.3 (Ar-C-j), 124.2 (Tph-*H*-c), 112.2 (Ar-C-g), 112.1 (Ar-C-i), 56.4 (OCH₃), 84.2 (pin-C(CH₃)₄), 24.8 (pin-C(CH₃)₄) ppm.³

¹¹B NMR (160 MHz, CDCl₃): δ = 28.5 ppm.

M.p.: 113 °C.

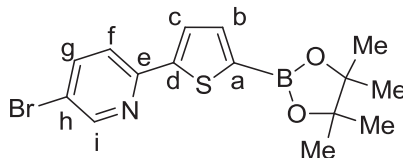
IR (ATR): $\tilde{\nu}$ = 2977 (w), 1731 (w), 1615 (m), 1529 (m), 1487 (m), 1459 (s), 1348 (s), 1139 (s), 1066 (m), 1019 (m), 851 (s), 812 (s), 663 (s) cm⁻¹.

MS (EI, 70 eV): *m/z* (%) = 396/394 (100)/(80) [M]⁺.

MS (CI, *isobutane*): *m/z* (%) = 453/451 (6)/(12) [M + *isobutane* + H]⁺, 397/395 (100)/(88) [M + H]⁺.

HRMS (ESI): *m/z* found 417.0314; calcd. for C₁₇H₂₀BBrNaO₃S 417.0318.

4,4,5,5-Tetramethyl-2-(5-(2-(3-bromo)pyridin)thiophen-2-yl)-1,3,2-dioxaborolane (27)



4,4,5,5-Tetramethyl-2-(5-(trimethylstannyl)thiophen-2-yl)-1,3,2-dioxaborolane (374 mg, 1.00 mmol), [Pd(PPh₃)₄] (23 mg, 2 mol%) and the 5-bromo-2-iodopyridine (284 mg, 1.00 mmol) were dissolved in DMF (4 mL). The mixture was heated to 100 °C in a microwave for 300 min and was then filtered over a short plug of celite. The solvent was removed *in vacuo* and the crude product was purified by column chromatography (*n*-hexanes / ethyl acetate (9:1), R_f = 0.1) to afford the product as a colorless solid in a yield of 298 mg (81 %).

¹H NMR (500 MHz, CDCl₃): δ = 8.62 (dd, 1H, ⁴J = 2.4 Hz, ⁵J = 0.7 Hz, Pyr-*H*-i), 7.80 (dd, 1H, ³J = 8.5, ⁴J = 2.4 Hz, Pyr-*H*-g), 7.65 (d, 1H, ³J = 3.7 Hz, Tph-*H*), 7.60 (d, 1H, ³J = 3.7 Hz, Tph-*H*), 7.54 (dd, 1H, ³J = 8.5 Hz, ⁵J = 0.7 Hz, Pyr-*H*-f), 1.36 (s, 12H, (pin-C(CH₃)₄)) ppm.

¹³C NMR (125 MHz, CDCl₃): δ = 151.0 (Pyr-C-e), 150.7 (Pyr-C-i), 149.8 (Pyr-C-d), 139.2 (Pyr-C-g), 138.0 (Tph-CH), 126.4 (Tph-CH), 120.5 (Pyr-C-f), 118.9 (Pyr-C-h), 84.3 (pin-C(CH₃)₄), 24.8 (pin-C(CH₃)₄) ppm.³

¹¹B NMR (160 MHz, CDCl₃): δ = 28.7 ppm.

M.p.: 109 °C.

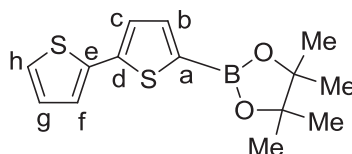
IR (ATR): $\tilde{\nu}$ = 2978 (w), 1571 (w), 1533 (m), 1486 (w), 1443 (s), 1346 (s), 1331 (s), 1302 (s), 1138 (s), 1071 (m), 1026 (m), 1001 (m), 853 (s), 813 (m), 742 (m), 662 (s) cm⁻¹.

MS (EI, 70 eV): *m/z* (%) = 367/365 (100)/(84) [M]⁺.

MS (CI, *isobutane*): *m/z* (%) = 410/408 (4)/(5) [M + *isobutane* + H]⁺, 368/366 (92)/(100) [M + H]⁺.

HRMS (ESI): Found 366.0337; calcd. for C₁₅H₁₈BBrNO₂S 366.0329.

2-([2,2'-Bithiophen]-5-yl)-4,4,5,5-tetramethyl-1,3,2-dioxaborolane (29)



This reaction was performed with two competing electrophiles to show that there is selectivity even if there are two electrophiles available.

4,4,5,5-Tetramethyl-2-(5-(trimethylstannyl)thiophen-2-yl)-1,3,2-dioxaborolane (374 mg, 1.00 mmol), [Pd(PPh₃)₄] (23 mg, 2 mol%), the standard triisopropylbenzene (100 μL) and the electrophiles 2-iodothiophene (205 mg, 1.00 mmol) and 2-bromothiophene (158 mg, 1.00 mmol) were dissolved in DMF (4 mL). The mixture was heated to 100 °C in a microwave for 20 min and was then filtered over a short plug of celite using ethyl acetate as solvent and used for GC measurements. The solvent was removed *in vacuo* and the crude product was purified by column chromatography (*n*-hexanes / ethyl acetate (9:1), R_f = 0.34) to afford the product as colorless oil in a yield of 228 mg (78 %).

¹H NMR (500 MHz, CDCl₃): δ = 7.52 (d, 1H, ³J = 3.6 Hz, Tph-*H*-b), 7.25 – 7.21 (m, 3H, Tph-*H*-c, *H*-f, *H*-h), 7.02 (t, 1H, ³J = 4.4 Hz Tph-*H*-g), 1.35 (s, 12H, pin-C(CH₃)₄) ppm.

¹³C NMR (126 MHz, CDCl₃): δ = 144.1 (Tph-C-d), 137.9 (Tph-C-b), 137.3 (Tph-C-e), 127.9 (Tph-C-g), 124.9, 124.9 (2 x Tph-CH), 124.5 (Tph-CH), 84.2 (pin-C(CH₃)₂), 24.7 (pin-C(CH₃)₂) ppm.³

¹¹B NMR (160 MHz, CDCl₃): δ = 28.7 ppm.

IR (ATR): $\tilde{\nu}$ = 2977 (w), 1510 (m), 1459 (s), 1360 (m), 1343 (s), 1267 (m), 1138 (s), 1064 (s), 1014 (m), 852 (m), 805 (m), 960 (s), 662 (s) cm⁻¹.

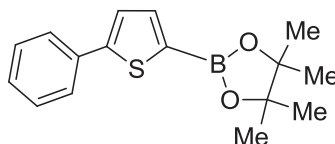
MS (EI, 70 eV): *m/z* (%) = 292 (100) [M]⁺.

MS (CI, isobutane): *m/z* (%) = 349 (23) [M + isobutane + H]⁺, 293 (100) [M+H]⁺.

HRMS (ESI): *m/z* found 293.0842; calcd. for C₁₄H₁₈BO₂S₂ 293.0836.

The NMR data are in agreement with the data found in the literature where the compound was prepared in a different way.¹¹

4,4,5,5-Tetramethyl-2-(5-phenylthiophen-2-yl)-1,3,2-dioxaborolane (31)



This reaction was performed with two competing electrophiles to show that there is selectivity even if there are two electrophiles available.

4,4,5,5-Tetramethyl-2-(5-(trimethylstannyl)thiophen-2-yl)-1,3,2-dioxaborolane (374 mg, 1.00 mmol), [Pd(PPh₃)₄] (23 mg, 2 mol%), the standard triisopropylbenzene (100 μL) and the electrophiles 1-iodobenzene (205 mg, 1.00 mmol) and 1-bromobenzene (158 mg, 1.00 mmol) were dissolved in DMF (4 mL). The mixture was heated to 100 °C in a microwave for 20 min and was then filtered over a short plug of celite using ethyl acetate as solvent and used for GC measurements. The solvent was removed *in vacuo* and the crude product was purified by column chromatography (*n*-hexanes / ethyl acetate (9:1), R_f = 0.41) to afford the product as a colorless solid in a yield of 263 mg (92 %).

¹H NMR (500 MHz, CDCl₃): δ = 7.66 – 7.63 (m, 2H, Ar-*H*), 7.60 (d, 1H, ³J = 3.6 Hz, Tph-*H*), 7.40 – 7.37 (m, 3H, Tph-*H*, 2 x Ar-*H*), 7.30 (t, 1H, ³J = 7.4 Hz, Ar-*H*), 1.35 (s, 12H, pin-C(CH₃)₄) ppm.

¹³C NMR (126 MHz, CDCl₃): δ = 151.5 (Tph-C), 138.3 (Tph-CH), 134.4 (Ar-C), 129.1 (Ar-CH), 128.1 (Ar-CH), 126.4 (Ar-CH), 124.6 (Tph-CH), 84.3 (pin-C(CH₃)₂), 24.9 (pin-C(CH₃)₄) ppm.³

¹¹B NMR (160 MHz, CDCl₃): δ = 28.8 ppm.

IR (ATR): $\tilde{\nu}$ = 2986 (m), 2932 (w), 1531 (s), 1499 (w), 1456 (s), 1443 (s), 1353 (s), 1331 (s), 1295 (s), 1137 (s), 1077 (m), 1020 (m), 854 (s), 813 (s), 758 (s), 662 (s) cm⁻¹.

MS (EI, 70 eV): *m/z* (%) = 286 (100) [M]⁺.

MS (CI, isobutane): *m/z* (%) = 287 (100) [M + H]⁺.

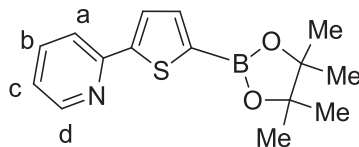
M.p.: 65 °C.

(11) A. Del-Grosso, M. D. Helm, S. A. Solomon, D. Caras-Quintero, M. J. Ingleson, *Chem. Comm.* **2011**, 47, 12459.

HRMS (ESI): m/z found 287.1279; calcd. for $C_{16}H_{20}BO_2S$ 287.1279.

The NMR data are in agreement with the data found in the literature where the compound was prepared in a different way.¹²

2-(5-(4,4,5,5-Tetramethyl-1,3,2-dioxaborolan-2-yl)thiophen-2-yl)pyridine (33)



This reaction was performed with two competing electrophiles to show that there is selectivity even if there are two electrophiles available.

4,4,5,5-Tetramethyl-2-(5-(trimethylstannyl)thiophen-2-yl)-1,3,2-dioxaborolane (374 mg, 1.00 mmol), $Pd(PPh_3)_4$ (23 mg, 2 mol%), the standard triisopropylbenzene (100 μ L) and the electrophiles 2-iodopyridine (205 mg, 1.00 mmol) and 2-bromopyridine (158 mg, 1.00 mmol) were dissolved in DMF (4 mL). The mixture was heated to 100 $^{\circ}C$ in a microwave for 20 min and was then filtered over a short plug of celite using ethyl acetate as solvent and used for GC measurements. The solvent was removed *in vacuo* and the crude product was purified by column chromatography (*n*-hexanes / ethyl acetate (9:1), $R_f = 0.36$) to afford the product as a colorless solid in a yield of 255 mg (89 %).

1H NMR (500 MHz, $CDCl_3$): $\delta = 8.53$ - 8.49 (m, 1H, Pyr-*H*-c), 7.64 - 7.58 (m, 3H, Pyr-*H*-b, Pyr-*H*-d, Tph-*H*), 7.55 (d, 1H, $^3J = 3.6$ Hz, Tph-*H*), 7.09 (ddd, 1H, $^3J = 6.7$, $^3J = 4.9$, $^4J = 1.7$ Hz, Pyr-*H*-a), 1.29 (s, 12H, pin- $C(CH_3)_4$) ppm.

^{13}C NMR (125 MHz, $CDCl_3$): $\delta = 152.4$ (Tph-*C*), 152.1 (Pyr-*C*), 151.0 (Tph-*C*), 149.7 (Pyr-*C*-c), 137.9 (Pyr-*C*-d), 136.6 (Tph-*CH*), 125.9 (Tph-*CH*), 122.2 (Pyr-*C*-a), 119.5 (Pyr-*C*-b), 84.2 (pin- $C(CH_3)_4$), 24.8 (pin- $C(CH_3)_4$) ppm.³

^{11}B NMR (160 MHz, $CDCl_3$): $\delta = 28.8$ ppm.

M.p.: 52 $^{\circ}C$.

IR (ATR): $\tilde{\nu} = 2976$ (m), 2929 (w), 1583 (m), 1532 (m), 1485 (m), 1447 (s), 1428 (s), 1350 (s), 1330 (s), 1303 (s), 1136 (s), 1079 (m), 1024 (m), 991 (m), 956 (m), 852 (s), 775 (s), 664 (s), 618 (w) cm^{-1} .

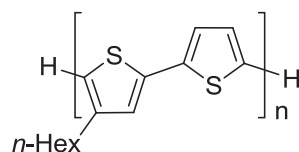
MS (EI, 70 eV): m/z (%) = 287 (100) $[M]^+$.

MS (CI, isobutane): m/z (%) = 288 (100) $[M + H]^+$.

HRMS (ESI): m/z found 288.1231; calcd. for $C_{15}H_{19}BNO_2S$ 288.1224.

(12) J. J. Apperloo, L. B. Groenendaal, H. Verheyen, M. Jayakannan, R. A. J. Janssen, A. Dkhissi, D. Beljonne, R. Lazzaroni, J.-L. Brédas, *Chem. Eur. J.* **2002**, 8, 2384.

Poly[4-hexyl-2,2'-bithiophene] (34)



4,4,5,5-Tetramethyl-2-(5-(5-bromo-3-*n*-hexylthiophen)thiophen-2-yl)-1,3,2-dioxaborolane (200 mg, 0.540 mmol) was placed in a flask and vacuum was applied. The flask was flooded with N₂. THF (stabilizer free, 30 mL) and 2 mol/L aqueous solution of sodium carbonate (6 mL) were added, and the mixture was stirred at 13 °C. Then, a solution of [Pd(*t*Bu₃)₂] (5.52 mg, 0.011 mmol, 2 mol % based on the monomer) in THF (2 mL) was added. Within 30 seconds, the solution became clear yellow, then orange and subsequently dark red. After 30 min a dark red particulate visible was found. The residue was precipitated in methanol (500 mL) and collected by solution centrifugation. This procedure was repeated another two times until the methanol remained colorless. The particulate was dried *in vacuo* to afford a dark red polymer in a yield of 151 mg (61 %).

The polymer was insoluble in CHCl₃, Pyridine, THF and pentane.

The images show the reaction progress:

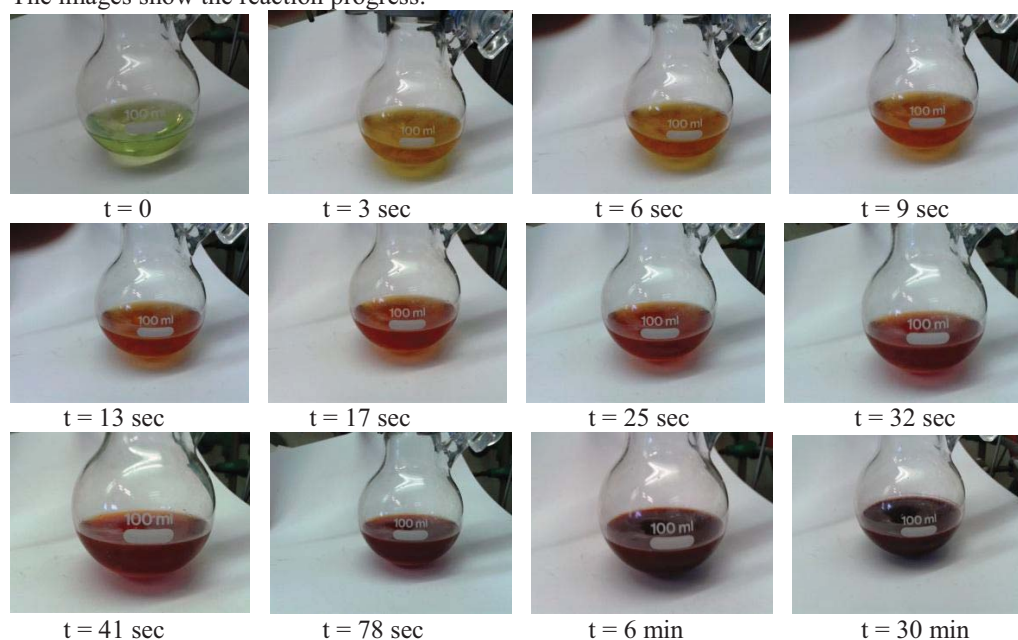


Figure SI 9. Images of the reaction mixture during the polymerization progress to afford the polymer **34**.

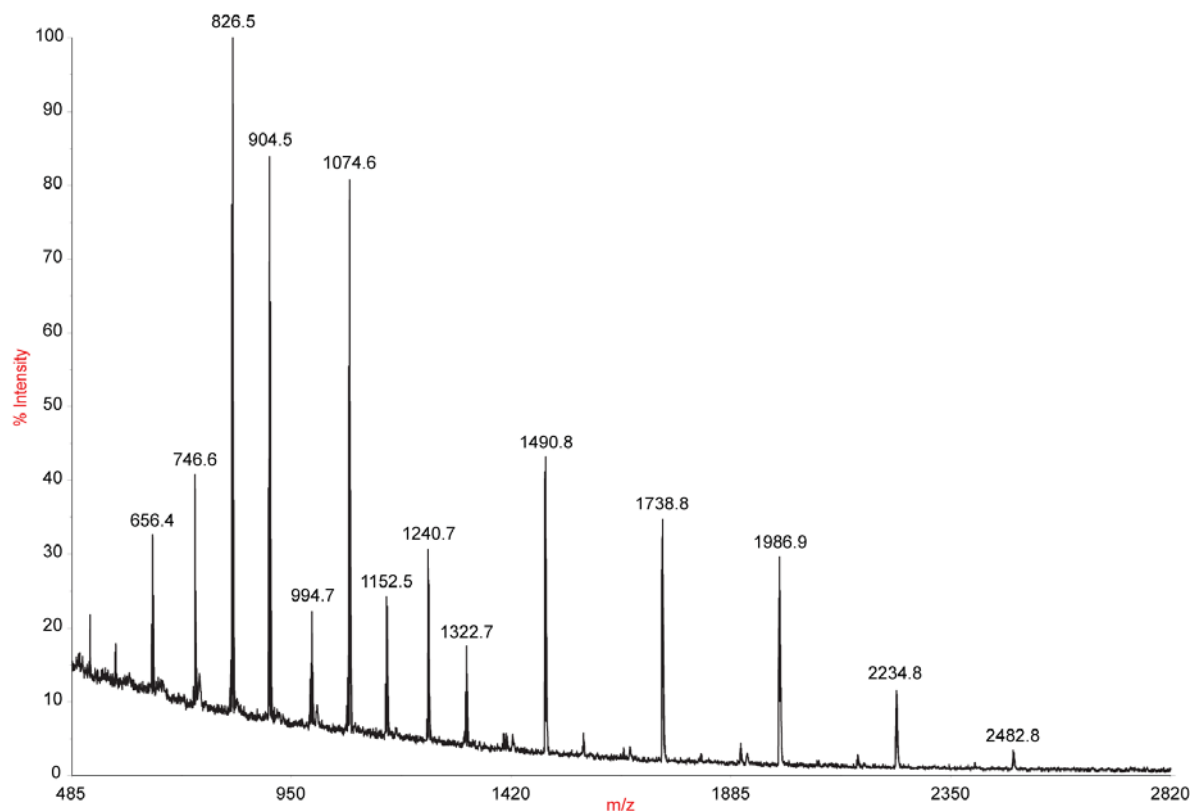


Figure SI 10. MALDI-ToF-ToF-MS of **34**, using dithranol as a matrix. The Peak with the mass 2482.8 m/z shows an oligomer of 10 repeating units with H-atoms as end groups. The mass difference between the peaks is exactly one monomer with a molecular weight of 284 g/mol.

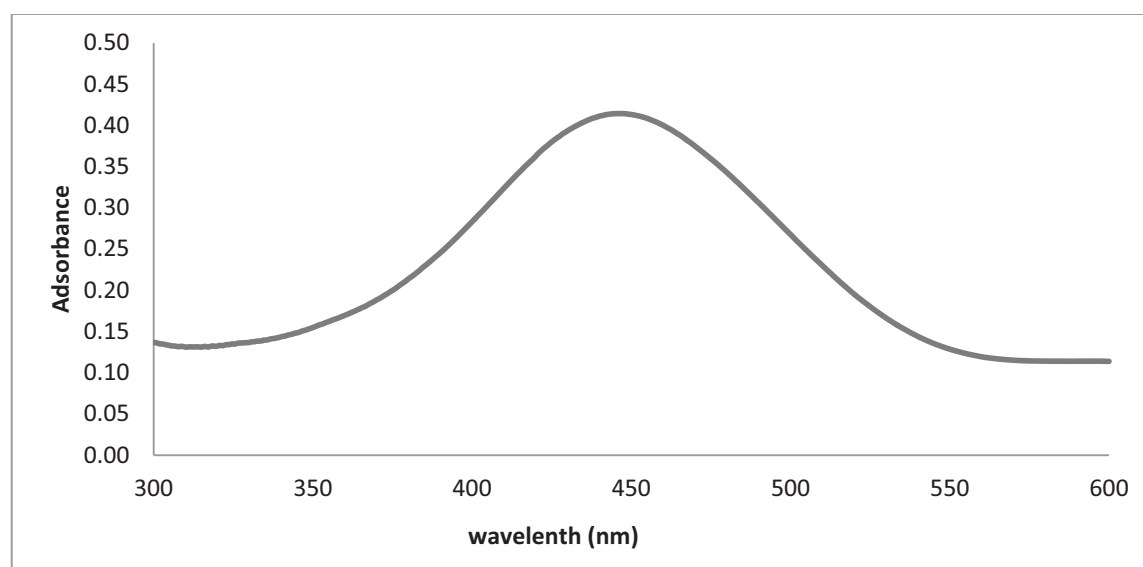
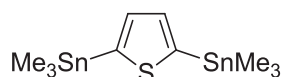


Figure SI 11. UV-Vis spectrum of the soluble fraction of **34** in chloroform, with $\lambda_{\max} = 446$ nm, which is close to regioregular P3HT with $\lambda_{\max} = 449$ nm.¹³

(13) I. F. Perepichka, D. F. Perepichka, *Handbook of Thiophene-Based Materials: Applications in Organic Electronics and Photonics*, 1st ed., John Wiley & Sons, Ltd., Chichester, UK, 2009.

2,5-Bis(trimethylstannyl)thiophene (35)

2,5-Bis(trimethylstannyl)thiophene was prepared similar to a method described in the literature by Seitz et al.^[13] and was modified as follows:

n-Butyllithium (16.0 mL, 40.0 mmol, 2.50 M in *n*-hexane) was added within 10 min to a solution of thiophene (1.56 g, 20.0 mmol) and TMEDA (5.96 mL, 40.0 mmol) in *n*-hexane (40 mL) at 0 °C. The reaction mixture was heated to reflux for 45 min and after cooling the suspension to 0 °C, a solution of trimethyltin chloride (7.97 g, 40.0 mmol) dissolved in THF (20 mL), was added over the course of 10 min. After removal of the cooling bath, the reaction mixture was stirred for 15 h at 24 °C and was then quenched with a saturated solution of ammonium chloride (50 mL). The aqueous layer was extracted with diethyl ether (3 x 50 mL) and the combined organic layers were washed with brine (2 x 40 mL). The organic layer was dried over magnesium sulfate and the volatiles were removed *in vacuo* to afford 7.65 g (93 %, Lit.¹⁴: 82 %) of a bright yellow solid.

¹H NMR (200 MHz, CDCl₃): δ = 7.40 (s, 2H, Tph-H), 0.39 (s, 18H, Sn(CH₃)₃) ppm.

¹³C NMR (50 MHz, CDCl₃): δ = 143.0 (Tph-C), 135.8 Tph-CH), -8.2 (Sn(CH₃)₃) ppm.

¹¹⁹Sn NMR (187 MHz, CDCl₃): δ = -27.9 ppm.

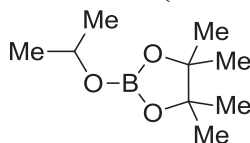
M.p.: 101 °C.

IR (ATR): $\tilde{\nu}$ = 3057 (w), 2982 (w), 2913 (w), 1564 (w), 1477 (w), 1390 (w), 1199 (w), 1255 (w), 1187 (w), 953 (m), 921 (w), 797 (s), 761 (s), 734 (s), 531 (s), 515 (s) cm⁻¹.

MS (EI, 70 eV): *m/z* (%) = 411 (8) [M]⁺, 395 (100) [M-CH₃]⁺, 365 (6) [M-C₃H₉]⁺.

MS (CI, isobutane): *m/z* (%) = 412 (17) [M + H]⁺, 411 (40) [M]⁺, 165 (100) [SnMe₃]⁺.

The NMR data are in agreement with the data found in the literature.¹³

2-Isopropoxy-4,4,5,5-tetramethyl-1,3,2-dioxaborolane (*i*PrO-BPin; 36)

2-Isopropoxy-4,4,5,5-tetramethyl-1,3,2-dioxaborolane was prepared similar to a method described in the literature by Andersen et al.^[14] and was modified as follows:

From a solution of triisopropyl borate (16.9 g, 90.0 mmol) and pinacol (10.6 g, 90.0 mmol) in *n*-hexane (130 mL), an isopropanol / *n*-hexane azeotrope was slowly distilled at 55-60 °C. The residue was distilled (90 °C, 1.00 mbar) to give 13.7 g (89 %, Lit.¹⁴: 89 %) of a colorless liquid.

¹H NMR (200 MHz, CDCl₃): δ = 4.29 (septet, 1H, ³J = 6.2 Hz, CH(CH₃)₂), 1.20 (s, 12H, pin-C(CH₃)₃), 1.15 (d, 6H, ³J = 6.2 Hz, CH(CH₃)₂) ppm.

¹³C NMR (50 MHz, CDCl₃): δ = 82.5 (pin-C(CH₃)₂), 67.4 (CH(CH₃)₂), 24.6 (pin-CH(CH₃)₂), 24.4 (CH(CH₃)₂) ppm.

¹¹B NMR (160 MHz, CDCl₃): δ = 21.8 ppm.

IR (ATR): $\tilde{\nu}$ = 2979 (w), 1504 (w), 1473 (w), 1444 (m), 1373 (w), 1345 (w), 1319 (m), 1148 (m), 1121 (m), 958 (w), 905 (s), 852 (m), 727 (s), 672 (m), 648 (m) cm⁻¹.

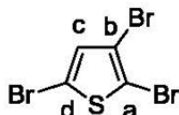
MS (EI, 70 eV): *m/z* (%) = 185 (12) [M]⁺, 170 (100) [M-CH₃]⁺.

MS (CI, isobutane): *m/z* (%) = 186 (2) [M + H]⁺, 171 (9) [M-CH₃ + H]⁺, 145 (100) [M-C₃H₇ + H]⁺.

The NMR data are in agreement with the data found in the literature.¹⁵

(14) D. E. Seitz, S.-H. Lee, R. N. Hanson, J. C. Bottaro, *Synth. Commun.* **1983**, *13*, 121.

(15) M. W. Andersen, B. Hildebrandt, G. Köster, R. W. Hoffmann, *Chem. Ber.* **1989**, *122* 1777.

2,3,5-Tribromothiophene (37)

2,3,5-Tribromothiophene was prepared similar to a method described by Brandsma et al.¹⁶ and was modified as follows:

A solution of bromine (16.7 mL, 325 mmol) in hydrobromic acid (48 %, 50 mL) was added to a mixture of thiophene (8.00 mL, 100 mmol), hydrobromic acid (48 %, 50 mL) and diethyl ether (12.5 mL) within 3.5 h with vigorous stirring while the internal temperature was kept below 10 °C. After the addition was finished, the mixture was warmed up to 20 °C and was stirred for 16 h. Then, sodium thiosulfate (200 mL) was added and the layers were separated. The aqueous layer was extracted (3 x 150 mL) with dichloromethane and the combined organic solutions were washed with brine (2 x 150 mL), dried over magnesium sulfate and subsequently concentrated *in vacuo*. The product was obtained as a colorless solid by sublimation (2×10^{-1} mbar, 20 °C) in a yield of 80 % (25.7 g).

¹H NMR (500 MHz, CDCl₃): δ = 6.92 (s, 1H, Tph-*H-c*) ppm.

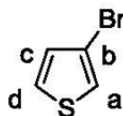
¹³C NMR (125 MHz, CDCl₃): δ = 132.5 (Tph-*C-c*), 113.7 (Tph-*C-d*), 112.2 (Tph-*C-a*), 110.8 (Tph-*C-b*) ppm.

M.p.: 28 °C.

IR (ATR): $\tilde{\nu}$ = 3091 (m), 1626 (w), 1500 (s), 1406 (s), 1295 (s), 1128 (s), 991 (s), 968 (s), 810 (s) cm⁻¹.

MS (EI, 70 eV): m/z (%) = 318/320/322/324 (34/90/100/30) [M]⁺, 239/241/243 (12/20/12) [M-Br]⁺, 160/162 (45/39) [M-2Br]⁺.

MS (CI, isobutane): m/z (%) = 318/320/322/324 (3/7/6/2) [M+H]⁺.

3-Bromothiophene (38)

3-Bromothiophene was prepared similar to a method described by Gronowitz and Raznikiewicz¹⁶ and was modified as follows:

A solution of 2,3,5-tribromothiophene (128.0 g, 400.0 mmol) in acetic acid (30 mL) was added dropwise a refluxing suspension of zinc (65.4 g, 1.00 mol), acetic acid (30.0 mL) and water (155 mL) over a course of 30 min using a cooling bath (0 °C). After the addition was complete, the reaction mixture was heated for another 4.5 h to reflux. The mixture was then allowed to cool to 20 °C and filtered. The filter cake was washed with *n*-hexane (300 mL). Then the liquid phases were separated and the aqueous phase was extracted with *n*-hexane (3 x 50 mL). The combined organic phases were dried over magnesium sulfate and subsequently concentrated *in vacuo*. The crude product was purified by Kugelrohr distillation (110 °C, 500 mbar) to yield slightly yellow oil in a yield of 45.8 g (70 %).

¹H NMR (500 MHz, CDCl₃): δ = 7.28 (dd, 1H, ³*J* = 4.9 Hz, ⁴*J* = 3.2 Hz, Tph-*H-d*), 7.24 (dd, 1H, ⁴*J* = 3.2 Hz, ⁴*J* = 1.5 Hz, Tph-*H-a*), 7.03 (dd, 1H, ³*J* = 4.9 Hz, ⁴*J* = 1.5 Hz, Tph-*H-c*) ppm.

¹³C NMR (125 MHz, CDCl₃): δ = 130.1 (Tph-*C-c*), 126.8 (Tph-*C-d*), 122.9 (Tph-*C-a*), 110.2 (Tph-*C-b*) ppm.

MS (EI, 70 eV): m/z (%) = 164/162 (100/100) [M]⁺.

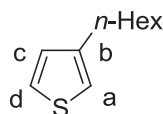
MS (CI, isobutane): m/z (%) = 164/162 (100/98) [M]⁺.

IR (ATR): $\tilde{\nu}$ = 3111 (m), 1493 (s), 1399 (w), 1353 (m), 1195 (m), 1086 (w), 880 (s), 845 (s), 758 (s) cm⁻¹.

The NMR data are in agreement with the data found in the literature.¹⁷

(16) L. Brandsma, H. D. Verkruisje, *Synth. Commun.* **1988**, *18*, 1763.

(17) S. R. Gronowitz, T., *Organic Syntheses* **1973**, *Coll. Vol. 5*, 149.

3-*n*-Hexylthiophene (39)

2-Bromo-3-*n*-hexylthiophene was prepared similar to a method described by Zhang et al.¹⁸ and was modified as follows:

Magnesium (9.72 g, 400 mmol) was stirred without solvent under nitrogen for 1 h in order to activate the surface. A solution of 1-bromohexane (57.4 g, 350 mmol) in diethyl ether (100 mL) was added dropwise over a course of 30 min to a suspension of the activated magnesium in diethyl ether (150 mL) and the reaction mixture was heated to reflux for 1 h.

The Grignard reagent was added to a solution of 3-bromothiophene (24.3 g, 280 mmol) and Ni(dppp)Cl₂ (380 mg, 0.25 mol%) in diethyl ether (100 mL) at 0 °C and the orange solution was stirred for 12 h at 20 °C. The reaction mixture was cooled to 0 °C and quenched with HCl (1 M, 100 mL). The aqueous layer was extracted with diethyl ether (4 x 80 mL). The combined organic layers were dried over magnesium sulfate and the volatiles were removed *in vacuo*. The residue was distilled (Kugelrohr; 0.03 mbar; 40 °C) to afford the product as a colorless oil in a yield of 38.1 g (81 %).

¹H NMR (500 MHz, CDCl₃): δ = 7.24 (dd, 1H, ³J = 4.9 Hz, ⁴J = 2.9 Hz, Tph-*H*-c), 6.94 (dd, 1H, ³J = 4.9 Hz, ⁴J = 0.9 Hz, Tph-*H*-d), 6.92 (dd, 1H, ³J = 2.9 Hz, ⁴J = 0.9 Hz, Tph-*H*-a), 2.63 (t, 2H, ³J = 7.7 Hz, Tph-CH₂), 1.62 (m, 2H, Tph-CH₂-CH₂), 1.38-1.22 (m, 6H, Tph-CH₂-CH₂-(CH₂)₃CH₃), 2.63 (dt, 3H, ³J = 6.9 Hz, ⁴J = 6.1 Hz, Tph-(CH₂)₅CH₃) ppm.

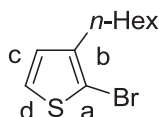
¹³C NMR (125 MHz, CDCl₃): δ = 143.3 (Tph-C-b), 128.3 (Tph-C-c), 125.0 (Tph-C-d), 119.7 (Tph-C-a), 31.9-29.0, 22.7 (Tph-(CH₂)₅CH₃), 14.1 (Tph-(CH₂)₅CH₃) ppm.

IR (ATR): $\tilde{\nu}$ = 2956 (m), 2923 (s), 2853 (s), 1466 (m), 1378 (w), 857 (w), 835 (w), 770 (m) cm⁻¹.

MS (EI, 70 eV): *m/z* (%) = 168 (21) [M]⁺, 111 (13) [M - C₄H₉]⁺, 98 (100) [M - C₅H₁₀]⁺.

MS (CI, isobutane): *m/z* (%) = 169 (100) [M + H]⁺.

The NMR data are in agreement with the data found in the literature.¹⁷

2-Bromo-3-*n*-hexylthiophene (40)

2-Bromo-3-*n*-hexylthiophene was prepared similar to a method described by Hoffmann et al.¹⁸ and was modified as follows:

N-Bromosuccinimide (534 mg, 3.00 mmol) was added in one portion to 3-*n*-hexylthiophene (505 mg, 3.00 mmol) in glacial acetic acid (8 mL) at 15 °C. The reaction mixture was stirred for 2.5 h. Then, water (20 mL) was added and the reaction mixture was extracted with diethyl ether (3 x 20 mL). The organic layer was washed with 1 M sodium hydroxide solution (50 mL) followed by drying over magnesium sulfate. The solvent was removed *in vacuo* and gave the crude product which was distilled by Kugelrohr distillation (130 °C, 0.04 mbar) to afford 577 mg (78 %) of a colorless oil.

¹H NMR (500 MHz, CDCl₃): δ = 7.18 (d, 1H, ³J = 5.6 Hz, Tph-H), 6.79 (d, 1H, ³J = 5.6 Hz, Tph-H), 2.50 (t, 2H, ³J = 7.8 Hz, Tph-CH₂), 1.72-1.12 (m, 8H, Tph-CH₂(CH₂)₄-CH₃), 0.89 (t, 3H, ³J = 7.0 Hz, Tph-(CH₂)₅-CH₃) ppm.

¹³C NMR (125 MHz, CDCl₃): δ = 141.9 (Tph-C-a), 128.2, 125.1 (Tph-C-c, C-d), 108.8 (Tph-C-b), 31.9, 29.7, 29.4, 28.9, 22.6 (Tph-(CH₂)₅CH₃), 14.1 (Tph-(CH₂)₅CH₃) ppm.

IR (ATR): $\tilde{\nu}$ = 2954 (s), 2923 (s), 2954 (s), 2850 (m), 1460 (m), 1408 (m), 1376 (w), 1228 (w), 991 (s), 829 (m), 771 (s), 683 (s), 634 (s), 580 (m) cm⁻¹.

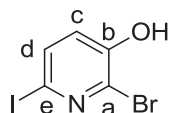
MS (EI, 70 eV): *m/z* (%) = 246/248 (35)/(40) [M]⁺, 174/176(100)/(96) [M - C₅H₁₁]⁺.

MS (CI, isobutane): *m/z* (%) = 247/249 (100)/(86) [M + H]⁺.

The NMR data are in agreement with the data found in the literature.¹⁹

(18) Y. Zhang, C. Zhao, J. Yang, M. Kapiamba, O. Haze, L. J. Rothberg, M.-K. Ng, *J. Org. Chem.* **2006**, *71*, 9475.

(19) K. J. Hoffmann, P. H. J. Carlsen, *Synth. Commun.* **1999**, *29*, 1607.

2-Bromo-6-iodopyridin-3-ol (41)

2-Bromopyridin-3-ol (5.00 g, 28.7 mmol) was added to a solution of potassium carbonate (7.95 g, 57.5 mmol) and iodine (7.51 g, 29.6 mmol) in water (40 mL) at 20 °C. The solution was stirred for 2 h before being acidified (to pH 6.5) with 1 M HCl. The precipitate was filtered, washed with water (2 x 40 mL), and dissolved in ethyl acetate (100 mL) and washed with 10 % solution of Na₂S₂O₃ (30 mL), brine (30 mL), dried over magnesium sulfate and concentrated *in vacuo*. The solid was recrystallized from chloroform to give the desired product as an off-white solid in a yield of 6.20 g, 72 %.

¹H NMR (500 MHz, DMSO-*d*₆): δ = 11.08 (s, 1H, Pyr-*H*-b), 7.62 (d, ³*J* = 8.2 Hz, 1H, Pyr-*H*), 7.03 (d, ³*J* = 8.2 Hz, 1H, Pyr-*H*) ppm.

¹³C NMR (125 MHz, DMSO-*d*₆): δ = 152.2 (Pyr-*C*-b), 135.1 (Pyr-*CH*), 130.2 (Pyr-*C*-e), 126.3 (Pyr-*CH*), 101.7 (Pyr-*C*-a) ppm.

M.p.: 158 °C.

IR (ATR): $\tilde{\nu}$ = 2956 (w), 2820 (w), 2736 (w), 2655 (w), 2582 (w), 2523 (w), 2450 (w), 1548 (m), 1452 (m), 1386 (s), 1282 (s), 1218 (s), 1167 (m), 1130 (m), 1101 (m), 1069 (s), 822 (s), 681 (s), 610 (s), 568 (w) cm⁻¹.

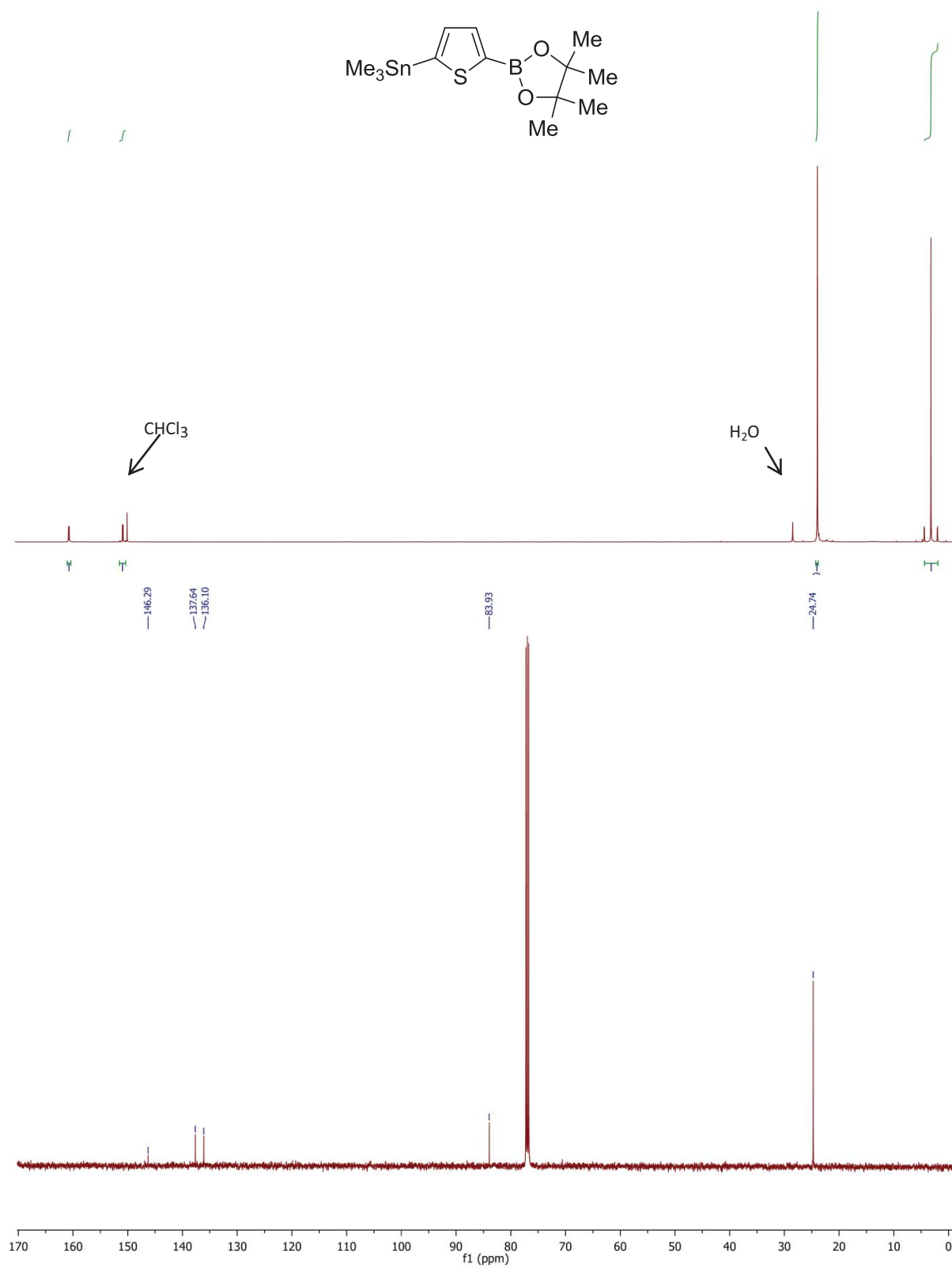
MS (EI, 70 eV): *m/z* (%) = 299 (100) [M]⁺.

MS (CI, isobutane): *m/z* (%) = 300 (100) [M + H]⁺.

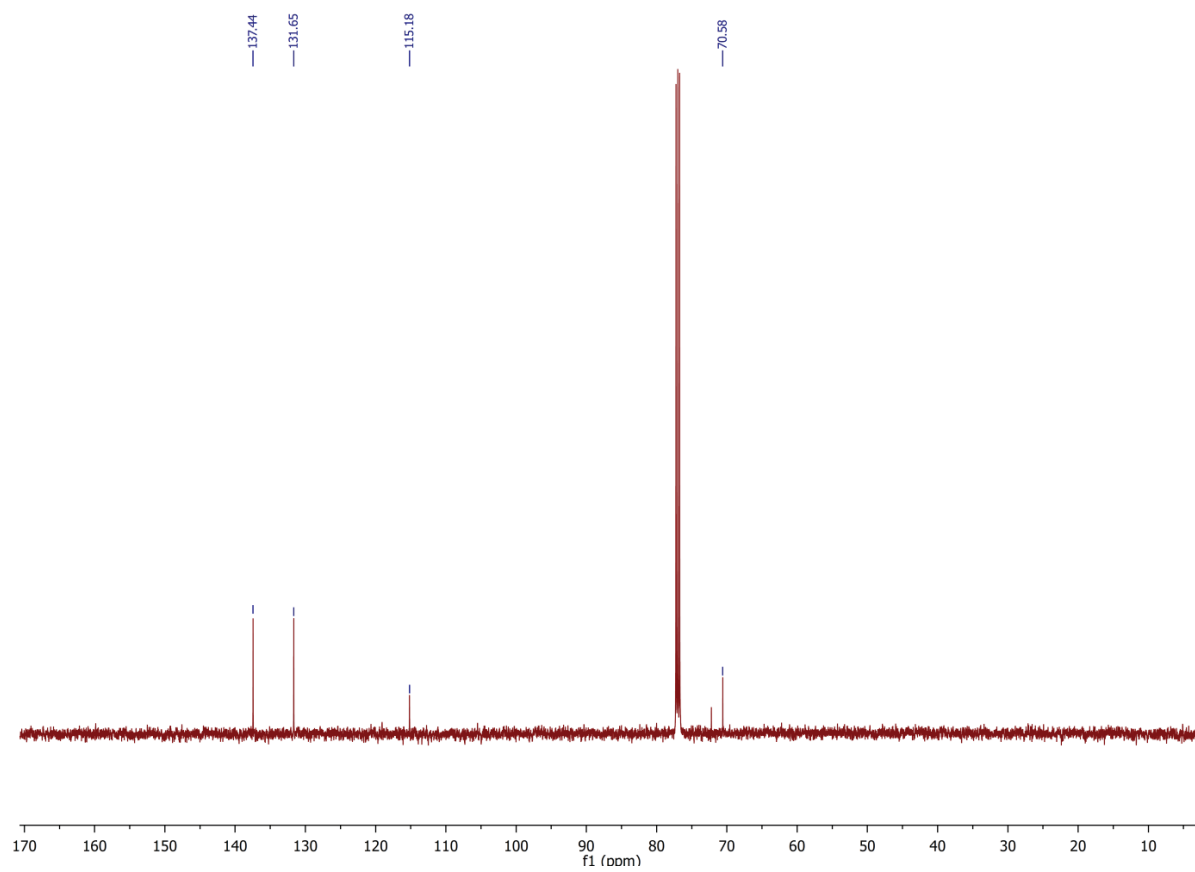
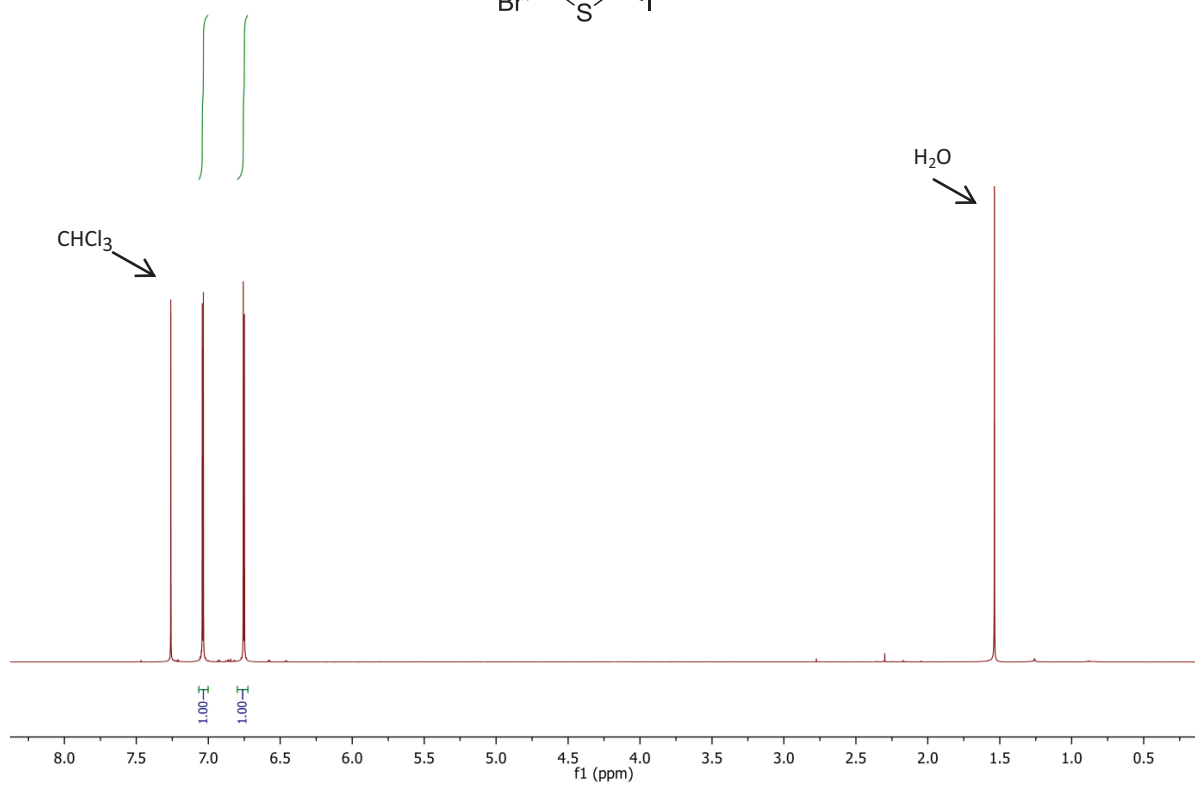
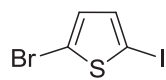
HRMS (EI): *m/z* found 298.8441; calcd. for C₅H₃BrIN 298.8443

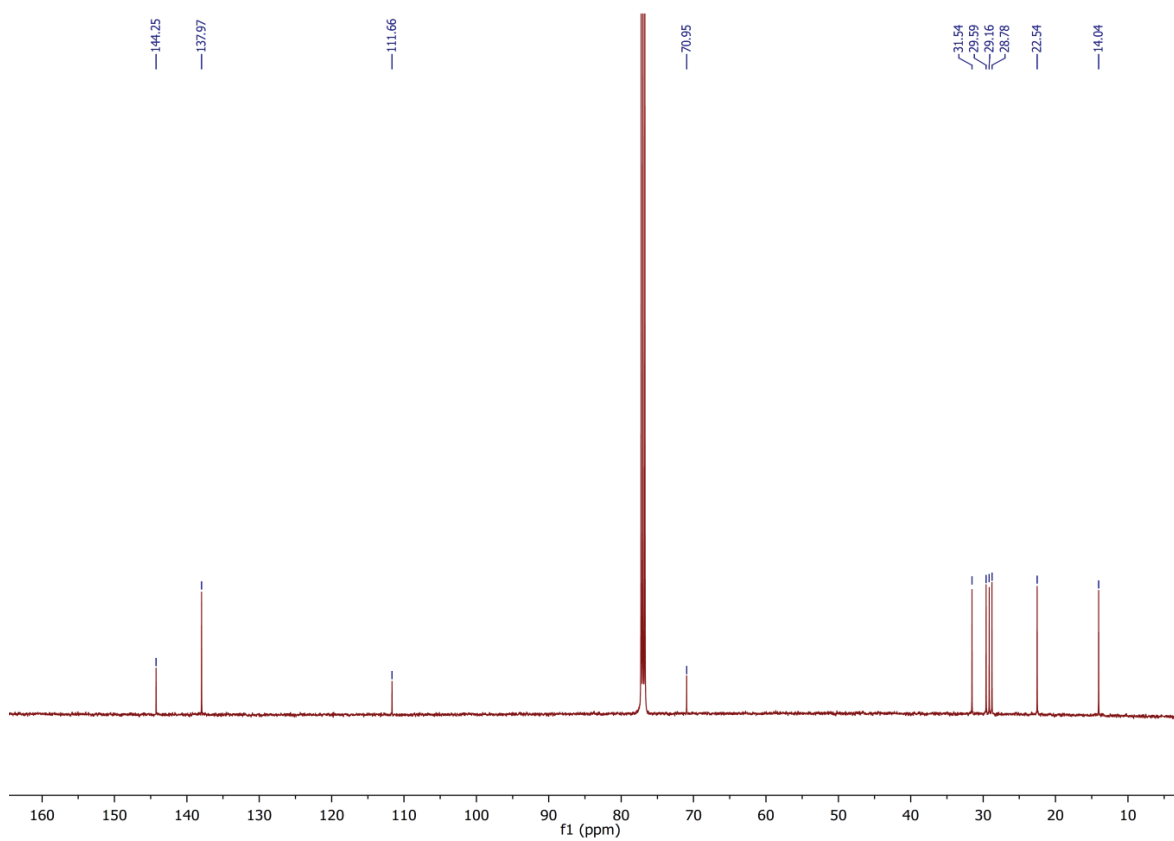
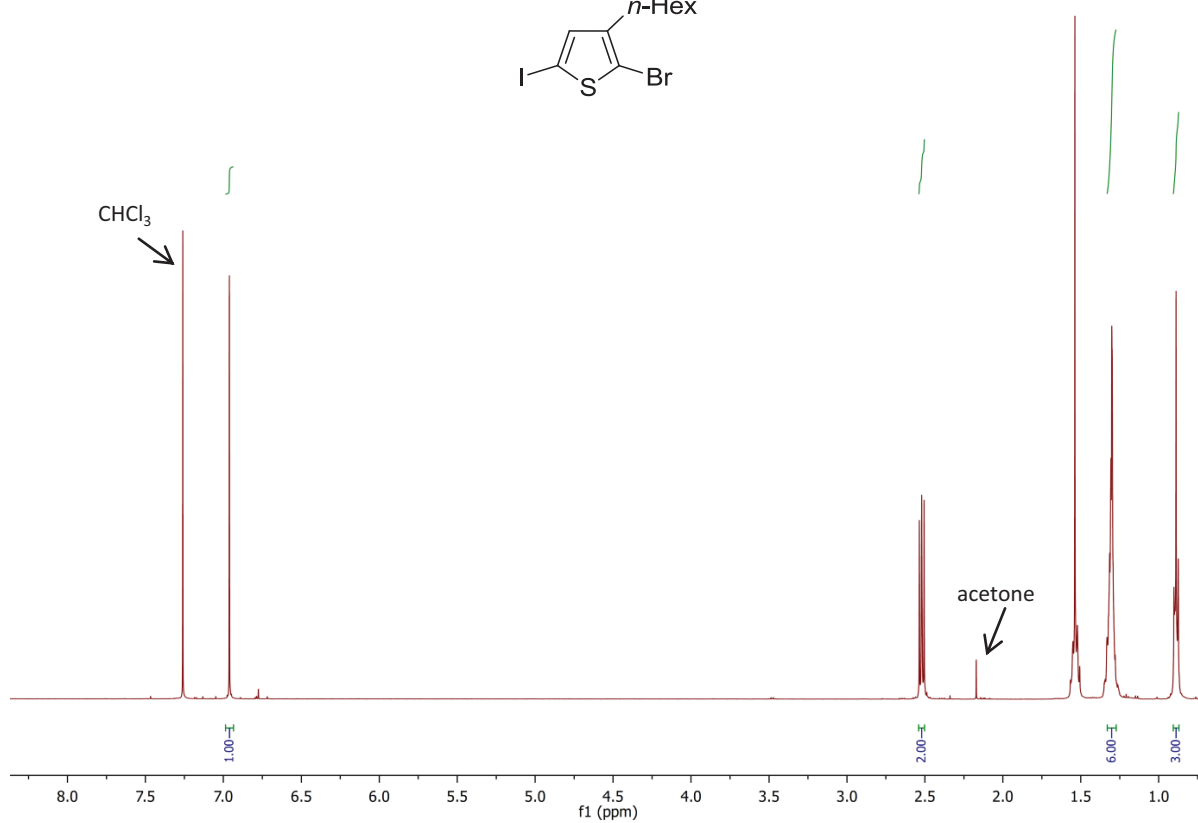
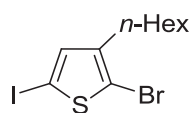
NMR Spectra

4,4,5,5-Tetramethyl-2-(5-(trimethylstannyl)thiophen-2-yl)-1,3,2-dioxaborolane (1)

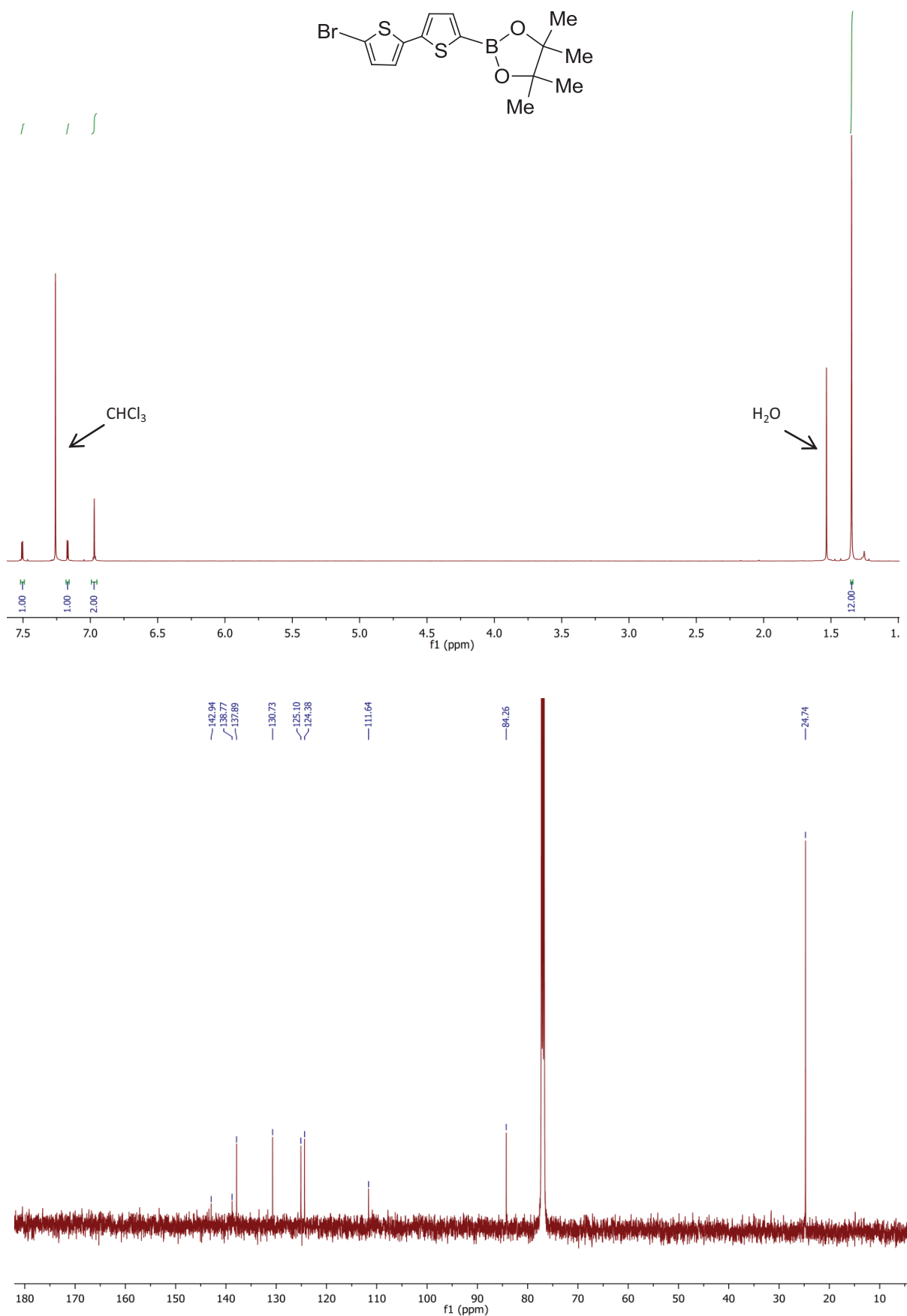


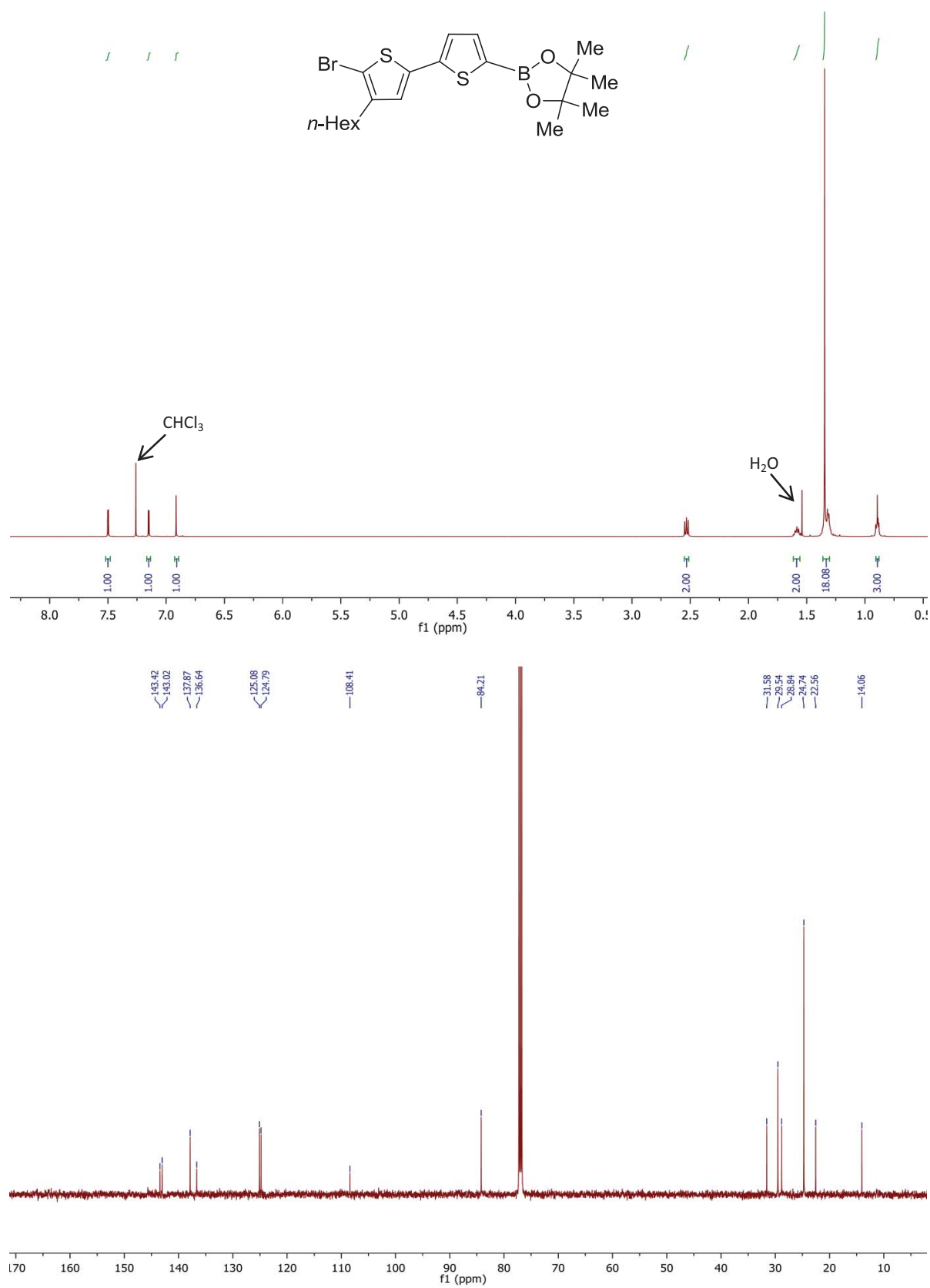
2-Bromo-5-iodothiophene (2)



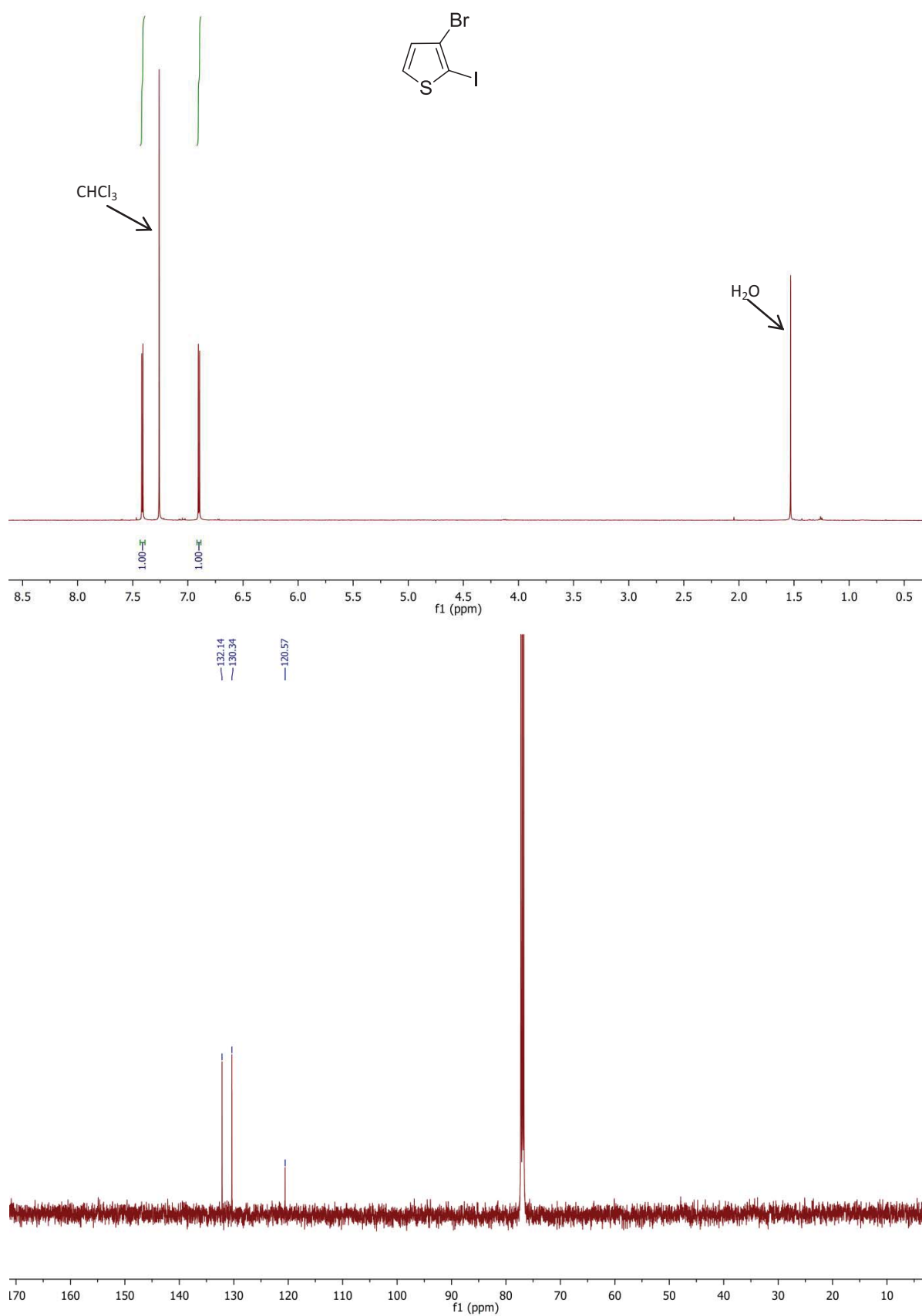
2-Bromo-3-*n*-hexyl-5-iodothiophene (3)

4,4,5,5-Tetramethyl-2-(5-(5-bromothiophen)thiophen-2-yl)-1,3,2-dioxaborolane (5a)

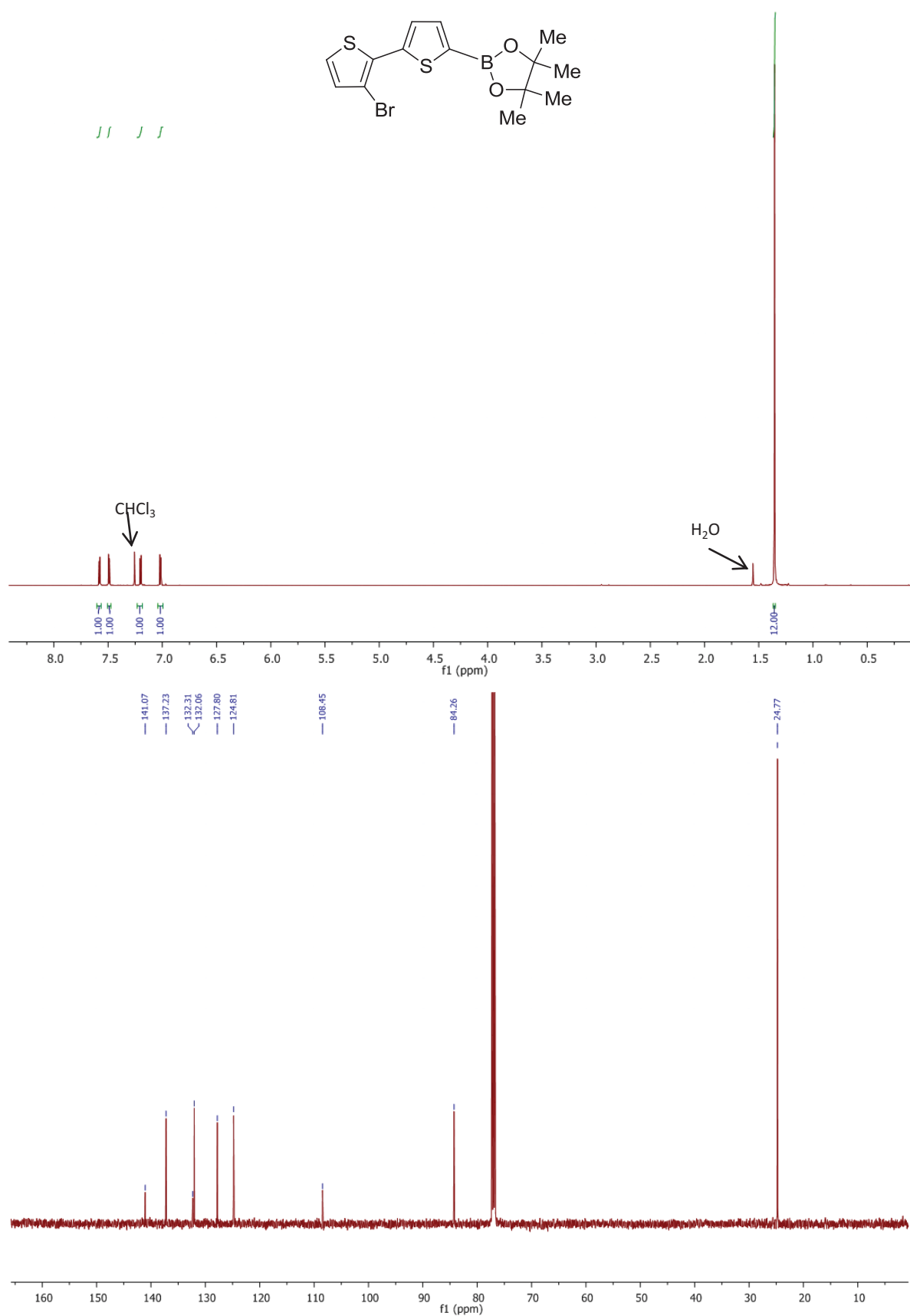


4,4,5,5-Tetramethyl-2-(5-(5-bromo-3-*n*-hexylthiophen)thiophen-2-yl)-1,3,2-dioxaborolane (5b)

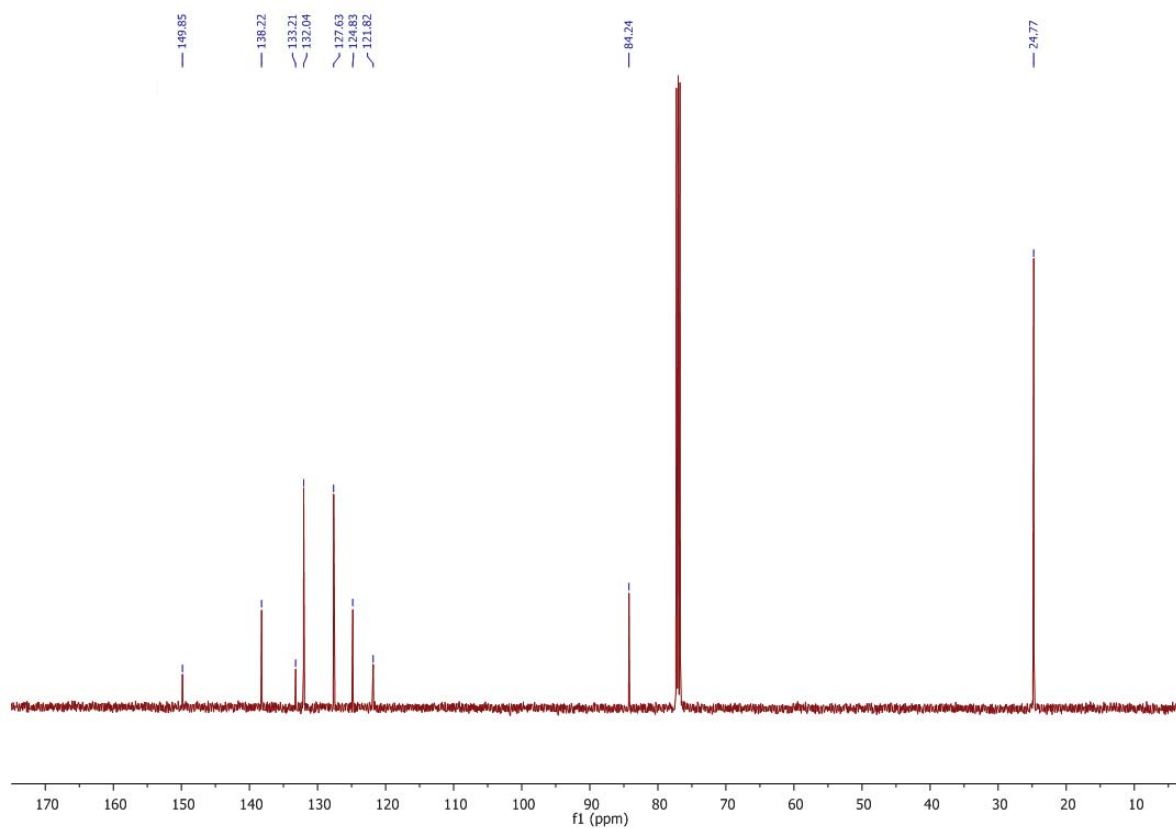
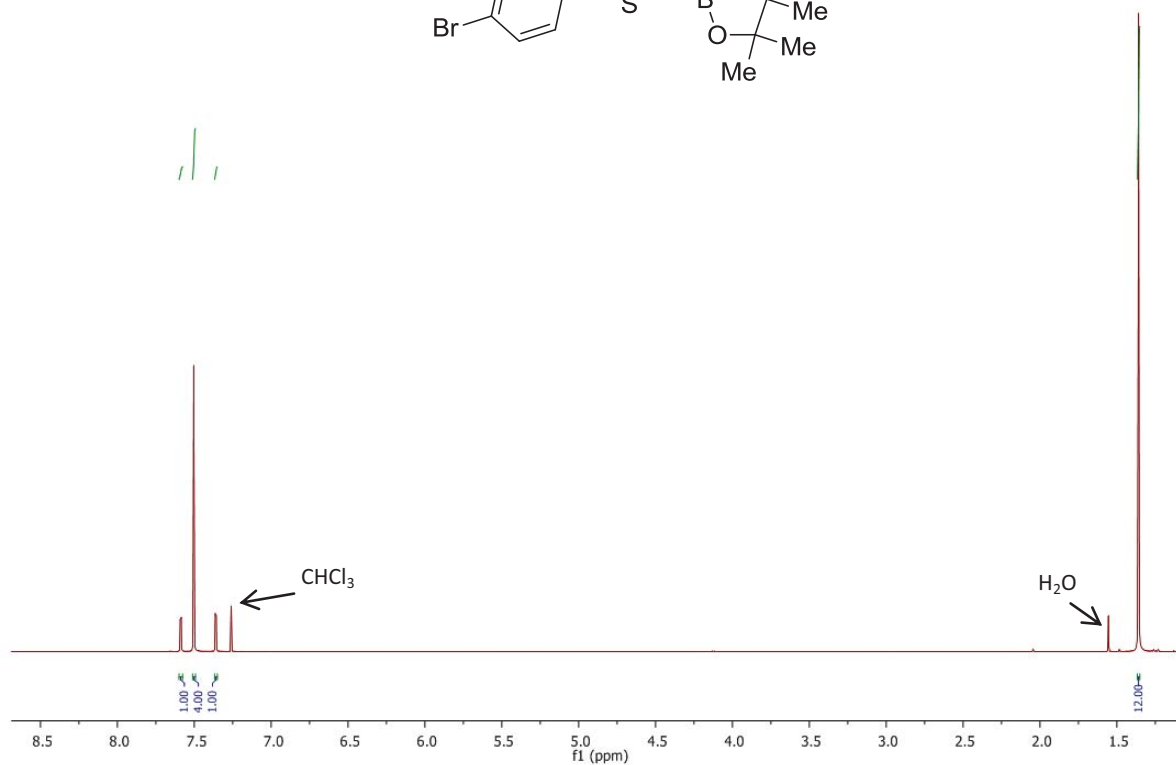
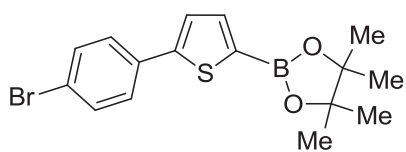
3-Bromo-2-iodothiophene (6)



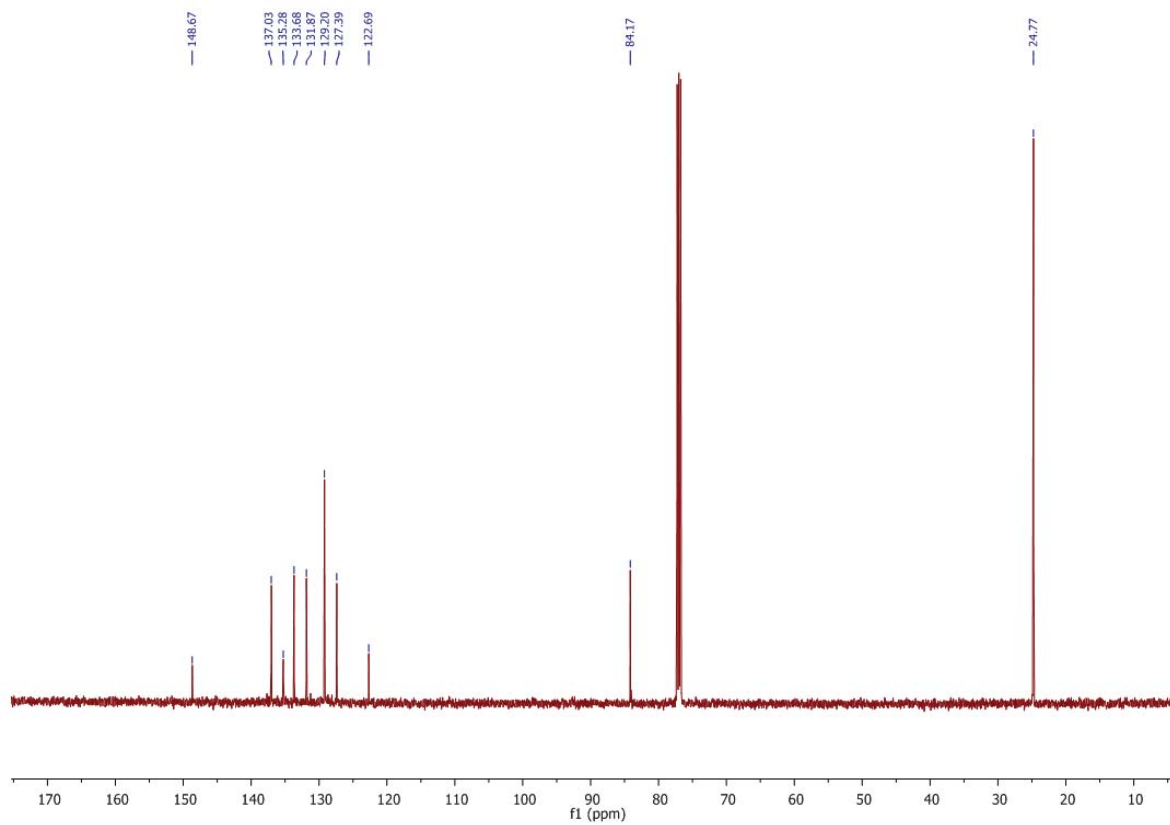
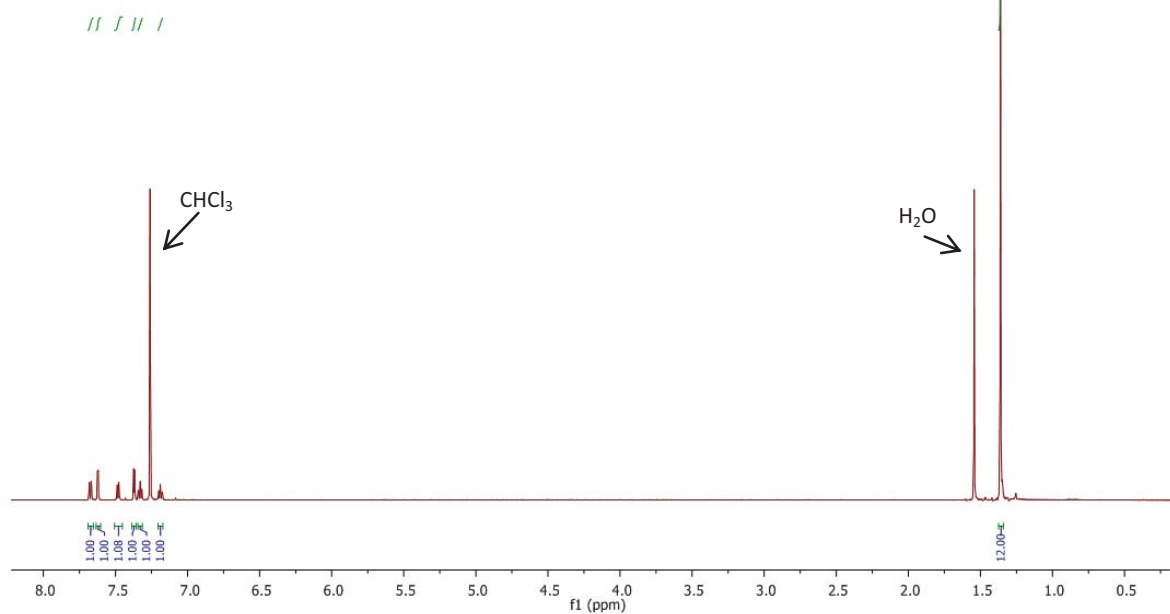
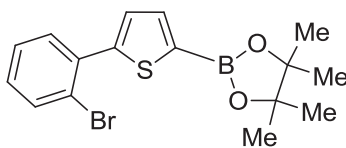
4,4,5,5-Tetramethyl-2-(5-(3-bromothiophen)thiophen-2-yl)-1,3,2-dioxaborolane (7)



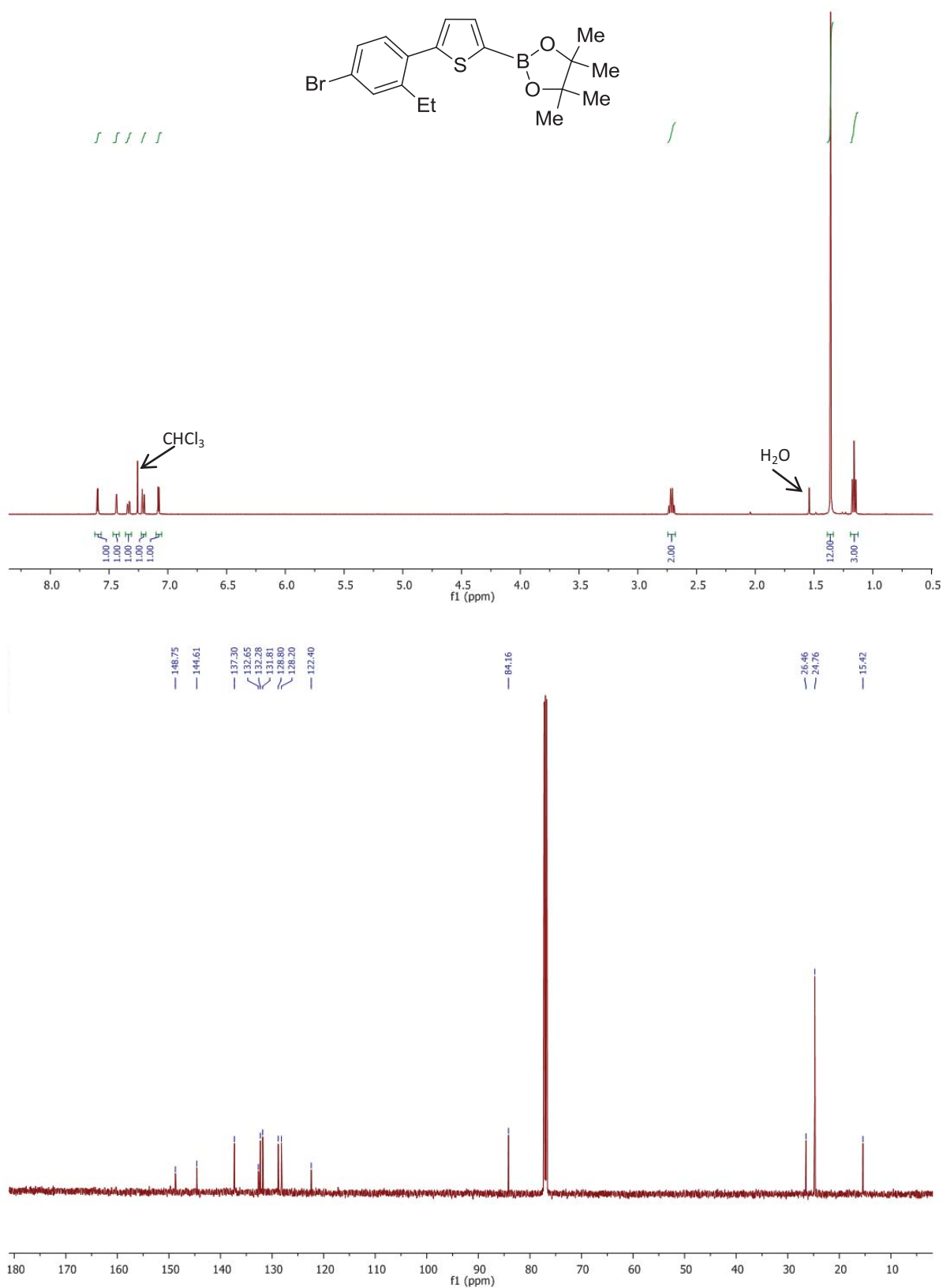
4,4,5,5-Tetramethyl-2-(5-(4-bromophenyl)thiophen-2-yl)-1,3,2-dioxaborolane (9)



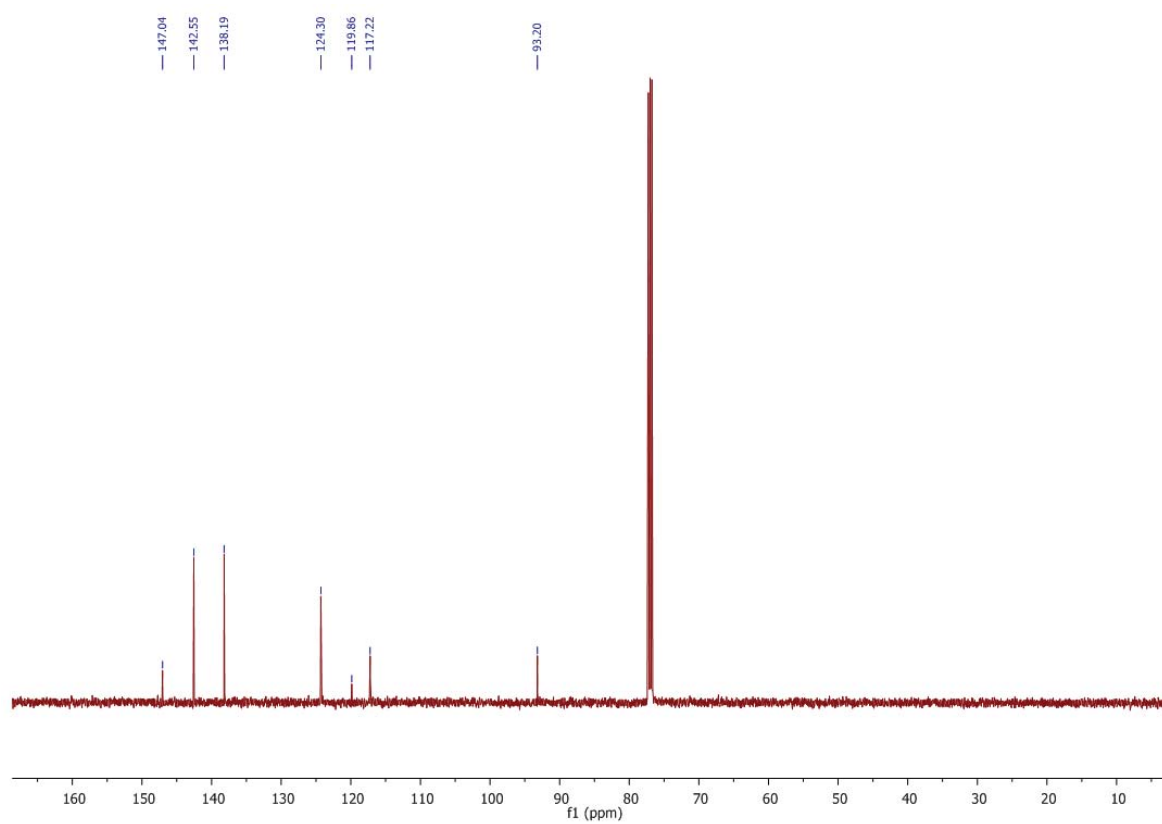
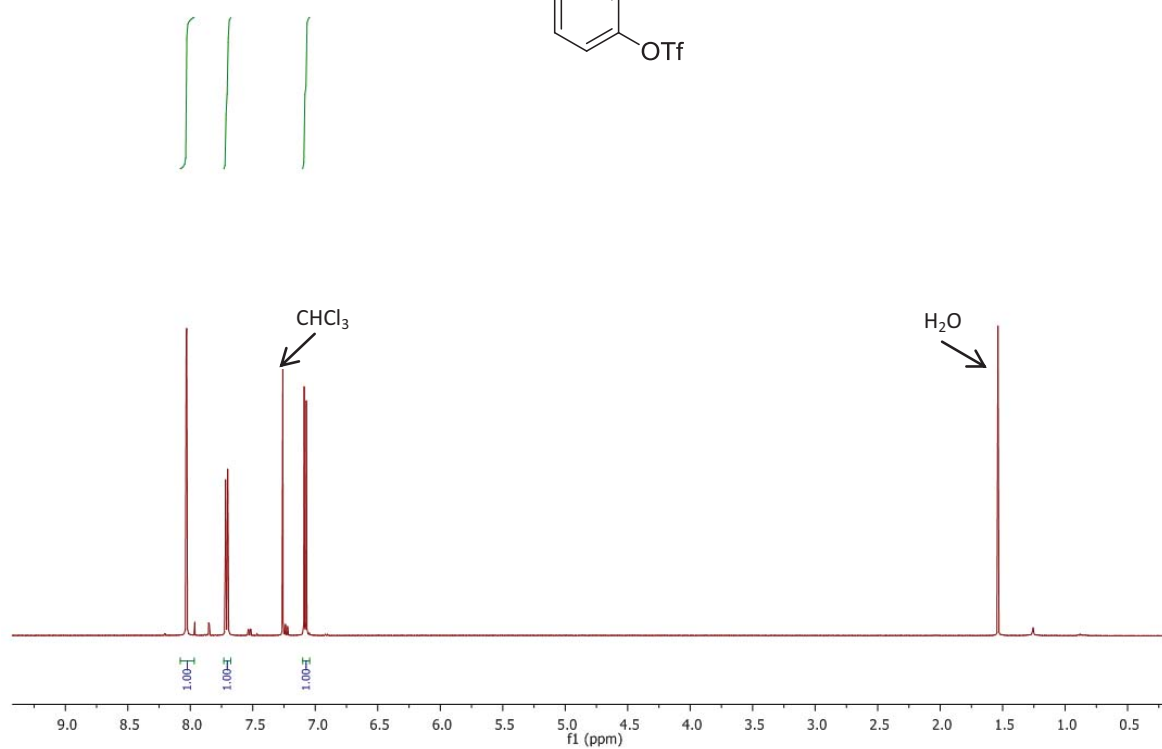
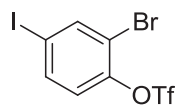
4,4,5,5-Tetramethyl-2-(5-(2-bromophenyl)thiophen-2-yl)-1,3,2-dioxaborolane (11)

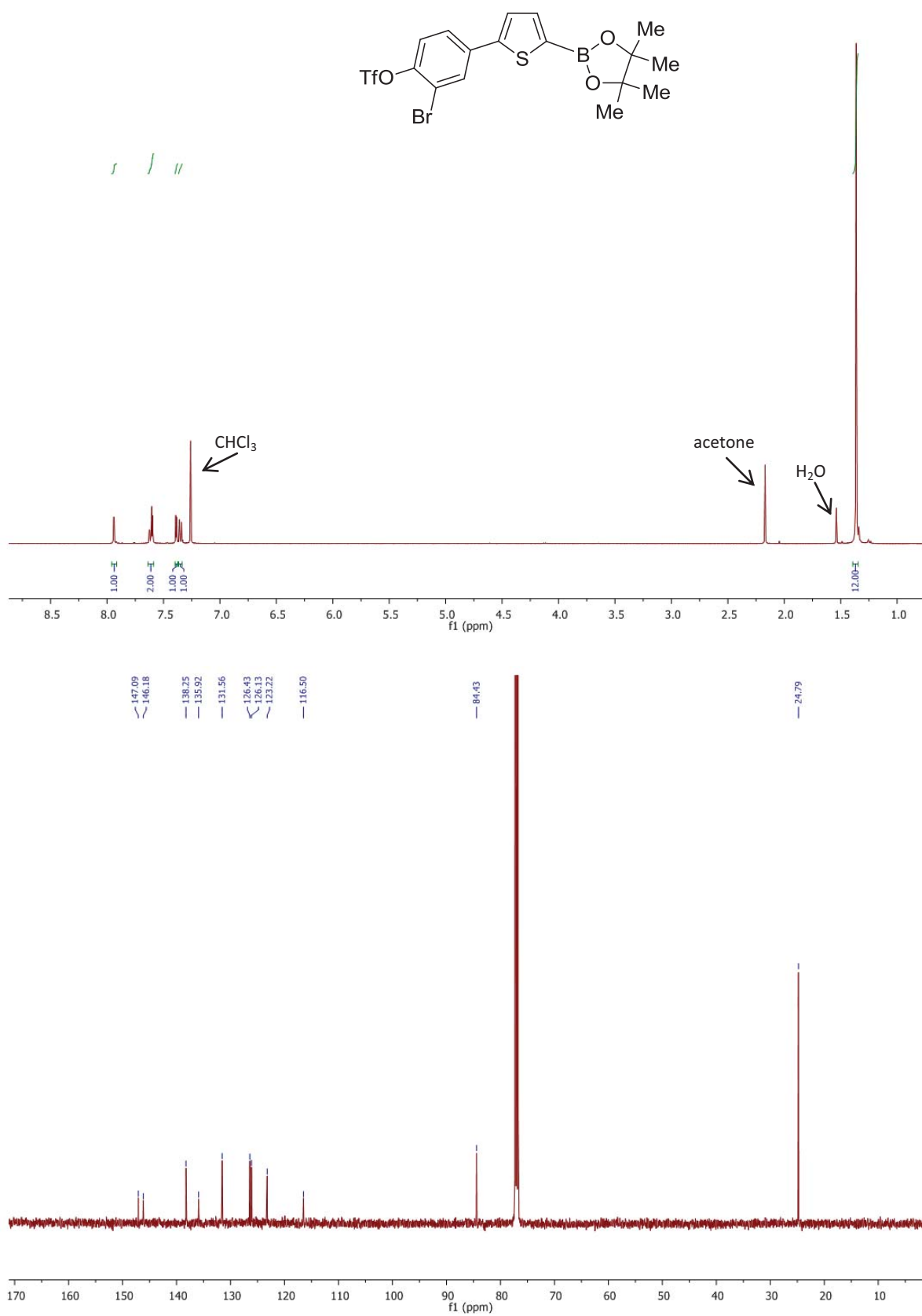


4,4,5,5-Tetramethyl-2-(5-(4-bromo-2-ethylphenyl)thiophen-2-yl)-1,3,2-dioxaborolane (13)

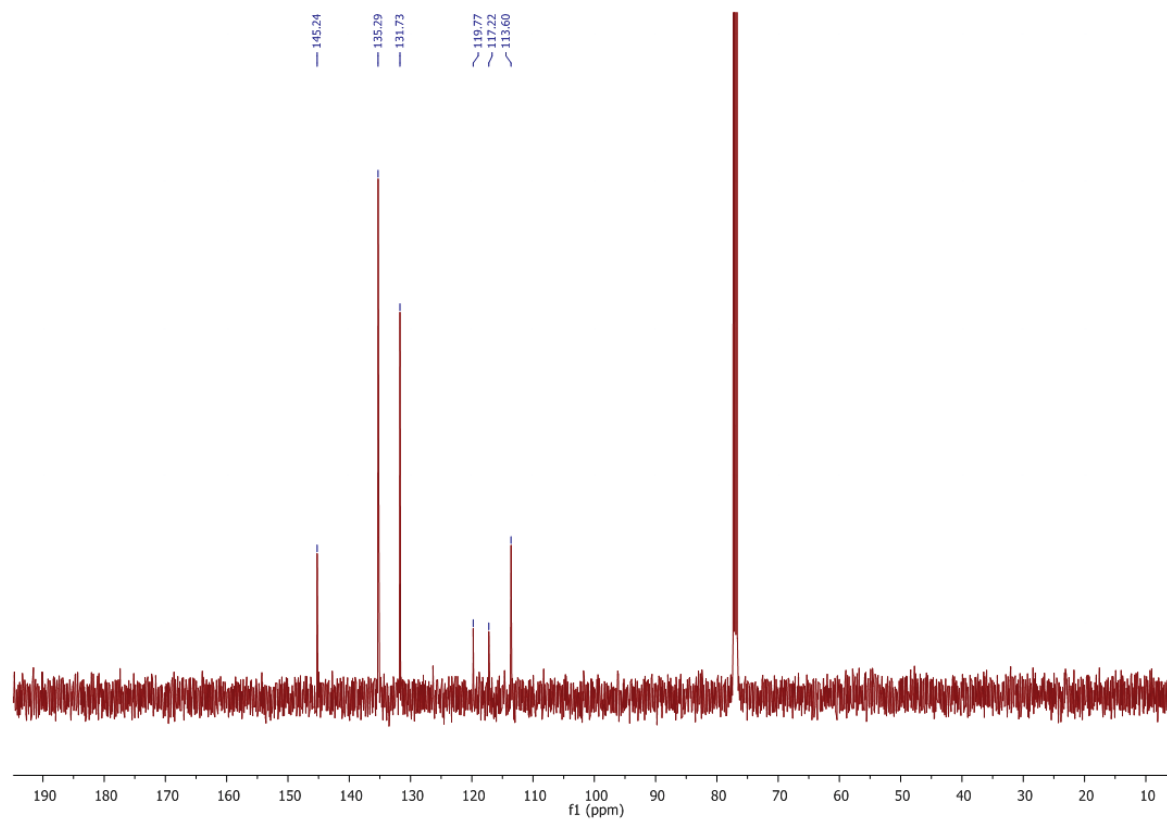
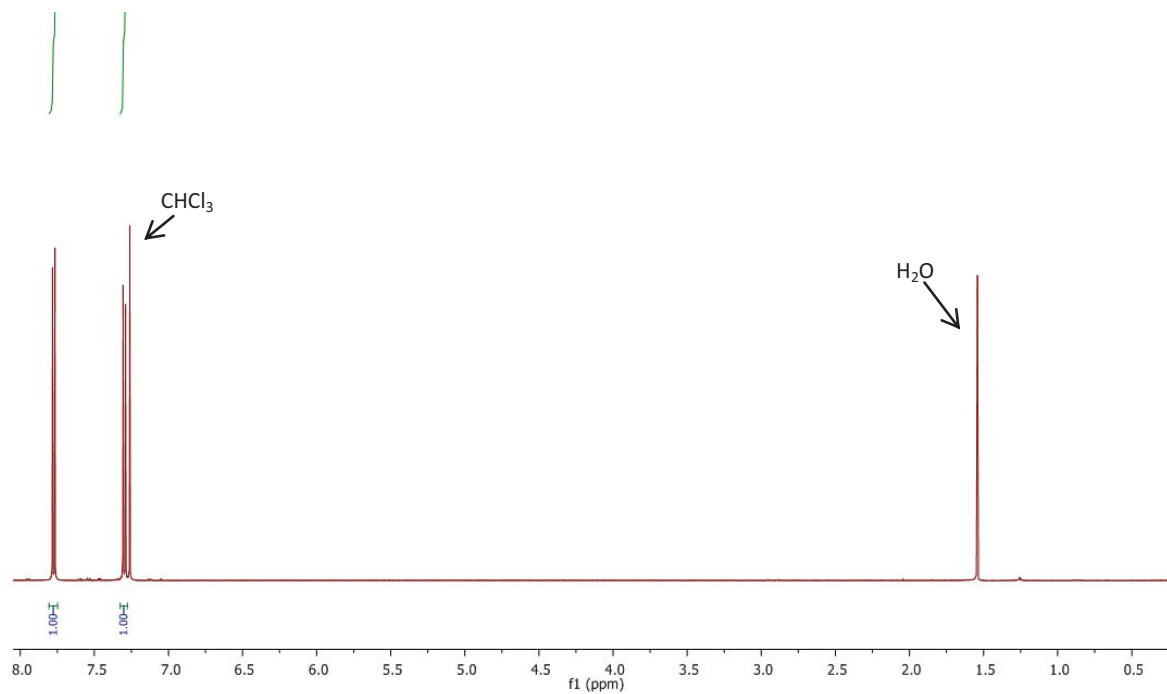
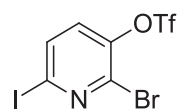


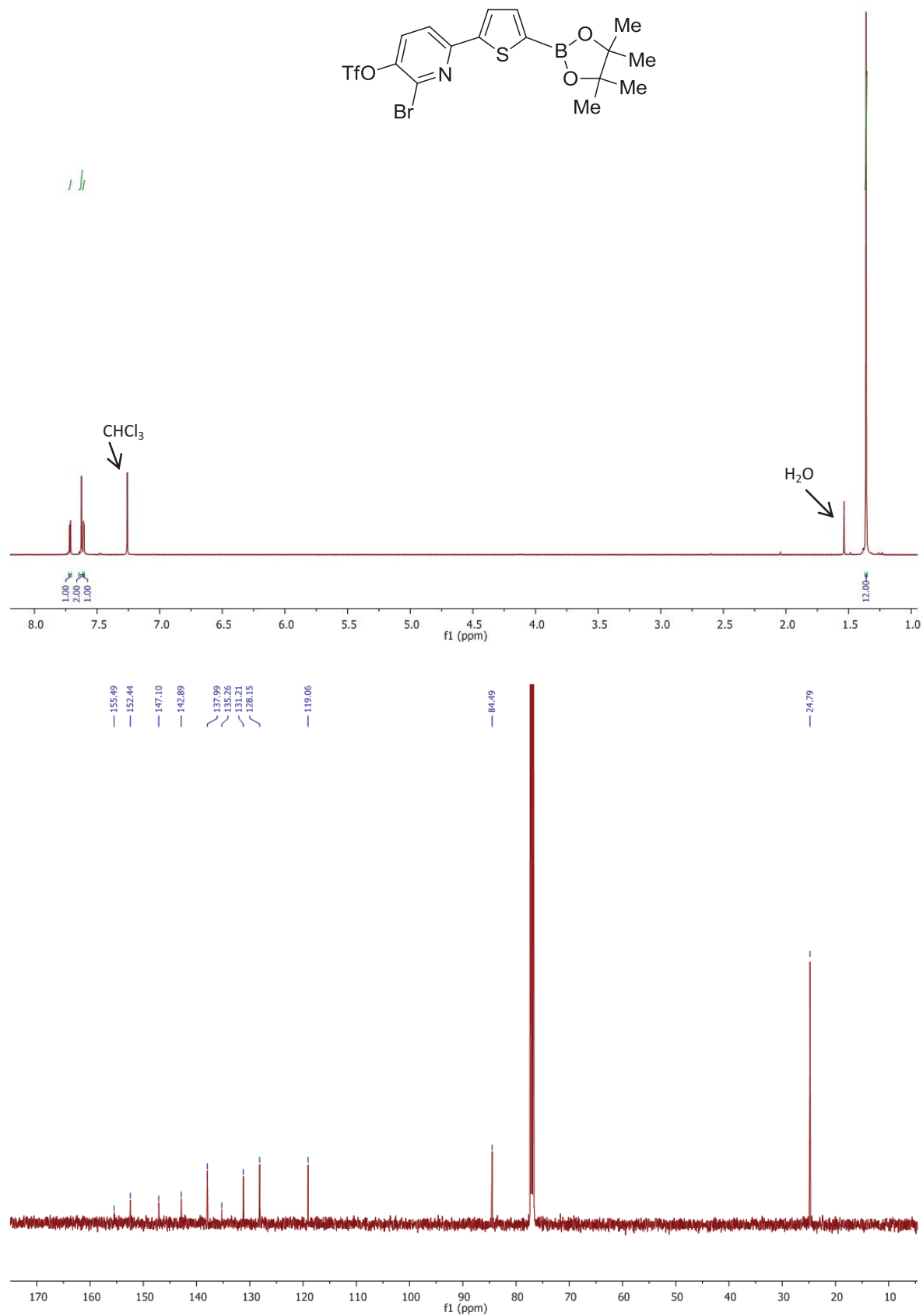
2-Bromo-4-iodophenyl trifluoromethanesulfonate (14)



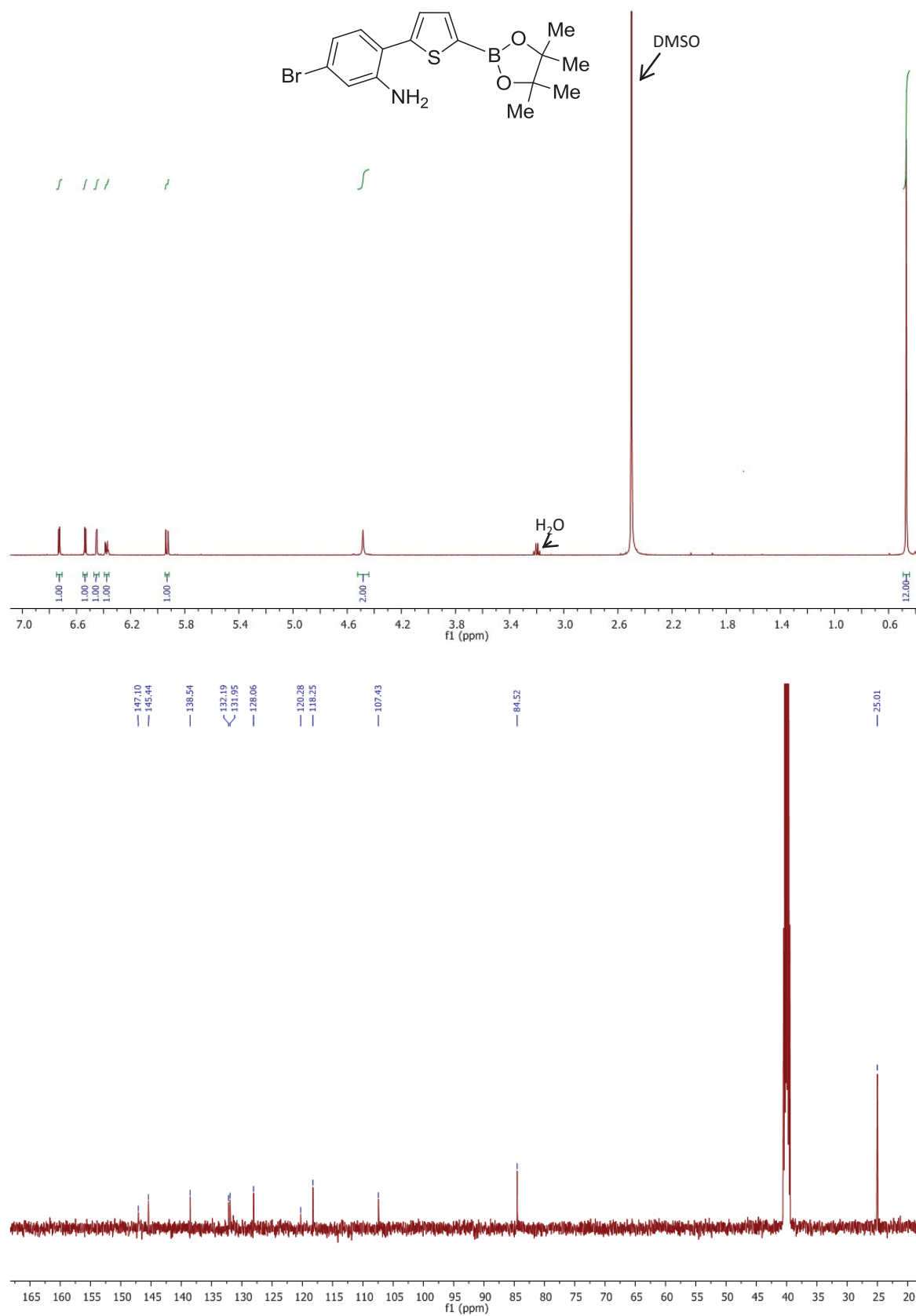
4,4,5,5-Tetramethyl-2-(5-(3-bromo-4-trifluoromethanesulfonatephenyl)-thio-phen-2-yl)-1,3,2-dioxaborolane (15)

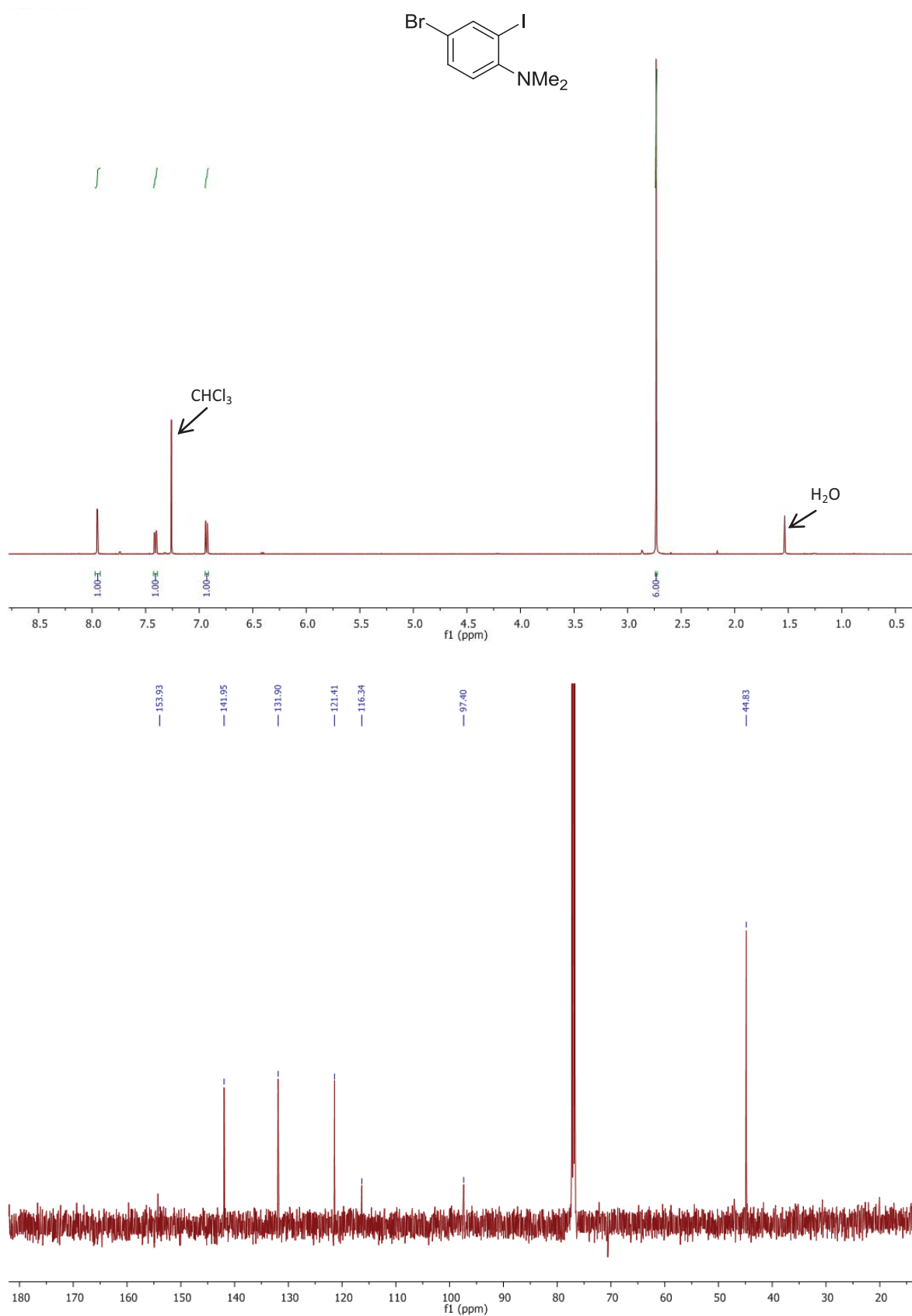
2-Bromo-6-iodopyridine-3-yl trifluoromethanesulfonate (16)



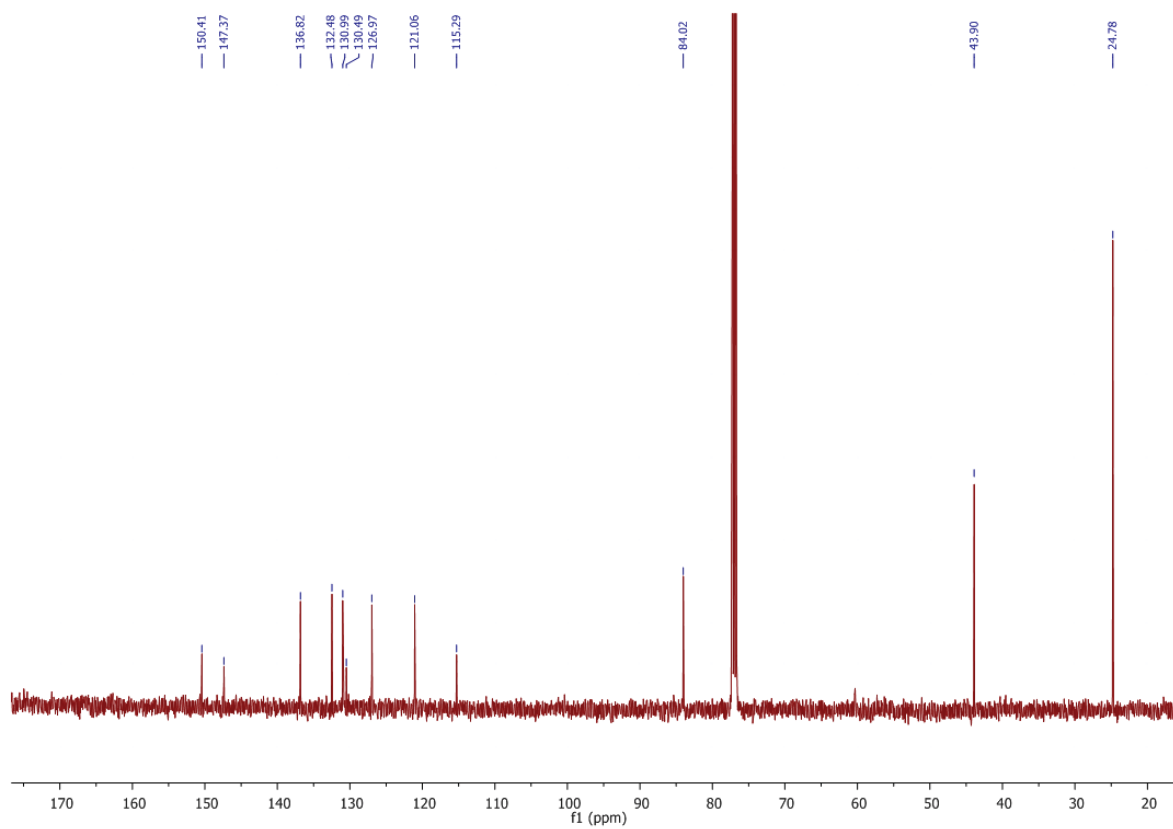
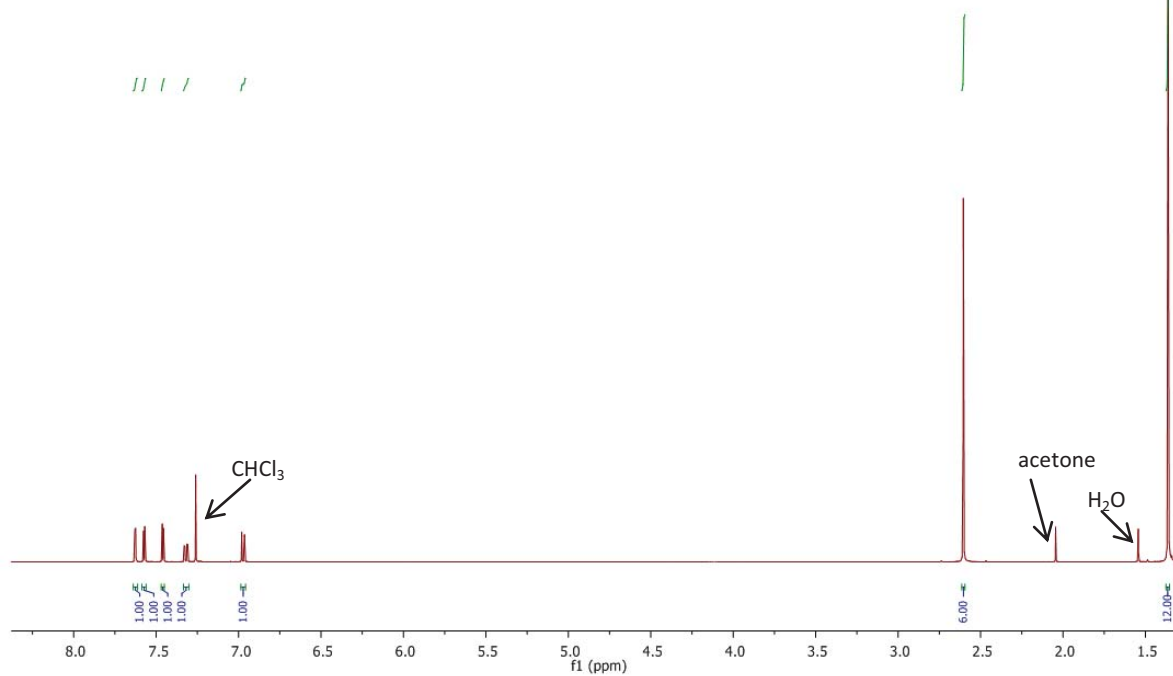
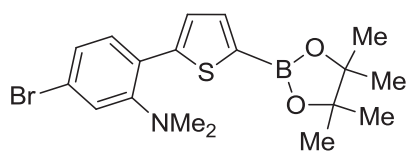
4,4,5,5-Tetramethyl-2-(5-(2-bromo-3-trifluoromethanesulfonate)pyridine-6-yl)-thiophen-2-yl)-1,3,2-dioxaborolane (17)

5-Bromo-2-(5-(4,4,5,5-tetramethyl-1,3,2-dioxaborolan-2-yl)thiophen-2-yl)aniline (19)

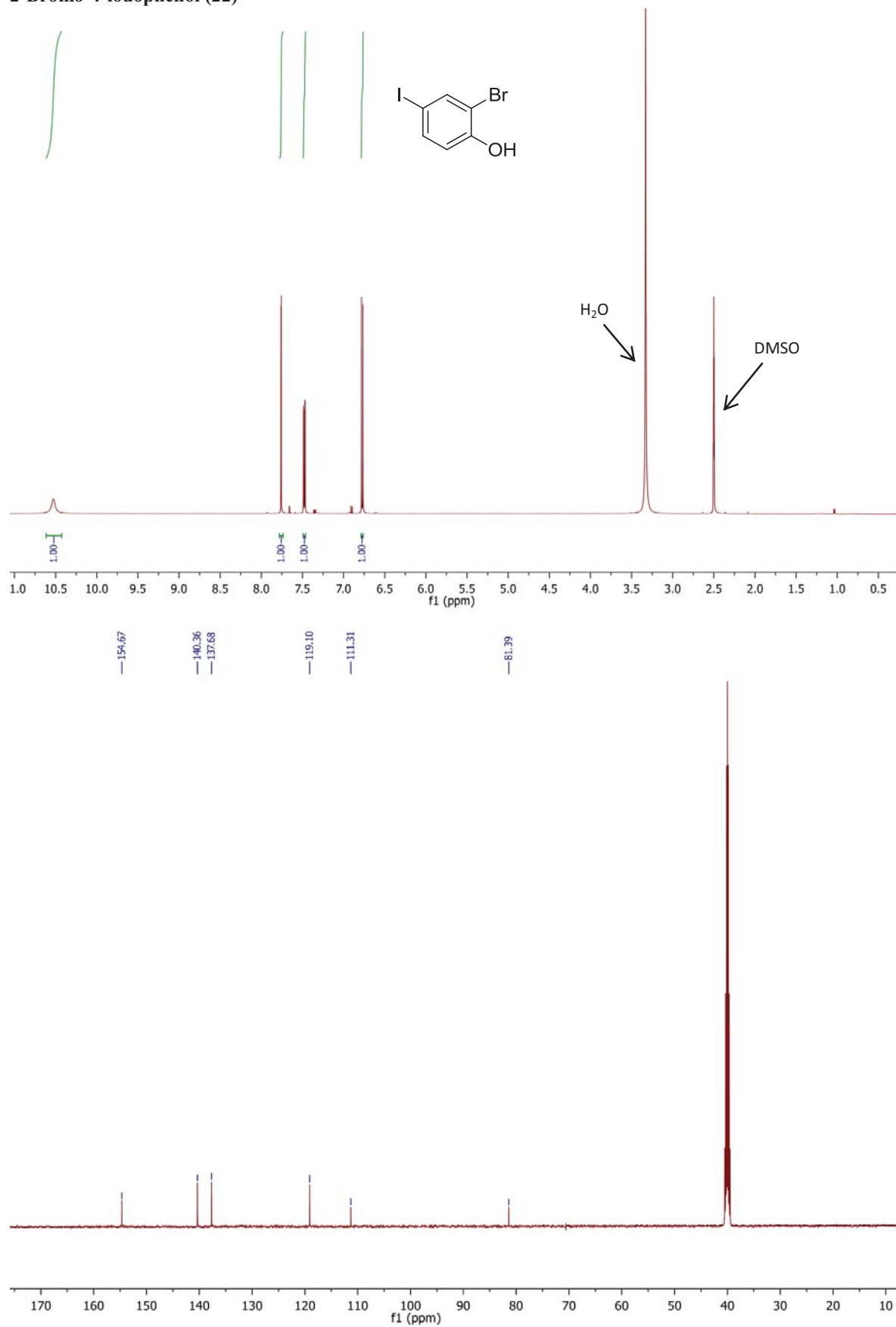


4-Bromo-2-iodo-*N,N*-dimethylaniline (20)

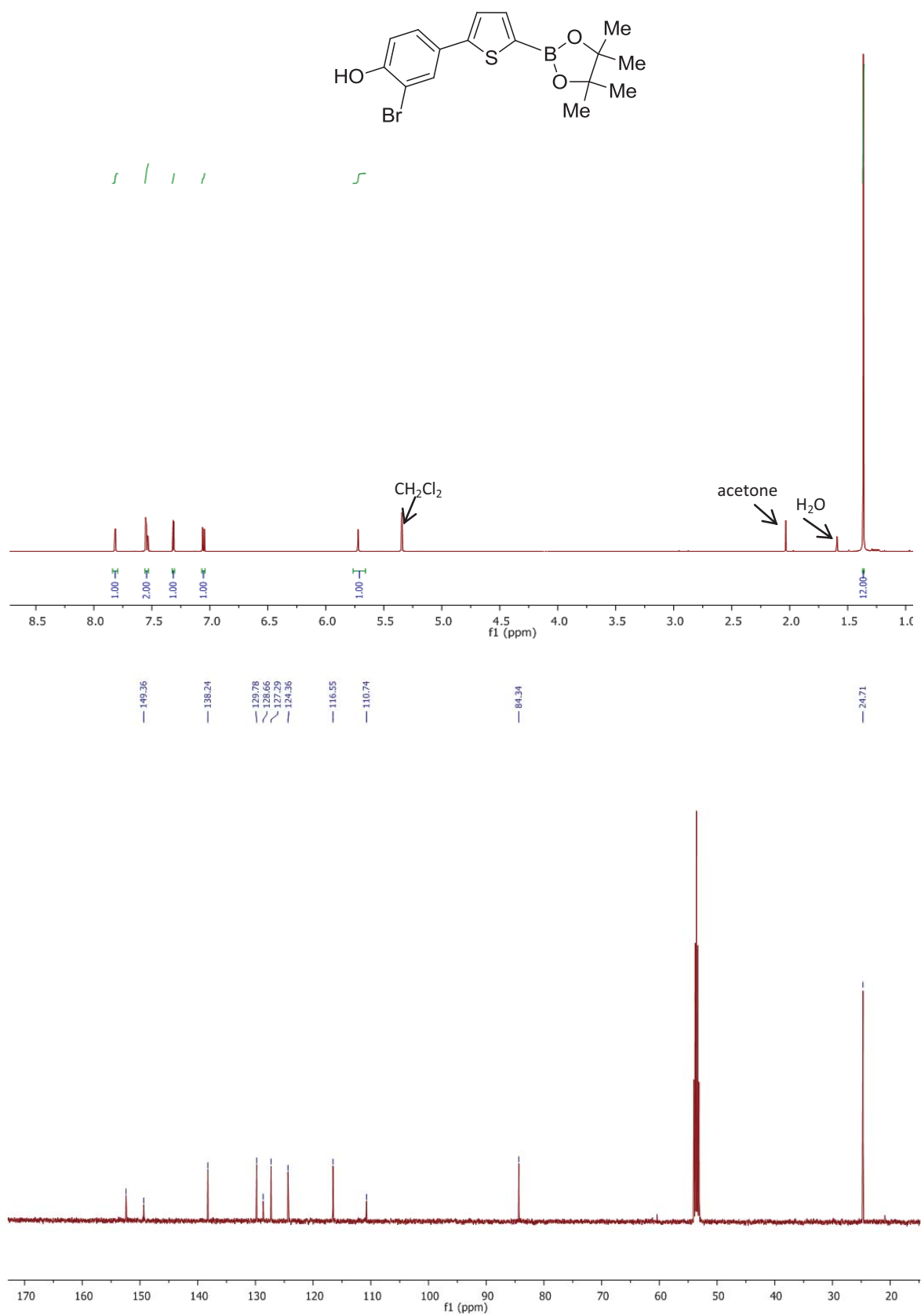
5-Bromo-N,N-dimethyl-2-(5-(4,4,5,5-tetramethyl-1,3,2-dioxaborolan-2-yl)thiophen-2-yl)aniline (21)



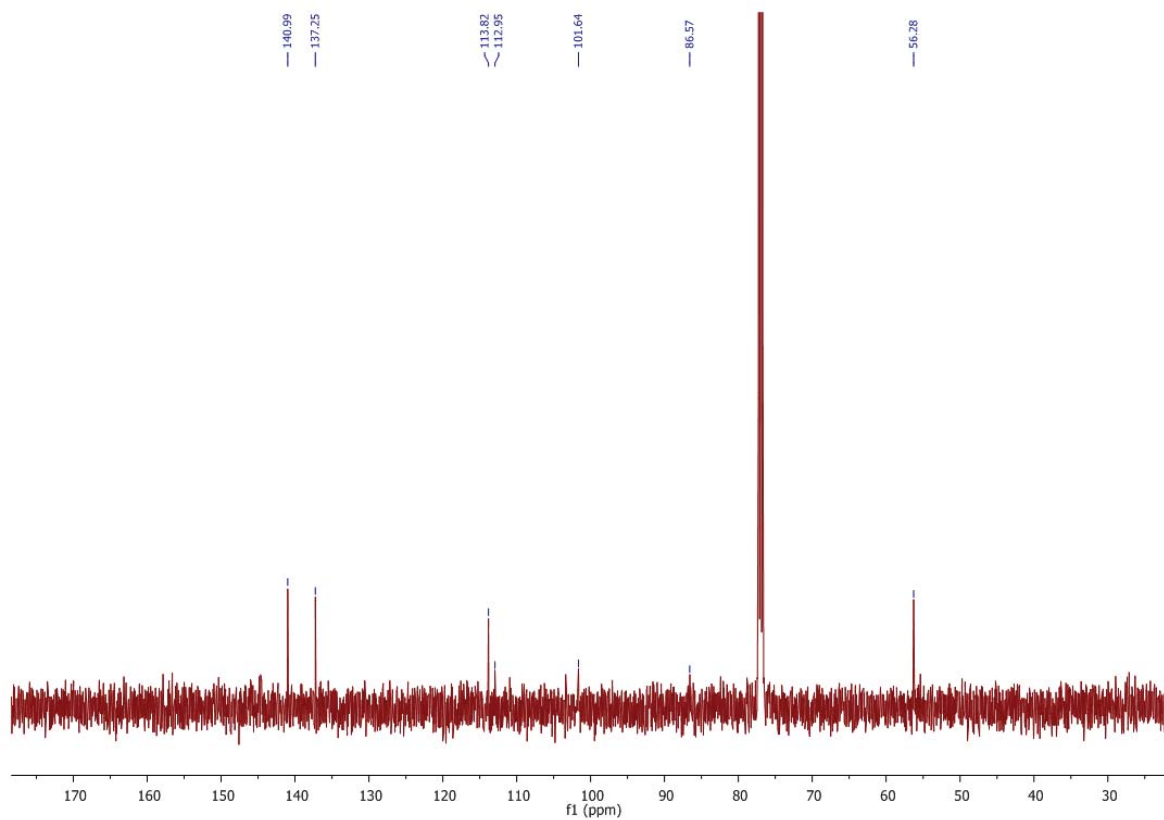
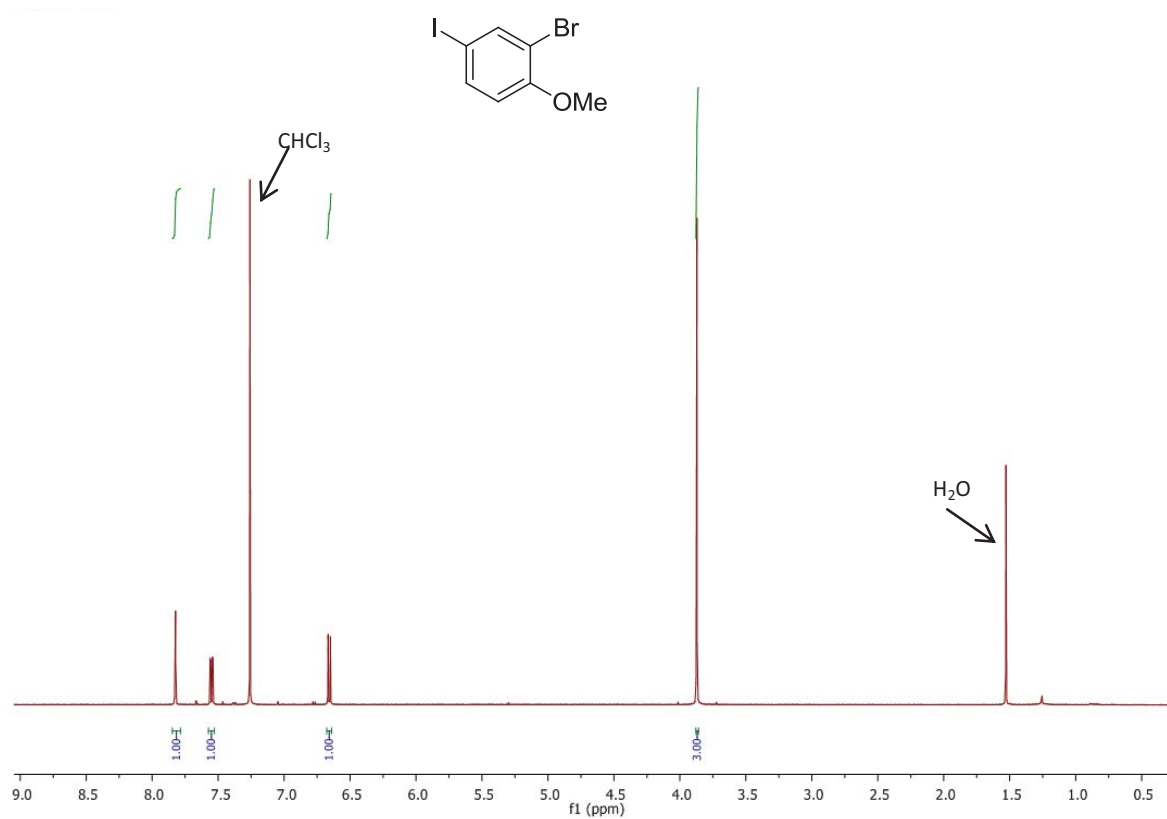
2-Bromo-4-iodophenol (22)



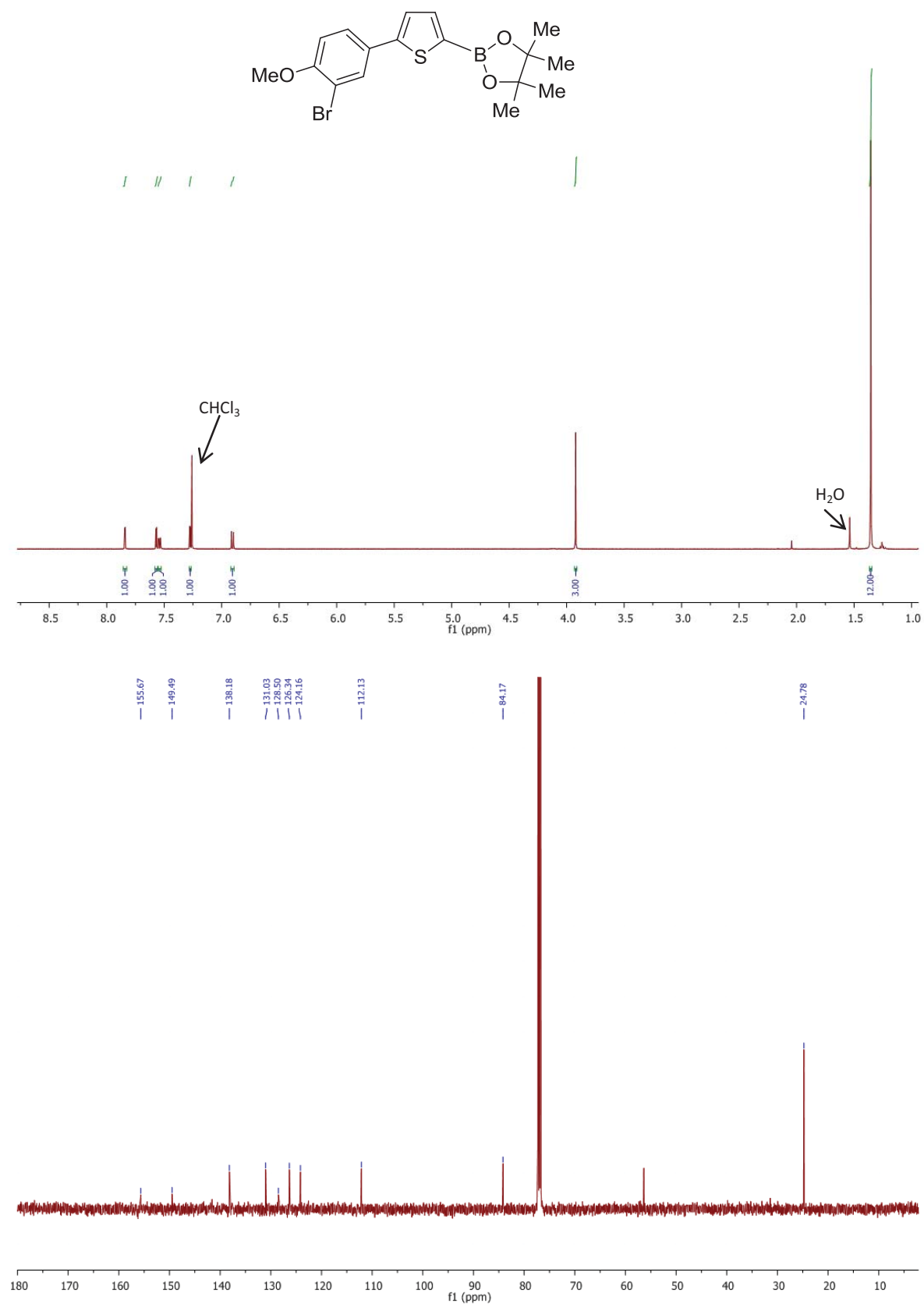
4,4,5,5-Tetramethyl-2-(5-(3-bromo-phen-4-ol)thiophen-2-yl)-1,3,2-dioxaborolane (23)



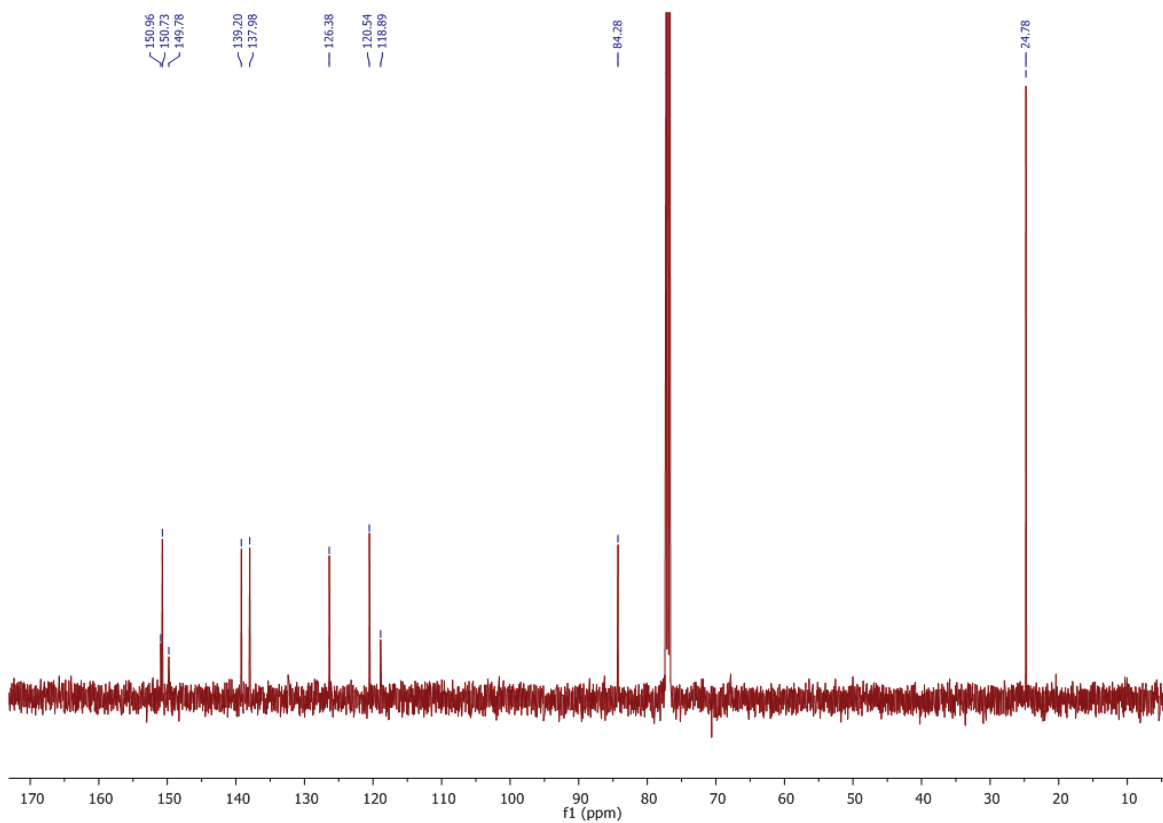
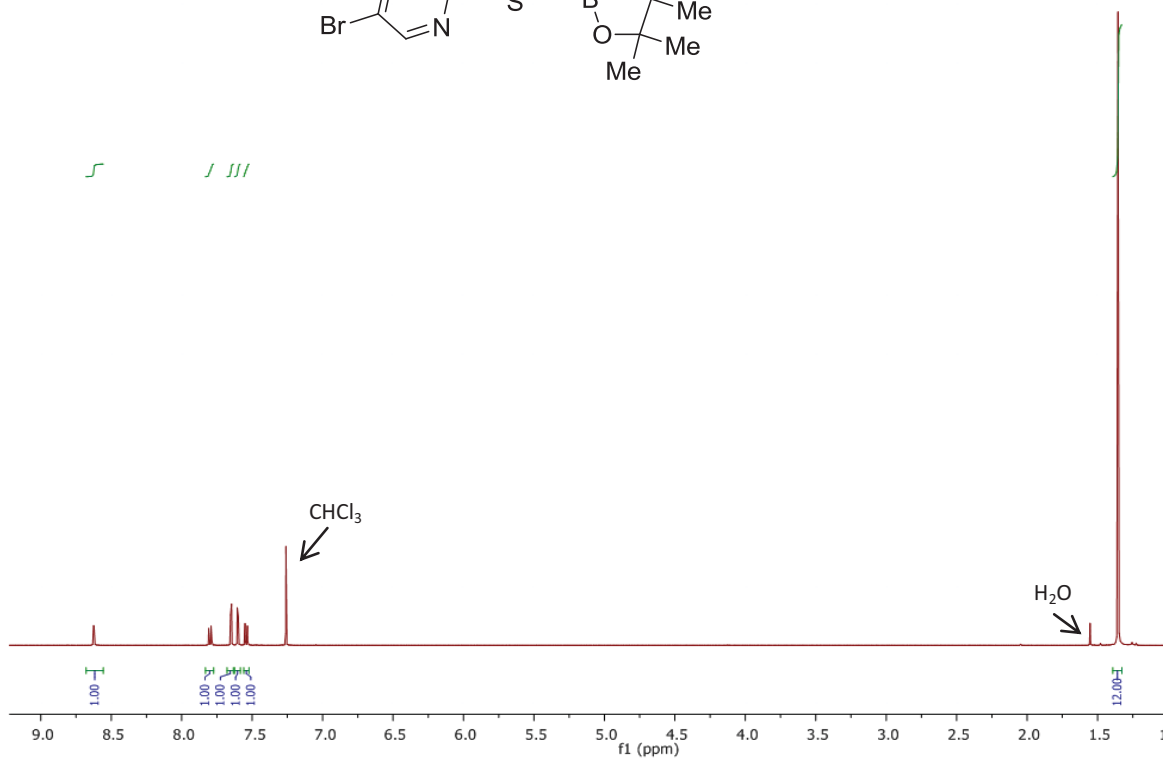
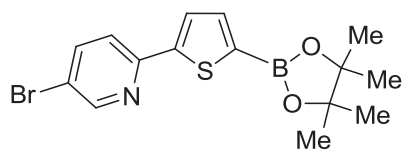
2-Bromo-4-iodo-1-methoxybenzene (24)



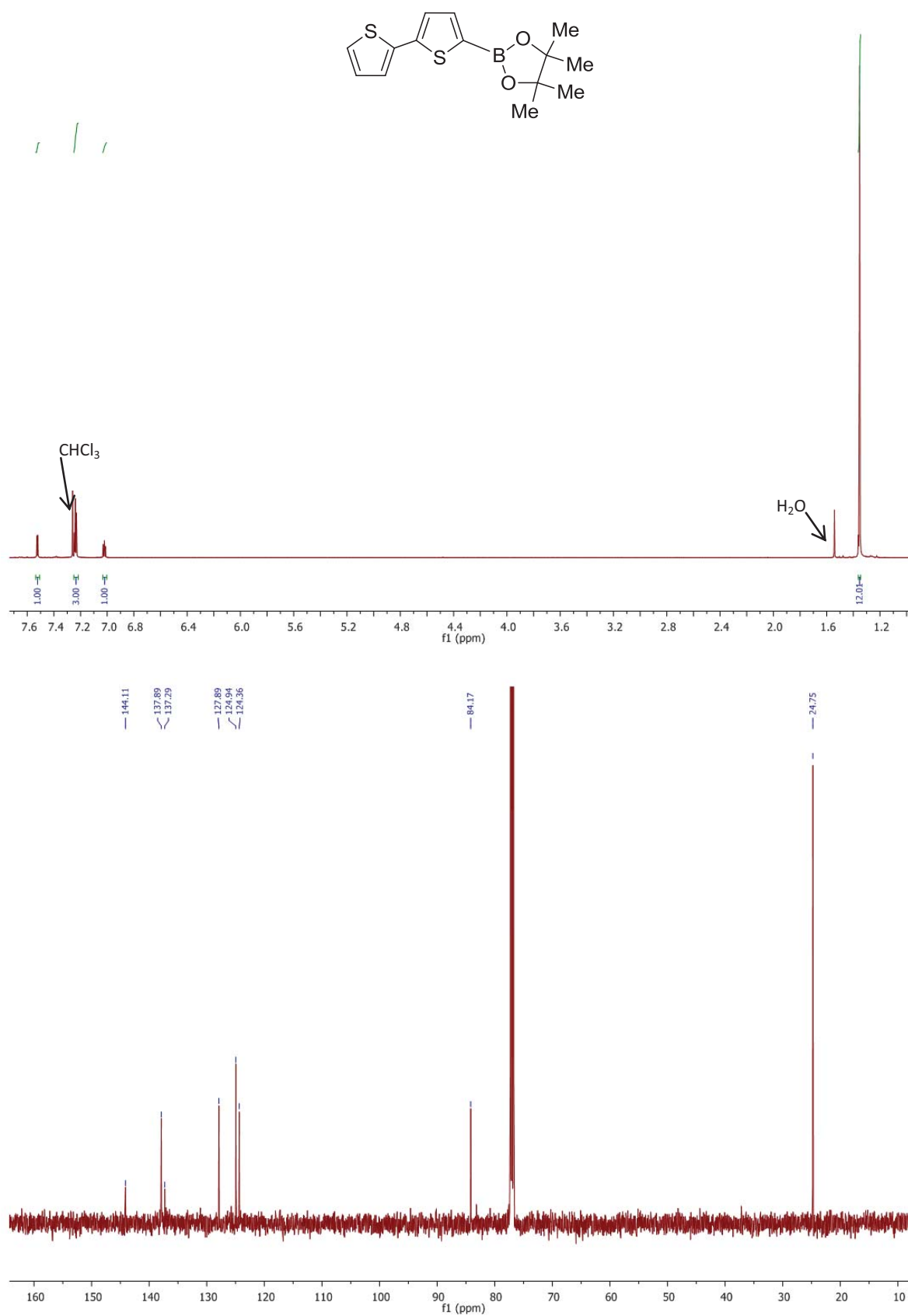
4,4,5,5-Tetramethyl-2-(5-(3-bromo-phen-4-methoxy)thiophen-2-yl)-1,3,2-dioxaborolane (25)



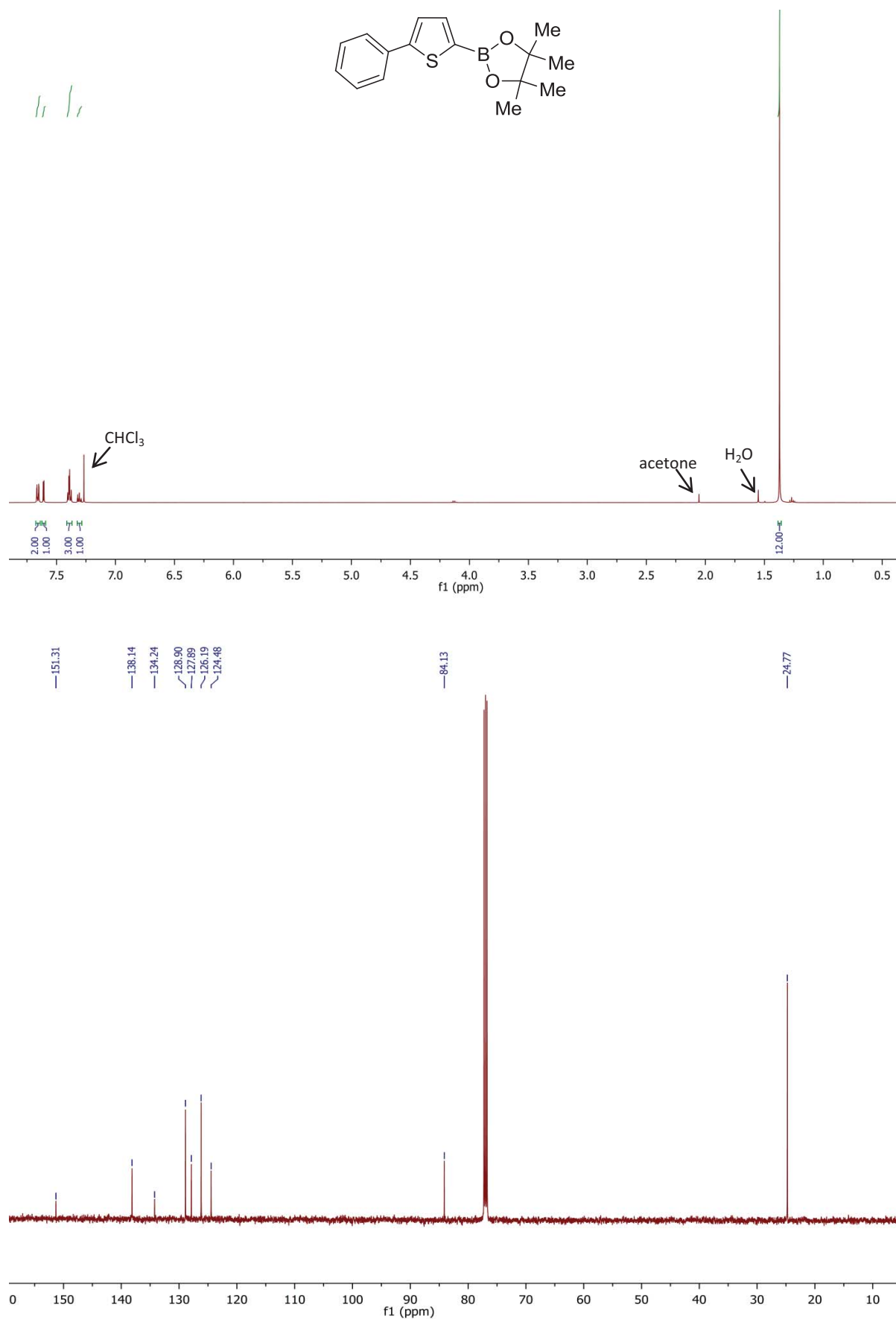
4,4,5,5-Tetramethyl-2-(5-(2-(3-bromo)pyridin)thiophen-2-yl)-1,3,2-dioxaborolane (27)



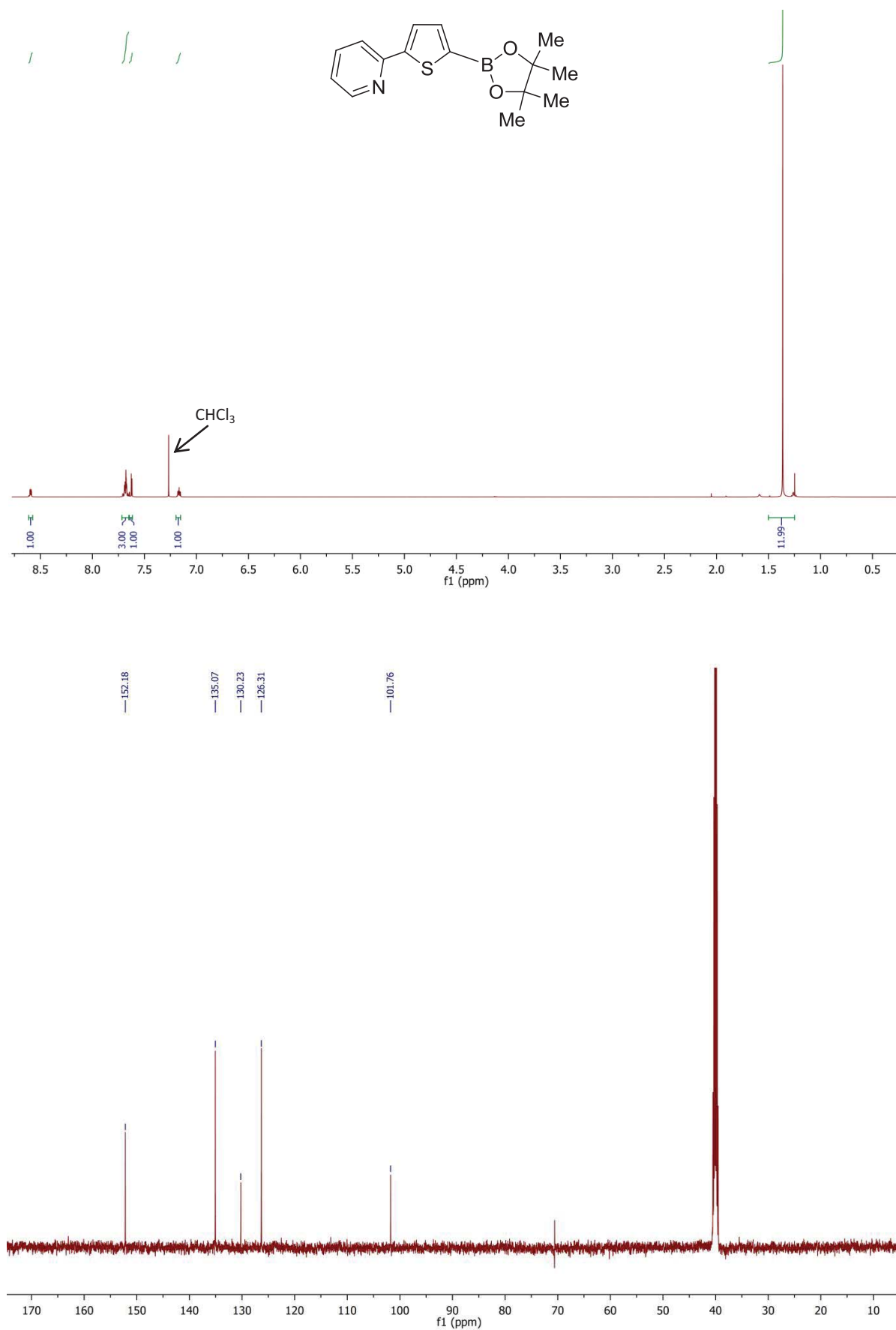
2-((2'-Bithiophen)-5-yl)-4,4,5,5-tetramethyl-1,3,2-dioxaborolane (29)



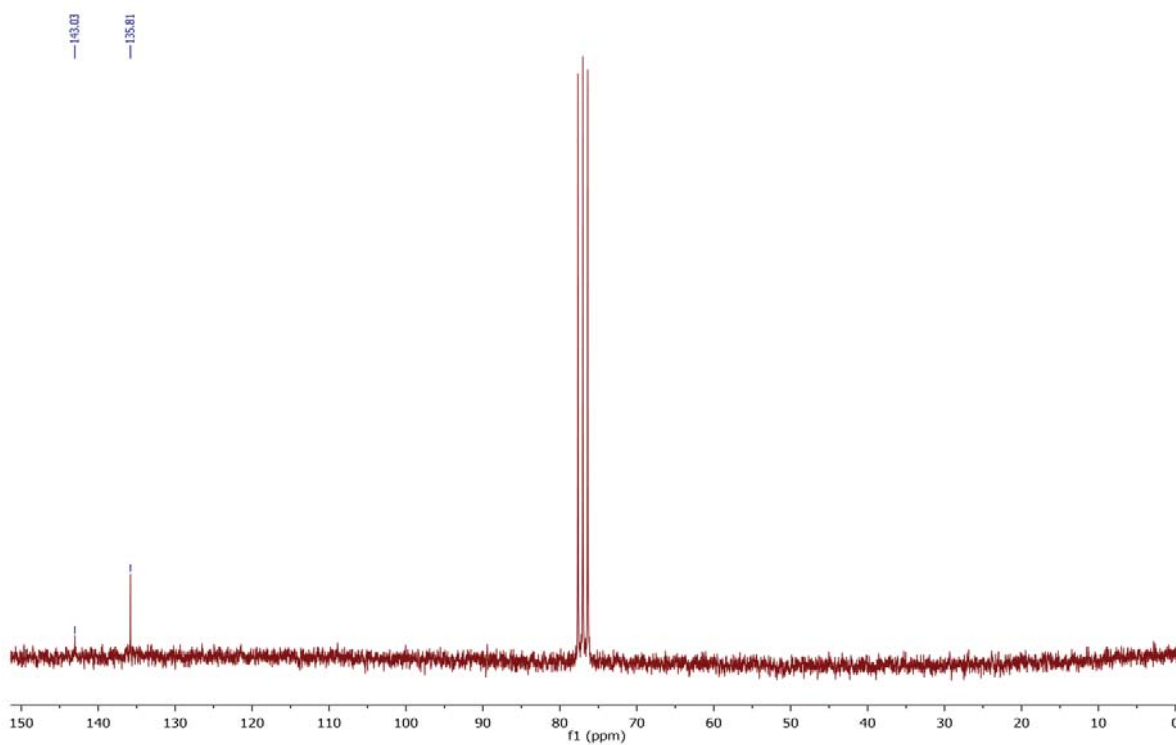
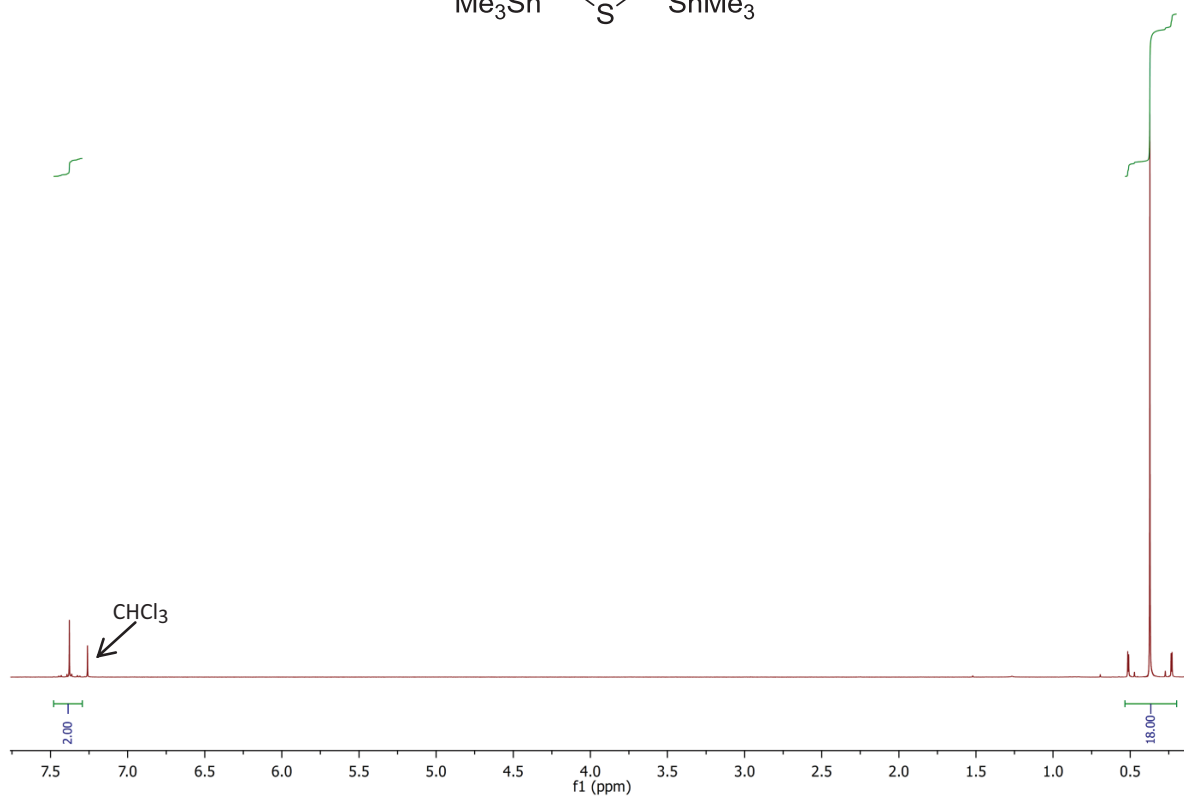
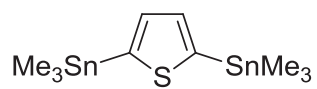
4,4,5,5-Tetramethyl-2-(5-phenylthiophen-2-yl)-1,3,2-dioxaborolane (31)



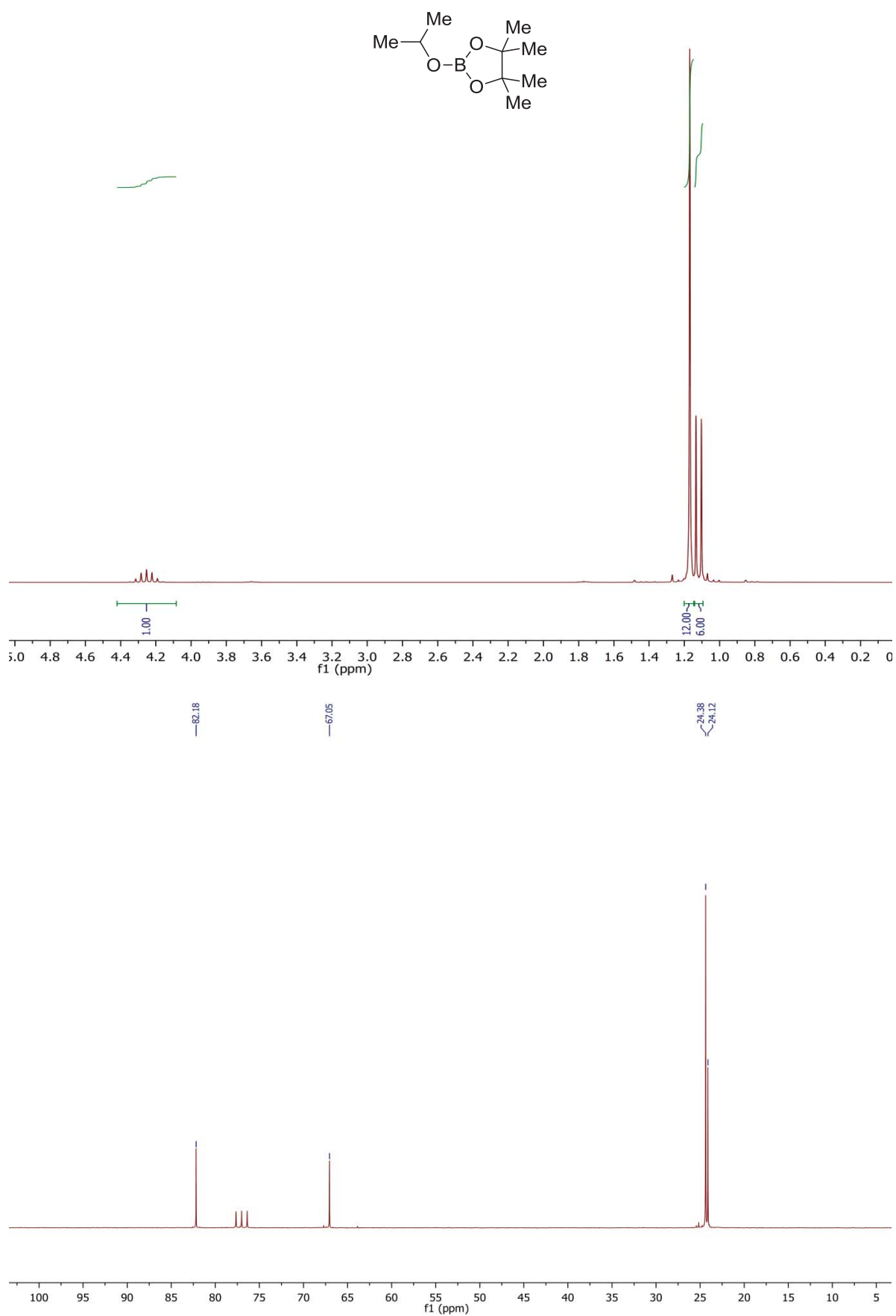
2-(5-(4,4,5,5-Tetramethyl-1,3,2-dioxaborolan-2-yl)thiophen-2-yl)pyridine (33)



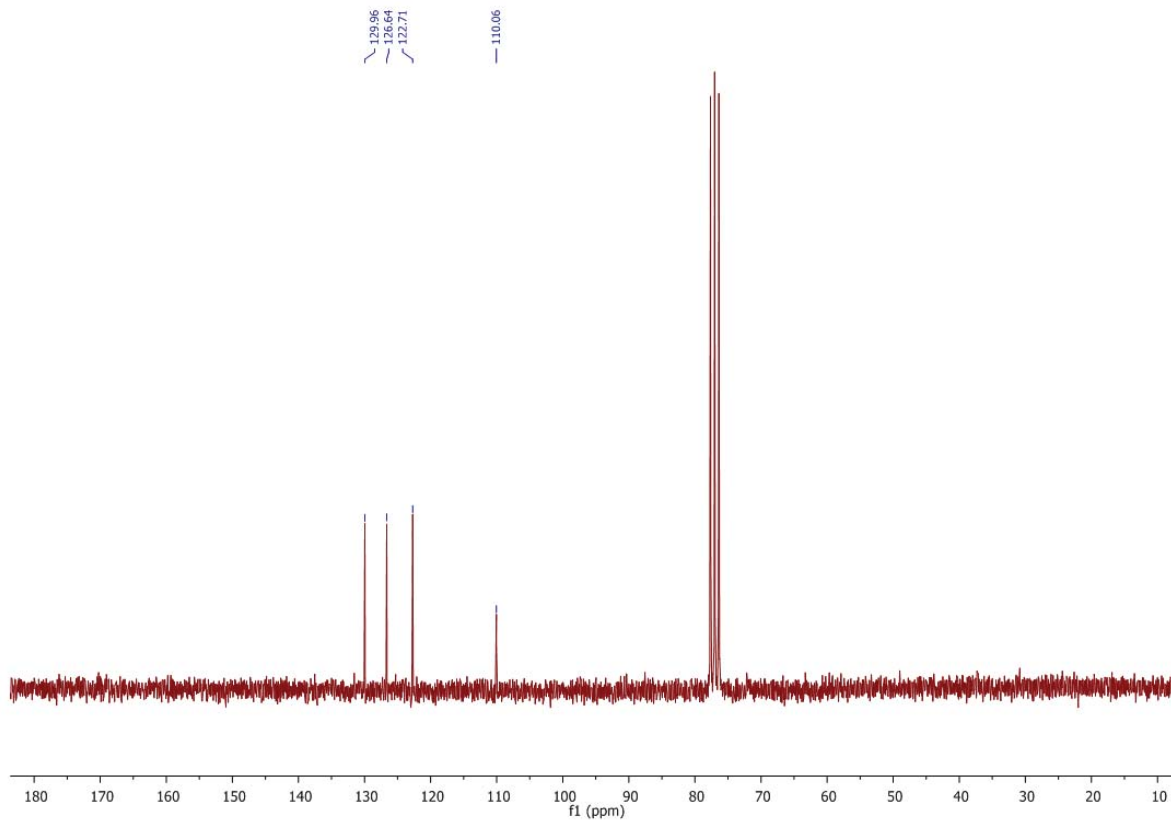
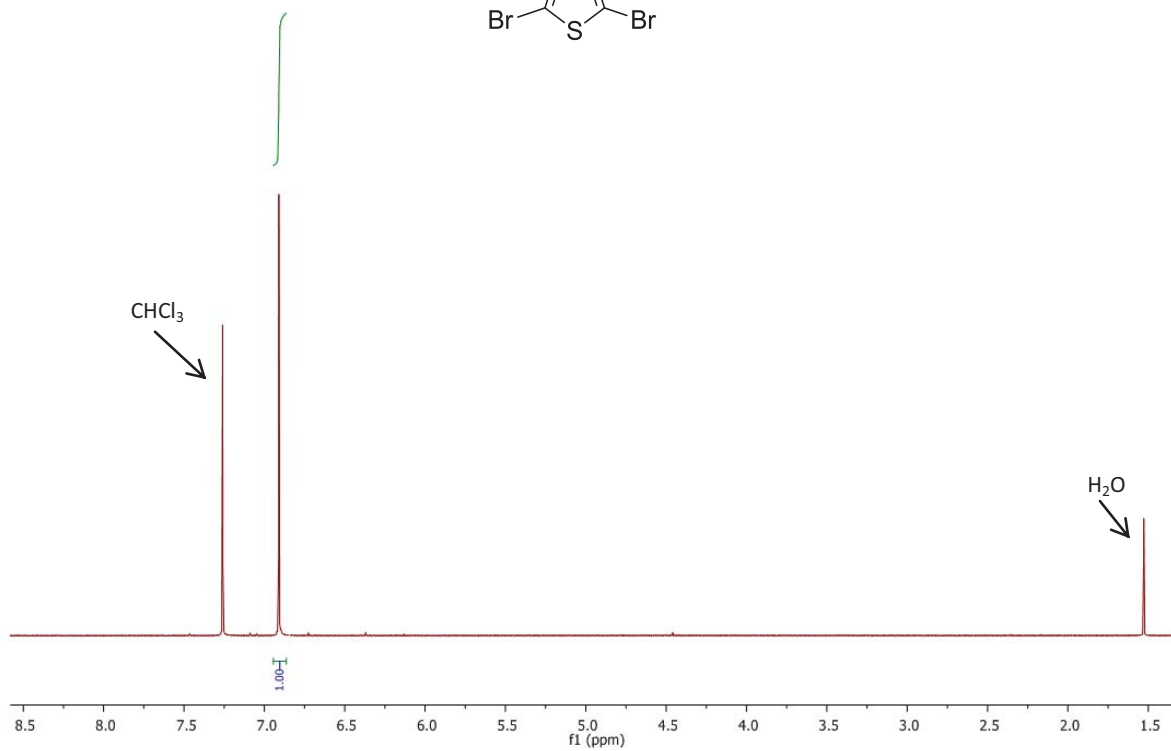
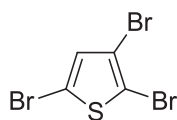
2,5-Bis(trimethylstannyl)thiophene (35)



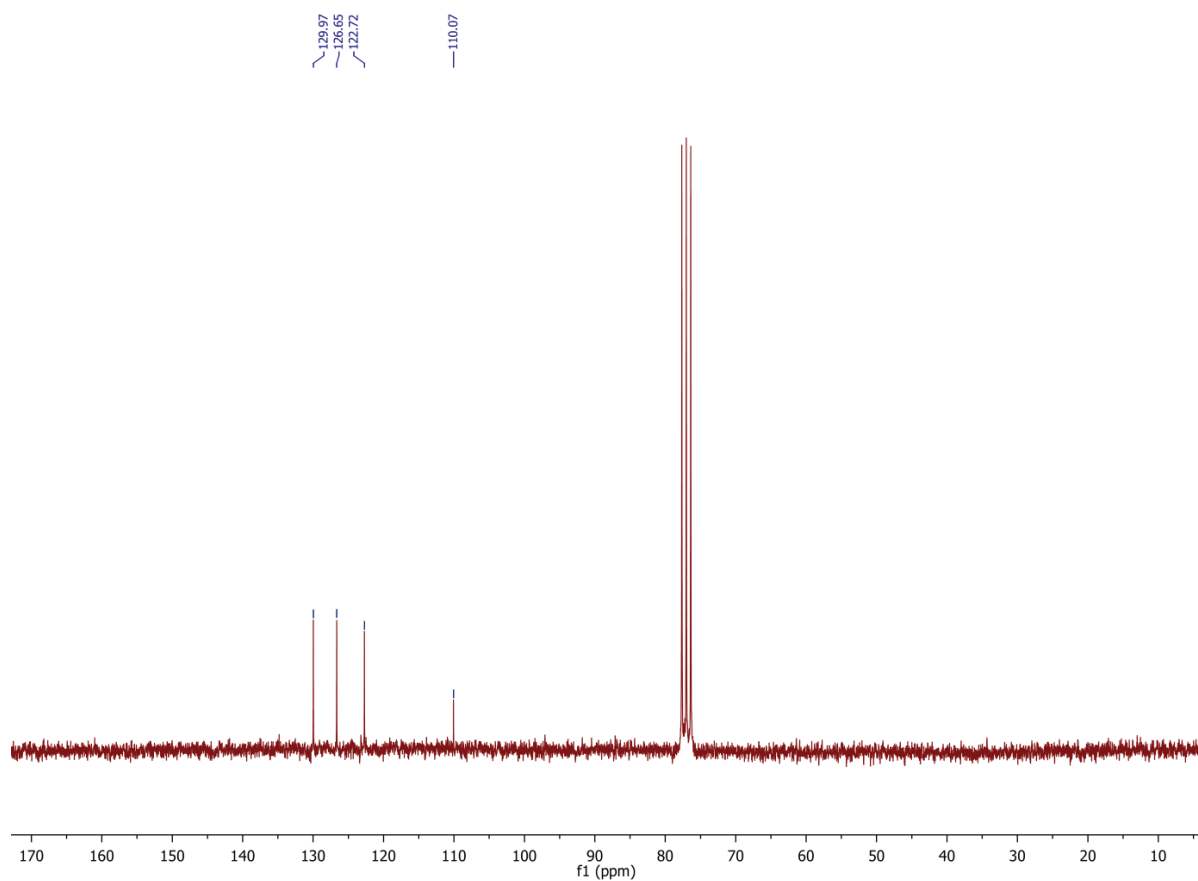
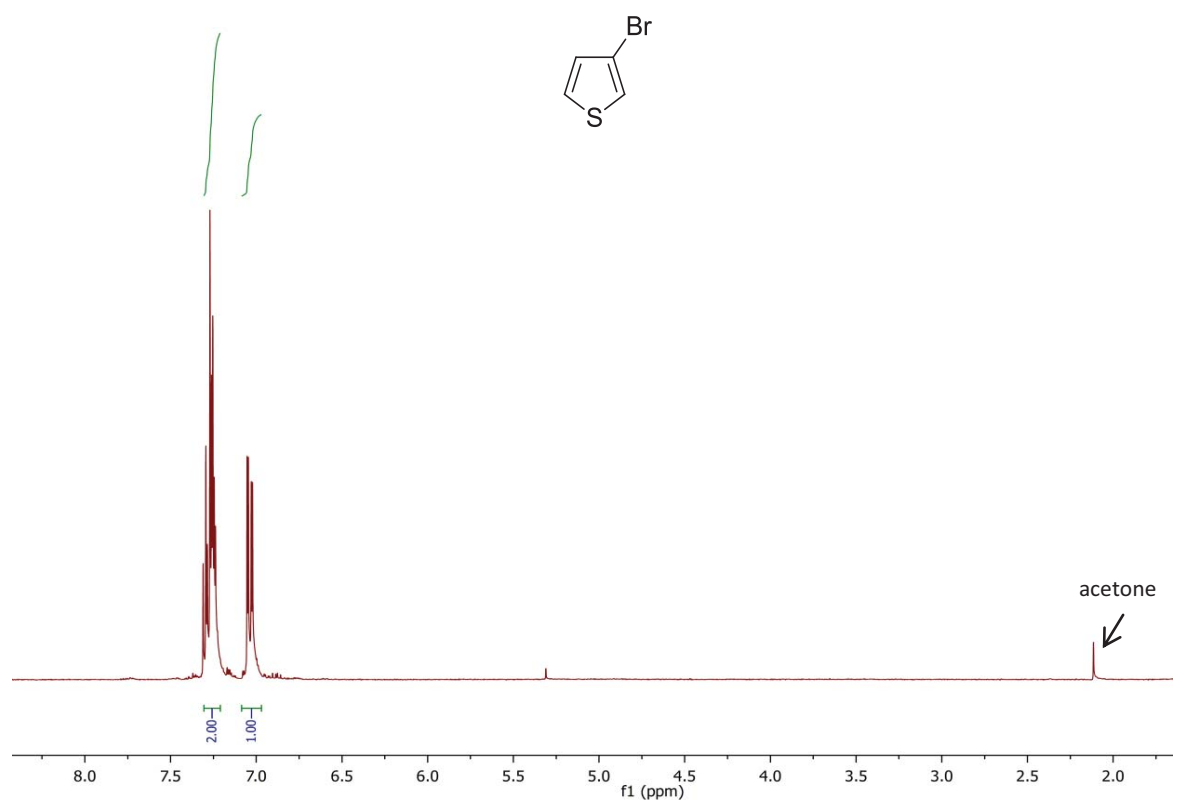
2-Isopropoxy-4,4,5,5-tetramethyl-1,3,2-dioxaborolane (iPrO-BPin; 36)

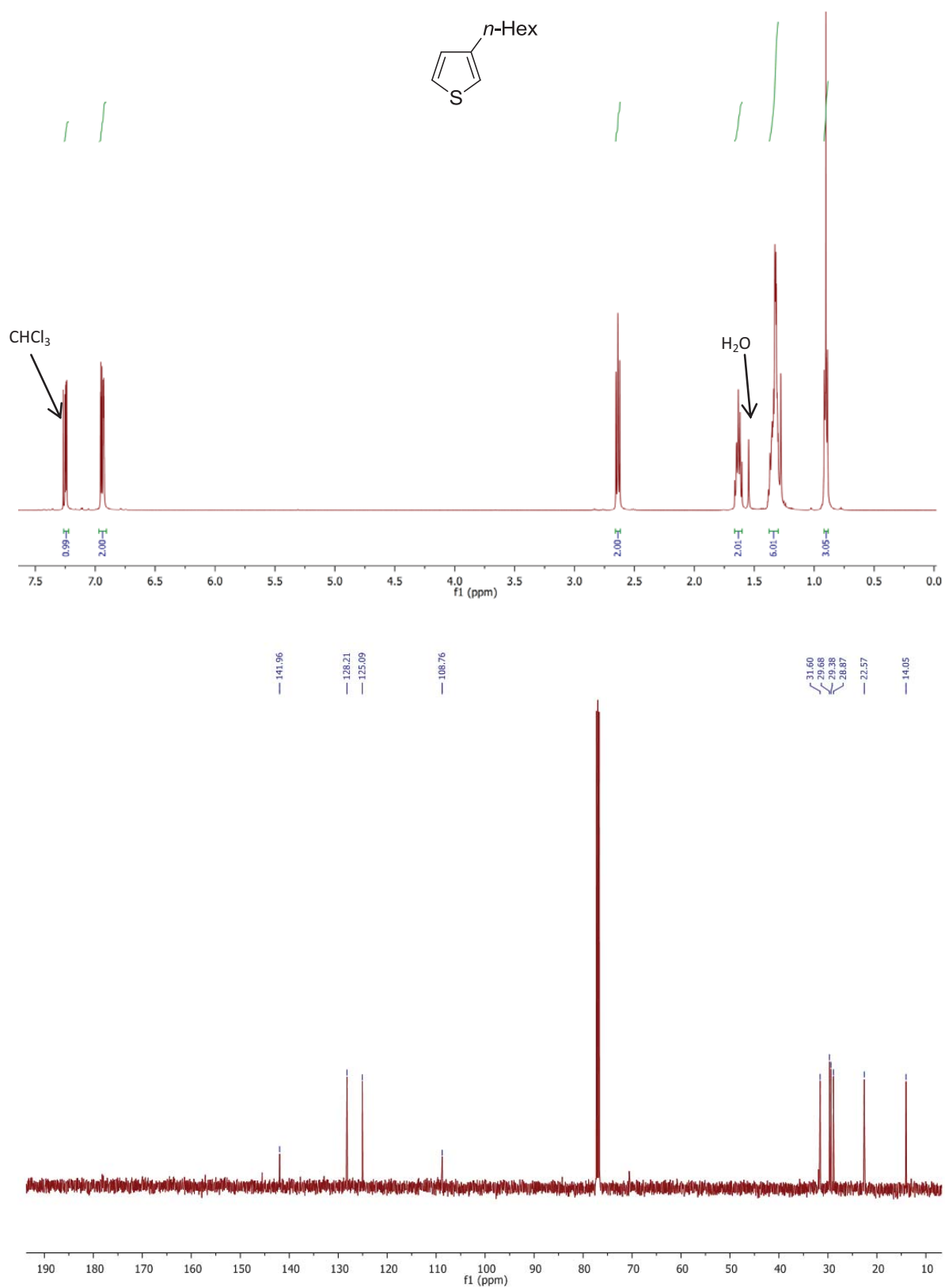


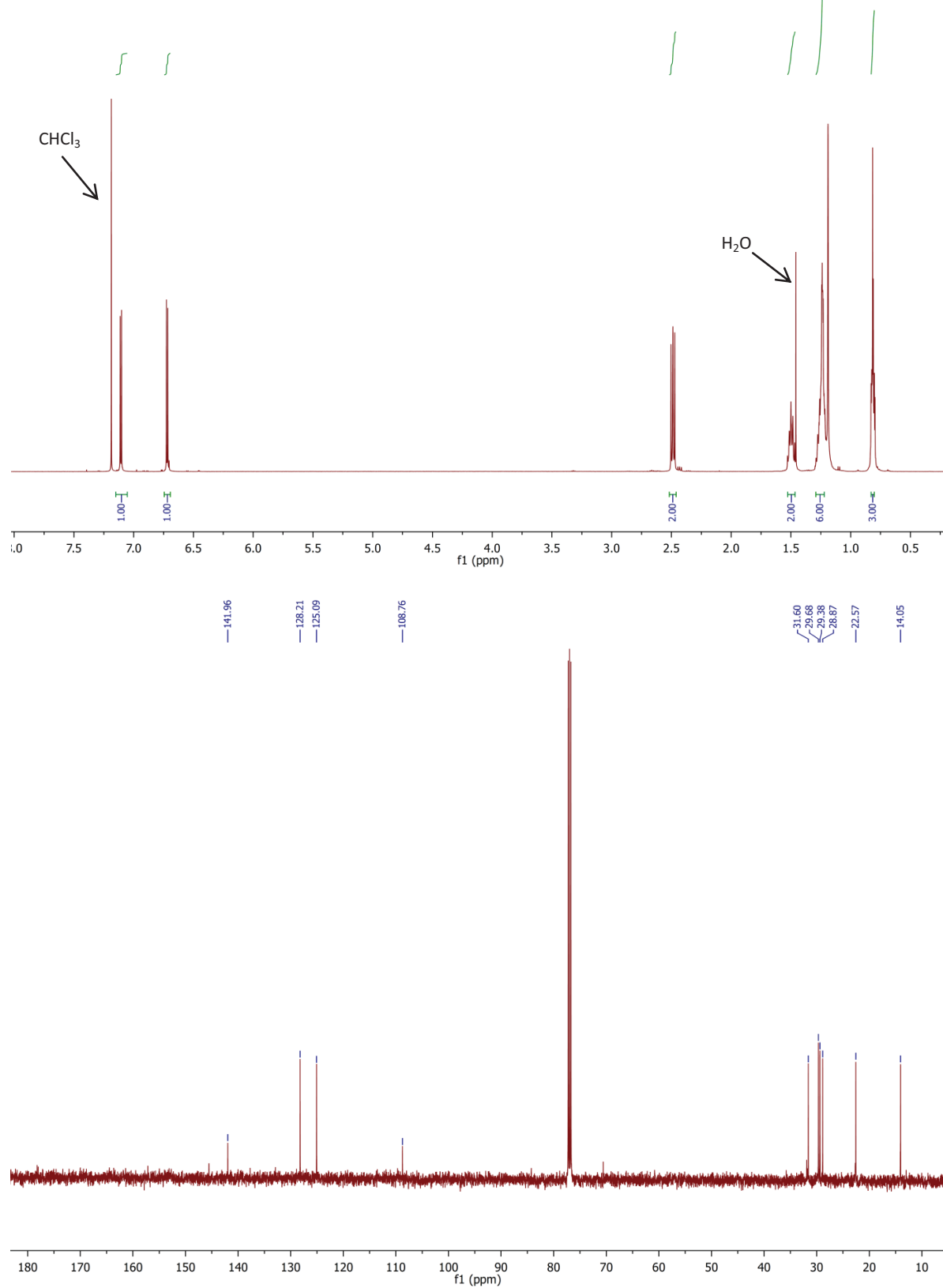
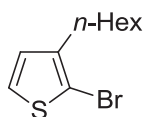
2,3,5-Tribromothiophene (37)



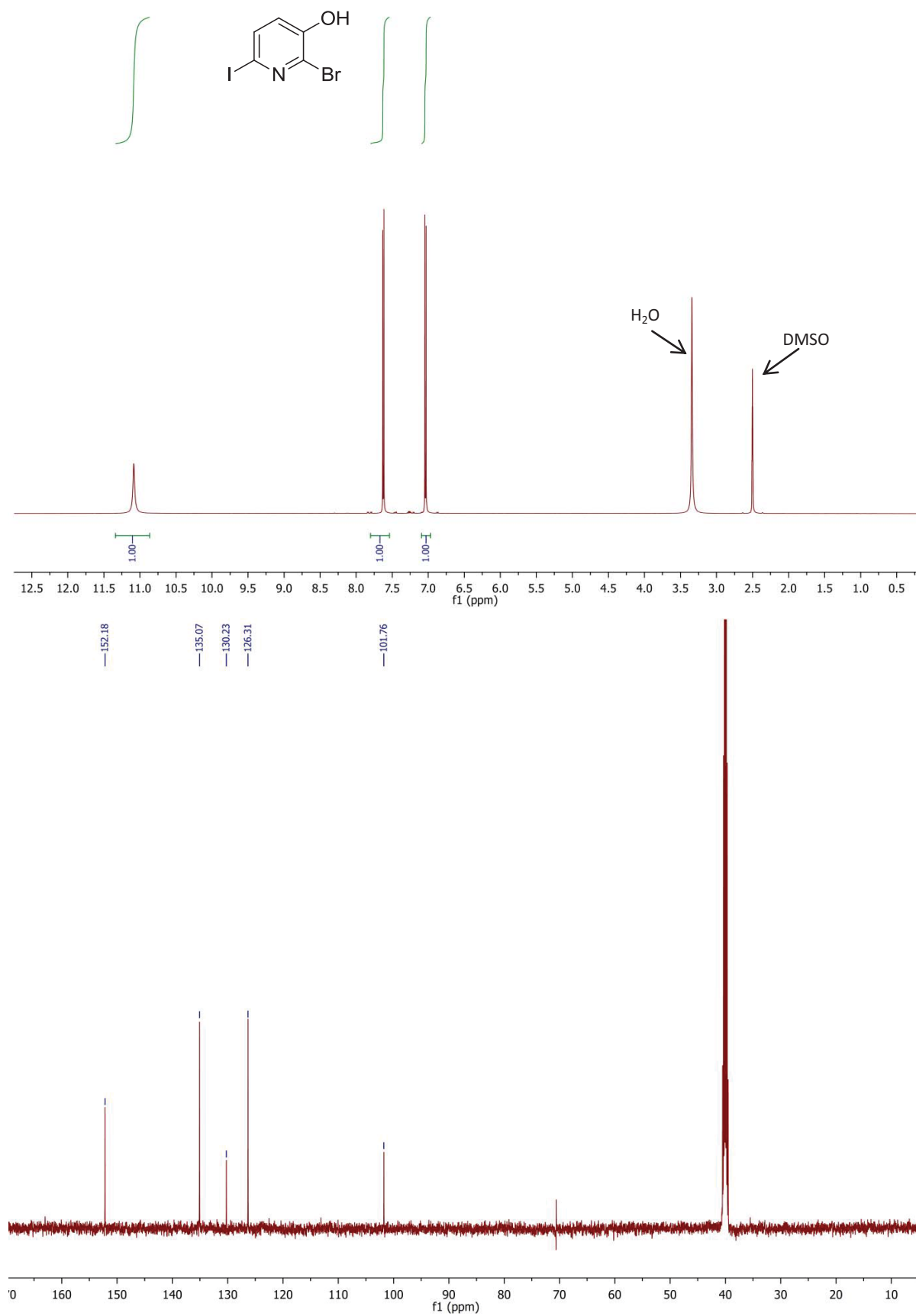
3-Bromothiophene (38)



3-*n*-Hexylthiophene (39)

2-Bromo-3-*n*-hexylthiophene (40)

2-Bromo-6-iodopyridin-3-ol (41)

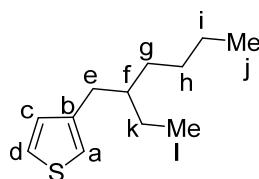


5.1.2 Further Experimental Data on Chapter 3.1

For general methods and materials see beginning of this chapter 5.2. The synthesis of 3-bromothiophene is described in the main SI (chapter 5.1.1). 1-Bromo-2-ethylhexane was purchased from VWR Inc. in a purity of 98%. Compounds **65**, **66** and **67** (Outlook) were prepared by M. Ried under my supervision during an internship.

5.1.2.1 Syntheses

3-(2-Ethylhexyl)thiophene (**65**)

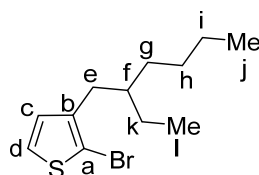


A solution of 1-bromo-2-ethylhexane (10.2 mL, 10.9 g, 56.0 mmol) in diethyl ether (30 mL) was added dropwise to a suspension of activated magnesium (1.36 g, 56.0 mmol) in ether (40 mL) over a course of 20 min. [Ni(dppp)Cl₂] (60 mg, 0.11 mmol) in ether (3 mL) was added at 19 °C in one portion, followed by addition of 3-bromothiophene (5.20 mL, 9.13 g, 56.0 mmol) in ether (20 mL) dropwise over a course of 30 min. The reaction mixture was heated to reflux for 15 h, was allowed to cool to 20 °C, poured into a mixture of crushed ice and 2 M HCl, and extracted with ether (3 x 100 mL). The combined organic layers were washed with a saturated solution of sodium hydrogen carbonate, brine and water and dried over sodium sulfate. The solvent was removed *in vacuo* and the crude product was purified by silica gel column chromatography (*n*-hexane, R_f = 0.8) to afford the product as colorless oil in a yield of 5.09 g (25.9 mmol, 46%).

¹H NMR (500 MHz, CDCl₃): δ = 7.22 (dd, 1H, ³J = 4.9 Hz, 3.0 Hz, Tph-H-d), 6.93-6.86 (m, 2H, Tph-H-a, c), 2.56 (d, 2H, ³J = 6.9 Hz, e), 1.62-1.48 (m, 1H, f), 1.36-1.20 (m, 8H, g, h, i, k), 0.94-0.80 (m, 6H, l, j) ppm.

¹³C NMR (126 MHz, CDCl₃): δ = 141.9 (Tph-C-b), 128.7 (Tph-CH-a/c), 124.7 (Tph-CH-d), 120.6 (Tph-CH-a/c), 40.3 (f), 34.2 (e), 32.5, 28.9, 25.6, 23.0 (g, h, i, k), 14.1 (j), 10.8 (l) ppm.

HRMS (EI⁺): *m/z* found 196.1284 (60) [M]⁺; calcd. for C₁₂H₂₀S 196.1286; found 98.1 (100) [M-C₇H₁₅]⁺.

2-Bromo-3-(2-ethylhexyl)thiophene (66)

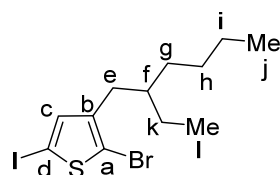
N-Bromosuccinimide (2.22 g, 12.5 mmol) was added to 3-(2-Ethyl)-hexylthiophene (2.47 g, 12.5 mmol) in glacial acetic acid (75 mL) at 15 °C and the mixture was stirred for 2.5 h. Then, water (100 mL) was added and the reaction mixture was extracted with diethyl ether (3 x 40 mL). The organic layer was washed with 1 M sodium hydroxide solution followed by drying over magnesium sulfate. The solvent was removed *in vacuo* and gave the crude product which was distilled by Kugelrohr distillation (140 °C, 0.1 mbar) to afford the product as colorless oil in a yield of 1.48 g (5.40 mmol, 43%).

¹H NMR (500 MHz, CDCl₃): δ = 7.17 (d, 1H, ³*J* = 5.6 Hz, Tph-*H*-d), 6.76 (d, 1H, ³*J* = 5.6 Hz, Tph-*H*-c), 2.50 (d, 2H, ³*J* = 7.2 Hz, e), 1.66-1.55 (m, 1H, f), 1.37-1.16 (m, 8H, g, h, i, k), 0.88 (m, 6H, j, l) ppm.

¹³C NMR (126 MHz, CDCl₃): δ = 141.1 (Tph-C-b), 128.7 (Tph-CH-c), 124.9 (Tph-CH-d), 109.4 (Tph-C-a), 39.9 (f), 33.6 (e/k), 32.4 (e/k), 28.7, 25.6, 23.0 (g, h, i), 14.0 (j), 10.8 (l) ppm.

IR (ATR): $\tilde{\nu}$ = 2957 (s), 2924 (s), 2857 (s), 1458 (m), 1410 (w), 1378 (m), 1232 (w), 991 (m), 829 (m), 718 (s), 684 (s), 640 (m) cm⁻¹.

HRMS (EI⁺): *m/z* found 274.0386 (55) [M]⁺; calcd. for C₁₂H₁₉SBr 274.0391; found 197.3/195.2 (90) [M-Br]⁺; found 177.9 (100) [M-C₇H₁₅]⁺.

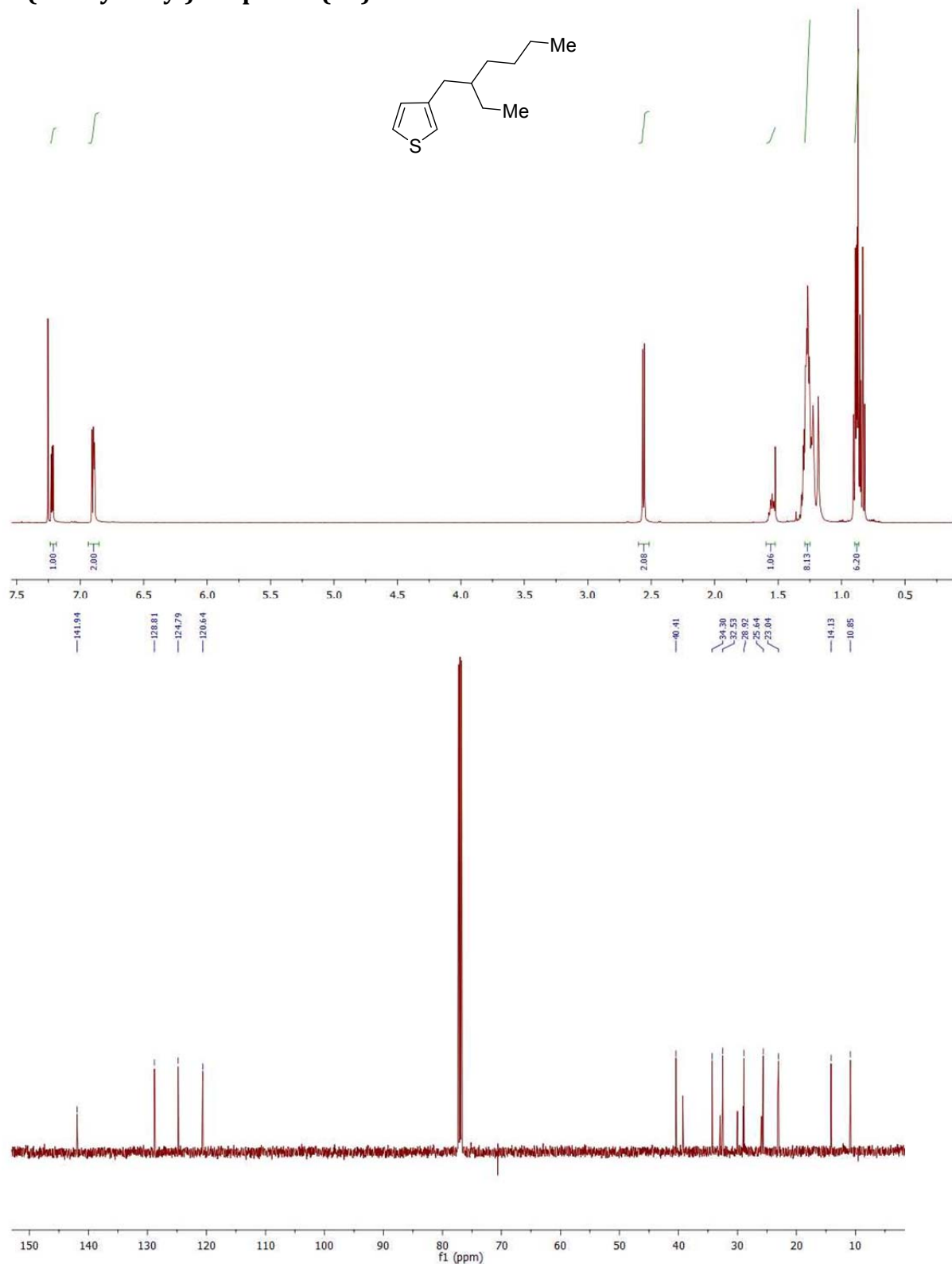
2-Bromo-5-Iodo-3-(2-ethylhexyl)thiophene (67)

To a solution of 2-bromo-3-(2-ethyl)-hexylthiophene (910 mg, 3.30 mmol) in DCM (20 mL), iodine (420 mg, 1.65 mmol) and iodobenzene diacetate (530 mg, 1.65 mmol) were added at 0 °C over a course of 3 min. The mixture was stirred at 20 °C for 4 h. Then, a solution of sodium dithiosulfate (10% in water) was added and the mixture was extracted with diethyl ether (3 x 30 mL). The organic layer was dried over magnesium sulfate. The solvent and iodobenzene were removed *in vacuo*. The residue was purified by silica gel column chromatography (*n*-hexane, $R_f = 0.92$) followed by vacuum distillation (85 °C, 4.2×10^{-2} mbar) to afford the product as colourless oil in a yield of 670 mg (1.65 mmol, 50%).

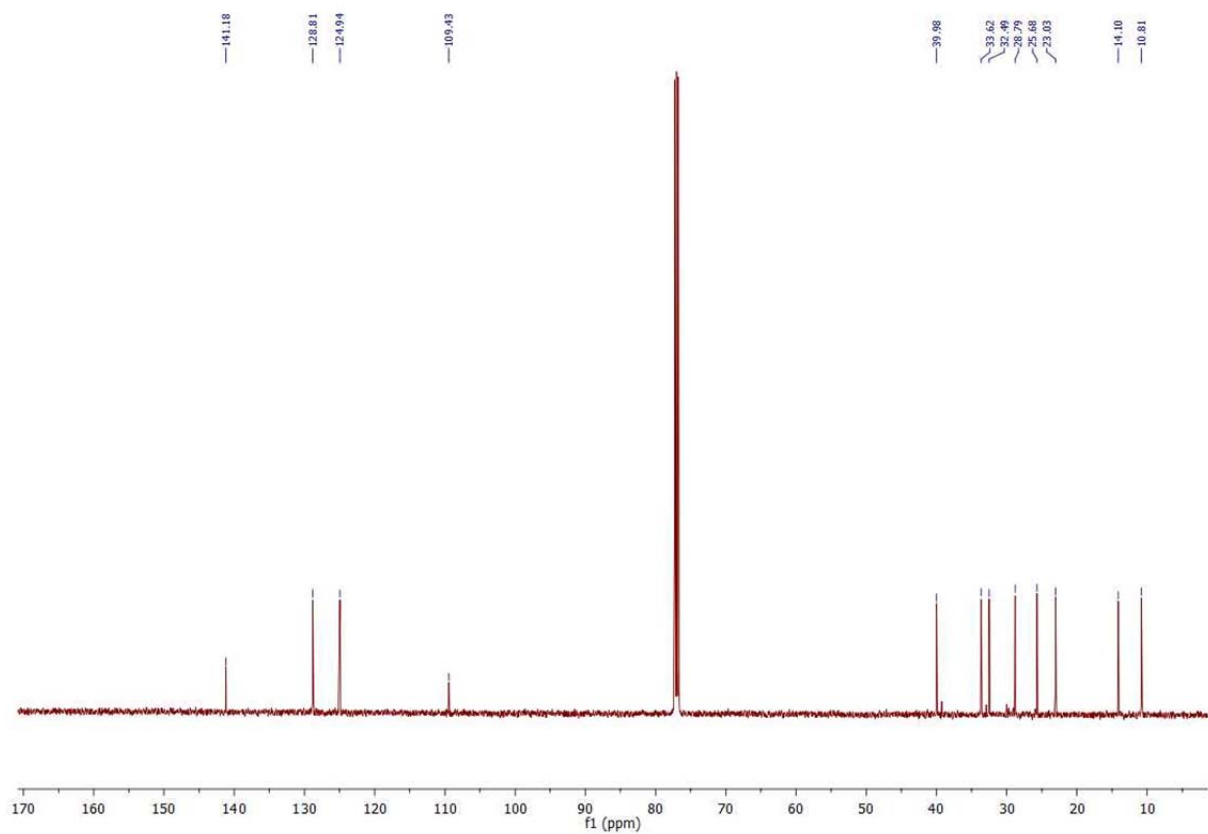
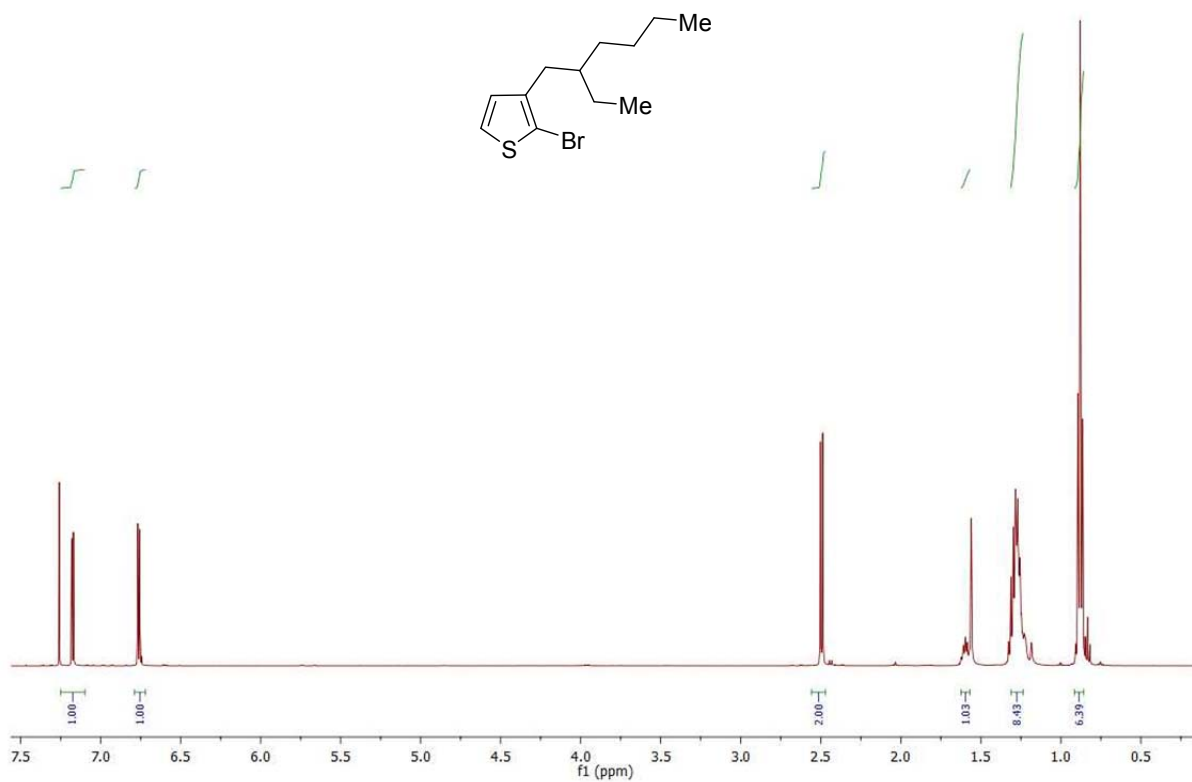
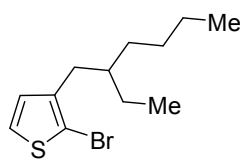
$^1\text{H NMR}$ (500 MHz, CDCl_3): $\delta = 6.93$ (s, 1H, Tph-*H*-c), 2.46 (d, 2H, $^3J = 7.1$ Hz, e), 1.65-1.48 (m, 1H, f), 1.36-1.14 (m, 8H, g, h, i, k), 0.95-0.81 (m, 6H, j, l) ppm.

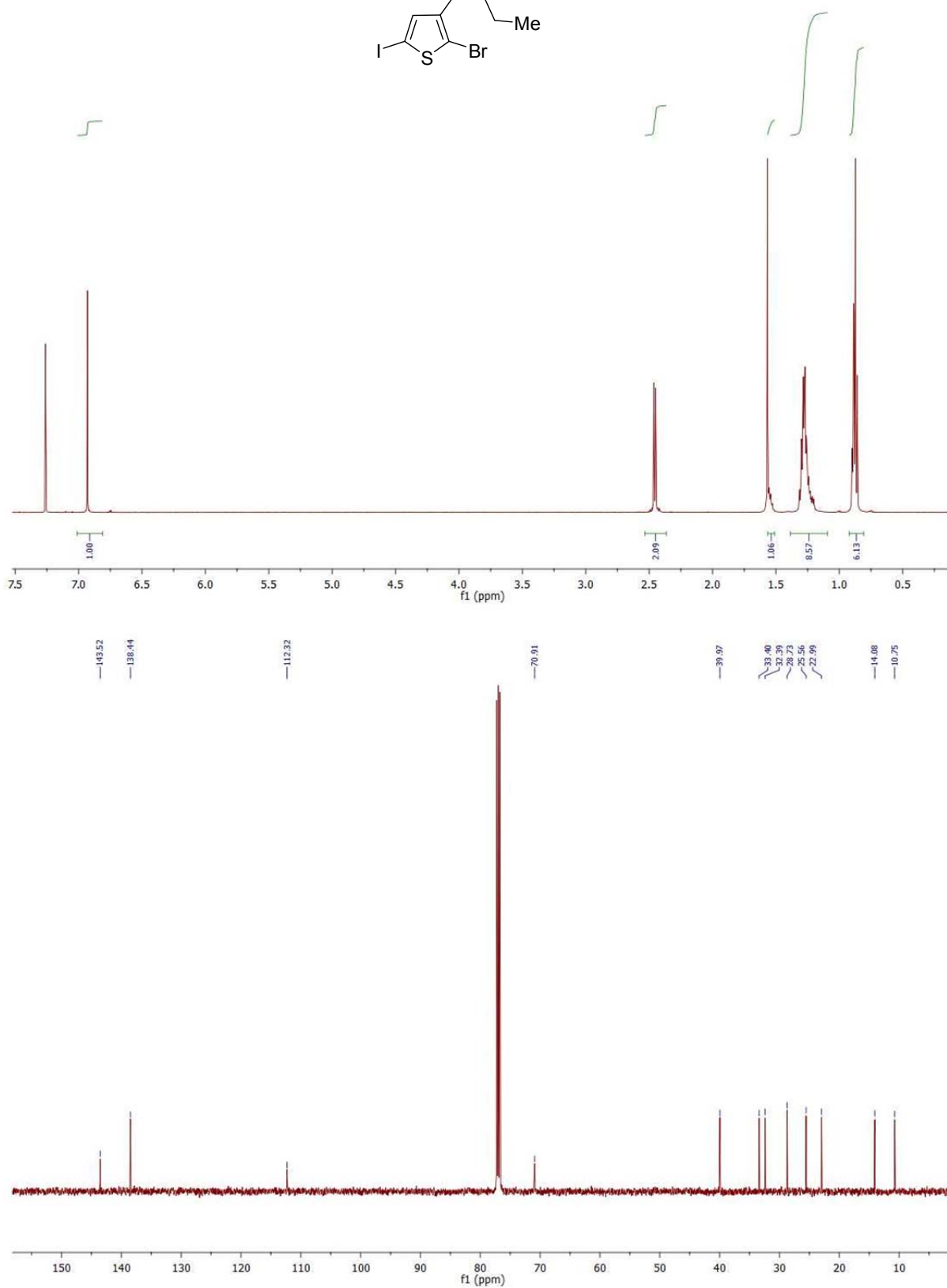
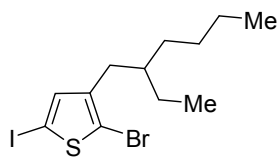
$^{13}\text{C NMR}$ (126 MHz, CDCl_3): $\delta = 143.5$ (Tph-C-b), 138.4 (Tph-CH-c), 112.3 (Tph-C-a), 70.9 (Tph-C-d), 39.9 (f), 33.4 (e), 32.3 (g), 28.7 (h), 25.5 (k), 22.9 (i), 14.0 (l), 10.7 (j) ppm.

IR (ATR): $\tilde{\nu} = 2956$ (s), 2924 (s), 2856 (s), 1458 (m), 1403 (w), 1378 (m), 1175 (w), 1005 (m), 915 (w), 831 (s), 469 (s) cm^{-1} .

5.1.2.2 ^1H NMR Spectra and $^{13}\text{C}\{^1\text{H}\}$ NMR Spectra3-(2-Ethylhexyl)thiophene (65)¹

¹ The compound shows impurities in the alkyl region. This impurity is caused by unreacted alkylation reagent and is removed in the next step.

2-Bromo-3-(2-ethylhexyl)thiophene (66)

2-Bromo-5-Iodo-3-(2-ethylhexyl)thiophene (67)

5.2 Supporting Information on Chapter 3.2

5.2.1 Supporting Information for the Manuscript *Aromatic Dinucleophiles*

Supporting Information

for

Aromatic Dinucleophiles

*Annika C. J. Heinrich, Paul J. Gates, Christian Näther and Anne Staubitz**

Abbreviations

General Methods and Materials

GC Optimization Reactions

Syntheses

^1H NMR Spectra and $^{13}\text{C}\{^1\text{H}\}$ NMR Spectra

Single Crystal Data of (5-(4,4,5,5-Tetramethyl-1,3,2-dioxaborolan-2-yl)thiophen-2-yl)(triphenylphosphine)gold **35**

Single Crystal Data of (5-Iodothiophen-2-yl)(triphenylphosphine)gold **37**

Single Crystal Data of (5-Iodophenyl-2-yl)(triphenylphosphine)gold **39**

Abbreviations

A	area
ATR	attenuated total reflectance
calcd.	calculated
CI	chemical ionization
COSY	correlated spectroscopy
d	doublet (NMR)
DCM	dichloromethane
dd	doublet of doublets (NMR)
Decomp. temp.	decomposition temperature
DMF	<i>N,N</i> -dimethylformamide
dppe	1,2-bis(diphenylphosphino)ethane
dppf	1,1'-bis(diphenylphosphino)ferrocene
EI	electron ionization
GC	gas chromatography
GC-MS	gas chromatography-mass spectrometry
HMBC	heteronuclear multiple bond coherence
HSQC	heteronuclear single quantum coherence
Ind	indole scaffold
IR	infrared
LDA	lithium diisopropylamide
m	medium (concerning the intensity) (IR)
m	multiplet (NMR)
M.p.	melting point
MS	mass spectrometry
MW	microwave
n	amount of substance
Phe	benzenescaffold
Pin	pinacol
Pyr	pyridine scaffold
R _f	response factor
s	strong (concerning the intensity) (IR)
s	singlet (NMR)
t	triplet (NMR)
THF	tetrahydrofuran
TMEDA	tetramethylethylenediamine
TMS	tetramethylsilane
TOF	time of flight
Tph	thiophene scaffold
w	weak (concerning the intensity) (IR)

General Methods and Materials

All syntheses were carried out using standard Schlenk techniques or in a glovebox under a dry and inert nitrogen atmosphere. In the cases in which argon was used or the reaction was not performed under inert reaction conditions, this is noted specifically in the procedure. Glassware and NMR-tubes were dried in an oven at 200 °C for at least 2 h before use. Reaction vessels were heated under vacuum and purged with nitrogen three times before adding reagents.

Analyses

^1H NMR, $^{13}\text{C}\{^1\text{H}\}$ NMR, ^{11}B NMR, ^{31}P NMR and ^{119}Sn NMR spectra were recorded at 300 K.

^1H NMR spectra were recorded on a Bruker DRX 500 (500 MHz) spectrometer or a Bruker Avance 600 spectrometer. $^{13}\text{C}\{^1\text{H}\}$ NMR spectra were recorded on a Bruker DRX 500 (126 MHz) spectrometer or a Bruker Avance 600 spectrometer. ^{11}B NMR, ^{31}P NMR and ^{119}Sn NMR spectra were recorded on a Bruker DRX 500 (160 MHz, 202 MHz and 187 MHz) spectrometer.

^1H NMR and $^{13}\text{C}\{^1\text{H}\}$ NMR spectra were referenced against the solvent residual proton signals (^1H) or the solvent itself (^{13}C). ^{11}B NMR spectra were referenced against $\text{BF}_3\cdot\text{OEt}_2$ in CDCl_3 , the reference of the ^{119}Sn NMR spectra was calculated based on the ^1H NMR signal of TMS.

The exact assignment of the peaks was proved by ^1H , ^{13}C DEPT and two-dimensional NMR spectroscopy such as ^1H COSY, ^{13}C HSQC or $^1\text{H}/^{13}\text{C}$ HMBC when possible.

All melting points were recorded on an Electrothermal melting point apparatus LG 1586 and are uncorrected.

IR spectra were recorded on a Perkin Elmer Paragon 1000 FT-IR spectrometer with a A531-G Golden-Gate-ATR-unit.

Ultra High resolution ESI mass spectra were recorded on a Bruker Daltonics Apex IV Fourier Transform Ion Cyclotron resonance mass spectrometer or on a Bruker Daltonics micrOTOF II mass spectrometer. The high resolution EI mass spectra were run on a VG Analytical Autospec apparatus or a Jeol AccuTOF JMS-T100GCV mass spectrometer.

GC-MS analysis was performed on a Hewlett Packard 5890A gas chromatograph, equipped with a Hewlett Packard 5972A mass selective detector and an Agilent Technologies

poly(dimethylsiloxane) column (19091S-931E, nominal length 15 m, 0.25 mm diameter, 0.25 μm grain size).

GC analysis was performed on an Agilent Technologies 6890N gas chromatograph, equipped with an Agilent Technologies 7683 Series Injector, an Agilent Technologies (5 %-phenyl)-poly(methylsiloxane) column (19091J-413, nominal length 30 m, 0.32 mm diameter, 0.25 μm grain size) and a flame ionization detector (FID).

All microwave irradiation reactions were carried out on a Biotage[®] Initiator+ SP Wave synthesis system, with continuous irradiation power from 0 to 300 W. All reactions were carried out in 5 mL oven-dried Biotage microwave vials sealed with an aluminum/Teflon[®] crimp top, which can be exposed to a maximum of 250 °C and 20 bar internal pressure. The reaction temperature was measured by an external IR sensor.

The single crystal data were measured using an Imaging Plate Diffraction System (IPDS-1) from STOE & CIE and were corrected for absorption using X-Red and X-Shape from STOE & CIE (Min/max. transmission: 0.4839/0.7604). The structure was solved with direct methods using SHELXS-97 and refinement was performed against F^2 using SHELXL-97.

Chemicals

All reagents were used without further purification unless noted otherwise.

The preparation of *i*PrO-BPin (2-isopropoxy-4,4,5,5-tetramethyl-1,3,2-dioxaborolane, **P1-36**), 2-bromo-3-*n*-hexylthiophene (**P1-40**) and 2-bromo-3-*n*-hexyl-5-iodothiophene (**P1-3**) was already described in the supporting information of *Org. Lett.* **2013**, *15*, 4666 (see chapter 5.1). 3-*n*-Hexylthiophene was either bought (see following table) or prepared, starting with thiophene, which is described in the supporting information *Org. Lett.* **2013**, *15*, 4666 (see chapter 5.1).

Name	Supplier	Purity	Comment
Acetic acid	Merck Inc.	99.8%	anhydrous
Ammonium chloride	Grüssing Inc.	99.5%	
Glacial acetic acid	Grüssing	99%	
Gold	Degussa Inc.	99.9%	
1-Boc-5-bromoindole-2-boronic acid	Alfa Aesar Inc.	95%	
2-(4-Iodophenyl)-4,4,5,5-tetramethyl-1,3,2-dioxaborolane	Sigma Aldrich Inc.	97%	

2-Bromopyridine-5-boronic acid	TCI Inc.	≥96%	
2-Iodothiophene	Acros Inc.	98%	
3- <i>n</i> -Hexylthiophene	Sigma Aldrich Inc.	>99%	
Hexamethyldistannane	VWR Inc.	99%	
Hydrochloric acid	Grüssing Inc.	37%	
Magnesium sulfate	Grüssing Inc.	99%	
Molecular sieves, 3 Å	Alfa Aesar Inc.		
Nitric acid	Grüssing Inc.	68%	
<i>N</i> -Bromosuccinimide	Alfa Aesar Inc.	99%	
<i>N</i> -Iodosuccinimide	Molekula	95%	
<i>n</i> -Butyllithium	Acros Inc.		2.5 M in hexanes
Pinacol	ABCR Inc.	99%	
Sodium	Merck Inc.	≥ 99%	
Sodium chloride	Grüssing Inc.	99.5%	
Sodium hydroxide	Grüssing Inc.	99.5%	
Sodium hydrogen carbonate	Grüssing Inc.	99%	
Thiophene	VWR Inc.	99%	distilled
Triisopropyl borate	Strem Chemicals Inc.	>98%	
Trimethyltin chloride	Acros Inc.	99%	
Triphenylphosphine	Alfa Aesar Inc.	99%	

Chromatography

For the chromatographic purification, silica gel (Macherey-Nagel Inc., grain size 0.040 - 0.063 mm) was used. Thin layer chromatography was performed using pre-coated plates from Macherey-Nagel Inc., ALUGRAM[®] Xtra SIL G/UV254. Most chromatography purifications were carried out using an Interchim Puriflash[®] 430 system, where cartridges of Interchim (silica HC, grain size 50 µm, 120 g or 80 g) were used.

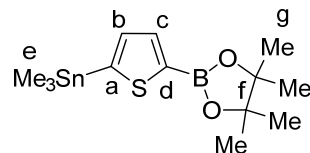
Solvents

All solvents were used freshly distilled after refluxing for several hours over the specified drying agent under nitrogen and were stored in a J. Young's-tube. If no drying agent is noted, the solvents were only distilled for purification purposes.

Solvent	Comment
Acetic acid	Grüssig Inc.
CDCl ₃	Deutero Inc.
Chloroform	VWR Inc., HPLC grade
Dichloromethane	BCD Inc.
DMF	Acros Inc., CaH ₂ ; stored over 3 Å molecular sieves
Ethyl acetate	BCD Inc.
Methanol	Baker Inc., HPLC grade
<i>n</i> -Hexane	Walter CMP Inc., sodium with benzophenone as an indicator; degassed by freeze-pump-thaw technique, stored over 3 Å molecular sieves
<i>n</i> -Pentane	Walter CMP Inc., lithium aluminium hydride; degassed by freeze-pump-thaw technique, stored over 3 Å molecular sieves
THF	Sigma Aldrich Inc., CaH ₂ with triphenylmethane as an indicator; degassed by freeze-pump-thaw technique, stored over 3 Å molecular sieves
Toluene	BCD Inc., sodium with benzophenone as an indicator; degassed by freeze-pump-thaw technique, stored over 3 Å molecular sieves

Syntheses

4,4,5,5-Tetramethyl-2-(5-(trimethylstannyl)thiophen-2-yl)-1,3,2-dioxaborolane (9)



Method (A)

n-Butyllithium (8.00 mL, 20.0 mmol, 2.50 M in *n*-hexane,) and TMEDA (2.33 g, 20.0 mmol) were dissolved in THF (30 mL) at -78 °C. 2,5-Dibromothiophene (2.40 g, 10.0 mmol) was added dropwise within 5 min to the solution, and the mixture was stirred for 30 min. Then, trimethyltin chloride (1.99 g, 10.0 mmol) in THF (24 mL) was added to the stirred solution over a period of 3 h via a syringe pump. The reaction mixture was stirred for another 5 h and then 2-isopropoxy-4,4,5,5-tetramethyl-1,3,2-dioxaborolane (1.86 g, 10.0 mmol) was added in one portion and the solution was allowed to warm to 20 °C and was stirred for 14 h. After aqueous workup and extraction with diethyl ether (3 x 20 mL), the combined organic layers were dried over sodium sulfate. The solvent was removed *in vacuo* and the by-products were removed by sublimation (25 °C, 2×10^{-2} mbar) to afford the product as a colorless solid in a yield of 3.18 g (8.02 mmol, 80%).

Method (B)

2-(5-Iodothiophen-2-yl)-4,4,5,5-tetramethyl-1,3,2-dioxaborolane (672 mg, 2.00 mmol), [Pd(PPh₃)₄] (0.50 mol%, 11.0 mg) and hexamethyldistannane (656 mg, 2.00 mmol) was dissolved in toluene (4 mL). The mixture was heated to 120 °C in the microwave for 20 min. Water (10 mL) was added to the reaction mixture and it was extracted with DCM (3 x 15 mL). After aqueous workup and extraction with diethyl ether (3 x 20 mL), the combined organic layers were dried over sodium sulfate. The solvent was removed *in vacuo* to afford the product a colorless solid in a yield of 754 mg (1.90 mmol, 95%) without further purification.

¹H NMR (500 MHz, CDCl₃): δ = 7.79 (d, 1H, ³J = 3.2 Hz, Tph-*H*-b/c), 7.33 (d, 1H, ³J = 3.2 Hz, Tph-*H*-b/c), 1.37 (s, 12H, g), 0.40 (s, 9H, e) ppm.

¹³C NMR (126 MHz, CDCl₃): δ = 146.5 (Tph-C-a), 137.8 (Tph-CH-b/c), 136.3 (Tph-CH-b/c), 84.1 (f), 24.9 (g), -8.1 (e) ppm.²

¹¹⁹Sn NMR (187 MHz, CDCl₃): δ = -26.8 ppm.

¹¹B NMR (160 MHz, CDCl₃): δ = 28.8 ppm.

IR (ATR): $\tilde{\nu}$ = 2978 (m), 2920 (w), 1510 (s), 1418 (s), 1331 (s), 1254 (m), 1138 (s), 1064 (s), 1021 (m), 957 (m), 928 (m), 853 (m), 820 (m), 770 (s), 665 (s), 533 (s) cm⁻¹.

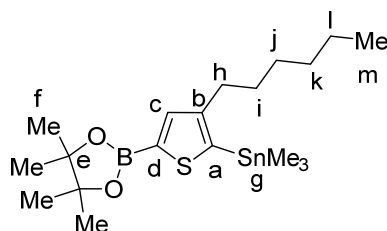
HRMS (ESI): *m/z* found 397.0432 (100) [M+Na]⁺; calcd. for C₁₃H₂₃BNaO₂SSn 397.0426.

M.p.: 84 °C.

The data agree with the literature, where the compound was prepared in a different way in a yield of 55%.³

² The carbon atom bound to boron was not visible due to the high quadrupole moment of the boron nucleus.

³ J. Linshoeft, A. C. J. Heinrich, S. A. W. Segler, P. J. Gates, A. Staubitz, *Org. Lett.* **2012**, *14*, 5644.

2-(4-*n*-Hexyl-5-(trimethylstannyl)thiophen-2-yl)-4,4,5,5-tetramethyl-1,3,2-dioxaborolane (14)

2-(4-*n*-Hexyl-5-iodothiophen-2-yl)-4,4,5,5-tetramethyl-1,3,2-dioxaborolane (919 mg, 1.00 mmol), [Pd(PPh₃)₄] (0.50 mol%, 6.0 mg) and hexamethyldistannane (393 mg, 1.20 mmol) were dissolved in toluene (4 mL). The mixture was heated to 120 °C in the microwave apparatus for 20 min. Water (10 mL) was added to the reaction mixture and it was extracted with DCM (3 x 15 mL). The organic layer was extracted with water (2 x 20 mL) and the aqueous layer was extracted with diethyl ether (3 x 20 mL). The combined organic layers were dried over sodium sulfate. The solvent was removed *in vacuo* to afford the product as yellow oil in a yield of 393 mg (0.86 mmol, quantitative) without further purification.

¹H NMR (500 MHz, CDCl₃): δ = 7.61 (s, 1H, Tph-*H*-c), 2.65-2.61 (m, 2H, h), 1.62-1.57 (m, 2H, i), 1.34-1.29 (m, 18H, j, k, l, f), 0.89 (t, 3H, ³J = 7.0 Hz, m), 0.37 (s, 9H, g) ppm.

¹³C NMR (126 MHz, CDCl₃): δ = 152.2 (Tph-C-b), 141.0 (Tph-CH-a), 138.9 (Tph-CH-c), 83.9 (e), 32.2 (h), 31.7, 29.3 (i, k), 26.9 (j), 24.7 (f), 22.6 (l), 14.1 (m), -8.1 (Sn(CH₃)₃) ppm.⁴

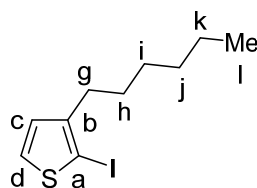
¹¹⁹Sn NMR (187 MHz, CDCl₃): δ = 35.6 ppm.

¹¹B NMR (160 MHz, CDCl₃): δ = 28.6 ppm.

IR (ATR): $\tilde{\nu}$ = 2977 (w), 2926 (m), 1526 (m), 1123 (m), 1369 (m), 1322 (s), 1267 (m), 1142 (s), 982 (m), 853 (s), 771 (s), 665 (s), 529 (s) cm⁻¹.

HRMS (ESI): *m/z* found 481.1358 (100) [M+Na]⁺; calcd. for C₁₉H₃₅BNaO₂SSn 481.1370.

⁴ The carbon atom bound to boron was not visible due to the high quadrupole moment of the boron nucleus.

2-Iodo-3-*n*-hexylthiophene (16)

This reaction was not performed under Schlenk conditions: *N*-Iodosuccinimide (6.75 g, 30.0 mmol) was added in one portion to 3-*n*-hexylthiophene (5.00 g, 40.0 mmol) in glacial acetic acid (50 mL) at 15 °C. The reaction mixture was stirred for 16 h at this temperature. Then, water (20 mL) was added and the reaction mixture was extracted with diethyl ether (3 x 20 mL). The organic layer was washed with sodium hydroxide solution (1 M, 5 x 50 mL) followed by drying over magnesium sulfate. The solvent was removed *in vacuo* and the crude product was distilled (kugelrohr, 8×10^{-3} mbar, 70 °C) to afford 7.72 g (26.3 mmol, 88%, Lit.⁵: 90% with impurities) of a slightly yellow oil.

¹H NMR (500 MHz, CDCl₃): δ = 7.38 (d, 1H, ³*J* = 5.5 Hz, Tph-*H*-d), 6.75 (d, 1H, ³*J* = 5.5 Hz, Tph-*H*-c), 2.60-2.51 (m, 2H, g), 1.61-1.52 (m, 2H, h), 1.39-1.28 (m, 6H, i, j, k), 0.94-0.86 (m, 3H, l) ppm.

¹³C NMR (126 MHz, CDCl₃): δ = 147.2 (Tph-C-b), 130.3 (Tph-CH-d), 127.9 (Tph-C-c), 73.9 (Tph-C-a), 32.1 (g), 31.6, 30.0, 28.9, 22.6 (h, i, j, k), 14.1 (l) ppm.

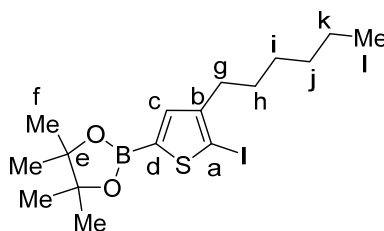
IR (ATR): $\tilde{\nu}$ = 2953 (m), 2923 (s), 2854 (s), 1456 (m), 1397 (m), 963 (m), 828 (s), 713 (s), 684 (s), 634 (s) cm⁻¹.

HRMS (EI⁺): *m/z* found 293.9937 (45) [M]⁺; calcd. for C₁₀H₁₅SI 293.9939; found 222.8 (100) [M-C₅H₁₁]⁺.

The NMR data are in agreement with the data found in the literature.⁶

⁵ T. Tkachov, V. Senkovskyy, H. Homber, A. Kiriya, *Macromolecules* **2011**, *44*, 2006.

⁶ T. Yokozawa, R. Suzuki, M. Nojima, Y. Ohta, A. Yokoyama, *Macromol. Rapid. Commun.* **2011**, *32*, 801.

2-(4-*n*-Hexyl-5-iodothiophen-2-yl)-4,4,5,5-tetramethyl-1,3,2-dioxaborolane (17)

A solution of diisopropylamine (2.42 g, 24.0 mmol) in THF (80 mL) was cooled to $-78\text{ }^{\circ}\text{C}$ and *n*-butyllithium (8.00 mL, 20.0 mmol, 2.5 M in *n*-hexane) was added dropwise over the course of 2 min. The mixture was warmed to $0\text{ }^{\circ}\text{C}$, cooled back to $-78\text{ }^{\circ}\text{C}$ and stirring was continued for 5 min. 2-Iodo-3-hexylthiophene (5.88 g, 20.0 mmol) was added dropwise over 5 min and the reaction mixture was stirred for 1 h at $-78\text{ }^{\circ}\text{C}$. *i*PrO-BPin (3.72 g, 20.0 mmol) was added dropwise over a course of 5 min to the orange-brown suspension and the reaction mixture was stirred at $-78\text{ }^{\circ}\text{C}$ for 15 min. Then the cooling bath was removed and the mixture was stirred for 3 h at $15\text{ }^{\circ}\text{C}$. The reaction was quenched with methanol (50 mL) and the solvents were removed *in vacuo*. The residue was dissolved in DCM (40 mL), washed with water (2 x 50 mL) and dried over magnesium sulfate. The solvent was removed *in vacuo* and the mixture was purified by silica gel column chromatography (pentane : ethyl acetate, $R_f = 0.65$, with a gradient starting with pure pentane to a mixture of pentane : ethyl acetate of 95 : 5) to afford the product in a yield of 7.07 g (16.8 mmol, 84%, Lit.⁷: 30%) as a dark red oil.

¹H NMR (500 MHz, CDCl₃): $\delta = 7.24$ (s, 1H, Tph-*H*-c), 2.52 (m, 2H, g), 1.63-1.53 (m, 2H, h), 1.40-1.26 (m, 18H, i, j, k, f), 0.89 (t, 3H, ³*J* = 7.9 Hz, l) ppm.

¹³C NMR (126 MHz, CDCl₃): $\delta = 148.6$ (Tph-C-b), 137.5 (Tph-CH-c), 84.2 (e), 82.7 (Tph-C-a), 31.9, 31.6, 29.9, 28.9 (g, h, i, j), 24.7 (f), 22.6 (k), 14.1 (l) ppm.

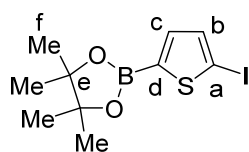
¹¹B NMR (160 MHz, CDCl₃): $\delta = 28.3$ ppm.

IR (ATR): $\tilde{\nu} = 2955$ (w), 2926 (m), 2855 (w), 1540 (m), 1428 (s), 1370 (m), 1327 (s), 1294 (s), 1267 (s), 1139 (s), 1025 (m), 956 (w), 851 (s), 662 (s) cm⁻¹.

HRMS (ESI): *m/z* found 443.0690 (100) [M+Na]⁺; calcd. for C₁₆H₂₆BI₂NaO₂S 443.0687.

The NMR data are in agreement with the data found in the literature.⁷

⁷ T. Yokozawa, R. Suzuki, M. Nojima, Y. Ohta, A. Yokoyama, *Macromol. Rapid. Commun.* **2011**, *32*, 801.

2-(5-Iodothiophen-2-yl)-4,4,5,5-tetramethyl-1,3,2-dioxaborolane (19)

A solution of diisopropylamine (1.05 g, 10.4 mmol) in THF (80 mL) was cooled to $-78\text{ }^{\circ}\text{C}$ and *n*-butyllithium (4.00 mL, 10.0 mmol, 2.5 M in *n*-hexane) was added dropwise over the course of 2 min. The mixture was warmed to $0\text{ }^{\circ}\text{C}$, cooled back to $-78\text{ }^{\circ}\text{C}$ and stirring was continued for 5 min. 2-Iodo-thiophene (2.94 g, 10.0 mmol) was added dropwise to the solution over the course of 5 min and the reaction mixture was stirred for 1 h at $-78\text{ }^{\circ}\text{C}$. The boronic ester (1.86 g, 10.0 mmol) dissolved in THF (5 mL) was added dropwise over a course of 5 min to the orange-brown suspension and the reaction mixture was stirred at $-78\text{ }^{\circ}\text{C}$ for 15 min. The mixture was allowed to warm to $15\text{ }^{\circ}\text{C}$ without removal of the cooling bath and stirred for 16 h. The reaction was quenched with a saturated solution of ammonium chloride (20 mL). The aqueous layer was extracted with ethyl acetate (3 x 30 mL) and the combined organic layers were dried over magnesium sulfate. The solvent was removed *in vacuo* and gave the product in a yield of 3.28 g (9.81 mmol, 98%) as a bright brown solid.

^1H NMR (200 MHz, CDCl_3): δ = 7.29 (d, 1H, 3J = 3.6 Hz, Tph-*H*-b/c), 7.72 (d, 1H, 3J = 3.6 Hz, Tph-*H*-b/c), 1.33 (s, 12H, f) ppm.

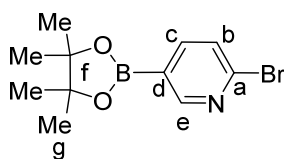
^{13}C NMR (126 MHz, CDCl_3): δ = 138.5 (Tph-CH-b/c), 138.3 (Tph-CH-b/c), 84.3 (e), 81.5 (Tph-C-a), 24.7 (f) ppm.⁸

^{11}B NMR (160 MHz, CDCl_3): δ = 28.2 ppm.

The NMR data are in agreement with the data found in the literature.⁹

⁸ The carbon atom bound to boron was not visible due to the high quadrupole moment of the boron nucleus.

⁹ G. A. Chotana, V. A. Kallepalli, R. E. Maleczka, M. R. Smith III, *Tetrahedron* **2008**, *64*, 6103.

2-Bromo-5-(4,4,5,5-tetramethyl-1,3,2-dioxaborolan-2-yl)pyridine (21)

2-Bromopyridine-5-boronic acid (3.00 g, 14.9 mmol), pinacol (1.88 g, 16.0 mmol) and molecular sieve (3 Å, 1.50 g, crushed) were placed in a Schlenk flask which was subsequently evacuated. Then, the flask was flushed with nitrogen, and diethyl ether (65 mL) was added to the mixture at 15 °C in one portion. Then the reaction mixture was stirred for 16 h at this temperature. Subsequently, the mixture was filtered over Celite, washed with diethyl ether (3 x 30 mL) and the solvents were removed *in vacuo* to afford the pure product as white solid in a yield of 3.44 g (12.2 mmol, 82%, Lit.¹⁰: 85%).

¹H NMR (500 MHz, CDCl₃): δ = 8.68 (dd, 1H, ⁴J = 2.0 Hz, ⁵J = 0.7 Hz, Pyr-H-e), 7.88 (dd, 1H, ³J = 7.9 Hz, ⁴J = 2.0 Hz, Pyr-H-c), 7.48 (dd, 1H, ³J = 7.9 Hz, ⁵J = 0.7 Hz, Pyr-H-b), 1.34 (s, 12H, g) ppm.

¹³C NMR (126 MHz, CDCl₃): δ = 155.9 (Pyr-CH-e), 145.4 (Pyr-C-a), 144.4 (Pyr-CH-c), 127.6, (Pyr-CH-b), 84.5 (f), 24.8 (g) ppm.¹¹

¹¹B NMR (160 MHz, CDCl₃): δ = 30.5 ppm.

IR (ATR): $\tilde{\nu}$ = 2981 (w), 2933 (w), 1577 (m), 1545 (w), 1455 (w), 1354 (s), 1278, (m), 1140 (s), 1100 (s), 1015 (m), 962 (w), 855 (m), 823 (s), 741 (s), 660 (s) cm⁻¹.

HRMS (ESI): *m/z* found 283.0377 (100) [M]⁺; calcd. for C₁₁H₁₅BNO₂Br 283.0379.

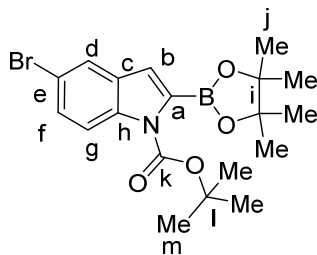
M.p.: 94 °C.

The NMR data are in agreement with the data found in the literature.¹⁰

¹⁰ C. G. Watson, V. K. Aggarwal, *Org. Lett* **2013**, *15*, 1346.

¹¹ The carbon atom bound to boron was not visible due to the high quadrupole moment of the boron nucleus.

***tert*-Butyl-5-bromo-2-(4,4,5,5-tetramethyl-1,3,2-dioxaborolan-2-yl)-1*H*-indole-1-carboxylate (23)**



2-Bromoindole-5-boronic acid (5.40 g, 15.2 mmol), pinacol (2.00 mg, 17.0 mmol) and molecular sieve (3 Å, 2.00 g, crushed) were placed in a Schlenk flask, which was subsequently evacuated. Then, the flask was flushed with nitrogen and diethyl ether (65 mL) was added to the mixture at 15 °C in one portion. The reaction mixture was stirred for 16 h at this temperature. Then, the mixture was filtered over Celite. The organic phase was washed with water (2 x 20 mL), saturated ammonium chloride solution (20 mL) and dried over magnesium sulfate. The solvent was removed *in vacuo* to afford a highly viscous orange oil which was dissolved in DCM (2 mL) and overlaid with *n*-hexane (10 mL). After storing the flask at 4°C, a white solid was formed which was removed by filtration. The solvent of the remaining mixture was removed *in vacuo* to afford a yellow oil which was filtered over silica (diethyl ether: ethyl acetate, 9 : 1, R_f = 0.30). After removing the solvent *in vacuo*, the product was obtained as orange oil in a yield of 5.83 g (14.5 mmol, 95%).

^1H NMR (500 MHz, CDCl_3): δ = 7.79 (d, 1H, 3J = 8.8 Hz, Ind-*H*-g), 7.65 (d, 1H, 4J = 2.0 Hz, Ind-*H*-d), 7.35 (dd, 1H, 3J = 8.8 Hz, 4J = 2.0 Hz, Ind-*H*-f), 6.76 (s, 1H, Ind-*H*-b), 1.67 (s, 9H, m), 1.40 (s, 12H, j) ppm.

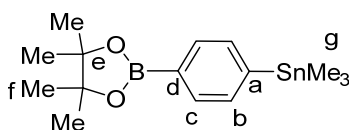
^{13}C NMR (126 MHz, CDCl_3): δ = 150.7 (k), 135.2 (e), 132.9 (Ind-*C*-c), 127.2 (Ind-*CH*-f), 123.5 (Ind-*CH*-d), 116.3 (Ind-*CH*-g), 115.7 (Ind-*C*-h), 114.7 (Ind-*CH*-b), 84.7 (l), 84.3 (i), 28.2 (m), 24.8 (j).¹²

^{11}B NMR (160 MHz, CDCl_3): δ = 28.6 ppm.

IR (ATR): $\tilde{\nu}$ = 2978 (w), 2924 (w), 1721 (s), 1557 (w), 1435 (w), 1364 (s), 1350 (s), 1315 (s), 1137 (s), 1060 (m), 965 (m), 849 (s), 788 (s), 665 (s), 665 (m), 455 (w) cm^{-1} .

HRMS (ESI): m/z found 421.1054 (100) $[\text{M}]^+$; calcd. for $\text{C}_{19}\text{H}_{25}\text{BNO}_4\text{Br}$ 421.1060.

¹² The carbon atom bound to boron was not visible due to the high quadrupole moment of the boron nucleus.

2-(4-(Trimethylstannyl)phenyl)-4,4,5,5-tetramethyl-1,3,2-dioxaborolane (24)

2-(4-Iodophenyl)-4,4,5,5-tetramethyl-1,3,2-dioxaborolane (330 mg, 1.00 mmol), [Pd(PPh₃)₄] (0.50 mol%, 6.0 mg) and hexamethyldistannane (393 mg, 1.20 mmol) were dissolved in toluene (4 mL). The mixture was heated to 120 °C in the microwave apparatus for 30 min. Water (10 mL) was added to the reaction mixture and it was extracted with DCM (3 x 15 mL). The organic layer was extracted with water (2 x 20 mL) and the aqueous layer was extracted with diethyl ether (3 x 20 mL). The combined organic layers were dried over sodium sulfate. The solvent was removed *in vacuo* to afford the product as a colorless solid in a yield of 342 mg (932 μmol, 93%) without further purification.

¹H NMR (500 MHz, CDCl₃): δ = 7.76 (d, 2H, ³J = 7.9 Hz, Phe-*H*-b), 7.51 (d, 2H, ³J = 7.9 Hz, Phe-*H*-c), 1.34 (s, 12H, f), 0.29 (s, 9H, g) ppm.

¹³C NMR (126 MHz, CDCl₃): δ = 146.7 (Phe-*C*-a), 135.3 (Phe-*CH*-c), 134.0 (Phe-*CH*-b), 83.7 (e), 24.8 (f), -9.6 (g) ppm.¹³

¹¹⁹Sn NMR (187 MHz, CDCl₃): δ = -28.1 ppm.

¹¹B NMR (160 MHz, CDCl₃): δ = 30.8 ppm.

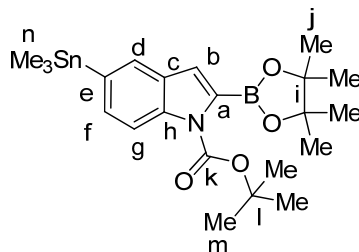
IR (ATR): $\tilde{\nu}$ = 3052 (w), 2980 (w), 2911 (w), 1592 (w), 1356 (s), 1324 (m), 1142 (s), 1100 (m), 1055(s), 1017 (w), 962(w), 858 (m), 767 (s), 655 (s), 530(s) cm⁻¹.

HRMS (ESI): *m/z* found 353.0741 (100) [M]⁺; calcd. for C₁₄H₂₂BO₂SSn 353.0735.

M.p.: 123 °C.

¹³ The carbon atom bound to boron was not visible due to the high quadrupole moment of the boron nucleus.

***tert*-Butyl-5-trimethylstannyl-2-(4,4,5,5-tetramethyl-1,3,2-dioxaborolan-2-yl)-1*H*-indole 1-carboxylate (25)**



tert-Butyl-5-bromo-2-(4,4,5,5-tetramethyl-1,3,2-dioxaborolan-2-yl)-1*H*-indole-1-carboxylate (422 mg, 1.00 mmol), [Pd(PPh₃)₄] (0.50 mol%, 6.0 mg) and hexamethyldistannane (393 mg, 1.20 mmol) were dissolved in toluene (4 mL). The mixture was heated to 100 °C in a microwave apparatus for 180 min. Water (10 mL) was added to the reaction mixture and it was extracted with DCM (3 x 15 mL). The combined organic phase was then extracted with water (2 x 20 mL) and the aqueous layer was extracted with diethyl ether (3 x 20 mL). The combined organic layers were dried over sodium sulfate. The solvent was removed *in vacuo* to afford the product as highly viscous oil in a yield 484 mg (956 μmol, 96%).

¹H NMR (500 MHz, CDCl₃): δ = 7.79 (d, 1H, ³J = 8.8 Hz, Ind-*H*-g), 7.65 (d, 1H, ⁴J = 1.8 Hz, Ind-*H*-d), 7.35 (dd, 1H, ³J = 8.8 Hz, ⁴J = 1.8 Hz, Ind-*H*-f), 6.76 (d, 1H, ⁴J = 0.7 Hz, Ind-*H*-b), 1.68 (s, 9H, m), 1.40 (s, 12H, j), 0.20 (s, 9H, n) ppm.

¹³C NMR (126 MHz, CDCl₃): δ = 150.7 (k), 135.2 (Ind-C-e), 132.9 (Ind-C-c), 127.2 (Ind-CH-f), 123.5 (Ind-CH-d), 116.3 (Ind-CH-g), 115.7 (Ind-C-h), 114.7 (Ind-CH-b), 84.7(l), 84.3 (i), 28.2 (m), 24.8 (i), -10.3 (n) ppm.¹⁴

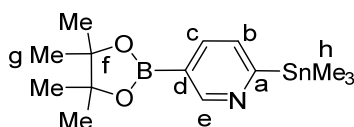
¹¹B NMR (160 MHz, CDCl₃): δ = 28.7 ppm.

¹¹⁹Sn NMR (187 MHz, CDCl₃): δ = -108.0 ppm.

IR (ATR): $\tilde{\nu}$ = 2977 (w), 2904 (w), 1725 (m), 1433 (m), 1366 (s), 1323 (s), 1138 (s), 1055 (m), 849 (m), 765 (m), 520 (m), 497 (m) cm⁻¹.

HRMS (ESI): *m/z* found 530.1490 (10) [M+Na]⁺; calcd. for C₂₂H₃₄BNNaO₄Sn 530.1503; found: 444.2037 (100) [M-C₆H₁₂]⁺.

¹⁴ The carbon atom bound to boron was not visible due to the high quadrupole moment of the boron nucleus.

2-Trimethylstannyl-5-(4,4,5,5-tetramethyl-1,3,2-dioxaborolan-2-yl)pyridine (26)

2-Bromo-5-(4,4,5,5-tetramethyl-1,3,2-dioxaborolan-2-yl)pyridine (284 mg, 1.00 mmol), [Pd(PPh₃)₄] (0.50 mol%, 6.0 mg) and hexamethyldistannane (393 mg, 1.20 mmol) were dissolved in toluene (4 mL). The mixture was heated to 100 °C in a microwave apparatus for 180 min. Water (10 mL) was added to the reaction mixture and it was extracted with DCM (3 x 15 mL). The organic layer was extracted with water (2 x 20 mL) and the aqueous layer was extracted with diethyl ether (3 x 20 mL). The combined organic layers were dried with sodium sulfate. The solvent was removed *in vacuo* to afford a dark red solid as a mixture of mainly product and starting material in a ratio of product and starting material of 21 : 26 = 60 : 40 by integration of an ¹H NMR spectrum. The mixture was purified by sublimation at 60 °C, 3 x 10⁻³ mbar to afford a white solid, as a pure mixture of starting material and product. A subsequent fractionation sublimation allowed to remove the starting material at 17 °C, 3 x 10⁻⁴ mbar to give the product as white solid in a yield 191 mg (540 μmol, 54%).

¹H NMR (500 MHz, CDCl₃): δ = 9.04 (dd, 1H, ⁴J = 1.7 Hz, ⁵J = 0.9 Hz, Pyr-H-e), 7.87 (dd, 1H, ³J = 7.3 Hz, ⁴J = 1.7 Hz, Pyr-H-c), 7.45 (dd, 1H, ³J = 7.3 Hz, ⁵J = 0.9 Hz, Pyr-H-b), 1.34 (s, 12H, g), 0.34 (s, 9H, h) ppm.

¹³C NMR (126 MHz, CDCl₃): δ = 177.1 (Pyr-C-a), 155.6 (Pyr-CH-e), 139.4 (Pyr-CH-c), 131.0 (Pyr-CH-b), 84.0 (f), 24.8 (g), -9.5 (h) ppm.¹⁵

¹¹B NMR (160 MHz, CDCl₃): δ = 30.8 ppm.

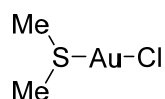
¹¹⁹Sn NMR (187 MHz, CDCl₃): δ = -108.7 ppm

IR (ATR): $\tilde{\nu}$ = 2968 (m), 2918 (w), 1584 (w), 1477 (w), 1347 (s), 1157 (s), 1072 (s), 1037 (s), 1016 (s), 851 (m), 807 (m), 768 (s), 753 (s), 656 (s), 524 (s), 509 (s) cm⁻¹.

HRMS (ESI): *m/z* found 354.0688 (100) [M]⁺; calcd. for C₁₃H₂₁BNO₂Sn 354.0687.

M.p.: 136 °C.

¹⁵ The carbon atom bound to boron was not visible due to the high quadrupole moment of the boron nucleus.

Dimethylsulfide gold(I) chloride (31)¹⁶

This procedure was not performed under Schlenk conditions.

Gold (4.00 g, 20.4 mmol) was dissolved in boiling *aqua regia* (65 mL, HCl/HNO₃, 3:1). The volume was reduced to ca. 10 mL by boiling and stirring at an external temperature of 150 °C, then HCl (ca. 50 mL, conc.) was added, and the volume again reduced to ca. 10 mL. This procedure was repeated until the vapors produced were no longer brown using a total of 25 mL HCl. The final solution (10 mL) was cooled to 20°C and methanol (100 mL) was added. Ensuring minimal light exposure, SMe₂ (ca. 4.25 g, 5 mL, 68 mmol, excess) was added dropwise over the course of 5 min, with continuous stirring. With the addition of each drop, a red coloration appeared. The reaction was finished when no red color appeared when adding SMe₂. The solution became colorless and a white precipitate formed. The white precipitate was isolated by filtration, washed with methanol (10 mL), diethyl ether (10 mL) and pentane (10 mL) and dried *in vacuo* to obtain the product as colorless solid in a yield of 5.65 g (19.2 mmol, 94%, Lit.²:93%).

¹H NMR (500 MHz, acetone-*d*₆): δ = 2.86 (s, 6H, CH₃) ppm.

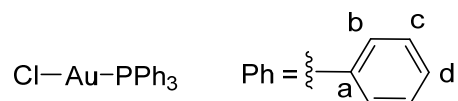
¹³C NMR (125 MHz, CDCl₃): δ = 25.6 (CH₃) ppm.

IR (ATR): $\tilde{\nu}$ = 2996 (w), 2921(w), 2954 (s), 1436 (m), 1421 (s), 1411 (s), 1317 (w), 1298 (w), 1032 (s), 993 (s), 953 (m) cm⁻¹.

HRMS (ESI): *m/z* found 316.6439 (25) [M+Na]⁺; calcd. for C₂H₆AuClNaS 316.9437; found 444.2037 (100) [M-C₂H₆+Na]⁺.

Decomp. temp.: 135°C

¹⁶ M.-C. Brandys, M. C. Jennings, R. J. Puddephatt *J. Chem. Soc., Dalton Trans.* **2000**, 24, 4601-4606.

Triphenylphosphine gold(I) chloride (32)¹⁷

Dimethylsulfide gold(I) chloride (1.20 g, 4.06 mmol) and triphenylphosphine (1.07 g, 4.06 mmol) were weighed at normal atmosphere into a flask. The flask was evacuated and flushed with nitrogen. DCM (350 mL) was added to these reagents, dissolving the starting materials. The mixture was stirred at 20 °C for 15 min monitoring the formation of the product by ³¹P NMR spectroscopy. The reaction mixture was worked up in air by reducing the volume of the solution to 50 mL *in vacuo* and *n*-hexane (350 mL) was added resulting in the precipitation of the complex. The solid was then filtered, washed with *n*-hexane (3 x 15 mL) and dried *in vacuo*, affording the product as a white solid in a yield of 1.93 g (3.90 mmol, 96%, Lit.³: quantitative).

¹H NMR (500 MHz, CDCl₃): δ = 7.60-7.40 (m, 15H) ppm.

¹³C NMR (125 MHz, CDCl₃): δ = 134.2 (d, ³J_{C-P} = 13.8 Hz, -b/c), 132.0 (d, ³J_{C-P} = 2.4 Hz, d), 129.2 (d, ³J_{C-P} = 11.9 Hz, b/c), 128.6 (d, ³J_{C-P} = 48.4 Hz, a) ppm.

³¹P NMR (202 MHz, CDCl₃, 300 K): δ = 33.0 ppm.

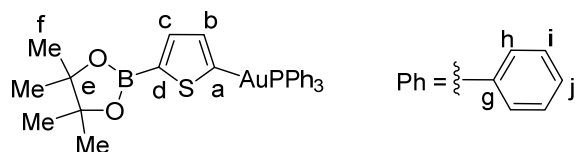
IR (ATR): $\tilde{\nu}$ = 3060 (w), 3005 (w), 1479 (m), 1433 (m), 1421 (s), 1101 (s), 997 (m), 747 (s), 712 (m), 690 (s), 544 (s), 499 (s) cm⁻¹.

HRMS (ESI): *m/z* found 517.0152 (100) [M+Na]⁺; calcd. for C₁₈H₁₅AuClNaP 517.0158.

M.p.: 236°C

¹⁷ N. Mezailles, L. Ricard, F. Gagosz *Org. Lett.* **2005**, *7*, 4133-4136.

(5-(4,4,5,5-Tetramethyl-1,3,2-dioxaborolan-2-yl)thiophen-2-yl)(triphenylphosphine)gold (35)



[ClAuPPh₃] (247 mg, 500 μmol) and 4,4,5,5-tetramethyl-2-(5-(trimethylstannyl)thiophen-2-yl)-1,3,2-dioxaborolane (186 mg, 500 μmol) were added under a nitrogen atmosphere. The reactants were suspended in anhydrous, degassed 2-propanol (15 mL), and the resulting yellow mixture was stirred under argon at 40 °C for 20 h. 2-Propanol was removed *in vacuo*. The remaining pale yellow residue was dissolved in anhydrous DCM (5 mL) and filtered twice through Celite pads to yield a yellow solution. The solvent was removed *in vacuo* to afford the crude product. This was diluted in DCM (5 mL) and a layer of pentane (10 mL) was carefully placed on top and the product was crystallized at 4 °C afford the product in a yield of 255 mg (382 μmol, 76%).

¹H NMR (600 MHz, CDCl₃): δ = 7.96 (d, 1H, ³J = 3.1 Hz, Tph-H-b/c), 7.63-7.57 (m, 5H, h, i), 7.53-7.44 (m, 10H, h, i), 7.26 (d, 1H, ³J = 3.1 Hz, Tph-H-b/c), 1.34 (s, 12H, f) ppm.

¹³C NMR (151 MHz, CDCl₃): δ = 137.3 (d, ³J_{C,P} = 7.8 Hz, Tph-CH-c), 134.4 (Tph-CH-b), 134.4 (d, ³J_{C,P} = 13.8 Hz, h/i), 131.3 (d, ³J_{C,P} = 2.3 Hz, j), 130.7 (g), 130.3 (Tph-C-a), 129.1 (d, ³J_{C,P} = 11.0 Hz, h/i), 83.4 (e), 24.8 (f) ppm.¹⁸

¹¹B NMR (160 MHz, CD₂Cl₂): δ = 29.1 ppm.

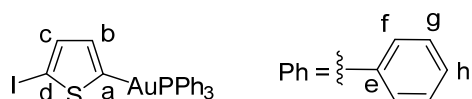
³¹P NMR (202 MHz, CD₂Cl₂): δ = -43.1 ppm.

IR (ATR): $\tilde{\nu}$ = 2977 (w), 1507 (m), 1406 (m), 1341 (s), 1315 (s), 1139 (m), 1104 (s), 1063 (m), 852 (m), 745 (s), 692 (s), 662 (s), 537 (s), 500 (s) cm⁻¹.

HRMS (ESI): *m/z* found 691.1273 (100) [M+Na]⁺; calcd. for C₂₈H₂₉AuBNaO₂PS 691.1282.

Decomp. temp.: 234 °C.

¹⁸ The carbon atom bound to boron was not visible due to the high quadrupole moment of the boron nucleus.

(5-Iodothiophene-2-yl)(triphenylphosphine)gold (37)

[ClAuPPh₃] (495 mg, 1.00 mmol) 2-(5-iodothiophen-2-yl)-4,4,5,5-tetramethyl-1,3,2-dioxaborolane ester (110 mg, 1.00 mmol), and Cs₂CO₃ (716 mg, 2.20 mmol) were added under an argon atmosphere. The reactants were suspended in anhydrous, degassed 2-propanol (30 mL), and the resulting yellow mixture was stirred under argon at 40 °C for 20 h. 2-Propanol was removed *in vacuo*. The remaining pale yellow residue was dissolved in anhydrous DCM (30 mL) and filtered twice through Celite pads to yield a yellow solution. The solvent was removed *in vacuo* obtaining a violet solid. This was diluted in DCM (6 mL). A layer of *n*-pentane (10 mL) was carefully placed on top and the product was crystallized at 4 °C to afford the product as colorless crystals in a yield of 640 mg (958 μmol, 96%).

¹H NMR (500 MHz, CDCl₃): δ = 7.60-7.55 (m, 6H, Tph-H-c/b and f/g/h), 7.52-7.42 (m, 10H, f/g/h), 6.88 (d, 1H, ³J = 3.3 Hz, Tph-H-c/b) ppm.

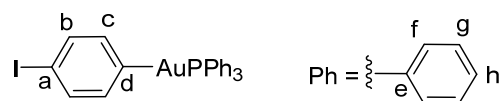
¹³C NMR (126 MHz, CDCl₃): δ = 136.8 (Tph-CH-c/b), 135.0 (Tph-CH-c/b), 134.3 (d, ³J_{C, P} = 13.7 Hz, f/g), 131.4 (h), 130.5 (Tph-C-a/e), 130.1 (Tph-C-a/e), 129.1 (d, ³J_{C, P} = 11.0 Hz, f/g), 74.4 (Tph-C-d) ppm.

³¹P NMR (202 MHz, CDCl₃): δ = 42.7 ppm.

IR (ATR): $\tilde{\nu}$ = 3044 (w), 1586 (w), 1477 (m), 1433 (s), 1383 (m), 1098 (s), 996 (m), 902 (m), 791 (m), 740 (s), 708 (s), 688 (s), 531 (s), 499 (s), 472 (s) cm⁻¹.

HRMS (ESI): *m/z* found 667.9493 (100) [M]⁺; calcd. for C₂₂H₁₇SAuIP 667.9499.

Decomp. temp.: 129 °C.

(5-Iodophenyl-2-yl)(triphenylphosphine)gold (39)

[ClAuPPh₃] (247 mg, 500 μmol), 5-iodophenylboronic ester (196 mg, 500 μmol) and Cs₂CO₃ (358 mg, 1.10 mmol) were added under an argon atmosphere. The reactants were suspended in anhydrous, degassed 2-propanol (15 mL), and the resulting yellow mixture was stirred under argon at 40 °C for 20 h. Then 2-propanol was removed *in vacuo*. The remaining pale yellow residue was dissolved in anhydrous DCM (30 mL) and filtered twice through Celite pads to yield a yellow solution. The solvent was removed *in vacuo* obtaining a violet solid. This was diluted in DCM (6 mL) and carefully overlaid with *n*-pentane (10 mL). The product was crystallized at 4 °C to afford the product as colorless crystals in a yield of 301 mg (455 μmol, 91%).

¹H NMR (600 MHz, CDCl₃): δ = 7.62-7.55 (m, 8H, f/g/h), 7.54-7.44 (m, 9H, Phe-*H*-c, f/g/h), 7.33 (dd, 2H, ³*J* = 7.8 Hz, ⁴*J* = 5.3 Hz, Phe-*H*-b) ppm.

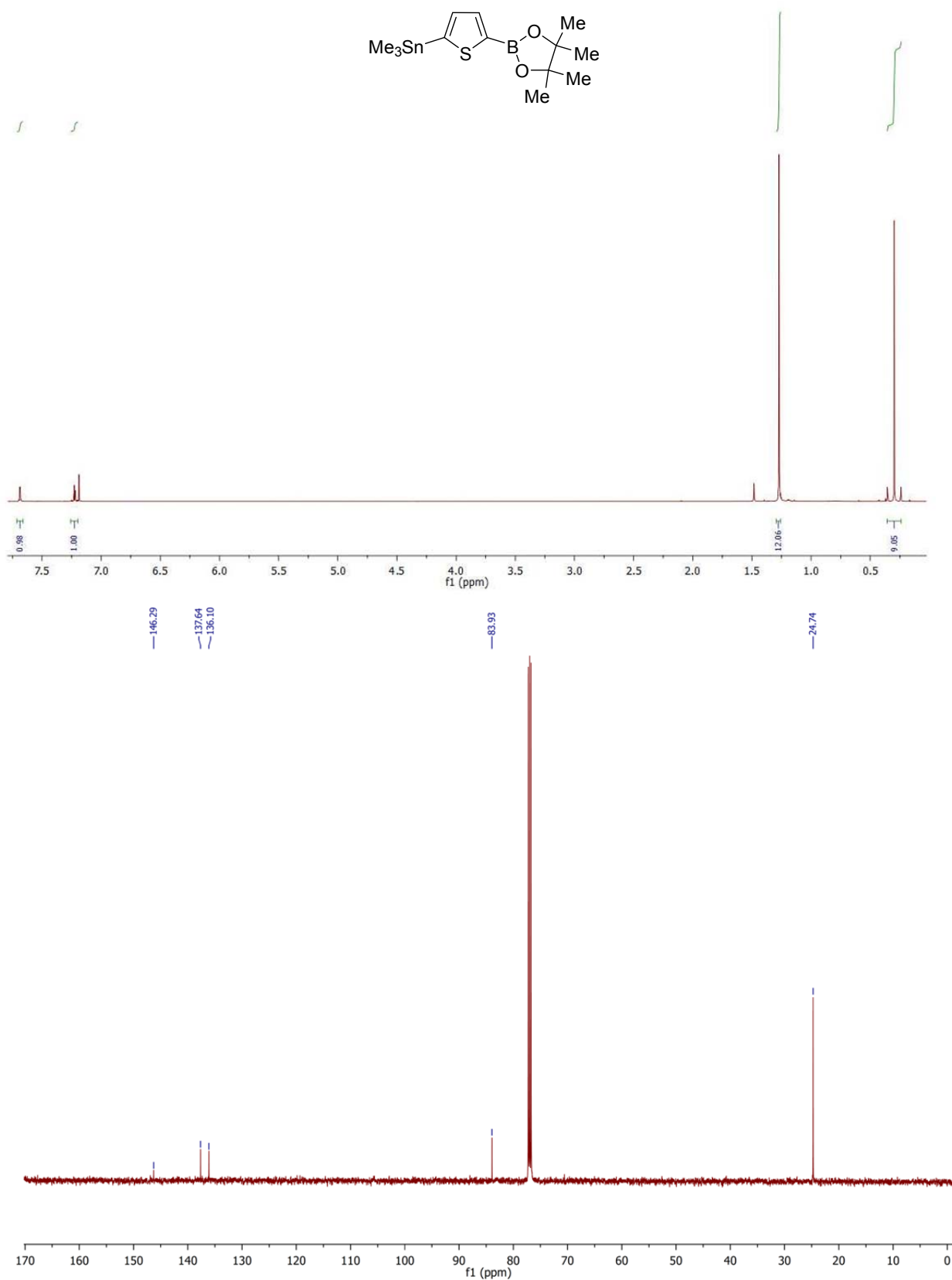
¹³C NMR (151 MHz, CDCl₃): δ = 171.2 (Phe-*C*-d), 141.1 (Phe-*CH*-b), 136.1 (d, *J* = 6.3 Hz, Ar-*CH*-c), 134.4 (d, ³*J*_{C,P} = 14.6 Hz, f/g), 131.2 (d, ³*J*_{C,P} = 2.2 Hz, h), 130.8 (d, ³*J*_{C,P} = 49.8 Hz, e), 129.1 (d, ³*J*_{C,P} = 11.7 Hz, f/g), 91.9 (Ar-*C*-a) ppm.

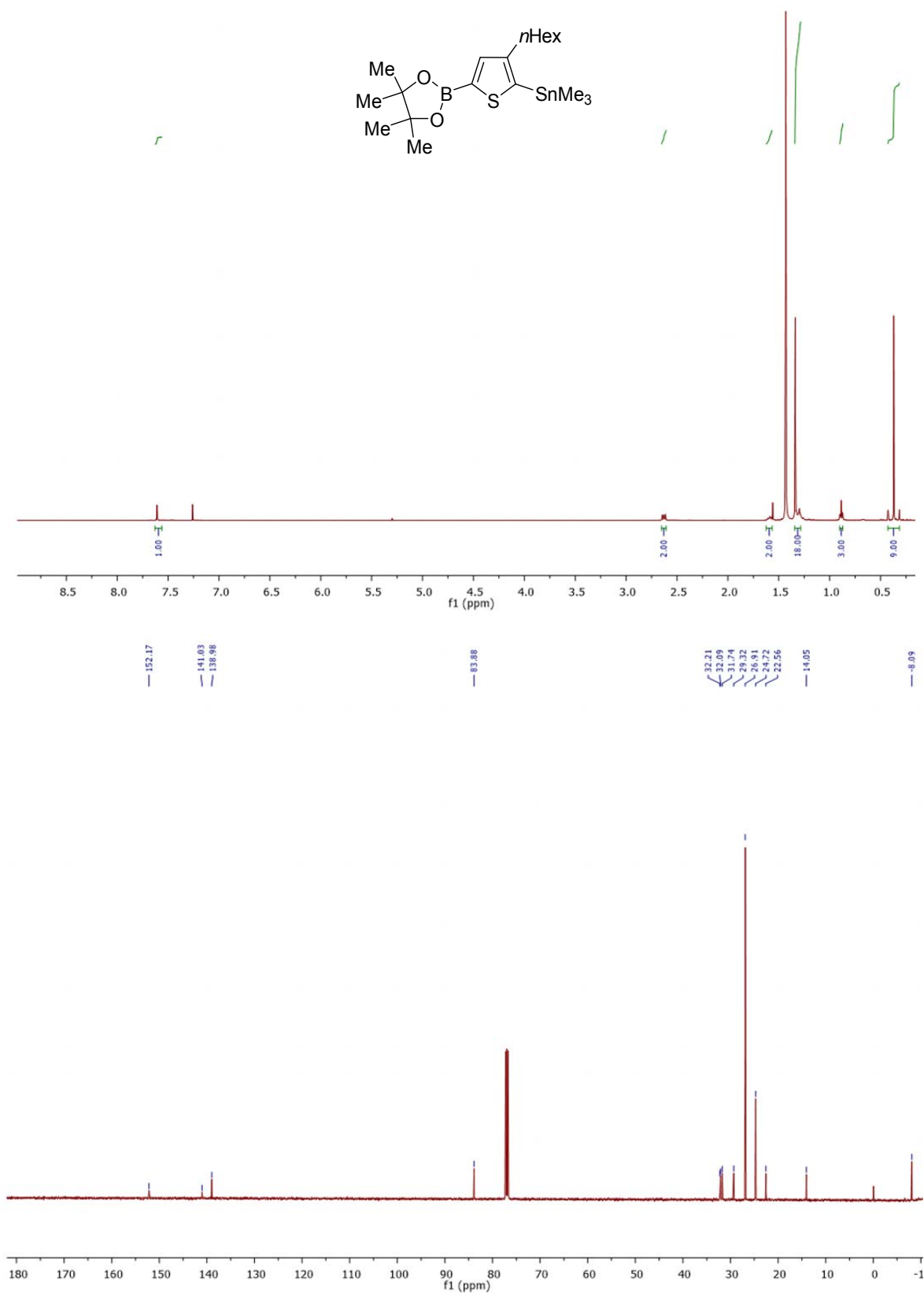
³¹P NMR (202 MHz, CDCl₃): δ = 43.6 ppm.

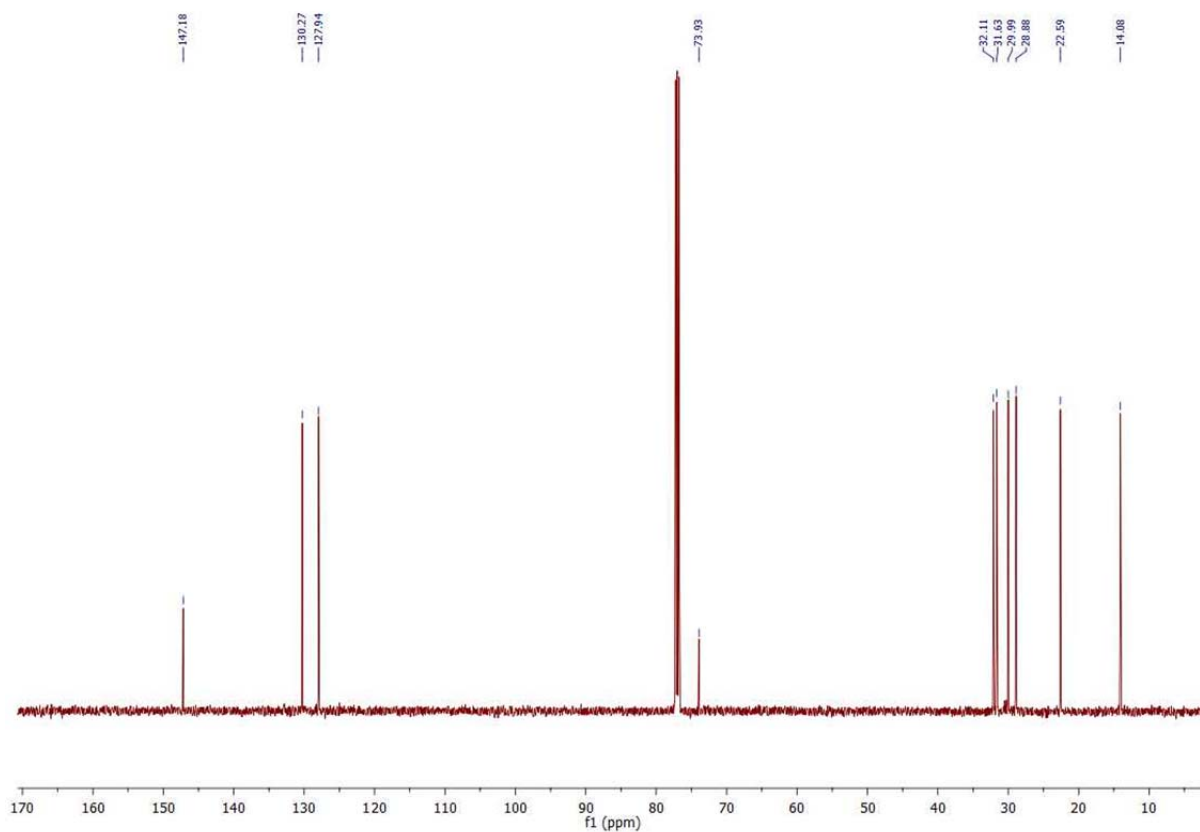
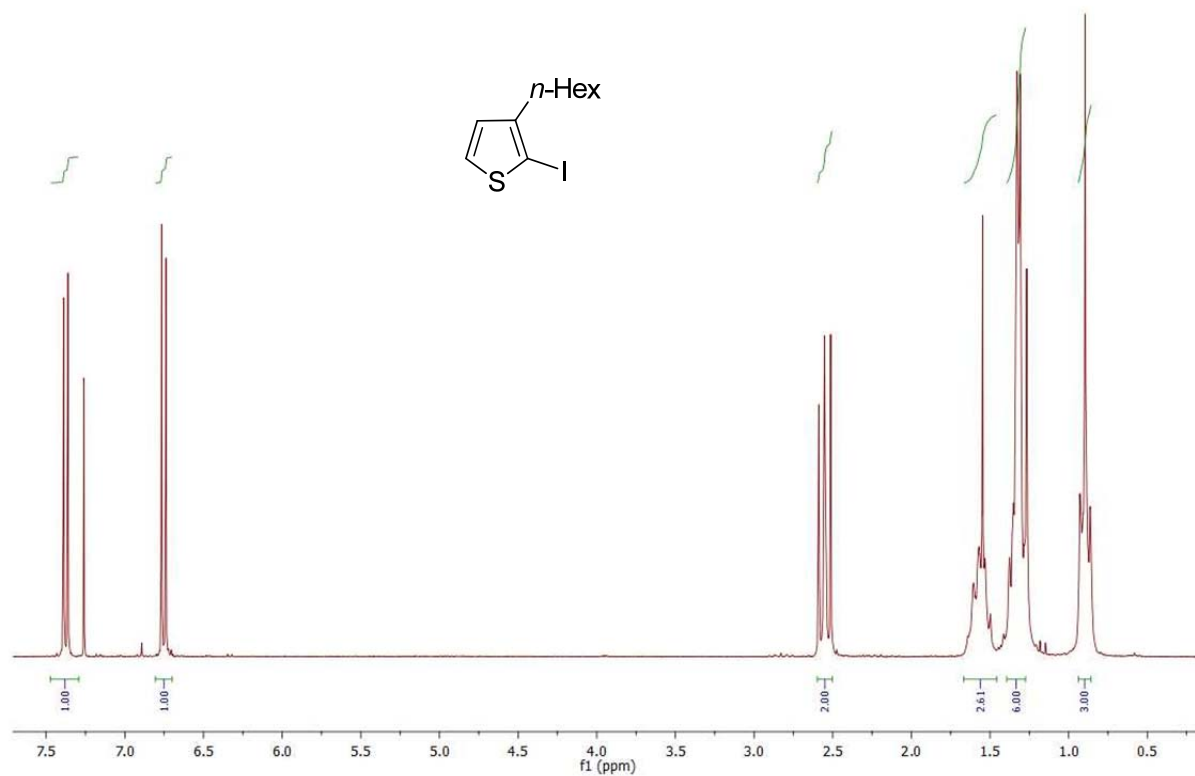
IR (ATR): $\tilde{\nu}$ = 3050 (w), 1478 (m), 1432 (s), 1365 (w), 1097 (s), 1092 (m), 1052 (m), 998 (s), 789 (s), 741 (s), 690 (s), 535 (s), 495 (s), 471 (s) cm⁻¹.

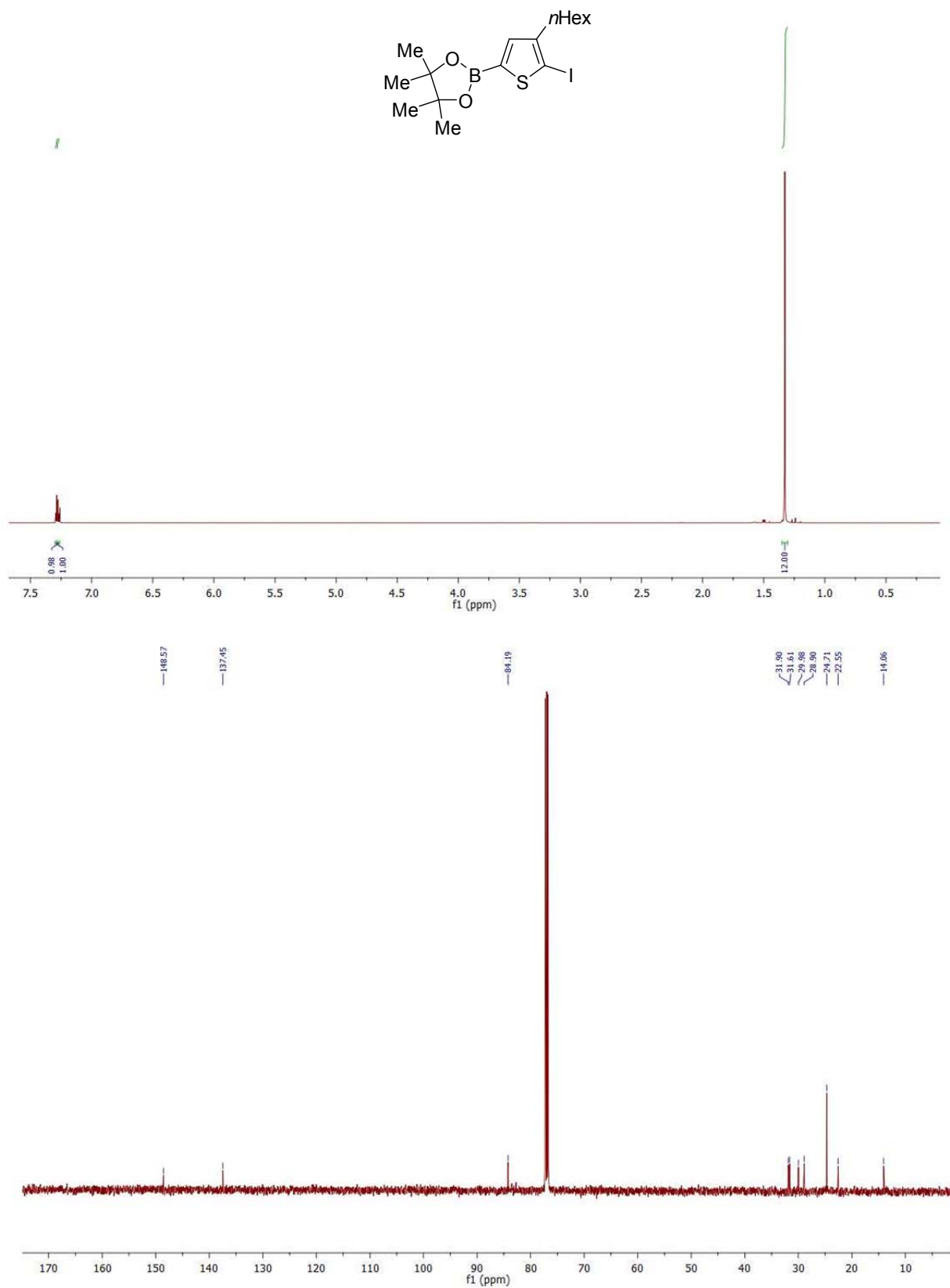
HRMS (ESI): *m/z* found 684.9824 (100) [M+Na]⁺; calcd. for C₂₄H₁₉AuINaP 684.9827.

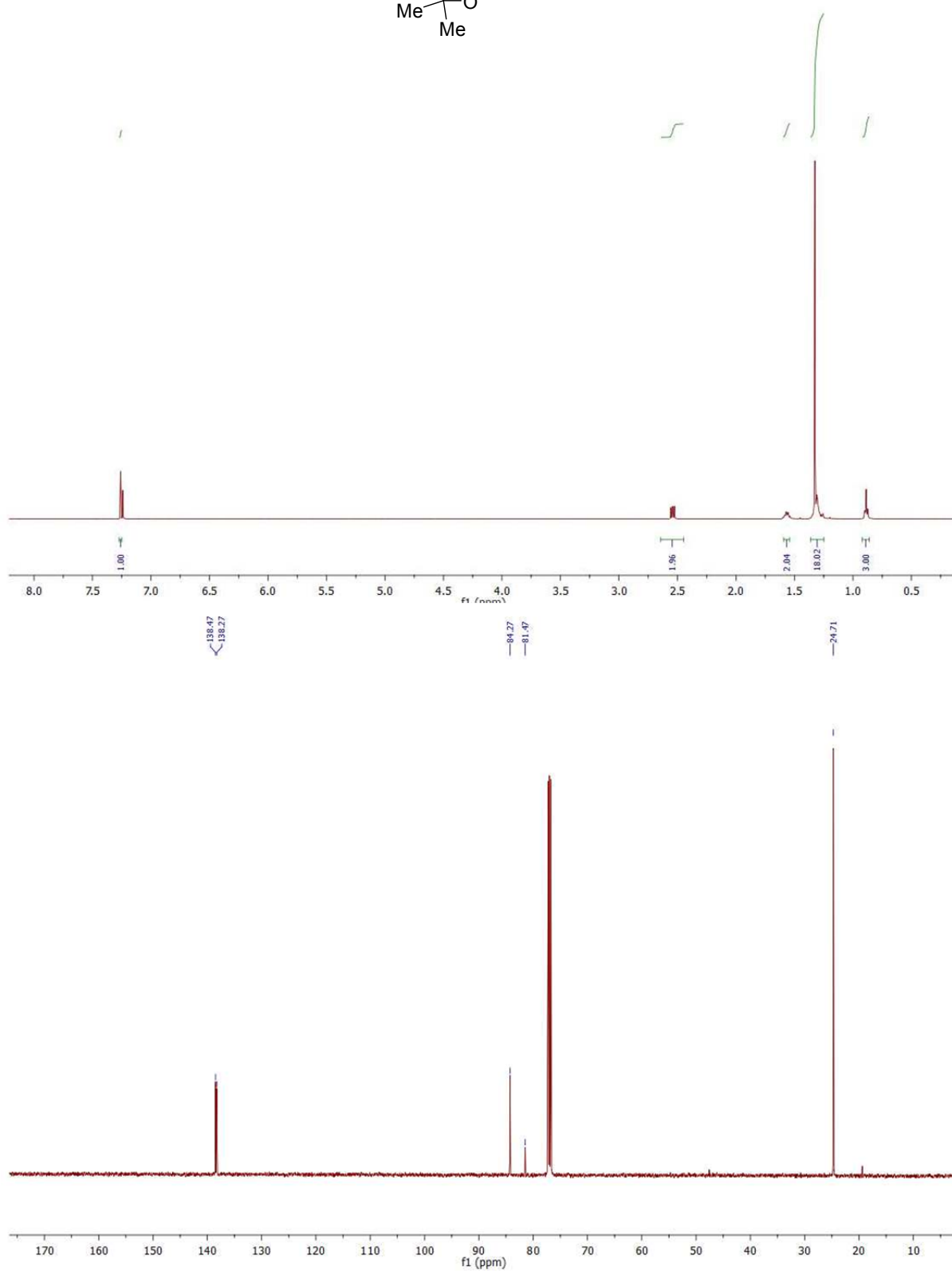
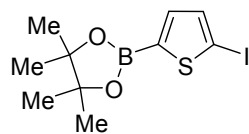
Decomp. temp.: 145 °C.

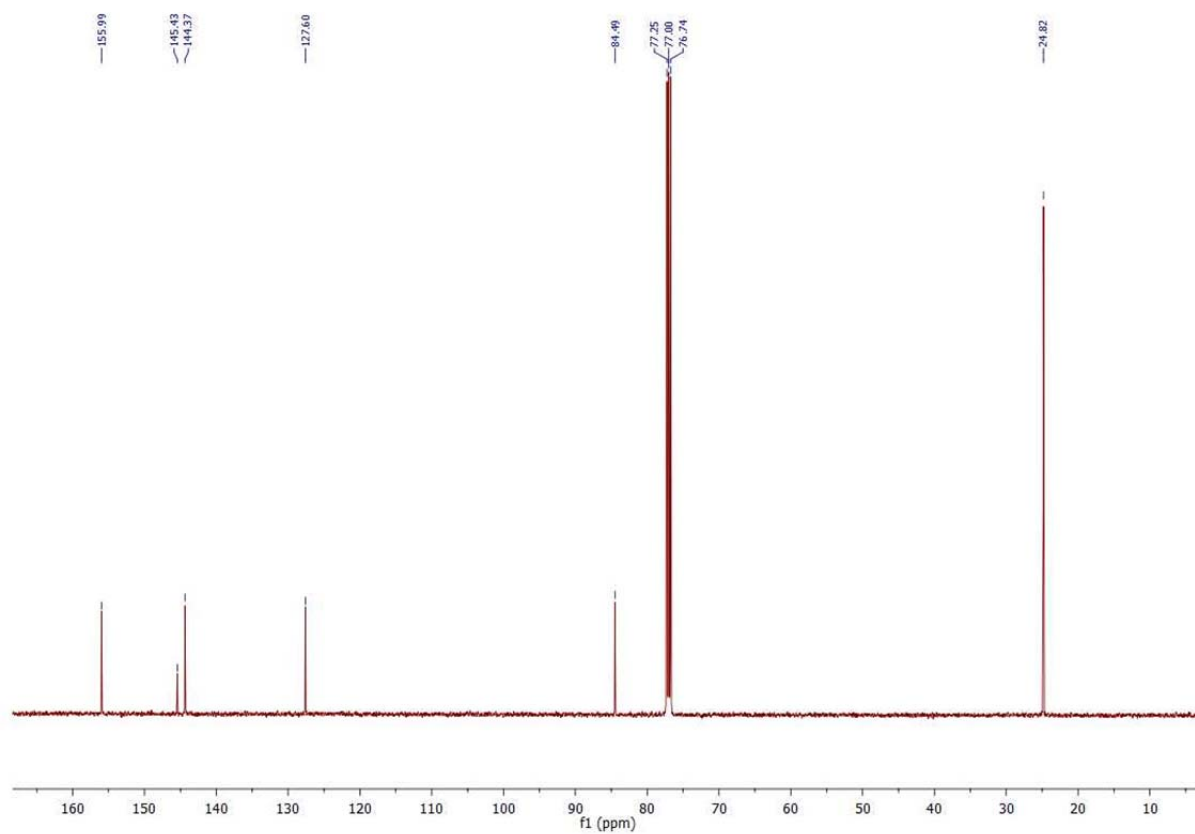
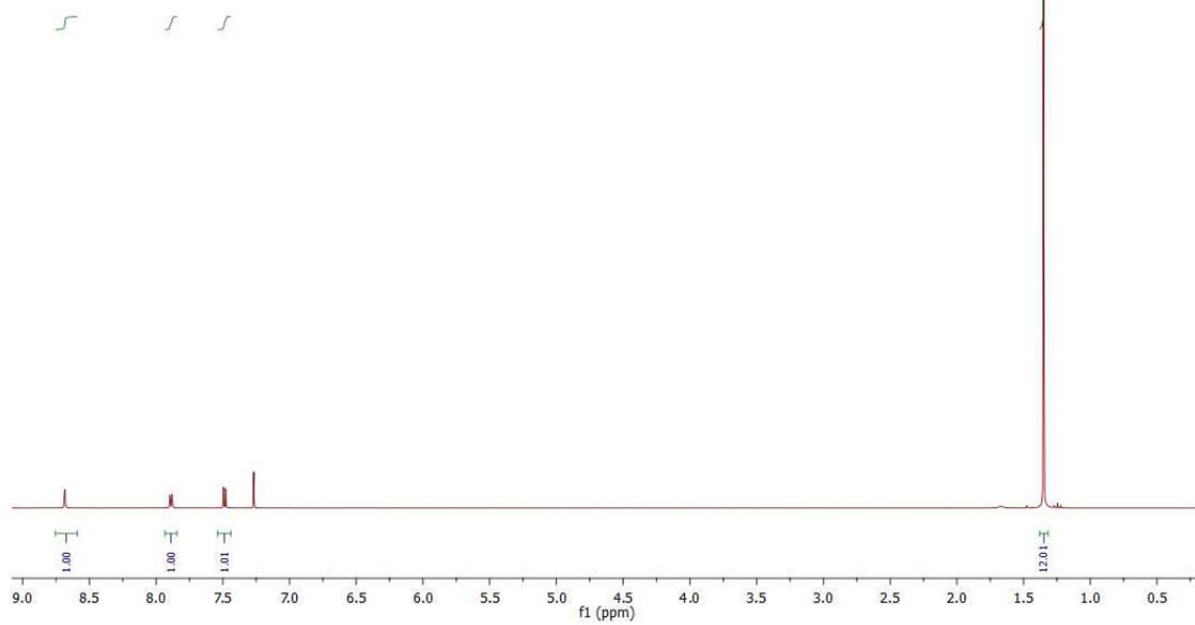
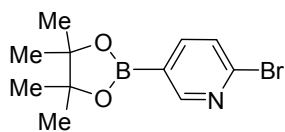
^1H NMR Spectra and $^{13}\text{C}\{^1\text{H}\}$ NMR Spectra**4,4,5,5-Tetramethyl-2-(5-(trimethylstannyl)thiophen-2-yl)-1,3,2-dioxaborolane (9, in CDCl_3)**

2-(4-*n*-Hexyl-5-(trimethylstannyl)thiophen-2-yl)-4,4,5,5-tetramethyl-1,3,2-dioxaborolane (14, in CDCl₃)

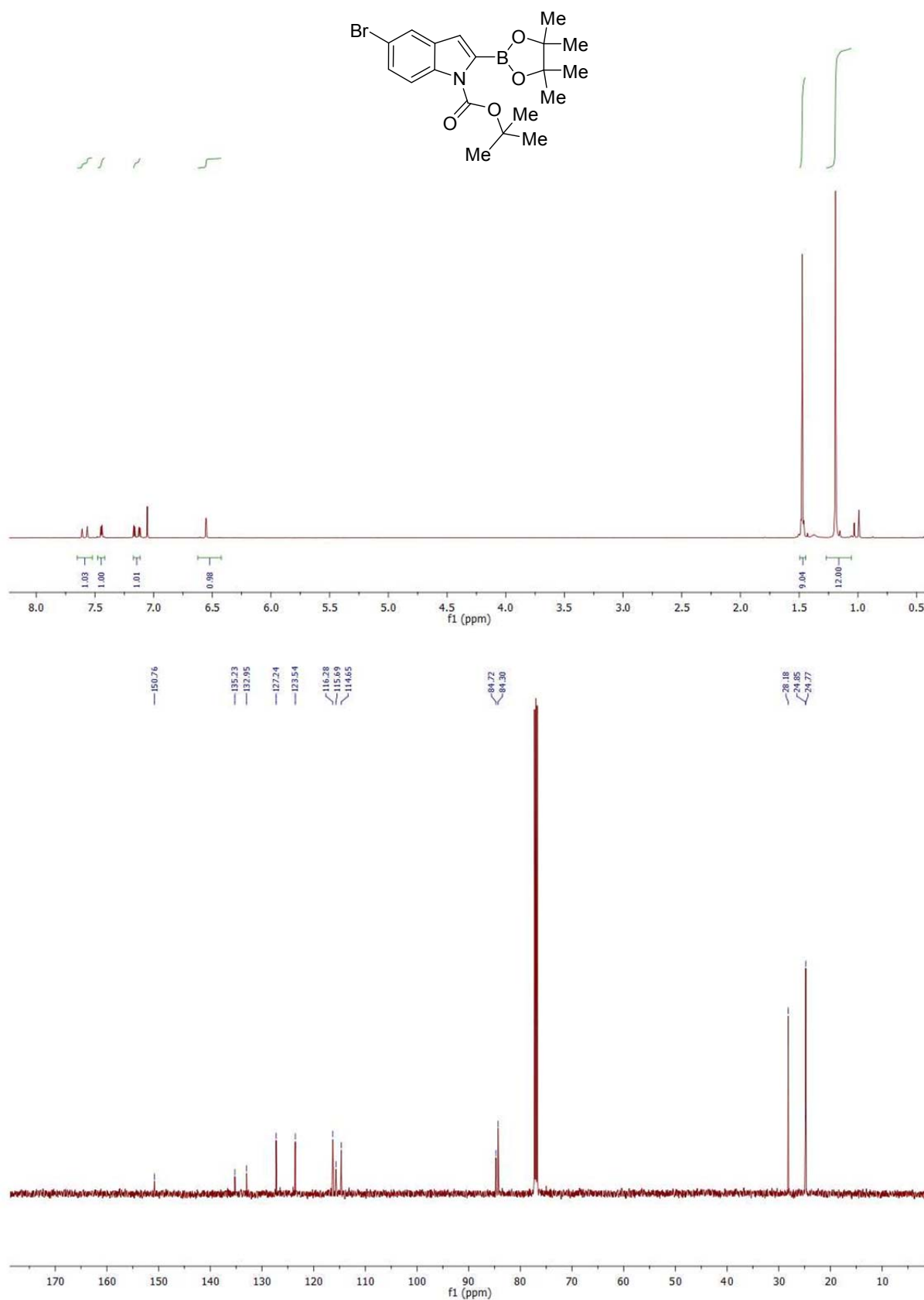
2-Iodo-3-*n*-hexyl-thiophene (16, in CDCl₃)

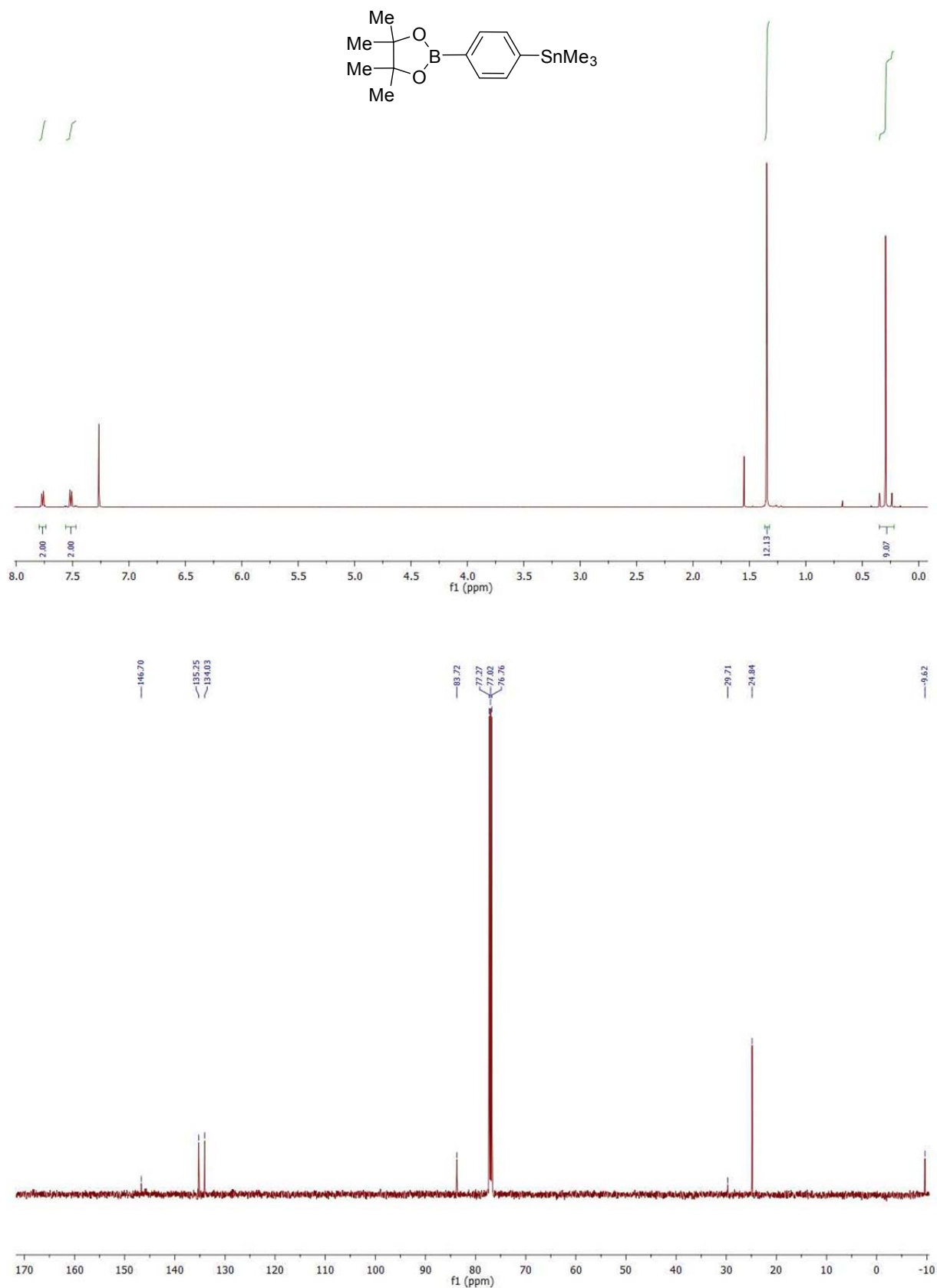
2-(4-*n*-Hexyl-5-iodothiophen-2-yl)-4,4,5,5-tetramethyl-1,3,2-dioxaborolane (17, in CDCl₃)

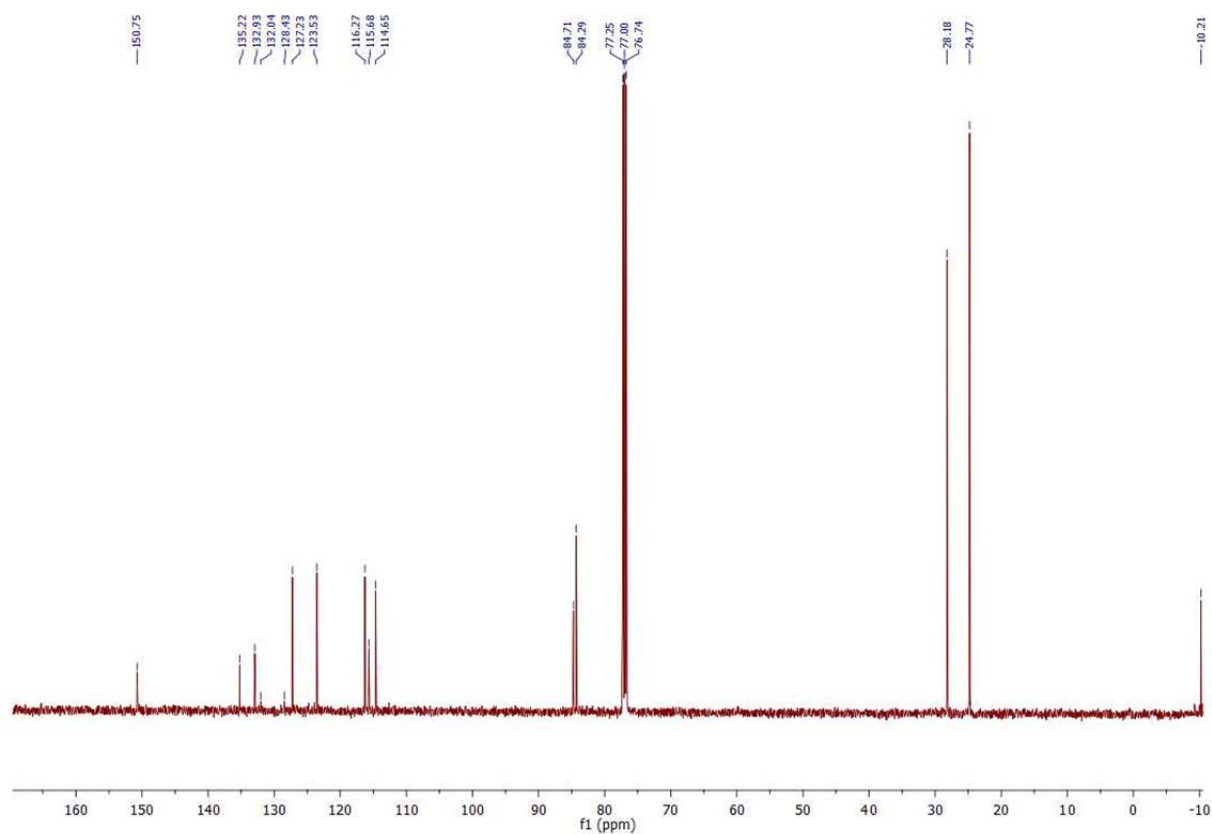
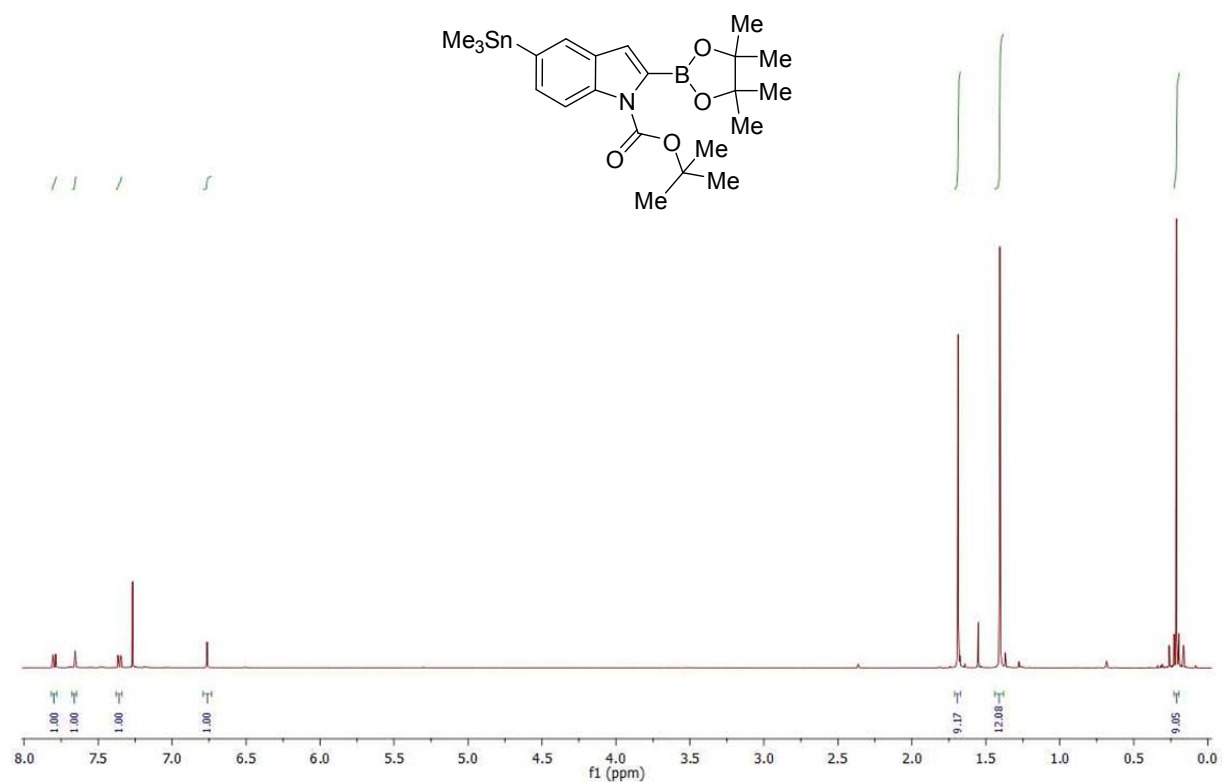
2-(5-Iodothiophen-2-yl)-4,4,5,5-tetramethyl-1,3,2-dioxaborolane (19, in CDCl₃)

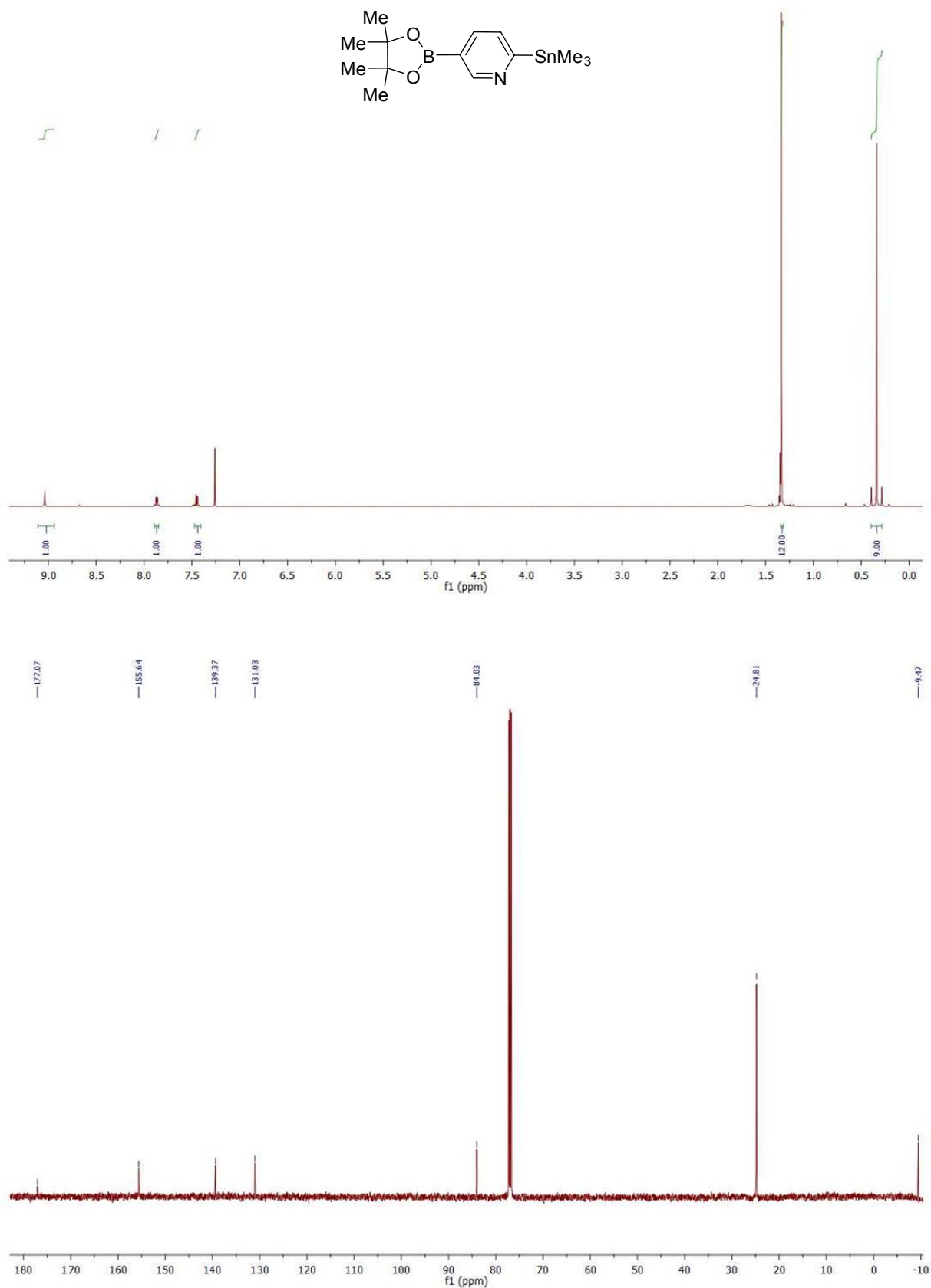
2-Bromo-5-(4,4,5,5-tetramethyl-1,3,2-dioxaborolan-2-yl)pyridine (21, in CDCl₃)

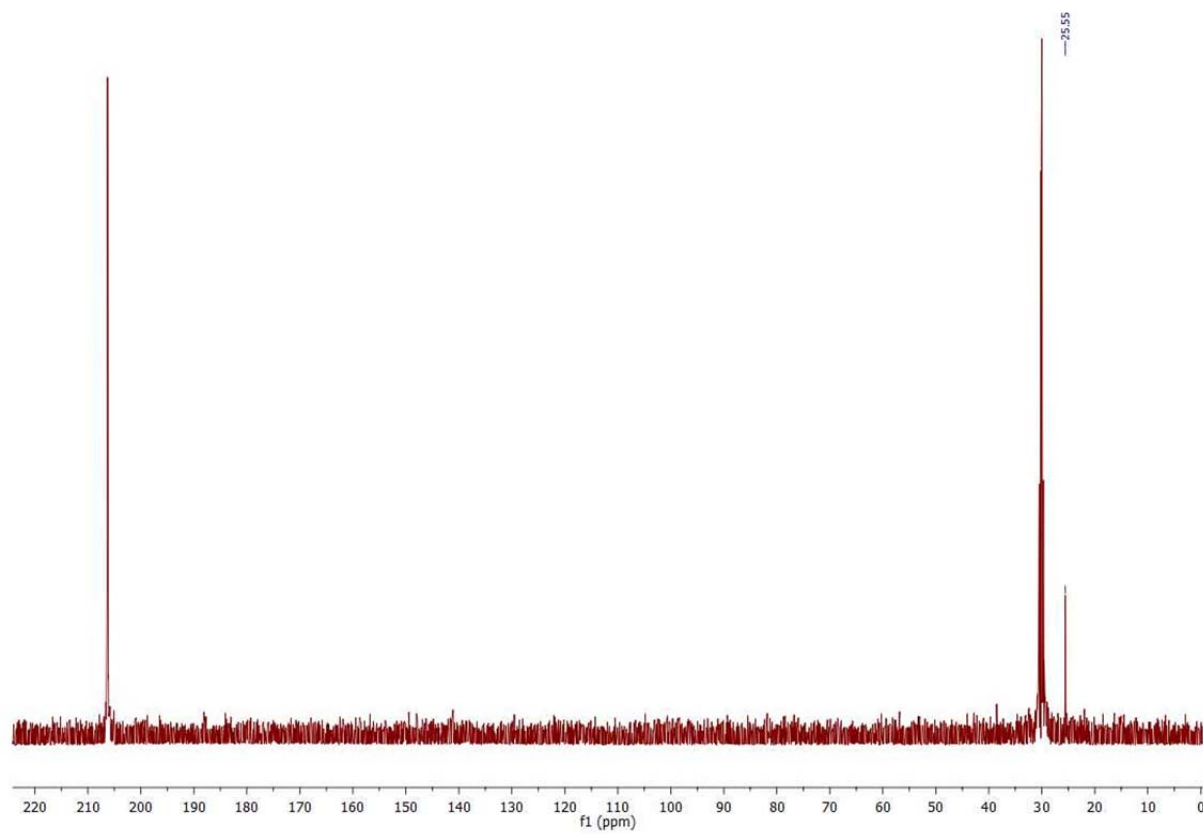
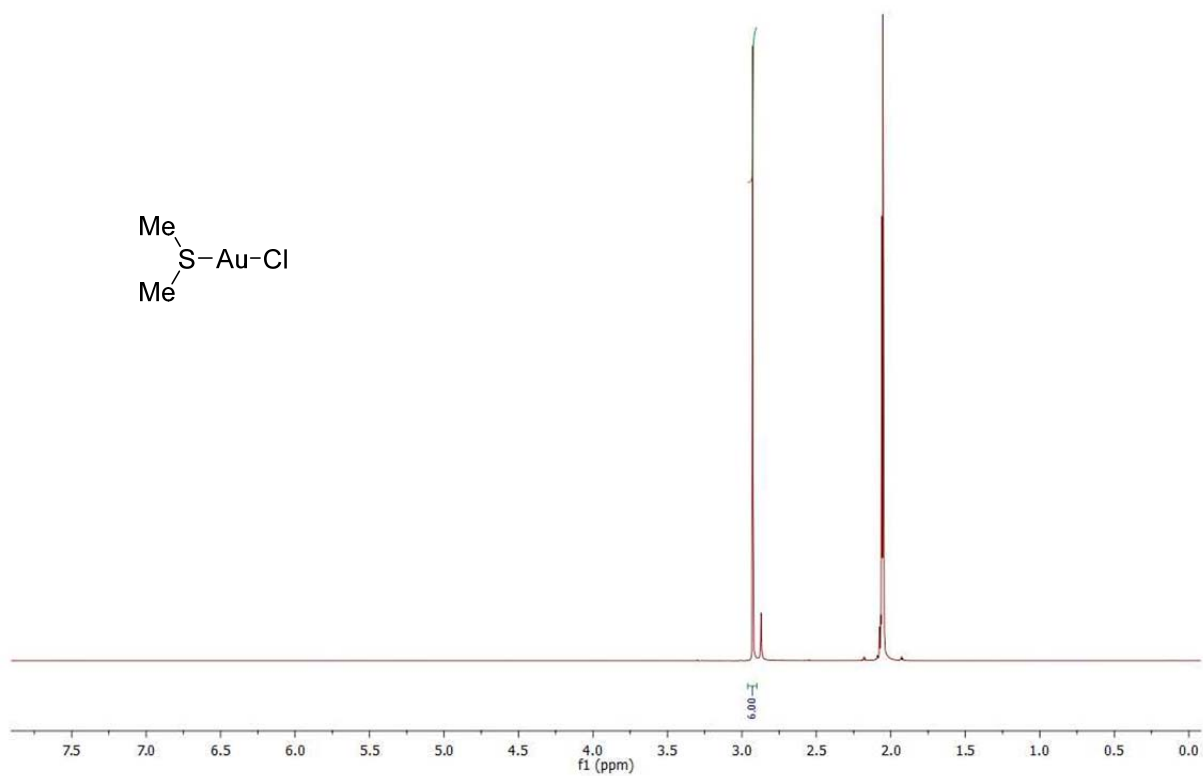
***tert*-Butyl-5-bromo-2-(4,4,5,5-tetramethyl-1,3,2-dioxaborolan-2-yl)-1*H*-indole-1-carboxylate (23, in CDCl₃)**

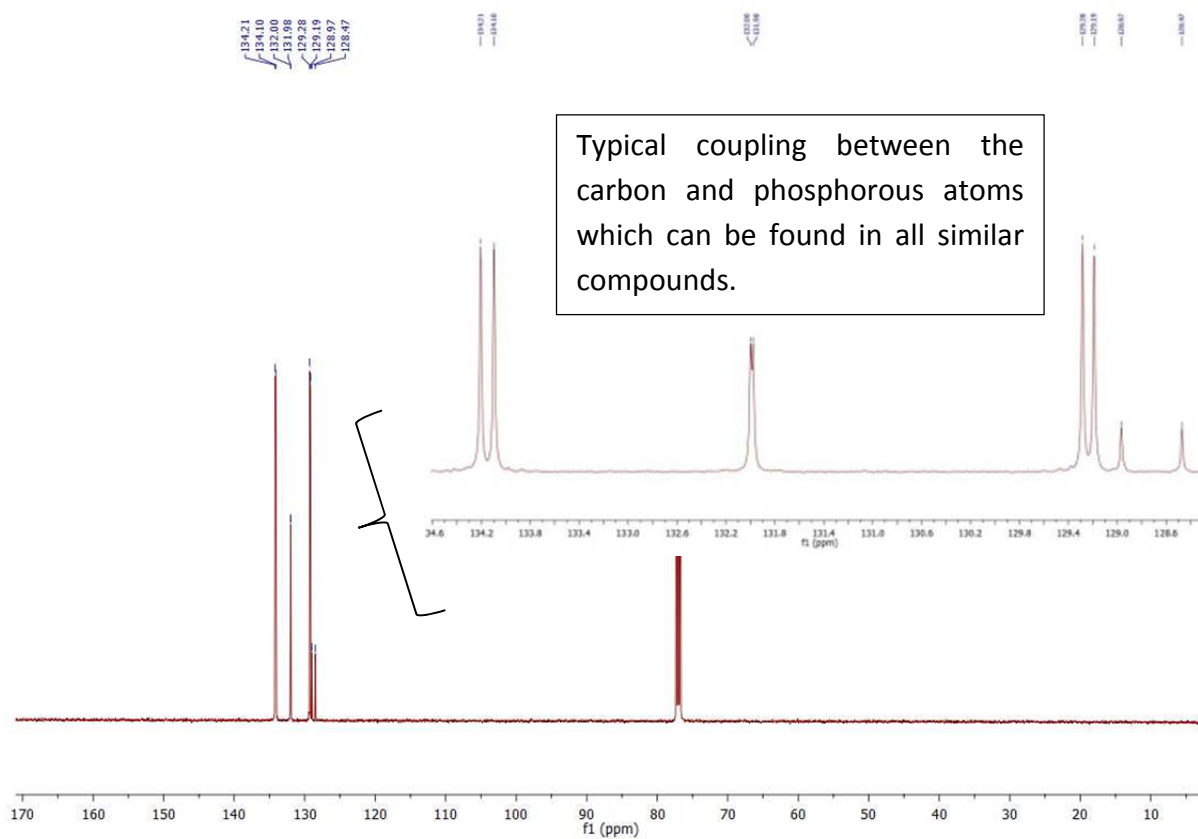
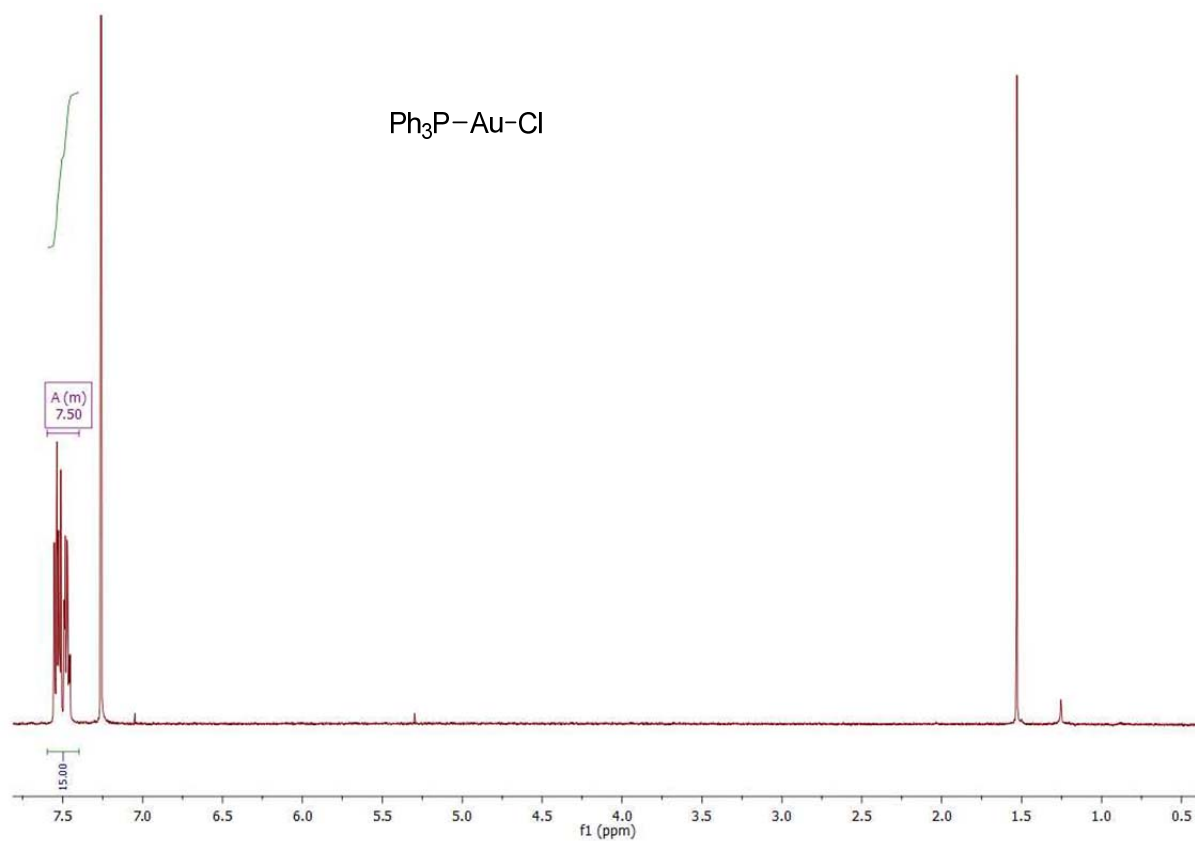


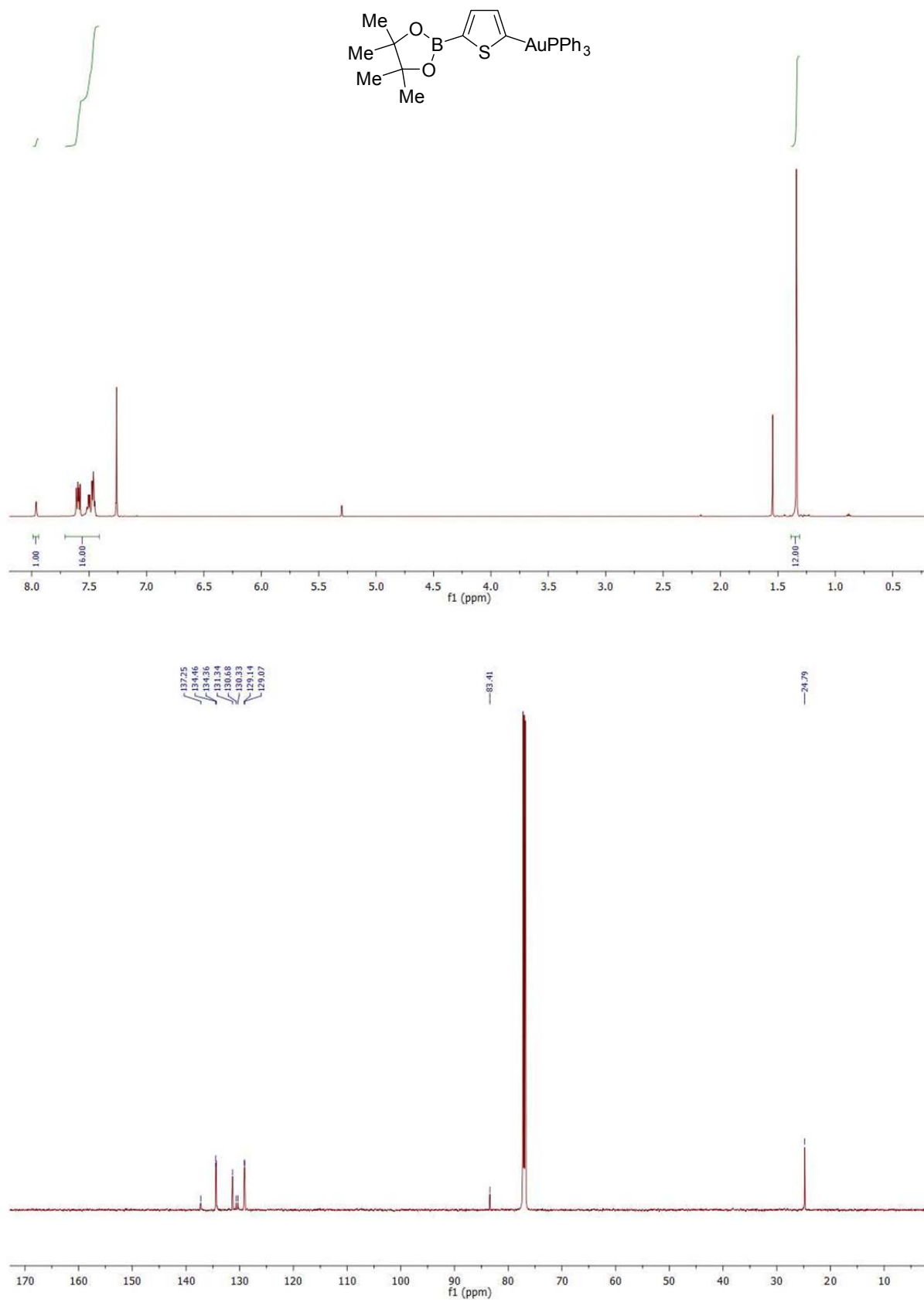
2-(4-(Trimethylstannyl)phenyl)-4,4,5,5-tetramethyl-1,3,2-dioxaborolane (24, in CDCl₃)

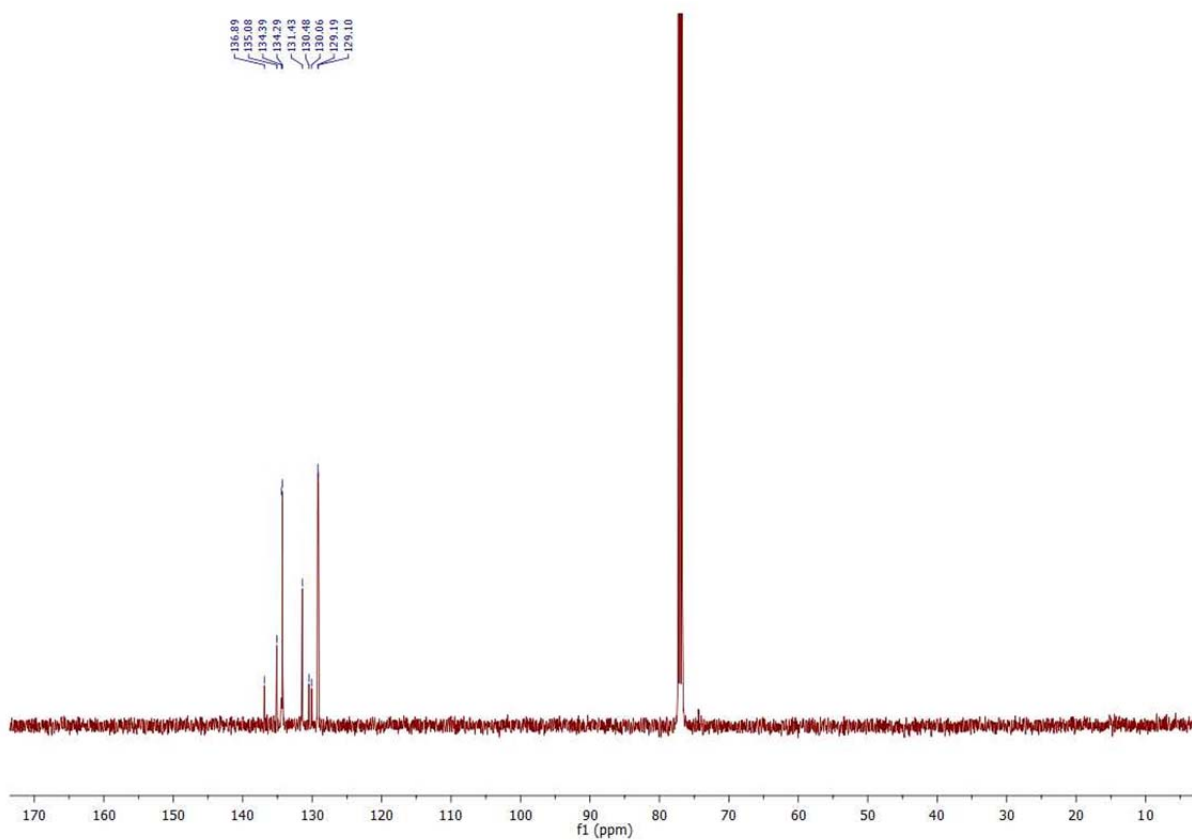
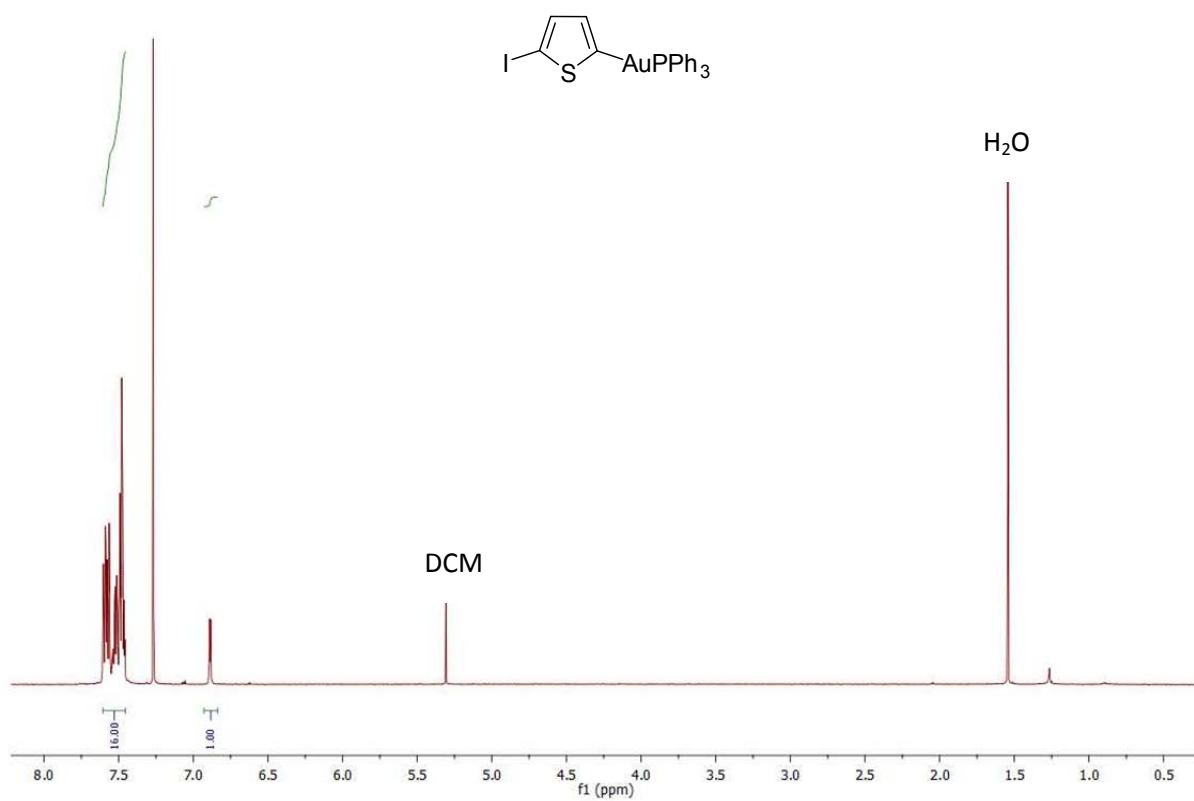
***tert*-Butyl-5-trimethylstannyl-2-(4,4,5,5-tetramethyl-1,3,2-dioxaborolan-2-yl)-1*H*-indole 1-carboxylate (25, in CDCl₃)**

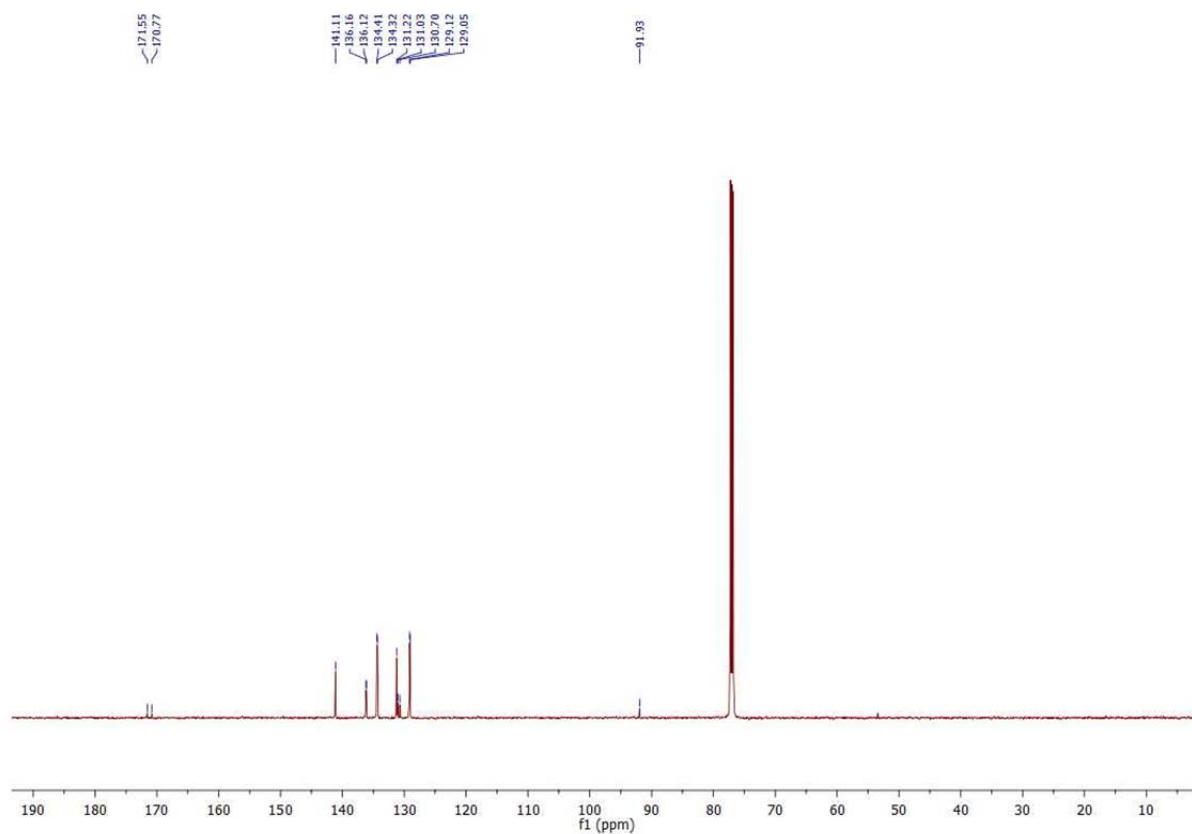
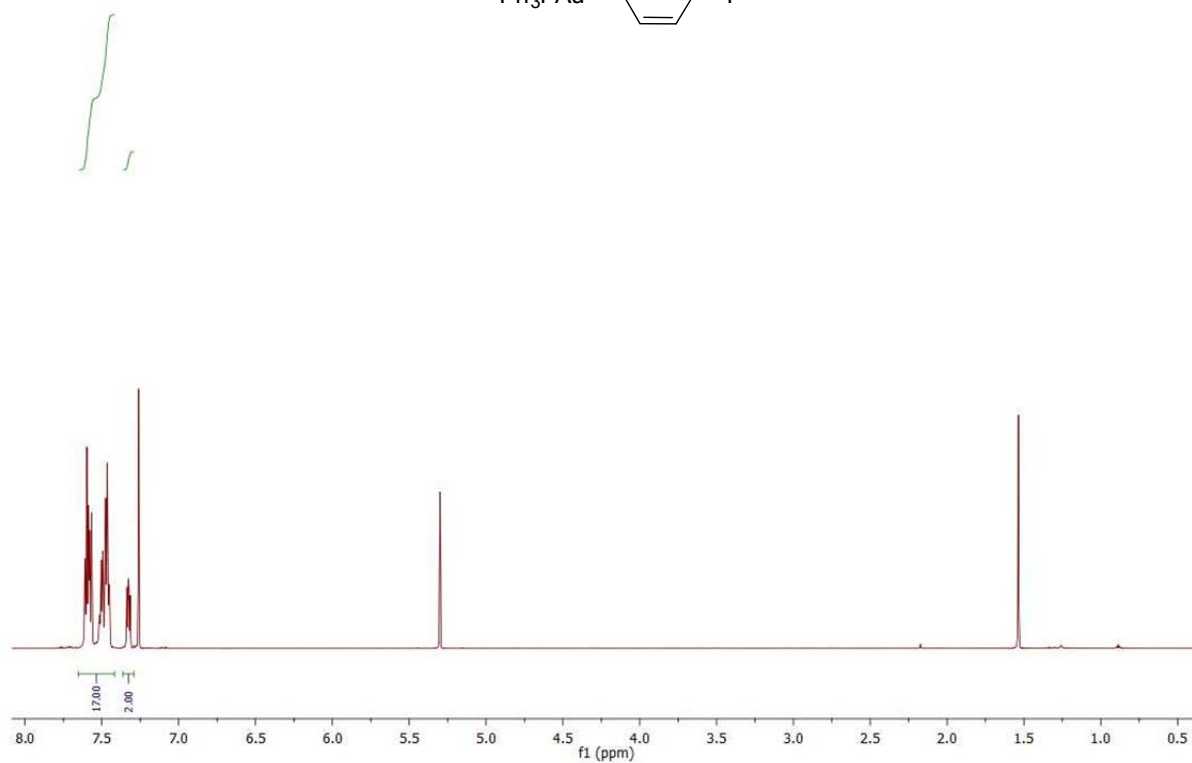
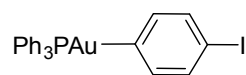
2-Trimethylstannyl-5-(4,4,5,5-tetramethyl-1,3,2-dioxaborolan-2-yl)pyridine (26, in CDCl₃)

Dimethylsulfide gold(I) chloride (31, in acetone- d_6)

Triphenylphosphine gold(I) chloride (32, in CDCl₃)

(5-(4,4,5,5-tetramethyl-1,3,2-dioxaborolan-2-yl)thiophen-2-yl)(triphenylphosphine)-gold (35, in CDCl₃)

(5-Iodothiophen-2-yl)(triphenylphosphine)gold (37, in CDCl₃)

(5-Iodophenyl-2-yl)(triphenylphosphine)gold (39, in CDCl₃)

Single Crystal Data

The data were measured using an Imaging Plate Diffraction System (IPDS-1) from STOE & CIE and were corrected for absorption using X-Red and X-Shape from STOE & CIE (Min/max. transmission: 0.4839/0.7604). The structure was solved with direct methods using SHELXS-97 and refinement was performed against F^2 using SHELXL-97. All non-hydrogen atoms were refined anisotropic. The C-H H atoms were positioned with idealized geometry and refined isotropic with $U_{\text{iso}}(\text{H}) = 1.2 \cdot U_{\text{eq}}(\text{C})$ (1.5 for methyl H atoms) using a riding model. Selected crystal data and details on the structure determination can be found in tables below.

(5-(4,4,5,5-tetramethyl-1,3,2-dioxaborolan-2-yl)thiophen-2-yl)(triphenylphosphine)gold (35)

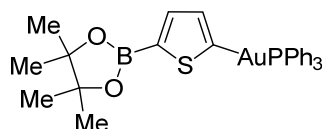


Table SI 1. Crystal data and structure refinement

Empirical formula	$\text{C}_{28}\text{H}_{29}\text{AuBO}_2\text{PS}$	
Formula weight	668.32	
Temperature	200(2) K	
Wavelength	0.71073 Å	
Crystal system	Triclinic	
Space group	P-1	
Unit cell dimensions	$a = 8.8487(3)$ Å	$\alpha = 86.810(3)^\circ$.
	$b = 11.1323(4)$ Å	$\beta = 89.161(3)^\circ$.
	$c = 13.7577(5)$ Å	$\gamma = 86.276(3)^\circ$.
Volume	$1350.18(8)$ Å ³	
Z	2	
Density (calculated)	1.644 Mg/m ³	
Absorption coefficient	5.607 mm ⁻¹	
F(000)	656	
Crystal size	0.04 x 0.10 x 0.14 mm ³	
Theta range for data collection	1.483 to 28.003°.	
Index ranges	-11<=h<=11, -14<=k<=14, -17<=l<=18	
Reflections collected	16713	
Independent reflections	6506 [R(int) = 0.0451]	
Completeness to theta = 25.242°	99.6 %	
Refinement method	Full-matrix least-squares on F^2	
Data / restraints / parameters	6506 / 0 / 308	
Goodness-of-fit on F^2	1.068	
Final R indices [I>2sigma(I)]	R1 = 0.0459, wR2 = 0.1209	

R indices (all data)	R1 = 0.0498, wR2 = 0.1240
Extinction coefficient	0.0188(12)
Largest diff. peak and hole	1.842 and -1.781 e.Å ⁻³

Comments:

All non-hydrogen atoms were refined anisotropic. The C-H atoms were positioned with idealized geometry and refined using a riding model. A numerical absorption correction was performed (Tmin/max: 0.2588/0.7723).

Table SI 2. Atomic coordinates ($\times 10^4$) and equivalent isotropic displacement parameters ($\text{\AA}^2 \times 10^3$) for staubitz10. $U(\text{eq})$ is defined as one third of the trace of the orthogonalized U^{ij} tensor.

	x	y	z	U(eq)
Au(1)	3495(1)	7251(1)	4208(1)	41(1)
C(1)	2780(6)	7151(5)	2817(4)	42(1)
S(1)	973(2)	7613(1)	2465(1)	48(1)
C(2)	1270(6)	7333(5)	1259(4)	43(1)
C(3)	2741(7)	6885(6)	1146(5)	52(1)
C(4)	3571(7)	6792(6)	2016(5)	56(2)
B(1)	63(7)	7561(6)	469(5)	43(1)
O(1)	-1417(5)	7933(4)	666(3)	52(1)
C(5)	-2137(7)	8230(6)	-274(5)	56(1)
C(6)	-1104(8)	7485(6)	-976(5)	55(1)
O(2)	343(5)	7407(4)	-483(3)	56(1)
C(7)	-2095(11)	9573(7)	-460(7)	79(2)
C(8)	-3765(8)	7877(9)	-192(7)	76(2)
C(9)	-1554(11)	6194(8)	-1045(7)	74(2)
C(10)	-856(10)	8065(9)	-2037(6)	76(2)
P(1)	4418(1)	7327(1)	5740(1)	37(1)
C(11)	6456(6)	7058(5)	5740(4)	40(1)
C(12)	7309(7)	7820(6)	5149(5)	51(1)
C(13)	8874(7)	7581(7)	5069(5)	61(2)
C(14)	9571(7)	6584(7)	5550(5)	60(2)
C(15)	8728(7)	5828(6)	6123(5)	54(1)
C(16)	7187(6)	6063(5)	6236(4)	44(1)
C(21)	3682(6)	6204(5)	6601(4)	40(1)
C(22)	3295(6)	5119(5)	6260(4)	44(1)
C(23)	2661(7)	4269(5)	6878(5)	54(1)
C(24)	2419(7)	4490(6)	7852(5)	57(2)
C(25)	2806(8)	5565(6)	8193(5)	61(2)
C(26)	3451(8)	6421(5)	7578(5)	54(1)

C(31)	3991(6)	8730(5)	6331(4)	43(1)
C(32)	2465(8)	9129(5)	6375(6)	57(2)
C(33)	2027(10)	10113(6)	6912(7)	74(2)
C(34)	3097(11)	10719(6)	7364(6)	73(2)
C(35)	4623(11)	10367(6)	7287(6)	70(2)
C(36)	5057(8)	9360(5)	6756(5)	54(1)

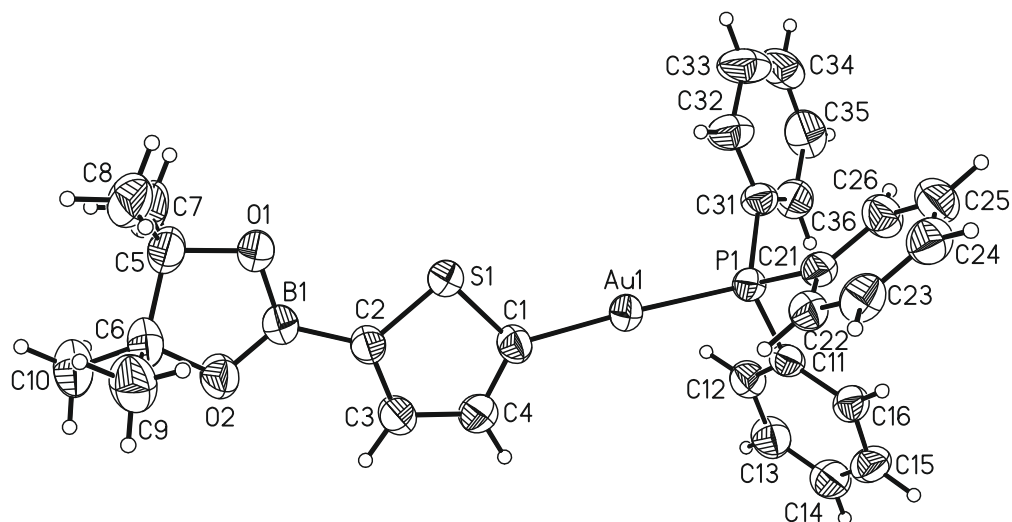


Table SI 3. Bond lengths [Å] and angles [°].

Au(1)-C(1)	2.036(6)	Au(1)-P(1)	2.2792(14)
C(1)-Au(1)-P(1)	176.99(15)	C(4)-C(1)-Au(1)	129.4(5)
C(11)-P(1)-Au(1)	110.81(18)	S(1)-C(1)-Au(1)	122.4(3)
C(31)-P(1)-Au(1)	115.8(2)	C(21)-P(1)-Au(1)	113.35(19)
C(1)-C(4)	1.361(8)	C(11)-C(12)	1.393(8)
C(1)-S(1)	1.715(6)	C(11)-C(16)	1.395(8)
S(1)-C(2)	1.718(6)	C(12)-C(13)	1.397(9)
C(2)-C(3)	1.373(8)	C(13)-C(14)	1.376(10)
C(2)-B(1)	1.534(8)	C(14)-C(15)	1.369(10)
C(3)-C(4)	1.409(9)	C(15)-C(16)	1.381(8)
B(1)-O(2)	1.348(8)	C(21)-C(22)	1.385(8)
B(1)-O(1)	1.375(7)	C(21)-C(26)	1.389(8)
O(1)-C(5)	1.463(8)	C(22)-C(23)	1.379(8)
C(5)-C(7)	1.506(10)	C(23)-C(24)	1.387(10)
C(5)-C(8)	1.519(10)	C(24)-C(25)	1.374(10)
C(5)-C(6)	1.556(10)	C(25)-C(26)	1.385(9)
C(6)-O(2)	1.453(8)	C(31)-C(36)	1.368(9)
C(6)-C(9)	1.524(11)	C(31)-C(32)	1.395(8)
C(6)-C(10)	1.580(10)	C(32)-C(33)	1.386(9)
P(1)-C(11)	1.808(5)	C(33)-C(34)	1.373(14)
P(1)-C(31)	1.817(5)	C(34)-C(35)	1.385(13)
P(1)-C(21)	1.819(6)	C(35)-C(36)	1.402(9)
C(4)-C(1)-S(1)	108.1(4)	C(31)-P(1)-C(21)	103.0(2)

C(1)-S(1)-C(2)	95.1(3)	C(12)-C(11)-C(16)	119.1(5)
C(3)-C(2)-B(1)	127.5(5)	C(12)-C(11)-P(1)	118.0(4)
C(3)-C(2)-S(1)	108.2(4)	C(16)-C(11)-P(1)	122.7(4)
B(1)-C(2)-S(1)	124.3(4)	C(11)-C(12)-C(13)	119.6(6)
C(2)-C(3)-C(4)	113.7(5)	C(14)-C(13)-C(12)	120.5(6)
C(1)-C(4)-C(3)	114.9(5)	C(15)-C(14)-C(13)	119.8(6)
O(2)-B(1)-O(1)	113.4(5)	C(14)-C(15)-C(16)	120.8(6)
O(2)-B(1)-C(2)	123.4(5)	C(15)-C(16)-C(11)	120.2(6)
O(1)-B(1)-C(2)	123.2(5)	C(22)-C(21)-C(26)	119.4(5)
B(1)-O(1)-C(5)	106.6(5)	C(22)-C(21)-P(1)	118.6(4)
O(1)-C(5)-C(7)	106.6(6)	C(26)-C(21)-P(1)	122.0(4)
O(1)-C(5)-C(8)	107.9(6)	C(23)-C(22)-C(21)	120.5(6)
C(7)-C(5)-C(8)	110.3(7)	C(22)-C(23)-C(24)	120.0(6)
O(1)-C(5)-C(6)	102.2(5)	C(25)-C(24)-C(23)	119.6(6)
C(7)-C(5)-C(6)	113.8(6)	C(24)-C(25)-C(26)	120.8(6)
C(8)-C(5)-C(6)	115.2(6)	C(25)-C(26)-C(21)	119.7(6)
O(2)-C(6)-C(9)	106.4(6)	C(36)-C(31)-C(32)	120.0(6)
O(2)-C(6)-C(5)	102.2(5)	C(36)-C(31)-P(1)	123.8(4)
C(9)-C(6)-C(5)	113.4(7)	C(32)-C(31)-P(1)	116.1(5)
O(2)-C(6)-C(10)	107.9(6)	C(33)-C(32)-C(31)	119.6(7)
C(9)-C(6)-C(10)	109.2(6)	C(34)-C(33)-C(32)	120.1(7)
C(5)-C(6)-C(10)	116.8(6)	C(33)-C(34)-C(35)	120.8(6)
B(1)-O(2)-C(6)	107.7(5)	C(34)-C(35)-C(36)	118.8(8)
C(11)-P(1)-C(31)	106.8(3)	C(31)-C(36)-C(35)	120.5(7)
C(11)-P(1)-C(21)	106.3(2)		

Table SI 4. Anisotropic displacement parameters ($\text{\AA}^2 \times 10^3$). The anisotropic displacement factor exponent takes the form: $-2\pi^2 [h^2 a^{*2} U^{11} + \dots + 2 h k a^* b^* U^{12}]$

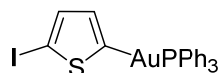
	U^{11}	U^{22}	U^{33}	U^{23}	U^{13}	U^{12}
Au(1)	40(1)	46(1)	37(1)	-2(1)	-4(1)	0(1)
C(1)	43(3)	49(3)	36(3)	-5(2)	-3(2)	-5(2)
S(1)	43(1)	60(1)	39(1)	-6(1)	-3(1)	8(1)
C(2)	48(3)	43(2)	36(2)	-2(2)	-3(2)	-1(2)
C(3)	45(3)	71(4)	41(3)	-12(3)	-1(2)	1(3)
C(4)	43(3)	74(4)	53(3)	-14(3)	-7(2)	8(3)
B(1)	46(3)	45(3)	37(3)	-2(2)	-2(2)	-3(2)
O(1)	45(2)	67(2)	42(2)	-1(2)	-4(2)	5(2)
C(5)	50(3)	67(4)	50(3)	3(3)	-11(3)	1(3)
C(6)	56(3)	69(4)	41(3)	0(3)	-10(2)	-11(3)
O(2)	46(2)	75(3)	46(2)	-6(2)	-4(2)	-5(2)
C(7)	90(6)	66(4)	81(6)	4(4)	-38(4)	9(4)
C(8)	43(3)	114(6)	72(5)	-7(4)	-13(3)	-4(4)

C(9)	82(5)	76(5)	68(5)	-14(4)	-16(4)	-16(4)
C(10)	76(5)	97(6)	56(4)	-1(4)	-18(4)	-14(4)
P(1)	36(1)	40(1)	36(1)	-5(1)	-2(1)	1(1)
C(11)	39(2)	43(2)	38(3)	-9(2)	1(2)	-1(2)
C(12)	48(3)	59(3)	44(3)	-1(2)	2(2)	-1(2)
C(13)	46(3)	82(4)	54(4)	-2(3)	3(3)	-7(3)
C(14)	41(3)	83(4)	56(4)	-14(3)	-5(3)	2(3)
C(15)	44(3)	56(3)	61(4)	-10(3)	-9(3)	8(2)
C(16)	44(3)	45(2)	45(3)	-7(2)	-7(2)	1(2)
C(21)	36(2)	44(2)	41(3)	-5(2)	-2(2)	2(2)
C(22)	47(3)	44(2)	42(3)	-3(2)	-2(2)	-1(2)
C(23)	56(3)	42(3)	66(4)	0(3)	-9(3)	-7(2)
C(24)	54(3)	52(3)	63(4)	8(3)	6(3)	-4(2)
C(25)	73(4)	60(3)	47(3)	-1(3)	12(3)	-2(3)
C(26)	74(4)	44(3)	44(3)	-5(2)	4(3)	-4(3)
C(31)	45(3)	37(2)	46(3)	-1(2)	5(2)	4(2)
C(32)	56(3)	45(3)	70(4)	-2(3)	13(3)	5(2)
C(33)	81(5)	47(3)	89(6)	1(3)	35(4)	14(3)
C(34)	120(7)	40(3)	58(4)	-6(3)	23(4)	10(3)
C(35)	110(6)	42(3)	59(4)	-5(3)	-3(4)	-8(3)
C(36)	62(3)	47(3)	52(3)	-10(2)	-8(3)	0(2)

Table SI 5. Hydrogen coordinates ($\times 10^4$) and isotropic displacement parameters ($\text{\AA}^2 \times 10^{-3}$).

	x	y	z	U(eq)
H(3)	3160	6659	538	63
H(4)	4604	6501	2042	68
H(7A)	-2569	9815	-1086	119
H(7B)	-2648	9985	61	119
H(7C)	-1041	9795	-476	119
H(8A)	-4273	8067	-815	114
H(8B)	-3778	7010	-26	114
H(8C)	-4295	8324	318	114
H(9A)	-2529	6200	-1374	112
H(9B)	-780	5739	-1416	112
H(9C)	-1643	5814	-389	112
H(10A)	-1818	8127	-2385	114
H(10B)	-485	8871	-1995	114
H(10C)	-111	7556	-2388	114
H(12)	6829	8498	4802	61
H(13)	9462	8112	4679	73
H(14)	10634	6420	5486	72

H(15)	9210	5133	6445	65
H(16)	6622	5546	6653	53
H(22)	3469	4960	5595	53
H(23)	2389	3530	6636	65
H(24)	1989	3903	8280	68
H(25)	2628	5722	8858	73
H(26)	3733	7155	7824	65
H(32)	1731	8729	6039	69
H(33)	985	10367	6968	88
H(34)	2787	11389	7734	88
H(35)	5361	10800	7589	84
H(36)	6100	9113	6690	64

(5-Iodothiophen-2-yl)(triphenylphosphine)gold (37)**Table SI 6.** Crystal data and structure refinement

Empirical formula	C ₂₂ H ₁₇ AuIPS	
Formula weight	668.25	
Temperature	200(2) K	
Wavelength	0.71073 Å	
Crystal system	Triclinic	
Space group	P-1	
Unit cell dimensions	a = 11.2623(8) Å	α = 89.835(9)°.
	b = 13.6294(10) Å	β = 84.181(9)°.
	c = 14.4792(12) Å	γ = 90.722(9)°.
Volume	2210.9(3) Å ³	
Z	4	
Density (calculated)	2.008 Mg/m ³	
Absorption coefficient	8.220 mm ⁻¹	
F(000)	1248	
Crystal size	0.08 x 0.11 x 0.14 mm ³	
Theta range for data collection	2.414 to 28.005°.	
Index ranges	-14 ≤ h ≤ 14, -17 ≤ k ≤ 17, -19 ≤ l ≤ 19	
Reflections collected	23241	
Independent reflections	10483 [R(int) = 0.0431]	
Completeness to theta = 25.242°	99.0 %	
Refinement method	Full-matrix least-squares on F ²	
Data / restraints / parameters	10483 / 0 / 515	
Goodness-of-fit on F ²	1.048	
Final R indices [I > 2σ(I)]	R1 = 0.0381, wR2 = 0.0940	
R indices (all data)	R1 = 0.0513, wR2 = 0.0997	
Extinction coefficient	0.0050(2)	
Largest diff. peak and hole	1.684 and -1.846 e.Å ⁻³	

Comments:

All non-hydrogen atoms were refined anisotropic. The H atoms were positioned with idealized geometry and refined using a riding model. A numerical absorption correction was performed (Tmin/max: 0.2202/0.4164). The asymmetric unit consists of two crystallographically independent molecules. In one of these molecules the five-membered ring is disordered in two orientations and was refined using a split model.

Table SI 7. Atomic coordinates ($\times 10^4$) and equivalent isotropic displacement parameters ($\text{\AA}^2 \times 10^3$).

$U(\text{eq})$ is defined as one third of the trace of the orthogonalized U^{ij} tensor.

	x	y	z	$U(\text{eq})$
Au(1)	9168(1)	24322(1)	-3129(1)	31(1)
C(1)	10467(4)	25376(4)	-3353(4)	32(1)
S(1)	10866(1)	26102(1)	-2450(1)	40(1)
C(2)	11931(4)	26729(4)	-3144(4)	31(1)
C(3)	11991(5)	26425(4)	-4028(4)	34(1)
C(4)	11152(5)	25648(4)	-4141(4)	36(1)
I(1)	12998(1)	27834(1)	-2644(1)	52(1)
P(1)	7665(1)	23168(1)	-2907(1)	27(1)
C(11)	7596(4)	22524(4)	-1801(4)	28(1)
C(12)	7872(6)	23048(5)	-1025(4)	42(1)
C(13)	7801(7)	22596(6)	-156(5)	55(2)
C(14)	7490(6)	21605(5)	-67(4)	47(2)
C(15)	7244(7)	21081(5)	-837(5)	50(2)
C(16)	7291(6)	21537(4)	-1707(4)	41(1)
C(21)	7721(5)	22213(4)	-3785(4)	33(1)
C(22)	8844(5)	21983(5)	-4248(4)	41(1)
C(23)	8920(7)	21257(6)	-4928(5)	56(2)
C(24)	7921(8)	20768(6)	-5150(5)	58(2)
C(25)	6811(7)	20991(6)	-4690(5)	58(2)
C(26)	6711(5)	21708(5)	-3999(4)	42(1)
C(31)	6216(4)	23739(4)	-2932(4)	31(1)
C(32)	5205(5)	23406(4)	-2366(4)	39(1)
C(33)	4142(5)	23908(5)	-2363(5)	49(2)
C(34)	4040(6)	24697(5)	-2931(6)	55(2)
C(35)	5031(7)	25010(6)	-3514(6)	61(2)
C(36)	6112(5)	24535(5)	-3513(5)	47(2)
Au(2)	15359(1)	19528(1)	-2484(1)	45(1)
S(2)	13201(4)	21071(4)	-2847(3)	36(1)
C(41)	14050(7)	20543(7)	-2068(8)	28(2)
S(2')	13400(5)	20950(4)	-1520(5)	51(1)
C(41')	14103(14)	20539(12)	-2583(15)	43(4)
C(42)	12379(4)	21693(4)	-2013(5)	39(1)
C(43)	12749(9)	21558(8)	-1167(8)	46(3)
C(44)	13744(15)	20874(12)	-1188(12)	56(4)
I(2)	11040(1)	22664(1)	-2318(1)	49(1)
C(43')	12511(13)	21586(14)	-2978(15)	56(5)
C(44')	13450(20)	20985(19)	-3190(20)	48(7)
I(2')	11037(1)	22431(1)	-1298(1)	86(1)
P(2)	16788(1)	18353(1)	-2580(1)	31(1)
C(51)	17082(5)	17733(4)	-3679(4)	33(1)
C(52)	16165(5)	17665(5)	-4263(4)	42(1)

C(53)	16335(6)	17116(6)	-5068(5)	54(2)
C(54)	17401(6)	16658(6)	-5315(5)	49(2)
C(55)	18313(6)	16730(5)	-4748(5)	46(2)
C(56)	18158(5)	17269(5)	-3937(4)	39(1)
C(61)	16370(5)	17407(5)	-1720(4)	42(1)
C(62)	15710(7)	17678(7)	-915(5)	67(2)
C(63)	15427(10)	17051(10)	-203(7)	98(4)
C(64)	15771(15)	16100(9)	-311(8)	132(6)
C(65)	16390(18)	15790(7)	-1123(9)	152(8)
C(66)	16665(12)	16454(6)	-1834(7)	98(4)
C(71)	18221(4)	18805(4)	-2293(4)	35(1)
C(72)	18741(6)	18489(6)	-1511(6)	64(2)
C(73)	19802(7)	18898(8)	-1300(7)	83(3)
C(74)	20389(7)	19607(7)	-1865(8)	75(3)
C(75)	19886(6)	19933(5)	-2636(6)	52(2)
C(76)	18801(5)	19540(5)	-2846(5)	41(1)

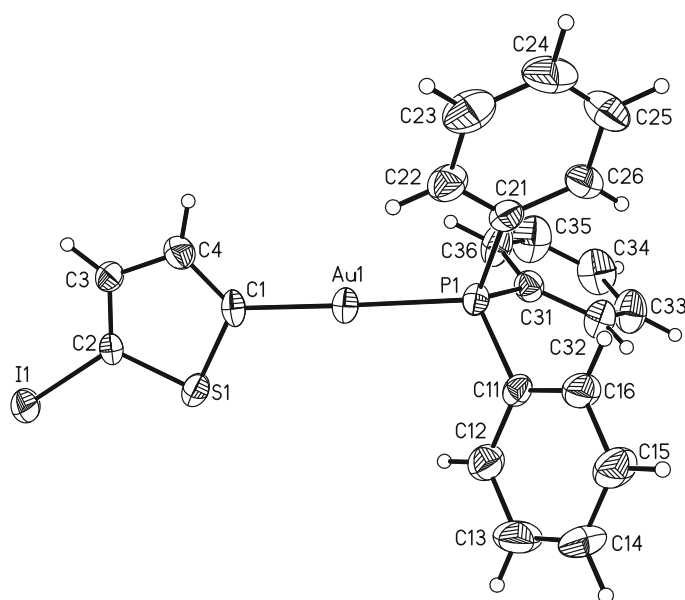


Table SI 8. Bond lengths [Å] and angles [°].

Au(1)-C(1)	2.039(5)	Au(1)-P(1)	2.2936(12)
C(1)-C(4)	1.359(8)	C(15)-C(16)	1.398(8)
C(1)-S(1)	1.733(6)	C(21)-C(26)	1.384(8)
S(1)-C(2)	1.704(5)	C(21)-C(22)	1.411(8)
C(2)-C(3)	1.342(8)	C(22)-C(23)	1.395(10)
C(2)-I(1)	2.090(5)	C(23)-C(24)	1.368(11)
C(3)-C(4)	1.430(7)	C(24)-C(25)	1.394(11)
P(1)-C(11)	1.818(5)	C(25)-C(26)	1.398(9)
P(1)-C(21)	1.819(6)	C(31)-C(36)	1.384(8)
P(1)-C(31)	1.821(5)	C(31)-C(32)	1.403(7)
C(11)-C(16)	1.388(8)	C(32)-C(33)	1.386(8)

C(11)-C(12)	1.392(8)	C(33)-C(34)	1.365(10)
C(12)-C(13)	1.393(9)	C(34)-C(35)	1.392(11)
C(13)-C(14)	1.393(10)	C(35)-C(36)	1.386(9)
C(14)-C(15)	1.375(10)		
C(1)-Au(1)-P(1)	178.01(16)	S(1)-C(1)-Au(1)	120.8(3)
C(4)-C(1)-Au(1)	130.8(4)	C(11)-P(1)-Au(1)	114.38(17)
C(21)-P(1)-Au(1)	114.53(17)	C(31)-P(1)-Au(1)	110.53(17)
C(4)-C(1)-S(1)	108.4(4)	C(11)-C(16)-C(15)	120.0(6)
C(2)-S(1)-C(1)	93.2(3)	C(26)-C(21)-C(22)	119.7(6)
C(3)-C(2)-S(1)	111.9(4)	C(26)-C(21)-P(1)	122.4(4)
C(3)-C(2)-I(1)	125.3(4)	C(22)-C(21)-P(1)	117.8(4)
S(1)-C(2)-I(1)	122.8(3)	C(23)-C(22)-C(21)	119.4(6)
C(2)-C(3)-C(4)	111.6(5)	C(24)-C(23)-C(22)	120.9(6)
C(1)-C(4)-C(3)	114.9(5)	C(23)-C(24)-C(25)	119.8(7)
C(11)-P(1)-C(21)	105.5(2)	C(24)-C(25)-C(26)	120.5(6)
C(11)-P(1)-C(31)	105.6(2)	C(21)-C(26)-C(25)	119.7(6)
C(21)-P(1)-C(31)	105.6(3)	C(36)-C(31)-C(32)	119.0(5)
C(16)-C(11)-C(12)	119.3(5)	C(36)-C(31)-P(1)	119.1(4)
C(16)-C(11)-P(1)	122.5(4)	C(32)-C(31)-P(1)	121.8(4)
C(12)-C(11)-P(1)	118.2(4)	C(33)-C(32)-C(31)	119.6(6)
C(11)-C(12)-C(13)	120.4(6)	C(34)-C(33)-C(32)	121.4(6)
C(12)-C(13)-C(14)	119.9(6)	C(33)-C(34)-C(35)	119.1(6)
C(15)-C(14)-C(13)	119.7(6)	C(36)-C(35)-C(34)	120.6(7)
C(14)-C(15)-C(16)	120.6(6)	C(31)-C(36)-C(35)	120.2(6)

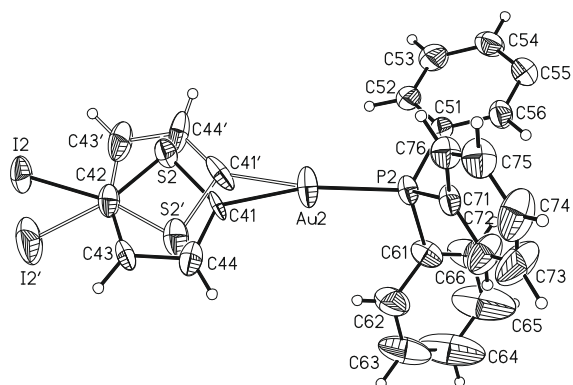


Table SI 9. Bond lengths [Å] and angles [°].

Au(2)-C(41')	2.002(19)	Au(2)-C(41)	2.079(9)
Au(2)-P(2)	2.2804(13)	S(2)-C(42)	1.683(7)
S(2)-C(41)	1.714(13)	C(52)-C(53)	1.384(10)
C(41)-C(44)	1.37(2)	C(53)-C(54)	1.375(10)
S(2')-C(42)	1.745(8)	C(54)-C(55)	1.381(10)
S(2')-C(41')	1.754(19)	C(55)-C(56)	1.385(9)
C(41')-C(44')	1.34(4)	C(61)-C(66)	1.352(11)
C(42)-C(43)	1.346(13)	C(61)-C(62)	1.371(9)
C(42)-C(43')	1.40(2)	C(62)-C(63)	1.348(12)

C(42)-I(2')	2.024(6)	C(63)-C(64)	1.361(18)
C(42)-I(2)	2.099(5)	C(64)-C(65)	1.376(17)
C(43)-C(44)	1.465(17)	C(65)-C(66)	1.378(13)
C(43')-C(44')	1.36(3)	C(71)-C(76)	1.395(8)
P(2)-C(51)	1.807(6)	C(71)-C(72)	1.396(10)
P(2)-C(71)	1.808(6)	C(72)-C(73)	1.375(10)
P(2)-C(61)	1.813(6)	C(73)-C(74)	1.382(12)
C(51)-C(56)	1.392(7)	C(74)-C(75)	1.376(12)
C(51)-C(52)	1.402(8)	C(75)-C(76)	1.390(8)
C(41')-Au(2)-P(2)	172.4(6)	C(41)-Au(2)-P(2)	166.7(3)
C(44)-C(41)-Au(2)	127.0(9)	C(44')-C(41')-Au(2)	143.1(19)
S(2)-C(41)-Au(2)	121.5(6)	S(2')-C(41')-Au(2)	115.2(13)
C(51)-P(2)-Au(2)	117.07(18)	C(71)-P(2)-Au(2)	113.04(18)
C(61)-P(2)-Au(2)	109.1(2)	C(42)-S(2)-C(41)	92.8(4)
C(44)-C(41)-S(2)	111.5(8)	C(54)-C(53)-C(52)	121.0(6)
C(42)-S(2')-C(41')	95.2(8)	C(53)-C(54)-C(55)	119.9(6)
C(44')-C(41')-S(2')	101.2(16)	C(54)-C(55)-C(56)	120.0(6)
C(43)-C(42)-S(2)	112.6(5)	C(55)-C(56)-C(51)	120.5(6)
C(43')-C(42)-S(2')	109.7(8)	C(66)-C(61)-C(62)	118.6(7)
C(43')-C(42)-I(2')	124.4(7)	C(66)-C(61)-P(2)	123.5(6)
S(2')-C(42)-I(2')	125.3(4)	C(62)-C(61)-P(2)	117.9(6)
C(43)-C(42)-I(2)	125.1(5)	C(63)-C(62)-C(61)	122.8(10)
S(2)-C(42)-I(2)	122.1(4)	C(62)-C(63)-C(64)	118.1(9)
C(42)-C(43)-C(44)	112.1(10)	C(63)-C(64)-C(65)	120.9(10)
C(41)-C(44)-C(43)	110.9(12)	C(64)-C(65)-C(66)	119.3(11)
C(44')-C(43')-C(42)	106.9(19)	C(61)-C(66)-C(65)	120.2(9)
C(41')-C(44')-C(43')	127(3)	C(76)-C(71)-C(72)	118.4(5)
C(51)-P(2)-C(71)	105.7(3)	C(76)-C(71)-P(2)	118.7(5)
C(51)-P(2)-C(61)	106.5(3)	C(72)-C(71)-P(2)	122.8(4)
C(71)-P(2)-C(61)	104.5(3)	C(73)-C(72)-C(71)	120.2(7)
C(56)-C(51)-C(52)	119.0(6)	C(72)-C(73)-C(74)	121.1(8)
C(56)-C(51)-P(2)	122.2(4)	C(75)-C(74)-C(73)	119.6(7)
C(52)-C(51)-P(2)	118.6(4)	C(74)-C(75)-C(76)	119.9(6)
C(53)-C(52)-C(51)	119.5(6)	C(75)-C(76)-C(71)	120.7(6)

Table SI 10. Anisotropic displacement parameters ($\text{\AA}^2 \times 10^3$). The anisotropic displacement factor exponent takes the form: $-2\pi^2 [h^2 a^{*2} U^{11} + \dots + 2 h k a^* b^* U^{12}]$

	U^{11}	U^{22}	U^{33}	U^{23}	U^{13}	U^{12}
Au(1)	25(1)	29(1)	38(1)	3(1)	0(1)	-5(1)
C(1)	23(2)	27(3)	44(3)	2(2)	-3(2)	-7(2)
S(1)	36(1)	49(1)	34(1)	-1(1)	6(1)	-15(1)
C(2)	22(2)	39(3)	33(3)	-1(2)	-2(2)	-7(2)
C(3)	35(3)	39(3)	29(3)	11(2)	-4(2)	-12(2)

C(4)	37(3)	35(3)	36(3)	-1(2)	-7(2)	-7(2)
I(1)	45(1)	68(1)	41(1)	-12(1)	1(1)	-28(1)
P(1)	24(1)	27(1)	30(1)	1(1)	1(1)	-4(1)
C(11)	23(2)	32(3)	27(2)	2(2)	3(2)	1(2)
C(12)	49(3)	40(3)	36(3)	-2(3)	2(2)	-6(2)
C(13)	72(5)	64(5)	30(3)	-9(3)	-10(3)	-1(3)
C(14)	66(4)	48(4)	26(3)	7(3)	-3(3)	6(3)
C(15)	69(4)	40(4)	41(4)	12(3)	-4(3)	-6(3)
C(16)	60(4)	31(3)	32(3)	4(2)	-8(2)	-9(2)
C(21)	38(3)	36(3)	26(3)	4(2)	-1(2)	-2(2)
C(22)	40(3)	47(3)	36(3)	-4(3)	5(2)	4(2)
C(23)	64(4)	56(4)	46(4)	-7(3)	12(3)	14(3)
C(24)	82(5)	53(4)	40(4)	-17(3)	-7(3)	7(4)
C(25)	66(4)	57(4)	51(4)	-16(3)	-18(3)	-11(3)
C(26)	42(3)	48(4)	35(3)	-9(3)	-5(2)	-4(2)
C(31)	31(2)	28(3)	33(3)	2(2)	-6(2)	-1(2)
C(32)	33(3)	37(3)	45(3)	7(3)	2(2)	0(2)
C(33)	28(3)	53(4)	67(4)	5(3)	-2(3)	3(2)
C(34)	42(3)	44(4)	80(5)	7(4)	-15(3)	13(3)
C(35)	55(4)	52(4)	78(6)	24(4)	-12(4)	7(3)
C(36)	36(3)	45(4)	58(4)	20(3)	-1(3)	0(2)
Au(2)	23(1)	27(1)	87(1)	-13(1)	-6(1)	2(1)
S(2)	27(2)	41(2)	41(2)	-10(1)	-2(1)	7(1)
C(41)	16(4)	25(4)	41(5)	-13(5)	11(4)	5(3)
S(2')	33(2)	44(3)	75(4)	-2(3)	0(2)	6(2)
C(41')	35(8)	31(8)	57(11)	-24(9)	25(8)	-11(6)
C(42)	21(2)	36(3)	58(4)	-1(3)	-3(2)	6(2)
C(43)	46(5)	49(6)	43(6)	-14(5)	4(4)	26(5)
C(44)	53(9)	55(8)	61(10)	0(7)	-13(6)	27(7)
I(2)	29(1)	50(1)	69(1)	-12(1)	-11(1)	18(1)
C(43')	25(7)	53(10)	92(15)	13(10)	-9(7)	9(7)
C(44')	12(8)	26(10)	110(20)	15(14)	-8(11)	-2(7)
I(2')	52(1)	75(1)	123(1)	2(1)	27(1)	28(1)
P(2)	22(1)	25(1)	46(1)	-3(1)	2(1)	1(1)
C(51)	30(2)	36(3)	31(3)	6(2)	0(2)	4(2)
C(52)	35(3)	56(4)	34(3)	6(3)	-3(2)	8(2)
C(53)	49(4)	73(5)	41(4)	3(3)	-11(3)	5(3)
C(54)	50(3)	65(4)	32(3)	-5(3)	0(2)	3(3)
C(55)	42(3)	52(4)	44(4)	-4(3)	4(3)	10(3)
C(56)	30(3)	43(3)	42(3)	-2(3)	-2(2)	5(2)
C(61)	45(3)	36(3)	41(3)	-5(3)	9(2)	-15(2)
C(62)	56(4)	95(7)	46(4)	4(4)	12(3)	3(4)
C(63)	113(8)	127(10)	46(5)	4(6)	26(5)	-42(7)
C(64)	237(16)	89(8)	59(6)	2(6)	26(8)	-99(10)
C(65)	330(20)	35(5)	75(8)	7(5)	40(11)	-14(8)
C(66)	185(12)	40(5)	58(6)	-2(4)	34(6)	-1(6)

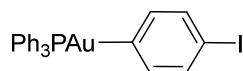
Table SI 11. Anisotropic displacement parameters ($\text{\AA}^2 \times 10^3$). The anisotropic displacement factor exponent takes the form: $-2\pi^2 [h^2 a^{*2} U^{11} + \dots + 2 h k a^* b^* U^{12}]$

	U^{11}	U^{22}	U^{33}	U^{23}	U^{13}	U^{12}
C(71)	25(2)	29(3)	50(3)	1(2)	4(2)	4(2)
C(72)	36(3)	72(5)	88(6)	37(4)	-19(3)	-11(3)
C(73)	52(4)	107(7)	97(7)	41(6)	-41(4)	-18(4)
C(74)	40(4)	67(5)	123(8)	15(5)	-27(4)	-11(3)
C(75)	39(3)	43(4)	72(5)	3(3)	0(3)	-12(3)
C(76)	33(3)	39(3)	49(4)	1(3)	-3(2)	-6(2)

Table SI 12. Hydrogen coordinates ($\times 10^4$) and isotropic displacement parameters ($\text{\AA}^2 \times 10^3$).

	x	y	z	U(eq)
H(3)	12524	26691	-4517	41
H(4)	11080	25345	-4723	43
H(12)	8110	23718	-1088	50
H(13)	7964	22963	374	66
H(14)	7448	21293	523	56
H(15)	7039	20404	-777	60
H(16)	7114	21170	-2234	49
H(22)	9543	22319	-4098	50
H(23)	9676	21101	-5241	68
H(24)	7984	20278	-5617	70
H(25)	6117	20653	-4847	69
H(26)	5955	21848	-3678	50
H(32)	5249	22839	-1988	47
H(33)	3471	23699	-1957	59
H(34)	3302	25027	-2929	66
H(35)	4967	25555	-3916	73
H(36)	6784	24756	-3912	56
H(43)	12405	21870	-620	56
H(44)	14126	20686	-660	67
H(43')	12033	21877	-3405	68
H(44')	13679	20869	-3827	58
H(52)	15433	17993	-4108	50
H(53)	15706	17056	-5456	65
H(54)	17509	16293	-5875	59
H(55)	19047	16408	-4915	56
H(56)	18792	17324	-3554	46
H(62)	15441	18335	-857	81
H(63)	15000	17266	358	118
H(64)	15580	15645	182	159

H(65)	16626	15125	-1193	182
H(66)	17064	16241	-2407	117
H(72)	18361	17990	-1123	77
H(73)	20138	18689	-757	100
H(74)	21134	19867	-1722	90
H(75)	20280	20426	-3023	62
H(76)	18451	19775	-3373	49

(5-Iodophenyl-2-yl)(triphenylphosphine)gold (39)**Table SI 13.** Crystal data and structure refinement

Empirical formula	C ₂₄ H ₁₉ AuIP	
Formula weight	662.23	
Temperature	200(2) K	
Wavelength	0.71073 Å	
Crystal system	Triclinic	
Space group	P-1	
Unit cell dimensions	a = 9.2321(19) Å	α = 75.90(3)°.
	b = 9.806(2) Å	β = 71.33(3)°.
	c = 12.743(3) Å	γ = 86.17(3)°.
Volume	1059.9(4) Å ³	
Z	2	
Density (calculated)	2.075 Mg/m ³	
Absorption coefficient	8.478 mm ⁻¹	
F(000)	620	
Crystal size	0.07 x 0.10 x 0.13 mm ³	
Theta range for data collection	1.735 to 29.003°.	
Index ranges	-12 ≤ h ≤ 12, -13 ≤ k ≤ 13, -17 ≤ l ≤ 17	
Reflections collected	18656	
Independent reflections	5641 [R(int) = 0.0293]	
Completeness to theta = 25.242°	100.0 %	
Refinement method	Full-matrix least-squares on F ²	
Data / restraints / parameters	5641 / 0 / 245	
Goodness-of-fit on F ²	1.027	
Final R indices [I > 2σ(I)]	R1 = 0.0257, wR2 = 0.0580	
R indices (all data)	R1 = 0.0325, wR2 = 0.0597	
Extinction coefficient	0.0018(2)	
Largest diff. peak and hole	0.967 and -0.961 e.Å ⁻³	

Comments:

All non-hydrogen atoms were refined anisotropic. The C-H atoms were positioned with idealized geometry and refined using a riding model. A numerical absorption correction was performed (Tmin/max: 0.2401/0.3412).

Table SI 14. Atomic coordinates ($\times 10^4$) and equivalent isotropic displacement parameters ($\text{\AA}^2 \times 10^3$).
 $U(\text{eq})$ is defined as one third of the trace of the orthogonalized U^{ij} tensor.

	x	y	z	U(eq)
Au(1)	3617(1)	2110(1)	5286(1)	32(1)
C(1)	3322(4)	796(4)	6854(3)	33(1)
C(2)	1874(4)	281(4)	7556(3)	38(1)
C(3)	1585(4)	-481(4)	8676(3)	38(1)
C(4)	2783(4)	-760(4)	9120(3)	33(1)
C(5)	4244(4)	-282(4)	8464(3)	40(1)
C(6)	4500(4)	491(4)	7337(3)	39(1)
I(1)	2393(1)	-1952(1)	10795(1)	45(1)
P(1)	3800(1)	3745(1)	3623(1)	30(1)
C(11)	3201(4)	3141(4)	2582(3)	33(1)
C(12)	3518(5)	3938(4)	1475(3)	40(1)
C(13)	3051(5)	3470(5)	689(4)	48(1)
C(14)	2274(5)	2205(5)	1014(4)	50(1)
C(15)	1938(5)	1415(5)	2113(4)	49(1)
C(16)	2397(4)	1879(4)	2911(4)	38(1)
C(21)	2607(4)	5263(4)	3897(3)	31(1)
C(22)	2903(4)	6038(4)	4589(3)	39(1)
C(23)	1997(5)	7171(5)	4836(4)	48(1)
C(24)	759(5)	7499(4)	4431(4)	46(1)
C(25)	432(5)	6707(5)	3778(3)	42(1)
C(26)	1361(4)	5585(4)	3506(3)	34(1)
C(31)	5741(4)	4408(4)	2834(3)	31(1)
C(32)	6837(4)	3409(4)	2551(4)	43(1)
C(33)	8344(5)	3820(5)	1954(4)	51(1)
C(34)	8764(4)	5214(5)	1671(4)	44(1)
C(35)	7687(5)	6210(5)	1958(4)	43(1)
C(36)	6165(4)	5819(4)	2535(3)	36(1)

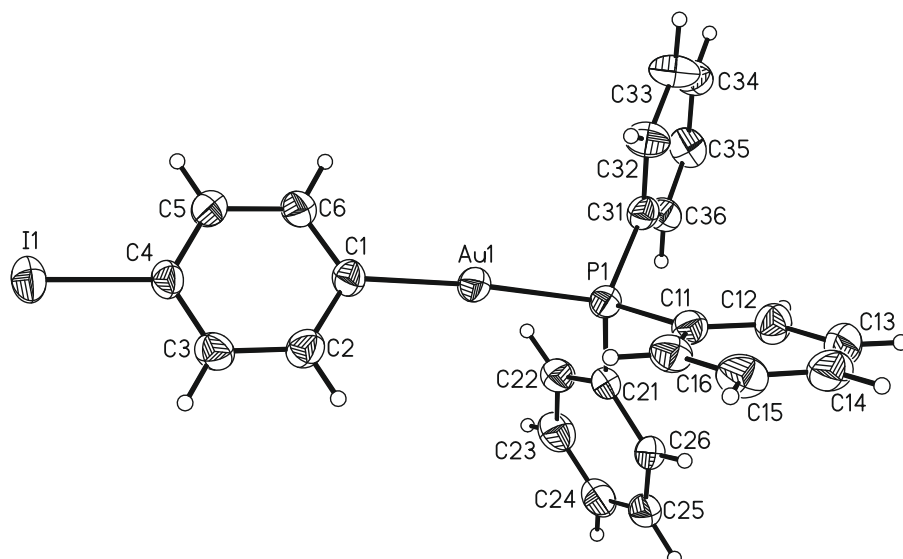


Table SI 15. Bond lengths [Å] and angles [°].

Au(1)-C(1)	2.043(4)	Au(1)-P(1)	2.2888(12)
C(1)-Au(1)-P(1)	174.16(10)	C(2)-C(1)-Au(1)	120.9(3)
C(11)-P(1)-Au(1)	115.51(13)	C(6)-C(1)-Au(1)	122.6(3)
C(31)-P(1)-Au(1)	113.69(12)	C(21)-P(1)-Au(1)	110.91(12)
C(1)-C(2)	1.395(5)	C(14)-C(15)	1.373(7)
C(1)-C(6)	1.395(5)	C(15)-C(16)	1.396(6)
C(2)-C(3)	1.390(6)	C(21)-C(26)	1.384(5)
C(3)-C(4)	1.380(5)	C(21)-C(22)	1.392(5)
C(4)-C(5)	1.382(5)	C(22)-C(23)	1.383(6)
C(4)-I(1)	2.098(4)	C(23)-C(24)	1.386(7)
C(5)-C(6)	1.404(6)	C(24)-C(25)	1.376(6)
P(1)-C(11)	1.820(4)	C(25)-C(26)	1.391(5)
P(1)-C(31)	1.824(4)	C(31)-C(32)	1.386(5)
P(1)-C(21)	1.828(4)	C(31)-C(36)	1.391(5)
C(11)-C(12)	1.384(6)	C(32)-C(33)	1.387(6)
C(11)-C(16)	1.389(5)	C(33)-C(34)	1.374(6)
C(12)-C(13)	1.387(5)	C(34)-C(35)	1.374(6)
C(13)-C(14)	1.380(7)	C(35)-C(36)	1.392(6)
C(2)-C(1)-C(6)	116.1(3)	C(11)-C(16)-C(15)	119.5(4)
C(3)-C(2)-C(1)	123.1(3)	C(26)-C(21)-C(22)	119.9(3)
C(4)-C(3)-C(2)	118.9(3)	C(26)-C(21)-P(1)	121.4(3)
C(3)-C(4)-C(5)	120.6(3)	C(22)-C(21)-P(1)	118.5(3)
C(3)-C(4)-I(1)	119.8(3)	C(23)-C(22)-C(21)	119.9(4)
C(5)-C(4)-I(1)	119.7(3)	C(22)-C(23)-C(24)	119.9(4)
C(4)-C(5)-C(6)	119.3(4)	C(25)-C(24)-C(23)	120.4(4)
C(1)-C(6)-C(5)	122.0(3)	C(24)-C(25)-C(26)	120.0(4)
C(11)-P(1)-C(31)	103.69(16)	C(21)-C(26)-C(25)	119.9(4)
C(11)-P(1)-C(21)	105.18(16)	C(32)-C(31)-C(36)	119.6(3)

C(31)-P(1)-C(21)	107.10(16)	C(32)-C(31)-P(1)	116.2(3)
C(12)-C(11)-C(16)	119.9(3)	C(36)-C(31)-P(1)	124.1(3)
C(12)-C(11)-P(1)	120.6(3)	C(31)-C(32)-C(33)	120.1(4)
C(16)-C(11)-P(1)	119.4(3)	C(34)-C(33)-C(32)	120.2(4)
C(11)-C(12)-C(13)	120.2(4)	C(33)-C(34)-C(35)	120.1(4)
C(14)-C(13)-C(12)	119.8(4)	C(34)-C(35)-C(36)	120.4(4)
C(15)-C(14)-C(13)	120.5(4)	C(31)-C(36)-C(35)	119.5(4)
C(14)-C(15)-C(16)	120.1(4)		

Table SI 16. Anisotropic displacement parameters ($\text{\AA}^2 \times 10^3$). The anisotropic displacement factor exponent takes the form: $-2\pi^2 [h^2 a^{*2} U^{11} + \dots + 2 h k a^* b^* U^{12}]$

	U^{11}	U^{22}	U^{33}	U^{23}	U^{13}	U^{12}
Au(1)	32(1)	31(1)	31(1)	-2(1)	-10(1)	1(1)
C(1)	36(2)	28(2)	30(2)	0(1)	-8(1)	2(1)
C(2)	36(2)	36(2)	41(2)	-2(2)	-16(2)	-4(2)
C(3)	32(2)	34(2)	40(2)	-3(2)	-6(2)	-5(1)
C(4)	38(2)	28(2)	28(2)	-2(1)	-8(1)	1(1)
C(5)	33(2)	45(2)	38(2)	0(2)	-13(2)	1(2)
C(6)	32(2)	40(2)	35(2)	1(2)	-5(2)	0(2)
I(1)	52(1)	42(1)	33(1)	0(1)	-10(1)	-3(1)
P(1)	30(1)	30(1)	29(1)	-5(1)	-10(1)	1(1)
C(11)	30(2)	35(2)	34(2)	-10(2)	-11(1)	1(1)
C(12)	41(2)	44(2)	37(2)	-9(2)	-15(2)	-5(2)
C(13)	43(2)	67(3)	38(2)	-15(2)	-16(2)	-4(2)
C(14)	39(2)	69(3)	54(3)	-31(2)	-20(2)	3(2)
C(15)	38(2)	52(2)	60(3)	-22(2)	-12(2)	-10(2)
C(16)	32(2)	40(2)	42(2)	-13(2)	-9(2)	-2(2)
C(21)	28(2)	37(2)	24(2)	-4(1)	-5(1)	0(1)
C(22)	36(2)	45(2)	36(2)	-14(2)	-10(2)	4(2)
C(23)	52(2)	47(2)	43(2)	-19(2)	-8(2)	5(2)
C(24)	49(2)	39(2)	35(2)	-3(2)	-2(2)	9(2)
C(25)	35(2)	49(2)	32(2)	-1(2)	-7(2)	7(2)
C(26)	32(2)	38(2)	28(2)	-1(1)	-9(1)	2(1)
C(31)	32(2)	33(2)	31(2)	-8(1)	-14(1)	-1(1)
C(32)	34(2)	38(2)	55(2)	-15(2)	-9(2)	-1(2)
C(33)	31(2)	50(2)	71(3)	-24(2)	-10(2)	7(2)
C(34)	31(2)	56(2)	46(2)	-15(2)	-10(2)	-7(2)
C(35)	45(2)	42(2)	41(2)	-13(2)	-9(2)	-10(2)
C(36)	35(2)	37(2)	36(2)	-12(2)	-8(2)	0(1)

Table SI 17. Hydrogen coordinates ($\times 10^4$) and isotropic displacement parameters ($\text{\AA}^2 \times 10^{-3}$).

	x	y	z	U(eq)
H(2)	1046	460	7252	45
H(3)	579	-806	9128	45
H(5)	5066	-474	8773	48
H(6)	5507	817	6889	47
H(12)	4057	4807	1253	48
H(13)	3266	4020	-70	57
H(14)	1970	1878	472	60
H(15)	1392	550	2331	58
H(16)	2161	1336	3673	46
H(22)	3727	5789	4890	46
H(23)	2221	7724	5283	57
H(24)	134	8274	4605	55
H(25)	-427	6926	3514	50
H(26)	1140	5041	3051	41
H(32)	6557	2442	2766	51
H(33)	9087	3137	1741	61
H(34)	9801	5488	1275	53
H(35)	7985	7172	1762	51
H(36)	5420	6512	2723	44

5.2.2 Further Experimental Data on Chapter 3.2

For general methods and materials see beginning of this chapter 5.2. **70** was purchased from ABCR with an purity of 99.5%, **75** was purchased from ABCR with an purity of 98%.

GC Optimization Reactions

The yields for the optimization reactions were determined by GC by a multiple point internal standard method, using 1,3,5-triisopropylbenzene as a standard. The following equation was used for the calculation of the yields:

$$n(\text{analyte}) = \frac{A(\text{analyte})}{A(\text{standard})} \times \frac{n(\text{standard})}{RF}$$

where n is the amount of substance, A the integrated area and RF a system specific response factor.

For the calibration curve, known amounts of the analyte and 1,3,5-triisopropylbenzene were used. The response factor RF was obtained from the slope of the resulting calibration curve (Figures SI 1, SI 2 and SI 3).

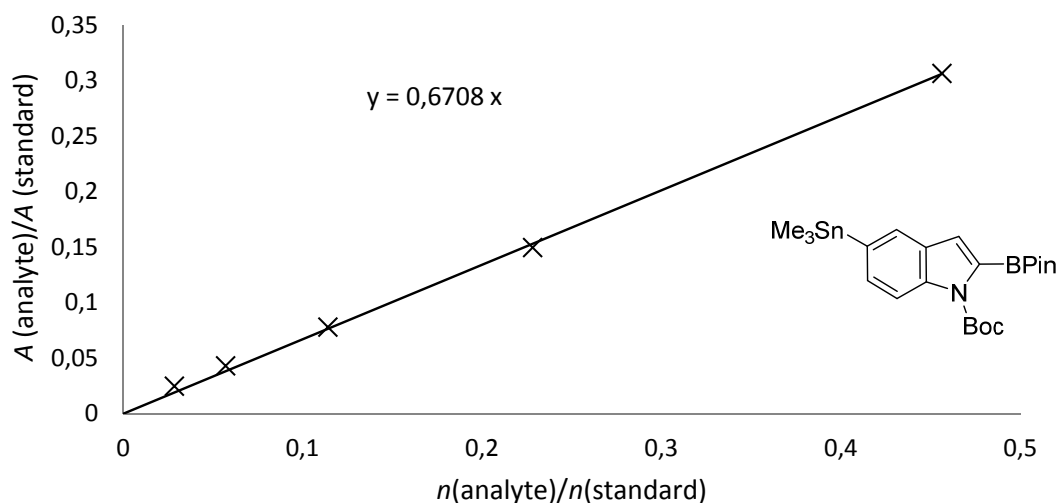


Figure SI 1. Calibration curve for *tert*-butyl-5-trimethylstannyl-2-(4,4,5,5-tetramethyl-1,3,2-dioxaborolan-2-yl)-1*H*-indole-1-carboxylate **M1-25** using 1,3,5-triisopropylbenzene as internal standard.

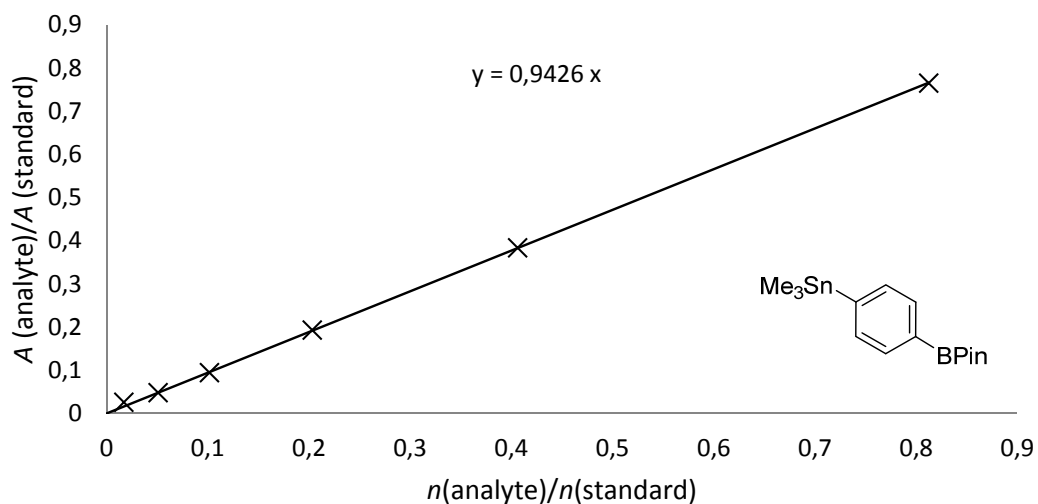


Figure SI 2. Calibration curve for 2-(4-(trimethylstannyl)phenyl)-4,4,5,5-tetramethyl-1,3,2-dioxaborolane **M1-24** using 1,3,5-triisopropylbenzene as internal standard.

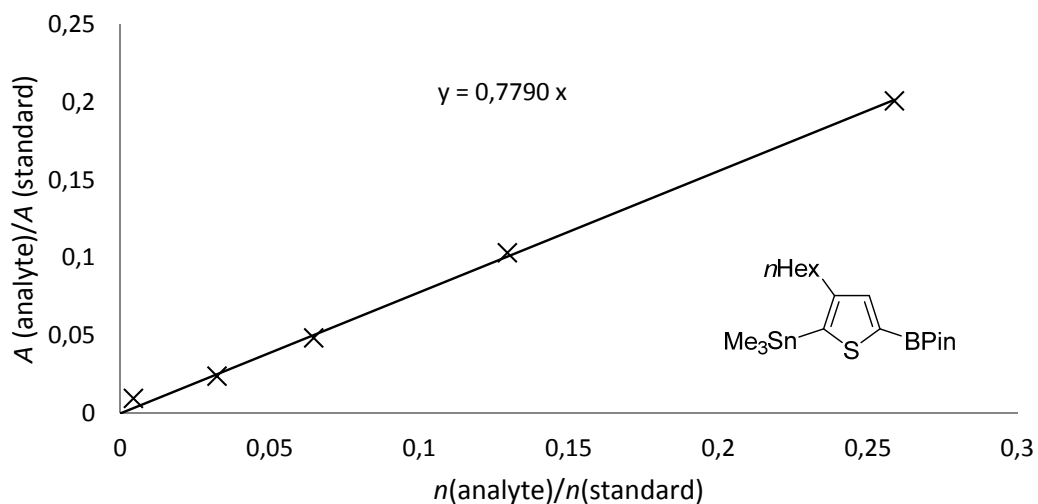
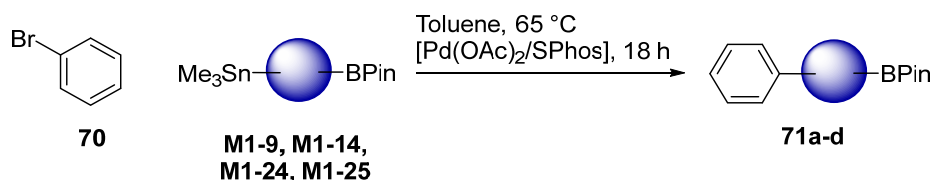


Figure SI 3. Calibration curve for 2-(4-(trimethylstannyl)-3-n-hexyl-thiophene)-4,4,5,5-tetramethyl-1,3,2-dioxaborolane **M1-9** using 1,3,5-triisopropylbenzene as internal standard.

General Procedures

These procedures were used for the attempts to perform cross-coupling reactions with the additional synthesized aromatic dinucleophiles.

General Procedure 1 (for CCR after *Org. Lett.* **2012**)



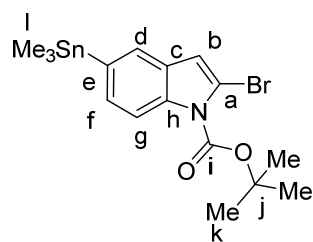
A solution of the organotin/organoboron containing species (1.00 mmol), bromobenzene (162 mg, 1.00 mmol), [Pd(OAc)₂] (2.3 mg, 0.01 mmol, 1 mol%) and SPhos (8.2 mg, 0.020 mmol, 2 mol%) in toluene (8 mL) was heated to 65 °C for 18 h. The reaction mixture was cooled to 20 °C, filtered through a short plug of silica (5 x 2 cm; eluent: ethyl acetate) and the volatiles were removed *in vacuo* and a crude ¹H NMR spectrum was taken.

Table SI 4. Results of the coupling reactions after general procedure 1.

Entry	Starting Material	Reaction time	Yield
1	 M1-9	18 h	83 % ^a
2	 M1-14	18 h	-
3	 M1-22	18 h	-
4	 M1-23	18 h	-

^aTo compare the reactions, this experiment is already reported in *Org. Lett.* **2012**.^[4b] The yield was isolated in this case, the conversion was not controlled by GC.

In one case, when the indole derivative was used as starting, a pure compound could be isolated:

2-Bromo-5-(trimethylstannyl)-1H-indole (74)

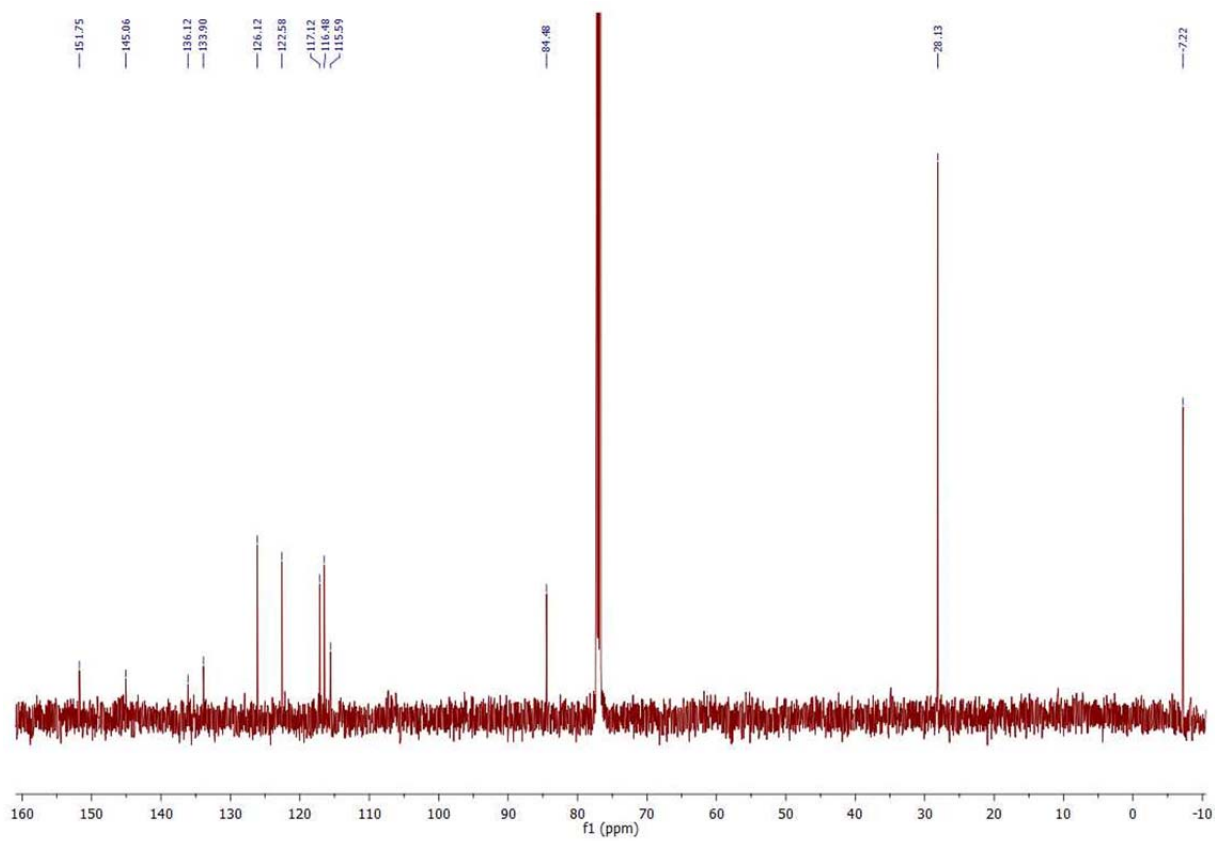
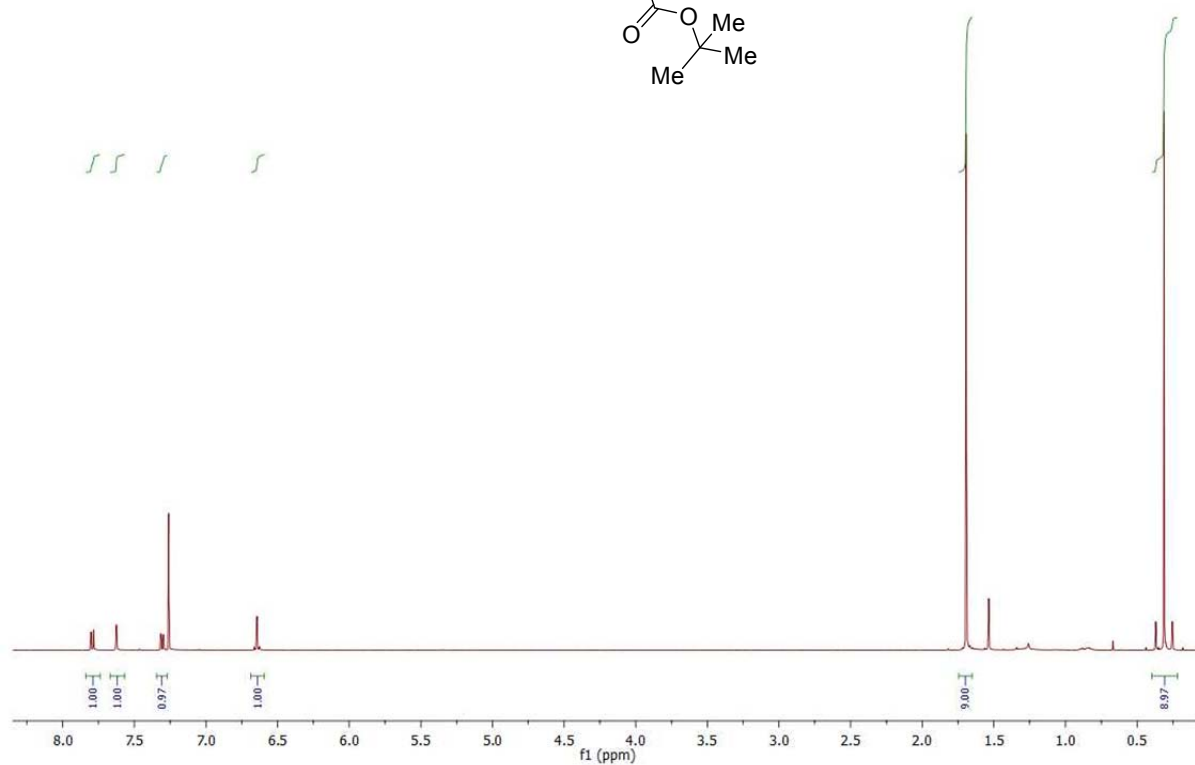
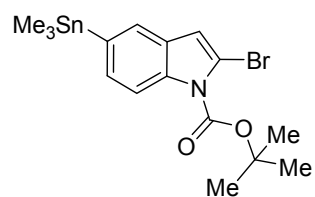
The reaction was performed following the general procedure 1. The crude product was purified by column chromatography (*n*-hexane, $R_f = 0.2$). One fraction gave the pure compound **74**, which must have been formed during the reaction.

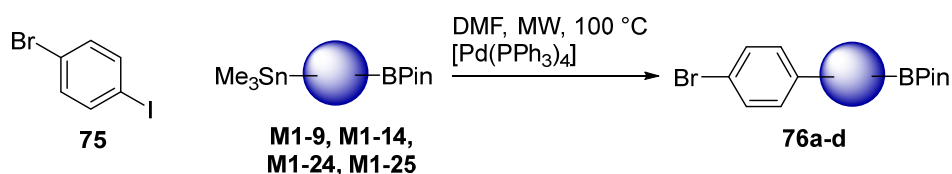
¹H NMR (500 MHz, CDCl₃): $\delta = 7.79$ (d, 1H, $^3J = 8.8$ Hz, Ind-*H*-g), 7.63 (d, 1H, $^4J = 2.0$ Hz, Ind-*H*-d), 7.31 (dd, 1H, $^3J = 8.8$, $^4J = 1.8$ Hz, Ind-*H*-f), 6.64 (d, 1H, $^4J = 0.7$ Hz, Ind-*H*-b), 1.69 (s, 9H, k), 0.31 (s, 9H, l) ppm.

¹³C NMR (126 MHz, CDCl₃): $\delta = 151.8$ (i), 145.1 (Ind-*C*-a) 136.1 (Ind-*C*-e), 133.9 (Ind-*C*-c), 126.1 (Ind-*CH*-f), 122.6 (Ind-*CH*-d), 117.31 (Ind-*CH*-g), 115.6 (Ind-*C*-h), 114.7 (Ind-*CH*-b), 84.5 (j), 28.1 (k), -7.2 (l) ppm.

¹¹⁹Sn NMR (187 MHz, CDCl₃): $\delta = -48.4$ ppm.

HRMS (EI⁺): *m/z* found 458.9848 (5) [M]⁺; calcd. for C₁₆H₂₂BrNO₂Sn 458.9856; found: 443.98(10) [M-CH₃]⁺; found: 387.91 (100) [M-C₄H₉O]⁺.

2-Bromo-5-(trimethylstannyl)-1H-indole (74)

General Procedure 2 (for CCR after *Org. Lett.* **2013**)

A solution of the organotin/organoboron containing species (1.00 mmol), 1-iodo-4-bromobenzene (314 mg, 1.00 mmol), $[\text{Pd}(\text{PPh}_3)_4]$ (4.5 mg, 0.010 mmol, 1 mol%) and the internal standard 1,3,5-triisopropylbenzene (100 μL , 86.0 mg, 0.430 mmol) were dissolved in DMF (4 mL) and the reaction mixture was heated to 100 $^\circ\text{C}$ for the specified reaction time. After certain time intervals, a sample (0.1 mL) was taken from each reaction vessel, filtered through a short plug of silica (5 x 3 mm; eluent: ethyl acetate) using a syringe filter (pore size 0.45 μm), and was then used for GC analysis. The reaction mixture was cooled to 20 $^\circ\text{C}$, filtered through a short plug of silica (5 x 2 cm; eluent: ethyl acetate) and the volatiles were removed *in vacuo*.

Table SI 5. Results of the coupling reactions after general procedure 2.

Entry	Starting Material	Reaction time	Conversion (GC)	Yield
1	 M1-9	60 min	>84%	84 % ^a
2	 M1-14	1 h	13 %	-
3	 M1-14	4 h	27%	-
4	 M1-22	1 h	31 %	-
5	 M1-22	17 h	100 %	-
6	 M1-23	90 min	100 %	-

^aTo compare the reactions, this experiment is already reported in *Org. Lett.* **2013**. The yield was isolated in this case, the conversion was not controlled by GC.

5.3 Supporting Information for Chapter 3.3

5.3.1 Supporting Information for the Manuscript *Gold-Functionalized Thiophene-Type Monomers in Polymerization Reactions*

Supporting Information

For

Gold-Functionalized Thiophene-Type Monomers in Polymerization Reactions

*Annika C. J. Heinrich, Paul J. Gates, Christian Näther and Anne Staubitz**

Abbreviations

General Methods and Materials

GC Optimization Reactions

Syntheses

Polymerization Kinetic Studies

¹H NMR Spectra and ¹³C{¹H} NMR Spectra

2-Bromo-3-*n*-hexyl-5-(triphenylphosphin)gold(I)-thiophene (**4**)

Abbreviations

A	area
ATR	attenuated total reflectance
calcd.	calculated
CI	chemical ionization
COSY	correlated spectroscopy
d	doublet (NMR)
DCM	dichloromethane
dd	doublet of doublets (NMR)
Decomp. temp.	decomposition temperature
DMF	<i>N,N</i> -dimethylformamide
dppe	1,2-bis(diphenylphosphino)ethane
dppf	1,1'-bis(diphenylphosphino)ferrocene
EI	electron ionization
GC	gas chromatography
GC-MS	gas chromatography-mass spectrometry
HMBC	heteronuclear multiple bond coherence
HSQC	heteronuclear single quantum coherence
IR	infrared
m	medium (concerning the intensity) (IR)
M_n	number average molecular weight
M.p.	melting point
MS	mass spectrometry
M_w	weight average molecular weight
MW	microwave
N	amount of substance
PDI	polydispersity index
Phe	benzene scaffold
PS	polystyrene
Pin	pinacol
R_f	response factor
s	strong (concerning the intensity) (IR)
s	singlet (NMR)
t	triplet (NMR)
THF	tetrahydrofuran
TMEDA	tetramethylethylenediamine
TMS	tetramethylsilane
TOF	time of flight
Tph	thiophene scaffold
w	weak (concerning the intensity) (IR)

General Methods and Materials

All syntheses were carried out using standard Schlenk techniques or in a glovebox under a dry and inert nitrogen atmosphere. In the cases in which argon was used or the reaction was not performed under inert reaction conditions, this is noted specifically in the procedure. Glassware and NMR-tubes were dried in an oven at 200 °C for at least 2 h before use. Reaction vessels were heated under vacuum and purged with nitrogen three times before adding reagents.

Analyses

^1H NMR, ^{13}C NMR, ^{11}B NMR, ^{31}P NMR and ^{119}Sn NMR spectra were recorded at 300 K.

^1H NMR spectra were recorded on a Bruker DRX 500 (500 MHz) spectrometer or a Bruker Avance 600 spectrometer. $^{13}\text{C}\{^1\text{H}\}$ NMR spectra were recorded on a Bruker DRX 500 (126 MHz) spectrometer or a Bruker Avance 600 spectrometer. ^{11}B NMR, ^{31}P NMR and ^{119}Sn NMR spectra were recorded on a Bruker DRX 500 (160 MHz, 202 MHz and 187 MHz) spectrometer.

^1H NMR and $^{13}\text{C}\{^1\text{H}\}$ NMR spectra were referenced against the solvent residual proton signals (^1H) or the solvent itself (^{13}C). ^{11}B NMR spectra were referenced against $\text{BF}_3\cdot\text{OEt}_2$ in CDCl_3 , the reference of the ^{119}Sn NMR spectra was calculated based on the ^1H NMR signal of TMS.

The exact assignment of the peaks was proved by ^1H , ^{13}C DEPT and two-dimensional NMR spectroscopy such as ^1H COSY, ^{13}C HSQC or $^1\text{H}/^{13}\text{C}$ HMBC when possible.

All melting points were recorded on an electrothermal melting point apparatus LG 1586 and are uncorrected.

IR spectra were recorded on a Perkin Elmer Paragon 1000 FT-IR spectrometer with a A531-G Golden-Gate-ATR-unit.

UV/Vis spectra were recorded on a Perkin Elmer Lambda14 spectrometer.

Ultra High resolution ESI mass spectra were recorded on a Bruker Daltonics Apex IV Fourier Transform Ion Cyclotron resonance mass spectrometer or on a Bruker Daltonics micrOTOF II mass spectrometer. The high resolution EI mass spectra were run on a VG Analytical Autospec apparatus or a Jeol AccuTOF JMS-T100GCV mass spectrometer.

The MALDI-TOF-TOF mass spectra were recorded on a Applied Biosystems 4700 Proteomics analyzer spectrometer and a dithranol matrix in methanol. The polymer was dissolved in THF.

GC-MS analysis was performed on a Hewlett Packard 5890A gas chromatograph, equipped with a Hewlett Packard 5972A mass selective detector and an Agilent Technologies poly(dimethylsiloxane) column (19091S-931E, nominal length 15 m, 0.25 mm diameter, 0.25 μm grain size).

GC analysis was performed on an Agilent Technologies 6890N gas chromatograph, equipped with an Agilent Technologies 7683 Series Injector, an Agilent Technologies (5 %-phenyl)-poly(methylsiloxane) column (19091J-413, nominal length 30 m, 0.32 mm diameter, 0.25 μm grain size) and a flame ionization detector (FID).

M_n and M_w were determined on a Viscotec GPCmax VE2001, equipped with a Viscotec VE3580 RI detector (columns: Viscotec LT50000L 300 x 7.8 mm and LT4000L 300 x 7.8 mm).

All microwave irradiation reactions were carried out on a Biotage[®] Initiator+ SP Wave synthesis system, with continuous irradiation power from 0 to 300 W. All reactions were carried out in 5 mL oven-dried Biotage microwave vials sealed with an aluminum/Teflon[®] crimp top, which can be exposed to a maximum of 250 °C and 20 bar internal pressure. The reaction temperature was measured by an external IR sensor.

The single crystal data were measured using an Imaging Plate Diffraction System (IPDS-1) from STOE & CIE and were corrected for absorption using X-Red and X-Shape from STOE & CIE (Min/max. transmission: 0.4839/0.7604). The structure was solved with direct methods using SHELXS-97 and refinement was performed against F^2 using SHELXL-97.

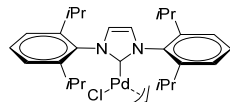
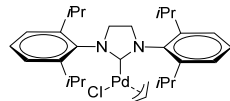
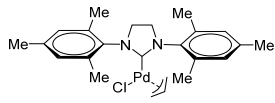
Chemicals

All reagents were used without further purification unless noted otherwise. The preparation of *i*PrO-BPin (2-isopropoxy-4,4,5,5-tetramethyl-1,3,2-dioxaborolane, **P1-36**) and 2-bromo-3-*n*-hexylthiophene (**3**, **P1-40**), 2-bromo-3-*n*-hexyl-5-iodothiophene (**12**, **P1-3**) was described in the supporting information of *Org. Lett.* **2013**, *15*, 4666 (see chapter 5.1). 3-*n*-Hexylthiophene was either bought (see following table) or prepared, starting with thiophene, which is described in the supporting information of *Org. Lett.* **2013**, *15*, 4666 (see

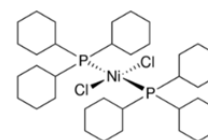
chapter 5.1). Dimethylsulfide gold(I) chloride (**M1-31**) was prepared as described in Chapter 5.2.

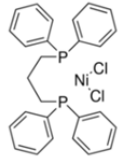
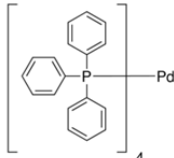
Name	Supplier	Purity	Comment
Acetic acid	Merck Inc.	99.8 %	anhydrous
Ammonium chloride	Grüssing Inc.	99.5 %	
Glacial acetic acid	Grüssing	99 %	
Gold	Degussa Inc.	99.9 %	
2-Iodothiophene	Acros Inc.	98 %	
3- <i>n</i> -Hexylthiophene	Sigma Aldrich Inc.	>99 %	
Hydrochloric acid	Grüssing Inc.	37 %	
Magnesium sulfate	Grüssing Inc.	99 %	
Nitric acid	Grüssing Inc.	68 %	
<i>N</i> -Bromosuccinimide	Alfa Aesar Inc.	99 %	
<i>N</i> -Iodosuccinimide	Molekula	95 %	
<i>n</i> -Butyllithium	Acros Inc.		2.5 M in hexanes
Pinacol	ABCR Inc.	99 %	
Sodium	Merck Inc.	≥ 99 %	
Sodium chloride	Grüssing Inc.	99.5 %	
Sodium hydroxide	Grüssing Inc.	99.5 %	
Sodium hydrogen carbonate	Grüssing Inc.	99 %	
Thiophene	VWR Inc.	99 %	distilled
Triisopropyl borate	Strem Chemicals Inc.	>98 %	
Trimethyltin chloride	Acros Inc.	99 %	
Triphenylphosphine	Alfa Aesar Inc.	99 %	
(Triphenylphosphin)gold(I)-bromide	Alfa Aesar Inc.	99.99%	(metals basis)

Catalyst species

Name	Abbreviation	Supplier (CAS-No)	Formula
Allylchloro[1,3-bis(2,6-diisopropyl-phenyl)imidazol-2-ylidene]palladium(II)	[(<i>i</i> Pr)Pd(allyl)Cl]	Umicore Inc. (478980-03-9)	
Allylchloro[1,3-bis-(2,6-diisopropyl-phenyl)imidazol-2-idinylidene]palladium(II)	[(<i>Si</i> Pr)Pd(allyl)Cl]	Umicore Inc. (478980-01-7)	
Allylchloro[1,3-bis-(2,4,6-trimethylphenyl)imidazol-2-ylidene]palladium(II)	[(<i>i</i> Mes)Pd(allyl)Cl]	Umicore Inc. (478980-04-0)	

1,1'-Bis(diphenylphosphino)-ferrocene]dichloropalladium(II), complex with dichloromethane	[Pd(dppf)Cl ₂ ·CH ₂ Cl ₂]	Sigma Aldrich Inc. (379670)
[1,3-Bis(2,4,6-trimethylphenyl)-2-imidazolidinylidene][1,3-divinyl-1,1,3,3-tetramethyldisiloxane]palladium(0)	[(<i>S</i> iMes)Pd(vs)]	Umicore Inc. (1004291-85-3)
[1,3-Bis(2,4,6-trimethylphenyl)imidazol-2-ylidene][1,3-divinyl-1,1,3,3-tetramethyldisiloxane]palladium(0)	[(<i>i</i> Mes)Pd(vs)]	Umicore Inc. (441018-46-8)
Bis(1,4-naphthoquinone)bis[1,3-bis(2,6-diisopropylphenyl)-imidazole-2-ylidene]-dipalladium(0)	[[(<i>i</i> Pr)Pd(NQ)] ₂]	Umicore Inc. (649736-75-4)
Bis(1,4-naphthoquinone)bis[1,3-bis(2,4,6-trimethylphenyl)imidazol-2-ylidene]dipalladium(0)	[[(<i>i</i> Mes)Pd(NQ)] ₂]	Umicore Inc. (467220-49-1)
Bis(tri- <i>tert</i> -butylphosphine)palladium(0)	[Pd(P <i>t</i> Bu ₃) ₂]	Sigma Aldrich Inc. (53199-31-8)
Bis(di- <i>tert</i> -butylphenylphosphine)palladium(0)	[Pd(P <i>t</i> Bu ₂ Ph) ₂]	Alfa Aesar Inc. (52359-17-8)
Bis(tricyclohexylphosphine)-nickel(II) dichloride	[Ni(PCy ₃) ₂ Cl ₂]	Sigma Aldrich Inc. (19999-87-2)
Chlorophenylallyl[1,3-bis(2,6-diisopropylphenyl)-2-imidazolidinylidene]palladium(II)	[(<i>S</i> iPr)Pd(cinnamyl)Cl]	Umicore Inc. (884879-24-7)



Dichloro(di- μ -chloro)bis[1,3-bis(2,6-diisopropylphenyl)imidazol-2-ylidene]-dipalladium(II)	$[[(\textit{iPr})\text{PdCl}_2]_2]$	Umicore Inc. (444910-17-2)	
(1,3-Divinyl-1,1,3,3-tetramethyldisiloxane)[1,1'-bis(diisopropylphosphino)ferrocene]palladium(0) toluene solution	$[\text{Pd}(\text{dippf})(\text{vs})\text{tol}]$	Umicore Inc. (252062-59-2)	
[1,3-Bis(diphenylphosphino)propane]dichloronickel(II)	$[\text{Ni}(\text{dppp})\text{Cl}_2]$	Sigma Aldrich Inc. (15629-92-2)	
Tetrakis-(triphenylphosphin)palladium(0)	$[\text{Pd}(\text{PPh}_3)_4]$	Sigma Aldrich Inc. (14221-01-3)	

Chromatography

For the chromatographic purification, silica gel (Macherey-Nagel Inc., grain size 0.040 - 0.063 mm) was used. Thin layer chromatography was performed using pre-coated plates from Macherey-Nagel Inc., ALUGRAM[®] Xtra SIL G/UV254. Most chromatography purifications were carried out using an Interchim Puriflash[®] 430 system, where cartridges of Interchim (silica HC, grain size 50 μm , 120 g or 80 g) were used.

Solvents

All solvents were used freshly distilled after refluxing for several hours over the specified drying agent under nitrogen and were stored in a J. Young's-tube. If no drying agent is noted, the solvents were only distilled for purification purposes.

Solvent	Comment
Acetic acid	Grüssig Inc.
CDCl ₃	Deutero Inc.
Chloroform	VWR Inc., HPLC grade
Dichloromethane	BCD Inc.
Diethyl ether	BDC Inc.
DME	Acros Inc., Sodium with benzophenone as an indicator; stored over 3 Å molecular sieves
DMF	Acros Inc., CaH ₂ ; stored over 3 Å molecular sieves
Ethyl acetate	BCD Inc.
Methanol	Baker Inc., HPLC grade
<i>n</i> -Hexane	Walter CMP Inc., sodium with benzophenone as an indicator; degassed by freeze-pump-thaw technique, stored over 3 Å molecular sieves
<i>n</i> -Pentane	Walter CMP Inc., lithium aluminium hydride; degassed by freeze-pump-thaw technique, stored over 3 Å molecular sieves
THF	Sigma Aldrich Inc., CaH ₂ with triphenylmethane as an indicator; degassed by freeze-pump-thaw technique, stored over 3 Å molecular sieves
Toluene	BCD Inc., sodium with benzophenone as an indicator; degassed by freeze-pump-thaw technique, stored over 3 Å molecular sieves

GC-Optimization Reactions

The yields for the optimization reactions were determined by GC by a multiple point internal standard method, using 1,3,5-triisopropylbenzene as a standard. The following equation was used for the calculation of the yields:

$$n(\text{analyte}) = \frac{A(\text{analyte})}{A(\text{standard})} \times \frac{n(\text{standard})}{RF}$$

where n is the amount of substance, A the integrated area and RF a system specific response factor.

For the calibration curve, known amounts of the analyte and 1,3,5-triisopropylbenzene were used. The response factor RF was obtained from the slope of the resulting calibration curve (Figures SI 1 and SI2).

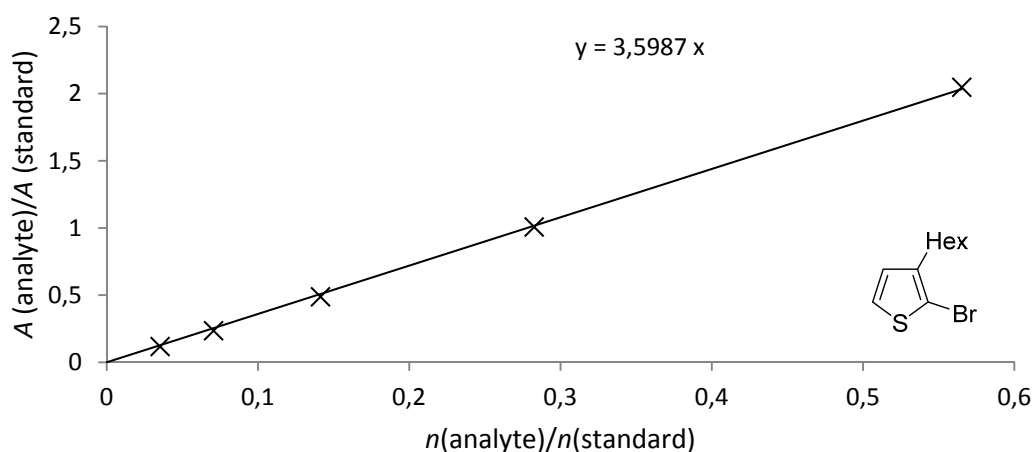


Figure SI 1. Calibration curve for 2-bromo-3-*n*-hexylthiophene (X), using 1,3,5-triisopropylbenzene as internal standard.

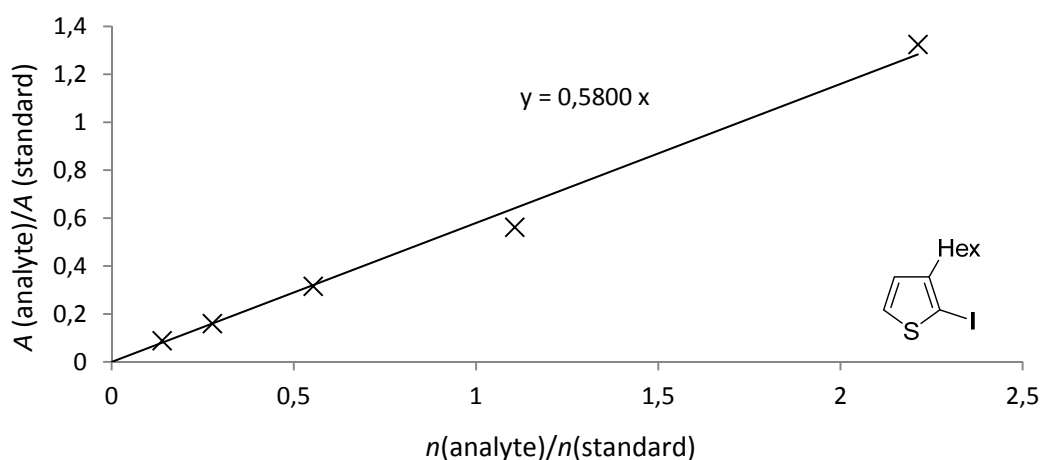
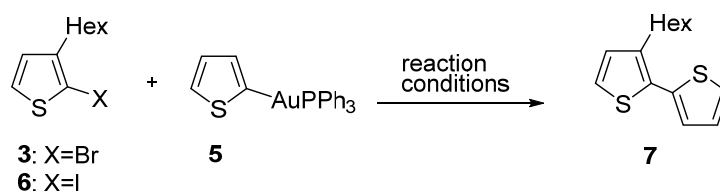


Figure SI 2. Calibration curve for 2-iodo-3-*n*-hexylthiophene (X), using 1,3,5-triisopropylbenzene as internal standard.

General procedure for Cross-Coupling Reactions with Organogoldthiophene:

A solution of the electrophilic component (0.500 mmol), 2-(triphenylphosphine)-gold(I)thiophene (374 mg, 0.550 mmol), catalyst (12 mg, 0.010 mmol, 2 mol%) and the internal standard 1,3,5-triisopropylbenzene (50 μ L, 43.0 mg, 0.213 mmol) in the solvent stated (4 mL) were stirred at the stated temperature for the specified time. A sample (0.1 mL) was taken from each reaction vessel, filtered through a short plug of silica (5 x 3 mm; eluent: ethyl acetate) and a syringe filter (pore size: 0.2 μ m) and was then used for GC analysis.

Table SI 3. Optimization of the Gold cross-coupling.



Entry	X	Solvent	Temperature	Time (h)	Conversion(%)
1	I	Acetonitrile	60 °C	2	63
2	I	Acetonitrile	60 °C	4	66
3	I	Toluene	60 °C	1.5	79
4	I	Toluene	60 °C	2.5	81
5	I	Toluene	60 °C	3.5	85
6	Br	Acetonitrile	60 °C	2	90
7	Br	Acetonitrile	60 °C	4	90
8	Br	Toluene	60 °C	1.5	94
9	Br	Toluene	60 °C	2.5	97
10	Br	Toluene	60 °C	3.5	98
11	Br	THF	60 °C	1.5	93
12	Br	THF	60 °C	2.5	95
13	Br	THF	60 °C	4	96
14	Br	DMF	60 °C	1.5	90
15	Br	DMF	60 °C	2.5	93
16	Br	DMF	60 °C	4	95
17	Br	Dioxane	60 °C	1.5	93
18	Br	Dioxane	60 °C	2.5	95
19	Br	Dioxane	60 °C	4	97
20	Br	Diethyl ether	reflux	1.5	84
21	Br	Diethyl ether	reflux	2.5	85
22	Br	Diethyl ether	reflux	4	93
23	Br	THF	20 °C	3	87

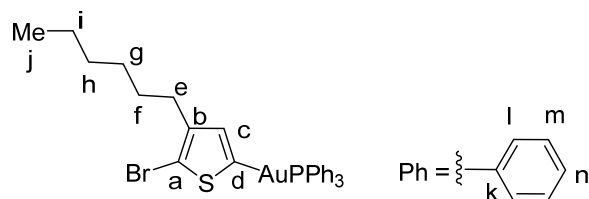
24	Br	THF	20 °C	5	88
25	Br	THF	20 °C	10	91
26	Br	DMF	20 °C	3	87
27	Br	DMF	20 °C	5	87
28	Br	DMF	20 °C	10	89
29	Br	Dioxane	20 °C	3	86
30	Br	Dioxane	20 °C	5	87
31	Br	Dioxane	20 °C	10	90
32	Br	Toluene	20 °C	3	88
33	Br	Toluene	20 °C	5	87
34	Br	Toluene	20 °C	10	94
35	Br	THF ^a	60°C	1.5	90
36	Br	THF ^a	60°C	2.5	93
37	Br	THF ^a	60°C	4	97
38	Br	THF ^a	20°C	1.5	85
39	Br	THF ^a	20°C	2.5	85
40	Br	THF ^a	20°C	5	97

The conversion was determined by GC, using triisopropylbenzene as an internal standard. Amount of catalyst: 2 mol%. ^aThe catalyst species was [Pd(PtBu₃)₂].

It was unexpected that the bromo-substituted electrophile gave higher yields than the iodo-derivative (Table SI 3, compare entries 1-5 with entries 6-10). Generally, at 60 °C independently of the solvent, all reactions gave very high yields of >90% within 4 hours (Table SI 3, entries 6-22), even if the gold starting material was poorly soluble (esp. in DMF, diethyl ether, dioxane and acetonitrile). It was also possible to lower the temperature to 20°C to obtain milder reaction conditions and by concomitant prolonging of the reaction time to 10 hours, we could obtain again yields of ca. 90% (Table SI 3, entries 23-34). To test a palladium (0) species, [Pd(PtBu₃)₂] was employed as an alternative catalyst species, which gave at both 60°C and 20°C overall very good results (Table SI 3, entries 35-40). Under all conditions we tested this reaction seemed very robust; especially the mild set of conditions were considered very suitable to be transferred to a polymerization of monomer **4**

Syntheses

2-Bromo-3-*n*-hexyl-5-(triphenylphosphin)gold(I)-thiophene (4)



A solution of diisopropylamine (111 mg, 1.10 mmol) in THF (10 mL) was cooled to $-78\text{ }^{\circ}\text{C}$ and *n*-butyllithium (0.40 mL, 1.0 mmol, 2.5 M in hexanes) was added dropwise over the course of 1 min. The mixture was warmed to $0\text{ }^{\circ}\text{C}$ over the course 3 min, then cooled to $-78\text{ }^{\circ}\text{C}$ and stirring was continued for another 5 min. 2-Bromo-3-hexylthiophene (247 mg, 1.00 mmol) was added dropwise over the course of 3 min and the reaction mixture was stirred for 1 h at $-78\text{ }^{\circ}\text{C}$. A solution of $[\text{ClAuPPh}_3]$ (495 mg, 1.00 mmol) in THF (10 mL) was added within 10 min to the orange-brown suspension and the reaction mixture was stirred at $-78\text{ }^{\circ}\text{C}$ for 30 min. Then the cooling bath was removed and the mixture was stirred for 3 h at $15\text{ }^{\circ}\text{C}$. The reaction was quenched with methanol (10 mL) and the solvents were removed *in vacuo*. The residue was diluted in DCM (15 mL) and washed with water (2 x 30 mL) and dried over magnesium sulfate. The solvent was removed *in vacuo* and the mixture was diluted DCM (1 mL) and in *n*-hexane (10 mL) to afford at $4\text{ }^{\circ}\text{C}$ the product as white crystals in a yield of 523 mg (741 μmol , 74%).

$^1\text{H NMR}$ (500 MHz, CDCl_3): $\delta = 7.56$ (m, 5H, l/m/n), 7.53-7.42 (m, 10H, l/ m/n), 6.84 (d, 1H, $^4J_{\text{H,P}} = 3.2$ Hz, Tph-*H-c*), 2.60-2.52 (m, 2H, e), 1.59 (dd, 2H, $^3J = 15.3$ Hz, 7.7 Hz, f), 1.40-1.22 (m, 6H, g, h, i), 0.88 (t, 3H, $^3J = 6.9$ Hz, j) ppm.

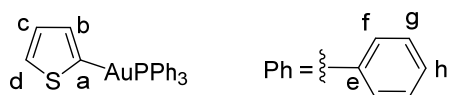
$^{13}\text{C NMR}$ (125 MHz, CDCl_3): $\delta = 141.7$ (Tph-*C-d*), 135.0 (Tph-*CH-c*), 134.3 (d, $^3J_{\text{C,P}} = 13.7$ Hz, l/ m), 131.4 (n), 130.5 (k/Tph-*C-b*), 130.1 (k/Tph-*C-b*), 129.2 (d, $^3J_{\text{C,P}} = 11.0$ Hz, l/m), 110.6 (Tph-*C-a*), 31.7 (e), 30.0, 29.6, 29.1, 22.6 (f, g, h, l, i), 14.1 (j) ppm.

$^{31}\text{P NMR}$ (202 MHz, CDCl_3): $\delta = 43.0$ ppm.

IR (ATR): $\tilde{\nu} = 2951$ (w), 2922 (m), 2852 (w), 1478 (w), 1434 (m), 1099 (m), 997 (w), 743 (s), 710 (m), 690 (s), 536 (s), 499 (s), 442 (m) cm^{-1} .

HRMS (MALDI-MS): *m/z* found 727.0469 (5) $[\text{M}+\text{Na}]^+$; calcd. for $\text{C}_{28}\text{H}_{29}\text{AuBrNaPS}$ 727.0474; found 721.1 (100) $[\text{Au}(\text{PPh}_3)_2]$.

M.p.: $104\text{ }^{\circ}\text{C}$.

2-(Triphenylphosphin)gold(I)-thiophene¹⁹ (5)

n-Butyllithium (0.80 mL, 2.00 mmol, 2.5 M in hexanes) was added to a stirred solution of thiophene (168 mg, 2.00 mmol) in THF (2 mL) at 0 °C over the course of 5 min. After 30 min, the reaction was warmed to 20 °C and stirred for 1 h. [ClAuPPh₃] (990 mg, 2.00 mmol) was added in one portion. After 3 h, the reaction was quenched by adding methanol (200 μL). Then, the solvents were removed *in vacuo*. DCM (20 mL) was added, and the organic layer was washed with water (3 x 15 mL), dried over sodium sulfate, filtered and concentrated under reduced pressure. The resulting gum was stirred overnight in *n*-hexane (5 mL). The resulting suspension was filtered. The solid was recrystallized from DCM/*n*-hexane to afford the product as colorless crystals in a yield of 865 mg (1.60 mmol, 80%, Lit.¹⁹: 65%).

¹H NMR (500 MHz, CDCl₃): δ = 7.63 (d, 1H, ³J = 4.8 Hz, Tph-*H*-b), 7.63-7.54 (m, 5H, f, g, h), 7.54-7.44 (m, 10H, f, g, h), 7.42 (dd, 1H, ³J = 4.8 Hz, ³J = 2.9 Hz, Tph-*H*-c), 7.19 (d, 1H, ³J = 2.9 Hz, Tph-*H*-d) ppm.

¹³C NMR (126 MHz, CDCl₃): δ = 134.4 (d, ³J_{C,P} = 13.7 Hz, f/g), 133.2 (Tph-CH-b/c/d), 131.3 (h), 130.7 (Ph-C-e), 130.3 (Tph-CH-b/c/d), 129.1 (d, ³J_{C,P} = 10.9 Hz, f/g), 127.0 (m, 1 x Tph-C-a, 1 x Tph-CH-b/c/d, e) ppm.

³¹P NMR (160 MHz, CDCl₃): δ = 43.3 ppm.

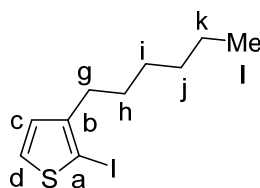
IR (ATR): $\tilde{\nu}$ = 3021 (w), 1478 (m), 1433 (s), 1100 (s), 997 (w), 834 (w), 812 (w), 744 (s), 709 (m), 687 (s), 532 (s), 501 (s), 474 (m), 442 (m), 432 (m) cm⁻¹.

HRMS (ESI): *m/z* found 565.0427 (100) [M+Na]⁺; calcd. for C₂₂H₁₈AuNaPS 565.0425.

Decomp. Temp.: 158 °C.

The NMR data are in agreement with the data found in the literature.¹⁹

¹⁹ F. Bonati, A. Burini, B. R. Pietroni, R. Galassi, *Gazz. Chim. Ital.* **1993**, *123*, 691.

2-Iodo-3-*n*-hexylthiophene (6)

This reaction was not performed under Schlenk conditions: *N*-Iodosuccinimide (6.75 g, 30.0 mmol) was added in one portion to 3-*n*-hexylthiophene (5.00 g, 40.0 mmol) in glacial acetic acid (50 mL) at 15 °C. The reaction mixture was stirred for 16 h at this temperature. Then, water (20 mL) was added and the reaction mixture was extracted with diethyl ether (3 x 20 mL). The organic layer was washed with sodium hydroxide solution (1 M, 5 x 50 mL) followed by drying over magnesium sulfate. The solvent was removed *in vacuo* and the crude product was distilled (kugelrohr, 8×10^{-3} mbar, 70 °C) to afford 7.72 g (26.3 mmol, 88% Lit.²⁰: 90% with impurities) of a slightly yellow oil.

¹H NMR (500 MHz, CDCl₃): δ = 7.38 (d, 1H, ³*J* = 5.5 Hz, Tph-*H*-d), 6.75 (d, 1H, ³*J* = 5.5 Hz, Tph-*H*-c), 2.60-2.51 (m, 2H, g), 1.61-1.52 (m, 2H, h), 1.39-1.28 (m, 6H, i, j, k), 0.94-0.86 (m, 3H, l) ppm.

¹³C NMR (126 MHz, CDCl₃): δ = 147.2 (Tph-C-b), 130.3 (Tph-CH-d), 127.9 (Tph-C-c), 73.9 (Tph-C-a), 32.1 (g), 31.6, 30.0, 28.9, 22.6 (h, i, j, k), 14.1 (l) ppm.

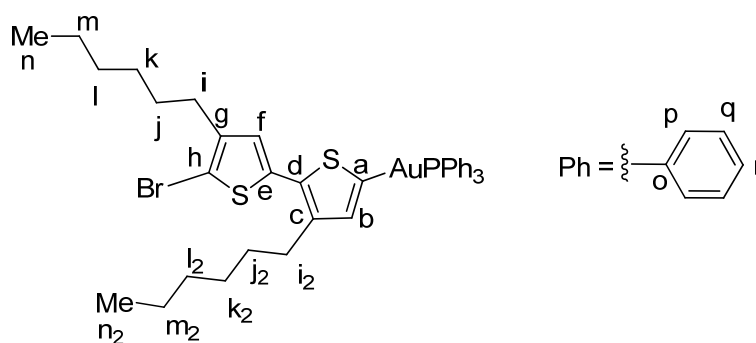
IR (ATR): $\tilde{\nu}$ = 2953 (m), 2923 (s), 2854 (s), 1456 (m), 1397 (m), 963 (m), 828 (s), 713 (s), 684 (s), 634 (s) cm⁻¹.

HRMS (EI⁺): *m/z* found 293.9937 (45) [M]⁺; calcd. for C₁₀H₁₅SI 293.9939; found 222.8 (100) [M-C₅H₁₁]⁺.

The NMR data are in agreement with the data found in the literature.²¹

²⁰ T. Tkachov, V. Senkovskyy, H. Homber, A. Kiriya, *Macromolecules* **2011**, *44*, 2006.

²¹ T. Yokozawa, R. Suzuki, M. Nojima, Y. Ohta, A. Yokoyama, *Macromol. Rapid. Commun.* **2011**, *32*, 801.

5'-Bromo-3,4'-dihexyl-5-triphenylphosphine-2,2'-bithiophene (8)

A solution of diisopropylamine (243 mg, 2.40 mmol) in THF (70 mL) was cooled to $-78\text{ }^{\circ}\text{C}$ and *n*-butyllithium (0.80 mL, 2.0 mmol, 2.5 M in hexanes) was added dropwise over the course of 2 min. The mixture was warmed to $0\text{ }^{\circ}\text{C}$ for 30 min, and then cooled to $-78\text{ }^{\circ}\text{C}$ while stirring was continued for 5 min. 2-Bromo-3-hexylthiophene (828 mg, 2.00 mmol) was added dropwise over the course of 3 min and the reaction mixture was stirred for 1 h at $0\text{ }^{\circ}\text{C}$. [ClAuPPh₃] (989 mg, 2.00 mmol) was added in one portion to the orange-brown suspension and the reaction mixture was stirred at $0\text{ }^{\circ}\text{C}$ for 15 min. Then the cooling bath was removed and the mixture was stirred for 5 h at $18\text{ }^{\circ}\text{C}$. The reaction was quenched with methanol (30 mL) and the solvents were removed *in vacuo*. The residue was diluted in benzene (2 mL) and filtered over Celite. The solvents were removed *in vacuo*. The residue was diluted in *n*-hexane (40 mL) at $50\text{ }^{\circ}\text{C}$ and stored at $4\text{ }^{\circ}\text{C}$ to crystallize the product. The product was washed with cold *n*-hexane ($4\text{ }^{\circ}\text{C}$, 3 x 30 mL) and dried *in vacuo* to afford pale yellow crystals (1.41 g, 1.62 mmol, 82%)

Note: In order to obtain high purities, it is essential to analyze the purification step by ³¹P NMR spectroscopy. If the ³¹P NMR spectrum still indicates the presence of impurities, the compound should be re-diluted in benzene, filtered over Celite and crystallized again until ³¹P NMR shows only one signal.

¹H NMR (500 MHz, CDCl₃): δ = 7.61-7.55 (m, 6H, p/q/r), 7.53-7.44 (m, 9H, p/q/r), 6.96 (d, 1H, ³J = 2.6 Hz, Tph-H-b), 6.75 (s, 1H, Tph-H-f), 2.75-2.69 (m, 2H, i), 2.56-2.49 (m, 2H, i²), 1.65-1.59 (m, 6H, j, j², k/k²), 1.32 (m, 10H, k/k², l, m, l², m²), 0.90-0.86 (m, 6H, n, n²) ppm.

¹³C NMR (126 MHz, CDCl₃): δ = 142.0 (Tph-C-g), 140.1 (Tph-C-a), 138.0 (Tph-C-e), 137.1 (Tph-CH-b), 134.3 (d, ³J_{C, p} = 13.8 Hz, p/q), 132.2 (Tph-C-d), 131.3 (r), 130.6 (o), 130.2 (Tph-C-c),

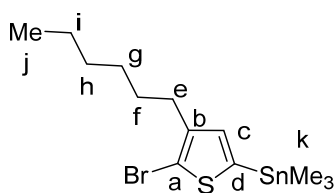
129.1 (d, $^3J_{C,P} = 11.0$, Hz, p/q), 125.3 (Tph-CH-f), 106.9 (Tph-C-h), 31.8, 31.6, 30.9, 29.7, 29.6, 29.5, 29.4, 28.9, 22.6, 22.6 (all i-m, i²-m²), 14.1, 14.1 (n, n²) ppm.

³¹P NMR (202 MHz, CDCl₃): δ = 43.2 ppm.

IR (ATR): $\tilde{\nu}$ = 2953 (m), 2923 (s), 2854 (s), 1457 (m), 1410 (w), 1377 (w), 1195 (w), 1004 (w), 831 (s), 722 (s), 687 (m), 648 (s), 467 (w) cm⁻¹.

HRMS (EI⁺): *m/z* found 870.1387 (5) [M]⁺; calcd. for C₃₈H₄₃AuBrPS₂ 870.1393; found 721.1 (100) [Au(PPh₃)₂]⁺.

M.p.: 63 °C.

2-Bromo-3-*n*-hexyl-5-trimethyltin-thiophene (9)

A solution of diisopropylamine (3.04 g, 30.0 mmol) in THF (80 mL) was cooled to $-78\text{ }^{\circ}\text{C}$ and *n*-butyllithium (11.2 mL, 28.0 mmol, 2.5 M in hexanes) was added over the course of 5 min. The mixture was warmed to $0\text{ }^{\circ}\text{C}$ for 30 min, then cooled to $-78\text{ }^{\circ}\text{C}$ and stirring was continued for another 5 min. Then, 2-bromo-3-*n*-hexylthiophene (6.92 mg, 28.0 mmol) in THF (20 mL) was added dropwise over the course of 10 min and the reaction mixture was stirred for 1 h at $-78\text{ }^{\circ}\text{C}$. ClSnMe_3 (5.58 g, 28.0 mmol) in THF (20 mL) was added dropwise over the course of 10 min to the bright yellow suspension. The suspension was stirred at $-78\text{ }^{\circ}\text{C}$ for 15 min. Then the cooling bath was removed and the mixture was stirred for 3 h at $17\text{ }^{\circ}\text{C}$. The reaction was quenched with water (60 mL). DCM (70 mL) was added and the phases were separated. The organic layer was washed with water (100 mL) and dried over magnesium sulfate. The solvent was removed *in vacuo* to afford the crude product as orange oil, which was distilled (kugelrohr, 3×10^{-2} mbar, $90\text{ }^{\circ}\text{C}$) to yield 9.69 g (23.6 mmol, 84% Lit.²²: 79%) of a slightly yellow oil.

^1H NMR (500 MHz, CDCl_3): δ = 6.86 (s, 1H, Tph-*H*-c), 2.59-2.55 (m, 2H, e), 1.62-1.55 (m, 2H, f), 1.39-1.30 (m, 6H, g, h, i), 0.90 (t, 3H, $^3J = 7.0\text{ Hz}$, j), 0.36 (s, 9H, k) ppm.

^{13}C NMR (126 MHz, CDCl_3): δ = 143.1 (Tph-C-b), 137.9 (Tph-C-d), 136.3 (Tph-CH-c), 113.4 (Tph-CH-a), 31.6 (e), 29.9, 29.2, 29.0, 22.6 (f, g, h, i), 14.1 (j), -8.3 (k) ppm.

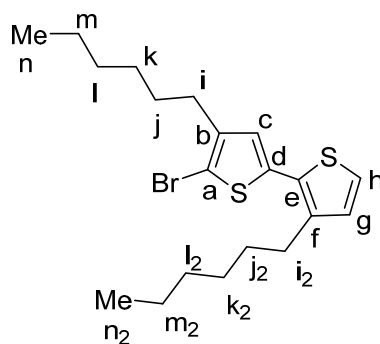
^{119}Sn NMR (187 MHz, CDCl_3): δ = -24.5 ppm.

IR (ATR): $\tilde{\nu}$ = 2955 (w), 2924 (m), 2855 (w), 1457 (w), 1396 (w), 1191 (m), 956 (w), 909 (w), 833 (m), 770 (s), 720 (m), 531 (s), 513 (s), 491 (m) cm^{-1} .

HRMS (EI^+): m/z found 409.9731 (20) $[\text{M}]^+$; calcd. for $\text{C}_{13}\text{H}_{23}\text{BrSSn}$ 409.9726; 359.0 (100) $[\text{M}-\text{CH}_3]^+$.

The NMR data are in agreement with the data found in the literature.²²

²² B. Burkhart, P. P. Khlyabich, T. Cakir Canak, T. W. LaJoie, B. C. Thompson, *Macromolecules* **2011**, *44*, 1242.

5'-Bromo-3,4'-dihexyl-2,2'-bithiophene (10)**Method (A)**

2-Bromo-3-*n*-hexyl-5-trimethyltin-thiophene (374 mg, 1.00 mmol), [Pd(PPh₃)₄] (23 mg, 0.020 mmol, 2.0 mol%) and 3-bromo-2-iodothiophene (289 mg, 1.00 mmol) were dissolved in DMF (4 mL). The mixture was heated to 100 °C in a microwave apparatus for 45 min. The reaction mixture was diluted with ethyl acetate (30 mL), washed with water (20 mL) and brine (20 mL). The residue was distilled by kugelrohr distillation (starting material: 70 °C, 4 x 10⁻² mbar and product: 2 x 10⁻³ mbar, 150 °C) to afford the product as a bright yellow oil 396 mg (957 μmol, 96%).

Method (B)

To a solution of 2-bromo-3-*n*-hexyl-5-iodothiophene (2.03 g, 5.44 mmol) in DME (25 mL), [Pd(PPh₃)₄] (243 mg, 0.210 mmol, 4.00 mol%) was added. After the mixture was stirred for 10 min at 18 °C, 2-(3-hexylthiophen-2-yl)-4,4,5,5-tetramethyl-1,3,2-dioxaborolane (1.60 g, 5.44 mmol) and an aqueous solution of sodium hydrogen carbonate (1 M, 16 mL) were added. The reaction mixture was heated to reflux under vigorous stirring for 18 h. Then, the reaction was cooled to 20 °C and quenched with water (100 mL). The organic layer was separated and the aqueous layer was extracted with diethyl ether (3 x 30 mL). The combined organic layers were dried over sodium sulfate followed by the removal of the solvent *in vacuo*. The crude product was purified by flash chromatography (petrol ether, R_f = 0.40) to afford the product as a bright yellow oil in a yield of 1.88 g (4.57 mmol, 84%, Lit.²³: 62%).

²³ T. Beryozkina, V. Senkovskyy, E. Kaul, A. Kiriya, *Macromolecules* **2008**, *41*, 7817.

¹H NMR (500 MHz, CDCl₃): δ = 7.16 (d, 1H, ³J = 5.2 Hz, Tph-H-h), 6.91 (d, 1H, ³J = 5.2 Hz, Tph-H-g), 6.79 (s, 1H, Tph-H-c), 2.72-2.68 (m, 2H, i²), 2.58-2.54 (m, 2H, i), 1.63-1.58 (m, 4H, j, j²), 1.36-1.29 (m, 12H, k, l, m, k², l², m²), 0.91-0.88 (m, 6H, n, n²) ppm.

¹³C NMR (126 MHz, CDCl₃): δ = 142.6 (Tph-C-b), 139.9 (Tph-C-f), 135.7 (Tph-C-d), 130.0 (Tph-C-e), 129.9 (Tph-CH-g), 126.8 (Tph-CH-c), 123.9 (Tph-CH-h), 108.5 (Tph-C-a), 31.6, 31.6, 30.7, 29.6, 29.6, 29.2, 29.1, 28.9, 22.6, 22.6 (i-m, i²-m²), 14.1, 14.1 (n, n²) ppm.

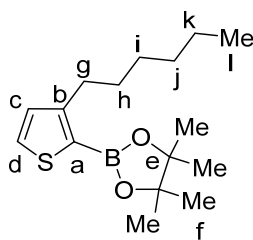
IR (ATR): $\tilde{\nu}$ = 2953 (m), 2923 (s), 2854 (s), 1457 (m), 1410 (w), 1377 (w), 1195 (w), 1004 (w), 831 (s), 722 (s), 687 (m), 648 (s), 467 (w) cm⁻¹.

HRMS (EI⁺): *m/z* found 412.0888 (100) [M]⁺; calcd. for C₂₀H₂₉BrS₂ 412.0894.

The NMR data are in agreement with the data found in the literature.²⁴

²⁴ T. Beryozkina, V. Senkovskyy, E. Kaul, A. Kiriya, *Macromolecules* **2008**, *41*, 7817.

2-(3-Hexylthiophen-2-yl)-4,4,5,5-tetramethyl-1,3,2-dioxaborolane (11)



n-Butyllithium (6.40 mL, 15.0 mmol, 2.5 M in *n*-hexane) was dissolved in THF (50 mL) at -78 °C. Then, 2-bromo-3-*n*-hexylthiophene (3.71 g, 15.0 mmol) was added dropwise over the course of 10 min to the yellow solution and the mixture was stirred for 60 min. 2-Isopropoxy-4,4,5,5-tetramethyl-1,3,2-dioxaborolane (2.97 g, 15.0 mmol) was added in one portion to the yellow solution. The mixture was allowed to warm to 15 °C within 12 h and was then quenched with a saturated aqueous solution of ammonium chloride (15 mL). The aqueous layer was extracted with diethyl ether (3 x 30 mL), the combined organic layers were washed with brine (20 mL) and were dried over magnesium sulfate. The solvent was removed *in vacuo* and the crude product was purified by flash chromatography (*n*-pentane, $R_f = 0.25$) as eluent to yield 3.56 g (12.1 mmol, 81%, Lit.²⁵: 92%) of a slightly yellow oil.

¹H NMR (200 MHz, CDCl₃): δ = 7.48 (d, 1H, ³J = 4.7 Hz, Tph-CH-d), 7.01 (d, 1H, ³J = 4.7 Hz, Tph-CH-c), 2.92-2.85 (m, 2H, g), 1.61-1.53 (m, 2H, h), 1.40-1.15 (m, 18H, i, j, k, f), 0.88 (m, 3H, l) ppm.

¹³C NMR (126 MHz, CDCl₃): δ = 154.7 (Tph-C-b), 131.2 (Tph-CH-d), 130.3 (Tph-CH-c), 83.5 (e), 31.8 (g), 31.7, 30.1, 28.9, 22.6 (h, i, j, k), 24.8 (f), 14.1 (l) ppm.²⁶

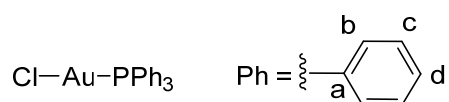
¹¹B NMR (160 MHz, CDCl₃): δ = 29.1 ppm.

IR (ATR): $\tilde{\nu}$ = 2956 (w), 2977 (w), 2926 (m), 2856 (w), 1529 (m), 1467 (w), 1430 (s), 1379 (m), 1370 (m), 1334 (s), 1303 (s), 1270 (m), 1165 (m), 1142 (s), 1101 (w), 1028 (m), 958 (w), 855 (s), 738 (m), 667 (w), 644 (m), 578 (w) cm⁻¹.

HRMS (EI⁺): *m/z* found 294.1819 (50) [M]⁺; calcd. for C₁₆H₂₇O₂SB 294.1825; found 224.1 (100) [M-C₅H₁₁]⁺.

²⁵ E. J. Dell, B. Capozzi, K. H. DuBay, T. C. Berkelbach, J. R. Morneo, D. R. Reichman, L. Venkataraman, L. M. Campos, *J. Am. Chem. Soc.* **2013**, *135*, 11724.

²⁶ The carbon atom bound to boron was not visible due to the high quadrupole moment of the boron nucleus.

Triphenylphosphine gold(I) chloride (13)²⁷

Dimethylsulfide gold(I) chloride (1.20 g, 4.06 mmol) and triphenylphosphine (1.07 g, 4.06 mmol) were weighed at normal atmosphere into a flask. The flask was evacuated and flushed with nitrogen. DCM (350 mL) was added to these reagents, dissolving the starting materials. The mixture was stirred at 20 °C for 15 min monitoring the formation of the product by ³¹P NMR spectroscopy. The reaction mixture was worked up in air by reducing the volume of the solution to 50 mL *in vacuo* and *n*-hexane (350 mL) was added resulting in the precipitation of the complex. The solid was then filtered, washed with *n*-hexane (3 x 15 mL) and dried *in vacuo*, affording the product as a white solid in a yield of 1.93 g (3.90 mmol, 96%; Lit.³: quantitative).

¹H NMR (500 MHz, CDCl₃, 300 K): δ = 7.60-7.40 (m, 15H, b, c, d) ppm.

¹³C NMR (125 MHz, CDCl₃): δ = 134.15 (d, ³J_{C-P} = 13.8 Hz, b/c), 131.99 (d, ³J_{C-P} = 2.4 Hz, d), 129.24 (d, ³J_{C-P} = 11.9 Hz, b/c), 128.6 (d, ³J_{C-P} = 48.4 Hz, a) ppm.

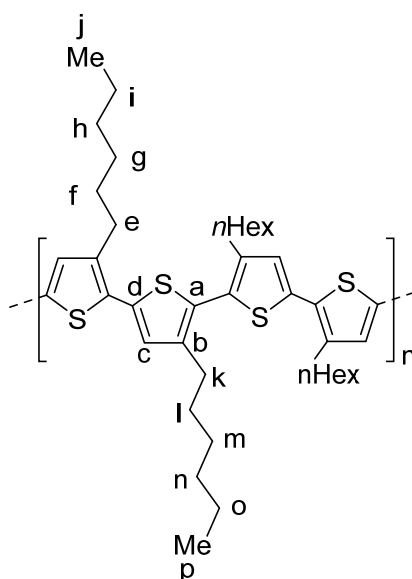
³¹P NMR (202 MHz, CDCl₃, 300 K): δ = 33.0 ppm.

IR (ATR): $\tilde{\nu}$ = 3060 (w), 3005 (w), 1479 (m), 1433 (m), 1421 (s), 1101 (s), 997 (m), 747 (s), 712 (m), 690 (s), 544 (s), 499 (s) cm⁻¹.

HRMS (ESI): *m/z* found 517.0152 (100) [M+Na]⁺; calcd. for C₁₈H₁₅AuClNaP 517.0158.

M.p.: 236°C.

²⁷ N. Mezailles, L. Ricard, F. Gagosz *Org. Lett.* **2005**, *7*, 4133-4136.

***rr*-HH-TT-P3HT (14)**

In the glove box, 5'-bromo-3,4'-dihexyl-5-triphenylphosphine-2,2'-bithiophene (174 mg, 200 μmol) and $[\text{Pd}(\text{P}t\text{Bu}_2\text{Ph})_2]$ (5 mol%) were placed in a Schlenk flask, which was closed and removed from the glovebox. Then, under Schlenk conditions, THF (8 mL) was added to the solution and the mixture was stirred at 70 $^\circ\text{C}$ for 12 h. The reaction mixture was cooled to 20 $^\circ\text{C}$ and quenched by adding a 1 M solution of HCl in methanol (5 mL). DCM (10 mL) and water (5 mL) was added. The layers were separated and the organic phase was dried over sodium sulfate, filtered and the solvents were removed *in vacuo*. Half of the resulting red residue was diluted in chloroform (HPLC grade, 4 mL) and used for GPC analysis. The other half was used for NMR analysis. Due to this procedure, no yield was determined.

$^1\text{H NMR}$ (500 MHz, CDCl_3): δ = 6.99-6.85 (m, 10H, Tph-*H-c*), 2.77-2.62 (m, 12H, e), 2.56-2.42 (m, 8H, k), 1.66-1.52 (m, 20H, f, l), 1.37-1.20 (m, 60H, g, h, i, m, n, o), 0.88-0.72 (m, 30H, j, p) ppm.²⁸

$^{13}\text{C NMR}$ (126 MHz, CDCl_3): δ = 142.9 (Tph-C), 140.2 (Tph-C), 139.7 (Tph-C), 135.3 (Tph-C), 128.6 (Tph-CH), 128.1 (Tph-C), 127.1 (Tph-C), 126.6 (Tph-CH), 30.7, 30.5, 29.6, 29.5, 29.1, 28.9, 26.9, 26.9, 22.6, 22.6 (e-l, k-o), 14.1 (j, p) ppm.

λ_{max} (CHCl_3) = 431 nm.

M_n (GPC in CHCl_3 , calibrated against PS) = 17 kDa.

²⁸ NMR signals show a pentamer (10 thiophene units) as repeating units, calculated from the $^1\text{H NMR}$ spectra.

M_w (GPC) = 40 kDa.

PDI (GPC) = 2.4.

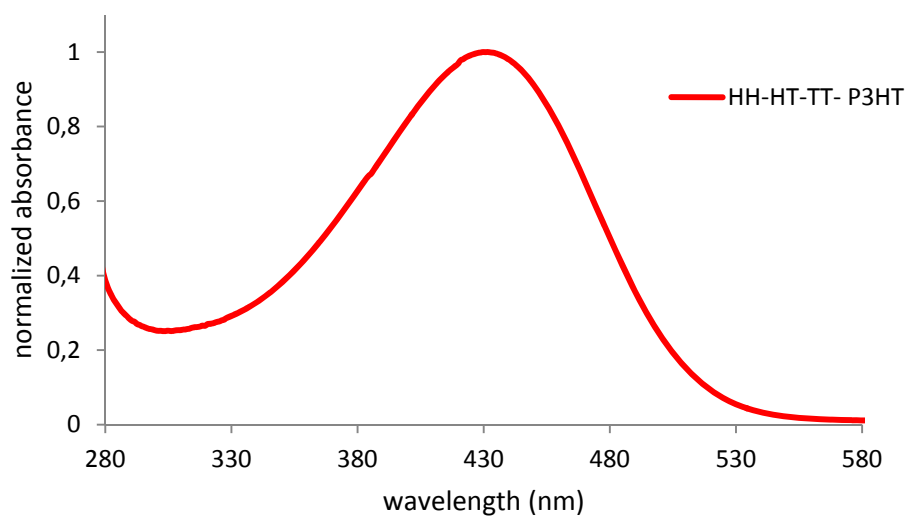
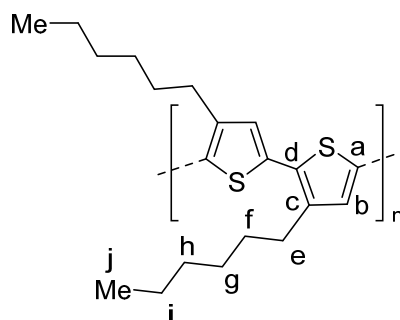


Figure SI 4. Full absorption spectrum of *rr*-HH-TT-P3HT in solution (CHCl₃).

***rr*-HT-P3HT (15)**

In the glove box, 5'-bromo-3,4'-dihexyl-5-triphenylphosphinegold-2,2'-bithiophene (174 mg, 200 μmol) and $[\text{Pd}(\text{PtBu}_3)_2]$ (5.10 mg, 10.0 μmol , 5.00 mol%) were placed in a Schlenk flask. THF (8 mL) was added to the solution and the mixture was stirred at 70 $^\circ\text{C}$ for 14 h. The reaction mixture was cooled to 20 $^\circ\text{C}$ and quenched by adding a 1 M solution of HCl in methanol (5 mL). A dark red solid started directly to precipitate. This was collected by filtration, and diluted in a minimum of DCM (1 mL) and precipitated into stirring methanol (100 mL). A dark red solid was collected by filtration, washed with methanol (3 x 5 mL) and dried *in vacuo* to yield the regio regular polymer as product in a yield of 4.00 mg (12.0 μmol , 61%).

^1H NMR (600 MHz, CDCl_3): δ = 6.98 (s, 1H, Tph-*H*-b), 2.88-2.74 (m, 2H, e), 1.76-1.65 (m, 2H, f), 1.46-1.30 (m, 6H, g, h, i), 0.91 (t, 3H, 3J = 6.7 Hz, j) ppm.

^{13}C NMR (126 MHz, CDCl_3): δ = 139.9 (Tph-C-d/b), 133.79 (Tph-C-a), 130.5 (Tph-C-d/b), 128.6 (Tph-CH-c), 31.9, 31.7, 29.6, 29.4, 22.7 (e, f, g, h, i), 14.1 (j) ppm.

λ_{max} (CHCl_3) = 451 nm.

M_n (GPC, in CHCl_3 , calibrated against PS) = 26 kDa.

M_w (GPC) = 54 kDa.

PDI (GPC) = 2.0.

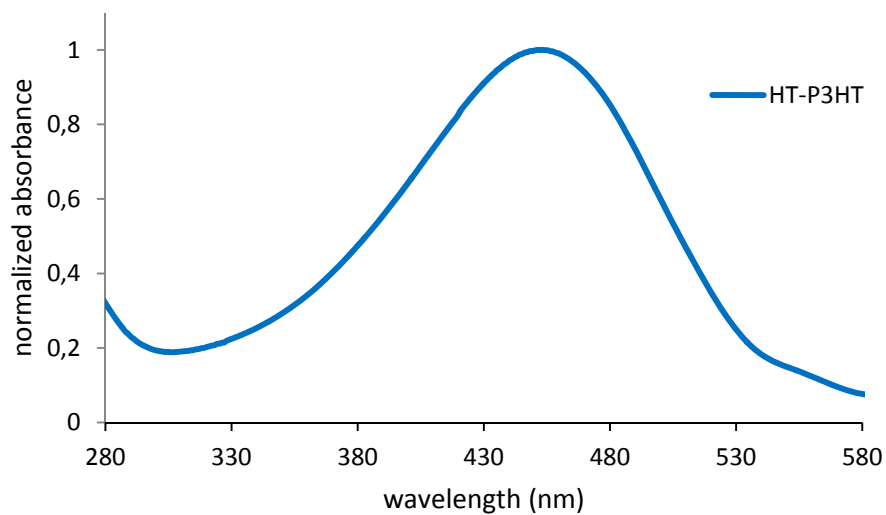
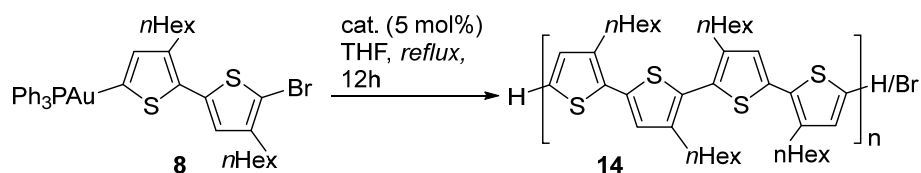


Figure SI 3. Full absorption spectrum of *rr*-HT-P3HT in solution (CHCl₃).

Polymerization Catalyst Screening

For the synthesis of P3HT, different catalyst species were used for a screening. All reactions (Table SI 4) were performed similar to the following procedure (analysis see above):

General Procedure:



In the glove box, 5'-bromo-3,4'-dihexyl-5-triphenylphosphine-2,2'-bithiophene (174 mg, 200 μmol) and catalyst (5 mol%) were placed in a Schlenk flask, which was closed and removed from the glovebox. Then, under Schlenk conditions, THF (8 mL) was added to the solution and the mixture was stirred at 70 $^{\circ}\text{C}$ for 12 h. The reaction mixture was cooled to 20 $^{\circ}\text{C}$ and quenched by adding a 1 M solution of HCl in methanol (5 mL). DCM (10 mL) and water (5 mL) were added. The layers were separated and the organic phase was dried over sodium sulfate, filtered and the solvents were removed *in vacuo*. Half of the resulting red residue was diluted in chloroform (HPLC grade, 4 mL) and used for GPC analysis. The other half was used for NMR analysis.

Table SI 4. Catalyst screening with **8** as monomer.

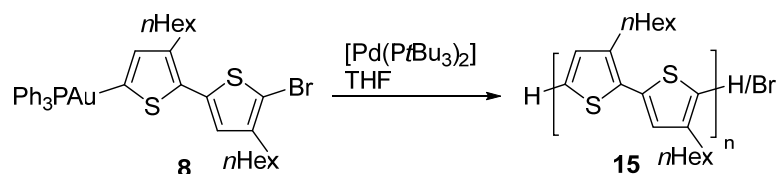
Entry	Catalyst ^a	Polymer ^b	M _n ^c	M _w ^c	PDI ^c
1	[Pd(dppf)Cl ₂ ·CH ₂ Cl ₂]	HH-TT, 5:3:2	16016	55723	3.48
2	[Pd(PPh ₃) ₄]	HH-TT, 5:3:2	2218	3398	1.53
3	[Pd(PtBu ₂ Ph) ₂]	HH-TT, 5:3:2	16745	39778	2.4
4	[[<i>i</i> PrPd(NQ)] ₂]	-	431	1771	4.11
5	[[<i>i</i> MesPd(NQ)] ₂]	-	385	848	2.20
6	[[<i>i</i> PrPd(allyl)Cl]	HH-TT, 5:3:2	1152	1796	1.55
7	[[<i>i</i> MesPd(allyl)Cl]	HH-TT, 5:3:2	1815	3297	1.82
8	[[<i>S</i> iPrPd(allyl)Cl]	HH-TT, 5:3:2	1289	2570	1.99
9	[[<i>S</i> iPrPd(cinnamyl)Cl]	HH-TT, 5:3:2	7794	18169	2.33
10	[[<i>i</i> PrPdCl ₂] ₂]	HH-TT, 5:3:2	9023	23136	2.56
11	[[<i>i</i> MesPd(vs)]	HH-TT, 5:3:2	8981	25480	2.84
12	[[<i>S</i> iMesPd(vs)]	HH-TT, 5:3:2	9547	28701	3.0
13	[Pd(dippf)(vs)tol]	HH-TT, 5:3:2	1573	2796	1.78
14	[Pd(PtBu ₃) ₂]	HT-HT, 1:1	26390	54376	2.06
15	[Pd(PtBu ₃) ₂] ^d	HT-HT, 1:1	25243	64430	2.55
16	[Pd(PtBu ₃) ₂] ^e	HT-HT, 1:1	20638	46854	2.27
17	[Pd(PtBu ₃) ₂] ^f	HT-HT, 1:1	23736	122802	5.17

All reactions were carried out in THF as a solvent at 70 °C, if not noted otherwise. ^a5 mol% of the catalyst species was used. ^bDetermined by ¹H NMR spectra: Integration of the first alkyl-CH₂ groups. ^cDetermined by GPC, using polystyrene as calibration standard. ^d2 mol% catalyst species. ^eThe reaction temperature was 45 °C. ^fToluene was used as solvent and the reaction temperature was 90 °C.

Polymerization Kinetic Studies

a) Kinetic for *rr*-HT-P3HT with different catalyst loadings

General Procedure:



In the glove box, 5'-bromo-3,4'-dihexyl-5-triphenylphosphinegold-2,2'-bithiophene (174 mg, 200 μmol) and $[\text{Pd}(\text{P}t\text{Bu}_3)_2]$ (2 mol% and 5 mol%, respectively) were placed in a Schlenk flask. THF (8 mL) was added to the solution and the mixture was stirred at 70 $^\circ\text{C}$ for the specified time. In regular intervals (see tables SI 5 and 6), a sample (0.3 mL) was taken out of the reaction mixture and quenched with a 1 M solution of HCl in methanol (3 mL). The sample was taken out of the glovebox, opened to air and diluted with DCM (4 mL) and water (2 mL). After shaking the vial, the layers were separated. The organic phase was dried over sodium sulfate, filtered and the solvents were removed *in vacuo*. Half of the resulting red residue was diluted in chloroform (HPLC grade, 4 mL) and used for GPC analysis. The other half was diluted in CDCl_3 and used for NMR analysis.

Table SI 5. Results for polymerization reaction with **8** as monomer. The reactions were performed in THF as solvent at 70 $^\circ\text{C}$, the catalyst species was $[\text{Pd}(\text{P}t\text{Bu}_3)_2]$ with a catalyst loading of 2 mol%.

time (min)	M_n	M_w	PDI
0.3	-	-	-
0.75	4709	6519	1.38
1.5	4084	6143	1.5
3	4080	6716	1.65
6	4458	7858	1.76
12	5357	9343	1.74
25	5879	10423	2.14
50	5947	10890	2.11
90	5100	10504	2.06
150	5594	11227	2
210	5860	11615	1.98
310	6145	12412	2.02
420	6162	13442	2.1
620	7777	15565	2
900	10743	25150	2.3

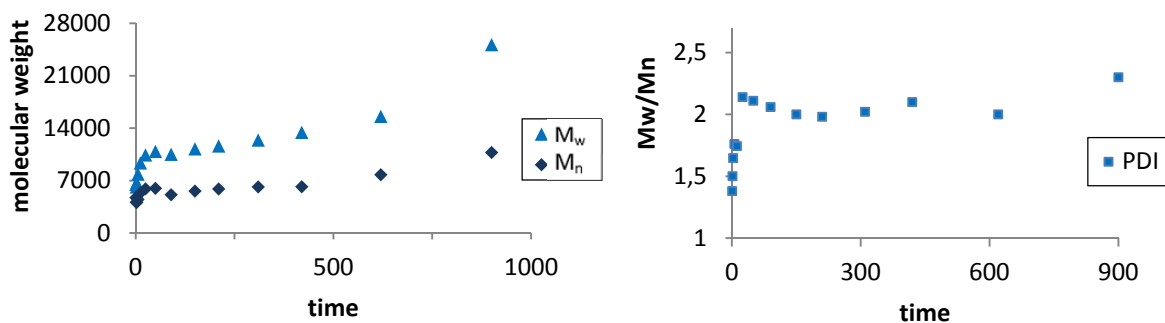


Chart SI 1. Kinetic control of the polymerization reaction at 70 °C with 2 mol% of the catalyst species (left: M_n and M_w ; right PDI).

Table SI 6. Results for polymerization reaction with **8** as monomer. The reactions were performed in THF as solvent at 70 °C, the catalyst species was $[Pd(PtBu_3)_2]$ with 5 mol%.

time (min)	M_n	M_w	PDI
0.3	3801	4967	1.3
0.75	3944	5801	1.47
1.5	4065	6814	1.67
3	4330	7778	1.7
6	5497	8951	1.72
12	5899	10393	1.76
25	7186	12860	1.83
50	7946	14708	1.95
90	9545	20789	2.1
150	9926	22610	2.27
210	9883	22870	2.3
310	9700	21953	2.29
420	9487	21837	2.28
620	9671	21896	2.29
900	9097	20813	2.29

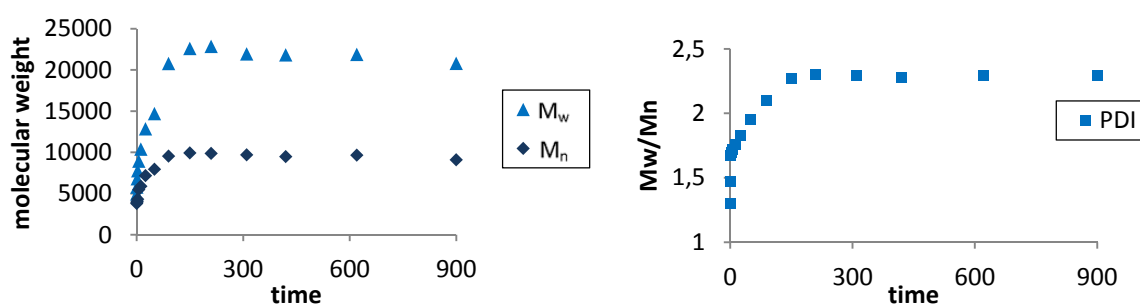


Chart SI 2. Kinetic control of the polymerization reaction at 70 °C with 5 mol% of the catalyst species (left: M_n and M_w ; right PDI).

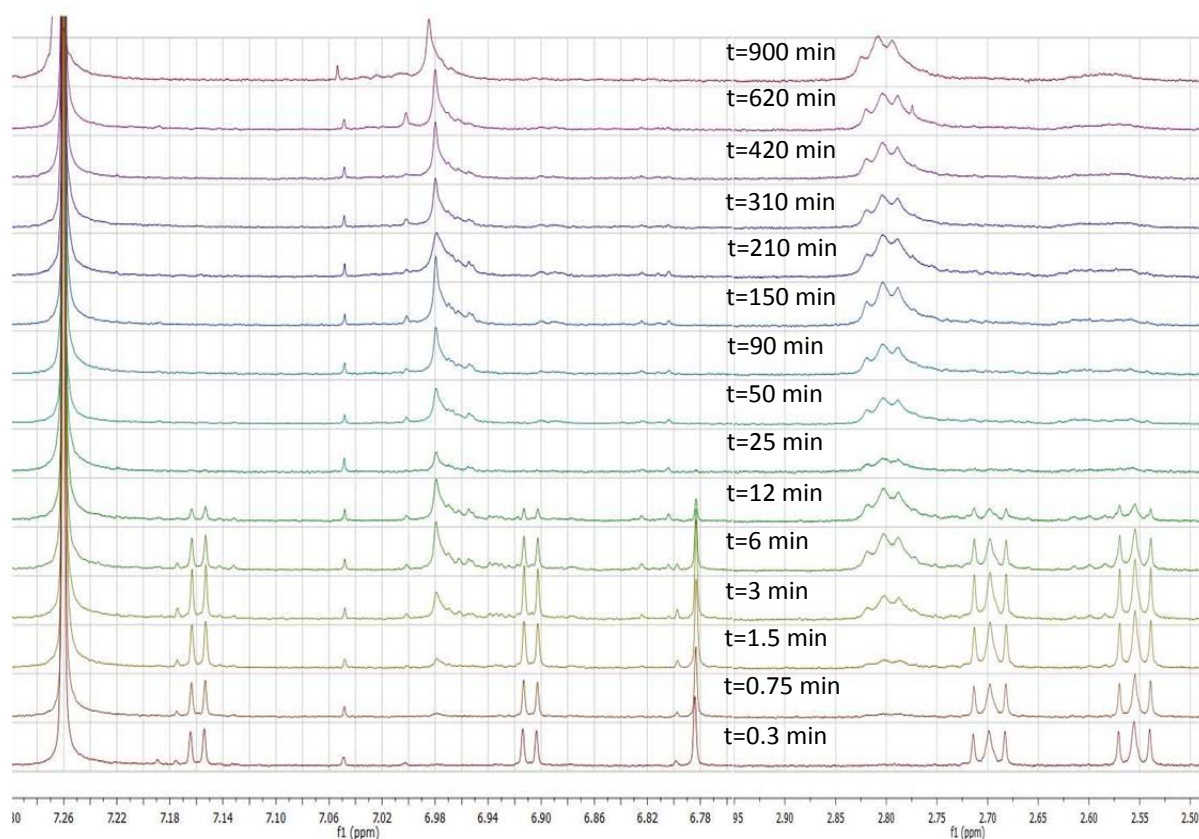


Chart SI 3. ^1H NMR spectra of the kinetic experiment, exemplary for the reaction described above at 70°C and with a catalyst loading of 5 mol% $[\text{Pd}(\text{PtBu}_3)_2]$. Shown are the aryl and alkyl region over a period of 900 min. The reactions were quenched by HCl. This procedure leads to a substitution of the gold group against a proton and results in 5'-bromo-3,4'-dihexyl-2,2'-bithiophene (proton signals at 6.78, 6.90 and 7.16 ppm). The singlet of the RR P3HT (6.98 ppm) is presented, its CH_2 group (2.8 ppm) and the CH_2 groups of the quenched monomer (2.70 and 2.55 ppm). Between 12 and 25 min, the monomer signals are disappearing. At this point of reaction, the monomer conversion is apparently complete.

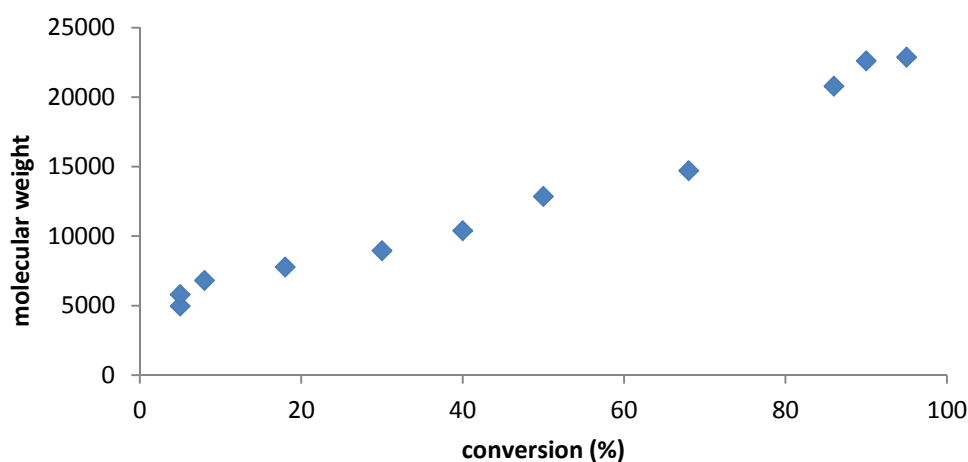
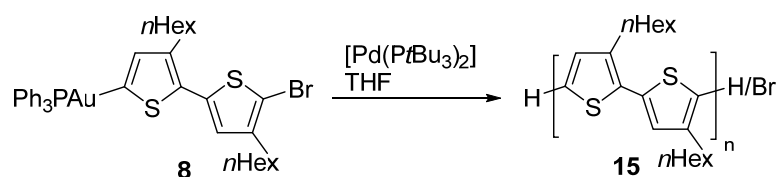


Chart 4. The conversion of the monomer **8** was calculated by integration of the peaks in the aromatic region of the corresponding ^1H NMR spectra. The error will be significant in this graphic due to the exchange of the phosphine ligands that occurs in the reaction. Nevertheless, it is visible that the polymerization kinetic is likely to be chain growth.

b) Kinetic for *rr*-HT-P3HT at different temperatures

General Procedure:



In the glove box, 5'-bromo-3,4'-dihexyl-5-triphenylphosphinegold-2,2'-bithiophene (174 mg, 200 μmol) and $[\text{Pd}(\text{PtBu}_3)_2]$ (5 mol%) were placed in a Schlenk flask. THF (Toluene) was added to the solution and the mixture was stirred at 45 $^\circ\text{C}$, 70 $^\circ\text{C}$ and 90 $^\circ\text{C}$ for the specified time. In regular intervals (see tables SI 7 and 8), a sample (0.3 mL) was taken out of the reaction mixture and quenched with a 1 M solution of HCl in methanol (3 mL). The sample was taken out of the glovebox, opened to air and diluted with DCM (4 mL) and water (2 mL). After shaking the vial, the layers were separated. The organic phase was dried over sodium sulfate, filtered and the solvents were removed *in vacuo*. Half of the resulting red residue was diluted in chloroform (HPLC grade, 4 mL) and used for GPC analysis. The other half was diluted in CDCl_3 and used for NMR analysis.

Table SI 7. Results for polymerization reaction with **8** as monomer. The reactions were performed in THF as solvent at 45 $^\circ\text{C}$, the catalyst species was $[\text{Pd}(\text{PtBu}_3)_2]$ (2 mol%).

The reaction was performed in THF at 45 $^\circ$			
time (min)	M_n	M_w	PDI
1	3644	5743	1.57
2,5	2838	4594	1.62
5	3268	5823	1.78
10	4495	7736	1.72
15	5802	10313	1.772
30	5996	10855	1.81
45	6850	11033	1.75
60	6616	11450	1.88
90	6439	11586	1.8
150	6562	11852	1.95
210	6857	12882	1.87
310	7265	13078	1.8
420	7158	13209	1.84
620	7671	13538	1.76
900	7084	12907	1.8

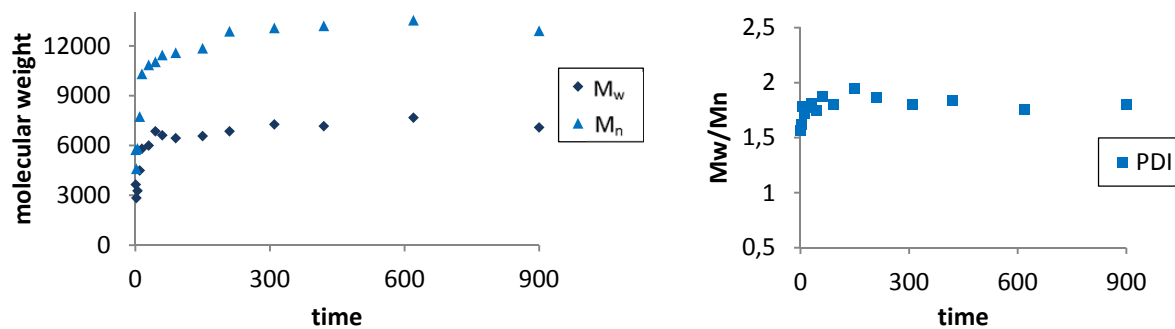


Chart SI 5. Kinetic control of the polymerization reaction at 45 °C with 2 mol% of catalyst species (left: M_n and M_w ; right PDI).

Table SI 8. Results for polymerization reaction with **8** as monomer. The reactions were performed in toluene as solvent at 90 °C, the catalyst species was $[Pd(PtBu_3)_2]$ (2 mol%).

The reaction was performed in toluene at 90 °C			
time (min)	M_n	M_w	PDI
0,3	1155	1220	1.056
0,75	1124	1364	1.213
1,5	1486	1880	1.265
3	2813	3789	1.37
6	3766	6589	1.75
12	4228	7803	1.82
25	12105	21052	2.1
50	9783	22003	2.249
90	21894	55468	2.53
150	15940	38904	2.44
210	20579	60464	2.94
310	20929	57993	2.77
420	21789	69079	3.17
620	22539	68042	3.019
900	30328	75494	2.489

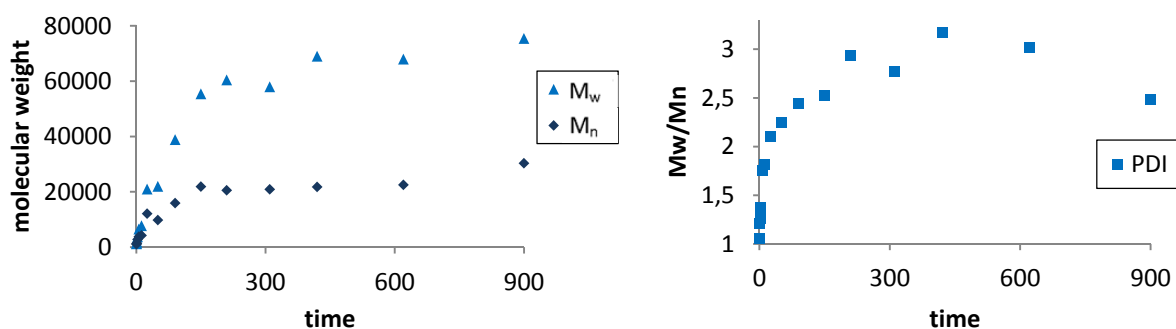


Chart SI 6. Kinetic control of the polymerization reaction at 90 °C with 2 mol% of catalyst species (left: M_n and M_w ; right: PDI).

c) Phosphin Ligand Exchange

As a control reaction, we tested if the triphenylphosphine ligands of the gold species **8** and **4** perform an exchange with the *tert*butylphosphine ligands of the catalyst species [Pd(P(*t*Bu₃)₂)]. The experiments were performed with 2 different ratios of monomer to ligand.

1) In a NMR tube, monomer **8** (9.0 eq, 78 mg, 90 μmol) was dissolved in THF-*d*₈ (0.6 mL) and tri(*tert*butyl)-phosphine (1.0 eq, 2.0 mg, 10 μmol) was added. These ratios are the same as for the polymerization reactions with 10 mol% of catalyst. The reaction was monitored by ³¹P NMR spectroscopy at 65 °C. When the first NMR spectra were recorded, the signal of the tri(*tert*butyl)-phosphine at 63 ppm had already disappeared. A new signal was visible at 92.5 ppm (species **16**). The monomer **8** gave a very broad, slightly shifted signal at 39.7 ppm. The signal ratio stayed constant over the period of 3 h, indicating that a ligand exchange takes place to give a stable equilibrium.

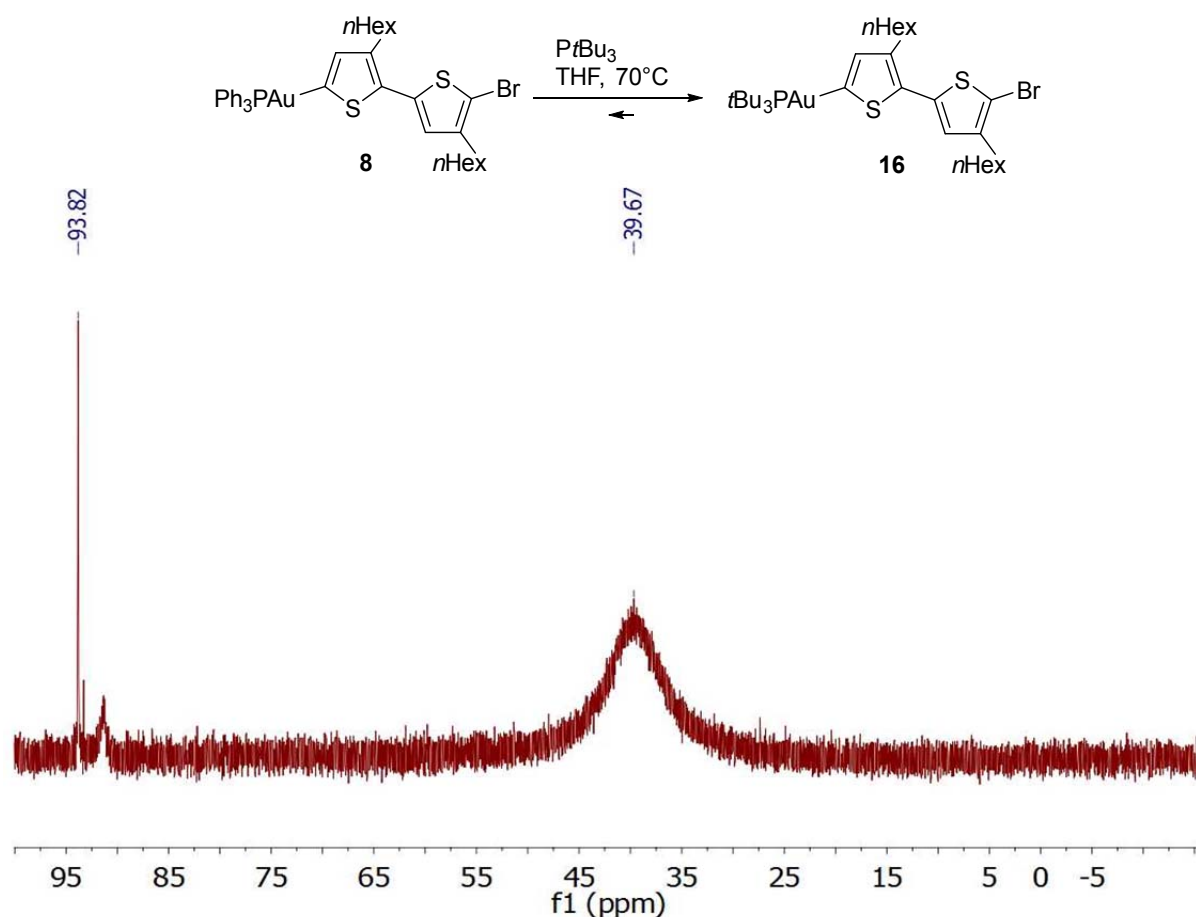


Figure SI 5. Blank test for ligand exchange reaction. In this case, the monomer **8** (broad signal at 39.7 ppm) was used in an excess (9:1) to the ligand. When the first ³¹P NMR spectra were recorded, the signal of the tri(*tert*butyl)-phosphine at 63 ppm had already disappeared. A new signal was visible at 93.8 ppm.

2) To prove that the new signal resulted from the formation of compound **16**, another experiment was performed, where tri(*tert*butyl)-phosphine was used in an excess (9:1): In a NMR tube, Monomer **8** (1.0 eq, 8.7mg, 10 μ mol) was dissolved in THF-*d*₈ (0.6 mL) and tri(*tert*butyl)-phosphine (9.0 eq, 18 mg, 90 μ mol) was added. The reaction was monitored by ³¹P NMR spectroscopy. Here, the signal of the starting material **8** at 43 ppm disappeared entirely (see Figure SI 6). The spectrum displayed peaks at 92.5 ppm indicative of the newly formed compound **16** at, a peak at 63 ppm, which could be attributed to the excess tri(*tert*butyl)phosphine and, as triphenylphosphine is liberated, its signal at -5.4 ppm (Figure 6). This experiment suggests that an entirely different process takes place in the case of [Pd(P*t*Bu₃)₂] as opposed to all other catalysts that were analyzed: When using [Pd(P(*t*Bu₃)₂)] as catalyst species, the butyl ligands are exchanged with the phenyl phosphine ligands of the gold species.

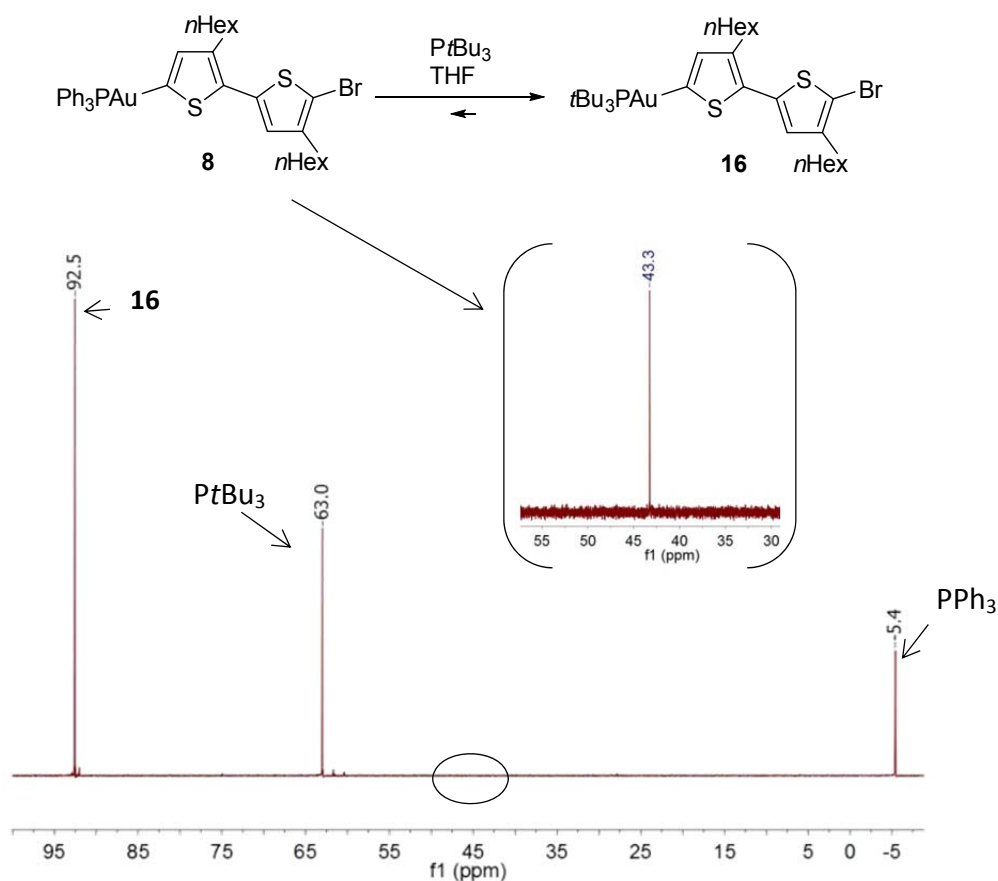
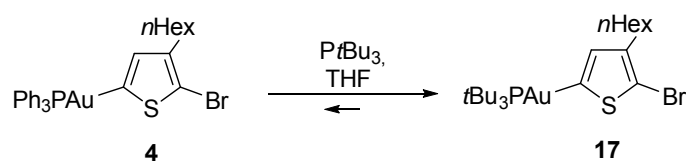


Figure SI 6. Ligand exchange reaction. In this case, PtBu₃ (63.0 ppm) was used in an excess (9:1) to the monomer **8** (not visible at 43.3 ppm). As the whole monomer was converted into the organogold species **16**, 92.5 ppm), PPh₃ became a free ligand (-5.4 ppm).

Both experiments with monomer **4** were performed similar to those with monomer **8**:



3) In a NMR tube, monomer **4** (9.0 eq, 63 mg, 90 μmol) was dissolved in THF- d_8 (0.6 mL) and tri(*tert*butyl)-phosphine (1.0 eq, 2.0 mg, 10 μmol) was added. These ratios are the same as for the polymerization reactions with 10 mol% of catalyst. The reaction was monitored by ^{31}P NMR spectroscopy (Figure SI 7, b)).

4) In a NMR tube, Monomer **4** (1.0 eq, 7.2 mg, 10 μmol) was dissolved in THF- d_8 (0.6 mL) and tri(*tert*butyl)-phosphine (9.0 eq, 18 mg, 90 μmol) was added. The reaction was monitored by ^{31}P NMR spectroscopy.

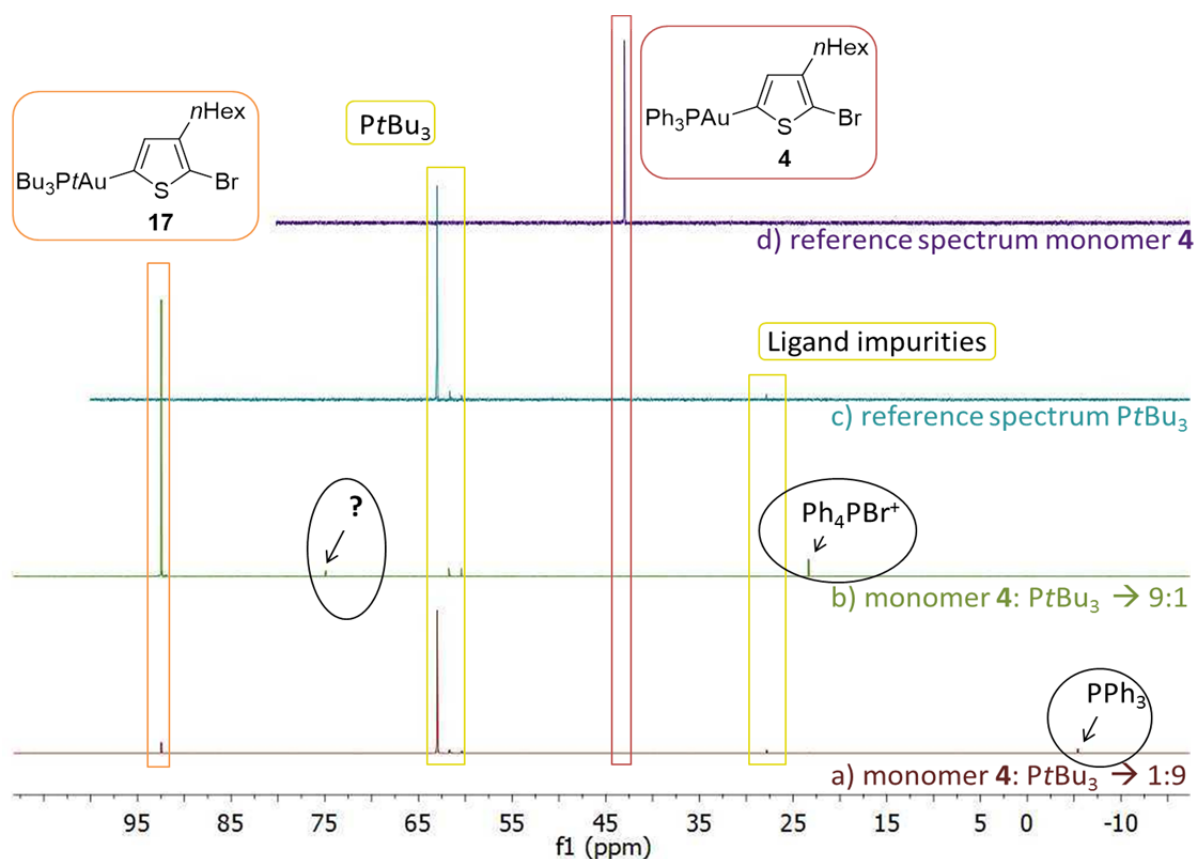
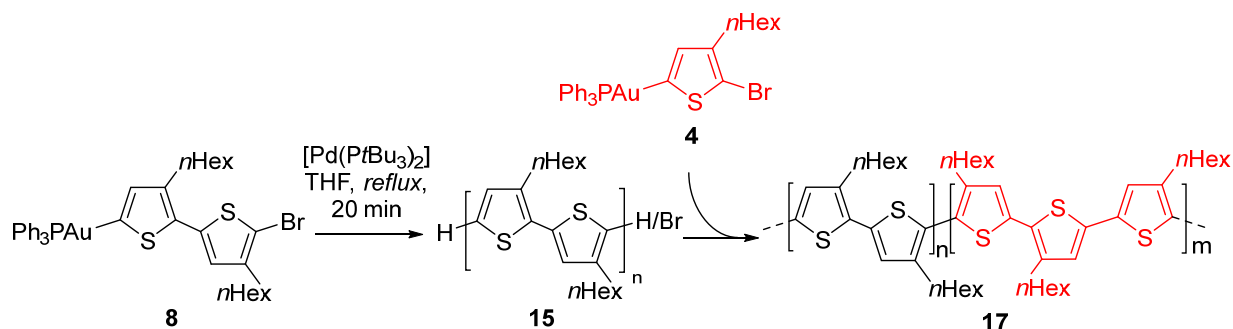


Figure SI 7. Ligand exchange reaction with monomer **4**. Reference spectra show the monomer **4** (spectrum d), 43 ppm) and the ligand itself, PtBu₃ (spectrum c), 63 ppm). In experiment a), PtBu₃ was used in an excess (9:1) with respect to the monomer **4** (no longer visible at 43.3 ppm). As the whole monomer was converted into the organogold species **17**, 92.5 ppm), PPh₃ dissociated (-5.4 ppm). In reaction b), the monomer **4** (no longer visible at 43.3 ppm) was used in an excess (9:1) with respect to PtBu₃ (no longer visible at 63.0 ppm). The newly formed, expected organogold species **17** was formed. However, in addition to this, the excess of **4** was converted to another, undefined species (74 ppm); the formation of [Ph₄PBr⁺]^[29] was confirmed as well (24 ppm).

d) Kinetic Studies II: Addition of monomer 4 to a growing polymer chain to analyze if the reaction follows a living mechanism.



In the glove box, 5'-bromo-3,4'-dihexyl-5-triphenylphosphinegold-2,2'-bithiophene (174 mg, 200 μ mol) and $[\text{Pd}(\text{tBu}_3)_2]$ (5.1 mg, 10 μ mol, 5 mol%) were placed in a Schlenk flask. THF (8 mL) was added to the solution and the mixture was stirred at 70 $^\circ\text{C}$ for 20 min. In another flask, 2-bromo-3-n-hexyl-5-triphenylphosphinegold-thiophene (3 eq., 211 mg, 0.300 mmol) was diluted in THF (2 mL) and warmed to 70 $^\circ\text{C}$. After 20 min, 4 mL of the polymerization mixture was added to the stirring mixture of the monomer 4. After the 25, 40, 60, 90, 150, 210, 330, 600 and 900 min, a sample (0.3 mL) was taken out of the reaction mixture and quenched with a 1 M solution of HCl in methanol (3 mL). The sample was taken out of the glovebox, opened to air and diluted with DCM (4 mL) and water (2 mL). After shaking the vial, the layers were separated. The organic phase was dried over sodium sulfate, filtered and the solvents were removed in vacuo. Half of the resulting red residue was diluted in chloroform (HPLC grade, 4 mL) and used for GPC analysis. The other half was diluted in CDCl_3 and used for NMR analysis.

Table SI 9. Results for polymerization reaction where 2-bromo-3-n-hexyl-5-triphenyl-phosphinegold-thiophene (**4**) was added after 20 min to a growing polymer chain to analyze if the reaction follows a living mechanism.

time (min)	M_n	M_w	PDI	$M_n (+)$	$M_w (+)$	PDI (+)
25	9195	19827	2.15	8013	17705	2.2
40	9046	19414	2.1	7946	14708	1.95
60	9097	20381	2.2	2207	9318	4.2
90	9113	20970	2.3	3292	11017	3.3
150	10947	23690	2.2	4838	14741	3.04
210	8809	20519	2.3	11463	26367	2.3
330	9343	21281	2.2	11466	25459	2.2
600	9209	21987	2.3	12495	32587	2.6
900	8621	20717	2.4	22324	58321	2.6

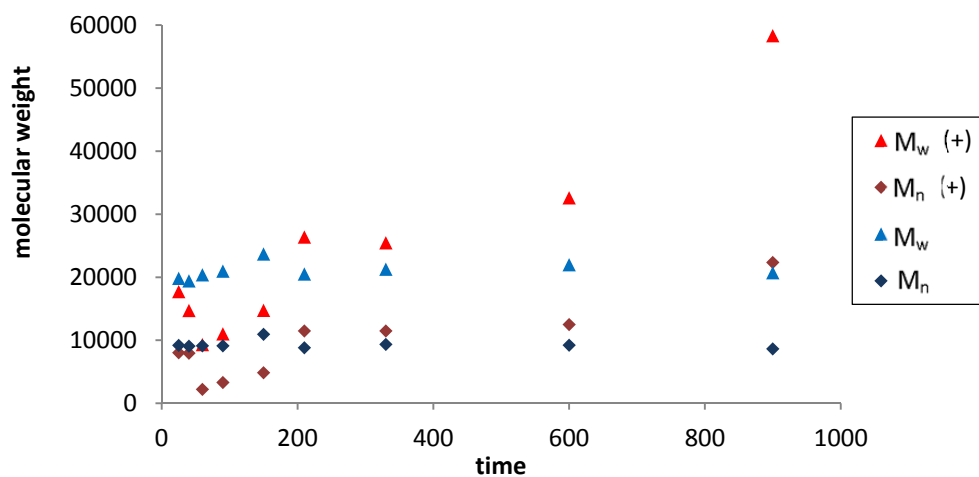


Chart SI 7. Shown are the results of kinetic control. M_n (+) and M_w (+) (red) present the reaction with addition of the second monomer **4**, where M_n and M_w (blue) present the control reaction that was running in parallel.

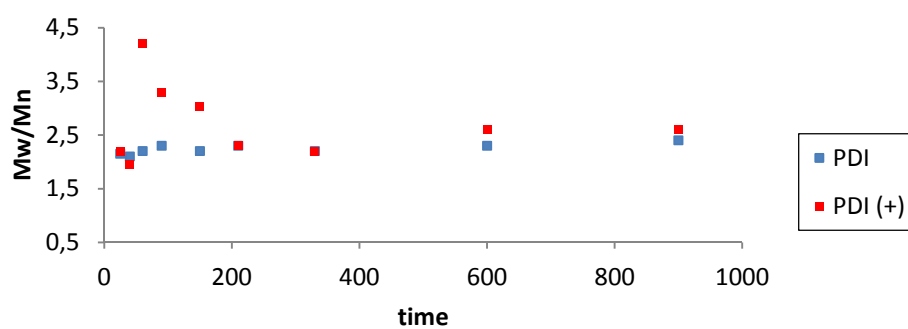


Chart SI 8. Shown are the PDI results of kinetic control. PDI (+) (red) present the reaction with addition of the second monomer **4**, where PDI (blue) present the control reaction that was running parallel.

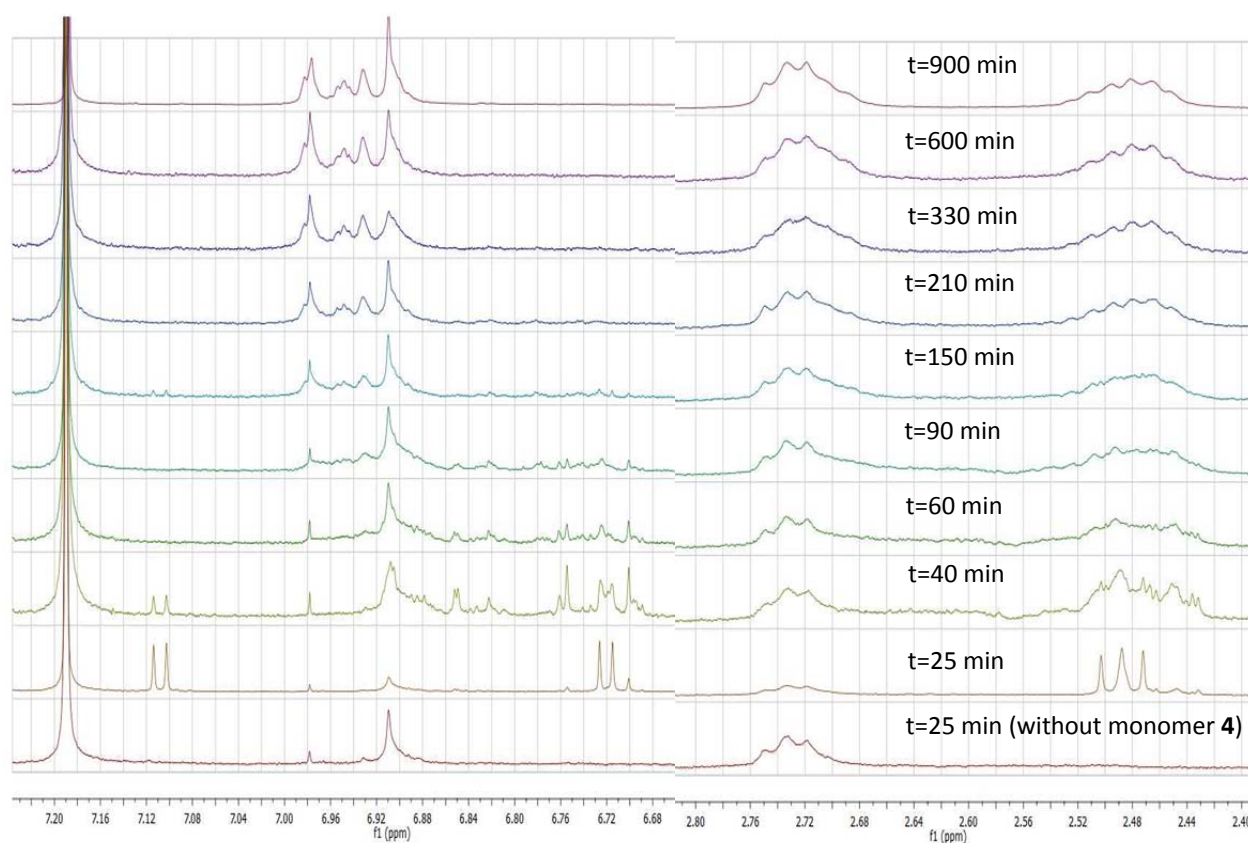
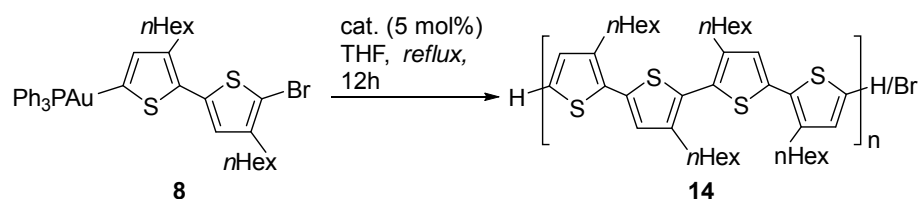


Chart SI 9. Shown are the ^1H NMR results of kinetic control (aryl and alkyl region). At $t = 25$ min, without monomer **4**, the reference spectrum of the parallel running polymerization reaction without addition of the monomer **4** is shown (at 6.98 ppm, the signal presents a satellite of chloroform.) At $t = 25$ min, two clear doublets are shown. During the work-up, the added monomer **4** was quenched by HCl, resulting in 2-bromo-3-*n*-hexylthiophene. In addition, the singlet of the *rr*-P3HT (6.9 ppm) is present, its CH_2 group (2.7 ppm) and the CH_2 group of the monomer (2.5 ppm). At $t = 40$ min, it is clearly visible that a lot of smaller chains are formed which are getting longer until at $t = 210$ min, a “homogenous” polymer is formed. These results corresponding will with the GPC data. The ratio of CH_2 groups at 2.7 ppm and 2.5 ppm = 50 : 50.

e) For *rr*-HH-TT-P3HT with [Pd(PPh_tBu₂)₂] as catalyst species at 70 °C



In the glove box, 5'-bromo-3,4'-dihexyl-5-triphenylphosphinegold-2,2'-bithiophene (174 mg, 200 μ mol) and [Pd(PPh_tBu₂)₂] (5 mol%) were placed in a Schlenk flask. THF (8 mL) was added to the solution and the mixture was stirred at 70 °C for the specified time. In regular intervals (see table SI 10), a sample (0.3 mL) was taken out of the reaction mixture and quenched with a 1 M solution of HCl in methanol (3 mL). The sample was taken out of the glovebox, opened to air and diluted with DCM (4 mL) and water (2 mL). After shaking the vial, the layers were separated. The organic phase was dried over sodium sulfate, filtered and the solvents were removed *in vacuo*. Half of the resulting red residue was diluted in chloroform (HPLC grade, 4 mL) and used for GPC analysis. The other half was diluted in CDCl₃ and used for NMR analysis.

Table SI 10. Kinetic Data measured by GPC.

Entry	M _n	M _w	PDI
1	683	739	1
2	675	710	1
3	798	852	1
4	915	1114	1.21
5	1353	2369	1.75
6	8202	14290	1.87
7	10856	26383	2.4
8	14971	36133	2.41
9	16745	39778	2.4

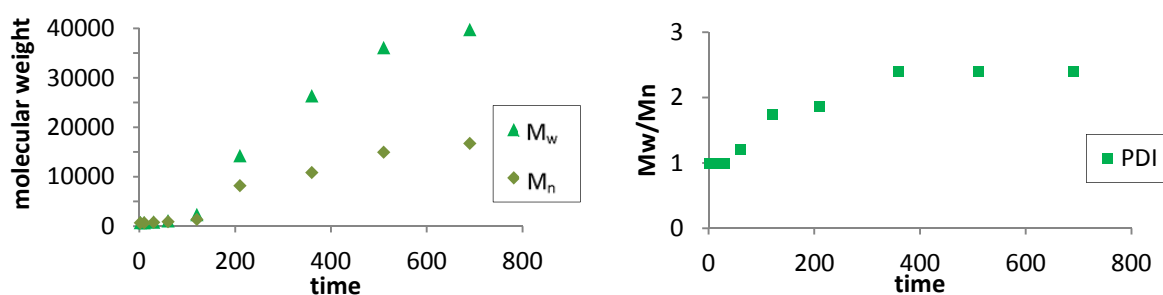


Chart SI 10. Shown are the results of the kinetic control reaction with [Pd(PPh_tBu₂)₂] as catalyst species at 70 °C.

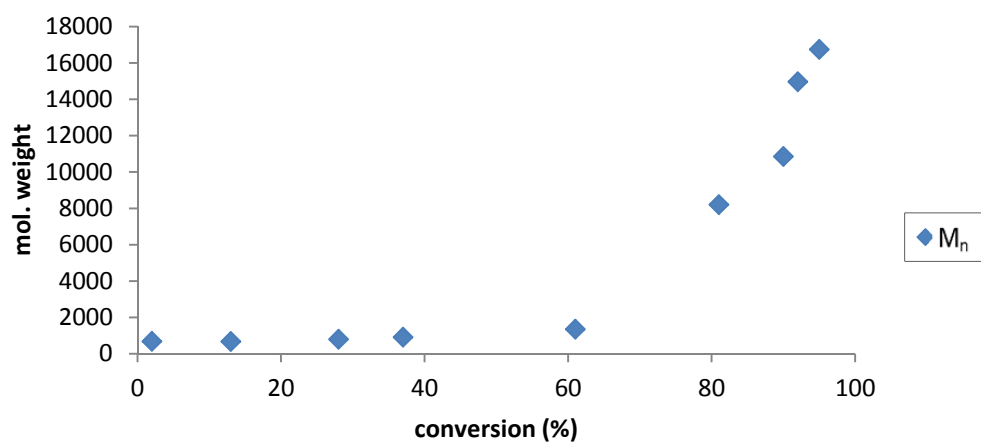


Chart SI 11. The conversion of the monomer **8** was calculated by integration of the corresponding ^1H NMR spectra which may result in some error. Nevertheless it is clearly visible that the polymerization to give high molecular weights starts very slowly. The molecular weight starts to increase after a conversion of 60%.

f) Comparing Data of *rr*-HT-P3HT and *rr*-HH-TT-P3HT

Many data points for the different polymers were measured. Here, some of the most significant differences are presented to a better comparison of the two species:

Kinetic

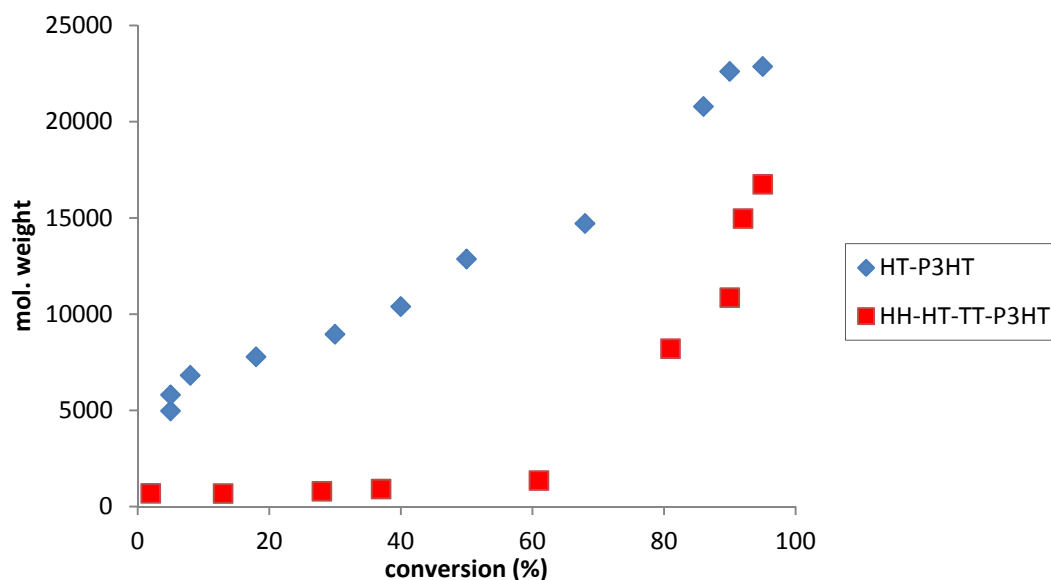


Chart SI 12. The polymers HT-P3HT (**15**, blue) and HH-TT-P3HT (**14**, red) were prepared by using the same monomers but different catalyst species. The chain growth shows distinct differences: while HH-TT-P3HT was formed slowly and high molecular weight can be observed at high conversion (>70%), the HT-P3HT was formed in a continuous way of chain growth.

UV-Vis

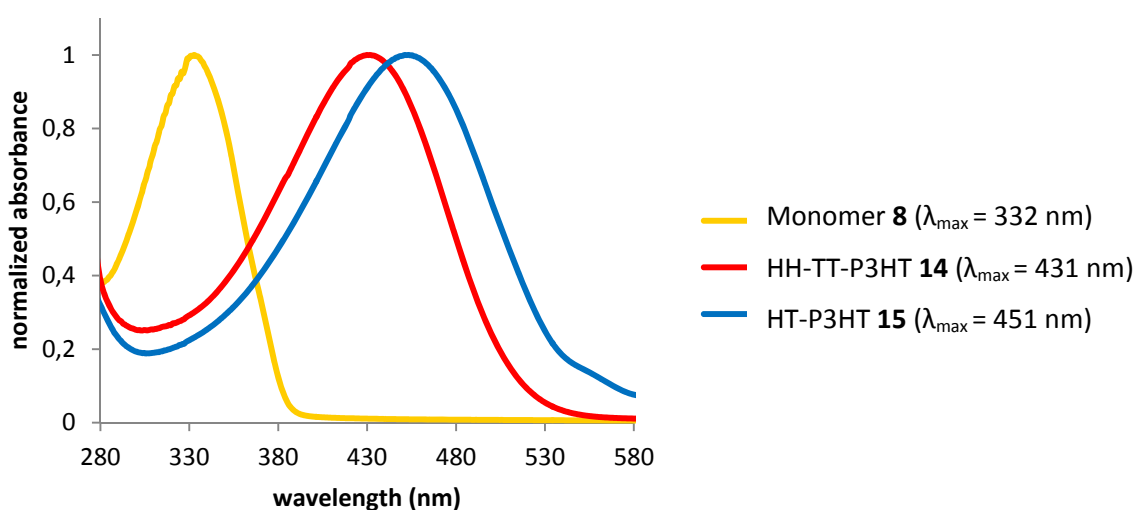


Figure SI 7: UV spectra of the monomer (**8**, yellow), HH-TT-P3HT (**14**, red) and the HT-P3HT (**15**, blue).

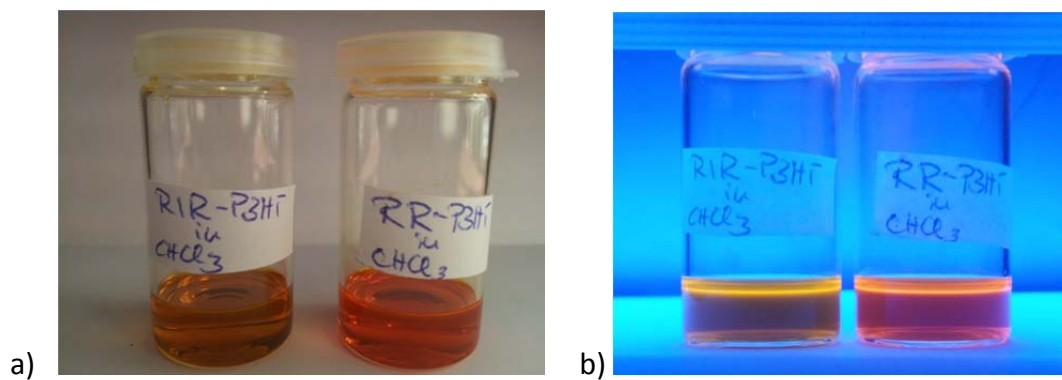
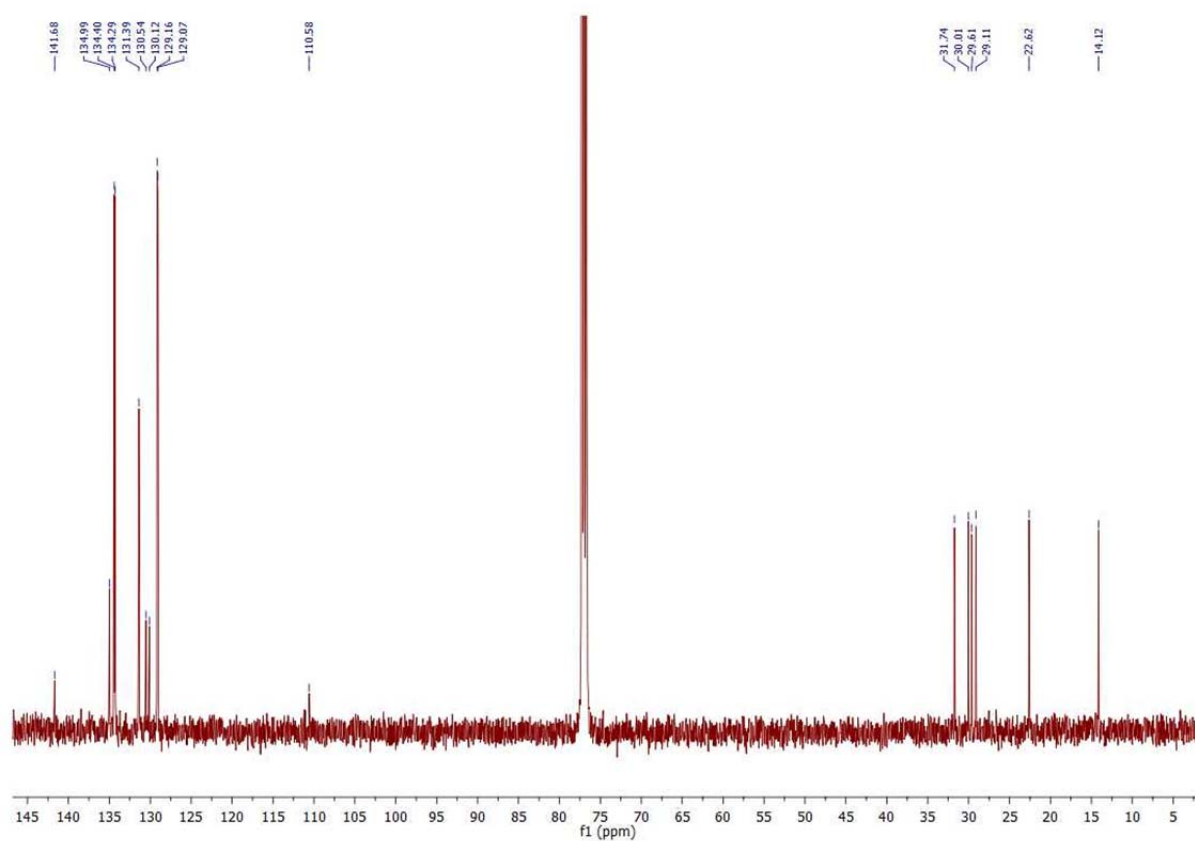
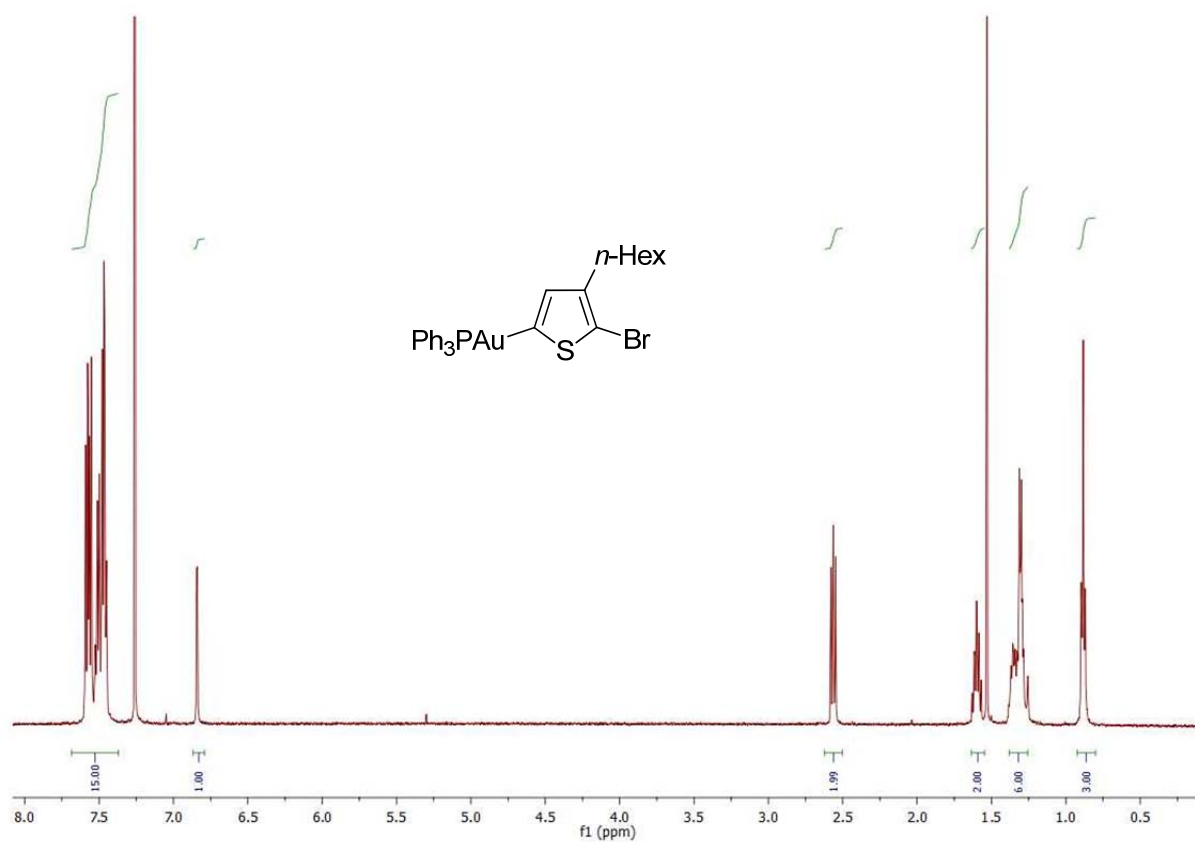
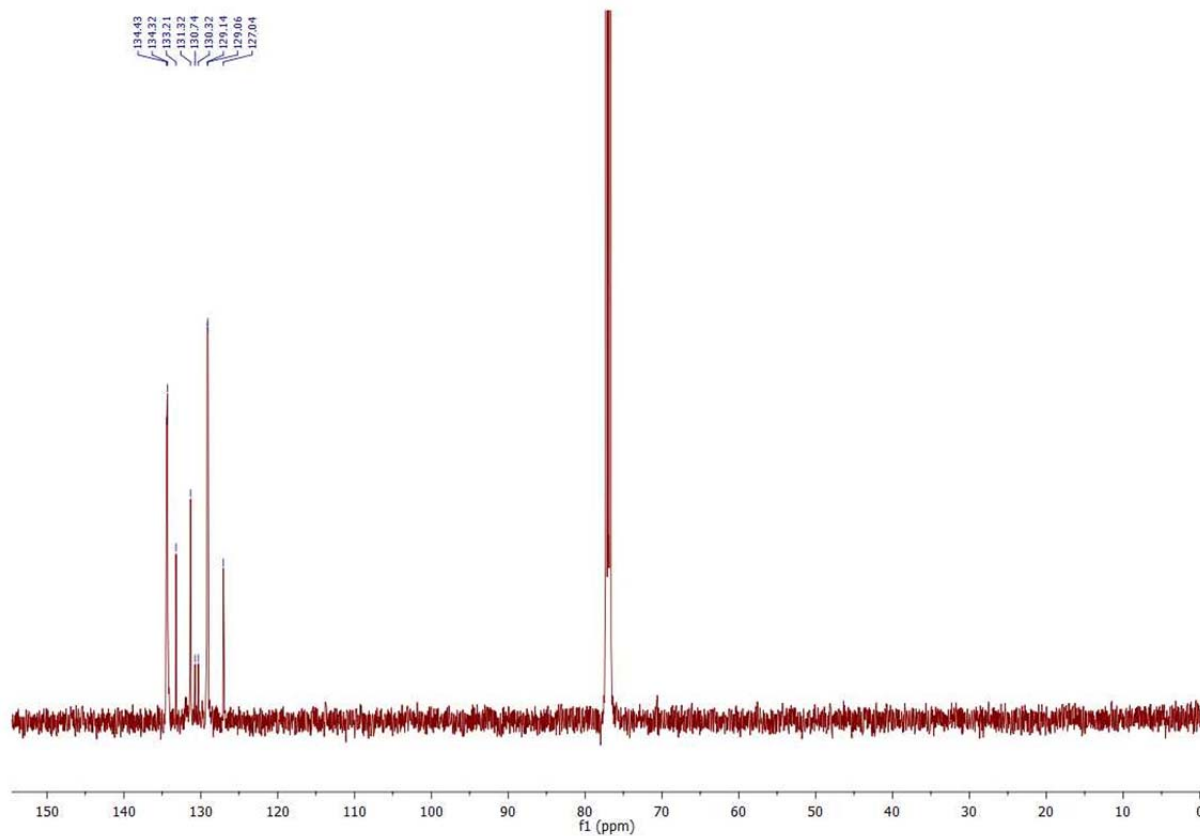
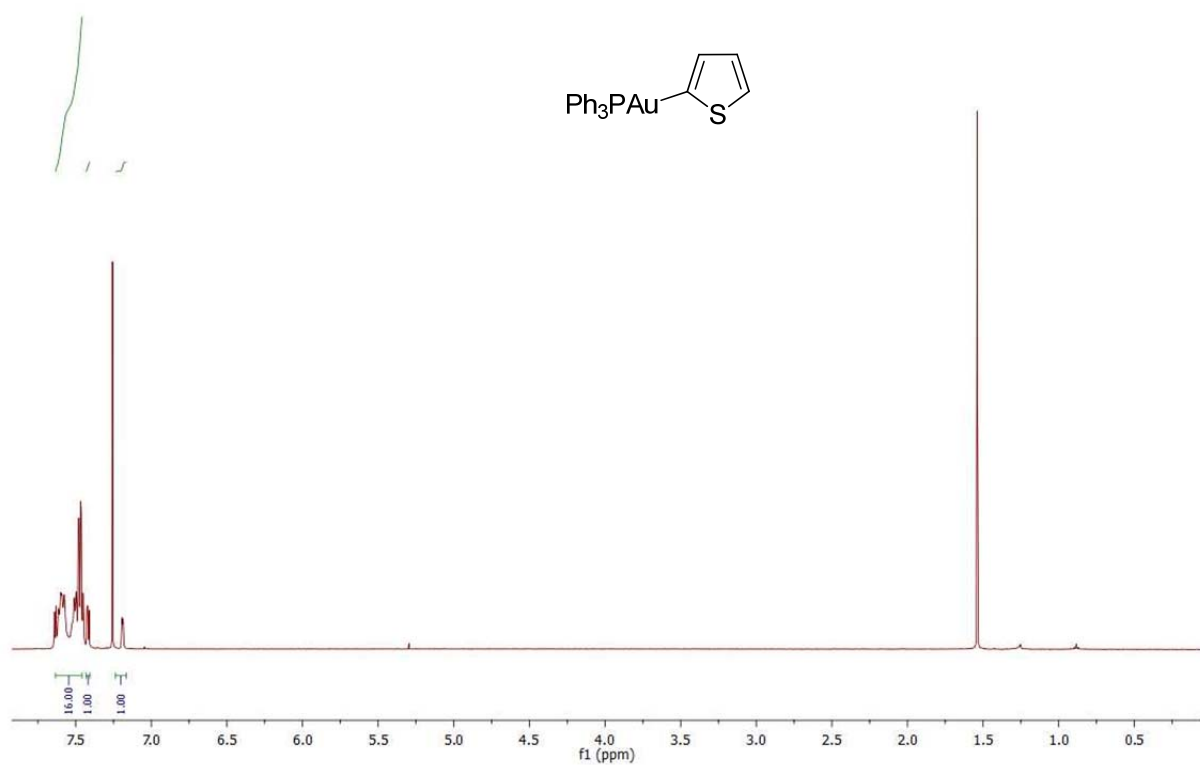
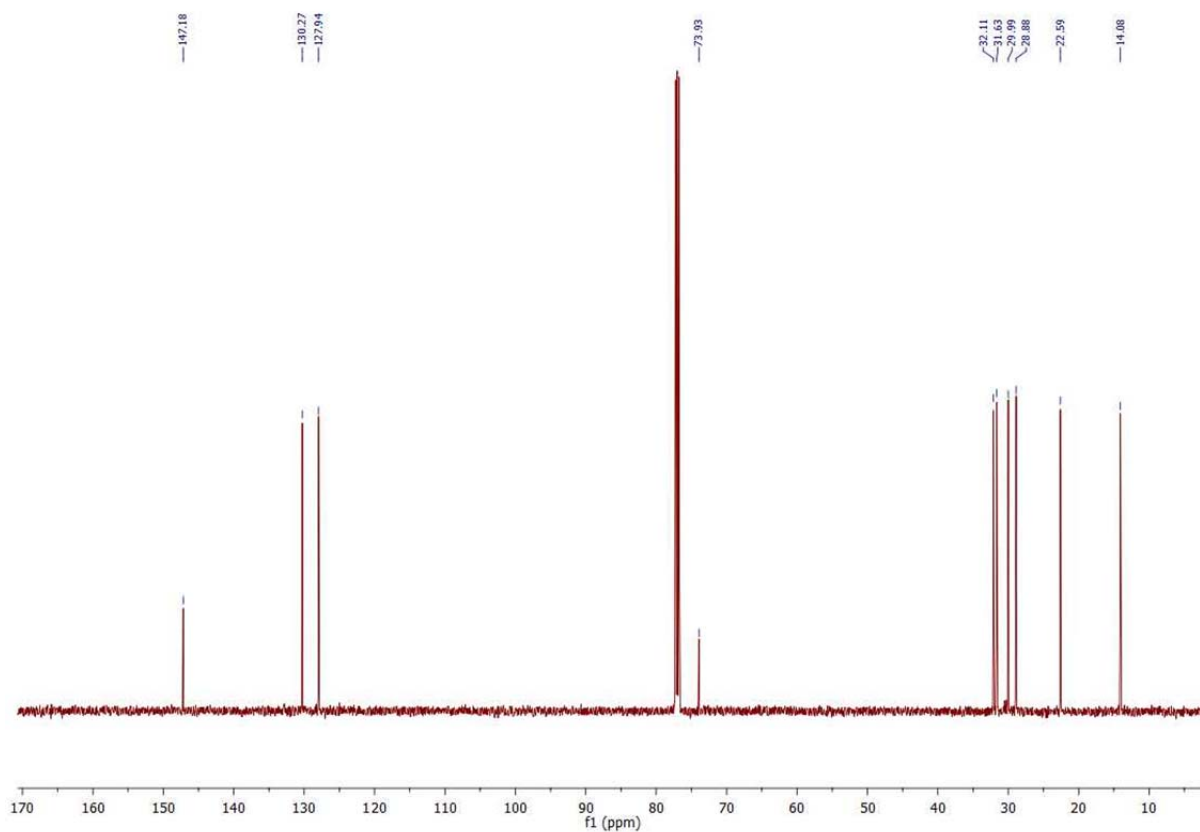
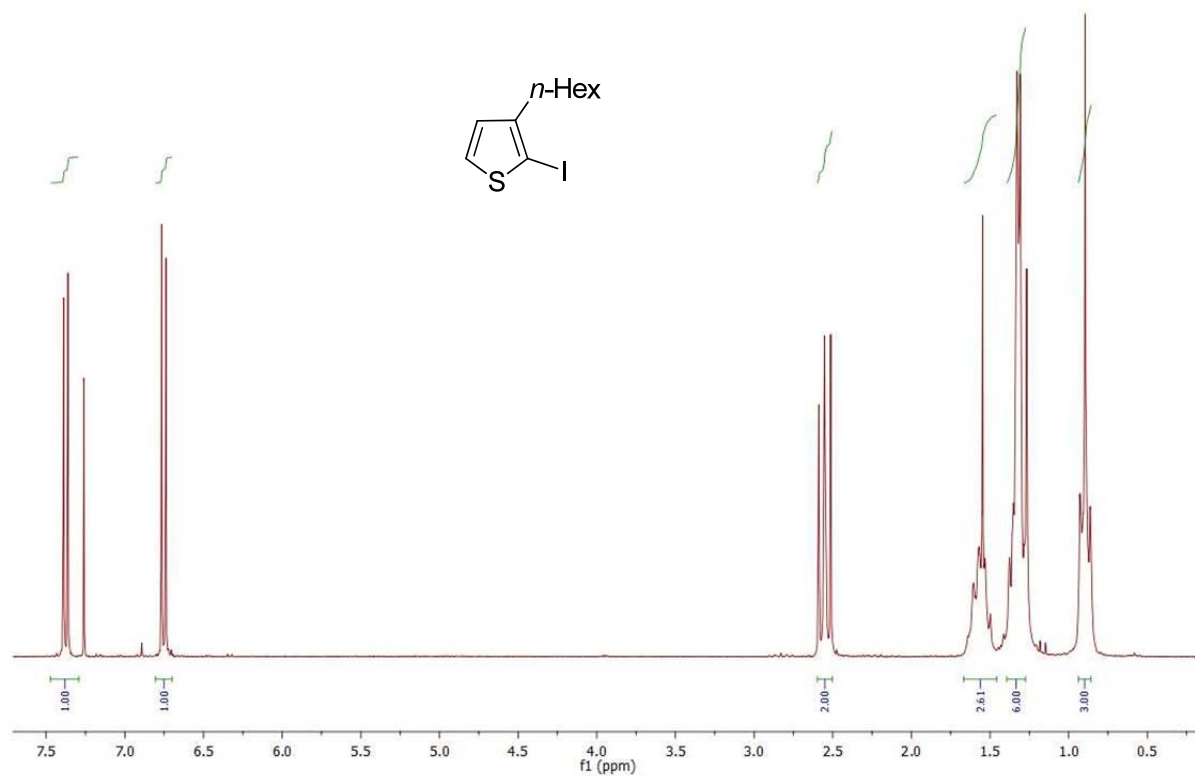
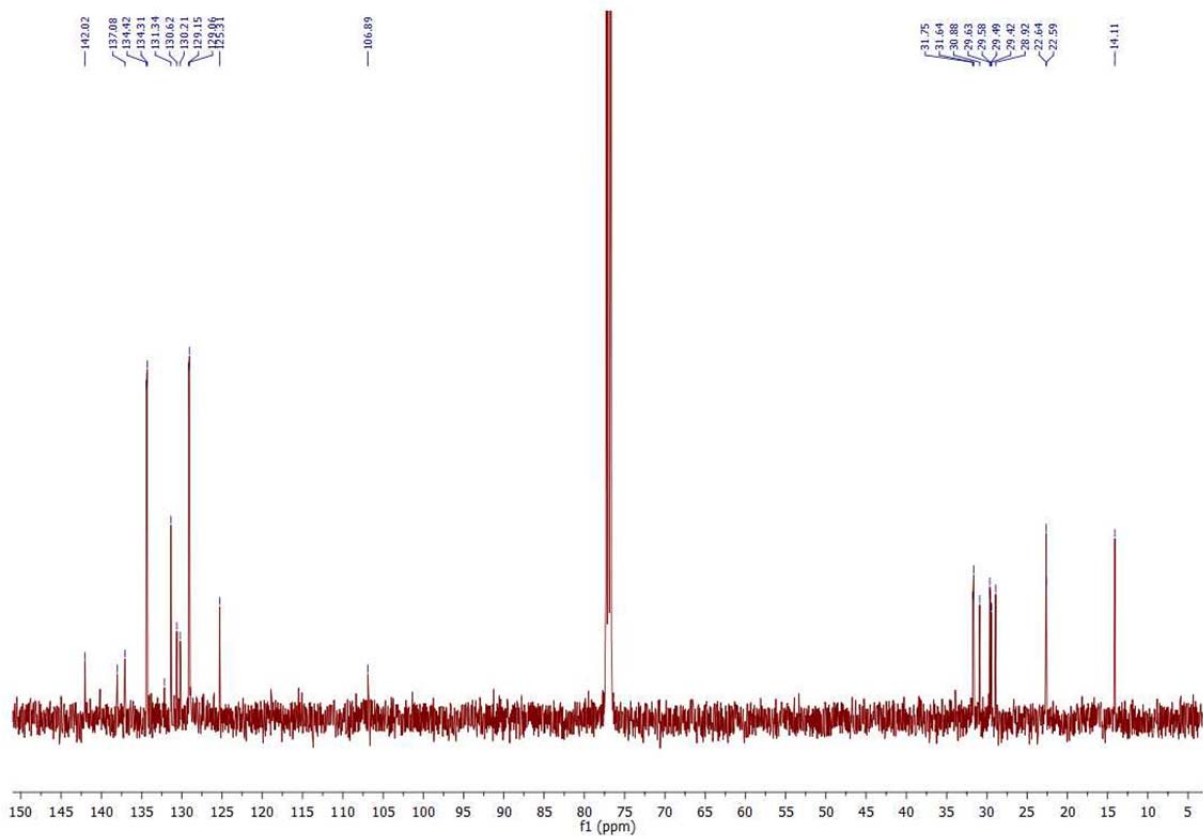
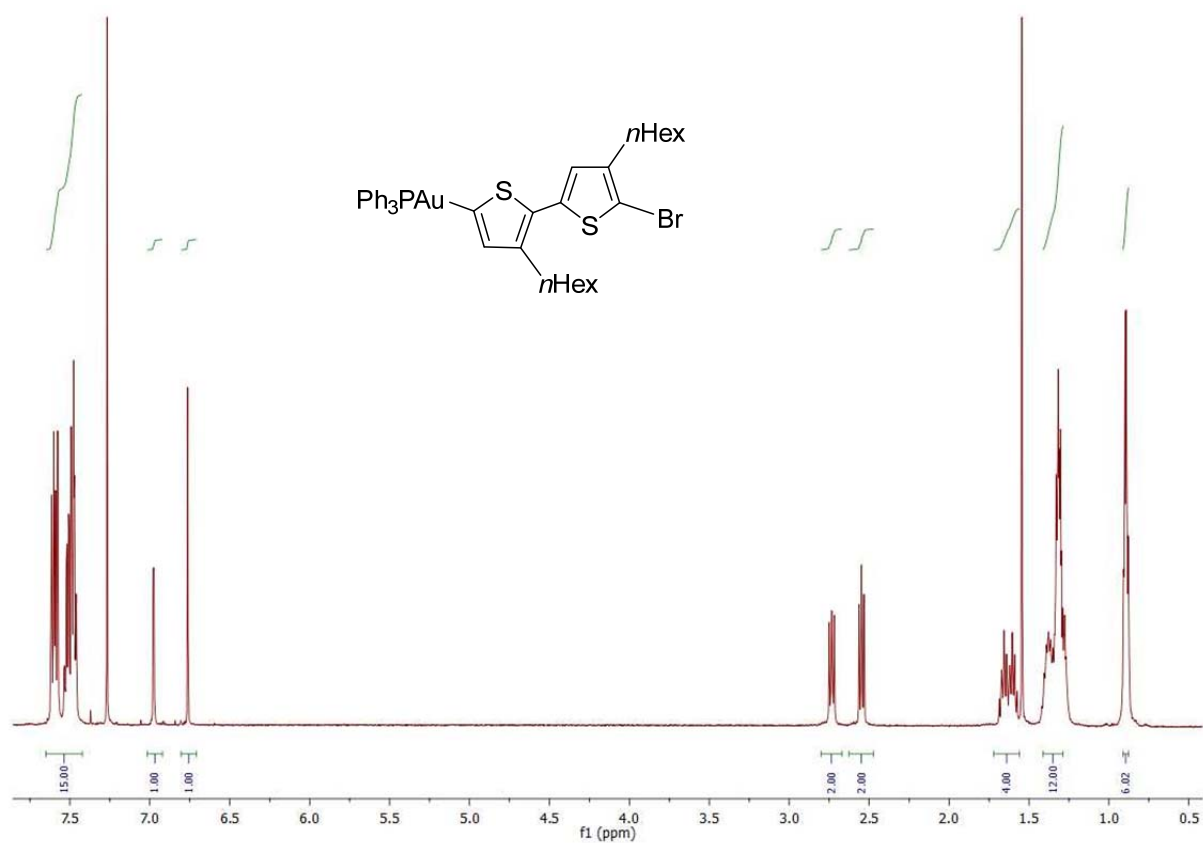


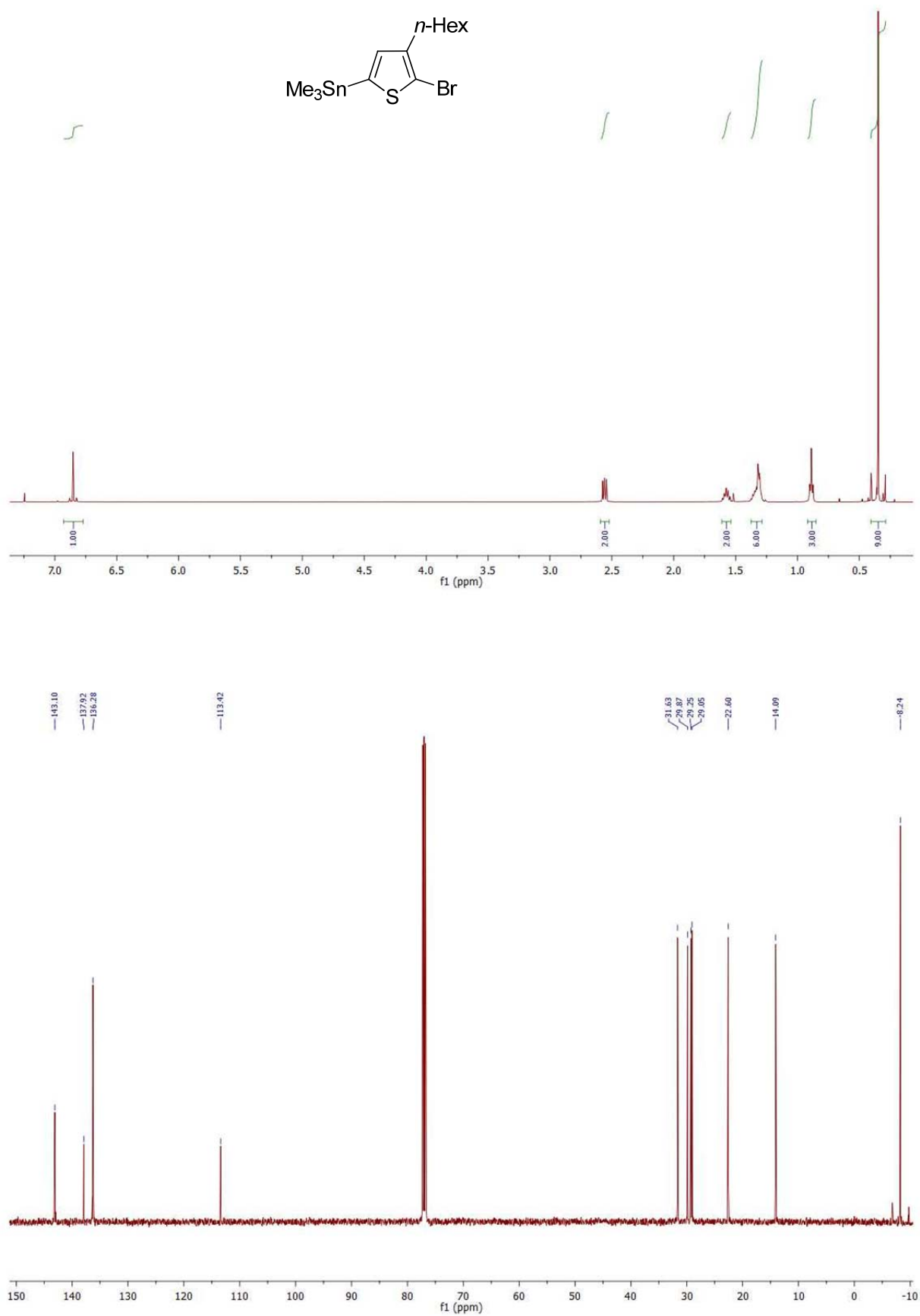
Figure SI 8. Pictures of the two P3HT species in solution (CHCl_3); a) under day light; b) under UV-light (420 nm). Clear color differences are visible.

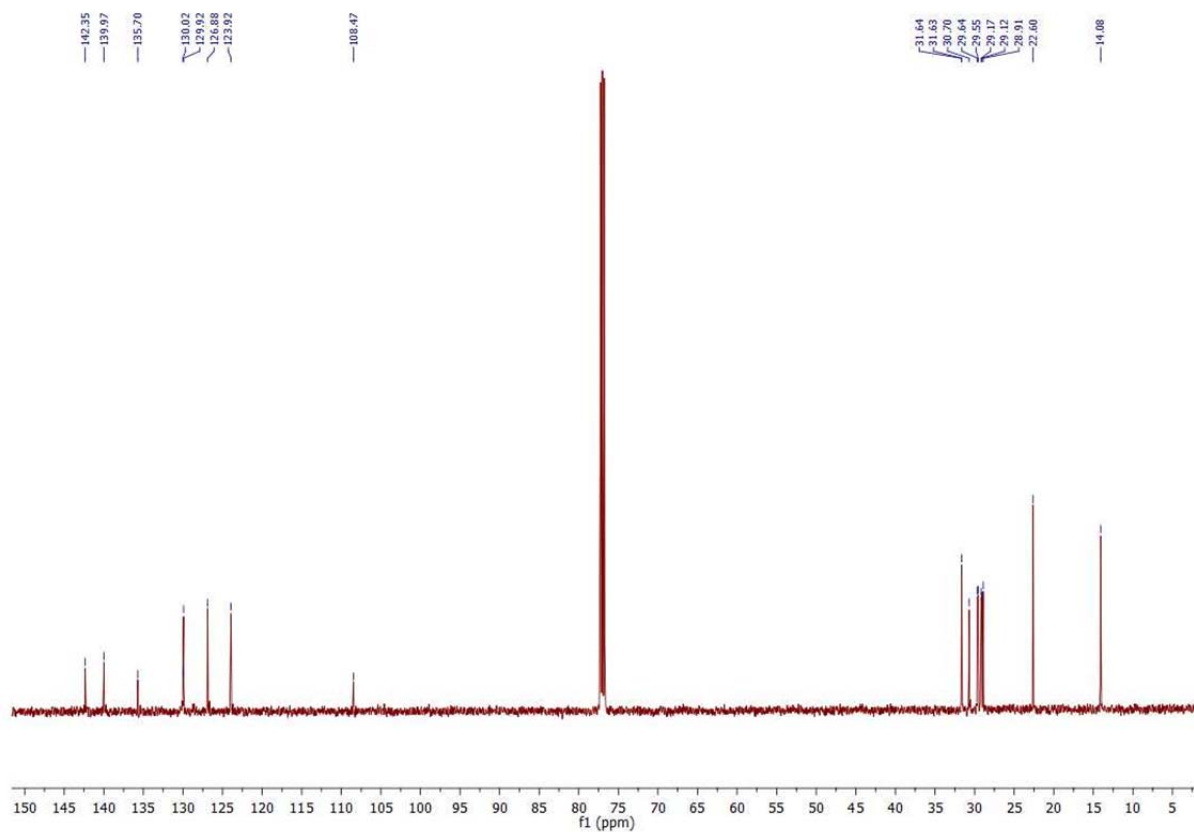
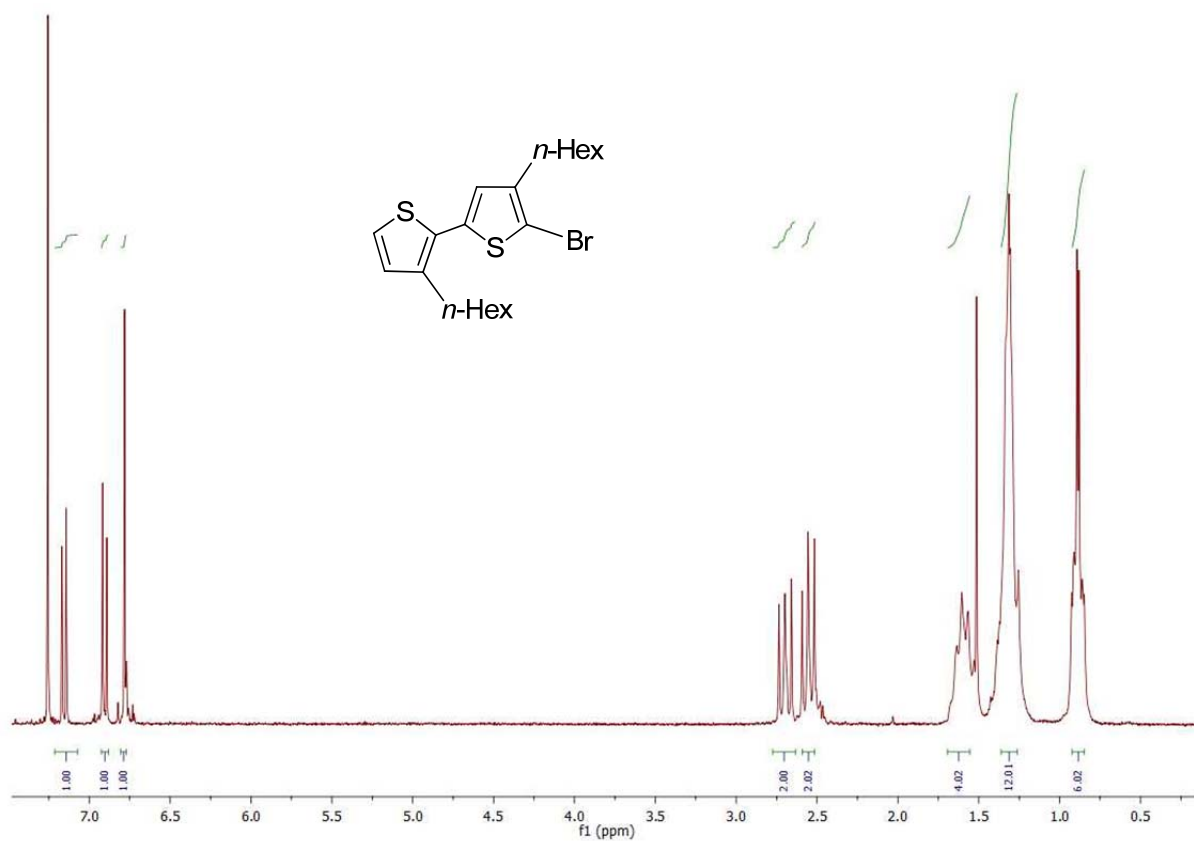
^1H NMR Spectra and $^{13}\text{C}\{^1\text{H}\}$ NMR Spectra**2-Bromo-3-*n*-hexyl-5-(triphenylphosphin)gold(I)-thiophene (4, CDCl_3)**

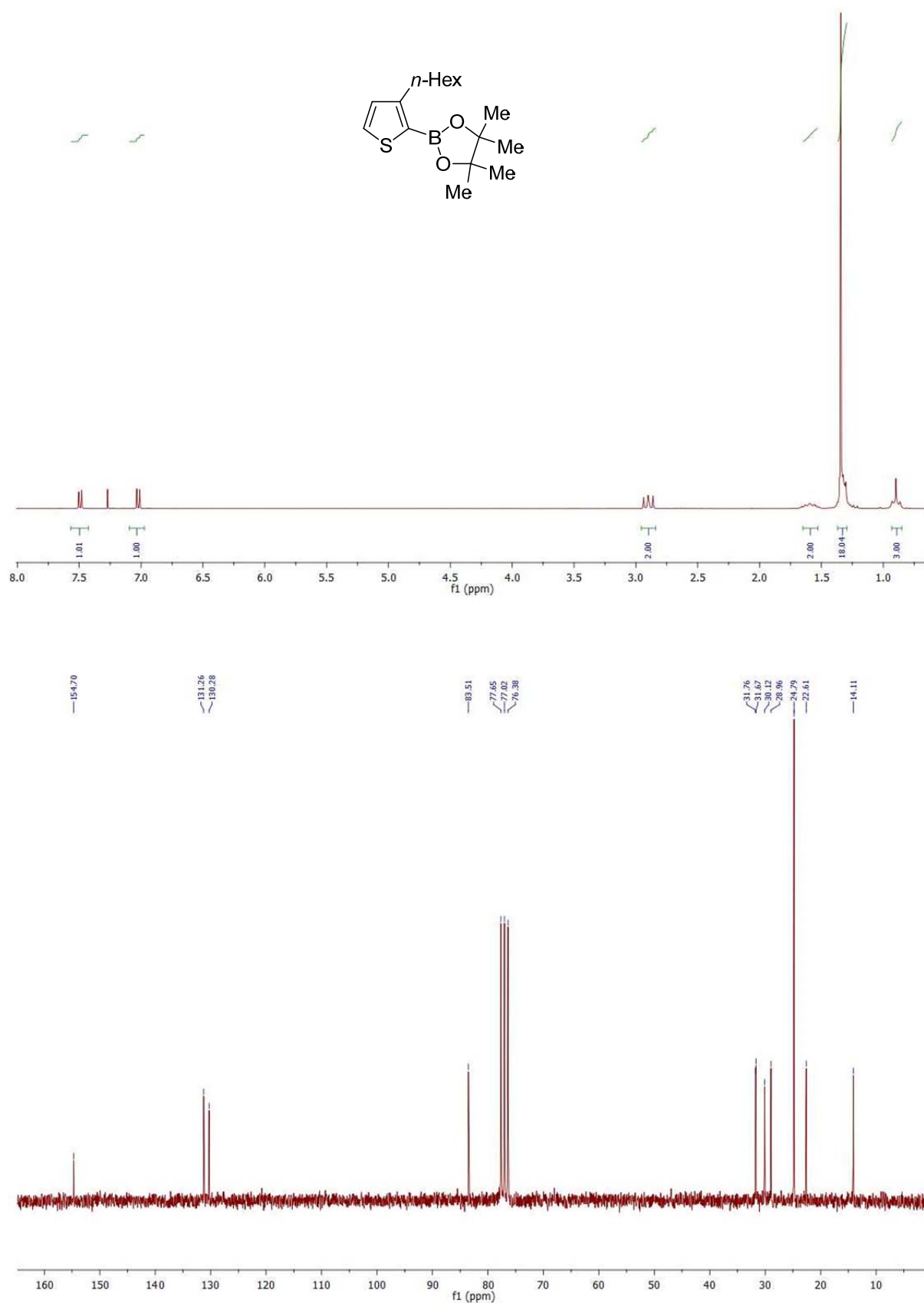
2-(Triphenylphosphin)gold(I)-thiophene (5, in CDCl₃)

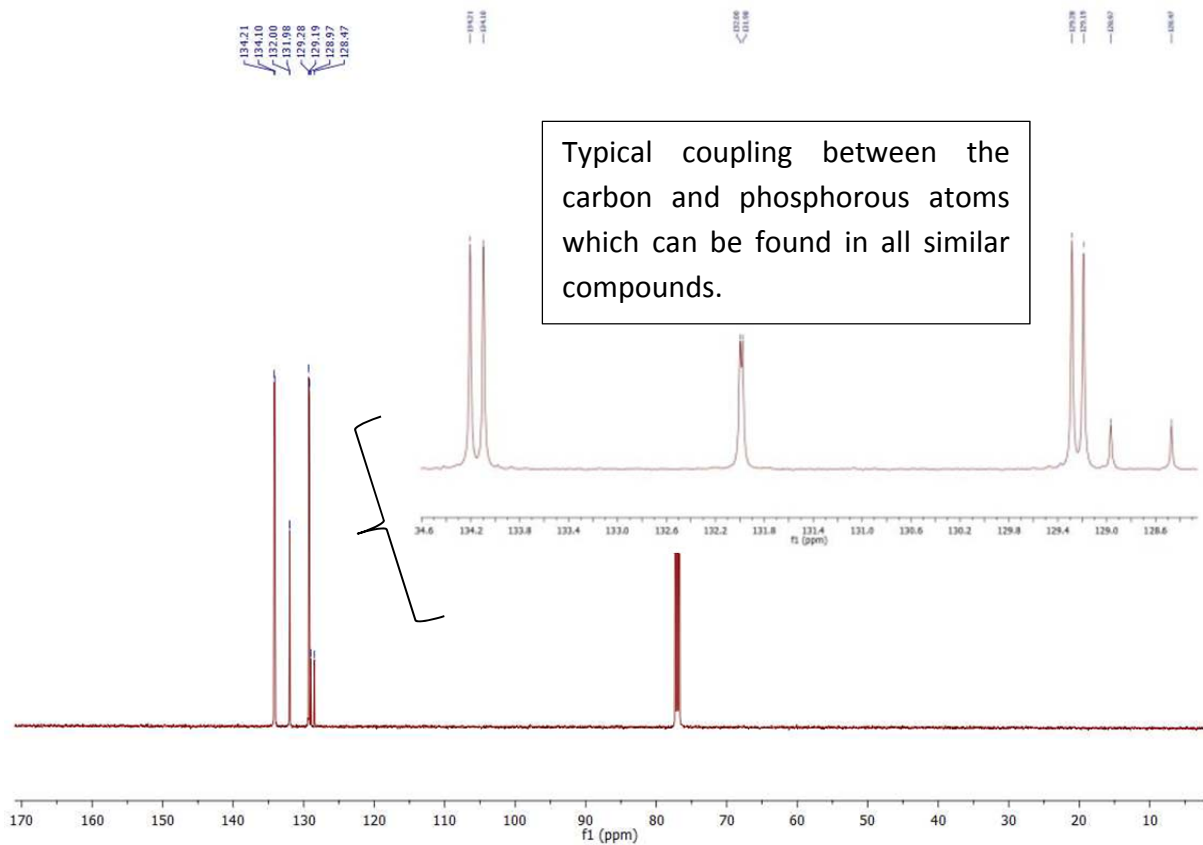
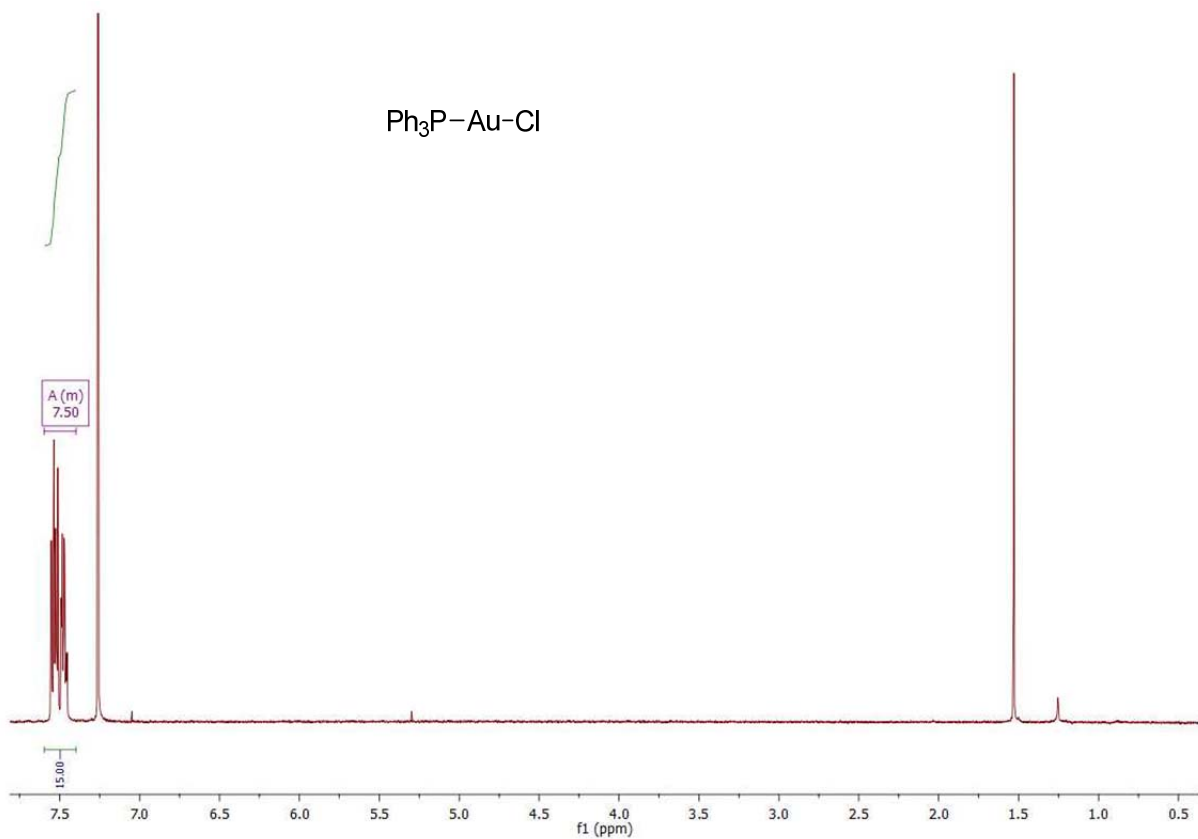
2-Iodo-3-*n*-hexyl-thiophene (6, in CDCl₃)

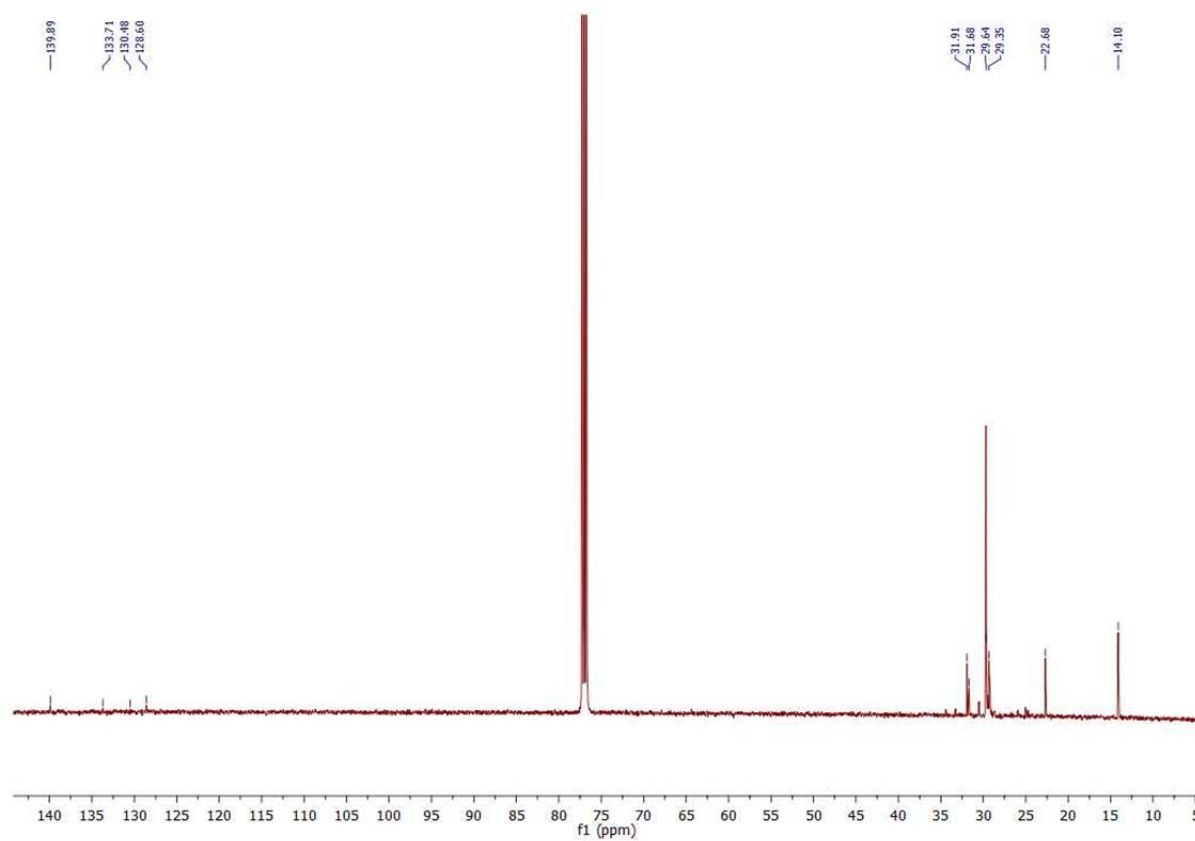
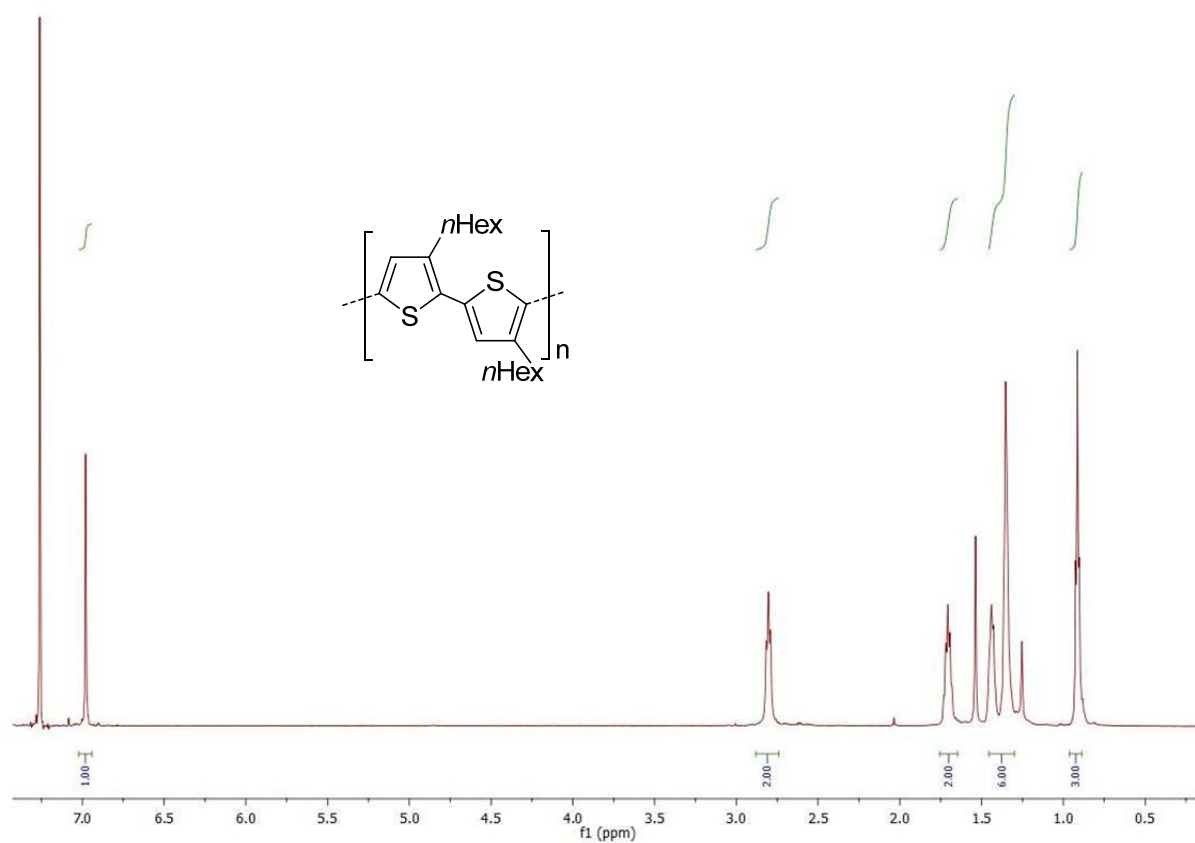
5'-Bromo-3,4'-dihexyl-5-triphenylphosphine-2,2'-bithiophene (8, in CDCl₃)

2-Bromo-3-*n*-hexyl-5-trimethyltin-thiophene (9, in CDCl₃)

5'-Bromo-3,4'-dihexyl-2,2'-bithiophene (10, in CDCl₃)

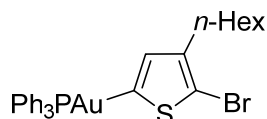
2-(3-Hexylthiophen-2-yl)-4,4,5,5-tetramethyl-1,3,2-dioxaborolane (11, in CDCl₃)

Triphenylphosphine gold(I) chloride (13, in CDCl₃)

RR-P3HT (15, in CDCl₃)

Single Crystal Data

2-Bromo-3-*n*-hexyl-5-(triphenylphosphin)gold(I)-thiophene (4)



The data were measured using an Imaging Plate Diffraction System (IPDS-1) from STOE & CIE and were corrected for absorption using X-Red and X-Shape from STOE & CIE (Min/max. transmission: 0.4839/0.7604). The structure was solved with direct methods using SHELXS-97 and refinement was performed against F^2 using SHELXL-97. All non-hydrogen atoms were refined anisotropic. The C-H H atoms were positioned with idealized geometry and refined isotropic with $U_{\text{iso}}(\text{H}) = 1.2 \cdot U_{\text{eq}}(\text{C})$ (1.5 for methyl H atoms) using a riding model. A numerical absorption correction was performed (Tmin/max: 0.2761/0.3969). Selected crystal data and details on the structure determination can be found in table 11-15 (see below).

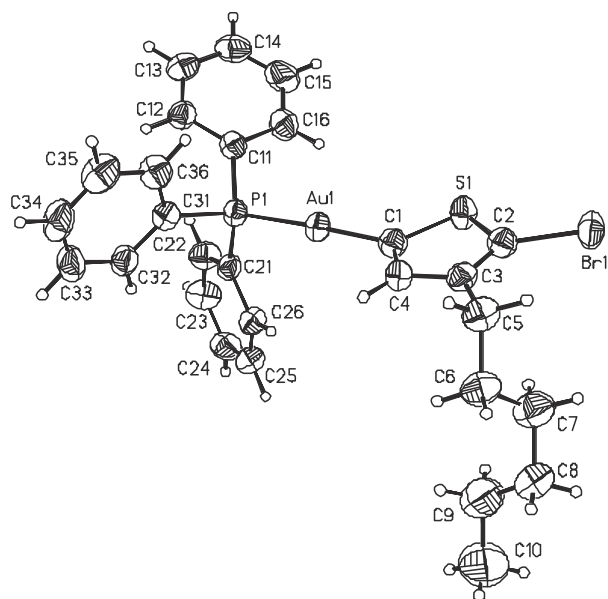
Table SI 11. Crystal data and structure refinement for $\text{C}_{28}\text{H}_{29}\text{SPBrAu}$.

Empirical formula	$\text{C}_{28}\text{H}_{29}\text{AuBrPS}$	
Formula weight	705.42	
Temperature	200(2) K	
Wavelength	0.71073 Å	
Crystal system	triclinic	
Space group	P-1	
Unit cell dimensions	$a = 8.9278(3)$ Å	$\alpha = 70.108(3)^\circ$.
	$b = 10.9973(4)$ Å	$\beta = 77.035(3)^\circ$.
	$c = 14.8969(5)$ Å	$\gamma = 89.177(3)^\circ$.
Volume	$1337.21(8)$ Å ³	
Z	2	
Density (calculated)	1.752 Mg/m ³	
Absorption coefficient	7.147 mm ⁻¹	
F(000)	684	
Crystal size	0.12 x 0.09 x 0.06 mm ³	
Theta range for data collection	1.97 to 27.00°.	
Index ranges	-11 ≤ h ≤ 11, -14 ≤ k ≤ 14, -19 ≤ l ≤ 18	
Reflections collected	16381	
Independent reflections	5813 [R(int) = 0.0377]	
Completeness to theta = 27.00°	99.7 %	
Refinement method	Full-matrix least-squares on F^2	
Data / restraints / parameters	5813 / 0 / 279	
Goodness-of-fit on F^2	1.074	

Final R indices [$I > 2\sigma(I)$]	R1 = 0.0310, wR2 = 0.0669
R indices (all data)	R1 = 0.0379, wR2 = 0.0693
Largest diff. peak and hole	1.043 and -0.800 e.Å ⁻³

Table SI 12. Atomic coordinates ($\times 10^4$) and equivalent isotropic displacement parameters ($\text{Å}^2 \times 10^3$). U(eq) is defined as one third of the trace of the orthogonalized U_{ij} tensor.

	x	y	z	U(eq)
Au(1)	3803(1)	7589(1)	4439(1)	39(1)
C(1)	3402(5)	8135(4)	3070(4)	41(1)
S(1)	1913(1)	9086(1)	2768(1)	44(1)
C(2)	2422(5)	9167(4)	1559(4)	42(1)
Br(1)	1262(1)	10075(1)	669(1)	53(1)
C(3)	3676(5)	8489(4)	1374(3)	39(1)
C(4)	4207(5)	7915(4)	2256(4)	40(1)
C(5)	4389(6)	8322(5)	421(4)	50(1)
C(6)	4087(6)	6957(6)	420(5)	57(1)
C(7)	2417(7)	6650(6)	477(6)	70(2)
C(8)	2038(8)	5274(6)	512(6)	71(2)
C(9)	2008(12)	4262(8)	1472(7)	101(3)
C(10)	1542(11)	2908(8)	1553(9)	115(3)
P(1)	4339(1)	6911(1)	5953(1)	35(1)
C(11)	3883(5)	8008(4)	6631(3)	39(1)
C(12)	4797(5)	8202(5)	7220(4)	44(1)
C(13)	4370(6)	9016(5)	7747(4)	52(1)
C(14)	3019(6)	9631(5)	7710(5)	59(1)
C(15)	2112(7)	9451(6)	7131(5)	67(2)
C(16)	2529(6)	8648(5)	6587(4)	54(1)
C(21)	3315(4)	5372(4)	6760(4)	39(1)
C(22)	2889(6)	5052(5)	7768(4)	50(1)
C(23)	2057(6)	3882(5)	8359(5)	58(1)
C(24)	1643(6)	3041(5)	7934(5)	55(1)
C(25)	2069(6)	3349(5)	6933(5)	56(1)
C(26)	2898(5)	4516(5)	6339(4)	46(1)
C(31)	6380(5)	6673(4)	5864(3)	38(1)
C(32)	6929(5)	5469(5)	6241(4)	47(1)
C(33)	8504(6)	5335(6)	6102(5)	58(1)
C(34)	9520(6)	6393(7)	5600(5)	66(2)
C(35)	8994(6)	7595(7)	5231(5)	65(2)
C(36)	7418(5)	7747(5)	5352(4)	52(1)

**Table SI 13.** Bond lengths [Å] and angles [°].

Au(1)-C(1)	2.035(5)	C(11)-C(16)	1.394(6)
Au(1)-P(1)	2.2804(11)	C(12)-C(13)	1.378(7)
C(1)-C(4)	1.360(7)	C(13)-C(14)	1.378(8)
C(1)-S(1)	1.723(5)	C(14)-C(15)	1.368(9)
S(1)-C(2)	1.728(5)	C(15)-C(16)	1.385(8)
C(2)-C(3)	1.365(6)	C(21)-C(22)	1.383(7)
C(2)-Br(1)	1.874(5)	C(21)-C(26)	1.391(6)
C(3)-C(4)	1.433(6)	C(22)-C(23)	1.395(7)
C(3)-C(5)	1.491(7)	C(23)-C(24)	1.381(8)
C(5)-C(6)	1.529(7)	C(24)-C(25)	1.374(9)
C(6)-C(7)	1.511(8)	C(25)-C(26)	1.392(8)
C(7)-C(8)	1.535(8)	C(31)-C(32)	1.381(7)
C(8)-C(9)	1.478(11)	C(31)-C(36)	1.392(7)
C(9)-C(10)	1.510(11)	C(32)-C(33)	1.388(6)
P(1)-C(11)	1.810(5)	C(33)-C(34)	1.368(9)
P(1)-C(31)	1.819(4)	C(34)-C(35)	1.368(9)
P(1)-C(21)	1.820(5)	C(35)-C(36)	1.393(7)
C(11)-C(12)	1.390(6)	C(12)-C(11)-C(16)	118.8(5)
C(1)-Au(1)-P(1)	177.21(13)	C(12)-C(11)-P(1)	122.8(3)
C(4)-C(1)-S(1)	108.8(4)	C(16)-C(11)-P(1)	118.3(4)
C(4)-C(1)-Au(1)	129.7(3)	C(13)-C(12)-C(11)	120.5(4)
S(1)-C(1)-Au(1)	121.5(3)	C(12)-C(13)-C(14)	120.3(5)
C(1)-S(1)-C(2)	92.7(2)	C(15)-C(14)-C(13)	119.7(5)
C(3)-C(2)-S(1)	112.5(4)	C(14)-C(15)-C(16)	120.9(5)
C(3)-C(2)-Br(1)	127.0(4)	C(15)-C(16)-C(11)	119.8(5)
S(1)-C(2)-Br(1)	120.5(3)	C(22)-C(21)-C(26)	119.3(5)
C(2)-C(3)-C(4)	109.5(4)	C(22)-C(21)-P(1)	122.3(4)
C(2)-C(3)-C(5)	126.6(4)	C(26)-C(21)-P(1)	118.4(4)

C(4)-C(3)-C(5)	124.0(4)	C(21)-C(22)-C(23)	120.6(5)
C(1)-C(4)-C(3)	116.5(4)	C(24)-C(23)-C(22)	119.7(5)
C(3)-C(5)-C(6)	113.4(4)	C(25)-C(24)-C(23)	120.0(5)
C(7)-C(6)-C(5)	112.8(5)	C(24)-C(25)-C(26)	120.6(5)
C(6)-C(7)-C(8)	115.0(5)	C(21)-C(26)-C(25)	119.9(5)
C(9)-C(8)-C(7)	113.6(6)	C(32)-C(31)-C(36)	119.5(4)
C(8)-C(9)-C(10)	115.0(7)	C(32)-C(31)-P(1)	122.6(3)
C(11)-P(1)-C(31)	105.4(2)	C(36)-C(31)-P(1)	117.9(4)
C(11)-P(1)-C(21)	105.3(2)	C(31)-C(32)-C(33)	120.1(5)
C(31)-P(1)-C(21)	106.4(2)	C(34)-C(33)-C(32)	120.3(5)
C(11)-P(1)-Au(1)	115.39(15)	C(35)-C(34)-C(33)	120.4(5)
C(31)-P(1)-Au(1)	111.03(15)	C(34)-C(35)-C(36)	120.2(5)
C(21)-P(1)-Au(1)	112.63(15)	C(31)-C(36)-C(35)	119.6(5)

Table SI 14. Anisotropic displacement parameters ($\text{\AA}^2 \times 10^3$). The anisotropic displacement factor exponent takes the form: $-2\pi^2 [h^2 a^{*2} U^{11} + \dots + 2 h k a^* b^* U^{12}]$

	U ¹¹	U ²²	U ³³	U ²³	U ¹³	U ¹²
Au(1)	38(1)	46(1)	34(1)	-13(1)	-13(1)	4(1)
S(1)	37(1)	56(1)	39(1)	-16(1)	-11(1)	10(1)
Br(1)	50(1)	59(1)	49(1)	-9(1)	-27(1)	3(1)
C(3)	40(2)	38(2)	37(2)	-13(2)	-9(2)	-4(2)
C(4)	38(2)	43(2)	40(3)	-14(2)	-13(2)	4(2)
C(5)	53(3)	54(3)	39(3)	-17(2)	-2(2)	-4(2)
C(6)	60(3)	58(3)	53(3)	-26(3)	-5(3)	-2(2)
C(7)	67(3)	67(4)	81(5)	-34(4)	-17(3)	-4(3)
C(8)	78(4)	71(4)	77(5)	-36(4)	-28(4)	0(3)
C(9)	142(7)	79(5)	97(7)	-32(5)	-55(6)	6(5)
C(10)	121(7)	74(5)	144(9)	-24(6)	-40(7)	-15(5)
P(1)	34(1)	42(1)	33(1)	-14(1)	-11(1)	5(1)
C(11)	34(2)	40(2)	39(2)	-12(2)	-6(2)	3(2)
C(12)	45(2)	50(3)	43(3)	-22(2)	-11(2)	5(2)
C(13)	54(3)	55(3)	50(3)	-26(3)	-7(2)	-4(2)
C(14)	62(3)	52(3)	66(4)	-32(3)	-2(3)	6(2)
C(15)	54(3)	65(4)	90(5)	-39(4)	-12(3)	23(3)
C(16)	45(3)	60(3)	63(4)	-28(3)	-16(2)	15(2)
C(21)	29(2)	47(2)	46(3)	-22(2)	-12(2)	7(2)
C(22)	57(3)	50(3)	42(3)	-20(2)	-7(2)	1(2)
C(23)	60(3)	54(3)	50(3)	-17(3)	3(3)	-2(2)
C(24)	45(2)	41(3)	70(4)	-13(3)	-6(2)	-3(2)
C(25)	56(3)	48(3)	73(4)	-25(3)	-27(3)	1(2)
C(26)	49(2)	50(3)	49(3)	-24(2)	-20(2)	7(2)
C(31)	34(2)	45(2)	34(2)	-16(2)	-4(2)	2(2)
C(32)	38(2)	57(3)	53(3)	-26(2)	-15(2)	8(2)

C(33)	45(3)	72(4)	66(4)	-31(3)	-19(3)	21(3)
C(34)	32(2)	102(5)	74(4)	-46(4)	-10(3)	11(3)
C(35)	42(3)	82(4)	66(4)	-28(3)	3(3)	-13(3)
C(36)	40(2)	56(3)	53(3)	-14(3)	-4(2)	-1(2)

Table SI 15. Hydrogen coordinates ($\times 10^4$) and isotropic displacement parameters ($\text{\AA}^2 \times 10^{-3}$).

	x	y	z	U(eq)
H(4)	5078	7408	2270	48
H(5A)	5515	8520	269	60
H(5B)	3981	8954	-105	60
H(6A)	4731	6870	-186	68
H(6B)	4399	6318	986	68
H(7A)	2122	7278	-101	83
H(7B)	1777	6775	1070	83
H(8A)	1020	5244	358	85
H(8B)	2814	5079	-1	85
H(9A)	1284	4494	1988	121
H(9B)	3046	4262	1605	121
H(10A)	1533	2306	2214	172
H(10B)	2280	2647	1068	172
H(10C)	511	2890	1430	172
H(12)	5722	7770	7259	53
H(13)	5011	9154	8138	62
H(14)	2717	10178	8085	71
H(15)	1185	9882	7103	81
H(16)	1894	8534	6184	65
H(22)	3166	5634	8060	59
H(23)	1777	3665	9052	69
H(24)	1063	2249	8334	66
H(25)	1796	2762	6645	67
H(26)	3178	4727	5647	56
H(32)	6228	4732	6595	56
H(33)	8878	4504	6357	70
H(34)	10597	6294	5506	79
H(35)	9706	8327	4891	78
H(36)	7054	8579	5087	63

DFT Calculations on Chapter 3.3

All calculations were performed using the program Gaussian 9.0, revision D01.²⁹ The results were visualized with the program GaussView 5.0.³⁰ The optimizations and, based on these, more expensive and more accurate single point calculations were performed using the recommendations of Belanzoni and Belpassi and co-workers, who performed benchmark calculations on Au(I) complexes.³¹ The structures were optimized using the restricted PBE functional with the def2-svp basis set. To estimate the key thermochemical properties, full geometry optimization was followed by vibrational frequency calculations. These confirmed that true minima (only positive frequencies) or transition states (one negative frequency) were obtained. They also allowed obtaining corrections for zero-point energy, internal energy, and free energy (at 298.15 K) in the rigid-rotor harmonic oscillator limit. Charges were derived from calculating natural bond orbital (NBO) charges for optimized structures.³² All energies presented in this work are given in hartrees per particle and for comparison, the electronic energies, E , the zero-point energy corrected energies E_{ZPE} (at 0 K), enthalpies ΔH (at 298.15 K), and free energies ΔG (at 298.15 K) are given. To obtain more accurate energies, single point energies were calculated using B3LYP³³ as a functional and def2-tzvp as the basis. These energies are presented as $E_{\text{sglp-def2tzvp}}$.

²⁹ Gaussian 09, Revision D.01, M. J. Frisch, G. W. Trucks, H. B. Schlegel, G. E. Scuseria, M. A. Robb, J. R. Cheeseman, G. Scalmani, V. Barone, B. Mennucci, G. A. Petersson, H. Nakatsuji, M. Caricato, X. Li, H. P. Hratchian, A. F. Izmaylov, J. Bloino, G. Zheng, J. L. Sonnenberg, M. Hada, M. Ehara, K. Toyota, R. Fukuda, J. Hasegawa, M. Ishida, T. Nakajima, Y. Honda, O. Kitao, H. Nakai, T. Vreven, J. A. Montgomery, Jr., J. E. Peralta, F. Ogliaro, M. Bearpark, J. J. Heyd, E. Brothers, K. N. Kudin, V. N. Staroverov, T. Keith, R. Kobayashi, J. Normand, K. Raghavachari, A. Rendell, J. C. Burant, S. S. Iyengar, J. Tomasi, M. Cossi, N. Rega, J. M. Millam, M. Klene, J. E. Knox, J. B. Cross, V. Bakken, C. Adamo, J. Jaramillo, R. Gomperts, R. E. Stratmann, O. Yazyev, A. J. Austin, R. Cammi, C. Pomelli, J. W. Ochterski, R. L. Martin, K. Morokuma, V. G. Zakrzewski, G. A. Voth, P. Salvador, J. J. Dannenberg, S. Dapprich, A. D. Daniels, O. Farkas, J. B. Foresman, J. V. Ortiz, J. Cioslowski, and D. J. Fox, Gaussian, Inc., Wallingford CT, 2013. .

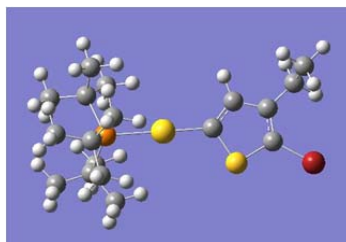
³⁰ Gaussian, Inc. 340 Quinipiac St Bldg 40, Wallingford, CT 06492 USA, Copyright 2000-2008 Semichem. Inc. Authors: R. D. Dennington II, T. A. Keith, J. M. Millam.

³¹ G. Ciancaleoni, S. Rampino, D. Zuccaccia, F. Tarantelli, P. Belanzoni, L. Belpassi, *J. Chem. Theory Comput.* **2014**, *10*, 1021.

³² a) A. E. Reed, L. A. Curtiss, F. Weinhold, *Chem. Rev.* **1988**, *88*, 899. b) NBO Version 3.1, E. D. Glendening, A. E. Reed, J. E. Carpenter, and F. Weinhold.

³³ a) A. D. Becke, *J. Chem. Phys.* **1993**, *98*, 5648; b) C. Lee, W. Yang, R. G. Parr, *Phys. Rev. B* **1988**, *37*, 785.

Structures of the compounds (optimization with the DFT functional PBE/PBE and def2svp)

a) DFT-*t*Bu₃-Au-Tph-Br

Center	Atomic Number	x	y	z
1	6	4.143238	-0.286304	-0.092950
2	6	3.928001	1.061854	-0.349042
3	6	2.519451	1.346117	-0.369527
4	6	1.678272	0.259595	-0.144175
5	16	2.656589	-1.169405	0.107091
6	1	2.138049	2.361218	-0.559757
7	35	5.815129	-1.156242	0.039919
8	79	-0.352603	0.120239	-0.070837
9	15	-2.717833	-0.038471	0.027310
10	6	5.009774	2.096804	-0.530973
11	1	5.900440	1.616129	-0.988001
12	1	4.656450	2.859779	-1.257189
13	6	5.420322	2.785515	0.780970
14	1	5.817851	2.047208	1.506473
15	1	6.206067	3.549164	0.605128
16	1	4.555112	3.289295	1.258524
17	6	-3.504180	1.581576	-0.704801
18	6	-3.268235	-0.253792	1.880428
19	6	-3.294305	-1.578286	-1.013967
20	6	-2.690510	1.983104	-1.957563
21	1	-1.612052	2.089234	-1.721510
22	1	-2.785745	1.270547	-2.794498
23	1	-3.061424	2.967266	-2.316277
24	6	-4.995511	1.461992	-1.069616
25	1	-5.356545	2.448957	-1.431384
26	1	-5.175934	0.736352	-1.885515
27	1	-5.627373	1.176961	-0.207385
28	6	-3.320871	2.730370	0.309273
29	1	-2.262987	2.841724	0.620683
30	1	-3.622325	3.679116	-0.183497
31	1	-3.949912	2.619689	1.211867
32	6	-4.763368	0.004460	2.142412
33	1	-4.980616	-0.202802	3.212522
34	1	-5.054063	1.056149	1.956910
35	1	-5.425747	-0.647106	1.542104
36	6	-2.911708	-1.683442	2.339244
37	1	-1.850204	-1.929228	2.135222
38	1	-3.058480	-1.742536	3.438651
39	1	-3.554180	-2.460542	1.884881
40	6	-2.411930	0.698935	2.746821
41	1	-2.640095	0.500006	3.815828
42	1	-1.328401	0.522724	2.589664
43	1	-2.613231	1.767422	2.560515
44	6	-3.132500	-1.246826	-2.512392
45	1	-2.110276	-0.886970	-2.745721

46	1	-3.295313	-2.179376	-3.093379
47	1	-3.866383	-0.504903	-2.878350
48	6	-2.316580	-2.741655	-0.726062
49	1	-2.388544	-3.135519	0.302038
50	1	-2.553789	-3.577821	-1.418162
51	1	-1.264767	-2.439299	-0.906050
52	6	-4.739532	-2.036881	-0.745636
53	1	-4.974932	-2.888988	-1.419242
54	1	-4.883400	-2.398967	0.290098
55	1	-5.488033	-1.246583	-0.944023

$$E_{\text{RPBE-PBE}} = -4152.55224302$$

$$E_{\text{ZPE}} = -4152.093523$$

$$\Delta H = -4152.062089$$

$$\Delta G = -4152.155900$$

$$E_{\text{sglpt-def2tzvp}} = -4155.6521113$$

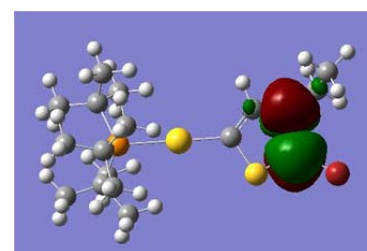
Charge at the C atom connected to Br = -0.347 (range: ± 0.933)

$$\text{LUMO}_{\text{RPBE-PBE}} = 0.01602 (\pi^* \text{ see below})$$

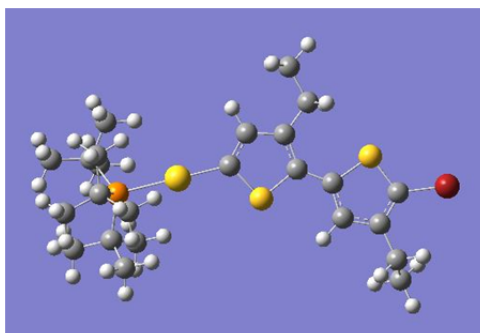
$$\text{LUMO}_{\text{sglpt-def2tzvp}} = 0.03192$$

$$\text{HOMO}_{\text{RPBE-PBE}} = -0.19049 (\text{at the S atom connected to P})$$

$$\text{HOMO}_{\text{sglpt-def2tzvp}} = -0.21703$$



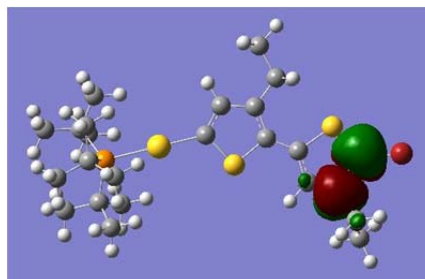
b) DFT-*t*Bu₃-Au-Tph₂-Br



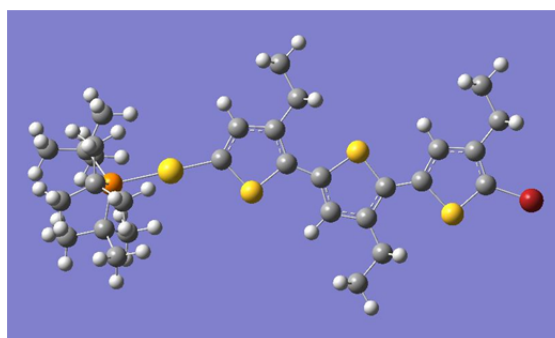
Center	Atomic Number	x	y	z
1	6	0.030342	0.745330	-0.006676
2	6	0.675946	1.979524	-0.069041
3	6	2.105928	1.930677	-0.046973
4	6	2.585605	0.611412	0.038984
5	16	1.232097	-0.511291	0.078654
6	1	0.119028	2.924636	-0.129526
7	6	3.933600	0.084607	0.100250
8	6	4.326592	-1.241099	0.291315
9	16	5.369916	1.095631	-0.079359
10	6	5.736557	-1.470736	0.301006
11	1	3.594663	-2.049282	0.436870
12	6	6.421587	-0.278958	0.104484
13	6	2.998790	3.150538	-0.106409
14	1	3.707651	3.122565	0.752485
15	1	3.648608	3.081447	-1.009202
16	6	6.377166	-2.826221	0.458932
17	1	5.771425	-3.426309	1.170725

18	1	7.377242	-2.700560	0.924100
19	6	2.278149	4.500522	-0.115935
20	1	3.009527	5.332720	-0.146618
21	1	1.615901	4.606100	-0.999230
22	1	1.653118	4.636437	0.790101
23	6	6.521686	-3.589219	-0.867905
24	1	6.984118	-4.584647	-0.706968
25	1	5.536340	-3.744820	-1.352635
26	1	7.158980	-3.027638	-1.580404
27	35	8.289437	-0.036381	0.041101
28	79	-1.946994	0.259604	-0.004271
29	15	-4.249516	-0.317271	0.001761
30	6	-4.463962	-2.080221	-0.790679
31	6	-3.958709	-3.143289	0.207961
32	1	-4.620133	-3.270453	1.085292
33	1	-3.924515	-4.121538	-0.317127
34	1	-2.931480	-2.923414	0.561582
35	6	-3.526775	-2.167179	-2.017863
36	1	-3.557243	-3.206449	-2.409642
37	1	-3.816510	-1.495133	-2.843157
38	1	-2.477802	-1.935351	-1.742677
39	6	-5.905122	-2.426175	-1.210154
40	1	-6.280233	-1.775297	-2.022703
41	1	-5.924430	-3.467299	-1.598592
42	1	-6.621488	-2.376317	-0.368656
43	6	-5.238939	0.995966	-1.035092
44	6	-6.763564	0.971309	-0.821041
45	1	-7.215240	-0.006414	-1.073647
46	1	-7.052309	1.229692	0.215401
47	1	-7.231223	1.730772	-1.484227
48	6	-4.932473	0.778721	-2.532025
49	1	-5.363448	1.629748	-3.101089
50	1	-3.842245	0.765172	-2.731854
51	1	-5.382611	-0.145011	-2.940633
52	6	-4.684396	2.396584	-0.684170
53	1	-5.147919	3.138730	-1.368898
54	1	-4.909443	2.715645	0.347841
55	1	-3.585266	2.442247	-0.825719
56	6	-4.901968	-0.337054	1.833378
57	6	-3.820794	-1.002219	2.717586
58	1	-4.133739	-0.912612	3.779982
59	1	-3.675519	-2.075472	2.506775
60	1	-2.840109	-0.496259	2.607060
61	6	-5.026595	1.117438	2.332821
62	1	-5.228088	1.093257	3.424838
63	1	-4.086535	1.685749	2.183633
64	1	-5.859717	1.671738	1.861648
65	6	-6.248109	-1.059249	2.029056
66	1	-6.187802	-2.138714	1.793588
67	1	-6.545766	-0.979106	3.096768
68	1	-7.066326	-0.620392	1.427376

$E_{\text{RPBE-PBE}} = -4782.24218047$
 $E_{\text{ZPE}} = -4781.683026$
 $\Delta H = -4781.643825$
 $\Delta G = -4781.756638$
 $E_{\text{sglpt-def2tzvp}} = -4786.2064138$
 Charge at the C atom connected to Br= -0.340 (range: ± 0.933)
 $\text{LUMO}_{\text{RPBE-PBE}} = 0.00313$ (π^* see below)
 $\text{LUMO}_{\text{sglpt-def2tzvp}} = 0.01888$
 $\text{HOMO}_{\text{RPBE-PBE}} = -0.18987$ (at the S atom connected to P)
 $\text{HOMO}_{\text{sglpt-def2tzvp}} = -0.21675$



c) DFT-*t*Bu₃P-Au-Tph₃-Br



Center	Atom number	x	y	z
1	6	-1.645271	0.688631	-0.035344
2	6	-0.986435	1.918497	-0.040114
3	6	0.441604	1.854933	-0.039757
4	6	0.909404	0.526436	-0.035207
5	16	-0.457535	-0.582950	-0.031260
6	1	-1.534311	2.870789	-0.042756
7	6	2.249730	-0.013458	-0.031492
8	6	2.628519	-1.359737	-0.035220
9	16	3.691967	0.989874	-0.017354
10	6	4.028654	-1.597069	-0.026251
11	1	1.880844	-2.163823	-0.044287
12	6	4.768187	-0.399001	-0.015031
13	6	1.345419	3.067626	-0.042740
14	1	2.020606	3.017582	0.842083
15	1	2.029728	3.006754	-0.919775
16	6	4.653997	-2.973548	-0.028379
17	1	5.325300	-3.065138	0.855914
18	1	5.333262	-3.058899	-0.907224
19	6	0.636632	4.423699	-0.054496
20	1	1.375582	5.249776	-0.056860
21	1	-0.002335	4.544388	-0.952932
22	1	-0.009591	4.556284	0.837038
23	6	3.671253	-4.146012	-0.037047

24	1	4.216202	-5.110810	-0.037132
25	1	3.012127	-4.134302	0.854780
26	1	3.021385	-4.129083	-0.935566
27	79	-3.631155	0.240468	-0.018299
28	15	-5.948543	-0.270598	0.018333
29	6	6.193016	-0.153234	-0.001725
30	6	6.847464	1.082531	0.017282
31	16	7.389566	-1.448443	-0.008179
32	6	8.272727	1.021228	0.026797
33	1	6.289953	2.029282	0.024900
34	6	8.697578	-0.302736	0.014509
35	6	9.210528	2.206301	0.047462
36	1	9.884336	2.106248	0.927280
37	1	9.887070	2.134965	-0.833127
38	6	8.532479	3.576447	0.068678
39	1	7.891417	3.703212	0.964929
40	1	9.288777	4.386167	0.083284
41	1	7.894750	3.732718	-0.825289
42	35	10.477919	-0.911227	0.021217
43	6	-6.230696	-2.033332	-0.752388
44	6	-6.577752	-0.251108	1.858020
45	6	-6.909712	1.063745	-1.019093
46	6	-7.688041	-2.335684	-1.147977
47	1	-8.052654	-1.680419	-1.961604
48	1	-7.747021	-3.379273	-1.525556
49	1	-8.389584	-2.253570	-0.296677
50	6	-5.745427	-3.103901	0.248164
51	1	-5.750158	-4.086592	-0.269671
52	1	-4.706654	-2.915254	0.585806
53	1	-6.397885	-3.203724	1.135620
54	6	-5.314107	-2.161657	-1.991612
55	1	-5.593451	-1.488811	-2.819824
56	1	-4.254331	-1.961568	-1.733276
57	1	-5.383182	-3.203076	-2.372817
58	6	-7.944857	-0.925716	2.077976
59	1	-7.923096	-2.009517	1.855354
60	1	-8.227186	-0.822802	3.147849
61	1	-8.754857	-0.467034	1.480113
62	6	-5.508938	-0.943995	2.735752
63	1	-4.513864	-0.470231	2.612376
64	1	-5.808235	-0.837532	3.800524
65	1	-5.400125	-2.022650	2.530965
66	6	-6.646267	1.211822	2.343076
67	1	-6.832099	1.206398	3.438118
68	1	-5.689765	1.746082	2.173664
69	1	-7.467164	1.789142	1.877819
70	6	-6.304215	2.448870	-0.691178
71	1	-6.754686	3.198868	-1.376040
72	1	-6.501613	2.785140	0.340873
73	1	-5.206665	2.456712	-0.851208
74	6	-6.632131	0.822005	-2.517825
75	1	-7.042649	1.681513	-3.089251
76	1	-5.545888	0.770490	-2.732632

77	1	-7.118838	-0.089989	-2.910478
78	6	-8.431178	1.093360	-0.782817
79	1	-8.694849	1.373681	0.254723
80	1	-8.881895	1.861607	-1.447658
81	1	-8.921448	0.129901	-1.017813

$$E_{\text{RPBE-PBE}} = -5411.93292796$$

$$E_{\text{ZPE}} = -5411.273087$$

$$\Delta H = -5411.226271$$

$$\Delta G = -5411.357207$$

$$E_{\text{sglpt-def2tzvp}} = -5416.7609219$$

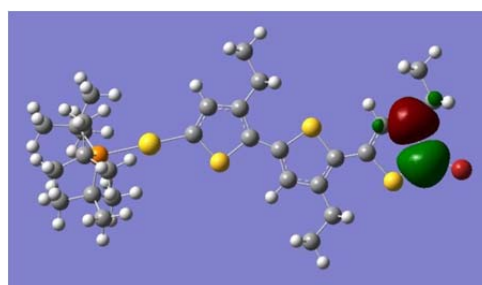
Charge at the C atom connected to Br= -0.339 (range: ± 0.933)

$$\text{LUMO}_{\text{RPBE-PBE}} = -0.00224 (\pi^* \text{ see below})$$

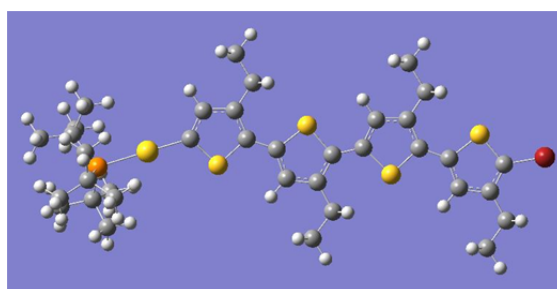
$$\text{LUMO}_{\text{sglpt-def2tzvp}} = 0.01318$$

$$\text{HOMO}_{\text{RPBE-PBE}} = -0.19117 (\text{at the S atom connected to P})$$

$$\text{HOMO}_{\text{sglpt-def2tzvp}} = -0.21765$$



d) DFT-*t*Bu₃P-Au-Tph₄-Br



Center	Atomic Number	x	y	z
1	6	-3.451588	0.796972	-0.033569
2	6	-2.864878	2.062968	-0.034730
3	6	-1.435670	2.081464	-0.036452
4	6	-0.891823	0.781861	-0.037334
5	16	-2.192816	-0.404147	-0.035159
6	1	-3.466728	2.982007	-0.033647
7	6	0.476242	0.319817	-0.038281
8	6	0.927431	-1.005213	-0.048835
9	16	1.861778	1.399385	-0.021848
10	6	2.336272	-1.168306	-0.043588
11	1	0.222903	-1.847223	-0.060411
12	6	3.012330	0.069169	-0.028475
13	6	-0.602337	3.343489	-0.036443
14	1	0.075934	3.328520	0.847310
15	1	0.082938	3.324131	-0.914621
16	6	3.032251	-2.510264	-0.053300
17	1	3.707306	-2.571019	0.830483
18	1	3.716240	-2.553770	-0.931197
19	6	-1.387799	4.656721	-0.042531

20	1	-0.697595	5.523898	-0.043307
21	1	-2.034255	4.743098	-0.939533
22	1	-2.038973	4.748749	0.850481
23	6	2.111926	-3.732247	-0.069823
24	1	2.706794	-4.667123	-0.076270
25	1	1.453363	-3.761690	0.822051
26	1	1.461866	-3.743980	-0.968336
27	79	-5.403319	0.216017	-0.017444
28	15	-7.669317	-0.486567	0.019889
29	6	4.418726	0.388344	-0.017499
30	6	5.008229	1.657737	-0.002124
31	16	5.680827	-0.834187	-0.020392
32	6	6.427542	1.666682	0.007983
33	1	4.401667	2.573201	0.002015
34	6	6.965340	0.365019	-0.000018
35	6	7.265798	2.924615	0.026058
36	1	7.941870	2.893098	0.910746
37	1	7.950442	2.913057	-0.852517
38	6	6.484039	4.239697	0.037226
39	1	5.831157	4.320604	0.929984
40	1	7.177367	5.103817	0.051698
41	1	5.841684	4.342358	-0.860901
42	6	8.331870	-0.105964	0.006230
43	6	8.779182	-1.431223	0.002614
44	16	9.721121	0.979742	0.019200
45	6	10.195285	-1.600189	0.009928
46	1	8.077947	-2.276851	-0.004930
47	6	10.827686	-0.361558	0.019341
48	6	10.929815	-2.920836	0.008254
49	1	11.607629	-2.946381	0.890197
50	1	11.611993	-2.941936	-0.870468
51	6	10.040173	-4.164259	0.002788
52	1	10.656493	-5.085070	0.002511
53	1	9.383756	-4.203201	0.896077
54	1	9.389101	-4.199276	-0.894571
55	35	12.682145	-0.047656	0.032291
56	6	-7.900939	-1.962537	-1.223229
57	6	-8.113758	-1.071854	1.820489
58	6	-8.818888	0.994981	-0.493715
59	6	-7.116729	-1.627555	-2.514018
60	1	-7.536285	-0.776324	-3.076389
61	1	-6.053589	-1.401171	-2.294509
62	1	-7.146984	-2.514278	-3.182886
63	6	-7.235223	-3.222592	-0.631287
64	1	-7.217371	-4.006541	-1.417949
65	1	-6.185230	-3.034335	-0.330095
66	1	-7.786499	-3.641830	0.230843
67	6	-9.366848	-2.280822	-1.572792
68	1	-9.863569	-1.453722	-2.114962
69	1	-9.391318	-3.165553	-2.244974
70	1	-9.977523	-2.527791	-0.683911
71	6	-6.917538	-1.882922	2.371212
72	1	-5.974480	-1.301573	2.318516

73	1	-7.115647	-2.116208	3.439293
74	1	-6.755806	-2.841734	1.850068
75	6	-9.401510	-1.909675	1.926610
76	1	-9.321943	-2.880128	1.400441
77	1	-9.591429	-2.140168	2.997103
78	1	-10.293964	-1.380715	1.542365
79	6	-8.240359	0.170336	2.728289
80	1	-8.320640	-0.176949	3.780268
81	1	-7.346262	0.822542	2.664164
82	1	-9.141411	0.776501	2.518731
83	6	-10.304841	0.813067	-0.132119
84	1	-10.470973	0.751681	0.959941
85	1	-10.872510	1.696673	-0.495538
86	1	-10.755926	-0.081816	-0.601008
87	6	-8.269230	2.275018	0.178392
88	1	-8.846775	3.145687	-0.199778
89	1	-8.358201	2.272827	1.277944
90	1	-7.202264	2.435560	-0.078446
91	6	-8.690078	1.225332	-2.013940
92	1	-9.213805	2.171784	-2.266360
93	1	-7.632159	1.339936	-2.324332
94	1	-9.156620	0.425413	-2.618528

$$E_{\text{RPBE-PBE}} = -6041.62482103$$

$$E_{\text{ZPE}} = -6040.864182$$

$$\Delta H = -6040.809780$$

$$\Delta G = -6040.957784$$

$$E_{\text{sglpt-def2tzvp}} = -6047.3169775$$

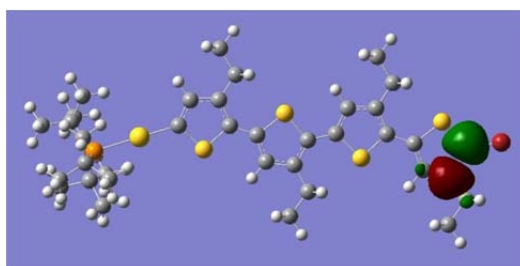
Charge at the C atom connected to Br= -0.338 (range: ± 0.933)

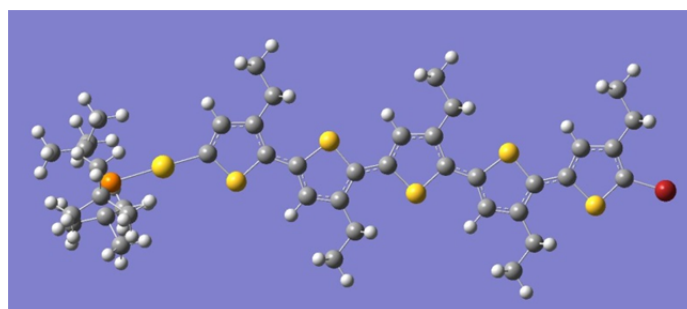
$$\text{LUMO}_{\text{RPBE-PBE}} = -0.00524 (\pi^* \text{ see below})$$

$$\text{LUMO}_{\text{sglpt-def2tzvp}} = 0.01029$$

$$\text{HOMO}_{\text{RPBE-PBE}} = -0.19264 (\text{at the S atom connected to P})$$

$$\text{HOMO}_{\text{sglpt-def2tzvp}} = -0.21878$$



e) DFT-*t*Bu₃P-Au-Tph₅-Br

Center	Atomic Number	x	x	z
1	6	-5.262027	0.800269	-0.032980
2	6	-4.662094	2.060159	-0.039676
3	6	-3.232909	2.063727	-0.044833
4	6	-2.702614	0.758326	-0.042607
5	16	-4.016061	-0.413958	-0.033479
6	1	-5.254375	2.985409	-0.040268
7	6	-1.339906	0.281719	-0.045164
8	6	-0.903570	-1.048688	-0.052858
9	16	0.057352	1.345859	-0.034652
10	6	0.502847	-1.227671	-0.049898
11	1	-1.617596	-1.882704	-0.060691
12	6	1.193193	0.002578	-0.039653
13	6	-2.386166	3.316726	-0.051202
14	1	-1.706428	3.297799	0.831362
15	1	-1.702831	3.286542	-0.930597
16	6	1.183770	-2.577233	-0.057012
17	1	1.859370	-2.642996	0.826004
18	1	1.866128	-2.630419	-0.935649
19	6	-3.157423	4.638300	-0.060977
20	1	-2.457883	5.497932	-0.066725
21	1	-3.804775	4.728003	-0.956997
22	1	-3.805630	4.741014	0.833015
23	6	0.249874	-3.788883	-0.069125
24	1	0.834293	-4.730306	-0.073847
25	1	-0.407776	-3.808613	0.823691
26	1	-0.401421	-3.795695	-0.966793
27	79	-7.218587	0.235441	-0.012240
28	15	-9.488016	-0.455664	0.028362
29	6	2.602281	0.305044	-0.032149
30	6	3.205732	1.569192	-0.021565
31	16	3.850712	-0.930692	-0.033137
32	6	4.623544	1.564144	-0.013876
33	1	2.608049	2.490523	-0.019166
34	6	5.149402	0.255302	-0.018932
35	6	5.473777	2.813910	-0.001236
36	1	6.149003	2.779017	0.883691
37	1	6.159368	2.789995	-0.878510
38	6	4.704474	4.136261	0.002613
39	1	4.052365	4.228759	0.894845
40	1	5.405908	4.993931	0.012359

41	1	4.063123	4.240332	-0.896114
42	6	6.507388	-0.229037	-0.013998
43	6	6.938693	-1.560763	-0.020300
44	16	7.908541	0.831208	0.002193
45	6	8.345781	-1.742751	-0.012494
46	1	6.225852	-2.395910	-0.030461
47	6	9.037579	-0.515607	0.000332
48	6	9.024233	-3.093651	-0.017321
49	1	9.696640	-3.160870	0.868193
50	1	9.707816	-3.149057	-0.895057
51	6	8.088616	-4.303995	-0.031230
52	1	8.671930	-5.245943	-0.033767
53	1	7.428988	-4.322520	0.860134
54	1	7.440215	-4.310792	-0.930970
55	6	10.451357	-0.215058	0.011641
56	6	11.057978	1.045219	0.023918
57	16	11.695886	-1.463905	0.012005
58	6	12.484242	1.037939	0.033700
59	1	10.465873	1.970841	0.025758
60	6	12.958716	-0.269520	0.028464
61	35	14.760051	-0.810446	0.036879
62	6	13.377135	2.257186	0.047560
63	1	14.051576	2.188683	0.929869
64	1	14.058231	2.203955	-0.830720
65	6	12.648510	3.601185	0.056464
66	1	12.008356	3.727081	-0.840544
67	1	12.000870	3.711014	0.950204
68	1	13.374322	4.438297	0.066919
69	6	-9.726582	-1.929913	-1.215632
70	6	-9.932966	-1.040258	1.829065
71	6	-10.631623	1.031151	-0.483017
72	6	-8.941897	-1.597497	-2.506760
73	1	-9.358138	-0.744058	-3.068248
74	1	-7.877603	-1.376052	-2.287798
75	1	-8.976566	-2.483640	-3.176172
76	6	-9.065694	-3.193049	-0.624820
77	1	-9.052231	-3.976836	-1.411717
78	1	-8.014504	-3.009315	-0.324988
79	1	-9.617611	-3.610120	0.237947
80	6	-11.194098	-2.241619	-1.564286
81	1	-11.687820	-1.411611	-2.104726
82	1	-11.222850	-3.125216	-2.237789
83	1	-11.804954	-2.487511	-0.675238
84	6	-11.223474	-1.873873	1.935389
85	1	-11.147674	-2.844342	1.408685
86	1	-11.413616	-2.104235	3.005869
87	1	-12.114323	-1.341676	1.551897
88	6	-8.739046	-1.855595	2.378444
89	1	-7.794334	-1.276882	2.326514
90	1	-8.937694	-2.089919	3.446195
91	1	-8.580155	-2.814048	1.855781
92	6	-10.055168	0.201649	2.737900
93	1	-10.136509	-0.146341	3.789564

94	1	-9.158864	0.850861	2.674348
95	1	-10.954194	0.811046	2.529043
96	6	-10.075882	2.308315	0.189517
97	1	-10.650266	3.181653	-0.187309
98	1	-10.163668	2.305552	1.289154
99	1	-9.008556	2.464738	-0.068390
100	6	-10.503336	1.261914	-2.003213
101	1	-11.024142	2.210217	-2.254718
102	1	-9.445310	1.373150	-2.314482
103	1	-10.973014	0.463762	-2.607679
104	6	-12.117995	0.855182	-0.120116
105	1	-12.283239	0.792635	0.971995
106	1	-12.682142	1.741879	-0.481464
107	1	-12.573537	-0.036922	-0.590004

$E_{\text{RPBE-PBE}} = -6671.31665534$

$E_{\text{ZPE}} = -6670.455222$

$\Delta H = -6670.393210$

$\Delta G = -6670.559328$

$E_{\text{sglpt-def2tzvp}} = -6677.872899$

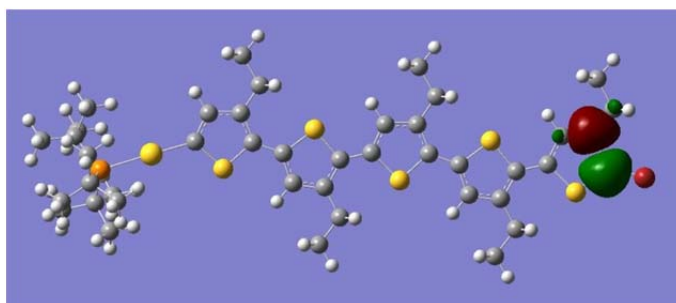
Charge at the C atom connected to Br= -0.337 (range: ± 0.933)

$\text{LUMO}_{\text{RPBE-PBE}} = -0.00715$ (π^* see below)

$\text{LUMO}_{\text{sglpt-def2tzvp}} = 0.00847$

$\text{HOMO}_{\text{RPBE-PBE}} = -0.19357$ (at the S atom connected to P)

$\text{HOMO}_{\text{sglpt-def2tzvp}} = -0.21946$



5.3.2 Further Experimental Data for Chapter 3.3

For general methods and materials see this chapter 5.3.1. BrAuPPh_3 (**83**) was purchased from Alfa Aesar Inc. in a purity of 98%.

Recycling

To determine the type of gold species formed during the polymerization, a quenching experiment of the reaction was performed by adding methanol. With this, it was possible to separate the species without the decomposition caused by HCl. A manual preparative column with GPC gel (PS beads from Sigma Aldrich Inc., in CHCl_3) was used for the separation of the polymer and the resulting gold species.

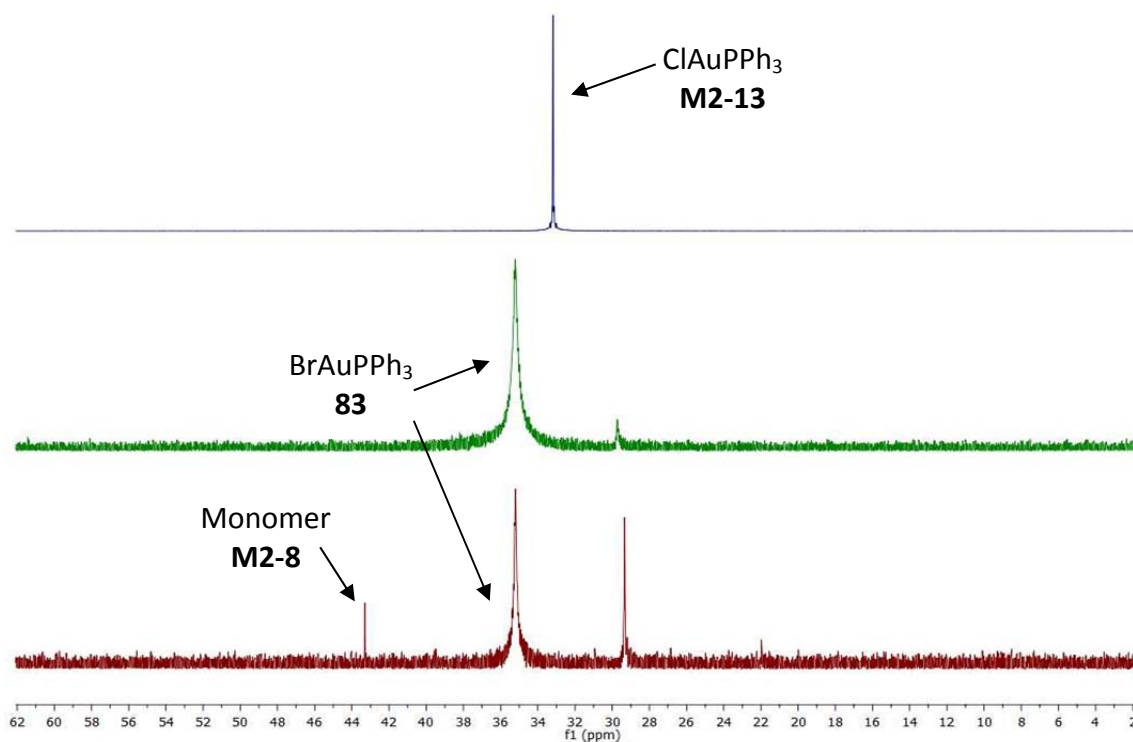
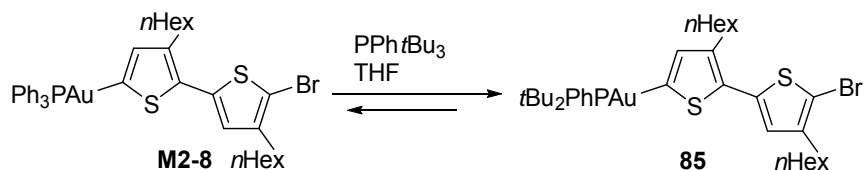


Figure SI 9. ^{31}P NMR of the synthesized ClAuPPh_3 (**M2-13**, blue), the commercially obtained BrAuPPh_3 (**83**, green) and the isolated gold species that was formed during the polymerization reaction (red).

The ^{31}P NMR spectrum showed that there were at least 3 phosphorus containing species in the reaction mixture: traces of monomer (**M2-8**, 43.3 ppm), BrAuPPh_3 (**83**, 35.2 ppm), which we expected to find and which is obviously the main product. Another undefined species was found at 29.3 ppm (red spectrum). In green the ^{31}P reference spectrum of BrAuPPh_3 (**83**) is shown, bought from Alfa Aesar. In blue, the ^{31}P NMR spectrum of the synthesized ClAuPPh_3 (**M2-13**) is shown. BrAuPPh_3 (**83**) was the main compound that was formed during the polymerization reaction.

Ligand exchange with PPh_tBu₂

1) In a J. Young's NMR tube, monomer **M2-8** (9.0 eq, 78 mg, 90 μmol) was dissolved in THF-*d*₈ (0.6 mL) and tri(*tert*butyl)-phosphine (1.0 eq, 2.02 mg, 10 μmol) was added. These ratios are the same as for the polymerization reactions with 10 mol% of catalyst. The reaction was monitored by ³¹P NMR spectroscopy.

2) In a J. Young's NMR tube, monomer **M2-8** (1.0 eq, 8.7mg, 10 μmol) was dissolved in THF-*d*₈ (0.6 mL) and tri(*tert*butyl)-phosphine (9.0 eq, 20 mg, 90 μmol) was added. The reaction was monitored by ³¹P NMR spectroscopy.

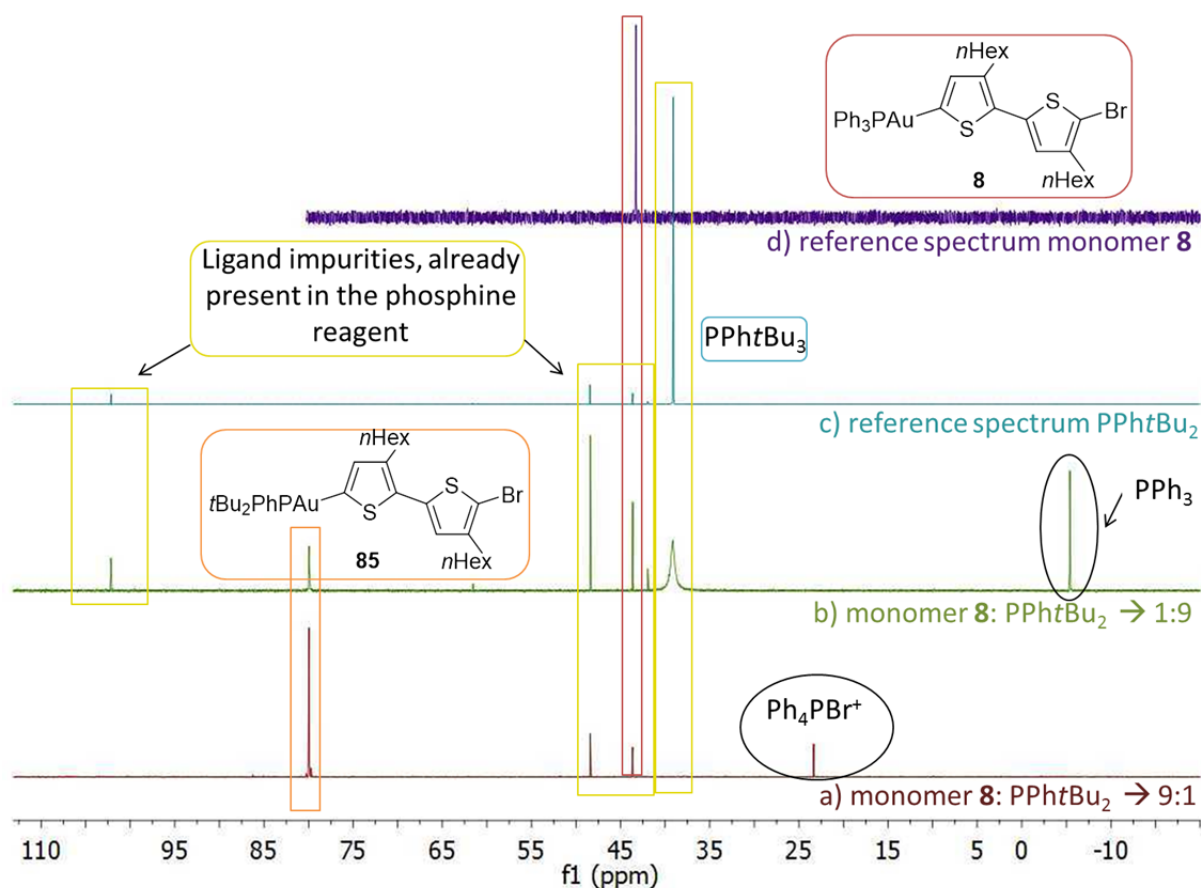


Figure SI 10. Ligand exchange reaction with monomer **M2-8**. Reference spectra show the monomer **M2-8** (spectrum d), 43 ppm and the ligand itself, PPh_tBu₃ (spectrum c), 39 ppm. In experiment a), the monomer **8** was used in an excess (9:1) with respect to PPh_tBu₃. In experiment b), PPh_tBu₃ was used in an excess (9:1) with respect to monomer **M2-8**.

This spectrum (very clear in spectrum b)) showed a large number of impurities (at 102, 48, 43 and 41 ppm) of the commercially obtained ligand, which should have a purity of 95 %. In experiment a), the monomer **M2-8** (no longer visible at 43 ppm) was used in an excess (9:1) with respect to PPh_tBu₃ (no longer visible at 63.0 ppm). The expected organogold species **85** (79 ppm) was formed. In addition to this, the signal at 23 ppm could be identified as [Ph₄PBr⁺].³⁴

Because of the monomer:ligand ratio of 9:1, the monomer would be expected to be still present, but no signal was visible at 43 ppm. Instead, the impurities that were already present in the batch of the commercially obtained ligand were found in a higher relative intensity than was to be expected from the addition of ligand. In addition, their intensity relative to one another appeared to have changed: The signals at 102 and 61 ppm disappeared, whereas the signals at 48 and 41 became much more intense. It would appear therefore that the monomer **M2-8** was transferred to other species, which could not be identified up to now.³⁵

Similar findings were made for the experiment b), where PPh_tBu₃ was used in an excess (9:1) with respect to the monomer **M2-8** (no longer visible at 43.3 ppm). Interestingly, besides the expected species **85** (80 ppm), free PPh₃ (-5.4 ppm) was detected, but in such a high amount that another ligand transfer at the phosphine itself may have occurred. In this case, two more species were found at 61 ppm and 40 ppm as well as the PPh_tBu₃ ligand itself (39 ppm, broad signal). These species could not be identified up to now.

³⁴ D. Marcoux, A. B. Charette, *Adv. Synth. Catal.* **2008**, *350*, 2967.

³⁵ The species that were initially considered could be excluded due to their reported chemical shifts: PPh₂tBu, BrPPh₂, BrPPh₃⁺, BrPtBu₂, BrPPh_tBu. For other species, no chemical shifts are reported, so that they cannot be confirmed or excluded at this point: BrPPh₂tBu⁺, BrPPh_tBu₂⁺, Br₂PPh_tBu⁺ or corresponding THF containing species.

6 References

- [1] (a) H. Shirakawa, E. J. Louis, A. G. MacDiarmid, C. K. Chiang, A. J. Heeger, *J. Chem. Soc.* **1977**, 578; (b) A. J. Heeger, *Angew. Chem., Int. Ed.* **2001**, *40*, 2591; (c) H. Shirakawa, *Angew. Chem., Int. Ed.* **2001**, *40*, 2575; (d) A. G. MacDiarmid, *Angew. Chem., Int. Ed.* **2001**, *40*, 2581.
- [2] D. Astruc, *Anal. Bioanal. Chem.* **2011**, *399*, 1811.
- [3] R. F. Heck, J. P. Nolley, *J. Org. Chem.* **1972**, *37*.
- [4] E.-I. Negishi, A. O. King, N. Okukado, *J. Org. Chem.* **1977**, *42*, 1821.
- [5] A. Suzuki, N. Miyaura, *J. Chem. Soc. Chem. Commun.* **1979**, 866.
- [6] (a) G. Yu, J. Gao, J. C. Hummelen, F. Wudl, A. J. Heeger, *Science* **1995**, *270*, 1789; (b) P. M. Beaujuge, J. M. J. Fréchet, *J. Am. Chem. Soc.* **2011**, *133*, 20009; (c) C. Li, M. Liu, N. G. Pschirer, M. Baumgarten, K. Müllen, *Chem. Rev.* **2010** *110*, 6817; (d) J. L. Delgado, P.-A. Bouit, S. Filippone, M. Á. Herranz, N. Martín, *Chem. Commun.* **2010**, *46*, 4853; (e) J. Peet, A. J. Heeger, G. C. Bazan, *Acc. Chem. Res.* **2009**, *42*, 1700; (f) S. Günes, H. Neugebauer, N. S. Sariciftci, *Chem. Rev.* **2007**, *107*, 1324; (g) C. Groves, O. G. Reid, D. S. Ginger, *Acc. Chem. Res.* **2010**, *43*, 612; (h) F. C. Krebs, *Polymer Photovoltaics A Practical Approach*, SPIE Press, Bellingham, Washington, USA, **2008**.
- [7] (a) W. Wu, Y. Liu, D. Zhu, *Chem. Soc. Rev.* **2010**, *39*, 1489; (b) D. Braga, G. Horowitz, *Adv. Mater.* **2009**, *21*, 1473; (c) H. Usta, A. Facchetti, T. J. Marks, *Acc. Chem. Res.* **2011**, *44*, 501; (d) C. Wang, H. Dong, W. Hu, Y. Liu, D. Zhu, *Chem. Rev.* **2013**, *112*, 2208; (e) W. Wu, Y. Liu, D. Zhu, *Chem. Soc. Rev.* **2010**, *39*, 1489.
- [8] (a) O. Nuyken, S. Jungermann, V. Wiederhirn, E. Bacher, K. Meerholz, *Monatsh. Chem.* **2006**, *137*, 811; (b) D. Braun, *Mater. Today* **2002**, *5*, 32; (c) A. P. Kulkarni, C. J. Tonzola, A. Babel, S. A. Jenekhe, *Chem. Mater.* **2004**, *16*, 4556; (d) D. Kabra, L. P. Lu, M. H. Song, H. J. Snaith, R. H. Friend, *Adv. Mater.* **2010**, *22*, 3194.
- [9] Reprinted with permission of LG: <http://www.lg.com/au/images/pressrelease/lg-oled-tv-curved-screen.jpg> (20.02.2015)
- [10] (a) C. D. Dimitrakopoulos, P. R. L. Malenfant, *Adv. Mater.* **2002**, *14*, 99; (b) H. E. Katz, J. Huang, *Annu. Rev. Mater. Res.* **2009**, *39*, 71; (c) A. Facchetti, *Chem. Mater.* **2011**, *23*, 733; (d) A. P. Kulkarni, C. J. Tonzola, A. Babel, S. A. Jenekhe, *Chem. Mater.* **2004**, *16*, 4556; (e) N. Koch, *ChemPhysChem* **2007**, *8*, 1438; (f) Y. Shirota, *J. Mater. Chem.* **2000**, *10*, 1; (g) R. R. Sondergaard, M. Hoesel, F. C. Krebs, *J. Polym. Sci., Part B: Polym. Phys.* **2013**, *13*, 16.
- [11] (a) S. R. Forrest, *Nature* **2004**, *428*, 911; (b) R. Sondergaard, M. Hösel, D. Angmo, T. T. Larsen-Olsen, F. C. Krebs, *Mater. Today* **2012**, *15*, 36; (c) T. M. Eggenhuisen, Y. Galagan, A. F. K. V. Biezemans, T. M. W. L. Slaats, W. P. Voorthuizen, S. Kommeren, S. Shanmugam, J. P. Teunissen, A. Hadipour, W. J. H. Verhees, S. C. Veenstra, M. J. J. Coenen, J. Gilot, R. Andriessen, W. A. Groen, *J. Mater. Chem.* **2015**, *3*, 7255.
- [12] (a) *Panasonic Press Release, 10 April 2014. Panasonic HIT® Solar Cell Achieves World's Highest Energy Conversion Efficiency of 25.6% at Research Level* (<http://panasonic.co.jp/corp/news/official.data/data.dir/2014/04/en140410-4/en140410-4.htm>) (20.02.2015) **2014**; (b) M. A. Green, K. Emery, Y. Hishikawa, W. Warta, E. D. Dumlop, *Prog. Photovoltaics Res. Appl.* **2015**, *23*, 1.
- [13] M. Hosoya, H. Oooka, H. Nakao, S. Mori, T. Gotanda, N. Shida, M. Saito, Y. Nakano, K. Todorii, *Abstract O-PV-6-2, Grand Renewable Energy Conference, Tokyo 2014, Module development for polymer solar cells*, p. 21.
- [14] B. S. Ong, Y. Wu, P. Liu, S. Gardner, *J. Am. Chem. Soc.* **2004**, *126*, 3378.
- [15] A. Patra, Y. H. Wijsboom, S. S. Zade, M. Li, Y. Sheynin, G. Leitius, M. Bendikov, *J. Am. Chem. Soc.* **2008**, *130*, 6734.
- [16] E. V. Anslyn, D. A. Dougherty, *Modern Physical Organic Chemistry 2006, Chemistry Science Books, Sausalito, CA*.
- [17] K. Vetenskapsakademien, *The Nobel Prize in Chemistry 2000*.
- [18] M. Rehan, *Chem. unserer Zeit* **2003**, *37*, 1.

- [19] I. F. Perepichka, D. F. Perepichka, *Handbook of Thiophene-Based Materials: Applications in Organic Electronics and Photonics*, 1st. ed., John Wiley & Sons, Ltd., Chichester, UK, **2009**.
- [20] D. Quintens, W. Fischer, F. Jonas, H. Ohst, H. Rehbein, *Agfa-Gevaert A.-G.* **1993**, EP570795A1.
- [21] E. Elmalem, A. Kiriya, W. T. S. Huck, *Macromolecules* **2011**, *44*, 9057.
- [22] F. F. Diaz, K. K. Kanazawa, G. P. Gardini, *J. Chem. Soc., Chem. Commun.* **1979**, 635.
- [23] (a) P. Kovacic, M. B. Jones, *Chem. Rev.* **1987**, *87*, 357; (b) T. Yokozawa, H. Kohno, Y. Ohta, A. Yokoyama, *Macromolecules* **2010**, *43*, 7095; (c) S. Kang, R. J. Ono, C. W. Bielawski, *J. Am. Chem. Soc.* **2013**, *135*, 4784.
- [24] (a) I. Osaka, R. D. McCullough, *Acc. Chem. Res.* **2008**, *41*, 1202; (b) T. Yokozawa, R. Suzuki, M. Nojima, Y. Ohta, A. Yokoyama, *Macromol. Rapid Commun.* **2011**, *32*, 801.
- [25] (a) M. Jayakannan, X. Lou, J. L. J. VanDongen, R. A. J. Janssen, *J. Polym. Sci., Part A: Polym. Chem.* **2005**, *43*, 1454; (b) J. Liu, E. Sheina, T. Kowalewski, R. D. McCullough, *Angew. Chem., Int. Ed.* **2002**, *41*, 329; (c) R. D. McCullough, P. C. Ewbank, R. S. Loewe, *J. Am. Chem. Soc.* **1997**, *119*, 633; (d) T. A. Chen, R. D. Rieke, *J. Am. Chem. Soc.* **1992**, *114*, 10087; (e) A. Yokoyama, H. Suzuki, Y. Kubota, K. Ohuchi, H. Higashimura, T. Yokozawa, *J. Am. Chem. Soc.* **2007**, *129*, 7236; (f) R. Grisorio, P. Mastroilli, G. P. Suranna, *Polym. Chem.* **2014**, *5*, 4304; (g) H.-H. Zhang, C.-H. Xing, Q.-S. Hu, *J. Am. Chem. Soc.* **2012**, *134*, 13156; (h) E. Elmalem, F. Biedermann, K. Johnson, R. H. Friend, W. T. S. Huck, *J. Am. Chem. Soc.* **2012**, *134*, 17769.
- [26] T. A. Skotheim, J. R. Reynolds, *Handbook of Conducting Polymers*, Third Edition ed., CRC Press Taylor & Francis Group, **2007**.
- [27] P. Kohn, S. Huettner, H. Komber, V. Senkovskyy, R. Tkachov, A. Kiriya, R. H. Friend, U. Steiner, W. T. S. Huck, J.-U. Sommer, M. Sommer, *J. Am. Chem. Soc.* **2012**, *134*, 4790.
- [28] J. L. Brédas, *J. Chem. Phys.* **1985**, *58*, 904.
- [29] (a) T. Matsuda, S. Kadowaki, Y. Yamaguchi, M. Murakami, *Org. Lett.* **2010**, *12*, 1056; (b) Y.-J. Cheng, S.-H. Yang, C.-S. Hsu, *Chem. Rev.* **2009**, *109*, 5868.
- [30] (a) B. Carsten, F. He, H. J. Son, T. Xu, L. Yu, *Chem. Rev.* **2011**, *111*, 1493; (b) W. Li, W. S. C. Roelofs, M. M. Wienk, R. A. J. Janssen, *J. Am. Chem. Soc.* **2012**, *134*, 13787; (c) J. Hou, Z. Tan, Y. Yan, Y. He, C. Yang, Y. Li, *J. Am. Chem. Soc.* **2006**, *128*, 4911; (d) Y. Liang, D. Feng, Y. Wu, S.-T. Tsai, G. Li, C. Ray, L. Yu, *J. Am. Chem. Soc.* **2009**, *131*, 7792; (e) H. Zhong, Z. Li, F. Deledalle, E. C. Fregoso, M. Shahid, Z. Fei, C. B. Nielsen, N. Yaacobi-Gross, S. Rossbauer, T. D. Anthopoulos, J. R. Durrant, M. Heeney, *J. Am. Chem. Soc.* **2013**, *135*, 2040; (f) H. T. Black, A. Dadvand, S. Liu, V. S. Ashby, D. F. Perepichka, *J. Mater. Chem. C* **2013**, *1*, 260.
- [31] (a) A. Zhang, J. Sakamoto, A. D. Schlüter, *Chimia* **2008**, *62*, 776; (b) C. S. Fischer, M. C. Baier, S. Mecking, *J. Am. Chem. Soc.* **2013**, *135*, 1148; (c) F. Zhang, W. Mammo, L. M. Andersson, S. Admassie, M. R. Andersson, O. Inganäs, *Adv. Mater.* **2006**, *18*, 2169; (d) N. Berton, F. Lemasson, J. Tittmann, N. Stürzl, F. Hennrich, M. M. Kappes, M. Mayor, *Chem. Mater.* **2011**, *23*, 2237.
- [32] (a) Although the living character of this type of polymerization was recognized in 2004, the polymerization itself has been reported much earlier: R. D. McCullough, R. D. Lowe, R., *J. Chem. Soc., Chem. Commun.* **1992**, 70; (b) A. Yokoyama, R. Miyakoshi, T. Yokozawa, *Macromolecules* **2004**, *37*, 1169; (c) E. E. Sheina, J. Liu, M. C. Iovu, D. W. Laird, R. D. McCullough, *Macromolecules* **2004**, *37*, 3526; (d) V. Senkovskyy, M. Sommer, A. Kiriya, *Macromol. Rapid Commun.* **2011**, *32*, 1503; (e) K. Okamoto, C. K. Luscombe, *Polym. Chem.* **2011**, *2*, 2424.
- [33] (a) C.-C. Ho, Y.-C. Liu, S.-H. Lin, W.-F. Su, *Macromolecules* **2012**, *45*, 813; (b) J. Hollinger, P. M. DiCarmino, D. Karl, D. S. Seferos, *Macromolecules* **2012**, *45*, 3772; (c) T. Yokozawa, A. Yokoyama, *Chem. Rev.* **2009**, *109*, 5595; (d) R. H. Lohwasser, M. Thelakkat, *Macromolecules* **2011**, *44*, 3388.
- [34] (a) S. D. Boyd, A. K.-Y. Jen, C. K. Luscombe, *Macromolecules* **2009**, *42*, 9387; (b) M. C. Iovu, E. E. Sheina, R. R. Gil, R. D. McCullough, *Macromolecules* **2005**, *38*, 8649; (c) R. Tkachov, V. Senkovskyy, H. Komber, J.-U. Sommer, A. Kiriya, *J. Am. Chem. Soc.* **2010**, *132*, 7803; (d) E. L. Lanni, A. J. McNeil, *J. Am. Chem. Soc.* **2009**, *131*, 16573.
- [35] A. Iraqi, G. W. Barker, *J. Mater. Chem.* **1998**, *8*, 25.

- [36] S. Guillerez, G. Bidan, *Synth. Met.* **1998**, *93*, 123.
- [37] U. Salzner, O. Karalti, S. Durdađi, *J. Mol. Model.* **2006**, *12*, 687.
- [38] (a) A. deMeijere, P. J. Stang, *Metal-Catalyzed Cross-Coupling Reactions, Vol. 2nd ed.*, **2004**;
(b) R. Chincilla, C. Nájera, *Chem. Rev.* **2007**, *107*, 874.
- [39] (a) A. Zapf, M. Beller, *Top. Catal.* **2002**, *19*, 101 ; (b) J. F. Hartwig, *Organotransition metal chemistry: from bonding to catalysis, 1st ed.*, University Science Books, **2010**.
- [40] V. F. Slagt, A. H. M. deVries, J. G. deVries, R. M. Kellogg, *Org. Process Res. Dev.* **2010**, *14*, 30.
- [41] D. Milstein, J. K. Stille, *J. Am. Chem. Soc.* **1978**, *100*, 3636.
- [42] M. Kosugi, K. Sasazawa, Y. Shimizu, T. Migita, *Chem. Lett.* **1977**, 301.
- [43] N. Miyaoura, K. Yamada, A. Suzuki, *Tetrahedron Lett.* **1979**, *19*, 3437.
- [44] Y. Hatanaka, T. Hiyama, *J. Org. Chem.* **1988**, *53*, 918.
- [45] K. S. K. Tamao, M. Kumada, *J. Am. Chem. Soc.* **1972**, *94*, 4374.
- [46] R. J. P. Corriu, J. P. Masse, *J. Chem. Soc., Chem. Commun.* **1972**, 144.
- [47] (a) N. Miyaoura, A. Suzuki, *Chem. Rev.* **1995**, *95*, 2457; (b) A. M. Echavarren, J. K. Stille, *J. Am. Chem. Soc.* **1987**, *109*, 5478.
- [48] (a) A. Leitner, M. Mèndez, H. Krause, A. Fürstner, *J. Am. Chem. Soc.* **2002**, *124*, 13856; (b) A. Leitner, A. Fürstner, *Angew. Chem. Int. Ed.* **2002**, *41*, 609.
- [49] (a) X.-F. Wu, P. Anbarasan, H. Neumann, M. Beller, *Angew. Chem. Int. Ed.* **2010**, *49*, 7316; (b) X.-F. Wu, P. Anbarasan, H. Neumann, M. Beller, *Angew. Chem.* **2010**, *122*, 7474; (c) S. Lou, G. C. Fu, *J. Am. Chem. Soc.* **2010**, *132*, 1264; (d) R. Martin, M. R. Rivero, S. L. Buchwald, *Angew. Chem. Int. Ed.* **2006**, *45*, 7079; (e) R. Martin, M. R. Rivero, S. L. Buchwald, *Angew. Chem.* **2006**, *118*, 7237; (f) M. Mosrin, P. Knochel, *Chem.--Eur. J.* **2009**, *15*, 1468; (g) A. Aranyos, D. W. Old, A. Kiyomori, J. P. Wolfe, J. P. Sadighi, S. L. Buchwald, *J. Am. Chem. Soc.* **1999**, *121*, 4369; (h) J. Bonnamour, M. Piedrafita, C. Bolm, *Adv. Synth. Catal.* **2010**, *352*, 1577; (i) A. Boyer, N. Isono, S. Lackner, M. Lautens, *Tetrahedron* **2010**, *66*, 6468; (j) G. Y. Cho, P. Rémy, J. Jansson, C. Moessner, C. Bolm, *Org. Lett.* **2004**, *6*, 3293; (k) Q. Shen, J. F. Hartwig, *J. Am. Chem. Soc.* **2007**, *129*, 7734; (l) M. Kienle, A. Unsinn, P. Knochel, *Angew. Chem. Int. Ed.* **2010**, *49*, 4751; (m) M. Kienle, A. Unsinn, P. Knochel, *Angew. Chem.* **2010**, *122*, 4860.
- [50] (a) J. Linshoef, A. C. J. Heinrich, S. A. W. Segler, P. J. Gates, A. Staubitz, *Org. Lett.* **2012**, *14*, 5644; (b) E. Elmalem, A. Kiriy, W. T. S. Huck, *Macromolecules* **2011**, *44*, 9057; (c) *For non-aromatic dinucleophiles, see: ;* (d) W. Kaim, H. Tesmann, H. Bock, *Chem. Ber.* **1980**, *113*, 3221; (e) M.-Z. Cai, Z. Zhou, P.-P. Wang *Synthesis* **2006**, *2006*, 789; (f) A. Sorg, R. Brückner, *Angew. Chem. Int. Ed.* **2004**, *43*, 4523; (g) M.-Z. Cai, Y. Wang, P.-P. Wang, *J. Organomet. Chem.* **2008**, *693*, 2954; (h) L. Iannazzo, K. P. C. Vollhardt, M. Malacria, C. Aubert, V. Gandon, *Eur. J. Org. Chem.* **2011**, *2011*, 3283; (i) M. Ogima, S. Hyuga, S. Hara, A. Suzuki, *Chem. Lett.* **1989**, *1959*; (j) C. Malan, C. Morin, *Synlett* **1996**, *167*; (k) P. M. Pihko, A. M. P. Koskinen, *Synlett* **1999**, *1966*; (l) A. Ros, R. López-Rodríguez, B. Estepa, E. Álvarez, R. Fernández, J. M. Lassaletta, *J. Am. Chem. Soc.* **2012**, *134*, 4573; (m) A. C. J. Heinrich, B. Thiedemann, P. J. Gates, A. Staubitz, *Org. Lett.* **2013**, *15*, 4666.
- [51] (a) M. Altendorfer, D. Menche, *Chem. Commun.* **2012**, *48*, 8267; (b) R. S. Coleman, X. L. Lu, I. Modolo, *J. Am. Chem. Soc.* **2007**, *129*, 3826; (c) F. Lehrmitte, B. Carboni, *Synlett* **1996**, 377.
- [52] (a) S. J. Lee, K. C. Gray, J. S. Paek, M. D. Burke, *J. Am. Chem. Soc.* **2008**, *130*, 466; (b) E. M. Woerly, A. H. Cherney, E. K. Davies, M. D. Burke, *J. Am. Chem. Soc.* **2010**, *132*, 6941; (c) G. A. Molander, D. L. Sandrock, *J. Am. Chem. Soc.* **2008**, *130*, 15792; (d) N. Iwadate, M. Sugionome, *J. Am. Chem. Soc.* **2010**, *132*, 2548; (e) J. C. H. Lee, R. McDonald, D. G. Hall, *Nature Chem.* **2011**, *3*, 894; (f) H. Nogouchi, T. Shioda, C. M. Chou, M. Sugionome, *Org. Lett.* **2008**, *10*, 377; (g) K. C. Gray, D. S. Palacios, I. Dailey, M. M. Endo, B. E. Uno, B. C. Wilcock, M. D. Burke, *Proc. Natl. Acad. Sci. USA* **2012**, *109*, 2234; (h) L. Xu, P. F. Li, *Synlett* **2014**, *25*, 1799.
- [53] Y. Yamamoto, T. Seko, H. Nemoto, *J. Org. Chem.* **1989**, *54*, 4736.
- [54] J. Linshoef, A. C. J. Heinrich, S. A. W. Segler, P. J. Gates, A. Staubitz, *Org. Lett.* **2012**, *14*, 5644.
- [55] C. Muschelkautz, C. Dostert, T. J. J. Müller, *Synlett* **2010**, *2010*, 415.
- [56] (a) E. Riedel, *Moderne Anorganische Chemie, Vol. 1*, de Gruyter, Berlin, **1999**; (b) R. Brückner, *Rektionsmechanismen, Vol. 2*, Spektrum Verlag, Heidelberg, **2002**.

- [57] Reprinted with permission of wikipedia, www.wikipedia.org/wiki/Tutanchamun, picture uploaded by user MykReeve (30.04.2015).
- [58] V. Milacic, D. Fregona, Q. P. Dou, *Histol Histopathol.* **2008**, *23*, 101.
- [59] (a) A. C. J. Heinrich, *Synlett* **2015**, *26*, 1135; (b) J. J. Hirner, Y. Shi, S. A. Blum, *Acc. Chem. Res.* **2011**, *44*, 603; (c) S. P. Nolan, *Acc. Chem. Res.* **2011**, *44*, 91; (d) A. S. K. Hashmi, *Chem. Rev.* **2007**, *107*, 3180; (e) A. S. K Hashmi, C. Lothschütz, R. Döpp, M. Rudolph, T. D. Ramamurthi, F. Rominger, *Angew. Chem. Int. Ed.* **2009**, *48*, 8243; (f) P. Garcia, M. Malacria, C. Aubert, V. Gandon, L. Fensterbank, *ChemCatChem* **2010**, *2*, 493; (g) A. S. K. Hashmi, G. J. Hutchings, *Angew. Chem. Int. Ed.* **2006**, *45*, 47; (h) E. Jiménez-Núñez, A. M. Echavarren, *Chem. Rev.* **2008**, *108*, 3326.
- [60] M. A. Cinellu, G. Minghetti, F. Cocco, S. Stoccoro, A. Zucca, *Angew. Chem. Int. Ed.* **2005**, *44*, 6892.
- [61] A. Arcadi, G. Bianchi, S. D. Guiseppe, F. Marinelli, *Green Chem.* **2003**, *5*, 443.
- [62] (a) M. Saramura, Y. Ito, *Chem. Rev.* **1992**, *92*, 857; (b) M. Sawamura, Y. Nakayama, T. Kato, Y. Ito, *J. Org. Chem.* **1995**, *60*, 1727.
- [63] Y. Ito, M. Sawamura, T. J. Hayashi, *J. Am. Chem. Soc.* **1986**, *108*, 6405.
- [64] (a) F. Rominger, T. D. Ramamurthi, A. S. K. Hashmi, *J. Organomet. Chem.* **2009**, *694*, 592; (b) Y. Shi, S. D. Ramgren, S. A. Blum, *Organometallics* **2009**, *28*, 1275; (c) L.-P.-. Liu, G. B. Hammond, *Chem. Soc. Rev.* **2012**, *41*, 3129; (d) J. J. Hirner, S. A. Blum, *Organometallics* **2011**, *30*, 1299.
- [65] A. S. K Hashmi, R. Döpp, C. Lothschütz, M. Rudolph, D. Riedel, F. Rominger, *Adv. Synth. Catal.* **2010**, *352*, 1307.
- [66] (a) Y. Shi, S. M. Peterson, W. W. Haberaecker(III), S. A. Blum, *J. Am. Chem. Soc.* **2008**, *130*, 2168; (b) M. Peña-López, M. Ayán-Varela, L. A. Sarandeses, J. P. Sestelo, *Chem. Eur. J.* **2010**, *16*, 9905.
- [67] (a) C. Lothschütz, R. Döpp, M. Rudolph, T. D. Ramamurthi, F. Rominger, A. S. K. Hashmi, *Angew. Chem.* **2009**, *121*, 8392; (b) Y. Shi, K. E. Roth, S. D. Ramgren, S. A. Blum, *J. Am. Chem. Soc.* **2009**, *131*, 18022.
- [68] P. J. Kocienski, *Protecting Groups*, Georg Thieme Verlag, Stuttgart, **1994**.
- [69] (a) K. Kent, *Critical Reviews in Toxicology* **1996**, *26*; (b) M. Hoch, *Appl. Geochem.* **2001**, *16*, 719; (c) K. Appel, *Drug Metab. Rev.* **2004**, *36*, 763; (d) F. Grun, B. Blumberg, *Endocrinology* **2006**, *147*, 550.
- [70] N. R. Panyala, E. Peña-Méndez, J. Havel, *J. Appl. Biomed.* **2009**, *7*, 75.
- [71] M. L. Wu, W. J. Tsai, J. Ger, J. F. Deng, S. H. Tsay, M. H. Yang, *Clin. Toxicol.* **2001**, *2001*, 739.
- [72] S. P. Fricker, *Metal Based Drugs* **1999**, *6*.
- [73] W. F. Kean, F. Forestier, Y. Kassam, W. W. Buchanan, P. J. Rooney, *Semin. Arthritis. Rheum.* **1985**, *14*, 180.
- [74] N. Meyer, S. Sivanathan, F. Mohr, *J. Organomet. Chem.* **2011**, *694*, 592.
- [75] F. K. Keter, I. A. Guzei, M. Nell, W. E. v. Zyl, J. Darkwa, *Inorg. Chem.* **2014**, *53*, 2058.
- [76] (a) A. Corma, E. Gutierrez-Puebla, M. Iglesias, A. Monge, S. Perez-Ferreras, F. Sanchez, *Adv. Synth. Catal.* **2006**, *348*, 1899; (b) J. Lu, H. P. Toy, *Chem. Rev.* **2009**, *109*, 815; (c) R. Nishio, M. Suigura, S. Kabayashi, *Org. Lett.* **2005**, *7*, 4831.
- [77] (a) R. D. McCullough, R. D. Lowe, *J. Chem. Soc., Chem. Commun.* **1992**, 70; (b) R. Miyakoshi, A. Yokoyama, T. Yokozawa, *Macromol. Rapid Commun* **2004**, *25*, 1663.
- [78] (a) R. Miyakoshi, K. Shimono, A. Yokoyama, T. Yokozawa, *J. Am. Chem. Soc.* **2006**, *128*, 16012; (b) L. Huang, S. Wu, Y. Qu, Y. Geng, F. Wang, *Macromolecules* **2008**, *41*, 8944; (c) M. C. Stefan, A. E. Javier, I. Osaka, R. D. McCullough, *Macromolecules* **2009**, *42*, 30; (d) L. Wen, B. C. Duck, P. C. Dastoor, S. C. Rasmussen, *Macromolecules* **2008**, *41*, 4576; (e) A. Yokoyama, A. Kato, R. Miyakoshi, T. Yokozawa, *Macromolecules* **2008**, *41*, 7271; (f) F. C. Krebs, V. Senkovskyy, A. Kiriya, *IEEE J. Sel. Top. Quant. Electron.* **2010**, *16*, 1821.
- [79] Work on this synthesis has already been embarked upon (during an internship of M. Ried under my guidance), although full characterizations of the products are pending. The data

obtained thus far are added as an appendix after the supporting information for the publication discussed in this chapter.

- [80] (a) H. Wu, J. J. Hynes, *Org. Lett.* **2010**, *12*, 1192; (b) P. N. Devine, D. R. Gauthier, R. P. Volante, R. H. Szumigala, *J. Org. Chem.* **2004**, *69*, 566.
- [81] G. Zhang, G. Lv, L. Li, F. Chen, J. Cheng, *Tetrahedron Lett.* **2011**, *52*, 1993.